



FOOD STORAGE, SPOILAGE AND SHELF LIFE: RECENT DEVELOPMENTS AND INSIGHTS

EDITED BY: Shalini Gaur Rudra, Santanu Basu and Anindya Chanda

PUBLISHED IN: *Frontiers in Microbiology* and
Frontiers in Sustainable Food Systems



frontiers

Frontiers eBook Copyright Statement

The copyright in the text of individual articles in this eBook is the property of their respective authors or their respective institutions or funders. The copyright in graphics and images within each article may be subject to copyright of other parties. In both cases this is subject to a license granted to Frontiers.

The compilation of articles constituting this eBook is the property of Frontiers.

Each article within this eBook, and the eBook itself, are published under the most recent version of the Creative Commons CC-BY licence.

The version current at the date of publication of this eBook is CC-BY 4.0. If the CC-BY licence is updated, the licence granted by Frontiers is automatically updated to the new version.

When exercising any right under the CC-BY licence, Frontiers must be attributed as the original publisher of the article or eBook, as applicable.

Authors have the responsibility of ensuring that any graphics or other materials which are the property of others may be included in the CC-BY licence, but this should be checked before relying on the CC-BY licence to reproduce those materials. Any copyright notices relating to those materials must be complied with.

Copyright and source acknowledgement notices may not be removed and must be displayed in any copy, derivative work or partial copy which includes the elements in question.

All copyright, and all rights therein, are protected by national and international copyright laws. The above represents a summary only. For further information please read Frontiers' Conditions for Website Use and Copyright Statement, and the applicable CC-BY licence.

ISSN 1664-8714

ISBN 978-2-88976-850-9

DOI 10.3389/978-2-88976-850-9

About Frontiers

Frontiers is more than just an open-access publisher of scholarly articles: it is a pioneering approach to the world of academia, radically improving the way scholarly research is managed. The grand vision of Frontiers is a world where all people have an equal opportunity to seek, share and generate knowledge. Frontiers provides immediate and permanent online open access to all its publications, but this alone is not enough to realize our grand goals.

Frontiers Journal Series

The Frontiers Journal Series is a multi-tier and interdisciplinary set of open-access, online journals, promising a paradigm shift from the current review, selection and dissemination processes in academic publishing. All Frontiers journals are driven by researchers for researchers; therefore, they constitute a service to the scholarly community. At the same time, the Frontiers Journal Series operates on a revolutionary invention, the tiered publishing system, initially addressing specific communities of scholars, and gradually climbing up to broader public understanding, thus serving the interests of the lay society, too.

Dedication to Quality

Each Frontiers article is a landmark of the highest quality, thanks to genuinely collaborative interactions between authors and review editors, who include some of the world's best academicians. Research must be certified by peers before entering a stream of knowledge that may eventually reach the public - and shape society; therefore, Frontiers only applies the most rigorous and unbiased reviews.

Frontiers revolutionizes research publishing by freely delivering the most outstanding research, evaluated with no bias from both the academic and social point of view. By applying the most advanced information technologies, Frontiers is catapulting scholarly publishing into a new generation.

What are Frontiers Research Topics?

Frontiers Research Topics are very popular trademarks of the Frontiers Journals Series: they are collections of at least ten articles, all centered on a particular subject. With their unique mix of varied contributions from Original Research to Review Articles, Frontiers Research Topics unify the most influential researchers, the latest key findings and historical advances in a hot research area! Find out more on how to host your own Frontiers Research Topic or contribute to one as an author by contacting the Frontiers Editorial Office: frontiersin.org/about/contact

FOOD STORAGE, SPOILAGE AND SHELF LIFE: RECENT DEVELOPMENTS AND INSIGHTS

Topic Editors:

Shalini Gaur Rudra, Indian Agricultural Research Institute, India

Santanu Basu, Swedish University of Agricultural Sciences, Sweden

Anindya Chanda, Mycologics LLC, United States

Citation: Rudra, S. G., Basu, S., Chanda, A., eds. (2022). Food Storage, Spoilage and Shelf Life: Recent Developments and Insights. Lausanne: Frontiers Media SA. doi: 10.3389/978-2-88976-850-9

Table of Contents

- 05 Editorial: Food storage, spoilage and shelf life: Recent developments and insights**
Shalini Gaur Rudra, Santanu Basu and Anindya Chanda
- 09 Markers to Rapidly Distinguish *Bacillus paralicheniformis* From the Very Close Relative, *Bacillus licheniformis***
Atinuke M. Olajide, Shu Chen and Gisèle LaPointe
- 19 Butylated Hydroxytoluene Induced Resistance Against *Botryosphaeria dothidea* in Apple Fruit**
Yan Huang, Cuicui Sun, Xiangnan Guan, Sen Lian, Baohua Li and Caixia Wang
- 30 Isolation and Molecular Identification of the Native Microflora on *Flammulina velutipes* Fruiting Bodies and Modeling the Growth of Dominant Microbiota (*Lactococcus lactis*)**
Qi Wei, Xinyuan Pan, Jie Li, Zhen Jia, Ting Fang and Yuji Jiang
- 41 Physical and Structural Characterization of Underutilized Climate-Resilient Seed Grains: Millets, Sorghum, and Amaranth**
Sarah Geisen, Kiruba Krishnaswamy and Rob Myers
- 54 Optimizing Pasteurized Fluid Milk Shelf-Life Through Microbial Spoilage Reduction**
Forough Enayaty-Ahangar, Sarah I. Murphy, Nicole H. Martin, Martin Wiedmann and Renata Ivanek
- 75 Smart and Active Food Packaging: Insights in Novel Food Packaging**
Hamed Ahari and Solmaz P. Soufiani
- 101 Antimicrobial Properties of Food Nanopackaging: A New Focus on Foodborne Pathogens**
Amir Ali Anvar, Hamed Ahari and Maryam Ataee
- 114 *Bacillus cereus* in Packaging Material: Molecular and Phenotypical Diversity Revealed**
Paul Jakob Schmid, Stephanie Maitz and Clemens Kittinger
- 125 Quantification of Viable *Brochothrix thermosphacta* in Cold-Smoked Salmon Using PMA/PMAxx-qPCR**
Agnès Bouju-Albert, Sabrina Saltaji, Xavier Dousset, Hervé Prévost and Emmanuel Jaffrès
- 137 Bruise Susceptibility and Impact on Quality Parameters of Pears During Storage**
Pankaj B. Pathare and Mai Al-Dairi
- 150 Microbial Diversity and Non-volatile Metabolites Profile of Low-Temperature Sausage Stored at Room Temperature**
Hongjiao Han, Mohan Li, Yanqi Peng, Zhenghan Zhang, Xiqing Yue and Yan Zheng
- 161 Warehouse Storage Management of Wheat and Their Role in Food Security**
Chandrasen Kumar, C. L. Ram, S. N. Jha and R. K. Vishwakarma

- 175** *Enabling Food Safety Entrepreneurship: Exploratory Case Studies From Nepal, Senegal, and Ethiopia*
Yevheniia Varyvoda, Thoric Cederstrom, Jenna Borberg and Douglas Taren
- 188** *Analysis of Microbial Diversity and Dynamics During Bacon Storage Inoculated With Potential Spoilage Bacteria by High-Throughput Sequencing*
Xinfu Li, Qiang Xiong, Hui Zhou, Baocai Xu and Yun Sun
- 202** *Mathematical Modeling of Total Volatile Basic Nitrogen and Microbial Biomass in Stored Rohu (Labeo rohita) Fish*
Pramod K. Prabhakar, Prem P. Srivastav, Sant S. Pathak and Kalyan Das
- 216** *Comparison of Physicochemical Changes and Water Migration of Acinetobacter johnsonii, Shewanella putrefaciens, and Cocultures From Spoiled Bigeye Tuna (Thunnus obesus) During Cold Storage*
Xin-Yun Wang and Jing Xie
- 226** *Evaluating the Effectiveness of Screened Lactic Acid Bacteria in Improving Crop Residues Silage: Fermentation Parameter, Nitrogen Fraction, and Bacterial Community*
Liwen He, Yimin Wang, Xiang Guo, Xiaoyang Chen and Qing Zhang



OPEN ACCESS

EDITED AND REVIEWED BY

Dike Ukuku,
Agricultural Research Service (USDA),
United States

*CORRESPONDENCE

Shalini Gaur Rudra
shalinigaur@iari.res.in

SPECIALTY SECTION

This article was submitted to
Agro-Food Safety,
a section of the journal
Frontiers in Sustainable Food Systems

RECEIVED 26 May 2022

ACCEPTED 11 July 2022

PUBLISHED 25 July 2022

CITATION

Rudra SG, Basu S and Chanda A (2022)
Editorial: Food storage, spoilage and
shelf life: Recent developments and
insights.
Front. Sustain. Food Syst. 6:953983.
doi: 10.3389/fsufs.2022.953983

COPYRIGHT

© 2022 Rudra, Basu and Chanda. This
is an open-access article distributed
under the terms of the [Creative
Commons Attribution License \(CC BY\)](#).
The use, distribution or reproduction
in other forums is permitted, provided
the original author(s) and the copyright
owner(s) are credited and that the
original publication in this journal is
cited, in accordance with accepted
academic practice. No use, distribution
or reproduction is permitted which
does not comply with these terms.

Editorial: Food storage, spoilage and shelf life: Recent developments and insights

Shalini Gaur Rudra^{1*}, Santanu Basu² and Anindya Chanda³

¹Division of Food Science and Postharvest Technology, Indian Agricultural Research Institute, New Delhi, India, ²Department of Molecular Sciences, Swedish University of Agricultural Sciences, Uppsala, Sweden, ³Mycologics LLC, Durham, NC, United States

KEYWORDS

trends, food safety, developments, detection, spoilage

Editorial on the Research Topic

Food storage, spoilage and shelf life: Recent developments and insights

The past few years have witnessed high levels of food production, processing and preservation due to advancements in crop production and protection. However, with global climate change, the pandemic, and the hindered food supply chain influenced by the ongoing geopolitical events, access to safe foods has become increasingly challenging. Besides, the pace of development in food storage has not been at par, leading to global problems of food spoilage and waste generation at various points of the supply chain and even at the consumers' end. Furthermore, with a rapidly increasing global population expected to cross 8.5 billion by 2030, there is a pressing need to reduce the amount of per capita global food waste at the retail and consumer levels by at least 50% to meet the Target 12.3 of the Sustainable Development Goals¹.

Improved storage conditions and technologies for combating foodborne pathogens will also lead to enhanced food safety. Consumption of unsafe foods amounts to 600 million reported foodborne illnesses and 420,000 deaths worldwide every year, with 30% of foodborne deaths occurring among children under 5 (Lee and Yoon, 2021). An estimated 33 million years² of healthy lives are lost because of eating unsafe food globally each year, although according to the WHO, this number is likely an under-estimation. Recent examples of foodborne illnesses include a multistate outbreak of *Salmonella* infections in the United States (<https://www.miamiherald.com/news/recalls/article261667272.html>), the Norovirus poisoning of oysters³ (> 100 cases) in Canada, the

1 <https://www.unep.org/thinkatsave/about/sdg-123-food-waste-index>

2 <https://www.who.int/activities/estimating-the-burden-of-foodborne-diseases>

3 <https://www.foodsafetynews.com/2022/04/fda-says-reports-nearing-450-in-outbreak-associated-with-lucky-charms-cereal/>

100 illnesses from *Staphylococcus aureus* exposure at the Coachella festival⁴ in California, the *Salmonella* outbreak in Finland⁵ that affected more than 700 people, and the 70 cases from Shigella toxin exposure in India⁶, including the death of a teenager. These examples are a grim reminder of the importance of proper food preparation, storage and rapid detection of food pathogens.

The objective of floating the Research Topic on Food storage, spoilage, and shelf life was to compile the advances in research toward preventing food spoilage, enhancing shelf life, and monitoring conditions during storage. The topic saw a tremendous response from researchers, with twenty-seven submissions and seventeen accepted articles contributed by sixty-seven authors worldwide. The total views numbering > 37,500 show the keen interest of researchers in this area.

The identification and distinction of pathogens from their close relatives pose a significant challenge to researchers and food safety professionals⁷. False detection of pathogens has enormous economic and legal implications, while missing out on the pathogens can lead to disease or even death. Olajide et al. from Canada identified the presence of fengycin operon in *B. paralicheniformis* through MADI-TOF. These two genetic markers (FenC and FenD) will help in reliable and quick differentiation of *Bacillus* species adequately, which cause spoilage in foods, including dairy. Bouju-Albert et al. developed a rapid and accurate *rpoC*-PMA-qPCR method to detect *Brochothrix thermosphacta*, a major food spoilage bacteria responsible for off-odors production in beef and seafood. This is the first report on the use of qPCR to quantify *B. thermosphacta*, along with the use of a viability dye (PMA or PMAXx) and the targeting of a single-copy gene (*rpoC* or *rpoB*). They could efficiently discriminate between live and dead cells and validated the test on industrially processed cold-smoked salmon filets. Their method could specifically and quickly enumerate *B. thermosphacta* within 3–4 h compared to 48 h for the STAA culture method.

Li et al. used high-throughput sequencing of the V3–V4 region of the 16S rRNA gene to study the dynamics, diversity, interaction, and succession of five food spoilage bacteria after inoculating sterilized smoked bacon with their culture. *Serratia liquefaciens*, *C. maltaromaticum*, and *L. mesenteroides* were identified as more competitive species over others. Similarly,

Han et al. generated helpful information for optimizing sausage storage conditions after studying the microbiota non-volatile metabolites in a model sausage after storage at 20°C for up to 12 days. Such a study on sausage samples exposed to an open environment during production, marketing, and distribution and characterization of quality and microbiota changes is rare and has seen > 1,000 views. Correct identification of the dominant species and their dynamism plays a key role in determining the strategies for preservation and prevention of disease outbreak during storage. Therefore studies like this would help improve the shelf life of meat products.

A similar study was conducted by Wei et al. to isolate and identify the dominant microorganism in *Flammulina velutipes* fruiting bodies using morphological examination and high-throughput sequencing. The kinetic models for describing the growth of predominant spoilage microorganism *L. lactis* can be used by regulatory agencies and food processors for conducting risk assessments and predicting the shelf-life of *Flammulina velutipes* fruiting bodies.

Prabhakar et al. studied the dynamic behavior of fish volatiles and the growth of microbes in stored Rohu fish through mathematical modeling. The findings of this study would help predict the freshness of rohu fish, and aid design and understand cold chain logistics for seafood.

Wang and Xie inoculated *Acinetobacter johnsonii*, *Shewanella putrefaciens*, and their co-cultures in bigeye tuna during cold storage and monitored quality changes and microbial dynamics. Trapped water, protein degradation, and lipid oxidation studies provide data for understanding the spoilage mechanism of co-cultures and enable estimation of aquatic food quality and shelf-life. Pathogens and spoilage microbes can enter at any point of food chain. Usually, toxin-producing strains of *B. cereus* originate from soil, water, and plants. But even packaging material can emerge as source of pathogen. From Austria, Schmid et al. have explored the presence and possible spoilage potential of *B. cereus* from packaging material. The first such study in this area showed that although a variety of *B. cereus* group strains can be found in packaging material, significant amounts of highly virulent strains and cereulide-producing strains are not present.

Milk spoilage due to spore-producing psychrotolerant microorganisms is an emerging problem since these spores can even tolerate pasteurization temperatures. Enayaty-Ahangar et al. have provided novel decision support tools to aid individual processors in identifying a suitable approach to achieving desired milk shelf-life as per their specific production conditions along with the motivation for the shelf-life extension. Such decision support systems can not only help in improving distribution efficiencies and ensure safe, long-lasting, high-quality dairy products for consumers, but also serve as guideline for other food chains.

The recent trend for preference for preservative-free and clean labels has seen developments in chemical-free

4 <https://www.foodsafetynews.com/2022/05/staph-blamed-for-foodborne-illness-outbreak-among-coachella-bus-drivers/>

5 <https://www.foodsafetynews.com/2022/05/large-salmonella-outbreak-dominates-finnish-figures/>

6 <https://indianexpress.com/article/india/kerala/shigella-food-poisoning-girl-died-shawarma-kerala-health-dept-7899820/>

7 [https://www.who.int/news-room/fact-sheets/detail/food-safety#:~:siml\\$=text=An%20estimated%20600%20million%20E2%80%93%20almost%20healthy%20life%20years%20\(DALYs\)](https://www.who.int/news-room/fact-sheets/detail/food-safety#:~:siml$=text=An%20estimated%20600%20million%20E2%80%93%20almost%20healthy%20life%20years%20(DALYs))

food safety alternatives. Efficient packaging protects from contaminants. Modern packages have evolved to not only aid in preventing spoilage but indicate the state of quality while being environmentally friendly. Ahari and Soufiani have reviewed the latest developments in the field of packaging. Antimicrobial packaging can play an essential role in reducing the risk of pathogen contamination and improving foods' quality and shelf life. Various inorganic nanoparticles (silver, copper, gold, metal oxides) help induce antimicrobial attributes in packaging materials. They have discussed the issues related to degradation, indicator and scavenger functions of modern smart packages. Anvar et al. have reviewed the developments in these new antimicrobials for the improved shelf life of food products. In addition, they have provided advisory on food handling in COVID-19 scenario. The use of nanoparticles for intelligent food packages has also been reviewed.

On similar lines, scientists are working toward finding safer approaches for pathogen management during storage. Green postharvest solutions protect not just the fresh produce but also humankind. Ring rot spoilage of apples by *Botryosphaeria dothidea* is a major postharvest disease in bag-free cultivated apples. Plant activator butylated hydroxytoluene can emerge as an alternative to synthetic pesticides. Huang et al. reported that BHT confers resistance against *B. dothidea* in apple fruits, possibly by enhancing defensive enzyme activities and activating the salicylic acid signaling pathway. Alongside facing biotic challenges, fruits usually travel miles to reach the consumer. During this journey, mechanical damage in the form of bruises can lead to faster ripening, internal browning, and quality losses. Bruising can lead to increased surface area for microbial attachment, and survival due to nutrient leakage. The effect of such various drop impact levels, storage temperature, and storage duration on the quality of pears was studied by Pathare and Dairi. The findings of their study can help understand the mechanism of bruising and determine ways to reduce it.

Implementing food safety and sustainability through food safety entrepreneurship poses numerous challenges. In their research contribution, Varyvoda et al. have presented food safety solutions for Nepal, Senegal, and Ethiopia, including diversification, use of underutilized food sources, marrying traditional knowledge with innovations and use of digital technology. They suggest that in scenarios where the local context of business operations influences food safety practices, the intervention programs should consider their influence and consequence for effective implementation in the field. Among such underutilized food sources are millets, sorghum, and amaranth. These climate-resilient crops can provide sustainable solutions for production and nutrition. Geisen et al. demonstrated that while millets appear similar to the human eye, there is a considerable variation in mechanical properties like bulk density, color, porosity, etc. They have proposed a methodology for their physical characterization and highlighted the need for focused breeding programs and

product development based on the specific attribute of each millet grain.

In practice, sustainable grain storage systems offer numerous challenges in sub-tropical climates like that of India. Kumar et al. have documented the storage management practices of wheat in the Food Corporation of India (handling > 70 million tons of cereals annually) in their warehouse system and quantified the storage losses based on field study. They have reported that adopting proper storage management practices for wheat in warehouse storage has brought the level of storage losses (0.3% in 3 years) equivalent to silo storage.

Conversion of agricultural waste to safe animal feed is another dimension of food sustainability. He et al. have studied the effectiveness of two lactic acid bacterial strains for ensiling sweet potato vine and peanut straw. Effective and safe animal feed translates to safety for humans also, especially in the wake of zoonotic disease spread like COVID-19.

The research contributions to this topic showcased the multiple dimensions of food safety and sustainability with élan. For example, the use of genetic markers, mathematical modeling, non-synthetic chemicals, nanomaterials, packaging aids, decision support systems, etc. to identify and contain food spoilage agents, along with other considerations like reducing mechanical damage, alternative food sources, on-field efficient storage practices, all pave the way to safe and sustainable food environment for future generations.

Author contributions

All authors contributed to the review of manuscripts and preparation of this editorial. All authors contributed to the article and approved the submitted version.

Acknowledgments

We are immensely grateful to all peer reviewers who genially took the time to review the manuscripts and helped improve the quality of manuscripts for this Research Topic. We appreciate the promptness and patience of authors for clarifying and attending to suggestions by learned reviewers and editors. The guidance and consistent support by the Frontiers team is also noteworthy for providing shape to this Research Topic.

Conflict of interest

Author AC was employed by Mycologics LLC.

The remaining authors declare that the research was conducted in the absence of any commercial or financial relationships that could be construed as a potential conflict of interest.

Publisher's Note

All claims expressed in this article are solely those of the authors and do not necessarily represent those of their affiliated

organizations, or those of the publisher, the editors and the reviewers. Any product that may be evaluated in this article, or claim that may be made by its manufacturer, is not guaranteed or endorsed by the publisher.

References

- Lee, H., and Yoon, Y. (2021). Etiological agents implicated in foodborne illness world wide. *Food Sci. Anim. Resour.* 41, 1–7. doi: 10.5851/kosfa.2020.e75



Markers to Rapidly Distinguish *Bacillus paralicheniformis* From the Very Close Relative, *Bacillus licheniformis*

Atinuke M. Olajide^{1*}, Shu Chen² and Gisèle LaPointe^{1*}

¹CRIFS, Department of Food Science, University of Guelph, Ontario, ON, Canada, ²Agriculture and Food Laboratory, Laboratory Services Division, University of Guelph, Ontario, ON, Canada

OPEN ACCESS

Edited by:

Anindya Chanda,
Mycologics LLC, United States

Reviewed by:

Colin Harwood,
Newcastle University, United Kingdom
Kaoru Nakasone,
Kindai University, Japan

*Correspondence:

Gisèle LaPointe
glapoint@uoguelph.ca
Atinuke M. Olajide
atinuke@uoguelph.ca

Specialty section:

This article was submitted to
Food Microbiology,
a section of the journal
Frontiers in Microbiology

Received: 20 August 2020

Accepted: 07 December 2020

Published: 11 January 2021

Citation:

Olajide AM, Chen S and
LaPointe G (2021) Markers to Rapidly
Distinguish *Bacillus paralicheniformis*
From the Very Close Relative,
Bacillus licheniformis.
Front. Microbiol. 11:596828.
doi: 10.3389/fmicb.2020.596828

As close relatives, *Bacillus paralicheniformis* is often wrongly identified as *Bacillus licheniformis*. In this study, two genetic markers are presented based on *fenC* and *fenD* from the fengycin operon of *B. paralicheniformis* to rapidly distinguish it from *B. licheniformis*. The fengycin operon is one of the few present in *B. paralicheniformis* but absent in *B. licheniformis* up to date. Using these markers, two presumptive *B. paralicheniformis* isolates each were recovered from a set of isolates previously identified as *B. licheniformis* by Matrix-assisted laser desorption ionization–time of flight (MALDI-TOF) or identified only to genus level as *Bacillus* by 16S ribosomal RNA (rRNA) gene sequencing, respectively. Whole genome sequencing of the four isolates confirmed their identity as *B. paralicheniformis* having the closest similarity with *B. paralicheniformis* ATCC 9945a (GenBank: CP005965.1) with a 7,682 k-mer score and 97.22% Average Nucleotide Identity (ANI). ANI of 100% suggests that the four isolates are highly similar. Further analysis will be necessary to determine if finer differences exist among these isolates at the level of single nucleotide polymorphisms.

Keywords: *Bacillus paralicheniformis*, markers, fengycin, dairy, draft genome

INTRODUCTION

In the *Bacillus* genus, many species within the assigned groups are very closely related so that 16S ribosomal RNA (rRNA) gene sequences cannot be used to distinguish them (Branquinho et al., 2014a). For instance, in the *Bacillus cereus* group, more than 97% sequence similarity exists among the 16S rRNA genes of *Bacillus anthracis*, *B. cereus*, *Bacillus weihenstephanensis*, *Bacillus thuringiensis*, *Bacillus mycoides*, *Bacillus pseudomyoides*, *Bacillus cytotoxicus*, *Bacillus gaemokensis*, and *Bacillus manliponensis* (Guinebretière et al., 2013). Furthermore, in the *Bacillus pumilus* group, *B. pumilus*, *Bacillus safensis*, *Bacillus altitudinis*, *Bacillus stratosphericus*, *Bacillus aerophilus*, *Bacillus xiamenensis*, and *Bacillus invictae* have over 99.5% similarity in their 16S rRNA gene sequences (Satomi et al., 2006; Liu et al., 2013; Lai et al., 2014; Branquinho et al., 2014b). Likewise, based on the comparative analysis of the 16S rRNA gene, *Bacillus paralicheniformis* strain KACC 18426 (KJ-16^T) is 99.5% similar to *Bacillus sonorensis* KCTC-13918^T and 99.4% similar to *Bacillus licheniformis* DSM 13^T (Dunlap et al., 2015).

Due to the close relatedness of *B. paralicheniformis* to *B. licheniformis*, the former has been wrongly identified as *B. licheniformis* up until 2015. The phylogenetic analysis of nine *B. paralicheniformis* and 46 *B. licheniformis* showed that most of the former belonged to lineage P while the latter clustered together in lineage L (Du et al., 2019). However, the researchers observed that a few *B. licheniformis* clustered with *B. paralicheniformis* in lineage P rather than in lineage L. The genome comparative study by Du et al. (2019) revealed differences existing in the operons implicated in secondary metabolite synthesis among many *Bacillus* species. Some examples are the fengycin, paralichenicidin, and bacitracin operons, encoded by the genomes of *B. paralicheniformis* but absent in those of *B. licheniformis* analyzed to date (Harwood et al., 2018; Du et al., 2019).

Fengycins belong to a group of non-ribosomally synthesized antifungal lipopeptides, produced by certain strains of *Bacillus* species, such as *B. subtilis*, *B. velezensis*, *B. paralicheniformis*, and *B. amyloliquefaciens* (Steller et al., 1999; Stein, 2005; Harwood et al., 2018; Du et al., 2019). Also, fengycin lowered the numbers of *Staphylococcus aureus* in the human intestine (Piewngam et al., 2018). Fengycin synthetase consists of five non-ribosomal peptide synthetases (NRPSs) FenA – FenE encoded by *fenA* – *fenE* (Figure 1; Vanittanakom et al., 1986; Steller et al., 1999; Chen et al., 2007). Fengycin is a cyclic lipodecapeptide (CLP) containing a β -hydroxy fatty acid side chain of up to 19 carbon atoms (Steller et al., 1999) while the peptide portion contains at least four amino acids (Steller et al., 1999). The structure and function of the fengycin synthetase of *B. subtilis* origin have been reviewed previously by Steller et al. (1999).

Although Dunlap et al. (2015) attempted to differentiate *B. paralicheniformis* from *B. licheniformis* based on 16S rRNA gene phylogenetic and phenotypic analyses; there are no genetic markers that have been used to rapidly achieve this. To adequately identify *Bacillus* species, known to cause spoilage in foods including dairy, it is important to develop markers that work rapidly and efficiently in distinguishing these close relatives. Hence, *B. paralicheniformis* specific markers were designed based on the *fenC* gene (7,640 bp) and the *fenD* (10,780 bp). The markers were used to screen a collection of isolates previously identified as *B. licheniformis* or *Bacillus* spp. by 16S rRNA gene sequencing, matrix-assisted laser desorption ionization–time of flight (MALDI-TOF), or *B. licheniformis* specific primers. To the best of our knowledge, dairy *B. paralicheniformis* isolates of Canadian origin have not yet been reported.

MATERIALS AND METHODS

Isolate Identification

Three hundred and nineteen (319) isolates were obtained after spore pasteurization (80°C for 12 min) or laboratory pasteurization (63°C for 30 min) of samples (raw milk, HT-milk, whey, curds, and environmental swabs) from a Cheddar cheese making plant and incubation on BHI agar (Oxoid) at 30°C for 48 h (aerobic). The identification was carried out by Sanger sequencing of the 16S rRNA gene, MALDI-TOF mass spectroscopy or *B. licheniformis* specific primers by de Almeida (2014). Sanger sequencing of at least 750 bp of the 16S rRNA gene was carried out using the FD1 forward primer (5' AGAGTTTGATCCTGGCTCAG-3') and the RD1 reverse primer (5' AAGGAGGTGATCCAGCCGCA-3'; Weisburg et al., 1991). Colony PCR was carried out with the condition as follows: 94°C for 2 min, 35 cycles of 94°C for 15 s, 55°C for 30 s, 72°C for 1.5 min and finally, and 72°C for 10 min. After amplification, the amplicons were separated by agarose gel electrophoresis (1% w/v, 70 v for 30 min) and visualized using a ChemiDoc Imaging System (Bio-Rad, Canada). Once the appropriate bands were purified, the products were sequenced at Eurofins (Canada). The sequences obtained per isolate were assembled (using DNA Baser v4) and compared against the National Center for Biotechnology Information (NCBI) database using the Ribosomal Database Project (Michigan State University) to obtain identification (> 99% similarity to species level).

Matrix-assisted laser desorption ionization–time of flight was used to identify isolates at the Animal Health Laboratory, University of Guelph (Guelph, ON, Canada) on the MALDI Biotyper (Bruker, Canada) with the software Compass v 4.1.80 (PYTH) 1022017-08-226_04-55-52. Each isolate to be identified was struck on a plate (Brain Heart Infusion agar at 30°C for 1 day) to obtain single and distinct colonies. After incubation, the isolates were maintained at room temperature until they were transported to the MALDI-TOF analysis facility. A bacterial colony was directly transferred to a 96-spot stainless steel target plate. One microliter of HCCA matrix (α -Cyano-4-hydroxycinnamic acid) was applied to each spot and left to dry (at room temperature). One microliter 70% formic acid was applied to the spot and allowed to dry followed by the addition of another 1 μ l HCCA matrix after which it was left to dry. Identification was completed using a Bruker MALDI Biotyper and the software “Compass version 4.1.80 (PYTH) 1022017-08-226_04-55-52.” Calibration of each run was

Fengycin

B. paralicheniformis MDJK30 (CP020352.1)

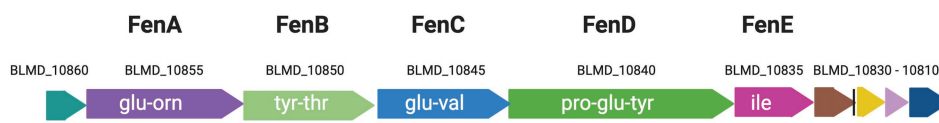


FIGURE 1 | Genetic organization of the cluster coding for fengycin biosynthesis from the genome of *B. paralicheniformis* MDJK30 (Du et al., 2019).

completed by applying a Bacterial Test Standard (BTS) to each target. The BTS was an *Escherichia coli* extract spiked with two high molecular weight proteins that was developed for the quality control process of the MALDI Biotyper System. The specific composition of the BTS covered the entire mass range of proteins used for precise identification of microorganisms. This control was run at every MALDI identification procedure, and the calibration must pass in flex control with a score greater than 2.0. A MALDI-TOF spectrum was automatically generated by the software and instantly matched against the reference library to give identification. For taxonomy allocation, if an organism obtained a score (x): $x < 1.7$, the ID was reported as “not reliable identification”; a score between $1.7 \leq x \leq 1.99$ was reported to genus level only and with a score $x \geq 2.0$, the ID was reliably reported to species level.

Lastly, four *B. licheniformis* specific primer sets (in pairs per PCR) were applied to crude DNA from *Bacillus* isolates with undetermined species as described by de Almeida (2014) (Table 1) using DNA from *B. licheniformis* ATCC 14580 and *B. paralicheniformis* KACC 18426 as positive and negative control, respectively. The PCR reaction mixture (23.5 μ l) contained 1 \times PCR Supermix (Invitrogen), 0.25 μ l (12.5 μ M) of each primer, and 10 μ l of template DNA. The amplification was as follows: initial denaturation for 5 min at 95°C, 35 cycles of 30 s at 95°C, 30 s at 58°C, and 90 s at 72°C followed by a final extension step for 10 min at 72°C. The amplification products were separated on a 2% agarose gel at 100 V for 35 min. Isolates for which amplicons were obtained by all four primer sets were assigned to *B. licheniformis*.

Identification of the Fengycin Operon in the *B. paralicheniformis* Genome

The genes making up the fengycin operon were searched using BLAST within the six *B. paralicheniformis* whole genomes present in the NCBI GenBank (NZ_CP023666.1, NZ_CP023168.1, NC_021362.1, NZ_CP020352.1, NZ_CP023665.1, and NZ_CP033389.1). Genes were located using their arrangement in the genome of strain MDJK30 as a reference. The two longest genes (*fenC* and *fenD*) of the operon were chosen for designing primers. The sequences of these two genes from the six genomes listed above were aligned (MEGA 7; default settings) and observed to be 100% identical.

Primer Design and PCR

A primer set for each of *fenC* and *fenD* genes were designed (using PrimerQuest tool on IDT.com) based on the *B. paralicheniformis* MDJK30 genome sequence (GenBank: NZ_CP020352.1). Once specificity for *B. paralicheniformis* was ascertained *in silico*, primers were synthesized by Eurofins (Canada) and the PCR conditions were optimized using *B. paralicheniformis* KACC 18426.

Crude DNA was extracted from all the isolates identified as *B. licheniformis* isolates and *Bacillus* spp. isolates using Instagene matrix according to the manufacturers' recommendations

(Bio-Rad, Canada) and screened (Table 2). The PCR reaction mix of 23.5 μ l contained 1 \times PCR Supermix (Invitrogen), 10 μ M (0.5 μ l) each of forward and reverse primers and 10 μ l of template DNA (approx. 10–100 ng). The PCR cycle was carried out on Biometra professional thermocycler as follows: 2 min at 95°C, 40 cycles of 30 s at 95°C, 30 s at 53°C, and 1.5 min at 72°C, followed by a final extension step at 72°C for 5 min.

Confirmation of Presumptive *Bacillus paralicheniformis* Isolates

The isolates which gave amplicons (of correct sizes) with the two sets of *B. paralicheniformis* specific primers were sequenced using the Sanger method which was carried out at Eurofins (Canada). Also, whole genome sequencing of the presumptive *B. paralicheniformis* isolates was carried out for confirmation of their identity and diversity. For each isolate, genomic DNA was extracted from a single colony (picked from freshly prepared plates) using the Ultraclean Microbial DNA Isolation Kit (Qiagen, Canada), following the manufacturer's protocol. The sequencing was carried out at the Laboratory Services, University of Guelph (Guelph, Ontario). The sequence library preparation was done using the Nextera DNA Flex library preparation kit (Illumina, Canada) following the manufacturer's protocol. A MiSeq sequencer was used for sequencing with a MiSeq V2 reagent kit (Illumina) and 2 \times 250 paired-end cycles, according to the manufacturer's recommendation.

The MiSeq sequencer system software v3.1 (Illumina) was used to process the raw sequence reads. Furthermore, short sequences were filtered using FastQC 1.0.0 in BaseSpace.¹ The sequences that passed a quality score of 30 were assembled *via de novo* assembly following an overlap-layout-consensus method using SPAdes v3.9.0 Genome Assembler (Bankevich et al., 2012) to generate contigs and scaffolds. Bacterial Analysis Pipeline v1.0.4 was used to predict the bacterial species following a k-mer based approach (Larsen et al., 2014). An Average Nucleotide Identity (ANI) calculator on EZBioCloud (<https://www.ezbiocloud.net/>; Yoon et al., 2017) was used to determine the percentage of nucleotide identity. NCBI Prokaryotic Genome Annotation Pipeline (PGAP) v4.10 was used to predict, name, and annotate genes using the best-placed reference protein set method (Tatusova et al., 2016). Default parameters were used for all software.

Maximum Likelihood Dendrogram

Using the genomes of *B. subtilis* (168 and ATCC 13952), *B. velezensis* (UCMB5033 and BZB42), *B. amyloliquefaciens* (IT-45 and DSM 7), and *B. paralicheniformis* MDJK30 and a presumptive *B. paralicheniformis* isolate, a maximum likelihood dendrogram was constructed. Consensus sequences of the fengycin operon were extracted from each genome and aligned in the CLC workbench genomics (v10.0), after which the tree was created using MEGA (K2 + I model).

¹<https://basespace.illumina.com>

TABLE 1 | *Bacillus licheniformis* specific primer sequences and amplification conditions.

PCR	ORF	Products	Marker	Primers	Primer sequence (5' – 3')	Amplicon size (bp)	Limitation (observed during the <i>in-silico</i> primer verification via NCBI)
PCR 1	BL00303	hypothetical protein	BL5B	Forward	CGCTCACCATATGCACAGCTCT	332	Amplified at least 1 <i>B. paralicheniformis</i> genome
	serA2	3-phosphoglycerate dehydrogenase	BL8A	Reverse	CGGTTTATCGCTTGAGACYCGG		
PCR 2	BLi00806	hypothetical protein	BL13C	Forward	TCACAACCCGTTGACGACAA	247	Amplified at least 1 <i>B. paralicheniformis</i> or <i>B. glycinifermentans</i> genome
				Reverse	CGTGTCCGAGTGTGCGTTATAT		
	ligD	ATP-dependent DNA ligase	BL18A	Forward	TTGTGCGTATCTCCGGGCCA	376	Amplified at least 1 <i>B. paralicheniformis</i> genome
				Reverse	AGGCATTGTCCCAGTGGTGG		
				Forward	GTCAACGACACAATTCCCCGT	216	Amplified about 6 <i>B. paralicheniformis</i> genomes with 2 mismatched nucleotides
				Reverse	AGCTCCCTCAGGCGGCAATT		

Letter Y = nucleotides T/C. Marker BL5B was not present in all genomes deposited as *B. licheniformis* in National Center for Biotechnology Information (NCBI) while marker BL8A gave unspecific amplification with other *Bacillus* species.

TABLE 2 | PCR primer sequences and amplification conditions for *fenC* and *fenD*.

Gene	Primer name	Direction	5' to 3'	Start	Stop	Length	Tm	GC %	Amplicon length
<i>fenC</i>	FenCf	Forward	CCGCAAGACTGAGAGAAATA	6,204	6,224	20	59	45	446
	FenCr	Reverse	CGACGACCAAATGATGAATG	6,630	6,650	20	59	45	
<i>fenD</i>	FenDf	Forward	GGATAGTCCTGGTGTTCATAG	6,695	6,716	21	59	47.6	803
	FenDr	Reverse	CAGAGAGTGGAAGCTGTATT	7,478	7,498	20	59	45	

RESULTS

Identification of *Bacillus* Isolates

Out of 319 isolates, 124 were identified as *B. licheniformis* while 116 were identified to the genus level as *Bacillus* by 16S rRNA sequencing and MALDI-TOF. Using the species-specific primers, 17 additional *B. licheniformis* isolates were obtained (Figure 2) out of the 116 isolates previously identified to the genus level as *Bacillus*. However, the negative control, *B. paralicheniformis* KACC 18426, was amplified by three out of the four primer sets (BL13C, BL18A, and BL8A). Overall, 141 *B. licheniformis* and 85 *Bacillus* spp. were identified, resulting in a total of 226 isolates for screening.

Detection of *B. paralicheniformis* Isolates

Out of the 226 isolates tested, four (9MF010A, 9MF10B, 7CS50, and 7WI3) gave amplicons with both the *fenC* and *fenD* gene primer sets (Table 3). On all occasions, DNA from *B. licheniformis* ATCC 14580 (negative control) and the no-template control were not amplified by both sets of primers (Figure 3). Sanger sequencing of the amplicons from *fenD* confirmed that they were 99% identical to *B. paralicheniformis* ATCC 9945a as top match.

Whole Genome Sequencing of Presumptive *Bacillus paralicheniformis* Isolates

Whole genome sequencing of the four *B. paralicheniformis* isolates showed an ANI of 100%, therefore, only one genome

(7CS50) is presented here. The genome was closest to *B. paralicheniformis* ATCC 9945a (GenBank: CP005965.1) with a k-mer score of 7,682 and ANI of 97.22% was identified as *B. paralicheniformis*. With 137x coverage, 2,302,435 reads were generated for strain 7CS50 which were trimmed to 250 bp and assembled into 26 contigs. Strain 7CS50 has an estimated genome size of 4,199,730 bp and a 46.07% GC content (Figure 4). In total, 3,981 protein-coding sequences, 111 RNAs and 4,217 genes were found. The fengycin operon in *B. paralicheniformis* 7CS50 is closest in overall nucleotide identity to strain MDJK30 (97%) and farthest from the other species (78–87%; Figure 5).

TABLE 3 | Isolates newly identified as *Bacillus paralicheniformis*.

Isolate code	Isolation source	Isolation method	Initial method of identification	Initial identity
7WI3	Whey	ASC	16S rRNA gene Sanger sequencing	<i>Bacillus</i> spp.
9MF10A	HT-milk	ASC	MALDI-TOF	<i>B. licheniformis</i>
9MF10B	HT-milk	ASC	MALDI-TOF	<i>B. licheniformis</i>
7CS50	Cheese curd	ASC	16S rRNA gene Sanger sequencing	<i>Bacillus</i> spp.

HT-milk refers to heat-treated (thermized) milk.

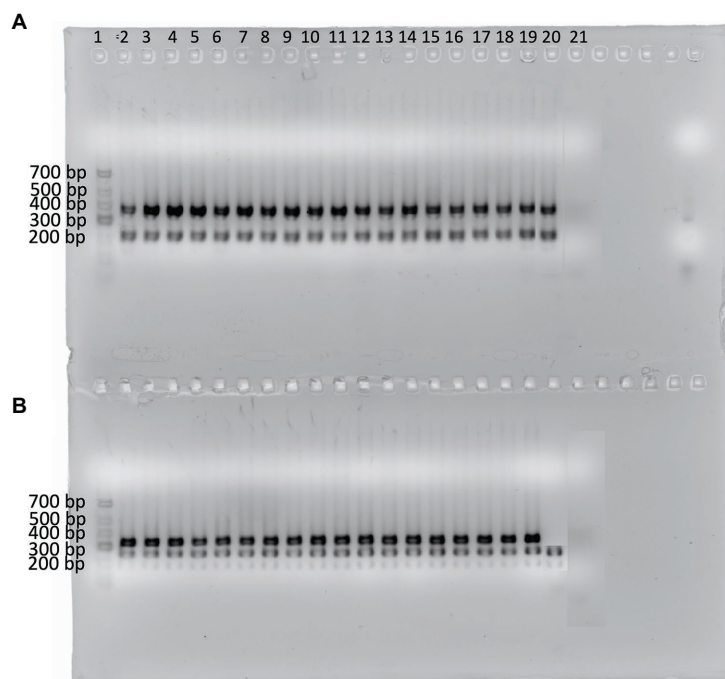


FIGURE 2 | Agarose gel showing the amplicons from 17 isolates identified as *B. licheniformis* using the four *B. licheniformis* specific markers (de Almeida, 2014). (A) Multiplex 1: primer sets 18A and 13C; (B) Multiplex 2: primer sets 5B and 8A. Lane 1 contains the GeneRuler Low range DNA ladder (ThermoScientific). Lanes 2–18 represent the additional *B. licheniformis* isolates while lane 19 contains *B. licheniformis* ATCC 14580 (positive control), lane 20 contains *B. paralicheniformis* KACC 18426 (negative control), and lane 21 contains the no template control.

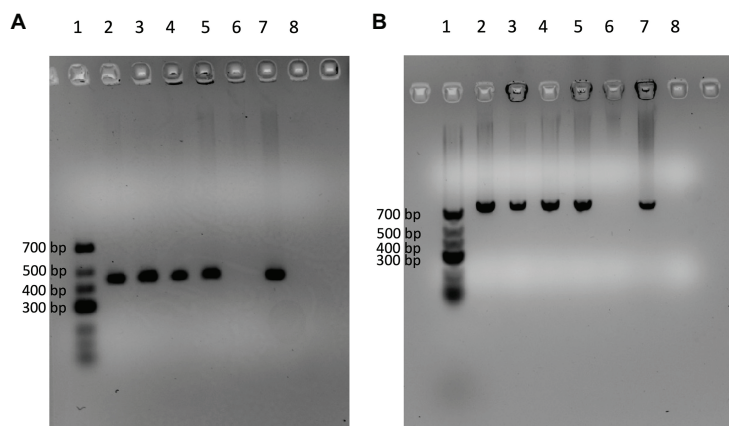


FIGURE 3 | Agarose gels showing four isolates (Lanes 2–5) which were amplified by the DNA markers [*fenC* (A) and *fenD* (B)] designed specifically for *B. paralicheniformis* using *B. licheniformis* ATCC 14580 as negative control (Lane 6) and *B. paralicheniformis* KACC 18426 (NRRL – B65293) as positive control (Lane 7). Lane 8 contains the no-template control of the PCR reaction. Lane 1 contains the GeneRuler Low range DNA ladder (ThermoScientific).

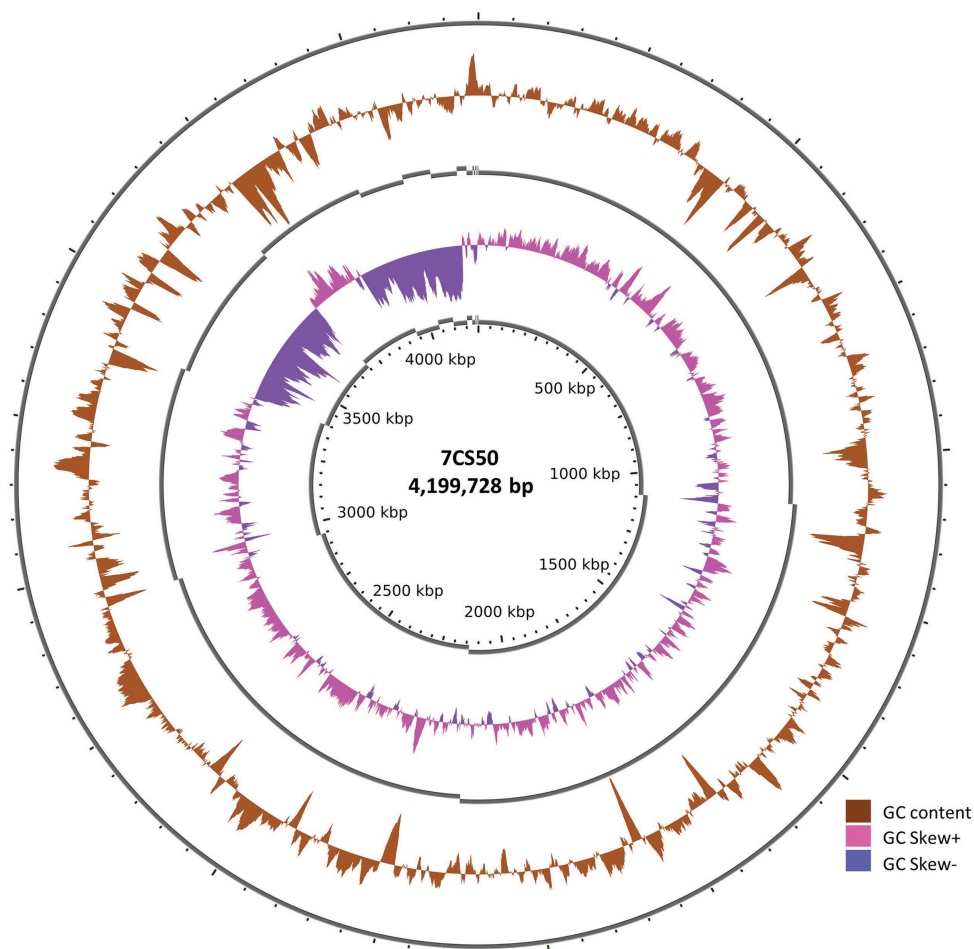
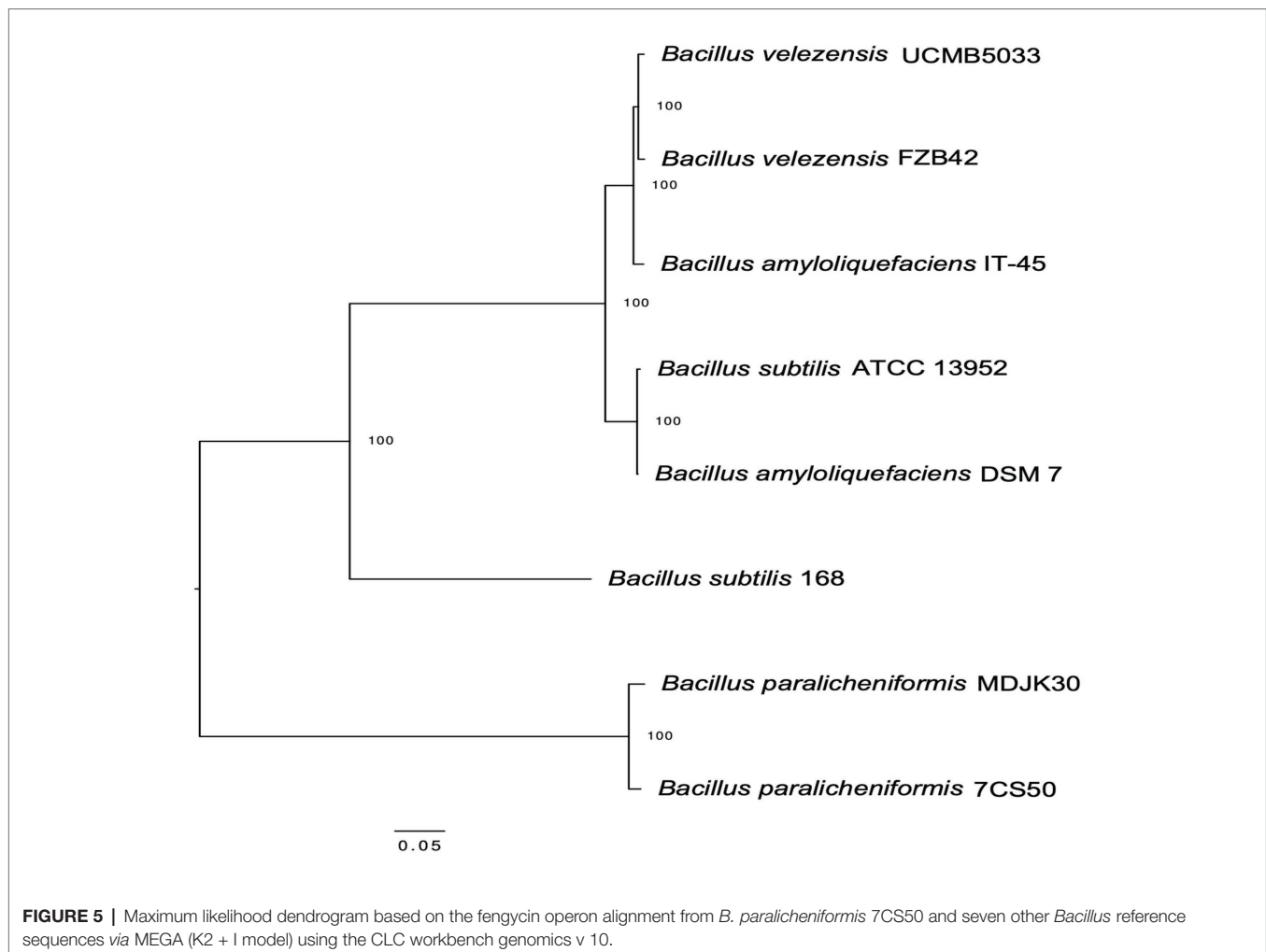


FIGURE 4 | The circular genome of *B. paralicheniformis* 7CS50 using the CGViewer and a command line (<https://github.com/paulstothard/cgview>) for multiple contigs (Grant and Stothard, 2008).



DISCUSSION

Fengycin was selected for the design of the *B. paralicheniformis* specific primers due to the ease of locating the operon in at least five publicly available genomes coupled with the ease of primer design. As most relevant literature target *B. licheniformis* for marker design, developing markers based on *B. paralicheniformis* should be explored. Of the five large proteins in the fengycin operon, only *fenC* and *fenD* were present in the six genomes with complete genome sequence data in the NCBI GenBank database.

The four isolates which were amplified by the designed primers were confirmed to be *B. paralicheniformis* using *B. paralicheniformis* ATCC 9945a as the reference genome. The four genomes encode the fengycin A–D operon, specific to *B. paralicheniformis* (Du et al., 2019). Two of the isolates were obtained from winter cheese and whey samples from separate vats while the other two were from a heat-treated (HT) milk samples collected in spring, all from a cheese making plant. These isolates were obtained after spore pasteurization (80°C for 12 min) of dairy samples obtained from a cheese processing system during the aerobic spore

former count (ASC). These four isolates were highly similar as their sequences showed an ANI score of 100%. *Bacillus licheniformis* ATCC 14580 DNA was not amplified by the primer sets, implying that the sets were indeed specific for *B. paralicheniformis*.

Bacillus paralicheniformis specific markers have not been reported to date, to the best of our knowledge. These markers provide a fast detection of *B. paralicheniformis* among presumptive *B. licheniformis* isolates or even isolates identified to genus level as *Bacillus*. These markers are very promising as they provide a better approach to distinguishing this closely related *Bacillus* in comparison to previous phylogenetic and the phenotypic approaches. The four new *B. paralicheniformis* isolates had been previously identified as *B. licheniformis* by MALDI-TOF or as *Bacillus* spp. by Sanger sequencing of the 16S rRNA gene. It can be inferred that these approaches cannot adequately identify this bacterial species, as seen with many other close relatives among the genera *Bacillus*, *Anoxybacillus*, and *Geobacillus* (Randazzo et al., 2009; Weng et al., 2009; Burgess et al., 2010; Branquinho et al., 2014a). The misidentification of *B. paralicheniformis* by MALDI-TOF may have been due to either the quality and size of the

protein database itself or due to the instability of the proteins produced by the isolates (Stingu et al., 2008; Seng et al., 2009; Starostin et al., 2015). Adding the protein profile of these isolates to the MALDI-TOF database will improve future discrimination of the species using this method. Although 16S rRNA gene sequencing has been the gold standard for bacterial identification and for inferring phylogenetic relationships, it shows insufficient variation between closely related species (Zeigler, 2005). Similarly, species-specific primers of *B. licheniformis* that are not designed based on operons lacking in *B. paralicheniformis* will likely amplify the latter. This probably means that many of the primers previously designed specifically for *B. licheniformis* might also detect *B. paralicheniformis*. Even though *fenC* and *fenD* are not housekeeping genes which are alternative options for providing accurate taxonomic resolution of close relatives, they may be suitable to provide presumptive species identification. These markers could be used singly or in duplex to distinguish these two closely related species.

Across *Bacillus* species that possess a fengycin operon, the level of homology in terms of protein identity was low, ranging from 62 to 74%, indicating divergence from a common ancestor rather than horizontal transfer of these genes (Du et al., 2019). The fengycin operon from strain 7CS50 shows less than 90% nucleotide identity with the fengycin operons from seven other *Bacillus* species, which also suggests divergence, not horizontal transfer. Horizontal gene transfer (HGT) can occur in three main ways: transformation, transduction, and conjugation (Thomas and Nielsen, 2005). Genes (even if they are not accompanied by mobile elements) can be integrated into genomes if there is an active recombination system in the strain. Similarly, cells must be competent to take up DNA and integrate it into their genome (Johnston et al., 2014). Therefore, if *fenC* or *fenD* were transferred to *B. licheniformis*, then the strain would become indistinguishable from *B. paralicheniformis* with these markers. To mitigate this problem, it would be prudent to combine these markers with additional types of taxonomic identification or other markers based on secondary metabolites such as paralichenicidin (specific to *B. paralicheniformis*) or lichenicidin (specific to *B. licheniformis*). There appears to be a lower risk of HGT with the diverse polyketide synthase (pks) and NRPS-type operons (Grubbs et al., 2017), even though they are often found on genomic islands. Other approaches can be considered, such as Single Nucleotide Polymorphisms (SNPs) or a k-mer based approach as well as the use of smaller individual genes.

Structures, such as transposons, genomic islands, and integrases could suggest the possibility of HGT (Bose and Grossman, 2010). At this time, an *in silico* search using the IslandViewer online tool (v4 – www.pathogenomics.sfu.ca/islandviewer/query.php) predicted no genomic island close to the fengycin operon in the three *B. paralicheniformis* genomes analyzed (NZ_CP020352.1, NZ_CP023168.1, and NZ_CP023666.1; Bertelli et al., 2017). However, in the *B. amyloliquefaciens* FZB42 genome (now *B. velezensis* FZB42), there is a Tn1546 transposase encoded close to the fengycin

operon located on genomic island 10 (Rückert et al., 2011). Similarly, the *bmy* (bacillomycin D) operon (located on a genomic island) is closely inserted by the fengycin operon in the FZB42 genome (Koumoutsis et al., 2004). A low (74%) nucleotide similarity between the fengycin-related gene (*fenD*) in *B. velezensis* (*amyloliquefaciens*) FZB42 and *B. paralicheniformis* MDJK30 suggests that they are only distantly related. For these markers to remain relevant, the possible occurrence of horizontal gene transfer of specific fengycin operons from *B. paralicheniformis* to *B. licheniformis* accompanied by recombination should continue to be monitored.

CONCLUSION

Two markers for the reliable and quick differentiation of *B. licheniformis* from *B. paralicheniformis* were established. They can be useful for presumptive identification of *B. paralicheniformis*. A new dairy *B. paralicheniformis* strain of Canadian origin was discovered using the *fenC* and *fenD* markers. Unlike lanthipeptides, such as bacitracin, the operons encoding fengycin-type NRPS metabolites do not show any evidence of HGT as yet but display a significant level of diversity among *Bacillus* species. The draft genome assembly of strain 7CS50 provides more data for future research on the species such as exploring the genomic diversity and functions of dairy *B. paralicheniformis* strains in comparison with those obtained from other environments.

DATA AVAILABILITY STATEMENT

The draft genome data were deposited at DDBJ/EMBL/GenBank (BioProject ID PRJNA580480) under the accession number WLWZ00000000 with SRA accession number SRX7224652 (Olajide et al., 2019).

AUTHOR CONTRIBUTIONS

AO: methodology, investigation, writing, original draft and revising, formal analysis, and visualization. SC: supervision, resources, formal analysis, writing, reviewing, and editing. GL: conceptualization, supervision, project administration, funding acquisition, resources, writing – review and editing, and data curation. All authors contributed to the article and approved the submitted version.

FUNDING

Funding for this research was provided by Genome Canada [Genomic Applications Partnership Program (GAPP) Round 7] and the NSERC/Dairy Farmers of Ontario Industrial Research Chair in Dairy Microbiology held by GL.

ACKNOWLEDGMENTS

The ARS Culture Collection is appreciated for providing us with *B. paralicheniformis* NRRL B65293 (KACC

18426 = KJ-16^T), the type strain of *B. paralicheniformis* free of charge in this study. We are grateful for the help of Myra Siddiqi in constructing the sequence alignment dendrogram.

REFERENCES

- Bankevich, A., Nurk, S., Antipov, D., Gurevich, A. A., Dvorkin, M., Kulikov, A. S., et al. (2012). SPAdes: a new genome assembly algorithm and its applications to single-cell sequencing. *J. Comput. Biol.* 19, 455–477. doi: 10.1089/cmb.2012.0021
- Bertelli, C., Laird, M. R., Williams, K. P., Simon Fraser University Research Computing Group, Lau, B. Y., Hoad, G., et al. (2017). IslandViewer 4: expanded prediction of genomic islands for larger-scale datasets. *Nucleic Acids Res.* 45, W30–W35. doi: 10.1093/nar/gkx343
- Bose, B., and Grossman, A. D. (2010). Regulation of horizontal gene transfer in *Bacillus subtilis* by activation of a conserved site-specific protease. *J. Bacteriol.* 193, 22–29. doi: 10.1128/JB.01143-10
- Branquinho, R., Meirinhos-Souares, L., Carriço, J. A., Pintado, M., and Peixe, L. V. (2014a). Phylogenetic and clonality analysis of *Bacillus pumilus* isolates uncovered a highly heterogeneous population of different closely related species and clones. *FEMS Microbiol. Ecol.* 90, 689–698. doi: 10.1111/1574-6941.12426
- Branquinho, R., Sousa, C., Lopes, J., Pintado, M. E., Peixe, L. V., and Osorio, H. (2014b). Differentiation of *Bacillus pumilus* and *Bacillus safensis* using MALDI-TOF-MS. *PLoS One* 9:e110127. doi: 10.1371/journal.pone.0110127
- Burgess, S. A., Lindsay, D., and Flint, S. H. (2010). Thermophilic *Bacilli* and their importance in dairy processing. *Int. J. Food Microbiol.* 144, 215–225. doi: 10.1016/j.ijfoodmicro.2010.09.027
- Chen, X. H., Koumoutsis, A., Scholz, R., Eisenreich, A., Schneider, K., and Heinemeyer, I. (2007). Comparative analysis of the complete genome sequence of the plant growth-promoting bacterium *Bacillus amyloliquefaciens* FZB42. *Nat. Biotechnol.* 25, 1007–1014. doi: 10.1038/nbt1325
- de Almeida, E. M. M. (2014). *Bacillus licheniformis* specific DNA markers for identification and culture independent monitoring. Master thesis. Portugal: Departamento de Biologia, Universidade do Porto.
- Du, Y., Ma, J., Yin, Z., Liu, K., Yao, G., Xu, W., et al. (2019). Comparative genomic analysis of *Bacillus paralicheniformis* MDJK30 with its closely related species reveals an evolutionary relationship between *B. paralicheniformis* and *B. licheniformis*. *BMC Genomics* 20:283. doi: 10.1186/s12864-019-5646-9
- Dunlap, C. A., Kwon, S. -W., Rooney, A. P., and Kim, S. -J. (2015). *Bacillus paralicheniformis* sp. nov., isolated from fermented soybean paste. *Int. J. Syst. Evol. Microbiol.* 65, 3487–3492. doi: 10.1099/ijsem.0.000441
- Grant, J. R., and Stothard, P. (2008). The CGView server: a comparative genomics tool for circular genomes. *Nucleic Acids Res.* 36, W181–W184. doi: 10.1093/nar/gkn179
- Grubbs, K. J., Bleich, R. M., Santa Maria, K. C., Allen, S. E., Farag, S., AgBiome Team et al. (2017). Large-scale bioinformatics analysis of *Bacillus* genomes uncovers conserved roles of natural products in bacterial physiology. *mSystems* 2, e00040–e00057. doi: 10.1128/mSystems.00040-17
- Guinebretière, M. H., Auger, S., Galleron, N., Contzen, M., De Sarrau, B., De Buyser, M., et al. (2013). *Bacillus cytotoxicus* sp. nov. is a novel thermotolerant species of the *Bacillus cereus* group occasionally associated with food poisoning. *Int. J. Syst. Evol. Microbiol.* 63, 31–40. doi: 10.1099/ijss.0.030627-0
- Harwood, C. R., Mouillon, J., Pohl, S., and Arnau, J. (2018). Secondary metabolite production and the safety of industrially important members of the *Bacillus subtilis* group. *FEMS Microbiol. Rev.* 42, 721–738. doi: 10.1093/femsre/fuy028
- Johnston, C., Martin, B., Fichant, G., Polard, P., and Claverys, J. -P. (2014). Bacterial transformation: distribution, shared mechanisms and divergent control. *Nat. Rev. Microbiol.* 12, 181–196. doi: 10.1038/nrmicro3199
- Koumoutsis, A., Chen, X., Henne, A., Liesegang, H., Hitzeroth, G., Franke, P., et al. (2004). Structural and functional characterization of gene clusters directing nonribosomal synthesis of bioactive cyclic lipopeptides in *Bacillus amyloliquefaciens* strain FZB42. *J. Bacteriol.* 186, 1084–1096. doi: 10.1128/JB.186.4.1084–1096.2004
- Lai, Q., Liu, Y., and Shao, Z. (2014). *Bacillus xiamenensis* sp. nov., isolated from intestinal tract contents of a flathead mullet (*Mugil cephalus*). *Antonie Van Leeuwenhoek* 105, 99–107. doi: 10.1007/s10482-013-0057-4
- Larsen, M. V., Cosentino, S., Lukjancenko, O., Saputra, D., Rasmussen, S., Hasman, H., et al. (2014). Benchmarking of methods for genomic taxonomy. *J. Clin. Microbiol.* 52, 1529–1539. doi: 10.1128/jcm.02981-13
- Liu, Y., Lai, Q., Dong, C., Sun, F., Wang, L., Li, G., et al. (2013). Phylogenetic diversity of the *Bacillus pumilus* group and the marine ecotype revealed by multilocus sequence analysis. *PLoS One* 8:e800097. doi: 10.1371/journal.pone.0085660
- Olajide, A. M., Chen, S., Mitterboeck, T. F., and LaPointe, G. (2019). *Data from Bacillus paralicheniformis* 7CS50 whole genome shotgun sequencing project draft genome data. NCBI Database (GenBank). 1.0. Available at: <https://www.ncbi.nlm.nih.gov/nucleotide/WLVZ000000000> (Accessed December 16, 2020).
- Piewngam, P., Zheng, Y., Nguyen, T. H., Dickey, S. W., Joo, H. -S., Villaruz, A. E., et al. (2018). Pathogen elimination by probiotic *Bacillus* via signalling interference. *Nature* 562, 532–537. doi: 10.1038/s41586-018-0616-y
- Randazzo, C., Caggia, C., and Neviani, E. (2009). Application of molecular approaches to study lactic acid bacteria in artisanal cheeses. *J. Microbiol. Methods* 78, 1–9. doi: 10.1016/j.mimet.2009.04.001
- Rückert, C., Blom, J., Chenb, X., Reva, O., and Borris, R. (2011). Genome sequence of *B. amyloliquefaciens* type strain DSM7T reveals differences to plant-associated *B. amyloliquefaciens* FZB42. *J. Biotechnol.* 155, 78–85. doi: 10.1016/j.jbiotec.2011.01.006
- Satomi, M., La Duc, M. T., and Venkateswaran, K. (2006). *Bacillus safensis* sp. nov., isolated from spacecraft and assembly-facility surfaces. *Int. J. Syst. Evol. Microbiol.* 56, 1735–1740. doi: 10.1099/ijss.0.64189-0
- Seng, P., Drancourt, M., Gouriet, F., La Scola, B., Fournier, P., Rolain, J. M., et al. (2009). Ongoing revolution in bacteriology: routine identification of bacteria by matrix-assisted laser desorption/ionization time-of-flight mass spectrometry. *Clin. Infect. Dis.* 49, 543–551. doi: 10.1086/600885
- Starostin, K. V., Demidov, E. A., Bryanskaya, A. V., Efimov, V. M., Rozanov, A. S., and Peltek, S. E. (2015). Identification of *Bacillus* strains by MALDI TOF MS using geometric approach. *Sci. Rep.* 5:16989. doi: 10.1038/srep16989
- Stein, T. (2005). *Bacillus subtilis* antibiotics: structures, syntheses and specific functions. *Mol. Microbiol.* 56, 845–857. doi: 10.1111/j.1365-2958.2005.04587.x
- Steller, S., Vollenbroich, D., Leenders, F., Stein, T., Conrad, B., and Hofemeister, J. (1999). Structural and functional organization of the fengycin synthetase multienzyme system from *Bacillus subtilis* b213 and A1/3. *Chem. Biol.* 6, 31–41. doi: 10.1016/S1074-5521(99)80018-0
- Stingu, C. S., Rodloff, A. C., Jentsch, H., Schaumann, R., and Eschrich, K. (2008). Rapid identification of oral anaerobic bacteria cultivated from subgingival biofilm by MALDI-TOFMS. *Oral Microbiol. Immunol.* 23, 372–376. doi: 10.1111/j.1399-302X.2008.00438.x
- Tatusova, T., DiCuccio, M., Badretdin, A., Chetvernin, V., Nawrocki, E. P., Zaslavsky, L., et al. (2016). NCBI prokaryotic genome annotation pipeline. *Nucleic Acids Res.* 44, 6614–6624. doi: 10.1093/nar/gkw569
- Thomas, C., and Nielsen, K. (2005). Mechanisms of, and barriers to, horizontal gene transfer between bacteria. *Nat. Rev. Microbiol.* 3, 711–721. doi: 10.1038/nrmicro1234
- Vanittanakom, N., Loeffler, W., Koch, U., and Jung, G. (1986). Fengycin—a novel antifungal lipopeptide antibiotic produced by *Bacillus subtilis* F-29-3. *J. Antibiot.* 39, 888–901. doi: 10.7164/antibiotics.39.888
- Weisburg, W., Barns, S., Pelletier, D., and Lane, D. (1991). 16S ribosomal DNA amplification for phylogenetic study. *J. Bacteriol.* 173, 697–703. doi: 10.1128/JB.173.2.697-703.1991
- Weng, F. Y., Chiou, C. S., Lin, P. H. P., and Yang, S. S. (2009). Application of *recA* and *rpoB* sequence analysis on phylogeny and molecular identification of *Geobacillus* species. *J. Appl. Microbiol.* 107, 452–464. doi: 10.1111/j.1365-2672.2009.04235.x
- Yoon, S. H., Ha, S. M., Lim, J. M., Kwon, S. J., and Chun, J. (2017). A large-scale evaluation of algorithms to calculate average nucleotide identity. *Antonie Van Leeuwenhoek* 110, 1281–1286. doi: 10.1007/s10482-017-0844-4

Zeigler, D. R. (2005). Application of a *recN* sequence similarity analysis to the identification of species within the bacterial genus *Geobacillus*. *Int. J. Syst. Evol. Microbiol.* 55, 1171–1179. doi: 10.1099/ijs.0.63452-0

Conflict of Interest: The authors declare that the research was conducted in the absence of any commercial or financial relationships that could be construed as a potential conflict of interest.

Copyright © 2021 Olajide, Chen and LaPointe. This is an open-access article distributed under the terms of the Creative Commons Attribution License (CC BY). The use, distribution or reproduction in other forums is permitted, provided the original author(s) and the copyright owner(s) are credited and that the original publication in this journal is cited, in accordance with accepted academic practice. No use, distribution or reproduction is permitted which does not comply with these terms.



Butylated Hydroxytoluene Induced Resistance Against *Botryosphaeria dothidea* in Apple Fruit

Yan Huang¹, Cuicui Sun¹, Xiangnan Guan², Sen Lian¹, Baohua Li¹ and Caixia Wang^{1*}

¹ Key Laboratory of Integrated Crop Pest Management of Shandong Province, College of Plant Health and Medicine, Qingdao Agricultural University, Qingdao, China, ² Knight Cancer Institute, Oregon Health & Science University, Portland, OR, United States

OPEN ACCESS

Edited by:

Santanu Basu,
Swedish University of Agricultural
Sciences, Sweden

Reviewed by:

Koushik Mazumder,
National Agri-Food Biotechnology
Institute, India
Wenxing Xu,
Huazhong Agricultural University,
China

*Correspondence:

Caixia Wang
cxwang@qau.edu.cn

Specialty section:

This article was submitted to
Food Microbiology,
a section of the journal
Frontiers in Microbiology

Received: 26 August 2020

Accepted: 03 December 2020

Published: 14 January 2021

Citation:

Huang Y, Sun C, Guan X, Lian S,
Li B and Wang C (2021) Butylated
Hydroxytoluene Induced Resistance
Against *Botryosphaeria dothidea*
in Apple Fruit.
Front. Microbiol. 11:599062.
doi: 10.3389/fmicb.2020.599062

Apple ring rot caused by *Botryosphaeria dothidea* is an important disease in China, which leads to serious economic losses during storage. Plant activators are compounds that induce resistance against pathogen infection and are considered as a promising alternative strategy to traditional chemical treatment. In the present study, butylated hydroxytoluene (BHT), a potential plant activator, was evaluated for its induced resistance against *B. dothidea* in postharvest apple fruits. The physiological and molecular mechanisms involved in induced resistance were also explored. The results showed that BHT treatment could trigger strong resistance in apple fruits against *B. dothidea*, and the optimum concentration was 200 $\mu\text{mol L}^{-1}$ by immersion of fruits. BHT treatment significantly increased the activities of four defensive enzymes and alleviated lipid peroxidation by increasing antioxidant enzyme activities. In addition, salicylic acid (SA) content was enhanced by BHT treatment as well as the expression of three SA biosynthesis-related genes (*MdSID2*, *MdPAD4*, and *MdEDS1*) and two defense genes (*MdPR1* and *MdPR5*). Our results suggest that BHT-conferred resistance against *B. dothidea* might be mainly through increasing the activities of defense-related enzymes and activating SA signaling pathway, which may provide an alternative strategy to control apple ring rot in postharvest fruits.

Keywords: butylated hydroxytoluene, apple fruit, induced resistance, *Botryosphaeria dothidea*, defense-related enzyme, salicylic acid signaling

INTRODUCTION

Apple (*Malus domestica* Borkh.) is one of the most important fruit and is widely consumed worldwide. However, the apple fruit is susceptible to pathogenic fungi, one of which is *Botryosphaeria dothidea* (Tang et al., 2012). *B. dothidea* is a plant hemi-biotrophic fungi and causes apple ring rot, a severe disease that reduces the yield and quality of apple, especially in China. Infected fruits show soft, sunken lesions with alternating tan and brown rings. *B. dothidea* infects fruits at the growth stage and causes fruit rot during the ripening or in the postharvest period (Zhang Q. M. et al., 2016), making it difficult to control apple ring rot. In addition, *B. dothidea* also infects apple tree branches, resulting in warts, canker, necrotic bark lesions, and even the death of the branches (Zhao et al., 2016).

Currently, the main strategy to control apple ring rot is the eradication of the fungal inoculum combined with application of bagging technology and scheduled spraying of protective fungicides

(Zhao et al., 2016). As the cost of bagging is increasing yearly, the bagless cultivation of apple has become an inevitable trend in China. However, apple fruit ring rot is the key problem that remains to be solved in bagless cultivation (Zhao et al., 2016; Yu et al., 2018). Furthermore, issues associated with chemical residue, fungicide resistance in pathogens, and serious environmental pollution have motivated to develop new, effective, and eco-friendly agents for the control of apple ring rot (Fan et al., 2016, 2018).

Plant activators that induce plant defense response have attracted considerable interest due to their broad-spectrum resistance and long-term disease control while reducing the environmental burden (Yang et al., 2015; Liu et al., 2019). As an alternative strategy to traditional chemical treatment, the application of activators has gained increasing attention (Yu et al., 2014; Zhang Y. et al., 2016). The plant activators include physical, biological, and chemical inducers, while most are compounds. Complex signaling networks, such as the pathways mediated by salicylic acid (SA), jasmonic acid (JA), and ethylene (ET), are activated by plant activators, leading to plant defense response (Van Bockhaven et al., 2015; Yu et al., 2019). SA-mediated signaling plays important roles in fighting against (hemi)-biotrophic pathogens (Glazebrook, 2005) as well as in the activation of robust systemic resistance marked by the increased expression of many defense proteins including pathogenesis-related (PR) proteins. In contrast, JA- and/or ET-mediated signaling is mainly involved in plant defense against necrotrophic pathogens.

As metabolic by-products in plants, reactive oxygen species (ROS) play a pivotal role in the regulation of plant defense response against pathogen invasion (Torres, 2010; Wang et al., 2014). However, ROS produced in excess can cause oxidative damage and induce membrane lipid peroxidation in the cellular environment (Marschall and Tudzynski, 2016). To protect cells from oxidative damage, plants employ a complex ROS-antioxidative system to scavenge harmful ROS. The main scavenging mechanism includes enzymatic antioxidants and metabolites that facilitate their degradation (Mittler, 2002).

In the previous work, we demonstrated that *Streptomyces rochei* A-1 could induce resistance against *B. dothidea* infection in postharvest apple fruit and did not affect the external and internal fruit appearance (Zhang Q. M. et al., 2016). It was recently found that butylated hydroxytoluene (BHT) was one of the main metabolites of *S. rochei* A-1 and that low concentration of BHT could effectively inhibit the postharvest apple fruit decay caused by *B. dothidea*. However, low concentration of BHT has no effect on mycelial growth and spore germination of *B. dothidea* (Yu et al., 2018), suggesting other possible mechanisms of BHT in inhibiting postharvest decay in apple fruits. Moreover, BHT could inhibit postharvest gray mold caused by *Botrytis cinerea* and bitter rot caused by *Colletotrichum gloeosporioides* (data not published). As a synthetic phenolic antioxidant, BHT has been widely used in foods and food-related products, such as packing (Babich, 1982). Furthermore, BHT could activate several antioxidases and regulate endogenous nitric oxide against abiotic stress conditions in *Haematococcus pluvialis* (Zhao et al., 2018).

In this study, we set out to investigate the effectiveness of BHT on the control of apple ring rot caused by *B. dothidea* in postharvest apple fruit. The possible mechanisms of action underlying BHT-induced resistance to *B. dothidea* and the association with the SA signaling pathway in apple fruits were also explored. Our results suggested BHT treatment as a promising strategy to protect fruits from pathogen infection.

MATERIALS AND METHODS

Butylated Hydroxytoluene, Fungal Pathogen, and Fruit Materials

Butylated hydroxytoluene was purchased from Sigma-Aldrich (St. Louis, United States). The stock solution (1 M in methanol) was filtered through a 0.22- μ m filter for sterilization and stored at -20°C . The working concentration of BHT in this study was 0 (0.1% methanol as control), 50, 100, 200, and 500 $\mu\text{mol L}^{-1}$.

In this study, the fungal pathogen *Botryosphaeria dothidea* LXS030101, which was used in our previous study (Zhang Q. M. et al., 2016), was isolated from infected “Red Fuji” fruits with typical apple ring rot symptoms. The pathogen was maintained on potato dextrose agar (PDA: the extract of 200 g of potato, 20 g of glucose, and 15 g of agar in 1 L of water) at 4°C and was revived on PDA plates for 3 days to obtain the culture. Conidia were harvested from young apple fruits following the method described by Leng et al. (2009). Spore concentration was determined by a hemocytometer and adjusted with sterile distilled water to the concentration of 1×10^5 spores ml^{-1} .

Apple (cv. “Fuji”) fruits were harvested at a commercial mature stage from a commercial orchard in Qingdao, China. For this study, fruits with uniform shape, size, and no physical injuries were selected. Before treatment, fruits were surface disinfected with 2% (v/v) sodium hypochlorite for 2 min, washed with tap water, and then air-dried for use in the experiments.

Induction of Apple Fruit Resistance Against *Botryosphaeria dothidea* by Butylated Hydroxytoluene

Prior to pathogen inoculation, apple fruits were pre-treated with BHT according to the previous procedure with some modifications (Yang et al., 2017). Briefly, apple fruits were immersed in the BHT solution for 15 min at different concentrations (0, 50, 100, 200, and 500 $\mu\text{mol L}^{-1}$). Then, all fruits were taken out, air-dried for 2 h at room temperature, and stored in plastic boxes. After 48 h of incubation at 25°C , three uniform wounds (5 mm wide and 3 mm deep) around the apple equator were punctured with a sterile borer (Zhang Q. M. et al., 2016). Each wound was inoculated with 10 μl of *B. dothidea* spore suspension at 1×10^5 spores ml^{-1} . All treated fruits were incubated at 25°C and high relative humidity of 90–95%. Disease severity was expressed by disease incidence and lesion areas, which were recorded at 3, 5, and 7 days post inoculation (dpi). Disease incidence was calculated as the percentage of infected wounds, and lesion diameter was measured for infected wounds only. The experiment was

conducted three times in triplicates with 10 fruits in each replicate group.

Treatment of Apple Fruit and Sample Collection

Apple fruits were divided into two groups, immersed in 0 $\mu\text{mol L}^{-1}$ (0.1% methanol as control) or 200 $\mu\text{mol L}^{-1}$ of BHT solution, air-dried for 2 h, and then stored at 25°C with high relative humidity. Sample collection was performed following the method of Zheng et al. (2011). Peels from the fruit equator area were excised and cut into small pieces at time points 0, 0.5, 1, 2, 3, 5, and 7 days after treatment. Each treatment included three replicates, and each replicate consisted of five fruits. The excised tissues from five fruits were mixed and encased in aluminum foil, snap frozen in liquid nitrogen, and then stored at -86°C until further biochemical assays and gene expression analysis. All the experiments were repeated thrice.

Determination of Defensive Enzyme Activities

Phenylalanine ammonia lyase (PAL; EC 4.3.1.5), polyphenol oxidase (PPO; EC 1.10.3.1), β -1,3-glucanase (GLU; EC 3.2.1.58), and chitinase (CHI, EC 3.2.1.14) were assayed according to the method of Zhang Q. M. et al. (2016), Zhang Y. et al. (2016). Fruit tissues (0.5 g) were homogenized with 5 ml of 100 mmol L^{-1} of phosphate-buffered saline (PBS; pH 6.8–8.8) containing 1% (w/v) polyvinylpyrrolidone (PVP) for PPO and PAL, and 50 mmol L^{-1} of sodium acetate buffer (pH 5.0) for GLU and CHI. The homogenate was centrifuged for 15 min at 12,000 g at 4°C, and the supernatants were used to determine the enzyme activities. The activities of PAL, PPO, GLU, and CHI were calculated on the basis of fresh weight (FW), which were expressed as U g^{-1} FW. All measurements were performed in triplicate with samples collected from three biological replicates.

Determination of Antioxidant Enzyme Activities and Lipid Peroxidation

To determine the activities of main antioxidant enzymes including catalase (CAT, EC 1.11.1.6), peroxidase (POD, EC 1.11.1.7), and superoxide dismutase (SOD, EC 1.15.1.1), 0.5 g of fruit tissues was homogenized with 5 ml of 100 mmol L^{-1} PBS (pH 7.0) containing 1% PVP (w/v). The CAT Assay Kit A007, POD Assay Kit A084, and SOD Assay Kit A001 (Nanjing Jiancheng Bioengineering Institute, Nanjing, China) were used to measure the enzyme activities, following the protocol provided by the manufacturers. The final activity was expressed as U g^{-1} FW. Three biological replicates were used in each treatment.

To analyze the lipid peroxidation in apple fruits, four treatment groups were designed as follows: (i) control, fruits treated with 0.1% methanol; (ii) BHT, fruits treated with 200 μM of BHT solution; (iii) pathogen, fruits treated with 0.1% methanol followed by *B. dothidea* inoculation; (iv) BHT + pathogen, fruits treated with 200 $\mu\text{mol L}^{-1}$ of BHT followed by

B. dothidea inoculation. Fruit tissues were collected at various intervals (0, 1, 2, 3, 4, 5, and 7 dpi) as the description of Zhang Y. et al. (2016). Malondialdehyde (MDA) content was measured to determine lipid peroxidation in fruit tissues with an MDA Assay Kit A003 (Nanjing Jiancheng Bioengineering Institute, Nanjing, China). The MDA content was expressed as mmol per kg of FW . Three replicates were carried out in this experiment.

Analysis of Gene Expression by Quantitative Real-Time PCR

Spin column plant total RNA purification kit was used to extract total RNA from fruit tissues (Sangon Biotech, Shanghai, China). After quantification by micro spectrophotometry, a total of 2 μg of RNA was used for first-strand cDNA synthesis, using the Prime Script RT Reagent Kit with gDNA Eraser (Takara, Dalian, China).

qRT-PCR was performed using SYBR Premix Ex Taq kit (Takara, Dalian, China) according to the protocol provided by the manufacturer. Primers used for qRT-PCR are listed in Table 1. The qRT-PCR thermal cycling program was as follows: initial denaturation for 30 s at 95°C, 40 cycles of 5 s at 95°C, 15 s at 59°C (or 58°C or 56°C), and 15 s at 72°C. Elongation factor 1- α (*EF1a*) was used as a reference gene, and the relative gene expression was normalized to the *EF1a* Ct value according to the formula $2^{-\Delta \Delta C_t}$. All experiments were carried out with at least three biological replicates.

Determination of Salicylic Acid Content

Salicylic acid and SA glucoside (SAG) were extracted and measured from 0.3 g of fresh fruit tissue, as described by the previous method with some modifications (Verberne et al., 2002). The sample was homogenized with 1 ml of 90% methanol, and anisic acid was added as an internal standard. The homogenate was centrifuged at 6,000 g for 5 min, and the supernatant was collected and concentrated with nitrogen. Trichloroacetic acid was added to a concentration of 1 g L^{-1} . The sample was extracted three times with 1:1 ethylacetate:cyclohexane and used to detect the free SA. For SAG detection, 8 mol L^{-1} of HCl was added into the water phase collected from the abovementioned steps. The sample was boiled for 30 min and extracted as the abovementioned method. Samples were analyzed by an Agilent 1260 (Agilent Technologies, Palo Alto, CA, United States). SA and SAG contents were expressed as micrograms per kilogram of FW, and the results were the average of four independent extractions. The experiment was repeated twice.

Statistical Analysis

All the experiments were implemented using a completely randomized design. The biochemical and gene expression analyses of fruit tissues for each treatment were conducted in triplicate at each sampling point. The data were expressed as the mean \pm standard deviation (SD). All data were subjected to analysis of variance (ANOVA) followed by Duncan's multiple range tests. Statistical significance was determined with a *P* value of less than 0.05.

TABLE 1 | Specific primers used for quantitative real-time PCR to analyze gene expression.

Primer name	Forward primer 5' → 3'	Reverse primer 5' → 3'	Annealing temperature (°C)
<i>MdEF1α</i>	ACATTGCCCTGTGGAAGTT	GTCTGACCATCCTTGGAAG	59/58/56
<i>MdPR1</i>	GCAGCAGTAGGCGTTGGTCCCT	CCAGTGCTCATGGCAAGGTTTT	59
<i>MdPR5</i>	AGCAGCTTCCCTCCTCGGC	CCCAGAAGCGACCAGACC	58
<i>MdPDF1.2</i>	ATGTTTGGAAGTGTGTGGCAA	TCAACATCTGAAGTAGCAGAAG	58
<i>MdCOI1</i>	CTGACTTCCCTTAGGTACTTGTG	CAACTCGTCTCGGAGGAATCAA	58
<i>MdERF3</i>	TCCTTCAAAGCTCCGCTGACTT	CCAAGATGGTGCCTGGAAATCA	58
<i>MdCTR1</i>	AACTTGTCCATAGTCACGGAA	CCTTTGCCACATCATATGCC	58
<i>MdSID2</i>	TTATACTTCATTCGGCTGCT	GCCTCTAATTTCTTTGTATGCT	56
<i>MdEDS1</i>	GAGCTAGACAATGCCTTCGT	AGTATCCCTCATTGTGCTCGT	58
<i>MdPAD4</i>	GCTTCACCGTAAGTTACTCG	CAAGAACTCGCAACTGTC	58

RESULTS

Induction of Disease Resistance in Apple Fruit Against *Botryosphaeria dothidea* by Butylated Hydroxytoluene

The effectiveness of BHT for controlling apple ring rot in fruits was significantly affected by the concentrations of BHT (Figure 1). In the control fruits treated with 0.1% methanol, brown lesions with large zones appeared on the inoculation site and developed rapidly (Figure 1A). In contrast, the development of ring rot symptoms was significantly inhibited by BHT treatment, as indicated by the lower disease incidence and smaller lesion diameter in BHT-treated fruits compared with control until 7 dpi (Figures 1B,C). Meanwhile, BHT at the concentration of 200 $\mu\text{mol L}^{-1}$ showed the strongest effect on mitigating ring rot development (Figure 1A). Although disease incidence and lesion diameter increased from 3 to 7 dpi in all treatments, 200 $\mu\text{mol L}^{-1}$ of BHT treatment decreased disease incidence by 25.56% and lesion diameter by 78.22% as compared with control at 7 dpi (Figures 1B,C).

Effect of Butylated Hydroxytoluene on Defensive Enzyme Activities in Apple Fruit

To analyze whether BHT treatment was able to increase the defensive enzyme activities, PAL, PPO, GLU, and CHI activities were measured in apple fruits with or without BHT treatment. As shown in Figure 2, four defensive enzyme activities in the control apple fruits exhibited no obvious changes during the storage, whereas the enzyme activities in BHT-treated fruits increased significantly ($P < 0.05$) with varying patterns. PAL and PPO activities in BHT-treated fruits were remarkably enhanced at 2 days and then peaked at 5 and 3 days, which were 1.7-fold and 2.2-fold higher than those in the control fruits, respectively (Figures 2A,B). The activities of PAL and PPO in BHT-treated fruits then dropped sharply. The PPO activity decreased to the control level at 7 days, whereas the PAL activity in BHT-treated fruits was significantly ($P < 0.05$) higher than that in the control fruits during the storage (Figures 2A,B).

For CHI and GLU, BHT-treated fruits exhibited significantly higher enzyme activities from day 1 onward as compared

with the control fruits (Figures 2C,D). Particularly, in BHT-treated fruits, GLU activity increased continuously and peaked at 7 days, which was 1.7 times more than that of the control (Figure 2C). Meanwhile, CHI activity reached the highest level at 5 days, which was 2.5-fold higher than that in the control fruits (Figure 2D). These results suggested that BHT could enhance disease resistance against *Botryosphaeria dothidea* by heightening the activities of defensive enzymes PAL, PPO, GLU, and CHI.

Effect of Butylated Hydroxytoluene on Antioxidant Enzyme Activities and Lipid Peroxidation in Apple Fruit

To obtain more insights into the mechanisms of BHT in induced resistance against *B. dothidea*, antioxidant enzyme activities and lipid peroxidation were determined during apple fruit storage, with or without BHT treatment. In the control fruits, the antioxidant enzymes (CAT, POD, and SOD) activities showed no obvious changes throughout the experiment period; however, three enzyme activities markedly enhanced in BHT-treated fruits (Figures 3A–C). CAT activity increased slowly and reached the maximum levels at 3 days in fruits treated with BHT, which was 2.1-fold higher than that in the control fruits. Similarly, BHT treatment resulted in an evident increase of POD activity, and the maximum fold increase was reached at 2 days (3.6-fold higher than that in the control fruits). For SOD, two activity peaks appeared at 1 and 3 days after BHT treatment. Subsequently, three enzyme activities sharply decreased after the peaks in BHT-treated fruits; however, the enzyme activities remained significantly ($P < 0.05$) higher than those in the control fruits during the storage.

Malondialdehyde, a marker for monitoring lipid peroxidation caused by oxidative damage, was determined in four treatments and shown in Figure 3D. The MDA content in BHT-treated fruits still had no significant ($P > 0.05$) differences compared with that in the control fruits during the storage. Inoculation with *B. dothidea* resulted in a sharp rise of MDA content in apple fruits from 2 dpi, and the increase of MDA content was up to 197.77% and 251.86% more than the control at 4 and 7 dpi, respectively. However, MDA content in BHT plus *B. dothidea*-treated fruits increased slightly, and the enhancement was only 25.81 and 84.30% more than that of the control at 4 and 7 dpi, respectively.

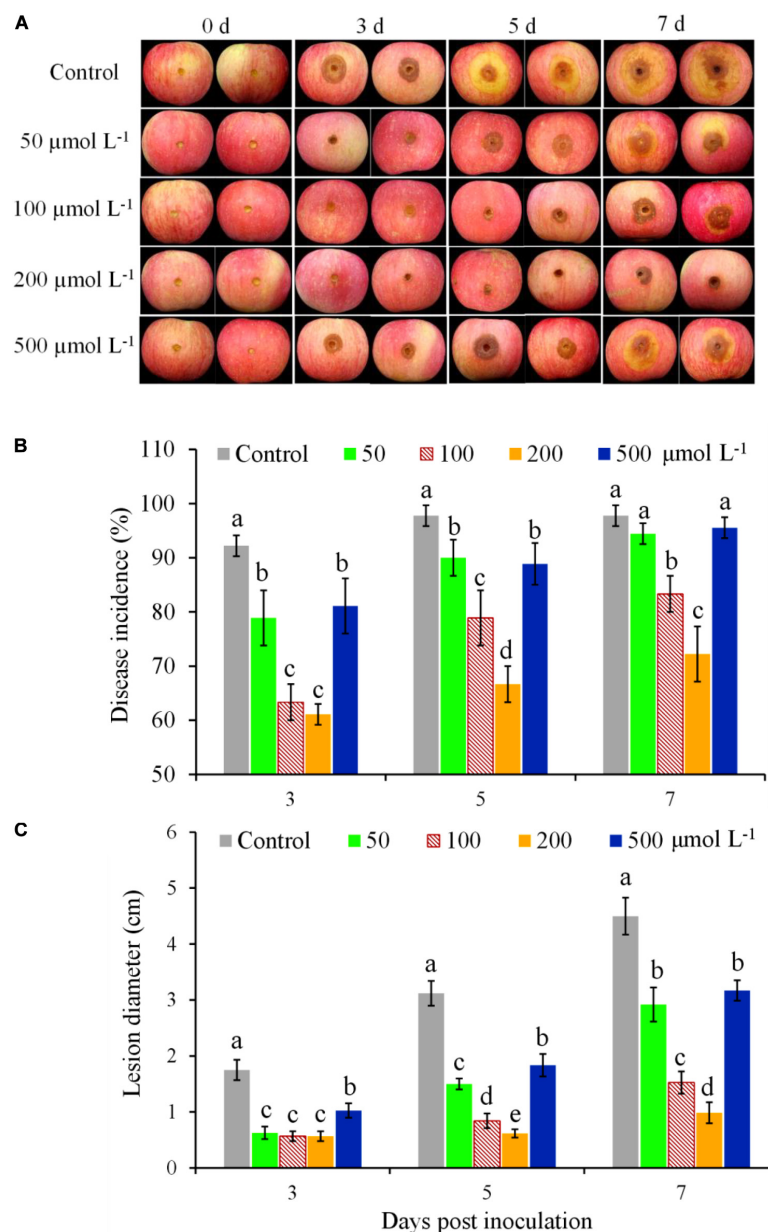


FIGURE 1 | Induced resistance at different butylated hydroxytoluene (BHT) concentrations against *Botryosphaeria dothidea* in apple fruits during postharvest storage. Apple fruits were immersed in 0.1% methanol (as the control) or BHT solution at different concentrations (50, 100, 200, and 500 $\mu\text{mol L}^{-1}$) for 15 min; 48 h after the treatment, all fruits were inoculated with 10 μl of *B. dothidea* conidia suspension (1×10^5 spores ml^{-1}) and then stored at 25°C and relative humidity (RH) of 90–95%. Images of representative samples (A) are shown for 3, 5, and 7 days post inoculation (dpi). Changes of disease incidence (B) and lesion diameter (C) in apple fruits were measured at 3, 5, and 7 dpi. Each column represents the mean of three replicates, and vertical bars represent the standard deviation (SD). Different letters above the bars indicate statistically significant differences ($P < 0.05$) within the same panel.

Effects of Butylated Hydroxytoluene on Relative Expression of Salicylic Acid/Jasmonic Acid/Ethylene Signaling Pathway Marker Genes in Apple Fruit

To determine the activation of signaling pathways by BHT, the relative expression levels of marker genes of SA/JA/ET signaling pathway at 0, 12, 24, and 48 h after treatment were analyzed.

PR1 and *PR5* are widely used molecular markers that correlate with SA signaling activation (Zhang Y. et al., 2016). Compared with the control, BHT treatment triggered significant ($P < 0.05$) increases of *MdPR1* and *MdPR5* transcript levels during the storage (Figures 4A,B). The expression of *MdPR1* in BHT-treated fruits showed 4.7-, 12.2-, and 11.8-fold increases at 12, 24, and 48 h, respectively, when compared with that in the control fruits (Figure 4A). Meanwhile, a similar pattern was observed in the

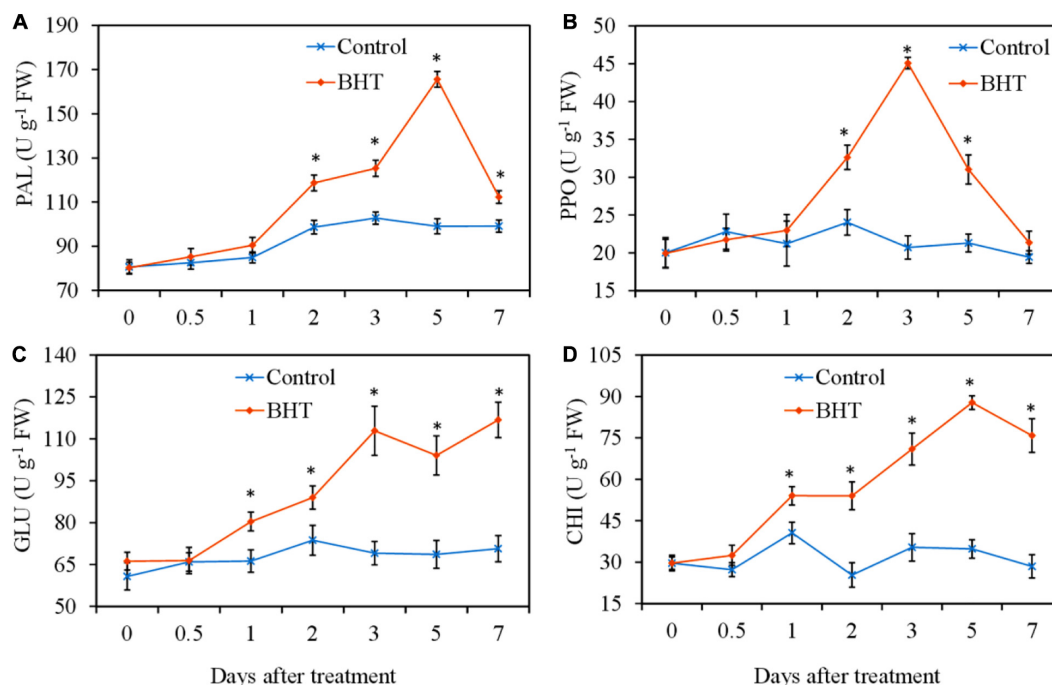


FIGURE 2 | Effects of $200 \mu\text{mol L}^{-1}$ of butylated hydroxytoluene (BHT) on the activities of phenylalanine ammonia lyase (PAL) (A), polyphenol oxidase (PPO) (B), β -1,3-glucanase (GLU) (C), and chitinase (CHI) (D) in apple fruits. The fruits were incubated for various time intervals at 25°C after BHT treatment. Each data point represents the mean \pm SD of three replicates. Asterisks denote significant difference from control at a given time point ($P < 0.05$).

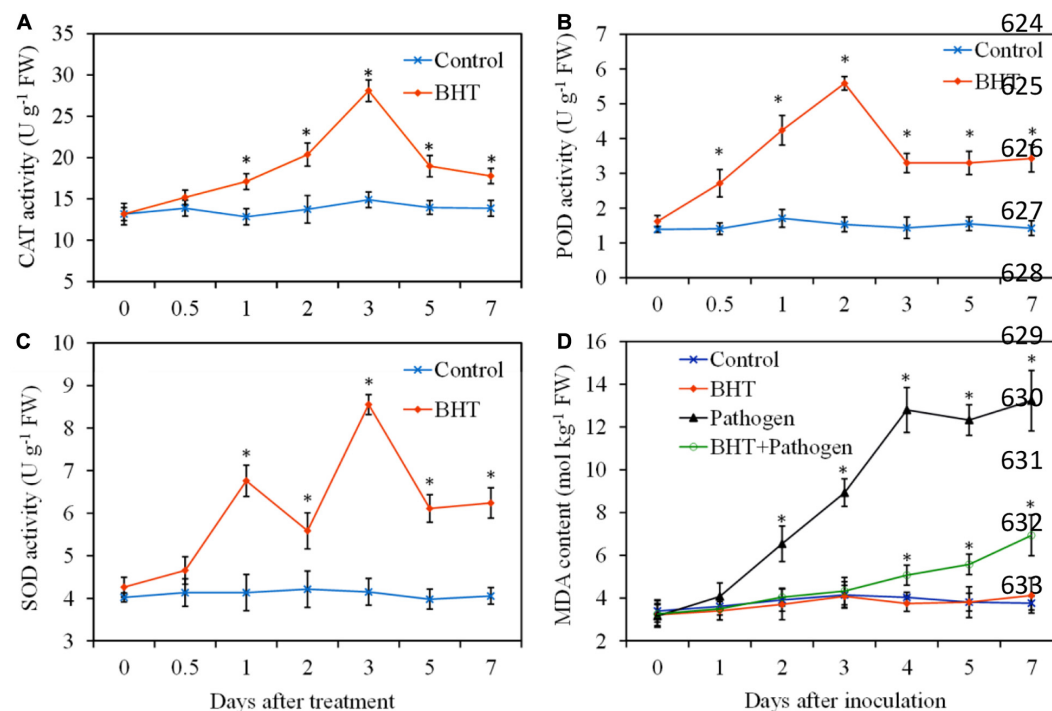


FIGURE 3 | Effects of $200 \mu\text{mol L}^{-1}$ of butylated hydroxytoluene (BHT) on catalase (CAT) (A), superoxide dismutase (SOD) (B), and peroxidase (POD) (C) activities and lipid peroxidation as measured by malondialdehyde (MDA) content (D) in apple fruits. The fruits were incubated for various time intervals at 25°C . Each data point represents the mean \pm SD of three replicates. Asterisks denote significant difference from control at a given time point ($P < 0.05$).

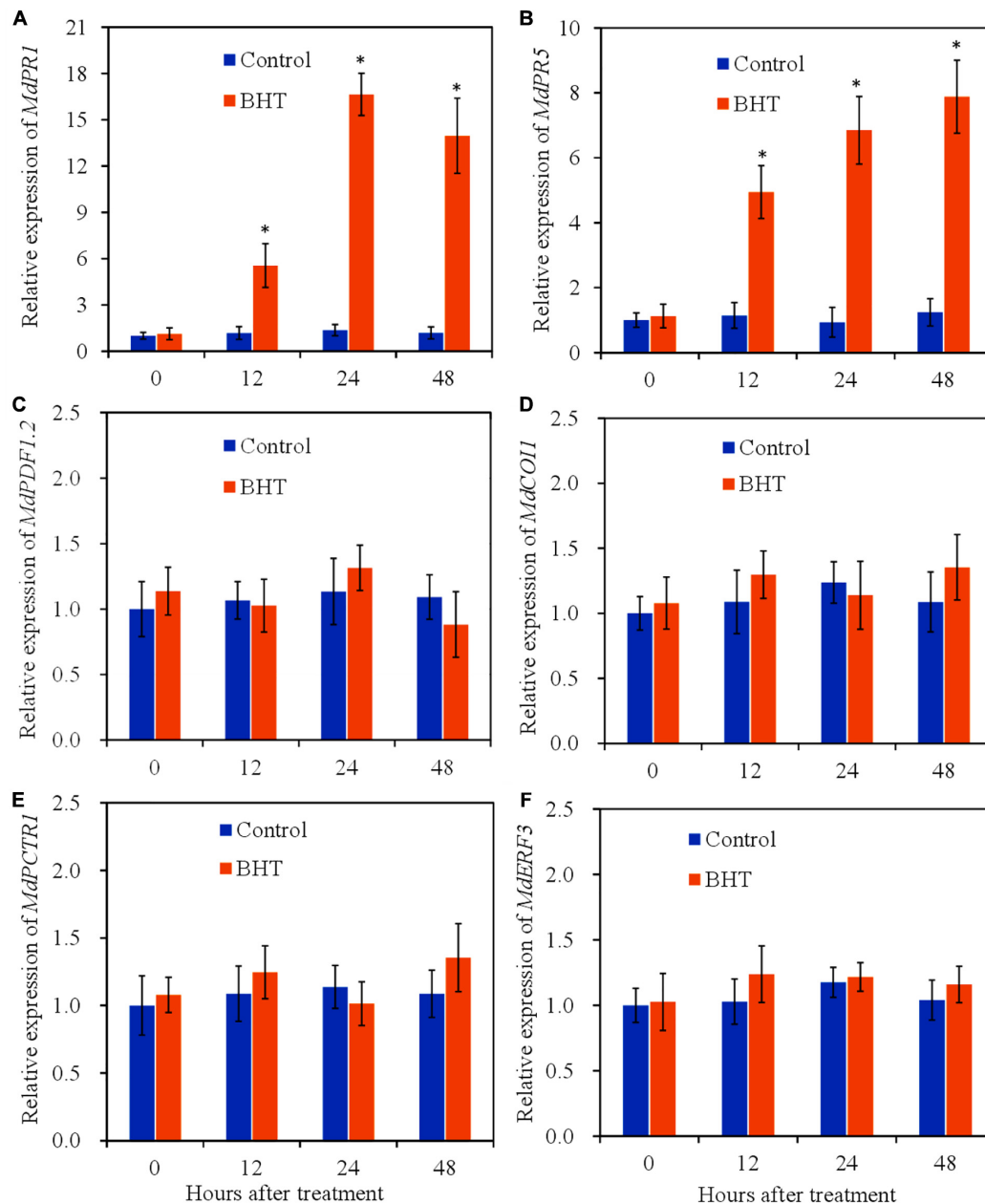


FIGURE 4 | Effects of 200 $\mu\text{mol L}^{-1}$ of butylated hydroxytoluene (BHT) on salicylic acid/jasmonic acid/ethylene (SA/JA/ET) signaling-related gene expressions in apple fruits: (A) *MdPR1*, (B) *MdPR5*, (C) *MdPDF1.2*, (D) *MdCOI1*, (E) *MdCTR1*, and (F) *MdERF3*. The fruits were incubated for various time intervals at 25°C. Each bar represents the mean \pm SD of three biological replicates. Asterisks denote significant difference from control at a given time point ($P < 0.05$).

expression of *MdPR5* in BHT-treated fruits, which were 4.3-, 7.4-, and 6.4-fold higher than that in the control fruits.

PDF1.2 (plant defensin 1.2), which encodes an antifungal peptide, is reported to be induced by pathogen and is required for the activation of JA response pathway (Penninckx et al., 1998). Coronatine insensitive 1 (*COI1*) is a JA receptor responsible for transducing JA signal to activate gene expression in JA signaling pathway (Browse, 2009). In the fruit treated with 0.1% methanol (control), no statistically significant differences

($P > 0.05$) were observed in the two JA signaling pathway marker genes (Figures 4C,D). Meanwhile, BHT treatment also did not induce the significant enhancement of *MdPDF1.2* and *MdCOI1* transcript levels during the storage.

Additionally, constitutive triple response 1 (*CTR1*) and ET response factor 3 (*ERF3*) are used as marker genes of ET signaling pathway (Guo and Ecker, 2004; Vahala et al., 2013). *CTR1* encodes a Raf-like protein kinase and functions as a negative regulator in ET signaling pathway, while *ERF3* is induced in

plants exposed to ET. As shown in **Figures 4E,F**, the expression profile of *CTR1* and *ERF3* exhibited a similar pattern in BHT-treated fruits. BHT treatment could not trigger the up-regulation of the two ET signaling pathway marker genes. These results together suggested that BHT treatment might mainly up-regulate SA signaling pathway.

Effects of Butylated Hydroxytoluene on Salicylic Acid Content and Salicylic Acid Synthesis-Related Gene Expressions in Apple Fruit

To investigate the regulation of SA signaling pathway mediated by BHT in apple fruits, SA content and relative expression of three genes related to SA biosynthesis were analyzed, with or without BHT treatment. The free SA content and SAG level changed slightly in the control apple fruits during the storage; however, free SA and SAG contents increased remarkably in BHT-treated fruits at 12 and 24 h, respectively (**Figures 5A,B**). Free SA and SAG levels continued to accumulate; and at 48 h, the levels were 3.2- and 2.3-fold higher than those in the control fruits, respectively.

SID2 (SA induction deficient 2), *PAD4* (phytoalexin deficient 4), and *EDS1* (enhanced disease susceptibility 1) are genes related to SA biosynthesis (Dempsey et al., 2011). The relative expression of *MdSID2* in the control fruits exhibited no obvious change

during the storage, while the transcript levels of *MdSID2* in BHT-treated fruits increased significantly ($P < 0.05$) at 24 and 48 h (**Figure 5C**). Similarly, BHT treatment up-regulated the expression of *MdPAD4* and *MdEDS1* during the storage. The transcript levels of *MdPAD4* and *MdEDS1* in BHT-treated fruits reached the highest at 24 and 48 h, which were 3.3- and 3.4-fold higher than those in the control fruits (**Figures 5D,E**).

DISCUSSION

As a promising alternative to synthetic chemical fungicides in managing plant diseases, many plant activators have been widely explored for their potential application, especially in controlling postharvest diseases (Worrall et al., 2012; Liu et al., 2019). In the past two decades, there has been growing interest in finding novel plant activators to meet the requirements of plant diseases controlling (Du et al., 2012). BHT is a most commonly used antioxidant in food containing fats, pharmaceuticals, etc. (Yehye et al., 2015). Furthermore, it has been found that BHT is effective as an antioxidant with radical-scavenging activity in living systems (Fujisawa et al., 2004). However, little knowledge was available regarding the effect of BHT applied for postharvest disease control. In the present study, our data showed the excellent efficacy of BHT to control postharvest apple ring rot. Especially, we investigated the mechanism of BHT induced

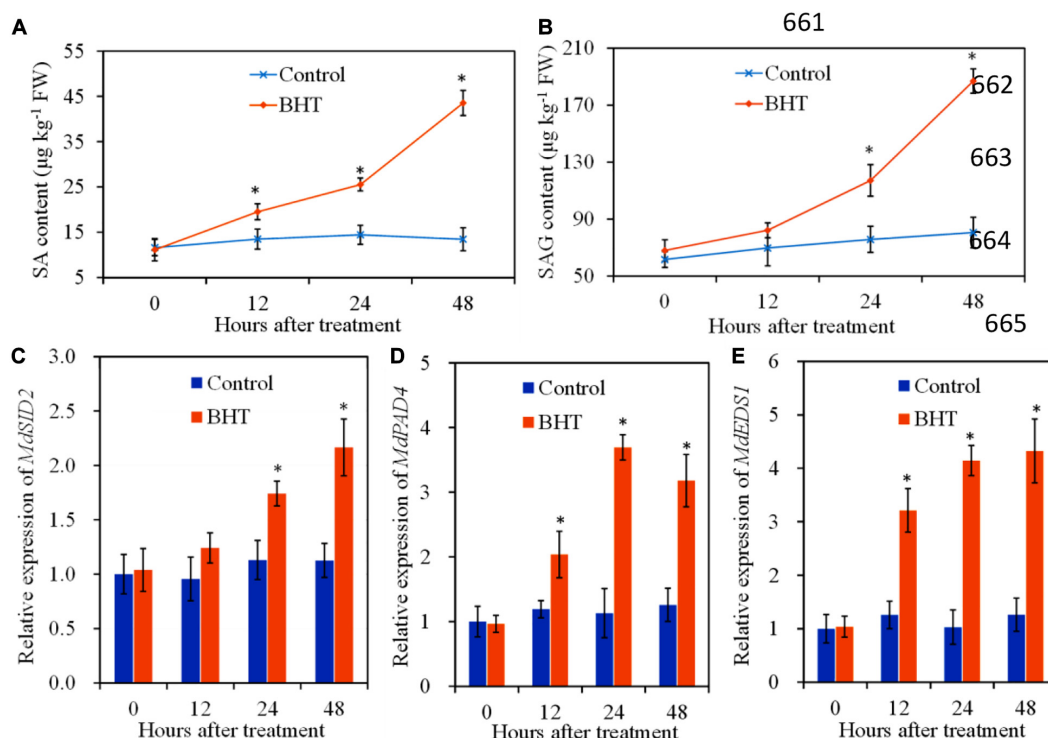


FIGURE 5 | Effects of 200 $\mu\text{mol L}^{-1}$ of butylated hydroxytoluene (BHT) on salicylic acid (SA) contents and SA synthesis-related gene expressions in apple fruits: **(A)** SA content; **(B)** SA glucoside (SAG) content; **(C)** *MdSID2*, **(D)** *MdPAD4*, and **(E)** *MdEDS1*. The fruits were incubated for various time intervals at 25°C. Each bar represents the mean \pm SD of four replicates. Asterisks denote significant difference from control ($P < 0.05$) at a given time point.

resistance against *Botryosphaeria dothidea* infection and found that SA signaling pathway was associated with BHT-mediated defense response in apple fruits.

To further study BHT-induced resistance in apple fruits against *B. dothidea*, we applied different concentrations of BHT by immersion of apple fruits and evaluated the effects of BHT on disease incidence and disease severity as measured by lesion diameter. As shown in **Figure 1**, BHT applied by immersion of fruits at 50~500 $\mu\text{mol L}^{-1}$ could effectively reduce disease incidence and lesion diameter as compared with the control, indicating that BHT played a positive role in apple fruits against *B. dothidea*. However, the inhibitory efficiency of BHT against *B. dothidea* did not depend on the dose. The disease incidence and lesion diameter on the fruits treated with 500 $\mu\text{mol L}^{-1}$ of BHT were significantly higher than those on the fruits treated with 100~200 $\mu\text{mol L}^{-1}$ of BHT. These results are consistent with previous reports that showed that the high doses of melatonin and L-arginine used on tomato had lower control efficiency against *Botrytis cinerea* than had low-dose compounds (Zheng et al., 2011; Liu et al., 2019). In addition, Zhao et al. (2018) reported that a high dose of BHT could affect the physiological response of *Haematococcus pluvialis*, which significantly decreased biomass production and astaxanthin content (Zhao et al., 2018). In this study, we speculate that 500 $\mu\text{mol L}^{-1}$ of BHT may cause cytotoxic effects on apple fruits, while it needs to be further confirmed. Because fruits treated with 200 $\mu\text{mol L}^{-1}$ of BHT had the least severe decay, we chose 200 $\mu\text{mol L}^{-1}$ of BHT immersion treatment to further investigate the mechanism of BHT-induced resistance against *B. dothidea*. Furthermore, we found that 200 $\mu\text{mol L}^{-1}$ of BHT had no effect on the color and sugar content of apple fruits (data not published). In the previous work, BHT applied by adding to fruit wounds at 50~1,000 $\mu\text{mol L}^{-1}$ could significantly reduce lesion size, and BHT at 100 $\mu\text{mol L}^{-1}$ was the most effective (Yu et al., 2018). Different methods of applying BHT may account for the inconsistency in these two studies.

The protection of plants from invasion by pathogens is largely dependent on the activation of a highly coordinated defense response. PAL, PPO, GLU, and CHI, the primary defensive enzymes, play important roles in plant defense responses against fungal infection and are widely used as markers to assess induced resistance (Zhang Q. M. et al., 2016; Liu et al., 2019). PAL is a key enzyme in the phenylpropanoid pathway that is involved in the biosynthesis of many compounds related to the structure and resistance of plants, such as lignin and SA, whereas PPO catalyzes the oxidation of phenolic compounds to produce antimicrobial substances (Tian et al., 2006). GLU and CHI encoded by *PR2* and *PR3* can directly inhibit fungal growth through the degradation of fungal cell walls or release oligosaccharide elicitors and induce a consequent chain of defense reactions (Edreva, 2005). Zheng et al. (2011) showed that the activities of these four enzymes in tomato fruits were triggered by L-arginine application, which induced resistance against *B. cinerea*. Zhang Y. et al. (2016) demonstrated that SA treatment increased PAL and PPO activities and up-regulated the expression of *GLU* and *CHI* in apple leaves, resulting in significantly enhanced host resistance against *Glomerella cingulata* infection. Our present study showed

that the four defensive enzymes are important components in BHT-treated fruits, which exhibited significant higher enzyme activities than the control ($P < 0.05$). In addition, our results also indicated that BHT treatment could enhance SA levels in apple fruits. These results suggested that BHT could regulate the phenylpropanoid pathway and stimulate the production of antimicrobial substances, which in turn contribute to the induced resistance in apple fruits against *B. dothidea*.

CAT, POD, and SOD are important antioxidant enzymes that regulate the metabolism of ROS and induce resistance in fruits against pathogen invasion (Mittler, 2002). A previous study showed that BHT has significant effect on the activities of these antioxidant enzymes, which is involved in mitigating abiotic stress-induced ROS and metabolite accumulation in *H. pluvialis* (Zhao et al., 2018). In the present study, the activities of CAT, POD, and SOD in BHT-treated fruits were remarkably increased and maintained at higher levels than those in the control fruits during the storage. Correspondingly, in BHT plus *B. dothidea*-treated fruits, the capacity of fruit tissues to scavenge redundant ROS was stimulated, and MDA content remained at a lower level than that in the fruits inoculated with *B. dothidea* alone. These results indicated that high activities of antioxidant enzymes induced by BHT played critical roles in alleviating oxidative stress, which agrees with previous reports (Tareen et al., 2012; Zhang et al., 2018). Additionally, recent research demonstrated that SA treatment could enhance fruit resistance against *B. dothidea* by magnifying the activities of CAT, POD, and SOD (Zhao et al., 2020). Our results also indicated that BHT induced resistance in apple fruits is partially due to the increased activities of antioxidant enzymes.

Salicylic acid, jasmonic acid, and ethylene are critical regulatory signals in plant defense against pathogens, and these signaling pathways are also known to crosstalk in antagonistic or synergistic manners (Mundy et al., 2006). Previous studies showed that SA is involved in the principal pathway in apple fruits to fight against *B. dothidea*, and exogenous SA application could enhance the resistance to *B. dothidea* in apple fruits (Zhao et al., 2020). In our study, *PR1* and *PR5* were strongly induced by BHT in apple fruits, indicating that effective manipulation of SA signaling pathway was essential for fruit resistance conferred by BHT treatment. The transcripts of *PDF1.2* and *CO11*, as well as *CTR1* and *ERF3*, were not induced by BHT, suggesting that JA and ET may be not the main signaling pathways in the BHT-induced resistance. Various studies demonstrated that JA signaling pathway is primarily induced by and effective in resistance against necrotrophic pathogens (Trusov et al., 2006). For example, melatonin induced resistance against *B. cinerea* in tomato fruits by stimulating JA signaling pathway (Liu et al., 2019). Moreover, the synergistic effects of JA and ET signaling pathways are reported to inhibit gray mold in tomato fruits (Yu et al., 2019).

Salicylic acid content and SA synthesis-related gene expression were also determined in this study, which helped us to further determine whether SA signaling pathway mediated the BHT-induced resistance in apple fruits against *B. dothidea*. *SID2* plays an essential role in SA accumulation and plant disease resistance (Dempsey et al., 2011). In apple fruits, *MdSID2* contributed to the

production of SA against *B. dothidea* infection (Zhao et al., 2020). *EDS1* and its interacting partner, *PAD4*, constitute a regulatory hub that is essential in the regulation of the plant defense to invasive (hemi-)biotrophic pathogens (Wiermer et al., 2005). Based on our results, the expression levels of *SID2*, *PAD4*, and *EDS1* were up-regulated significantly; and SA content increased remarkably in BHT-treated fruits, which led us to conclude that BHT-induced resistance against apple ring rot was mainly through the accumulation of SA content.

CONCLUSION

Butylated hydroxytoluene treatment triggered remarkable disease resistance against apple ring rot caused by *Botryosphaeria dothidea*. BHT could enhance the activities of defensive enzymes CHI, GLU, PAL, and PPO. Meanwhile, it increased antioxidant enzyme activities to alleviate lipid peroxidation. Furthermore, BHT treatment promoted SA content and up-regulated SA defense signaling, which is a crucial pathway in pathogen resistance. These data indicate that BHT confers resistance in apple fruits against *B. dothidea*, possibly by increasing defensive enzyme activities and activating SA signaling pathway. Therefore, our study strongly supports the application of BHT as a new plant activator to inhibit postharvest decay caused by *B. dothidea* in apple fruits.

REFERENCES

- Babich, H. (1982). Butylated hydroxytoluene (BHT): a review. *Environ. Res.* 29, 1–29. doi: 10.1016/0013-9351(82)90002-0
- Browse, J. (2009). Jasmonate passes muster: a receptor and targets for the defense hormone. *Annu. Rev. Plant Biol.* 60, 183–205. doi: 10.1146/annurev.arplant.043008.092007
- Dempsey, D. M. A., Vlot, A. C., Wildermuth, M. C., and Klessig, D. F. (2011). Salicylic acid biosynthesis and metabolism. *Arabidopsis Book* 9:e0156. doi: 10.1199/tab.0156
- Du, Q., Zhu, W., Zhao, Z., Qian, X., and Xu, Y. (2012). Novel benzo-1,2,3-thiadiazole-7-carboxylate derivatives as plant activators and the development of their agricultural applications. *J. Agric. Food Chem.* 60, 346–353. doi: 10.1021/jf203974p
- Edreva, A. (2005). Pathogenesis related proteins: research progress in the last 15 years. *Gen. Appl. Plant Physiol.* 31, 105–124.
- Fan, K., Wang, J., Fu, L., Li, X., Zhang, Y., Zhang, X., et al. (2016). Sensitivity of *Botryosphaeria dothidea* from apple to tebuconazole in China. *Crop Prot.* 87, 1–5. doi: 10.1016/j.cropro.2016.04.018
- Fan, K., Wang, J., Fu, L., Zhang, G. F., Wu, H. B., Feng, C., et al. (2018). Baseline sensitivity and control efficacy of pyraclostrobin against *Botryosphaeria dothidea* isolates in China. *Plant Dis.* 103, 1458–1463. doi: 10.1094/PDIS-07-18-1214-RE
- Fujisawa, S., Kadoma, Y., and Yokoe, I. (2004). Radical-scavenging activity of butylated hydroxytoluene (BHT) and its metabolites. *Chem. Phys. Lipids* 130, 189–195. doi: 10.1016/j.chemphyslip.2004.03.005
- Glazebrook, J. (2005). Contrasting mechanisms of defense against biotrophic and necrotrophic pathogens. *Annu. Rev. Phytopathol.* 43, 205–227. doi: 10.1146/annurev.phyto.43.040204.135923
- Guo, H., and Ecker, J. R. (2004). The ethylene signaling pathway: new insights. *Curr. Opin. Plant Biol.* 7, 40–49. doi: 10.1016/j.pbi.2003.11.011
- Leng, W. F., Li, B. H., Guo, L. Y., Dong, J. H., Wang, C. X., Li, G. F., et al. (2009). Method to promote sporulation of *Botryosphaeria berengeriana* f. sp. *piricola*. *Acta Phytopathol. Sinica* 39, 536–539. doi: 10.13926/j.cnki.apps.2009.05.017

DATA AVAILABILITY STATEMENT

The original contributions presented in the study are included in the article/supplementary material, further inquiries can be directed to the corresponding author.

AUTHOR CONTRIBUTIONS

YH and CS carried out the experiments and analyzed the data with the help of XG and SL. SL analyzed the data of gene expression and prepared the figure. YH and CW wrote the manuscript with help from all authors. BL performed the manuscript revision and provided part of the financial support. XG reviewed and edited the manuscript. All authors approved its final version.

FUNDING

The authors thank the financial support from projects of the Shandong Provincial Primary Research and Development Plan (No. 2019GSF109061), Qingdao Science and Technology Benefit People Demonstration and Guidance Project (No. 20-3-4-23-nsh), National Key Research and Development Project (No. 2016YFD0201122), and Chinese Modern Agricultural Industry Technology System (No. CARS-28).

- Liu, C., Chen, L., Zhao, R., Li, R., Zhang, S., Yu, W., et al. (2019). Melatonin induces disease resistance to *Botrytis cinerea* in tomato fruit by activating jasmonic acid signaling pathway. *J. Agric. Food Chem.* 67, 6116–6124. doi: 10.1021/acs.jafc.9b00058
- Marschall, R., and Tudzynski, P. (2016). Reactive oxygen species in development and infection processes. *Semin. Cell Dev. Biol.* 57, 138–146. doi: 10.1016/j.semcdb.2016.03.020
- Mittler, R. (2002). Oxidative stress, antioxidants and stress tolerance. *Trends Plant Sci.* 7, 405–410. doi: 10.1016/S1360-1385(02)02312-9
- Mundy, J., Nielsen, H. B., and Brodersen, P. (2006). Crosstalk. *Trends Plant Sci.* 11, 63–64. doi: 10.1016/j.tplants.2005.12.003
- Penninckx, I. A. M. A., Thomma, B. P. H. J., Buchala, A., Métraux, J. P., and Broekaert, W. F. (1998). Concomitant activation of jasmonate and ethylene response pathways is required for induction of a plant defense gene in *Arabidopsis*. *Plant Cell* 10:2103–2113. doi: 10.2307/3870787
- Tang, W., Ding, Z., Zhou, Z. Q., Wang, Y. Z., and Guo, L. Y. (2012). Phylogenetic and pathogenic analyses show that the causal agent of apple ring rot in China is *Botryosphaeria dothidea*. *Plant Dis.* 96, 486–496. doi: 10.1094/PDIS-08-11-0635
- Tareen, M. J., Abbasi, N. A., and Hafiz, I. A. (2012). Postharvest application of salicylic acid enhanced antioxidant enzyme activity and maintained quality of peach cv. 'Flordaking' fruit during storage. *Sci. Hortic.* 142, 221–228. doi: 10.1016/j.scienta.2012.04.027
- Tian, S., Wan, Y., Qin, G., and Xu, Y. (2006). Induction of defense responses against *Alternaria rot* by different elicitors in harvested pear fruit. *Appl. Microbiol. Biotechnol.* 70, 729–734. doi: 10.1007/s00253-005-0125-4
- Torres, M. A. (2010). ROS in biotic interactions. *Physiol. Plantarum* 138, 414–429. doi: 10.1111/j.1399-3054.2009.01326.x
- Trusov, Y., Rookes, J. E., Chakravorty, D., Armour, D., Schenk, P. M., and Botella, J. R. (2006). Heterotrimeric G proteins facilitate *Arabidopsis* resistance to necrotrophic pathogens and are involved in jasmonate signaling. *Plant Physiol.* 140, 210–220. doi: 10.1104/pp.105.069625

- Vahala, J., Felten, J., Love, J., Gorzsás, A., Gerber, L., Lamminmäki, A., et al. (2013). (ERFs) in hybrid aspen stem identifies ERF genes that modify stem growth and wood properties. *New Phytol.* 200, 511–522. doi: 10.1111/nph.12386
- Van Bockhaven, J., Spíchal, L., Novák, O., Strnad, M., Asano, T., Kikuchi, S., et al. (2015). Silicon induces resistance to the brown spot fungus *Cochliobolus miyabeanus* by preventing the pathogen from hijacking the rice ethylene pathway. *New Phytol.* 206, 761–773. doi: 10.1111/nph.13270
- Verberne, M. C., Brouwer, N., Delbianco, F., Linthorst, H. J. M., and Verpoorte, R. (2002). Method for the extraction of the volatile compound salicylic acid from tobacco leaf material. *Phytochem. Anal.* 13, 45–50. doi: 10.1002/pca.615
- Wang, C. X., El-Shetehy, M., Shine, M. B., Yu, K. S., Navarre, D., Wendehenne, D., et al. (2014). Free radicals mediate systemic acquired resistance. *Cell Rep.* 7, 348–355. doi: 10.1016/j.celrep.2014.03.032
- Wiermer, M., Feys, B. J., and Parker, J. E. (2005). Plant immunity: the EDS1 regulatory node. *Curr. Opin. Plant Biol.* 8, 383–389. doi: 10.1016/j.pbi.2005.05.010
- Worrall, D., Holroyd, G. H., Moore, J. P., Glowacz, M., Croft, P., Taylor, J. E., et al. (2012). Treating seeds with activators of plant defence generates long-lasting priming of resistance to pests and pathogens. *New Phytol.* 193, 770–778. doi: 10.1111/j.1469-8137.2011.03987.x
- Yang, J., Sun, C., Zhang, Y., Fu, D., Zheng, X., and Yu, T. (2017). Induced resistance in tomato fruit by γ -aminobutyric acid for the control of alternaria rot caused by *Alternaria alternata*. *Food Chem.* 221, 1014–1020. doi: 10.1016/j.foodchem.2016.11.061
- Yang, Q., Zhang, H., Zhang, X., Zheng, X., and Qian, J. (2015). Phytic acid enhances biocontrol activity of *Rhodotorula mucilaginosa* against *Penicillium expansum* contamination and patulin production in apples. *Front. Microbiol.* 6:1296. doi: 10.3389/fmicb.2015.01296
- Yehye, W. A., Rahman, N. A., Ariffin, A., Abd Hamid, S. B., Alhadi, A. A., Kadir, F. A., et al. (2015). Understanding the chemistry behind the antioxidant activities of butylated hydroxytoluene (BHT): a review. *Eur. J. Med. Chem.* 101, 295–312. doi: 10.1016/j.ejmech.2015.06.026
- Yu, C., Zeng, L., Sheng, K., Chen, F., Zhou, T., Zheng, X., et al. (2014). γ -aminobutyric acid induces resistance against *Penicillium expansum* by priming of defence responses in pear fruit. *Food Chem.* 159, 29–37. doi: 10.1016/j.foodchem.2014.03.011
- Yu, C. L., Meng, L. L., Lian, S., Li, B. H., Liang, W. X., and Wang, C. X. (2018). Control efficiency of BHT against apple fruit ring rot and its influence on the activity of defensive enzymes. *Plant Physiol. J.* 54, 819–826. doi: 10.13592/j.cnki.ppj.2018.0016
- Yu, W., Yu, M., Zhao, R., Sheng, J., Li, Y., and Shen, L. (2019). Ethylene perception is associated with methyl-jasmonate-mediated immune response against *Botrytis cinerea* in tomato fruit. *J. Agric. Food Chem.* 67, 6725–6735. doi: 10.1021/acs.jafc.9b02135
- Zhang, M., Liu, M., Pan, S., Pan, C., Li, Y., and Tian, J. (2018). Perillaldehyde controls postharvest black rot caused by *Ceratocystis fimbriata* in sweet potatoes. *Front. Microbiol.* 9:1102. doi: 10.3389/fmicb.2018.01102
- Zhang, Q. M., Yong, D. J., Zhang, Y., Shi, X. P., Li, B. H., Li, G. F., et al. (2016). *Streptomyces rochei* A-1 induces resistance and defense-related responses against *Botryosphaeria dothidea* in apple fruit during storage. *Postharvest Biol. Tec.* 115, 30–37. doi: 10.1016/j.postharvbio.2015.12.013
- Zhang, Y., Shi, X. P., Li, B. H., Zhang, Q. M., Liang, W. X., and Wang, C. X. (2016). Salicylic acid confers enhanced resistance to *Glomerella leaf spot* in apple. *Plant Physiol. Bioch.* 106, 64–72. doi: 10.1016/j.plaphy.2016.04.047
- Zhao, X., Qi, C., Jiang, H., Zhong, M., You, C., Li, Y., et al. (2020). MdWRKY15 improves resistance of apple to *Botryosphaeria dothidea* via the salicylic acid-mediated pathway by directly binding the MdICS1 promoter. *J. Integr. Plant Biol.* 62, 527–543. doi: 10.1111/jipb.12825
- Zhao, X., Zhang, G. L., Li, B. H., Xu, X. M., Dong, X. L., Wang, C. X., et al. (2016). Seasonal dynamics of *Botryosphaeria dothidea* infections and symptom development on apple fruits and shoots in China. *Eur. J. Plant Pathol.* 146, 507–518. doi: 10.1007/s10658-016-0935-5
- Zhao, Y., Yue, C., Ding, W., Li, T., Xu, J. W., Zhao, P., et al. (2018). Butylated hydroxytoluene induces astaxanthin and lipid production in *Haematococcus pluvialis* under high-light and nitrogen-deficiency conditions. *Bioresour. Technol.* 266, 315–321. doi: 10.1016/j.biortech.2018.06.111
- Zheng, Y., Sheng, J., Zhao, R., Zhang, J., Lv, S., Liu, L., et al. (2011). Preharvest L-arginine treatment induced postharvest disease resistance to *Botrytis cinerea* in tomato fruits. *J. Agric. Food Chem.* 59, 6543–6549. doi: 10.1021/jf2000053

Conflict of Interest: The authors declare that the research was conducted in the absence of any commercial or financial relationships that could be construed as a potential conflict of interest.

Copyright © 2021 Huang, Sun, Guan, Lian, Li and Wang. This is an open-access article distributed under the terms of the Creative Commons Attribution License (CC BY). The use, distribution or reproduction in other forums is permitted, provided the original author(s) and the copyright owner(s) are credited and that the original publication in this journal is cited, in accordance with accepted academic practice. No use, distribution or reproduction is permitted which does not comply with these terms.



Isolation and Molecular Identification of the Native Microflora on *Flammulina velutipes* Fruiting Bodies and Modeling the Growth of Dominant Microbiota (*Lactococcus lactis*)

OPEN ACCESS

Edited by:

Anindya Chanda,
Mycologics LLC, United States

Reviewed by:

Amit Kumar Singh,
Albany Medical College, United States

Theofania Tsironi,

Agricultural University of Athens,
Greece

Daniel Angelo Longhi,

Federal University of Paraná, Brazil

Jun-Fang Lin,

South China Agricultural University,
China

*Correspondence:

Zhen Jia
zhen-jia@uml.edu
Ting Fang
fangting930@163.com
Yuji Jiang
jyj1209@163.com

Specialty section:

This article was submitted to
Food Microbiology,
a section of the journal
Frontiers in Microbiology

Received: 06 February 2021

Accepted: 09 April 2021

Published: 21 May 2021

Citation:

Wei Q, Pan X, Li J, Jia Z, Fang T
and Jiang Y (2021) Isolation
and Molecular Identification of the
Native Microflora on *Flammulina
velutipes* Fruiting Bodies
and Modeling the Growth
of Dominant Microbiota (*Lactococcus
lactis*). *Front. Microbiol.* 12:664874.
doi: 10.3389/fmicb.2021.664874

Qi Wei^{1,2,3}, Xinyuan Pan^{1,4}, Jie Li¹, Zhen Jia^{1*}, Ting Fang^{1*} and Yuji Jiang^{1*}

¹ College of Food Science, Fujian Agriculture and Forestry University, Fuzhou, China, ² College of Life Science, Ningde Normal University, Ningde, China, ³ Fujian Higher Education Research Center for Local Biological Resources, Ningde, China, ⁴ Fujian Anjoy Food Co., Ltd., Xiamen, China

The objectives of this study were to isolate and identify the dominant microorganism in *Flammulina velutipes* fruiting bodies (FVFB) and to develop kinetic models for describing its growth. The native microflora community on FVFB was isolated and identified using morphological examination and high-throughput sequencing analysis. FVFB presented complex microbial communities with dominant microorganisms being *Lactococcus lactis*. Irradiated FVFB were inoculated with the isolated strain of *L. lactis* and cultivated at various temperatures (4, 10, 16, 20, 25, 32, and 37°C). Three primary models, namely the Huang, Baranyi and Roberts, and reparameterized Gompertz models, and three secondary models, namely the Huang square-root, Ratkowsky square-root, and Arrhenius-type models, were developed and evaluated. With the lowest values of mean square error (MSE, 0.023–0.161) and root mean square error (RMSE, 0.152–0.401) values, the reparameterized Gompertz model was more suitable to describe the growth of *L. lactis* on FVFB than both Huang and Baranyi and Roberts models. The Ratkowsky square-root model provided more accurate estimation for the effect of temperature on the specific growth rate of *L. lactis*. The minimum growth temperature predicted by the Ratkowsky square-root model was -7.1°C . The kinetic models developed in this study could be used to evaluate the growth behavior of *L. lactis* on FVFB and estimate the shelf-life of FVFB.

Keywords: *Flammulina velutipes*, microflora, mathematical model, *Lactococcus lactis*, growth

INTRODUCTION

Flammulina velutipes, known as golden needle mushroom, is one of the major edible mushrooms employed in factory cultivation in East Asia (Fang et al., 2015). *F. velutipes* had various distinct advantages, owing to its simple cultivation technique, ability of fast fruiting, high yield, desirable taste, and rich in nutrients (essential amino acids, dietary fiber, protein, vitamins, and low in

fat). Since *Flammulina velutipes* fruiting bodies (FVFB) have a variety of bioactivities, such as hepatoprotective, antitumor, antihyperlipidemia, immune regulation, and so on (Zhao et al., 2019; Wang and Zhang, 2021), the consumption demands of FVFB were increasing rapidly. The shelf-life of postharvest FVFB is very short (1~3 days) when stored under ambient condition. The deterioration of postharvest FVFB occurs easily during storage. The main reason might be microbial growth (Shi et al., 2018). Niu et al. (2020) reported that *Pseudomonas* spp. is spoilage organisms on postharvest FVFB. FVFB had a neutral pH value and high moisture content, which could be a suitable medium for the growth of pathogenic and spoilage bacteria.

Lactococcus lactis is a Gram-positive bacterium. It is one of the most important microorganisms used extensively in dairy products and other fermented foods (Odamaki et al., 2011). *L. lactis* could survive and grow well in many foods, which could utilize carbohydrates fermentatively and form lactic acid as an end-product. The increasing amount of *L. lactis* and lactic acid in FVFB could significantly reduce its quality by causing softening, browning, rotting, and deterioration. The texture and pH value of FVFB also could be significantly changed with the increasing population of *L. lactis*. Thus, the commercial value of postharvest FVFB could decrease during storage. Based on the beneficial use of *L. lactis* in food fermentation, *L. lactis* has generally been recognized as safe status (Wessels et al., 2004; Food and Drug Administration, 2012). However, some studies had also reported some species of *Lactococcus* to an opportunistic pathogen (Mannion and Rothburn, 1990; Aguirre and Collins, 1993). Rodrigues et al. (2016) suggested that the *Lactococcus* is a potential etiological agent in mastitis outbreak. Zhao et al. (2013) showed that the pathogen causing postharvest water-soaked and sunken lesions on the stipes and decay of *Pleurotus eryngii* was isolated and identified as *L. lactis* subsp. *lactis*. Therefore, *L. lactis* could be potential pathogenic microbes for the mushroom and food industry.

The predictive microbiology models were available to describe the microbial growth, survival, or inactivation in response to environmental conditions (Laurent, 2016; Akkermans et al., 2018). Primary models are used to describe microbial growth data as a function of time under constant environmental conditions (Whiting and Buchanan, 1993). The reparameterized Gompertz model (Zwietering et al., 1990; Buchanan et al., 1997), Huang model (Huang, 2013), Baranyi and Roberts model, and logistic model (Tashiro and Yoshimura, 2019) are generally reported as the primary models. A secondary model deals with the response of parameters appearing in primary modeling approaches as a function of one or more environmental conditions like temperature, pH, etc. (Whiting and Buchanan, 1993). The commonly described secondary models include the Huang square root, Arrhenius type, and Ratkowsky square root (Whiting and Buchanan, 1993; Huang, 2014).

However, there is limited information in the literature about microbial communities and *L. lactis* growth behavior on fresh postharvest FVFB. Therefore, in this study, native microflora on the surface of FVFB were analyzed and discriminated using

16S rRNA gene amplification and high-throughput sequencing. The growth behavior of dominant microflora (*L. lactis*) was studied at different storage temperatures. Mathematical models were fitted to the data and compared to select an accurate model for describing the growth of the dominant microflora. This study could provide useful information to predict the spoilage of FVFB caused by *L. lactis*. The models developed in this study may be used by the food industry and regulatory agencies to estimate the growth of *L. lactis* in FVFB.

MATERIALS AND METHODS

Sample Collection

The FVFB samples were purchased from five different local markets (FV1, FV2, FV3, FV4, and FV5) in Fuzhou, China. FV1 was from Laoguangcun market (farm market), FV2 from Yonghui superstore, FV3 from RT-Mart, FV4 from Walmart, and FV5 from Super Species.

Native Microflora Isolation and Identification

Twenty-five grams of FVFB were transferred into a sterile plastic bag (19 × 30 cm, Huankai Microbial Co., Ltd., Guangzhou, China) and homogenized in 225 ml 0.1% sterile peptone water (PW). Samples were serially diluted using 0.1% sterile PW. An aliquot of 100 µl was transferred onto Luria-Bertani (LB) agar plates (Huankai Microbial Co., Ltd., Guangzhou, China) and incubated at 37°C for 48 h. Different types of bacterial colonies on LB plates were isolated and transferred into 10 ml of LB broth (Huankai Microbial Co., Ltd., Guangzhou, China). The bacterial cultures were harvested after three consecutive transfers. The cultures were maintained in LB plates and stored at 4°C until use. Each isolated culture obtained was stained by Gram staining and examined using an Eclipse E100 microscope (Nikon, Japan).

Each isolated culture was mixed with 20 µl of double-distilled water and boiled for 2 mins. The bacterial suspension was centrifuged at 12,000 rpm for 1 min. DNA in the supernatants was extracted using a DNA extraction kit (Sangon Biotech, Shanghai, China) according to the manufacturer's protocol. PCR was carried out on a Mastercycler gradient (Eppendorf, Germany) using 50 µl reaction volumes, containing 2 µl primers (5 µM), 25 µl 2 × Taq PCR Master Mix, 2 µl template DNA, and 21 µl ddH₂O. The cycling conditions were as follows: initial denaturation at 94°C for 5 min, followed by 35 cycles of denaturation at 95°C for 45 s, annealing at 56°C for 45 s, extension at 72°C for 90 s, and final extension at 72°C for 10 min. The PCR products were qualified and visualized using 1% agarose gel electrophoresis (Sangon Biotech, Shanghai, China) and analyzed by 16S rRNA gene sequencing analysis. Sequences were compared with the National Center for Biotechnology Information (NCBI,¹) database using the basic local alignment search tool (BLAST) algorithm.

¹<https://www.ncbi.nlm.nih.gov/>

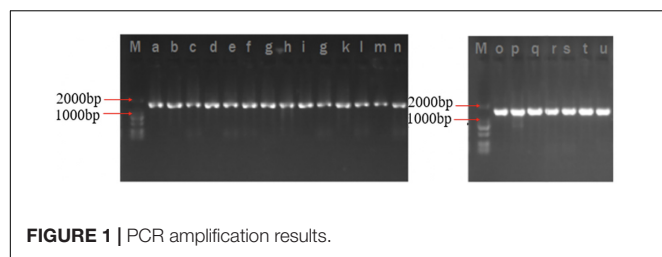


FIGURE 1 | PCR amplification results.

TABLE 1 | The species of bacteria in *Flammulina velutipes* fruiting bodies.

Organism	FV1	FV2	FV3	FV4	FV5
<i>Staphylococcus warneri</i>	+	–	–	–	–
<i>Ewingella americana</i>	+	+	+	+	+
<i>Bacillus amyloliquefaciens</i>	+	–	–	–	–
<i>Citrobacter freundii</i>	+	–	–	–	–
<i>Raoultella ornithinolytica</i>	+	–	–	–	–
<i>Kluyvera cryocrescens</i>	+	–	–	–	–
<i>Bacillus paramycoides</i>	–	+	–	–	+
<i>Pseudomonas aeruginosa</i>	–	+	–	–	–
<i>Lactococcus lactis</i>	–	+	+	+	–
<i>Klebsiella aerogenes</i>	–	–	–	+	–
<i>Chryseobacterium indologenes</i>	–	–	–	+	–
<i>Staphylococcus saprophyticus</i>	–	–	–	–	+

+Presence of the corresponding bacterium species based on 16S rRNA sequences.

–Absence of bacterium species.

High-Throughput Sequencing Analysis

The DNA of FVFB was extracted using PowerSoil DNA Isolation Kit (MoBio Laboratories, Carlsbad, CA, United States) according to the protocol provided by the manufacturer. The universal primer sets of 338F (5'-ACTCCTACGGGAGGCAGCAG-3') and 806R (5'-GGACTACHVGGGTWTCTAAT-3') were used to amplify the V3–V4 hypervariable region of 16S rRNA genes. High-throughput sequencing was conducted using the Illumina HiSeq 2500 platform at Allwegene Technology Co., Ltd., (Beijing, China). Qualified reads were separated using the sample-specific barcode sequences and trimmed with Illumina Analysis Pipeline Version 2.6. Sequences were

analyzed using QIIME (Version 1.8,²) software package and in-house Perl scripts to determine alpha diversity and beta diversity. Sequences with the level of 97% similarity were assigned to the same operational taxonomic units (OTUs). The Ribosomal Database Project classifier was used to annotate taxonomic information for each representative sequence.

Dominant Bacteria and Preparation

Lactococcus lactis was obtained from FVFB. The culture of *L. lactis* was revived by inoculating into 10 ml of LB tube and incubating at 37°C for 20 h. After incubation, the bacterial culture was centrifuged at 4,500 rpm for 15 min (4°C), washed three times using 0.1% sterile PW, and then resuspended in 10 ml of 0.1% sterile PW. The suspension was serially diluted to obtain a final concentration of 10⁵ to 10⁶ CFU/ml as working culture.

Sample Preparation and Inoculation

Flammulina velutipes fruiting bodies were purchased from a local market and irradiated (Rice Research Institute, Fujian Academy of Agricultural Sciences, Fuzhou, Fujian, China) at a dose of 5 kg. Afterward, 25 g of FVFB were placed into a sterile plastic bag and inoculated with 0.1 ml of *L. lactis* working culture. The inoculated FVFB samples were incubated at constant temperatures of 4, 10, 16, 20, 25, 32, and 37°C, respectively. Depending on the incubation temperature, samples were retrieved from the incubators at different time intervals. For each sample, 225 ml 0.1% sterile PW was added and homogenized in a stomacher for 20 s (Model BagMixer 400 W, Interscience Co., France). Each sample was serially diluted with PW. Each sample was mixed with 225 ml of 0.1% sterile PW and homogenized in a stomacher (Model BagMixer 400 W, Interscience Co., France). The liquid portion of the homogenized samples was serially diluted with 0.1% sterile PW and plated onto de Man–Rogosa–Sharpe (MRS, Huankai Microbial Co., Ltd., Guangzhou, China) agar plates. All plates were incubated at 37°C for 48 h. The *L. lactis* colonies were enumerated and converted to the logarithm of base 10 or natural

²<http://qiime.org/>

TABLE 2 | Morphological characteristics of identified bacteria in *Flammulina velutipes* fruiting bodies.

Organism	Diameter/mm	Form and color	Gram reaction	Shape
<i>Staphylococcus warneri</i>	0.71~0.76	Regular, smooth, white	Positive	Cocci
<i>Ewingella americana</i>	0.51~1.79	Regular, smooth, white	Negative	Rods
<i>Bacillus amyloliquefaciens</i>	2.27~4.98	Irregular, smooth, white	Positive	Rods
<i>Citrobacter freundii</i>	1.36~2.70	Regular, smooth, white	Negative	Rods
<i>Raoultella ornithinolytica</i>	1.71~2.63	Regular, smooth, white	Negative	Rods
<i>Kluyvera cryocrescens</i>	2.60~4.21	Regular, smooth, raised, white	Negative	Rods
<i>Bacillus paramycoides</i>	2.07~2.20	Irregular, raised, white	Positive	Rods
<i>Pseudomonas aeruginosa</i>	3.38~5.07	Regular, smooth, flat, pale green	Negative	Rods
<i>Lactococcus lactis</i>	1.15~1.47	Regular, smooth, white	Positive	Cocci
<i>Klebsiella aerogenes</i>	1.66~2.68	Regular, smooth, white	Negative	Rods
<i>Chryseobacterium indologenes</i>	0.74~1.11	Regular, smooth, raised, buff	Negative	Rods
<i>Staphylococcus saprophyticus</i>	1.27~1.60	Regular, smooth, buff	Positive	Cocci

base, recorded as log CFU/g or ln CFU/g. Each experiment was repeated three times.

Primary Models

In this study, three primary models were used for describing *L. lactis* growth: Huang model (Eqs 1, 2, Huang, 2013), Baranyi and Roberts model (Eqs 3, 4, Baranyi and Roberts, 1995), and

reparameterized Gompertz model (Eq. 5, Zwietering et al., 1990). The Huang model is expressed as

$$Y(t) = Y_0 + Y_{\max} - \ln \left\{ e^{Y_0} + [e^{Y_{\max}} - e^{Y_0}] e^{-\mu_{\max} B(t)} \right\} \quad (1)$$

$$B(t) = t + \frac{1}{\alpha} \ln \frac{1 + e^{-\alpha(t-\lambda)}}{1 + e^{\alpha\lambda}} \quad (2)$$

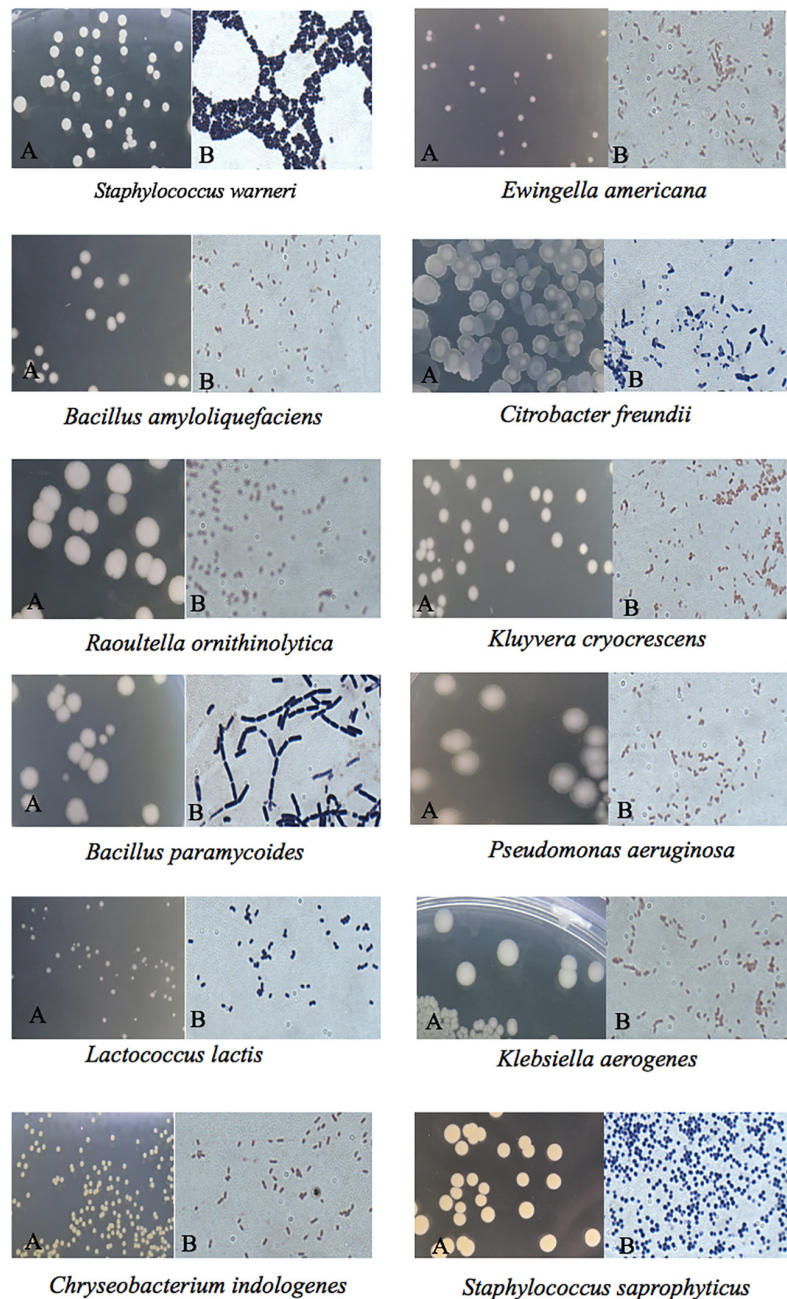


FIGURE 2 | Colony morphology of the identified native microflora in *Flammulina velutipes* fruiting bodies under a microscope: **(A)** without staining and **(B)** Gram staining.

where t is the time point (h), λ is the lag phase duration (h), $Y(t)$ represents the natural logarithm of microorganism count (ln CFU/g), Y_0 is the initial microorganisms count (ln CFU/g), Y_{\max} is the bacterial count (ln CFU/g) at the stationary phase, μ_{\max} is the maximum specific growth rate (h^{-1}), and α is a constant ($\alpha = 4$) that defines the transition from the lag phase to the exponential phase of a growth curve (Huang, 2013).

The Baranyi and Roberts model is expressed as

$$Y(t) = Y_0 + \mu_{\max} A(t) - \ln \left[1 + \frac{e^{\mu_{\max} A(t)} - 1}{e^{Y_{\max} - Y_0}} \right] \quad (3)$$

$$A(t) = t + \frac{1}{\mu_{\max}} \ln(e^{-\mu_{\max} t} + e^{-h_0} - e^{-\mu_{\max} t - h_0}) \quad (4)$$

where h_0 is the physiological state of the microorganism and equals to $\lambda \times \mu_{\max}$, and the other variables, i.e., $Y(t)$, Y_0 , Y_{\max} , and μ_{\max} , are defined as those used in the Huang model. Firstly, the h_0 values are estimated and an h_0 averaged value is established. Then, μ_{\max} , Y_0 , and Y_{\max} are estimated with fixed h_0 averaged value.

The reparameterized Gompertz model is expressed as

$$Y(t) = Y_0 + (Y_{\max} - Y_0) \exp \left\{ -\exp \left[\frac{\mu_{\max} e}{Y_{\max} - Y_0} (\lambda - t) + 1 \right] \right\} \quad (5)$$

where λ , t , $Y(t)$, Y_0 , Y_{\max} , and μ_{\max} are identical to those used in the Huang model.

Secondary Models

Secondary models were fitted to the maximum specific growth rates (μ_{\max}) estimated from the primary models under different incubation temperatures. The Ratkowsky square-root (Eq. 6, Ratkowsky et al., 1982), Huang square-root (Eq. 7, Huang, 2014), and Arrhenius-type (Eq. 8, Huang et al., 2011) models were used to evaluate the effect of temperature on growth rate.

$$\sqrt{\mu_{\max}} = a(T - T_0) \quad (6)$$

$$\sqrt{\mu_{\max}} = a(T - T_{\min})^{0.75} \quad (7)$$

$$\mu_{\max} = a(T + 273.15) \exp \left\{ - \left[\frac{\Delta G'}{R(T + 273.15)} \right]^n \right\} \quad (8)$$

In Equations 6–8a is a regression coefficient for each model, T is the incubation temperature ($^{\circ}\text{C}$) for microbial growth, T_0 is the nominal minimum temperature ($^{\circ}\text{C}$), T_{\min} is the estimated minimum growth temperature ($^{\circ}\text{C}$), and a and n are regression coefficients. In Eq. 8, R is the universal gas constant [8.314 J/(mol K)], and $\Delta G'$ is a type of activation energy related to bacterial growth (J/mol).

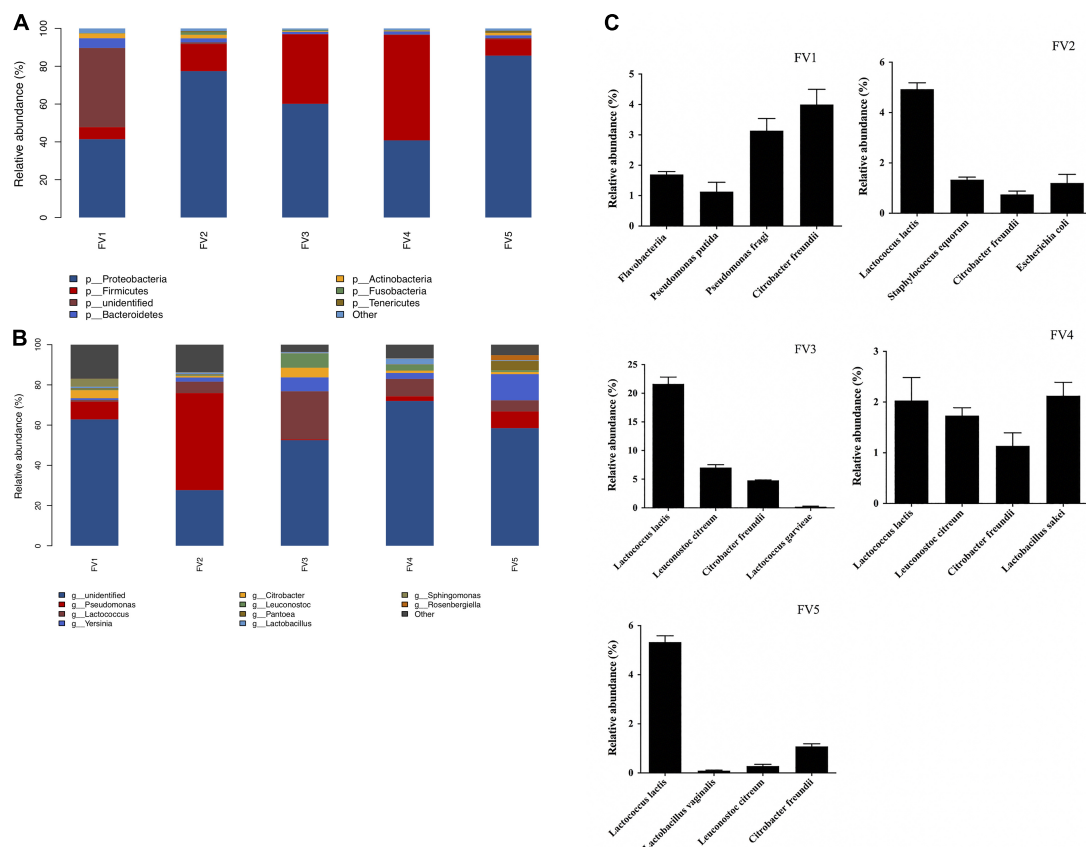


FIGURE 3 | Relative abundance of native microflora in *Flammulina velutipes* fruiting bodies. **(A)** Phylum level, **(B)** genus level, and **(C)** species level.

Modeling and Statistical Analysis

Growth curves of *L. lactis* on FVFB at different isothermal temperatures were analyzed using the United States Department of Agriculture (USDA) Integrated Pathogen Modeling Program (IPMP, Huang, 2014). Lag phase durations, specific growth rates, and maximum concentrations of *L. lactis* under different conditions were obtained from IPMP analysis.

RESULTS AND DISCUSSION

Identification of the Native Microbiota in FVFB

The 16S rRNA gene amplification and high-throughput sequencing analysis were used to identify the native microflora in FVFB. In this research, a total of 21 types of bacterial colonies were isolated and obtained from FVFB in different markets (FV1, FV2, FV3, FV4, and FV5). Each isolated culture was analyzed as shown in **Figure 1**, and the lengths of DNA fragments extracted from isolated cultures were similar and approximately 1,800 bp. DNA sequences obtained from high-throughput analysis were compared with the NCBI database using BLAST algorithm. A total of 12 species were identified and confirmed (**Table 1**). FV1 had more species of the bacteria than FV2, FV3, FV4, and FV5, which suggests that FVFB from the farm market (FV1) had a higher risk of being contaminated by the microorganism.

Morphological Examination

The cultural morphology of each selected bacteria was done and tested with Gram staining and used as a basic separation of bacteria into their taxonomy (**Table 2** and **Figure 2**). A total of five Gram-positive bacteria were obtained, including *Staphylococcus warneri*, *Bacillus amyloliquefaciens*, *Bacillus paramycoides*, *L. lactis*, and *Staphylococcus saprophyticus*. A total of seven Gram-negative bacteria were obtained as follows: *Ewingella americana*, *Citrobacter freundii*, *Raoultella ornithinolytica*, *Kluyvera cryocrescens*, *Pseudomonas aeruginosa*, *Klebsiella aerogenes*, and *Chryseobacterium indologenes*. The morphological examination results demonstrated that the number of Gram-negative bacteria was more than the Gram-positive bacteria isolated in FVFB. The most identified isolates showed the shape of rods except *S. warneri*, *L. lactis*, and *S. saprophyticus*.

Native Microflora Composition and Diversity

The bacterial community, relative abundance, and diversity on the surfaces of FVFB were investigated by high-throughput sequencing analysis. The relative abundance at the phylum level of different bacteria in FVFB is shown in **Figure 3A**. *Proteobacteria*, *Firmicutes*, *Bacteroidetes*, *Actinobacteria*, *Fusobacteria*, and *Tenericutes* were identified on the surface of FVFB. *Proteobacteria* and *Firmicutes* were found to be the dominant microflora in FVFB.

At the genus level, 212 bacteria genera were obtained (the top 10 genera are shown in **Figure 3B**). Results demonstrated

TABLE 3 | Estimated parameters for the primary models.

Primary models	4°C			10°C			16°C			20°C			25°C			32°C			37°C		
	Huang	Baranyi	Gompertz	Huang	Baranyi	Gompertz	Huang	Baranyi	Gompertz	Huang	Baranyi	Gompertz	Huang	Baranyi	Gompertz	Huang	Baranyi	Gompertz	Huang	Baranyi	Gompertz
Y_0 (ln CFU/g)	7.63	7.046	7.604	7.922	7.205	7.878	8.406	8.441	8.211	7.597	7.66	7.281	9.389	9.58	9.048	9.862	10.043	9.482	10.213	10.335	9.905
L_{95CI}	7.356	6.551	7.278	7.681	6.688	7.739	7.699	7.875	7.584	6.809	7.046	6.603	8.491	8.862	8.097	9.066	9.351	8.612	9.333	9.539	8.927
U_{95CI}	7.903	7.541	7.93	8.164	7.722	8.017	9.114	9.006	8.839	8.348	8.273	7.959	10.287	10.299	9.999	10.658	10.736	10.353	11.094	11.132	10.883
Y_{max} (ln CFU/g)	15.418	15.481	15.464	18.017	18.189	18.271	18.785	18.718	19.012	17.277	17.128	17.661	18.407	18.217	18.69	18.483	18.369	18.749	18.793	18.66	19.036
L_{95CI}	15.172	15.055	15.153	17.749	17.586	18.098	18.363	18.299	18.627	16.695	16.554	17.206	17.715	17.496	18.049	17.975	17.838	18.282	18.118	17.952	18.407
U_{95CI}	15.663	15.906	15.774	18.286	18.792	18.445	19.207	19.136	19.397	17.86	17.703	18.116	19.099	18.937	19.331	18.991	18.9	19.216	19.467	19.368	19.665
μ_{max} (h ⁻¹)	0.075	0.054	0.09	0.083	0.066	0.101	0.191	0.221	0.235	0.432	0.519	0.501	0.54	0.665	0.637	0.678	0.818	0.772	0.883	1.085	1.011
L_{95CI}	0.063	0.048	0.07	0.076	0.06	0.095	0.163	0.199	0.199	0.356	0.458	0.432	0.433	0.573	0.522	0.539	0.711	0.634	0.646	0.919	0.779
U_{95CI}	0.087	0.059	0.11	0.09	0.071	0.107	0.22	0.242	0.272	0.508	0.581	0.57	0.648	0.756	0.752	0.817	0.924	0.91	1.12	1.251	1.243
λ (h)	84.427	51.925	89.142	69	42.484	76.285	8.693	12.687	11.358	3.421	5.402	3.85	2.216	4.216	2.475	2.02	3.427	1.949	1.473	2.584	1.527
MSE (ln CFU/g)	0.119	0.319	0.161	0.076	0.321	0.023	0.202	0.219	0.113	0.242	0.284	0.082	0.212	0.303	0.119	0.251	0.318	0.136	0.226	0.302	0.126
RMSE (ln CFU/g) ²	0.345	0.564	0.401	0.276	0.566	0.152	0.449	0.468	0.337	0.492	0.533	0.303	0.46	0.55	0.345	0.501	0.564	0.368	0.476	0.549	0.356

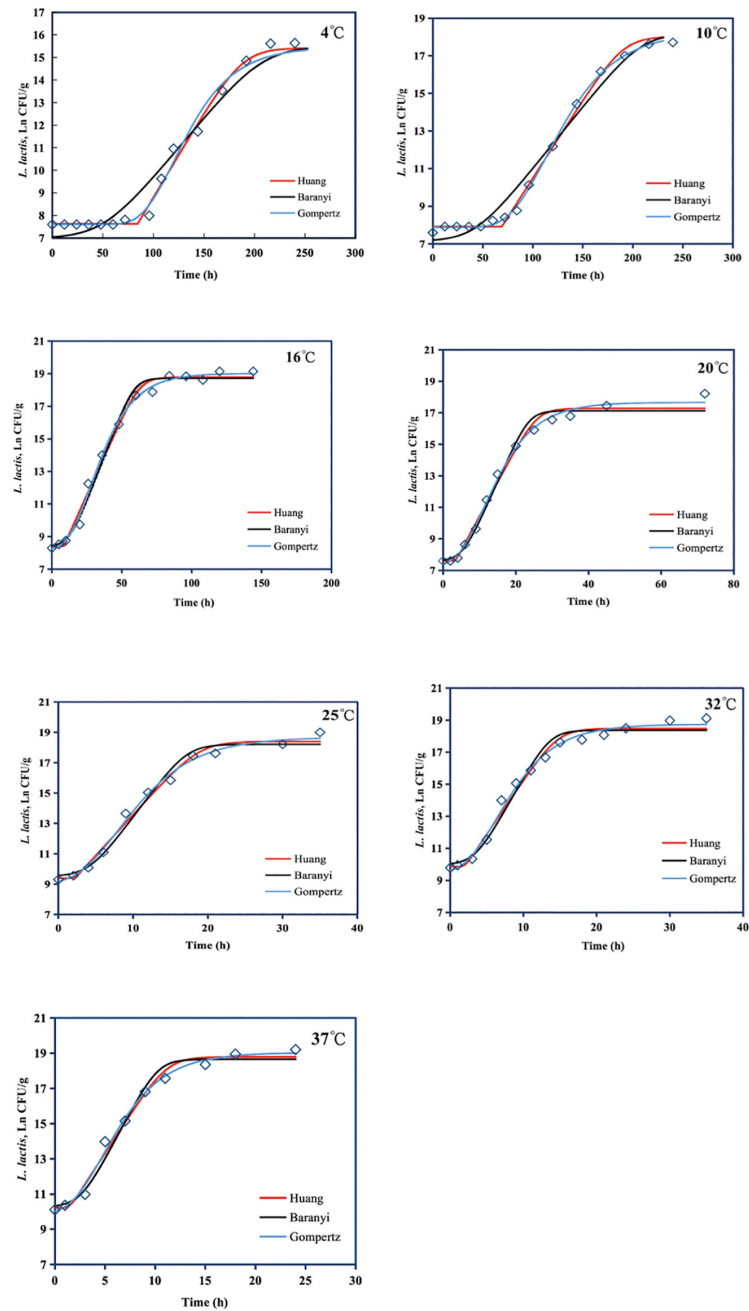


FIGURE 4 | Growth of *Lactococcus lactis* in *Flammulina velutipes* fruiting bodies at temperatures between 4 and 37°C. Solid red line: Huang model, solid black line: Baranyi and Roberts model, solid blue line: reparameterized Gompertz model, diamond: observed growth data.

TABLE 4 | Estimated parameters for the secondary models.

Secondary models	Parameters	Value	Standard deviation	t value	p value	MSE [(log CFU/g) ²]	RMSE (log CFU/g)
Huang square-root model	A	0.064	0.005	13.556	3.91E-05	0.005	0.068
	T _{min}	−1.7	2.142	−0.784	4.69E-01		
Ratkowsky square-root model	A	0.023	0.002	10.298	1.485E-04	0.004	0.065
	T ₀	−7.2	2.894	−2.48	5.581E-02		
Arrhenius-type model	A	0.004	0.001	3.254	3.13E-02	0.005	0.068
	ΔG	2,447.797	42.924	57.026	5.662E-07		
	N	20.957	8.61	2.434	7.17E-02		

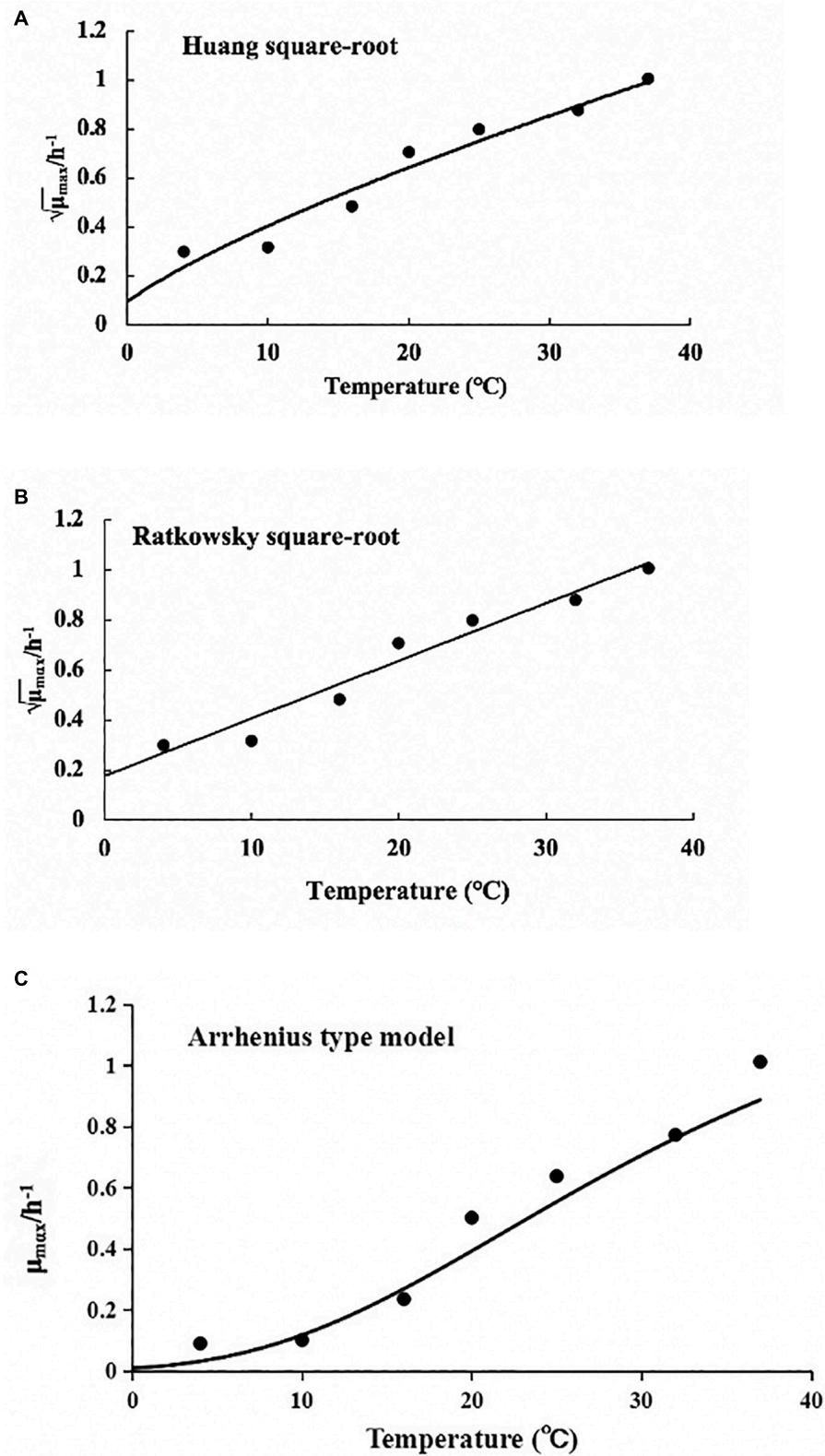


FIGURE 5 | Effect of temperature on the specific growth rate of *Lactococcus lactis* in *Flammulina velutipes* fruiting bodies. **(A)** Huang square-root model, **(B)** Ratkowsky square-root model, and **(C)** Arrhenius-type model.

that there were complex microbial communities in FVFB. *Pseudomonas* was determined as the dominant microflora in FV1 and FV2. Based on the observations of Li et al. (2020), the dominant population of microflora was *Pseudomonas* spp., along with small proportions of *Sphingobacterium*, *Pedobacter*, *Corynebacterium*, and *Pasteurella* in *Agaricus bisporus*. Therefore, *Pseudomonas* spp. had high relative abundances in bacterial community structure in mushrooms. *Lactococcus* was determined as the dominant microflora in FV3 and FV4. *Yersinia* was determined as the dominant microflora in FV5. As shown in **Figure 3C**, the dominant microflora was *Citrobacter freundii* (4%) in FV1 at the species level. However, the dominant microflora was *L. lactis* in FV2 (4.9%), FV3 (21.6%), FV4 (5.3%), and FV5 (2%). These results were the same as those shown in **Table 1**, which indicated that *L. lactis* was the dominant microflora in FVFB. Lee et al. (2016) demonstrated that lactic acid bacteria were isolated from traditional Korean fermented vegetable. *L. lactis* was one of the most important microorganisms in the dairy industry and generally recognized as safe status. Tormo et al. (2015) reported that *L. lactis* was the dominant species in raw goat milk. However, some studies reported that *L. lactis* was the causal agent of postharvest decay of mushroom (Zhao et al., 2013, 2018). Furthermore, *L. lactis* had a homofermentative metabolism, and it does not directly cause soft rot, but it can produce lactic acid from carbohydrates and create favorable conditions for soft rot symptoms of various vegetables (Baheyeldin and Gahan, 2010; Song et al., 2017). During storage, the increasing amount of *L. lactis* in FVFB could be harmful to its quality by causing softening, browning, sunken lesions, and deterioration in FVFB. Therefore, the growth of *L. lactis* isolated from FVFB was further investigated in this study.

Mathematical Modeling

Lactococcus lactis and other bacteria could grow well in FVFB. At chilled temperature, competition from other psychrotrophs may not allow *L. lactis* to grow well and reach the maximum population. Due to the limitations of MRS plates, a few other bacteria could also grow in the MRS plate, and *L. lactis* could not be accurately determined by MRS plating (Dave and Shah, 1996). Therefore, to accurately assess the growth of *L. lactis* in FVFB, FVFB was irradiated to eliminate the influence of background microorganisms.

The Huang, Baranyi, and reparameterized Gompertz models were fitted to the growth data of *L. lactis* in FVFB at different isothermal storage temperatures (4, 10, 16, 20, 25, 32, and 37°C). As shown in **Table 3** and **Figure 4**, the growth curves of *L. lactis* exhibited lag, exponential, and stationary phases at different temperatures. It can be seen that lag time (λ) and specific growth rate (μ_{\max}) of *L. lactis* were affected by temperature. As temperature increases, the lag time of *L. lactis* decreased, while the growth rates increased. The maximum population of *L. lactis* on FVFB could reach $19.11 \pm 0.10 \ln \text{CFU/g}$. For the Huang, Baranyi, and reparameterized Gompertz models, the values of mean square error (MSE) ranged from 0.076 to 0.251, 0.219 to 0.321, and 0.023 to 0.161, respectively, and the root mean square error (RMSE) ranged from 0.276 to 0.501, 0.468 to 0.566, and 0.152 to 0.401, respectively. Compared with the Huang

and Baranyi and Robert's models, the reparameterized Gompertz model had the lowest MSE and RMSE values, indicating that the model was more suitable for describing the growth of *L. lactis* than the Huang and Baranyi and Robert's models. Wang et al. (2017) demonstrated that the Gompertz model was suitable to estimate the shelf-life of the mushroom *A. bisporus*. Therefore, the Gompertz model was suitable for describing the microbial growth on mushroom.

The values of μ_{\max} and λ obtained from the reparameterized Gompertz model were used for secondary models' development (**Figure 5**). **Table 4** lists the estimated parameters of the Huang, Ratkowsky, and Arrhenius models. The minimum growth temperatures predicted by the Huang square-root model was -1.7°C . The minimum growth temperature estimated by the Ratkowsky square-root model was -7.2°C , which was close to the value (-12°C) reported by Zhou et al. (2014). However, the Arrhenius-type model did not predict minimum growth temperature. Additionally, the values of MSE and RMSE (0.004 and 0.065) for the Ratkowsky square-root model were much lower than those for the Huang square-root model and Arrhenius-type model. Therefore, the Ratkowsky-type model was more accurate to predict the effect of temperature on the specific growth rate of *L. lactis* on FVFB.

CONCLUSION

In this study, morphological examination and high-throughput sequencing were used to investigate the bacterial community in FVFB. *Proteobacteria*, *Firmicutes*, *Bacteroidetes*, *Actinobacteria*, *Fusobacteria*, and *Tenericutes* were the dominant phyla among all the FVFB samples collected from five different markets. *L. lactis* was the dominant microflora in FVFB. FVFB were most likely stored at a refrigerated temperature. However, it might be exposed to temperature abuse during storage. Due to their high moisture and delicate epidermal structure, FVFB were an ideal medium for bacteria growth, including *L. lactis*. The initial count of *L. lactis* in FVFB was estimated at around $9.73 \pm 0.41 \ln \text{CFU/g}$. The maximum population of *L. lactis* was $19.11 \pm 0.10 \ln \text{CFU/g}$ in the stationary phase. This study proved that the Huang, Baranyi, and reparameterized Gompertz models could describe the growth of *L. lactis* in FVFB. The reparameterized Gompertz model was recommended as the primary model for *L. lactis* growth in FVFB, with the lowest MSE and RMSE values, ranging from 0.023 to 0.161, and 0.152 to 0.401, respectively. This study also explored and compared three different secondary models, namely the Ratkowsky square-root model, Huang square-root model, and Arrhenius-type model, and estimated the minimum, optimum, and maximum growth temperatures and the optimum growth rate of *L. lactis* in FVFB. Also, the Ratkowsky square-root model might provide a more accurate estimation of the specific growth rate of *L. lactis* in FVFB.

The effect of temperature on the growth kinetics of *L. lactis* in FVFB was investigated in this study. The primary models and secondary models could be used to predict the growth of *L. lactis* in FVFB during refrigerated storage

and temperature abuse. The application of these models can also predict the shelf-life of spoilage microorganism shelf-life of FVFB and be used by regulatory agencies and food processors for conducting risk assessments of *L. lactis* in FVFB. The mathematical models could be used to describe the microbial growth under isothermal conditions in this study. However, temperature abuse during commercial production and distribution, isothermal studies were not suitable to investigate growth kinetics under fluctuating temperature conditions. Therefore, further studies are needed to develop dynamic models under fluctuating temperature conditions during storage.

DATA AVAILABILITY STATEMENT

The datasets presented in this study can be found in online repositories. The names of the repository/repositories and

accession number(s) can be found below: <https://www.ncbi.nlm.nih.gov/sra/PRJNA705553>.

AUTHOR CONTRIBUTIONS

All authors listed have made substantial, direct and intellectual contribution to the work, and approved it for publication.

FUNDING

This work was supported by the Key Cultivating Program of Ningde Normal University (Grant Number 2020ZDK03), the Scientific Research Foundation of Ningde Normal University (Grant Number 2020Y010), and the Scientific Research Fund for Young Teachers in Fujian Province (Grant Number JAT200689).

REFERENCES

- Aguirre, M., and Collins, M. D. (1993). Lactic acid bacteria and human clinical infection. *J. Appl. Bacteriol.* 75, 95–107. doi: 10.1111/j.1365-2672.1993.tb02753.x
- Akkermans, S., Logist, F., and Impe, J. F. V. (2018). Parameter estimations in predictive microbiology: statistically sound modelling of the microbial growth rate. *Food Res. Int.* 106, 1105–1113. doi: 10.1016/j.foodres.2017.11.083
- Baheyeldin, M., and Gahan, C. G. M. (2010). *Lactococcus lactis*: from the dairy industry to antigen and therapeutic protein delivery. *Discov. Med.* 9, 455–461. doi: 10.3109/14653241003587637
- Baranyi, J., and Roberts, T. A. (1995). Mathematics of predictive food microbiology. *Int. J. Food Microbiol.* 26, 199–218. doi: 10.1016/0168-1605(94)00121-L
- Buchanan, R. L., Whiting, R. C., and Damert, W. C. (1997). When is simple good enough: a comparison of the Gompertz, Baranyi, and three-phase linear models for fitting bacterial growth curves. *Food Microbiol.* 14, 313–326. doi: 10.1006/fmic.1997.0125
- Dave, R. I., and Shah, N. P. (1996). Evaluation of media for selective enumeration of *Streptococcus thermophilus*, *Lactobacillus delbrueckii* ssp. *bulgaricus*, *Lactobacillus acidophilus*, and *Bifidobacteria*. *J. Dairy Sci.* 79, 1529–1536. doi: 10.3168/jds.S0022-0302(96)76513-X
- Fang, D. L., Yang, W. J., Kimatu, B. M., and Hu, Q. (2015). Effect of nanocomposite-based packaging on storage stability of mushrooms (*Flammulina velutipes*). *Innov. Food Sci. Emerg. Technol.* 33, 489–497. doi: 10.1016/j.ifset.2015.11.016
- Food and Drug Administration (2012). *History of the GRAS List and SCOGS Reviews*. Silver Spring, MD: Food and Drug Administration.
- Huang, L. H. (2013). Optimization of a new mathematical model for bacterial growth. *Food Control.* 32, 283–288. doi: 10.1016/j.foodcont.2012.11.019
- Huang, L. H. (2014). IPMP 2013-A comprehensive data analysis tool for predictive microbiology. *Int. J. Food Microbiol.* 171, 100–107. doi: 10.1016/j.ijfoodmicro.2013.11.019
- Huang, L., Hwang, A., and Phillips, J. (2011). Effect of temperature on microbial growth rate-Mathematical analysis: the arrhenius and eyring-polanyi connections. *J. Food Sci.* 76, 553–560. doi: 10.1111/j.1750-3841.2011.02377.x
- Laurent, G. (2016). Predictive microbiology models and operational readiness. *Proc. Food Sci.* 7, 133–136. doi: 10.1016/j.profoo.2016.05.003
- Lee, K. W., Shim, J. M., Park, S. K., Heo, H. J., Ham, K. S., and Kim, J. H. (2016). Isolation of lactic acid bacteria with probiotic potentials from kimchi, traditional Korean fermented vegetable. *LWT Food Sci. Technol.* 71, 130–137. doi: 10.1016/j.lwt.2016.03.029
- Li, J., Wei, Q., Huang, L. X., Fang, T., Chen, B. Z., and Jiang, Y. J. (2020). Mathematical modeling *Pseudomonas* spp. growth and microflora composition variation in *Agaricus bisporus* fruiting bodies during chilled storage. *Postharvest Biol. Technol.* 163:111144. doi: 10.1016/j.postharvbio.2020.111144
- Mannion, P. T., and Rothburn, M. M. (1990). Diagnosis of bacterial endocarditis caused by *Streptococcus lactis* and assisted by immunoblotting of serum antibodies. *J. Infect.* 21, 317–318. doi: 10.1016/0163-4453(90)94149-T
- Niu, Y. X., Yun, J. M., Bi, Y., Wang, T., Zhang, Y., Liu, H., et al. (2020). Predicting the shelf life of postharvest *Flammulina velutipes* at various temperatures based on mushroom quality and specific spoilage organisms. *Postharvest Biol. Technol.* 176:111235. doi: 10.1016/j.postharvbio.2020.111235
- Odamaki, T., Xiao, J. Z., Yonezawa, S., Yaeshima, T., and Iwatsuki, K. (2011). Improved viability of bifidobacteria in fermented milk by cocultivation with *Lactococcus lactis* subspecies *lactis*. *J. Dairy Sci.* 94, 1112–1121. doi: 10.3168/jds.2010-3286
- Ratkowsky, D. A., Olley, J., McMeekin, T. A., and Ball, A. (1982). Relationship between temperature and growth rate of bacterial cultures. *J. Bacteriol.* 149, 1–5.
- Rodrigues, M. X., Lima, S. F., Higgins, C. H., Canniatti-Brazaca, S. G., and Bicalho, R. C. (2016). The *Lactococcus* genus as a potential emerging mastitis pathogen group: a report on an outbreak investigation. *J. Dairy Sci.* 99, 9864–9874. doi: 10.3168/jds.2016-11143
- Shi, C., Wu, Y. Y., Fang, D. L., Pei, F., Mariga, A. M., Yang, W. J., et al. (2018). Effect of nanocomposite packaging on postharvest senescence of *Flammulina velutipes*. *Food Chem.* 246, 414–421. doi: 10.1016/j.foodchem.2017.10.103
- Song, A. A. L., In, L. L. A., Lim, S. H. E., and Rahim, R. A. (2017). A review on *Lactococcus lactis*: from food to factory. *Microb. Cell Fact.* 16, 1–15. doi: 10.1186/s12934-017-0669-x
- Tashiro, T., and Yoshimura, F. (2019). A neo-logistic model for the growth of bacteria. *Physica A* 525, 199–215. doi: 10.1016/j.physa.2019.03.049
- Tormo, H., Lekhal, D. A. H., and Roques, C. (2015). Phenotypic and genotypic characterization of lactic acid bacteria isolated from raw goat milk and effect of farming practices on the dominant species of lactic acid bacteria. *Int. J. Food Microbiol.* 210, 9–15. doi: 10.1016/j.ijfoodmicro.2015.02.002
- Wang, J. M., Chen, J. R., Hu, Y. F., Hu, H. Y., Liu, G. H., and Yan, R. X. (2017). Application of a predictive growth model of *Pseudomonas* spp. for estimating shelf life of fresh *Agaricus bisporus*. *J. Food Prot.* 80, 1676–1681. doi: 10.4315/0362-028X.JFP-17-055
- Wang, Y. X., and Zhang, H. (2021). Advances in the extraction, purification, structural-property relationships and bioactive molecular mechanism of *Flammulina velutipes* polysaccharides: a review. *Int. J. Biol. Macromol.* 167, 528–538. doi: 10.1016/j.ijbiomac.2020.11.208
- Wessels, S., Axelsson, L., Hansen, E. B., Vuyst, L. D., Laulund, S., Hteenm, L. L., et al. (2004). The lactic acid bacteria, the food chain, and their regulation. *Trends Food Sci. Technol.* 15, 498–505. doi: 10.1016/j.tifs.2004.03.003
- Whiting, R. C., and Buchanan, R. L. (1993). A classification of models for predictive microbiology. *Food Technol.* 19, 175–177.

- Zhao, R. Q., Hu, Q. H., Ma, G. X., Su, A. X., Xie, M. H., Li, X. F., et al. (2019). Effects of *Flammulina velutipes* polysaccharide on immune response and intestinal microbiota in mice. *J. Funct Foods* 56, 255–264.
- Zhao, Y., Li, P., Hu, H., Wang, Y., Sun, Y., and Huang, K. (2013). Postharvest decay of the cultivated mushroom *Pleurotus eryngii* caused by *Lactococcus lactis* subsp. *lactis*. *J. Plant Pathol.* 95, 247–253. doi: 10.1614/IPSM-D-12-00059.1
- Zhao, Y. C., Zhu, R. J., Wang, Y., Song, Z. W., Shan, C. J., Qiu, J. P., et al. (2018). Complete genome sequence of *Lactococcus lactis* subsp. *lactis* SLPE1-3, a novel lactic acid bacterium causing postharvest decay of the mushroom *Pleurotus eryngii*. *J. Plant Pathol.* 100, 467–476. doi: 10.1007/s42161-018-0101-3
- Zhou, K., Wei, J., Jiang, C. L., Han, X. F., and Liu, S. L. (2014). Growth dynamics of *Lactococcus lactis* SQ117 under different temperatures and pHs. *Food Sci.* 35, 192–195. doi: 10.7506/spkx1002-6630-2014-07038
- Zwietering, M. H., Jongenburger, I., Rombouts, F. M., and van't Riet, K. (1990). Modeling of the bacterial growth curve. *Appl. Environ. Microbiol.* 56, 1875–1881.
- Conflict of Interest:** XP was employed by company Fujian Anjoy Foods Co., Ltd.
- The remaining authors declare that the research was conducted in the absence of any commercial or financial relationships that could be construed as a potential conflict of interest.
- Copyright © 2021 Wei, Pan, Li, Jia, Fang and Jiang. This is an open-access article distributed under the terms of the Creative Commons Attribution License (CC BY). The use, distribution or reproduction in other forums is permitted, provided the original author(s) and the copyright owner(s) are credited and that the original publication in this journal is cited, in accordance with accepted academic practice. No use, distribution or reproduction is permitted which does not comply with these terms.



Physical and Structural Characterization of Underutilized Climate-Resilient Seed Grains: Millets, Sorghum, and Amaranth

Sarah Geisen^{1,2}, Kiruba Krishnaswamy^{2,3*} and Rob Myers⁴

¹ Department of Mechanical Engineering, University of Missouri, Columbia, MO, United States, ² Department of Biomedical, Biological and Chemical Engineering, University of Missouri, Columbia, MO, United States, ³ Division of Food Systems and Bioengineering (Food Science and Nutrition), University of Missouri, Columbia, MO, United States, ⁴ Division of Plant Sciences, University of Missouri, Columbia, MO, United States

OPEN ACCESS

Edited by:

José Antonio Teixeira,
University of Minho, Portugal

Reviewed by:

Vetriventhan Mani,
International Crops Research Institute
for the Semi-Arid Tropics
(ICRISAT), India

Sean Mayes,
University of Nottingham,
United Kingdom

*Correspondence:

Kiruba Krishnaswamy
krishnaswamyk@umsystem.edu

Specialty section:

This article was submitted to
Sustainable Food Processing,
a section of the journal
Frontiers in Sustainable Food Systems

Received: 27 August 2020

Accepted: 20 April 2021

Published: 10 June 2021

Citation:

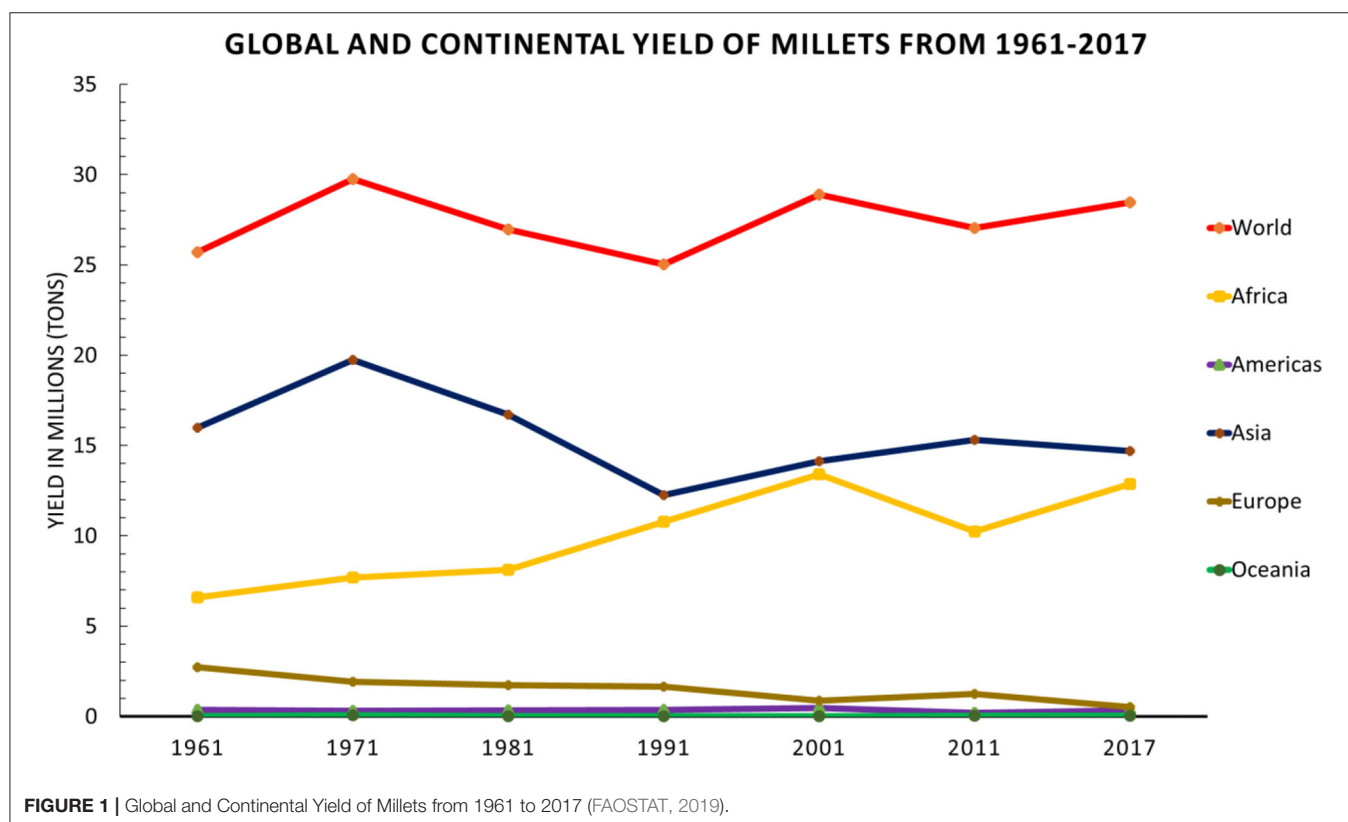
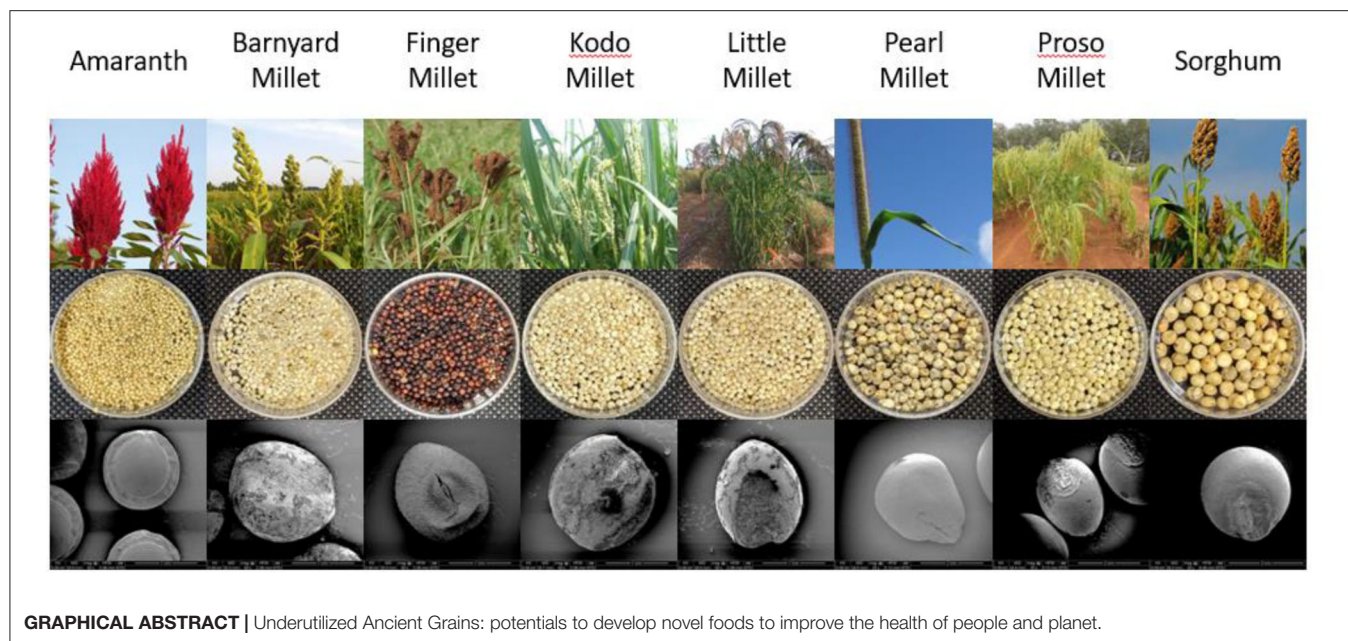
Geisen S, Krishnaswamy K and
Myers R (2021) Physical and
Structural Characterization of
Underutilized Climate-Resilient Seed
Grains: Millets, Sorghum, and
Amaranth.
Front. Sustain. Food Syst. 5:599656.
doi: 10.3389/fsufs.2021.599656

While the world is facing food and nutritional challenges leading to the multifaceted burden of malnutrition (underweight and overweight), there is a need to sustainably diversify and explore underutilized crops. Climate-resilient crops, which have the potential to withstand climate crises, have drought resistance, and provide healthy foods with essential vitamins and minerals. Ancient seed grains like amaranth, millets, and sorghum are highly nutritious seed grains that are underutilized, and there is a need for comprehensive research into their properties. This study will specifically investigate amaranth alongside barnyard, finger, kodo, little, pearl, proso millets, and sorghum. Physical and structural properties of the ancient seed grains can provide useful data for storage and food processing. The angle of repose, porosity, and water activity of the grains varied from 19.3° to 23.9°, 3.6 to 17.4%, and 0.533 to 0.660 at 25.5°C, respectively. Additionally, Scanning Electron Microscopy (SEM) was used to observe the surface characteristics and overall shape of each grain. SEM images of the millets shows the impact of dehulling on the surface morphology of the grains (little, barnyard, proso, and kodo millets). This calls for research and development of novel food processing technologies to minimize loss and damage during processing of climate-resilient crops.

Keywords: millet, scanning electron microscope, food and nutrition security, sustainable diets, SDG #2, ancient grains, UN sustainable development goal

INTRODUCTION

The bold and transformative 2030 Agenda for Sustainable Development was officially launched in September 2015 by 193 member states of the United Nations. The 2030 agenda calls on countries to begin efforts to achieve the 17 Sustainable Development Goals (SDGs) over the next 10 years (United Nations, 2020). SDG 2 focuses on Zero Hunger, to achieve food security, improved nutrition, and promote sustainable agriculture. Food and nutrition security are interconnected and in order to achieve them in the near future, there is a need to explore underutilized crops as food sources leading to diversification of healthy diets to feed 9 billion population in 2050. Millets are a group of small nutritious seed grains that are primarily grown in Africa and Asia. **Figure 1** shows production of millets by geographical region and year. The various millets



represent both cold and warm season crops that can be suited for dry and wet conditions, depending upon the species. Pearl millet, which originated in Africa, is suited for hot and dry climates with little rainfall but also tolerates hot and wet climates. By

contrast, proso millet is from a colder climate, originating from Central and Eastern Asia, so it performs better in cooler areas. Millets generally reach maturity faster than crops like maize or wheat. Foxtail and proso millet can mature in 60–90 days

while pearl and finger millet can mature in up to 100–110 days (Myers, 2018b). Millet uses vary from being processed into infant formula, fermented foods, flour, breads, beer, and snacks and can be prepared in a multitude of ways. Millets are a highly underutilized seed grain in the Western world, and in the US, they are often used as animal feed or cover crops to promote healthy soil (Myers, 2018b).

Amaranth is another ancient cereal grain that was first utilized by humans 6,000 years ago and was once an important crop to the Aztecs. Like millet, amaranth has drought resistance and includes many different varieties that are adaptable to a wide range of environments (Myers, 2018a). The leaves of the vegetable amaranth plant can be boiled and consumed like spinach, while the grain amaranth can be popped, ground into flour, or turned into many ready-to-eat products, such as millets (Robinson, 1986). In the US, amaranth has gained popularity in commercial products like sandwich bread, breakfast cereals, granola bars, and crackers (Myers, 2018a).

Millets and amaranth have the potential to help address climate change challenges (Saxena et al., 2018) and the need to find alternative crops to feed the growing population with nutritious food. To utilize and popularize these forgotten grains, novel value-added food product development, optimization, and research is required in this area. Ancient seed grains are gaining popularity among millennials and Gen Z for their low-calorie and low-fat contents. An ideal way to introduce consumers to an unfamiliar ingredient, like millet or amaranth, is to develop a familiar product with this new food ingredient. They also have potentials to be used in food fortification as natural alternatives due to rich micronutrient profile and create a new demand for millet and amaranth-based foods.

The health benefits of ancient seed grains are numerous, as there are several different varieties and each with its own strengths. All varieties of millets and amaranth are naturally free from gluten and have a lower caloric content than rice and wheat. Millets are also lower in carbohydrates than rice, which can help prevent the development of diabetes and obesity which has become a serious problem in our modern world. Pearl and proso millet are higher in protein than all other millets as well as rice. However, they both have a lower protein content than amaranth, (Valcárcel-Yamani and Caetano da Silva Lannes, 2012). Barnyard millet has a higher amount of fiber compared to rice, wheat, and other millets, which aids in digestion and nutrient retention. Finger millet contains a third of the daily recommended calcium intake, which is the most significant percentage of any essential mineral found in millets (Saleh et al., 2013). Other high percentages of essential minerals include iron in barnyard millet, zinc in foxtail and barnyard millets, niacin in proso millet, and riboflavin in barnyard millet.

Amaranth has a high protein content and contains almost twice as much protein as maize. Although the total protein content is not as high as a legume's, amaranth can be consumed as a source of "complete" protein because it has an ideal balance of the nine essential amino acids (Myers, 2018a). A more complete comparison between millets, amaranth, rice, and wheat can be seen in **Table 1**.

Hidden Hunger is a worldwide issue (deficiency due to vitamins and minerals): specifically, it is the double burden of malnutrition (stunting/underweight and obesity/overweight), which can affect any age, gender, or nationality. Children deficient in iron and zinc are shown to have stunted growth, impaired immune function, and irreversible neurological and psychomotor impairments (Mehta et al., 2017). Efforts to solve this crisis have recently included the biofortification of pearl millet in India, Govindaraj et al. (2019) have attempted to genetically improve cultivars of pearl millet to increase the densities of iron and zinc. There is a need to specifically design food processing equipment for ancient seed grains, develop new value-added food products, and expand the market needs for diversification of healthy diets.

The physical and structural properties of grains are critical and impact food processing parameters that are essential in the design of equipment for handling, harvesting, processing, and storing of grains (Baryeh, 2002). The shape of the grains is important in the design of sorting and sizing machines (Jain and Bal, 1997). Water activity, bulk density, true density, and porosity are important parameters to consider in the designing of storage structures for grains (Singh et al., 2010). The angle of repose is an important measure in the designing of storage, processing, and transporting structures (Bhadra et al., 2017). Scanning Electron Microscopy (SEM) is used to identify microstructural features of grains that would be otherwise hard to differentiate with human visual observations. The present study is investigating the physical and structural properties of barnyard millet, finger millet, kodo millet, little millet, pearl millet, proso millet, sorghum, and amaranth as an observational exercise to establish a physical characterization method. This information can help researchers and food industries explore the usage of the underutilized ancient seed grains in the development of new sustainable diets.

MATERIALS AND METHODS

Materials

Ancient Grains

The amaranth sample was provided by Dr. Rob Myers (Division of Plant Sciences, Columbia, MO), from his 2018 harvest of the Crimson Glow cultivar. The barnyard, little, kodo, and proso millets were obtained from Manna Foods (Southern Health Foods Pvt. Ltd, Chennai, India). The finger, pearl, and sorghum millets were supplied by Babco Foods International, LLC (Bridgewater, NJ 08807). All grain samples were stored at room temperature. The reasons for using commercial samples were based on the accessibility of raw materials and food availability to consumers/food start-up company interested to utilize ancient seed grains for new product development. Packaged food materials are subjected to food quality standards before entering commercial markets. Thus, for this study, we used commercially available ancient seed grains samples currently available for human consumption as an observational exercise to establish a physical characterization method. **Table 2** shows the whole grain image (photographic representation) used in this study along with information related to the geography of domestication, major producers of ancient seed grains.

TABLE 1 | Nutritional Comparison of Millets, Amaranth, Rice, and Wheat (per 100 g) (Valcárcel-Yamani and Caetano da Silva Lannes, 2012; Saleh et al., 2013; Kumar et al., 2018; Nithiyanantham et al., 2019).

Grain	Protein (g)	Carbohydrates (g)	Fat (g)	Calcium (mg)	Iron (mg)	Calorific value (kcal)
Amaranth	14.60	68.8–70.3	8.81	180.1–217.0	9.2–21.0	–
Barnyard Millet	6–13	55.0–56.88	3.53–3.9	18.33–22	15.47–19.7	300
Finger Millet	7.3–10	71.52–72.6	1.43–1.5	240–410	3.67–4.87	334–336
Kodo Millet	8.3–10	63.82–66.6	3.03–3.6	10–35	1.7–4.47	353
Little Millet	7.7–15	60.9	5.2	17.0–30	9.3	329
Pearl Millet	10.6–14	67.0–69.10	4.8	10–42	10.3–11.0	363
Proso Millet	10–13	67.09	3.09	14–23	1.0–3.4	352.5
Rice	3.61–6.8	75.33–90.39	0.87–2.7	0.05–10	0.47–2.03	341.2–396.8
Sorghum	10.4–10.82	70.7–72.97	3.1–3.23	25–35.23	4.01–6.57	329
Wheat	11.6–13.78	69.88–71.0	1.90–2.0	30–43.41	3.5–5.24	348–438

Methods

Angle of Repose

The angle of repose was calculated by filling a cylinder with grain that was then slowly lifted to create a conical mound (Akaaimo and Raji, 2006). The base diameter and the height of the cone were measured, and the following equation was used to calculate the angle of repose:

$$\phi = \tan^{-1} \frac{2H}{d}$$

where ϕ is the angle of repose, H is the height, and d is the diameter. The measurements were replicated ($n = 10$) times and the average value was reported. A plastic cylinder of 37 mm diameter was used. This value is an important property because it can impact the design of storage containers and processing equipment due to the differences in each grain.

Bulk Density

The bulk density of grains was measured using two methods: the water displacement method and mass/volume relationship. The variability between both methods was compared. The water displacement method was done by filling a 25 ml graduated cylinder with 15 ml of water, 4.5 grams of each grain was added, and the volume of water displaced was measured. For the mass/volume method bulk density was measured using the procedure described by Mariotti et al. (2006). Four gram of each grain was poured into a 25 ml graduated cylinder gently tapped 10 times and the volume was noted. The ratio of the mass of the sample of grain to its total volume was then calculated ($n = 5$). The results are expressed in Kg/m^3 .

True Density

The true density of the millets was measured using a Quantachrome Ultrapycnometer 1000 (Anton Paar, Graz, Austria). In total, 4.5 grams were weighed out and placed in the small cell for measurement. The equipment was operated using the multi-run setting with 5 runs and a standard deviation of 0.5%. The final three runs were averaged and reported by the equipment. This was repeated three times, each with a different sample of 4.5 grams to account for the variability in grain size and shape.

Color

The color of each millet sample was measured using a Konica Minolta Chroma Meter CR-400/410 (Konica Minolta, Chiyoda, Tokyo, Japan). The device utilizes an L^* , a^* , b^* color space system to quantify the color of an object. L^* represents lightness and darkness, a^* represents redness when positive and greenness when negative, and b^* represents yellowness when positive and blueness when negative. The device was calibrated using a white sample provided by the manufacturer. For each sample, a container was filled, and the meter was placed on the sample. Five measurements were taken ($n = 5$), with the average value reported.

Porosity

The porosity of the millet grains was calculated using the true density values determined by the pycnometer and the experimental bulk density with the following equation.

$$\% \text{ porosity} = 1 - \frac{\text{bulk density}}{\text{true density}}$$

Scanning Electron Microscopy

The internal and external structure of each millet type was determined using a Quanta 600F ESEM Scanning Electron Microscope located at the Electron Microscopy Core at the University of Missouri—Columbia. The grains were prepared by coating them with Platinum. Comparative analysis of multiple ancient seed grains at 5 KV power between 20 and 50X magnification.




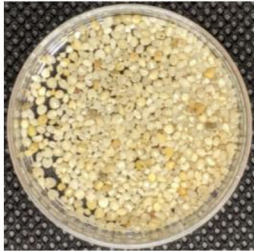

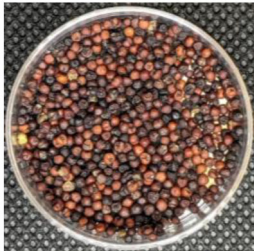




Shape

The shape of each grain was determined by evaluating the SEM images and using the data characterizations McDonough and Rooney (1989) determined to classify the different shapes of pearl millet they observed. These shape types include lanceolate, obovate, hexagonal, and globose.

Water Activity







The water activity was measured by the Aqua Lab Cx-2 Water Activity Meter (Decagon Devices, Inc., Pullman, Washington 99163). The equipment determines the water activity of a sample by measuring the relative humidity of the sample when the

TABLE 2 | Geography of domestication, major producers, and photographic representation of Ancient seed grains.

Grain	Scientific name	Geography of domestication	Year of domestication	Major producer(s)	Plant image	Whole grain image	Common name
Amaranth	<i>Amaranthus spp.</i>	Mexico & Central America (1)	8,000–7,000 BP (2, 3)	Latin America, USA, India, Africa, China, Eastern Europe, and Russia (1)			Spanish: Amaranto Hindi: Rajgira Kannada: Dhantina Soppu Tamil: Thandu Keerai Chinese: Hon-toi-moi Yoruba: Efo Tete Jamaican: Callaloo
Barnyard Millet	<i>Echinochloa esculenta</i>	Japan (4)	6,000 years ago (4, 5)	China, Korea, Japan, India (4)			Bengali: Shyama Hindi: Sanwa Kannada: Oodalulu Oriya: Khira Punjabi: Swank Tamil: Kuthiraivolly Telugu: Udalulu, Kodisama
Finger Millet	<i>Eleusine coracana</i>	East Africa (Ethiopia) (4)	5,000–4,000 years ago (4, 6)	Eastern and Southern Africa, India, Nepal, China (4)			Bengali: Marwa Gujarati: Nagli, Bavto Hindi: Ragi, Mandika Kannada: Ragi Oriya: Mandia Punjabi: Mandhuka, Mandhal Tamil: Keppai, Ragi Telugu: Ragi Chodi Hausa: Tamba Birom: Pwana Uganda: Bulo Swahili: Mandua Winbi
Kodo Millet	<i>Paspalum scrobiculatum</i>	India (4)	3,000 years ago (4, 7)	India (4)			Bengali: Kodo Gujarati: Kodra Hindi: Kodon Kannada: Harka Marathi: Kodra Oriya: Kodua Punjabi: Kodra Tamil: Varagu Telugu: Arikelu, Arika
Little Millet	<i>Panicum sumatrense</i>	India (4)	>6,400 BP (4, 8)	India, Nepal, Pakistan, Sri Lanka, Myanmar, Philippines (4)			Bengali: Sama Gujarati: Gajro, Kuri Hindi: Kutki, Shavan Kannada: Same, Save Marathi: Sava, Halvi, Vari Oriya: Suan Punjabi: Swank Tamil: Samai Telugu: Samalu

(Continued)

TABLE 2 | Continued

Grain	Scientific name	Geography of domestication	Year of domestication	Major producer(s)	Plant image	Whole grain image	Common name
Pearl Millet	<i>Pennisetum glaucum</i>	Northeast Mali (4)	4,500 BP (4, 9)	West and Central Africa, East and Southern Africa, India, Nigeria, USA (4)			Bengali: Bajra Gujarati: Bajri Hindi: Bajra Kannada: Sajje Marathi: Bajri Oriya: Bajra Punjabi: Bajra Tamil: Kambu Telugu: Sajja Marghi: Yadi Afrikaans: Bulrush Millet, Manna Sepedi: Leotsa Sesotho: Nyalothi isiNdebele: Inyouti Shangaan: Mhuga, Mhungu isiZulu: Unyaluthi, Unyawoti, Unyawothi
Proso Millet	<i>Panicum miliaceum</i>	Northern China (4)	10,300–8,700 BP (4, 10)	China, Kazakhstan, Afghanistan, India, Turkey, Romania, USA, Australia (4)			Bengali: Cheena Gujarati: Cheno Hindi: Chena; Barri Kannada: Baragu Marathi: Vari Oriya: China Bachari bagmu Punjabi: Cheena Tamil: Pani varagu Telugu: Variga
Sorghum	<i>Sorghum bicolor</i>	Northeast Africa (4, 11)	5,000 years ago (4, 12)	Nigeria, Burkina Faso, Niger, Mali, Sudan, Ethiopia, Cameroon, India, China, USA, South America, Australia (4)			Bengali: Jowar Gujarati: Jowari, Juar Hindi: Jowari, Juar Kannada: Jola Marathi: Jwari Oriya: Juara Punjabi: Jowar Tamil: Cholam Telugu: Jonna Yoruba: Okababa Hausa: Dawa, Jero Igbo: Soro South Africa: Mabele Thoro, Amazinba, Amabele East Africa: Mtama

BP-“Before Present” means before 1950—commonly used convention in radiocarbon dating.

Data Sources: FAO ICRISAT., 1996; ICAR- Indian Institute of Millets Research (IIMR), 2020; The United Sorghum Checkoff Program., 2020; (1) Arendt and Zannini, 2013; (2) Joshi et al., 2018; (3) Arreguez et al., 2013; (4) Taylor and Duodu, 2018; (5) Nasu and Momohara, 2016; (6) Hillu et al., 1979; (7) de Wet et al., 1983; (8) Fuller, 2011; (9) Manning et al., 2011; (10) Lu et al., 2009; (11) De Wet and Harlan, 1971; (12) Doggett, 1988; (13) Louw, 2020a; (14) Louw, 2020b. **Photo sources:** International Crops Research Institute for the Semi-Arid Tropics (ICRISAT), 2021, Indian Institute for Millet Research, Myers, 2018a, Amaranth: Pigweed Kin High in Protein., 2003, Food Engineering and Sustainable Technologies (FEAST Lab), University of Missouri.

sample water vapor pressure and air water vapor pressure reach equilibrium. The sample cups were filled less than half full and 5 measurements were made per sample. The average values were reported.

Statistical Analysis

A one-way ANOVA was conducted for all experiments. The number of replicates varies for different experiments with a minimum of ($n = 3$) for color, ($n = 10$) for the angle of repose, and ($n = 5$) for true density and water activity. All data

were analyzed using SASTM software, Version 9.4 of the System for Windows 10.

RESULTS AND DISCUSSION

Angle of Repose

While designing food processing equipment and storage systems, the angle of repose is an important physical parameter to be estimated for each grain. An ancient grain with a high angle of repose will pile higher and require more energy to transport than

a grain with a lower angle of repose. The angle of repose varied from 19.3° to 23.9° with kodo millet having the smallest angle and proso millet with the largest angle. The angle of repose values is shown in **Figure 2**. The base measurements for kodo, sorghum, little, finger, barnyard, and proso were not significantly different from each other. The height measurements for little, barnyard, and amaranth were not significantly different from each other, while proso, little, barnyard, amaranth, finger, sorghum, and kodo were not significantly different from each other. The values for base, height, and angle are presented in **Table 3**.

Previous studies on the angle of repose use two main methods: a cylindrical method that was employed in this study and a “box”

method. This method uses a plywood box with two plates, one fixed and the other unfixed. The box is filled with the samples and then either gradually inclined until a slope is formed or the front panel is quickly removed to allow a slope to form. Rough rice (Varnamkhasti et al., 2008), popcorn kernels (Karababa, 2006), and pearl millet (Baryeh, 2002) used this “box” method. These values are reported to vary from 37° to 38°, 25.3° to 30.8°, and 34.4° to 49°, respectively.

Soybean (Davies and El-Okene, 2009) has been found using the same method this study uses, along with *Prosopis africana* seeds (Akaaimo and Raji, 2006). The reported values vary with respect to moisture content from 30° to 51° and 21.57° to 22.71°,

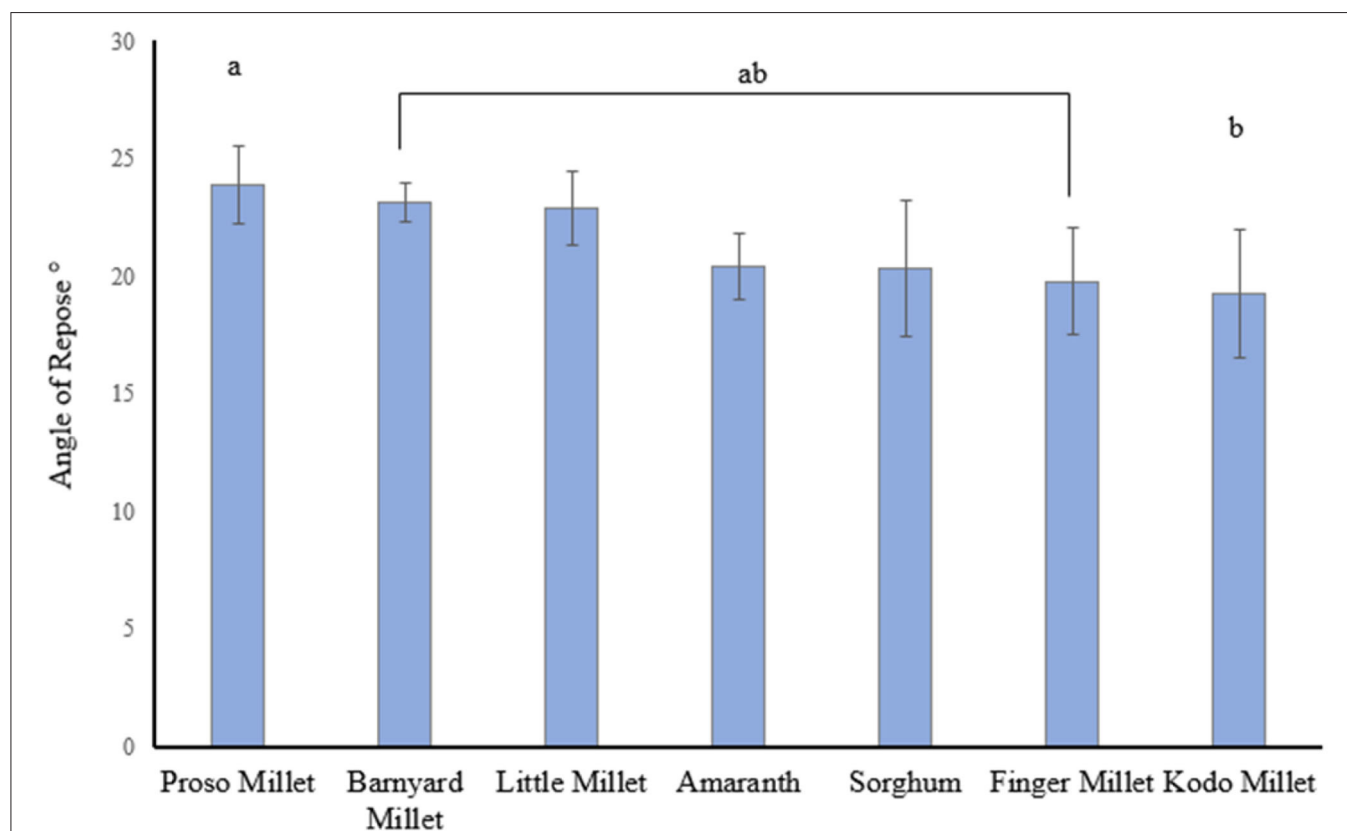


FIGURE 2 | Angle of Repose for Ancient Grains. Mean values not connected by the same letters are significantly different (Tukey's HSD, $P < 0.05$).

TABLE 3 | Color, shape, and water activity of ancient grains.

Ancient Grain	Color			Shape	Water activity		Angle of repose		
	L*	a*	b*		Temp (°C)		Diameter (cm)	Height (cm)	Angle (°)
Amaranth	58.08 ^d ± 0.91	5.86 ^b ± 0.18	24.71 ^a ± 0.82	Globose	0.583 ^b ± 0.003	25.2	10.44 ^a ± 0.32	1.94 ^{ab} ± 0.11	20.4 ^{ab} ± 1.55
Barnyard Millet	63.83 ^b ± 0.20	3.35 ^f ± 0.03	19.38 ^b ± 0.08	Globose	0.561 ^d ± 0.001	25.1	9.73 ^a ± 0.21	2.08 ^a ± 0.08	23.1 ^{ab} ± 0.97
Finger Millet	23.67 ^g ± 0.42	9.00 ^a ± 0.29	4.46 ^c ± 0.26	Obovate	0.533 ^f ± 0.003	25.5	10.26 ^a ± 0.4	1.84 ^{ab} ± 0.19	19.8 ^{ab} ± 2.56
Kodo Millet	59.12 ^d ± 0.52	4.68 ^d ± 0.05	18.79 ^d ± 0.17	Globose	0.563 ^d ± 0.002	25.3	10.12 ^a ± 0.67	1.76 ^b ± 0.18	19.3 ^b ± 3.04
Little Millet	57.69 ^c ± 0.45	3.24 ^e ± 0.03	19.57 ^e ± 0.16	Obovate	0.581 ^b ± 0.002	26.1	10.04 ^a ± 0.29	2.12 ^a ± 0.13	22.9 ^{ab} ± 1.76
Pearl Millet	52.86 ^e ± 0.08	2.48 ^g ± 0.02	16.40 ^f ± 0.03	Hexagonal	0.578 ^c ± 0.004	25.0	–	–	–
Proso Millet	72.64 ^a ± 0.19	2.22 ^e ± 0.04	30.93 ^g ± 0.09	Obovate	0.555 ^e ± 0.001	26.1	9.68 ^a ± 0.3	2.14 ^a ± 0.13	23.9 ^a ± 1.86
Sorghum	56.10 ^f ± 0.34	4.69 ^h ± 0.02	23.16 ^h ± 0.12	Globose	0.660 ^a ± 0.004	25.3	10.11 ^a ± 0.79	1.86 ^{ab} ± 0.21	20.3 ^{ab} ± 3.26

Mean values not followed by the same letter in the same column are significantly different (Tukey's HSD, $P < 0.05$).

L* = darkness to lightness, + = lighter, – = darker; a* = greenness to redness + = redder, – = greener; b* = blueness to yellowness + = yellower, – = bluer.

respectively. This study uses the cylindrical method as opposed to the box method because large amounts of grains are typically stored in cylindrical silos, so the values obtained would be the most applicable.

Bulk Density

Bulk density's values of the grains ranged from 1,153 to 1,408 kg/m^3 when using the water displacement method and 728.16–828.72 Kg/m^3 with the mass/volume method. The values of bulk density for both methods followed the same trend for the grains with sorghum showing the least bulk density at 1,153 Kg/m^3 for the water displacement method and 728.16 Kg/m^3 for mass/volume method and kodo millet showing the highest bulk density at 1,408 Kg/m^3 for water displacement method and 828.72 Kg/m^3 for mass/volume method.

Sorghum, while the largest in appearance, had the lowest bulk density, and kodo millet had the highest bulk density. Previous studies done on the bulk density of minor millets include a study by Subramanian and Viswanathan (2003), which employed a mass/volume method. A container of known volume was filled to the top with grain which was weighed. The bulk density was calculated as a ratio of the mass of grains to the volume of the container. In the study by Subramanian and Viswanathan (2003), the millet with the greatest bulk density was barnyard millet, at 888.7 kg m^{-3} and little millet had the lowest bulk density, at 748.1 kg m^{-3} . Similarly, the bulk density of soybeans (Kibar and Öztürk, 2008) and popcorn kernels (Karababa, 2006) have been previously found with similar values. Both use a similar method of filling a 1,000 mL container full of the respective samples which were then weighed. A ratio of sample mass to container volume was calculated. The bulk density of soybeans varied from 719 and 766 $\text{kg} \cdot \text{m}^{-3}$, while the popcorn kernels varied from 703 to 771 $\text{kg} \cdot \text{m}^{-3}$. The distributions of bulk density are shown in Figure 3.

The observed difference in the values expressed in the water displacement method and the mass/volume method may be due to the presence of air spaces between and/or within the grains (Manger, 1966). Bulk density calculation using the mass/volume method includes the volume of the grains, open and closed pores, and the interparticle voids (Lorraine and Flint, 2002) resulting in a higher volume and lower density. In the water

displacement method, water is absorbed by the grains and it adheres to the pores of the grains and between the grains resulting in a lower volume of water displaced and a larger bulk density value.

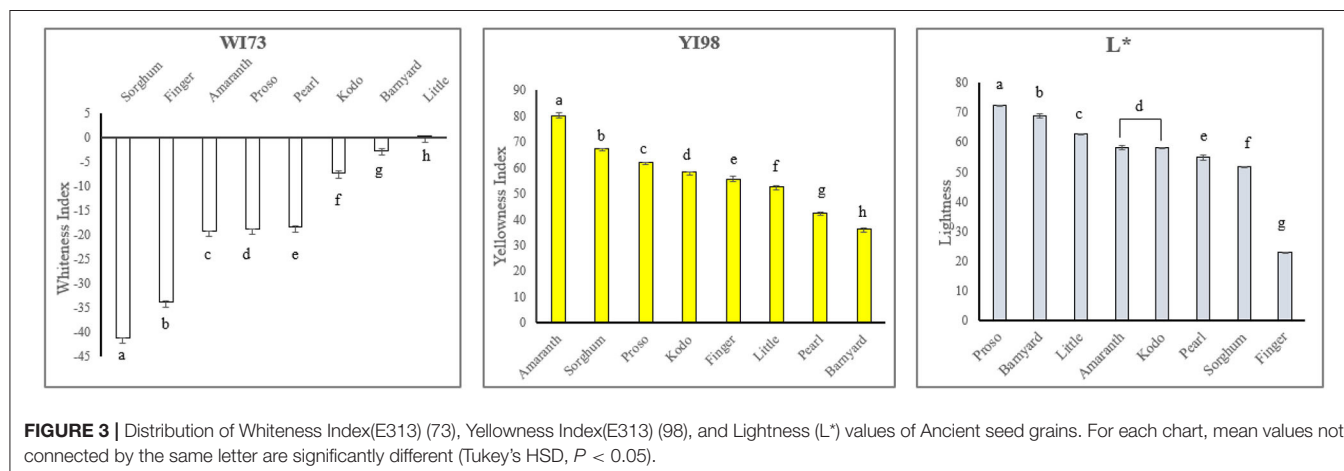
Two methods for bulk density measurements were analyzed in this study to observe which one would be more suitable for the ancient grains of smaller size profiles. The comparison results are presented in Table 4. In this study, we establish the water displacement method was not ideal for bulk density measurement of ancient grains of smaller size profile. The presence of pore spaces in the grains leads to the loading of gains on the water surface. As a result, the mass/volume method was determined to be more suitable for the bulk density measurement of ancient grains.

True Density

The true density of the grains, as shown in Table 4, varied from 1390.17 to 1459.4 $\text{kg} \cdot \text{m}^{-3}$ with amaranth having the lowest true density and kodo have the largest. The masses of proso, barnyard, little, kodo, and amaranth could be grouped and were not significantly different from each other, while amaranth, little, kodo, and sorghum can be grouped and were also not significantly different from each other. The volume of each grain was significantly different from each other, except for sorghum and proso. The density of each grain was significantly different from each other.

Previous work finding the true density of soybean and rough rice has been done using the toluene displacement method. Kibar and Öztürk (2008) used the liquid displacement method outlined by Baryeh (2001) and Abalone et al. (2004), with toluene instead of water because the soybeans would absorb that substance less than it would water. Varnamkhasti et al. (2008) also found the true density of rough rice by using the toluene displacement method outlined by Mohsenin (1986).

The true density of soybeans varied from 905 to 983 $\text{kg} \cdot \text{m}^{-3}$. The true density of rough rice of two different cultivars were 1269.1 and 1193.43 $\text{kg} \cdot \text{m}^{-3}$. While the method of this study differed from these two studies, the results are comparable. The true density of amaranth is most similar to the true density of



the densest rough rice cultivar determined by Varnamkhasti et al. (2008).

Color

Significant results of the color analysis show that the finger millet was the darkest, having the most redness and blueness of all of the grains. Oppositely, proso millet was the lightest, having the most yellowness and greenness of all of the grains. These values are shown in **Table 3**. The whiteness and yellowness indices were measured, WI(E313-73) and YI(E313-98), respectively. Deviation from whiteness can be perceived as yellowness, which is not always desirable in food. It is important to establish a base value for each grain in order to identify when one has spoiled, or in a comparison of grains like millets which can be very similar to the eye, it can be a way to differentiate between types. Barnyard millet had the greatest whiteness value, and proso millet had the highest yellowness value. The whiteness and yellowness of each grain were significantly different from each other, respectively. The L^* value of each grain was significantly different from each other except for amaranth and kodo. The a^* values for ancient grains were significantly different from each other except for proso and little. The b^* values for each grain were all significantly different from each other. The distributions of whiteness and yellowness indices Whiteness Index(E313-73) and Yellowness Index(E313-98) and L^* values are presented in **Figure 3**.

Porosity

The porosity, as shown in **Table 4**, varied from 3.6 to 17.4%, for water displacement method, and 44.5–48.1% with mass/volume method. Kodo millet and sorghum having the least and most porosity, respectively from both methods. The porosities of two rough rice cultivars were found to be 56.98 and 60.4% (Varnamkhasti et al., 2008). The porosity of popcorn kernels decreased from 42.56 to 40.87% when the moisture content of the kernels increased from 8.85 to 17.12% (Karababa, 2006). The porosity of *Prosopis africana* seed varied from 21.57 to 22.71% at 11% mc (Akaaimo and Raji, 2006).

Scanning Electron Microscopy

The scanning electron microscopy images shown in **Table 5** reveal the unique surface characteristics of each grain. Finger millet has a highly textured surface with numerous round protrusions over its entire surface compared to the rest of the grains. Sorghum and pearl millet appear to be relatively smooth. Barnyard millet, kodo millet, little millet, and proso millet all appear to have a rough surface. Amaranth is the only grain that has a distinct separation in its surface, with an outer ring around the grain itself. This is a unique structural feature present in amaranth grains. Wild-type rice is shown to have wax crystals on the outer surface, which gives it a similar appearance to finger millet (Bai et al., 2015). This is the first study to consolidate and report the structural morphology of the ancient grains: amaranth, millets, and sorghum using SEM micrographs.

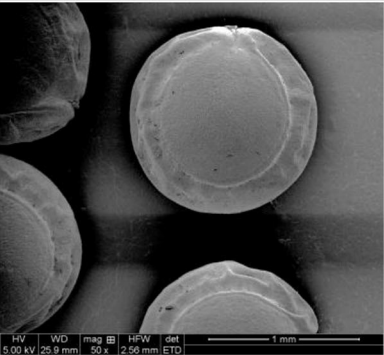
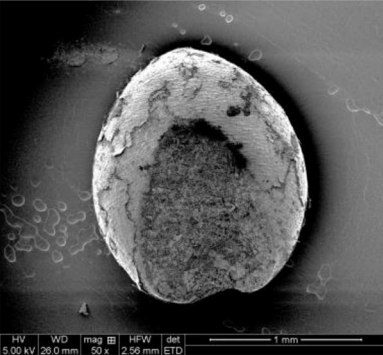
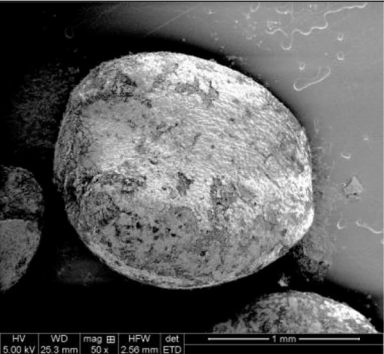
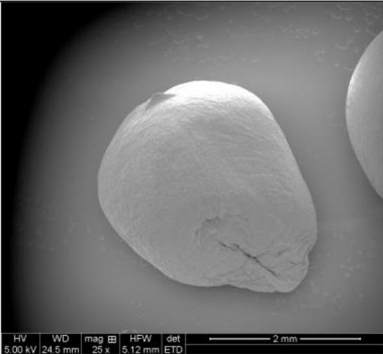
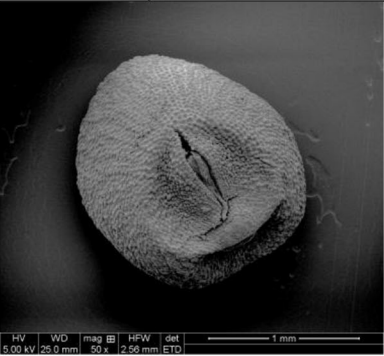

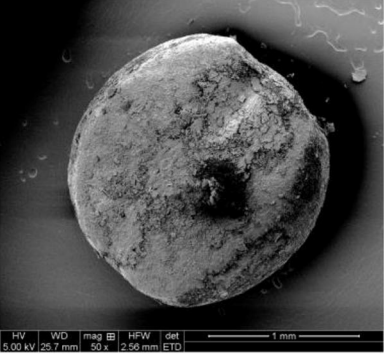

The surface features shown by the SEM photos can be explained due to the mechanical dehulling processes that the grains must undergo to be used as edible food and for further food processing. Little, barnyard, proso, and kodo millets must

TABLE 4 | True density, bulk density, porosity, and angle of repose of ancient grains.

Grain	Water displacement method				Porosity		Mass/Volume method			
	Mass (g)	True density Volume (cm ³)	Density ($\frac{kg}{m^3}$)	Mass (g)	Bulk density Displacement (mL)	Density ($\frac{kg}{m^3}$)	Mass (g)	Volume (cm ³)	Bulk Density ($\frac{kg}{m^3}$)	True Density ($\frac{kg}{m^3}$)
Amaranth	4.502 ± 0.003	3.239 ^a ± 0.003	1390.17 ^f ± 0.001	4.504	3.4	1,325	4.006 ± 0.002	5.117 ± 0.090	783.10 ^b ± 13.571	1415.57 ^{de} ± 8.987
Barnyard Millet	4.503 ± 0.001	3.112 ^e ± 0.003	1447.17 ^b ± 0.001	4.507	3.4	1,326	4.000 ± 0.000	5.017 ± 0.037	797.39 ^b ± 5.846	1462.85 ^b ± 3.744
Finger Millet	4.507 ± 0.002	3.188 ^c ± 0.009	1413.75 ^d ± 0.004	4.501	3.4	1,324	4.000 ± 0.000	5.083 ± 0.069	787.03 ^b ± 10.610	1428.75 ^{cd} ± 3.483
Kodo Millet	4.502 ± 0.001	3.085 ^f ± 0.001	1459.40 ^a ± 0.001	4.504	3.2	1,408	4.000 ± 0.003	4.833 ± 0.075	828.72 ^a ± 12.030	1492.13 ^a ± 5.079
Little Millet	4.502 ± 0.001	3.138 ^d ± 0.003	1434.60 ^c ± 0.002	4.502	3.4	1,324	4.000 ± 0.000	5.033 ± 0.047	794.77 ^b ± 7.395	1451.62 ^{bc} ± 10.519
Proso Millet	4.503 ± 0.003	3.214 ^b ± 0.002	1400.87 ^e ± 0.000	4.508	3.4	1,326	4.005 ± 0.002	5.133 ± 0.094	780.49 ^b ± 14.390	1432.90 ^{cd} ± 7.951
Sorghum	4.499 ± 0.003	3.222 ^b ± 0.007	1396.47 ^e ± 0.002	4.498	3.9	1,153	4.000 ± 0.000	5.500 ± 0.191	728.16 ^c ± 25.400	1403.30 ^e ± 25.285

Mean values not followed by the same letter in the same column are significantly different (Tukey's HSD, $P < 0.05$).

TABLE 5 | Scanning Electron Microscopic (SEM) images of ancient grains: Amaranth, Millets, and Sorghum.

 <p>HV WD mag B HFW det 5.00 kV 25.9 mm 50 x 2.56 mm ETO</p> <p>1 mm</p> <p><i>Amaranth</i></p>	 <p>HV WD mag B HFW det 5.00 kV 26.0 mm 50 x 2.56 mm ETO</p> <p>1 mm</p> <p><i>Little Millet</i></p>
 <p>HV WD mag B HFW det 5.00 kV 25.3 mm 50 x 2.56 mm ETO</p> <p>1 mm</p> <p><i>Barnyard Millet</i></p>	 <p>HV WD mag B HFW det 5.00 kV 24.5 mm 25 x 5.12 mm ETO</p> <p>2 mm</p> <p><i>Pearl Millet</i></p>
 <p>HV WD mag B HFW det 5.00 kV 25.0 mm 50 x 2.56 mm ETO</p> <p>1 mm</p> <p><i>Finger Millet</i></p>	 <p>HV WD mag B HFW det 5.00 kV 24.4 mm 25 x 5.12 mm ETO</p> <p>2 mm</p> <p><i>Proso Millet</i></p>
 <p>HV WD mag B HFW det 5.00 kV 25.7 mm 50 x 2.56 mm ETO</p> <p>1 mm</p> <p><i>Kodo Millet</i></p>	 <p>HV WD mag B HFW det 5.00 kV 29.3 mm 25 x 6.40 mm ETO</p> <p>3 mm</p> <p><i>Sorghum</i></p>

be dehulled before consuming. While dehulling, the grains experience shearing forces which cause the rough, irregular surfaces. The scanning electron microscopic images of the millets (**Table 5**) shows the impact of dehulling on the surface morphology of the grains. This is an important observation, as surface morphology affects various physical characterization, including the angle of repose, coefficient of friction, and porosity. This is the first report that provides a microscopic comparison of the surface morphology of ancient seed grains, which would be helpful to advance research related to millets.

Shape and Size

The ancient grains in this study were categorized in three out of the four shape types determined by McDonough and Rooney (1989). Amaranth, barnyard millet, kodo millet, and sorghum were globose in appearance, while finger millet, little millet, and proso millet were obovate. Pearl millet was the only grain with a hexagonal shape.

In increasing order, the size of the grains starts at the smallest with amaranth, followed by finger millet, little millet, barnyard millet, kodo millet, proso millet, pearl millet, and sorghum being the largest.

Baryeh (2002) observed lower bulk density with larger grains. Also showed that millet grains with a lower moisture content had a higher bulk density. Similar to Baryeh (2002), we also found that sorghum, having the larger grain size had lower bulk density using the water displacement method ($1,153 \frac{\text{kg}}{\text{m}^3}$) compared to ancient seed grains with smaller size like amaranth, finger millet, little millet, and barnyard millet ($1,324\text{--}1,326 \frac{\text{kg}}{\text{m}^3}$). While comparing the porosity data for sorghum (17.4%) and with other ancient seed grains (amaranth, finger, little, barnyard, kodo, and proso millets) the porosity range was between 3.6 and 8.5%. Similar trends were found for bulk density and porosity using mass/volume method. This could be explained by the fact that smaller grains could fill larger volumes by compactly packing themselves, filling interparticle voids, and minimizing porosity.

Water Activity (a_w)

Water activity is an important food safety parameter. Water activity value ranges from 1.0 (pure water) to 0.0 (complete dry conditions). The water activity value provides an indicator of microorganisms that can grow by utilizing the water in the food samples (ancient seed grains). Higher the water activity, bacteria, yeast, and mold can grow resulting in food spoilage during storage. Food products with a water activity below 0.60 have extended shelf-life during storage.

Water activity varied from 0.533 at a temperature of 25.5°C to 0.660 at a temperature of 25.3°C, with finger millet having the lowest water activity and sorghum having the greatest. The remaining values are shown in **Table 3**. This study did not study the effect of water activity based on different moisture content. The water activity was measured for all samples upon opening the sealed packaging from the suppliers. Amaranth, barnyard, and pearl can be grouped and were not significantly different from each other in terms of water activity. Likewise, kodo, sorghum, amaranth, and barnyard can be grouped. The water activity of

amaranth and little, little and pearl, and kodo and barnyard were not significantly different from each other.

CONCLUSIONS

The results of this study show that while the millets appear very similar to the human eye, they all vary with respect to the physical and structural properties. The potential for ancient seed grains to be grown in North America is far greater than what is currently being realized. They are commonly assumed to be useful only in developing countries, but field trials in Missouri and other locations show amaranth and millets to have good adaptation in temperate areas of North America (Myers, 2018b). Further research and breeding could help improve their potential even further, including improved yield and nutritional factors. Parts of the Midwestern and Great Plains areas of the U.S. are particularly viable areas to produce amaranth and other ancient seed grains. This, combined with the minimal water required to grow ancient seed grains like millet and amaranth compared to corn and wheat, could contribute to the growing effort to reduce freshwater consumption during climate crisis.

From the physical and structural characterization study, sorghum had a larger appearance, size, and the lowest bulk density, while kodo millet had the highest bulk density. Kodo millet had less porosity, while sorghum had high porosity from both density measurement methods. This is the first report that provides microstructural comparison clearly showing the impact of mechanical dehulling on the surface morphology of the ancient seed grains, which is invisible to human visual observation. Little, barnyard, proso, and kodo millets must be dehulled to make the seeds edible for human consumption. This study reports important microstructural observations that could directly impact physical characterization, including the angle of repose, coefficient of friction, porosity, and development of food processing equipment.

Color analysis shows that the finger millet was the darkest, having the most redness, and blueness of all the ancient seed grains. Barnyard millet had the greatest whiteness value (L), and proso millet had the highest yellowness value. The whiteness and yellowness of each ancient seed grain were significantly different from each other. This is an important food processing parameter to consider while developing new food products, ingredients from millets and would be of interest to food industries and plant-based food start-up companies.

This observational study establishes the methodology for physical characterizations of ancient grains. Further investigation on specific genetic traits, the effect of moisture content on the physio-chemical properties for different ancient seed grains is recommended. Since each ancient seed grain exhibits different physical and structural properties, further research, including chemical, functional properties, and nutrigenomics of the ancient seed grains for defined genetic lines, into environmental growth conditions is recommended to develop new products with enhanced health benefits. New value-added functional/nutraceutical food products can be formulated using single seed grains or the combination of amaranth as well as

barnyard, finger, kodo, little, pearl, proso millets, and sorghum to balance macro/micronutrient profiles.

To develop sustainable food processing technologies to utilize climate-resilient crops and improve agri-business, economic activity, and support for farming communities, a partnership between different stakeholders in food systems is critical. We conclude that ancient climate-resilient seed grains like millets, sorghum, and amaranth can lead to diversification of sustainable diets and have a positive impact to improve the health of people and the planet.

DATA AVAILABILITY STATEMENT

The original contributions presented in the study are included in the article/Supplementary Material, further inquiries can be directed to the corresponding author/s.

AUTHOR CONTRIBUTIONS

SG contributed to the formal analysis, investigation, visualization, and writing (original draft, reviewing, and editing). RM was responsible for the resources and

the writing (review and editing). KK carried out the conceptualization, resource management, methodology, visualization, writing (review and editing), supervision, funding acquisition, and project administration. All authors contributed to the article and approved the submitted version.

FUNDING

This work was supported by USDA Hatch Funds (MO-HAFE0003) Food Engineering and Sustainable Technologies (FEAST), University of Missouri.

ACKNOWLEDGMENTS

We would like to thank the University of Missouri Electron Microscopy Core for being inclusive and providing training to Undergraduate Students to use the Scanning Electron Microscope for analysis of ancient seed grains. We would like to thank Ms. Mercy Oghenerukewe Nani for the analysis and identifying local names for millets from the African continent context.

REFERENCES

- International Crops Research Institute for the Semi-Arid Tropics (ICRISAT) (2021). Retrieved from: <http://exploreit.icrisat.org/profile/Small%20millets/187> (accessed May 19, 2021).
- Abalone, R., Cassinera, A., Gaston, A., and Lara, M. A. (2004). Some physical properties of amaranth seeds. *Biosyst. Eng.* 89, 109–117. doi: 10.1016/j.biosystemseng.2004.06.012
- Akaaimo, D. I., and Raji, A. O. (2006). Some physical and engineering properties of *prosopis africana* seed. *Biosyst. Eng.* 95, 197–205. doi: 10.1016/j.biosystemseng.2006.06.005
- Amaranth: Pigweed Kin High in Protein. (2003). Retrieved from: <https://www.auri.org/2003/07/amaranth/> (accessed October 2, 2019).
- Arendt, E. K., and Zannini, E. (2013). *Cereal Grains for the Food and Beverage Industries*. Cambridge: Elsevier.
- Arreguez, G. A., Martínez, J. G., and Ponessa, G. (2013). *Amaranthus hybridus* L. ssp. *hybridus* in an archaeological site from the initial mid-Holocene in the Southern Argentinian Puna. *Quatern. Int.* 307, 81–85. doi: 10.1016/j.quaint.2013.02.035
- Bai, J., Zhu, X., Wang, Q., Zhang, J., Chen, H., Dong G., et al. (2015). Rice *TUTOU1* encodes a suppressor of cAMP receptor-like protein that is important for actin organization and panicle development. *Plant Physiol.* 169, 1179–1191. doi: 10.1104/pp.15.00229
- Baryeh, E. A. (2001). Physical properties of bambara groundnuts. *J. Food Eng.* 47, 321–326. doi: 10.1016/S0260-8774(00)00136-9
- Baryeh, E. A. (2002). Physical properties of millet. *J. Food Eng.* 51, 39–46. doi: 10.1016/S0260-8774(01)00035-8
- Bhadra, R., Casada, M. E., Thompson, S. A., Boac, J. M., Maghirang, R. G., Montross, M. D., et al. (2017). Field-observed angles of repose for stored grain in the United States. *Appl. Eng. Agric.* 33, 131–137. doi: 10.13031/aea.11894
- Davies, R. M., and El-Okene, A. M. (2009). Moisture-dependent physical properties of soybeans. *Int. Agrophys.* 23, 299–230.
- de Wet, J. M., Brink, D. E., Rao, K. P., and Mengesha, M. H. (1983). Diversity in kodo millet, *Paspalum scrobiculatum*. *Econ. Bot.* 37, 159–163.
- De Wet, J. M. J., and Harlan, J. R. (1971). The origin and domestication of Sorghum bicolor. *Econ. Bot.* 25, 128–135.
- Doggett, H. (1988). *Sorghum*. Harlow: Longman Scientific and Technical.
- FAO and ICRISAT. (1996). *The World Sorghum and Millet Economies: Facts, Trends and Outlook*. Retrieved from: <http://www.fao.org/3/W1808E/w1808e0c.htm> (accessed October 2, 2019).
- FAOSTAT. (2019). *Crops*. Retrieved from: <http://www.fao.org/faostat/en/#data/QC> (accessed October 2, 2019).
- Fuller, D. Q. (2011). Finding plant domestication in the Indian subcontinent. *Curr. Anthropol.* 52, S347–S362. doi: 10.1086/658900
- Govindaraj, M., Rai, K. N., Kanatti, A., Rao, A. S., and Shivade, H. (2019). Nutritional security in drylands: fast-track intra-population genetic improvement for grain iron and zinc densities in pearl millet. *Front. Nutr.* 6:74. doi: 10.3389/fnut.2019.00074
- Hilu, K. W., De Wet, J. M. J., and Harlan, J. R. (1979). Archaeobotanical studies of Eleusine coracana ssp. coracana (finger millet). *Am. J. Bot.* 66, 330–333.
- ICAR- Indian Institute of Millets Research (IIMR) (2020). Retrieved from: <https://millets.res.in/> (accessed May 19, 2021).
- Jain, R. K., and Bal, S. (1997). Properties of pearl millet. *J. Agric. Eng. Res.* 66, 85–91.
- Joshi, D. C., Sood, S., Hosahatti, R., Kant, L., Pattanayak, A., Kumar, A., et al. (2018). From zero to hero: the past, present and future of grain amaranth breeding. *Theor. Appl. Genet.* 131, 1807–1823. doi: 10.1007/s00122-018-3138-y
- Karababa, E. (2006). Physical properties of popcorn kernels. *J. Food Eng.* 72, 100–107. doi: 10.1016/j.jfoodeng.2004.11.028
- Kibar, H., and Öztürk, T. (2008). Physical and mechanical properties of soybean. *Int. Agrophys.* 22, 239–244.
- Kumar, A., Tomer, V., Kaur, A., Kumar, V., and Gupta, K. (2018). Millets: a solution to agrarian and nutritional challenges. *Agric. Food Sec.* 7, 1–15. doi: 10.1186/s40066-018-0183-3
- Lorraine, F., and Flint, A. (2002). Porosity. *Methods Soil Anal.* 4, 241–254. doi: 10.2136/sssabookser5.4.c11
- Louw, M. (2020a). *Sorghum in South Africa South African Indigenous Grains*. Available online at: <https://southafrica.co.za/sorghum-in-south-africa.html> (accessed September 25, 2020).
- Louw, M. (2020b). *What is Pearl Millet? South African Indigenous Grains*. Available online at: <https://southafrica.co.za/what-is-pearl-millet.html> (accessed September 25, 2020).
- Lu, H., Zhang, J., Liu, K. B., Wu, N., Li, Y., Zhou, K., et al. (2009). Earliest domestication of common millet (*Panicum miliaceum*) in East Asia extended to 10,000 years ago. *Proc. Natl. Acad. Sci. U.S.A.* 106, 7367–7372. doi: 10.1073/pnas.0900158106

- Manger (1966). Method-dependent values of bulk, grain, and pore volume as related to observed porosity. *Geological Survey Bulletin*. doi: 10.3133/b1203D
- Manning, K., Pelling, R., Higham, T., Schwenniger, J. L., and Fuller, D. Q. (2011). 4500-Year old domesticated pearl millet (*Pennisetum glaucum*) from the Tilemsi Valley, Mali: new insights into an alternative cereal domestication pathway. *J. Archaeol. Sci.* 38, 312–322. doi: 10.1016/j.jas.2010.09.007
- Mariotti, M., Alamprese, C., Pagani, M. A., and Lucisano, M. (2006). Effect of puffing on ultrastructure and physical characteristics of cereal grains and flours. *J. Cereal Sci.* 43, 47–56. doi: 10.1016/j.jcs.2005.06.007
- McDonough, C. M., and Rooney, L. W. (1989). Structural characteristics of *Pennisetum Americanum* (pearl millet) using scanning electron and fluorescence microscopy. *Food Struct.* 8, 137–149.
- Mehta, S., Finkelstein, J. L., Venkatramanan, S., Huey, S. L., Udipi, S. A., Ghugre, P., et al. (2017). Effect of iron and zinc-biofortified pearl millet consumption on growth and immune competence in children aged 12–18 months in India: study protocol for a randomized controlled trial. *BMJ Open* 7:e017631. doi: 10.1136/bmjopen-2017-017631
- Mohsenin, N. N. (1986). *Physical Properties of Plant and Animal Materials*, 2nd Edn. New York, NY: Gordon and Breach Science Publishers.
- Myers, R. (2018a). *Amaranth: An Ancient 3 Grain and Exceptionally Nutritious Food*. Columbia, MO: Harvest Road Publishing.
- Myers, R. (2018b). *Growing Millets for Grain, Forage or Cover Crop Use*. University of Missouri Extension Bulletin G4164. Retrieved from: <https://extension.missouri.edu/publications/g4164> (accessed May 19, 2021).
- Nasu, H., and Momohara, A. (2016). The beginnings of rice and millet agriculture in prehistoric Japan. *Quatern. Int.* 397, 504–512. doi: 10.1016/j.quaint.2015.06.043
- Nithiyanantham, S., Kalaiselvi, P., Mahomoodally, M. F., Zengin, G., Abirami, A., and Srinivasan, G. (2019). Nutritional and functional roles of millets-A review. *J. Food Biochem.* 43:e12859. doi: 10.1111/jfbc.12859
- Robinson, R. G. (1986). *Amaranth, Quinoa, Ragi, Tef, and Niger: Tiny Seeds of Ancient History and Modern Interest*. University of Minnesota Station Bulletin 571 AD-SB-2949. Retrieved from: <https://hdl.handle.net/11299/139533> (accessed May 19, 2021).
- Saleh, A. S. M., Zhang, Q., Chen, J., and Shen, Q. (2013). Millet grains: nutritional quality, processing, and potential health benefits. *Compreh. Rev. Food Sci. Food Saf.* 12, 281–295. doi: 10.1111/1541-4337.12012
- Saxena, R., Vanga, S. K., Wang, A., Orsat, A., and Raghavan, V. (2018). Millets for food security in the context of climate change: A review. *Sustainability* 10:2228. doi: 10.3390/su10072228
- Singh, K. P., Mishra, H. N., and Saha, S. (2010). Moisture-dependent properties of barnyard millet grain and kernel. *J. Food Eng.* 96, 598–606. doi: 10.1016/j.jfoodeng.2009.09.007
- Subramanian, S., and Viswanathan, R. (2003). Thermal properties of minor millet grains and flours. *Biosyst. Eng.* 84, 289–296. doi: 10.1016/S1537-5110(02)00222-2
- Taylor, J., and Duodu, K. G. (eds.). (2018). *Sorghum and Millets: Chemistry, Technology, and Nutritional Attributes*. Cambridge, MA: Elsevier.
- The United Sorghum Checkoff Program. (2020). *All About Sorghum*. Retrieved from: <https://www.sorghumcheckoff.com/all-about-sorghum> (accessed October 2, 2019).
- United Nations (2020). *The Sustainable Development Agenda*. Available online at: <https://www.un.org/sustainabledevelopment/development-agenda/> (accessed May 19, 2021).
- Valcárcel-Yamani, B., and Caetano da Silva Lannes, S. (2012). Applications of Quinoa (*Chenopodium Quinoa* Willd.) and Amaranth (*Amaranthus* Spp.) and their influence in the nutritional value of cereal based foods. *Food Public Health* 2, 265–275. doi: 10.5923/j.fph.20120206.12
- Varnamkhasti, M. G., Mobli, H., Jafari, A., Keyhani, A. R., Soltanabadi, M. H., Rafiee, S., et al. (2008). Some physical properties of rough rice (*Oryza Sativa* L.) grain. *J. Cereal Sci.* 47, 496–501. doi: 10.1016/j.jcs.2007.05.014

Conflict of Interest: The authors declare that the research was conducted in the absence of any commercial or financial relationships that could be construed as a potential conflict of interest.

Copyright © 2021 Geisen, Krishnaswamy and Myers. This is an open-access article distributed under the terms of the Creative Commons Attribution License (CC BY). The use, distribution or reproduction in other forums is permitted, provided the original author(s) and the copyright owner(s) are credited and that the original publication in this journal is cited, in accordance with accepted academic practice. No use, distribution or reproduction is permitted which does not comply with these terms.



Optimizing Pasteurized Fluid Milk Shelf-Life Through Microbial Spoilage Reduction

Forough Enayaty-Ahangar^{1*}, Sarah I. Murphy¹, Nicole H. Martin², Martin Wiedmann² and Renata Ivanek¹

¹ Population Medicine & Diagnostic Sciences, Cornell University, Ithaca, NY, United States, ² Department of Food Science, Cornell University, Ithaca, NY, United States

OPEN ACCESS

Edited by:

Santanu Basu,
Swedish University of Agricultural
Sciences, Sweden

Reviewed by:

Veronica Ortiz Alvarenga,
Federal University of Minas Gerais,
Brazil
Guadalupe Virginia Nevárez-Moorillón,
Autonomous University of Chihuahua,
Mexico

*Correspondence:

Forough Enayaty-Ahangar
forough.enayaty@cornell.edu

Specialty section:

This article was submitted to
Sustainable Food Processing,
a section of the journal
Frontiers in Sustainable Food Systems

Received: 20 February 2021

Accepted: 06 April 2021

Published: 08 July 2021

Citation:

Enayaty-Ahangar F, Murphy SI,
Martin NH, Wiedmann M and Ivanek R
(2021) Optimizing Pasteurized Fluid
Milk Shelf-Life Through Microbial
Spoilage Reduction.
Front. Sustain. Food Syst. 5:670029.
doi: 10.3389/fsufs.2021.670029

Psychrotolerant spore-forming bacteria, entering raw milk primarily on-farm, represent a major challenge for fluid milk processors due to the ability of these bacteria to survive heat treatments used for milk processing (e.g., pasteurization) and to cause premature spoilage. Importantly, fluid milk processors require tools to identify optimal strategies for reducing spore-forming bacteria, thereby extending product shelf-life by delaying spoilage. Potential strategies include (i) introducing farm-level premium payments (i.e., bonuses) based on spore-forming bacteria counts in raw milk and (ii) investing in spore reduction technologies at the processing level of the fluid milk supply chain. In this study, we apply an optimization methodology to the problem of milk spoilage due to psychrotolerant spore-forming bacteria and propose two novel mixed-integer linear programming models that assess improving milk shelf-life from the dairy processors' perspective. Our first model, imposed to a budgetary constraint, maximizes milk's shelf-life to cater to consumers who prefer milk with a long shelf-life. The second model minimizes the budget required to perform operations to produce milk with a shelf-life of a certain length geared to certain customers. We generate case studies based on real-world data from multiple sources and perform a comprehensive computational study to obtain optimal solutions for different processor sizes. Results demonstrate that optimal combinations of interventions are dependent on dairy processors' production volume and quality of raw milk from different producers. Thus, the developed models provide novel decision support tools that will aid individual processors in identifying the optimal approach to achieving a desired milk shelf-life given their specific production conditions and motivations for shelf-life extension.

Keywords: dairy supply chain, pasteurized fluid milk, microbial spoilage, premium/penalty system, optimization, mixed-integer linear programming

1. INTRODUCTION

Dairy products represent 17% of the total value of food wasted at the retail and consumer levels and are among the top food categories that contributed to the food waste in the United States in 2010 (United States Department of Agriculture, 2014). In the United States, the waste of fluid milk primarily occurs at point-of-retail and end-consumer levels (Buzby et al., 2014). For example, 31% of all dairy products and 32% of fluid milk were estimated to be wasted at these stages in

2010 (United States Department of Agriculture, 2014). A large portion of fluid milk waste is due to people throwing out (i) products that spoil before they are able to be consumed and (ii) products that are not spoiled based on organoleptic characteristics but are beyond their identified “best by” or “expiration” date (Hall-Phillips and Shah, 2017). Both of these are of concern to processors since they may lose customers because of short shelf-life or premature microbial spoilage of their product. Therefore, the microbial spoilage of milk leading to waste becomes a challenge for the dairy processors. Thus, they would benefit from decision support tools to determine optimal strategies to extend milk's shelf-life through microbial spoilage reduction in order to allow them to address their customers' needs by producing milk of a certain target shelf-life. A typical milk supply chain structure in the United States is described in the **Supplementary Material**.

There are two primary routes through which spoilage bacteria enter the fluid milk supply chain: (i) contamination of raw milk on farms with psychrotolerant Gram-positive spore-forming bacteria (Martin et al., 2019) and (ii) contamination of milk at the processing level with Gram-negative bacteria after pasteurization (i.e., post-pasteurization contamination) (Martin et al., 2018). When post-pasteurization contamination is prevented (e.g., through Good Manufacturing Practices), psychrotolerant Gram-positive spore-forming bacteria (e.g., *Bacillus* spp. and *Paenibacillus* spp.) are the primary causes of pasteurized fluid milk spoilage. This is because spores (i.e., the resistant structure produced by the spore-forming bacteria) can survive commonly used pasteurization methods (e.g., HTST) (Martin et al., 2019) and subsequently grow at refrigeration temperatures over a period of 14–17 days after pasteurization (Ranieri and Boor, 2009). Some technologies such as ultra-high pasteurization [e.g., pasteurization at 138°C (280°F) for 2 s (International Dairy Food Association, n.d.)] are known to effectively reduce bacterial spores in fluid milk. However, compared to HTST pasteurization, these alternative pasteurization methods are undesirable by processors, because of their considerably higher cost, and by many United States consumers, because higher pasteurization temperatures produce defects such as “cooked” and “stale” flavors (Mehta, 1980; Rysstad and Kolstad, 2006). As such, compared to alternative methods, the market for HTST pasteurized fluid milk remains strong. Thus, control of bacterial spores in HTST pasteurized fluid milk in the United States remains a considerable challenge for the dairy industry.

Factors that determine the concentration of spore-forming bacteria in pasteurized fluid milk include (i) the initial concentration of spores in the raw milk at the production level, (ii) spore reductions that can occur at the processing level, and (iii) bacterial growth that can take place at the transportation,

distribution, retail, and consumer levels. In order to reduce the spore-forming bacteria level of the final product, different strategies associated with each of the three factors need to be considered. Now, we provide more details about these strategies:

(i) Initial concentration of spores at the production level—The original source of spore-forming bacteria often is farms where spores are ubiquitous and can easily find their way (e.g., through dirty udders) to enter bulk tank raw milk. Efforts to reduce the initial concentration of spores in raw milk at the production level need to account for the heterogeneous quality of milk supplied by multiple producers. This means that even if the majority of the producers supply milk with low concentrations of spores, having a few producers with high spore concentrations can lead to high enough contamination levels in the silo milk to contaminate the majority of packaged products with >1 spore, which can subsequently grow and cause spoilage. Strategies to reduce the initial concentration of spores in raw milk require producers to perform on-farm interventions (e.g., training milking parlor employees). These interventions, with different impacts on raw milk's spore concentration, require a specific amount of time for implementation. More importantly, most United States producers do not currently have financial incentives to produce raw milk with low spore counts, making the producers reluctant to implement additional interventions. Statistical analysis in Saenger et al. (2013) shows that incentivizing producers for consistent high-quality milk and/or penalizing them for supplying low-quality milk encourages them to invest in quality-improving inputs that results in higher quality milk. Thus, one strategy for dairy processors to motivate the producers to perform on-farm interventions would be through a premium/penalty system by which the processors would test collected raw milk for spores and based on the result of each sample test, they would incentivize (or penalize) the producers for supplying raw milk with a desirable (or undesirable) quality. While such premium/penalty system would be new for the United States producers, there are examples of limited applications of such systems elsewhere, e.g., the Netherlands where some producers receive deduction on the milk price because of a high level of contamination of raw milk with spores (Vissers et al., 2007a).

Currently, in the United States, milk pricing is based on individual components (i.e., fat, protein, solids) and a blend price, which is based on the utilization of raw milk for different dairy products and geographic location, per 100 lb (i.e., CWT or hundredweight), along with additional potential premiums (i.e., quality premiums) based on different factors that will quantify its quality. According to Munch et al. (2020), premiums are often offered as a tool to reward/penalize producers for their milk's somatic cell counts. Based on data provided by three different dairy organizations in the United States, we estimate that premiums can vary between \$-0.60 to \$3 per CWT. Negative values mean the processors also apply penalties when the milk quality is not desirable. These premiums are currently paid based on raw milk quality parameters such as somatic cell count, added water (i.e., the freezing point of milk), laboratory pasteurization count, coliform bacteria count, and total bacteria count (but not spore count which is the focus

Abbreviations: BF, Bactofugation; CFU, Colony-forming units; HGP, Half-gallon package; HTST, High-temperature short-time; ISC, Initial spore count; MF, Microfiltration; MILP, Mixed-integer linear program; MPBOP, Milk processor budget optimization problem; MPN, Most probable number; MSLOP, Milk shelf-life optimization problem; OFV, Objective function value; SRT, Spore reduction technology.

of this study), which are tested for when raw milk is collected from the producers. As mentioned earlier, in the absence of post-pasteurization contamination, spore-forming bacteria are the primary bacterial agents that limit fluid milk shelf-life; therefore, in this paper, we propose a new flexible milk premium/penalty system that is solely based on raw milk's initial spore counts at the production level that would be implemented independently or instead of the current premium/penalty system described above and motivate producers to implement on-farm interventions. This novel system would require testing raw milk for the level of spores (i.e., spore counts) at the production stage of the supply chain.

(ii) Spore reduction at the processing level— The concentration of spores in raw milk can be reduced at the processing level, however, the spore reduction technologies (SRTs), such as microfiltration (MF) and bactofugation (BF), require units that are costly to purchase, install, and run. A brief description of these technologies can be found in the **Supplementary Material**.

(iii) Spore-forming bacteria growth after the processing level— Growth of bacteria in pasteurized fluid milk occurs when conditions are favorable for vegetative growth (e.g., refrigerated storage temperature). In such cases, certain strains of spore-forming bacteria are able to germinate (i.e., return to a metabolically active state from the dormant spore state) and then bacterial growth can occur (Huck et al., 2007; Masiello et al., 2014). Growth of bacteria in packaged pasteurized fluid milk after it leaves the processing facility has been studied by Buehler et al. (2018) who developed a Monte Carlo simulation model to estimate packaged milk's shelf-life given the distribution of initial concentration of spores in raw milk.

The strategies associated with each of these factors require operational and monetary resources; thus, their implementations need to be investigated first. The critical question is how a dairy processor should determine the optimal combination of strategies for their unique situation.

In this paper, the processor is defined as the entity in the chain that is responsible for purchasing raw milk from the producers and processing it prior to distribution. Thus, we consider the strategies that can be employed by the processor, which have effects on the initial concentration of spores at the production level and their reductions at the processing level. However, we use a Monte Carlo model, adapted from the model in Buehler et al. (2018), to simulate the bacterial growth after it leaves the processing facility. Note that it is unlikely for spores to germinate during the transportation between the suppliers and the processors due to (i) cold temperature at which the raw milk is kept in tanker trucks and (ii) the fact that the transportation time between farms and processing facilities is typically shorter than the amount of time needed for spore germination at low temperatures. Therefore, spore germination and subsequent bacterial growth at the transportation level is negligible and is not considered here.

Limited existing studies have focused on the reduction of spores at the production level (e.g., McKinnon and Pettipher, 1983; Christiansson et al., 1999; Ewanowski et al., 2020) and processor level (e.g., Guerra et al., 1997; Hurt et al., 2015; Doll

et al., 2017; Griep et al., 2018). However, these studies focus on only one level of the fluid milk supply chain and do not consider the strategies for more entities involved in the chain. There have been few mathematical modeling studies in the literature for improving the shelf-life for other dairy products. For example, Lütke Entrup et al. (2005) have developed a mixed-integer linear programming formulation for a yogurt production planning and scheduling problem. However, to the best of our knowledge, no optimization research has taken into account the effect of spore-forming bacteria at both the production and processing levels on the pasteurized fluid milk's shelf-life.

In this paper, using optimization techniques, we identify the best combinations of processing level interventions and production level incentive structures to optimize milk's shelf-life. We consider two types of interventions: (i) interventions that affect the production level: a flexible milk premium/penalty system based on milk quality categories, defined by raw milk's spore counts, that allows incentivizing and penalizing producers, and (ii) interventions at the processing level: implementing SRTs. These SRTs are (1) MF, (2) single-BF, and (3) double-BF which is performing BF twice.

Mathematical modeling has become a popular approach for solving real-world supply chain problems (e.g., McDonald and Karimi, 1997; Ahmadbeygi et al., 2009; Enayaty-Ahangar et al., 2019; Jabbarzare et al., 2019; Sheikh-Zadeh and Rossetti, 2020). In the past decades, researchers have been using different operation research tools to improve decision-making processes in the food supply chains in order to minimize the food loss along the chain or maximize the profit (Lemma et al., 2014). Among these tools, a few deterministic modeling techniques have been widely used to solve agricultural supply chains (Ahumada and Villalobos, 2009), such as linear programming [e.g., Apaiah and Hendrix (2005) for pea-based products, Jiao et al. (2005) for sugar cane farms, Glen (1986) for crop and beef production plans], mixed integer programming [e.g., Higgins (2002) for sugar cane farms], and dynamic programming [e.g., Stoecker et al. (1985) for irrigation and crop production]. Many planning models developed for perishable agri-foods lack consideration of the shelf-life aspect. This is mainly due to the added complexity that the shelf-life feature presents in the different echelons of the chain bring to the modeling of the problem (Ahumada and Villalobos, 2009). This could also be because of biological factors that impact the shelf-life and embedding these factors in an optimization model is difficult. A few research studies have taken into account the shelf-life of perishable products such as flowers, grapes, and tomatoes when optimizing the distribution, harvesting, and other operations in the chain (e.g., Widodo et al., 2006; Ferrer et al., 2008; de Keizer et al., 2017; Ghezavati et al., 2017). To the best of our knowledge, no optimization research study has focused on optimizing operations in a pasteurized fluid milk processing facility by considering factors that determine the concentration of spore-forming bacteria in pasteurized fluid milk and thus, have the most influence on milk's shelf-life. Here, we use mixed-integer linear programming (MILP) to model this fluid milk problem. Our objective is to determine the intervention strategies that maximize the milk shelf-life subject to the processor's

available budget or minimize the budget required to reach a set shelf-life target.

2. MATERIALS AND METHODS

2.1. Problem Definition

We define two optimization problems in this paper. In both, we try to identify the strategies for interventions that managers at the processing level should select to achieve their desired outcome (e.g., maximized average shelf-life of all pasteurized fluid milk packages) during a planning horizon. The decisions of the models consist of determining: (1) whether or not to implement the proposed novel premium/penalty system based on raw milk's spore counts and (2) whether or not to implement one or two of the SRTs. The primary restriction in model one is the processor's budget allocated to implement these strategies. The second model, on the other hand, requires to meet a minimum shelf-life. There are a set of assumptions in the problem which are presented as follows.

- ⇒ A large portion of fluid milk waste is due to people throwing out (i) products with unacceptable quality (i.e., spoiled product) and (ii) products with acceptable quality (i.e., not spoiled) that are past their "best by" dates. Processors desire to not lose customers because of a short shelf-life or premature microbial spoilage of their product and that requires them to find the optimal way to reduce that risk. Thus, the main focus of this paper is on extending pasteurized fluid milk's shelf-life.
- ⇒ Each day, the collected milk is stored in one or more silos at the processing facility and then goes through the same processing equipment for pasteurization; thus, we assume that the number of spores in milk packages in that day equals to the weighted average of spore counts of all the raw milk collected from the producers.
- ⇒ The spore counts are presented in logarithmic form because microbial counts are typically highly skewed. To match food microbiology practices regarding reduction in food contamination, any reduction of the spore count is presented in logarithmic (i.e., log10) values. Also, in rare cases, the initial spore count (ISC) can be so low that not all units of milk (i.e., half-gallon packages) will contain at least one spore. In these cases, we assume the number of the contaminated half-gallon packages (HGPs) is equal to the total number of spores, meaning that there is one spore per package, and consider the rest as not contaminated.
- ⇒ Due to the relatively high cost of a spore test, we assume testing for spore counts occurs once a week (rather than daily) for each producer if the premium/penalty system is implemented. Days on which raw milk sampling and testing occur are randomly selected by the processor so that daily routines do not change by the producers. Note that with this approach, the difference between two consecutive tests can be within the range of 1 to 13 days. Then, the producer would be paid premiums or penalized for the total volume of milk produced in that week based on the one-time sample test result. Note that these payments can occur at any time (e.g., at the end of each week or month). Paying producers for the milk's blend price (for the volume of sold milk) occurs regardless of any spore reduction strategies implemented by the producer and thus, milk blend price is not part of our optimization models.
- ⇒ To calculate the impact of the premium/penalty system on the initial spore count at the production level, we assume that each producer's main interest is in the premium that would be paid if the quality of their milk is improved one or two categories.
- ⇒ According to experts, there is about 1–1.25% of milk shrinkage (i.e., the difference between the processed milk volume and the raw milk volume) due to MF and BF in the processing facility. The milk shrinkage has impacts on the number of sold packages but not on the shelf-life. Due to the focus of this model being on the shelf-life extension of milk, we do not account for the shrinkage in this paper. However, we acknowledge that the shrinkage due to SRT implementations may affect processor decision making and will consider it for the future direction of this work.
- ⇒ We appreciate that the implementation of both BF and MF in a single given fluid milk processing plan is extremely unusual and may not be feasible; however, in our model, we allow the use of multiple SRTs and consider their impacts as independent from each other. Due to the lack of data, we do not account for any possible reductions in effectiveness when using multiple SRTs. Further research is needed to determine whether or not using two SRTs can have additive/reductive effects on spore counts.
- ⇒ Paying premiums is a continuous process and processors cannot stop doing it when the quality of milk is improved as the producers might stop doing on-farm interventions and return to their original production management and if so, their milk quality will diminish. Therefore, the premium payments occur until the end of the planning horizon in our models. This simulates a situation in which milk processors make a commitment to keep a certain bonus scheme. In agriculture, this can be enforced by a contract between dairy processors and milk producers. It is assumed that, for the length of a planning horizon, producers do not choose to stop supplying and/or switch between processors depending on their premium/penalty systems, and also, that producers would not be "dropped" (i.e., fired or let go by the processor). We also assume that it is feasible to establish a contract between the two parties and to set provisions about quality requirements and bonuses/penalties for a specific amount of time (e.g., 5 years). Note that similar contracts already exist in industries with livestock commodities such as chicken broilers, eggs, and milk (United States Department of Agriculture, 1996).
- ⇒ In this problem, we do not consider the processor facility is owned by the farmers since it only applies to a small fraction of the cases.

2.2. Definition and Explanation of Models

In this section, we present two novel MILP models for the production and processing stages of the milk supply chain: (1) milk shelf-life optimization problem (MSLOP) that focuses on

processors' desire to reach the longest shelf-life of their final product to please consumers who prefer longer shelf-life and (2) milk processor budget optimization problem (MPBOP) that needs to produce milk with a uniform shelf-life of certain length geared to certain customers.

2.2.1. Milk Shelf-Life Optimization Problem (MSLOP)

In this model, there is a set of producers $p \in P$ that supply milk for a processor in a fixed planning horizon (i.e., $|D|$ days or $|W|$ weeks). On day $d \in D$, raw milk supplied by producer $p \in P$ falls into one of the $|C|$ categories of raw milk based on its ISC value, ISC_{dp}^d , when collected by a tanker truck. Note that the superscripts in the parameters and variables' notations are part of their names and only the subscripts represent indices. Categories $c \in C$ are non-overlapping intervals $[C_c^{min}, C_c^{max}]$. Given the ISC_{dp}^d values, the weighted average of ISC, ISC_d^{avg} , for all the raw milk collected at the processing facility in day d is then calculated. Note that a smaller value of ISC_d^{avg} for day $d \in D$ means a longer shelf-life for all the HGP's of milk processed on that day.

To reduce the ISC_d^{avg} value, the processing facility can implement MF, single-BF, and double-BF. There are fixed (i.e., purchasing, installation, maintenance) and variable (i.e., electricity and operational) costs associated with each of these technologies which results in a different log reduction in the ISC_d^{avg} values. These parameters are presented in **Table 1**. There is a set of on-farm interventions $q \in Q$ that can occur to achieve premium payments. These interventions will result in a log reduction of producers' daily ISC values and subsequently in the average daily spore count values. These reductions can be different in size and starting time. For example, one of the short-term on-farm control strategies is laundering re-usable cloth towels, used for cleaning the udder and teats during milking preparation, through the use of detergent and chlorine bleach and fully drying (Evanowski et al., 2020); the impact of this strategy is immediate and here we assume it results in a fixed spore reduction for as long as it is performed. Another intervention can be investing in parlor employees training designed to teach them to focus on cleaning teat ends thoroughly during milking preparation.

The main variables in the model are x^{MF} , x^{BF1} , x^{BF2} , and x^{PR} that show whether or not the processor implements MF, single-BF, double-BF, and premium/penalty system, respectively. Given the premium/penalty system is implemented (i.e., $x^{PR} = 1$), variable PR_c , $c \in C$ denotes the premium paid for the raw milk in category c . Depending on the values the variables take, the average spore count of each day's milk will be reduced. As a result, the corresponding milk category $\bar{c} \in \bar{C}$ of the processed milk on day $d \in D$ and its shelf-life, $SL_{\bar{c}}$, are determined. Categories $\bar{c} \in \bar{C}$ are also non-overlapping intervals used to categorize the spore count values of packaged milk on day \bar{c} .

The problem is then to determine the set of values for the variables that maximize the average shelf-life of all the milk packages produced in the planning horizon, SL^{avg} , subject to the processor's daily budget, B , limit. We explain our model settings in the following paragraphs:

TABLE 1 | Notation - Sets and parameters.

Sets	
P	set of producers
W	set of weeks
D	set of days
C	set of categories of raw milk based on initial spore count values
\bar{C}	set of categories of packaged milk based on bacterial count values
Q	set of possible on-farm interventions at the production level
Parameters	
B	available daily budget (in \$ per day)
PR^{min}	minimum value of penalty that PR_5 (i.e., premium for the least desirable raw milk) can have (in \$ per HGP)
PR^{max}	maximum value of premiums (in \$ per HGP)
$\bar{P}R^{max}$	maximum value of $\bar{P}R$ (in \$ per HGP)
PC_p	category of producer $p \in P$
NP_{wp}^w	number of HGPs of milk supplied by producer $p \in P$ in week $w \in W$ (in HGP per week)
NP_{dp}^d	number of HGPs of milk supplied by producer $p \in P$ in day $d \in D$ (in HGP per day)
TP_d	total number of HGPs processed in day $d \in D$ (in HGP per day)
TP_d^0	total number of processed HGPs with no spores in day $d \in D$ (in HGP per day)
ISC_{wp}^w	ISC value of raw milk supplied by producer $p \in P$ tested in week $w \in W$ (in log10 MPN per HGP)
ISC_{dp}^d	ISC value of raw milk supplied by producer $p \in P$ in day $d \in D$ (in log10 MPN per HGP)
ISC_d^{avg}	weighted average of ISC values of all the raw milk collected at the processing facility in day $d \in D$ (in log10 MPN per HGP)
TC	cost of performing one spore test (in \$)
FC^{MF}	fixed cost per day associated with MF (in \$ per day)
VC^{MF}	variable cost associated with MF (in \$ per HGP)
FC^{BF1}	fixed cost per day associated with single-BF (in \$ per day)
VC^{BF1}	variable cost associated with single-BF (in \$ per HGP)
FC^{BF2}	fixed cost per day associated with double-BF (in \$ per day)
VC^{BF2}	variable cost associated with double-BF (in \$ per HGP)
R^{MF}	spore count log reduction as the result of MF implementation (in log10 MPN per HGP)
R^{BF1}	spore count log reduction as the result of single-BF implementation (in log10 MPN per HGP)
R^{BF2}	spore count log reduction as the result of double-BF implementation (in log10 MPN per HGP)
R_q^{PR}	ISC log reduction $q \in Q$ proportional to $\bar{P}R$ that occurs every I_q weeks (in log10 MPN per HGP)
S_q	binary parameter; 1, if the reduction $q \in Q$ occurs from the beginning of the planning horizon; 0, otherwise
I_q	number of weeks before a reduction of R_q^{PR} in ISC can be seen, $q \in Q$
a_q	scaling factor for on-farm intervention q
α	coefficient (between 0 and 1) that represents the effort a producer with $PC \geq 3$ wants to make to improve milk quality by one category and receive the corresponding premium
β	coefficient (between 0 and 1) that represents the effort a producer with $PC \geq 3$ wants to make to improve milk quality by two categories and receive the corresponding premium, $\beta = 1 - \alpha$

(Continued)

TABLE 1 | Continued

Parameters	
C_c^{min}	minimum ISC value of raw milk in category $c \in C$ (in log10 MPN per HGP)
C_c^{max}	maximum ISC value of raw milk in category $c \in C$ (in log10 MPN per HGP)
\bar{C}_c^{min}	minimum bacterial count value of processed milk in category $\bar{c} \in \bar{C}$ (in log10 MPN per HGP)
\bar{C}_c^{max}	maximum bacterial count value of processed milk in category $\bar{c} \in \bar{C}$ (in log10 MPN per HGP)
$SL_{\bar{c}}$	shelf-life of milk packages in category $\bar{c} \in \bar{C}$ (in days)
SL^{max}	shelf-life of milk packages with no spores (in days)
M	a sufficiently large positive constant

- ⇒ The produced and processed milk are represented by unit half-gallon package (HGP) throughout the supply chain. A half-gallon is approximately equal to 1,900 milliliters (mL).
- ⇒ Spore count and any reductions in it are measured in log10 MPN/HGP. The distribution of the initial concentration of spores in raw milk was determined by the most probable number (MPN) method described by Masiello et al. (2014) and Buehler et al. (2018). The MPN method estimates the population density of the microbial count on the basis of the probability theory without the actual count of single colonies (Alexander, 1983).
- ⇒ There are five categories of raw milk where categories one to five have the most to the least desirable qualities, respectively. Also, there are eight categories of packaged milk where categories one to eight, respectively have the lowest to highest bacterial counts.
- ⇒ Generally speaking, the shelf-life for one package of milk is defined as the period of time between processing/packaging until it no longer meets the consumer's acceptable quality standard; that is until it starts exhibiting any physical or organoleptic defects while it is kept under practical storage conditions (Bishop and White, 1986; Muir, 1996; Schroeter et al., 2016). The consumer threshold was quantified to be 6 log10 CFU/mL bacterial count by Carey et al. (2005) and Martin et al. (2012). Thus, we too define the shelf-life of all the processed milk packages in a day to be the number of days between the packaging and the first day when 5% of packages are defective meaning that they have bacterial counts in excess of 6 log10 CFU/mL (i.e., 9.3 log10 CFU/HGP). Note the CFU, colony-forming unit, is used to present bacterial level in the finished product, while MPN is used to determine spore counts due to their low concentrations in raw milk.
- ⇒ The shelf-life for each of the eight categories of packaged milk is equal to the shelf-life of a representative point in that category.

The complete sets and parameters; and variables are presented in Tables 1, 2, respectively, followed by the first MILP formulation.

$$\text{MSLOP: } \max SL^{Avg} \quad (1)$$

$$\text{s.t. } x^{BF1} + x^{BF2} \leq 1 \quad (2)$$

$$PR_c \geq PR_{c+1} \quad \forall c \in C, c \leq 4 \quad (3)$$

$$PR_5 \geq PR^{min} \quad (4)$$

TABLE 2 | Notation - Variables.

Decision variables	
x^{MF}	whether (1) or not (0) the processing facility implements microfiltration
x^{BF1}	whether (1) or not (0) the processing facility implements single-BF
x^{BF2}	whether (1) or not (0) the processing facility implements double-BF
x^{PR}	whether (1) or not (0) the processing facility decides to pay premiums
PR_c	premium paid per each HGP of raw milk in category $c \in C$ (in \$ per HGP)
Variables that are functions of the decision variables	
\hat{Z}_{wpc}	whether (1) or not (0) raw milk produced by producer $p \in P$ falls within category $c \in C$ on the day of test performed in week $w \in W$
Z_{dc}	whether (1) or not (0) processed milk in day $d \in D$ falls within category $\bar{c} \in \bar{C}$
PR_{wp}^{paid}	premium paid for each HGP of raw milk to producer $p \in P$ in week $w \in W$ (in \$ per HGP)
$\hat{P}R$	overall impact of premium payments on the ISC reduction at the production level (in \$ per HGP)
TR	total log reduction in spore counts due to selected SRTs at the processing facility (in log10 MPN per HGP)
SL^{Avg}	weighted average shelf-life of all milk packages (in days)

$$x^{PR} \geq PR_c \quad \forall c \in C \quad (5)$$

$$x^{PR} \geq -PR_5 \quad (6)$$

$$PR_c \leq PR^{max} \quad \forall c \in C \quad (7)$$

$$\begin{aligned} & \left(\sum_{d \in D} \sum_{p \in P, PC_p \geq 2} NP_{dp}^d \right) \hat{P}R \\ &= \sum_{d \in D} \left(\sum_{p \in P, PC_p \geq 3} NP_{dp}^d * (\alpha * PR_{PC_p-1} + \beta * PR_{PC_p-2}) \right. \\ & \quad \left. + \sum_{p \in P, PC_p=2} NP_{dp}^d * PR_{PC_p-1} \right) \end{aligned} \quad (8)$$

$$\hat{P}R \leq \hat{P}R^{max} \quad (9)$$

$$\hat{P}R \leq \sum_{p \in P, PC_p \geq 2} 1 \quad (10)$$

$$PR_5 \geq - \sum_{p \in P, PC_p \geq 3} 1 \quad (11)$$

$$\sum_{c \in C} \hat{Z}_{wpc} = 1 \quad w \in W, p \in P \quad (12)$$

$$\begin{aligned} & ISC_{wp}^w - \sum_{q \in Q, s_q=0} \lfloor w/l_q \rfloor * R_q^{PR} * a_q * \hat{P}R \\ & - \sum_{q \in Q, s_q=1} \lceil w/l_q \rceil * R_q^{PR} * a_q * \hat{P}R \end{aligned} \quad (13)$$

$$\geq \sum_{c \in C} \hat{Z}_{wpc} * C_c^{min} \quad \forall w \in W, p \in P \quad (14)$$

$$ISC_{wp}^w - \sum_{q \in Q, s_q=0} \lfloor w/l_q \rfloor * R_q^{PR} * a_q * \hat{P}R -$$

$$\sum_{q \in Q, s_q=1} [w/l_q] * R_q^{PR} * a_q * \hat{P}R$$

$$\leq \sum_{c \in C} \hat{z}_{wpc} * C_c^{max} \quad \forall w \in W, p \in P \quad (15)$$

$$PR_{wp}^{paid} \leq PR_c + M * (1 - \hat{z}_{wpc})$$

$$\forall w \in W, p \in P, c \in C \quad (16)$$

$$PR_{wp}^{paid} \geq PR_c - M * (1 - \hat{z}_{wpc})$$

$$\forall w \in W, p \in P, c \in C \quad (17)$$

$$\sum_{w \in W} \sum_{p \in P} (TC * X^{PR} + NP_{wp}^w * PR_{wp}^{paid})$$

$$+ \sum_{d \in D} (FC^{MF} * x^{MF} + \sum_{p \in P} (NP_{dp}^d * VC^{MF} * x^{MF})$$

$$+ FC^{BF1} * x^{BF1} + \sum_{p \in P} (NP_{dp}^d * VC^{BF1} * x^{BF1}) +$$

$$FC^{BF2} * x^{BF2} + \sum_{p \in P} (NP_{dp}^d * VC^{BF2} * x^{BF2})) \leq B * |D| \quad (18)$$

$$TR = R^{MF} * x^{MF} + R^{BF1} * x^{BF1} + R^{BF2} * x^{BF2} \quad (19)$$

$$\sum_{\bar{c} \in \bar{C}} z_{d\bar{c}} = 1 \quad \forall d \in D \quad (20)$$

$$ISC_d^{ave} - \sum_{q \in Q, s_q=0} \lfloor \frac{[d/7]}{l_q} \rfloor * R_q^{PR} * a_q * \hat{P}R$$

$$- \sum_{q \in Q, s_q=1} \lceil \frac{[d/7]}{l_q} \rceil * R_q^{PR} * a_q * \hat{P}R$$

$$- TR \geq \sum_{\bar{c} \in \bar{C}} z_{d\bar{c}} * \bar{C}_{\bar{c}}^{min} \quad \forall d \in D \quad (21)$$

$$ISC_d^{ave} - \sum_{q \in Q, s_q=0} \lfloor \frac{[d/7]}{l_q} \rfloor * R_q^{PR} * a_q * \hat{P}R$$

$$- \sum_{q \in Q, s_q=1} \lceil \frac{[d/7]}{l_q} \rceil * R_q^{PR} * a_q * \hat{P}R -$$

$$TR \leq \sum_{\bar{c} \in \bar{C}} z_{d\bar{c}} * \bar{C}_{\bar{c}}^{max} \quad \forall d \in D \quad (22)$$

$$SL^{Avg} = (\sum_{d \in D} \sum_{\bar{c} \in \bar{C}} ((TP_d - TP_d^0) * SL_{\bar{c}} * z_{d\bar{c}})$$

$$+ \sum_{d \in D} (TP_d^0 * SL^{max})) / (\sum_{d \in D} TP_d) \quad (23)$$

$$x^{MF}, x^{BF1}, x^{BF2}, x^{PR} \in \{0, 1\} \quad (24)$$

$$z_{d\bar{c}} \in \{0, 1\} \quad \forall d \in D, \bar{c} \in \bar{C} \quad (25)$$

$$\hat{z}_{wpc} \in \{0, 1\} \quad \forall d \in D, p \in P, c \in C \quad (26)$$

$$PR_c \geq 0 \quad \forall c \in C: c \leq 4 \quad (27)$$

$$PR_{wp}^{paid} \geq 0 \quad \forall w \in W, p \in P \quad (28)$$

$$TR, \hat{P}R \geq 0 \quad (29)$$

The objective function, (1), is to maximize the weighted average shelf-life of all the milk packages processed in the planning horizon. The only variable in the objective function, SL^{Avg} , is calculated in constraint (23) which is explained later. The processor can either implement single-BF or double-BF but not both; this is enforced by constraint (2). Constraint (3) ensures that the premiums do not decrease as the quality of the category increases. Constraint (4) sets a lower limit on the premium of category 5, PR_5 . This lower limit can be negative and act as a penalty for the producers who supply milk with the least desirable raw milk. If at least one of the categories' premiums takes a non-zero value, it means that the processor implements the premium/penalty system; therefore, x^{PR} should be equal to one. This restriction is enforced by constraints (5-6). Note that all premiums are defined only for an HGP and their absolute value is less than a small value (< 1). This means we do not need a coefficient on the right-hand side of the constraints to allow $\hat{P}R$ take the value of one in case one of the premiums is non-zero. Note that PR_5 is the only premium that can be negative and act as a penalty, hence constraint (6) is only defined for category five. Constraint (7) sets upper bounds for the premium variables to ensure that premiums do not have an unlimited impact on the raw milk spore reduction. The variable $\hat{P}R$, representing the overall impact of premium payments on the ISC reductions, is calculated in constraint (8). This variable is dependent on how much milk each producer produces and the usual quality of their milk (i.e., PC_p). For example, if a producer's milk is usually in category three ($PC_p = 3$), then the premiums of the next two better categories (i.e., two and one) act as incentives for them and motivate them to perform on-farm interventions so the category of their produced raw milk improves. Two parameters, α and β , define the producer's motivation to produce milk in those two categories. Note that if a producer's usual milk quality is in category two, then they merely consider the premium for category one as an incentive (i.e., $\alpha = 1$ and $\beta = 0$). Category-one producers are already producing the most desirable milk, therefore, they are not considered in the $\hat{P}R$ calculation. However, they will be paid the premium for category one. Constraint (9) sets an upper bound for $\hat{P}R$ which is later explained in section 2.3. If all the producers are already producing the most desirable milk, paying premiums will not change the objective function value (OFV), hence $\hat{P}R$ should be zero. This is ensured by constraint (10). On the other hand, constraint (11) ensures if there is no producer supplying undesirable milk (i.e., producers in categories 3-5), PR_5 cannot be negative, meaning no penalty is applied.

Constraints (12-17) are intended to calculate the total premiums the processor should pay the producers according to their quality of milk. The quality of raw milk for each producer is determined based on the weekly spore tests. The producers will be paid the premium based on (1) the spore category of tested milk and (2) the total volume of the milk produced in that week. Constraint (12) guarantees that each producer's milk is assigned to one category of milk based on the weekly test results. Constraints (14-15) determine the category of milk produced by producer p in week w after considering the impacts of the premium payments on the ISC. Such impact consists of the

overall $\hat{P}R$, R_q^{PR} , a_q , and how frequently the reductions can occur which are calculated by $\lfloor w/l_q \rfloor$ and $\lceil w/l_q \rceil$. If $s_q = 0$, it means that the impact of intervention q does not occur from the beginning of the planning horizon and requires l_q weeks before it shows any impact on the spore count. This reflects situations when a producer requires time to implement a strategy that improves the quality of their milk. Hence the floor of w/l_q is considered in constraints (14-15). For instance, for intervention q with $l_q = 52$ weeks, there will be no spore reductions occurring in $w = 1, \dots, 51$ since $\lfloor w/l_q \rfloor = 0$. However, starting week 52nd, the intervention at the production level will begin to show its impact and one $R_q^{PR} \log_{10}$ MPN/HGP occurs if $a_q * \hat{P}R = 1$. This remains the same until week 103rd. On the other hand, if $s_{q'} = 1$, we use $\lceil w/l_{q'} \rceil$ which means intervention q' at the production level shows its impact from the beginning of the planning horizon. For a similar case, where $l_{q'}$ is 52 weeks and $a_{q'} * \hat{P}R = 1$, reduction $R_{q'}^{PR}$ is seen once when $w = 1, \dots, 51$ since $\lceil w/l_{q'} \rceil = 1$. Constraints (16-17) capture the premium paid to each producer in each week. For each producer p in week w , the paid premium is equal to PR_c if the milk quality falls in category c (i.e., $\hat{z}_{wpc} = 1$). Note that for other categories where $\hat{z}_{wpc} = 0$, the two constraints do not pose any limit on the value of the paid premium (i.e., $-M \leq PR_{wp}^{paid} \leq M$). The total expenditure of the processor, including the spore tests' cost, premium payments, and the fixed and variable costs associated with the implementations of the SRTs (i.e., MF, single-BF, and double-BF), should not exceed the total budget in the planning horizon; this is imposed in constraint (18).

The purpose of constraints (19-23) is to calculate the weighted average shelf-life of all the HGPs during the planning horizon. The total reduction of spore count values due to the SRT implementations at the processing facility is calculated in constraint (19). Constraint (20), similarly to constraint (12), assigns all the packaged milk processed on a day to one category of milk. The two constraints (21-22) are similar to constraints (14-15) but they also consider the possible spore reductions that take place at the processing level (i.e., TR). Be reminded that all the units associated with the spore counts in the model are expressed as \log_{10} MPN/HGP; thus, any log reduction of the spore count values should be deducted from the initial logarithmic value. For instance, for an ISC value of $3 \log_{10}$ MPN/HGP (i.e., 1000 MPN/HGP) and TR of $1 \log_{10}$ MPN/HGP, which means it reduces the absolute spore count by 90% ($= 1 - 10^{-1}$), the final spore count is going to be 2 ($= 3 - 1 \log_{10}$ MPN/HGP (i.e., $1000 * 0.1 = 10^2$ MPN/HGP)). As the result of three constraints (20-22), the variable $z_{d\bar{c}}$ captures the category of milk processed on day d . Variables $z_{d\bar{c}}$ connect the daily spore count values to the daily shelf-life which is used to calculate the average shelf-life in constraint (23). Taking into account the amount of daily processed milk, constraint (23) calculates the weighted average shelf-life during the planning horizon. In this constraint, the shelf-life of the milk packages with at least one spore (i.e., $TP_d - TP_d^0$) and those packages with no spores since the production level are added. Finally, the sign constraints (24)-(29) declare the type of each variable.

2.2.2. Milk Processor Budget Optimization Problem (MPBOP)

In the MSLOP model, the goal is to determine how to allocate a fixed budget of a processor to different intervention options so that the final products' average shelf-life is maximized. However, in many cases, processors do not have a fixed and predefined value for the budget they can allocate to extend their milk's shelf-life. They first need to determine the financial benefits of shelf-life extension (e.g., \$ per day of extended shelf-life, which may not be linear) and then decide whether or not it is in their best interest to invest in interventions that target a specific shelf-life. To this end, we propose a second model, milk processor budget optimization problem (MPBOP), in which we assume that a processor's goal is to increase milk's shelf-life to a specific day and the model's objective is to determine how much daily budget they need to achieve that. There are a few differences between the two models. In MPBOP, B is a decision variable and there are one additional parameter that represents the shelf-life goal of the processor (SL^{min}) and one more constraint. The objective functions are also different in the two models. The MILP formulation of MPBOP is presented below.

$$\text{MPBOP: } \min B \quad (30)$$

$$\text{s.t. Constraints (2) – (23)}$$

$$SL^{Ave} \geq SL^{min} \quad (31)$$

$$B \geq 0 \quad (32)$$

$$\text{Constraints (24) – (28)}$$

Here, the objective, (30), is to minimize the daily budget required to reach the set shelf-life target. In constraint (31), the average shelf-life needs to be at least equal to SL^{min} and B is a non-negative continuous variable, as shown in (32). The rest of the constraints are the same as MSLOP. Note that B in constraint (18) is a parameter in MSLOP and a variable in MPBOP.

2.3. Experimental Design

In this section, we explain how instances, to be used for evaluating the proposed MSLOP and MPBOP models, are generated based on real-world data. We used a variety of sources for our data collection such as (1) experts in the Colleges of Agriculture and Life Sciences, Veterinary Medicine, and Business at Cornell University, (2) industry partners (names redacted to respect the confidentiality), (3) experts at SRT companies (names redacted to respect the confidentiality), (4) Journal articles (e.g., Pafylas et al., 1996; Rysstad and Kolstad, 2006; Masiello et al., 2014, 2017; Buehler et al., 2018), and (5) Online resources [e.g., The United States Department of Agriculture (U.S. Energy Information Administration, 2019)].

2.3.1. Instance Generation Process

There are a variety of fluid milk processing facilities that differ in size. Processing facilities can be categorized into three groups based on annual lb of milk processed: small (less than 10M lb/yr), medium ([10M, 100M) lb/yr), and large (100M and

more lb/yr) (Martin et al., 2012). We generated two different sizes for each category. Other parameters are determined by the following steps:

Number of producers and their herd sizes – The first step includes generating producers and their herd sizes in order to have enough lactating cows to produce a targeted annual milk volume for each processor. Producers' herd sizes follow the probability distribution presented in the last row of **Table 3**. This data was obtained from National Agricultural Statistics Service (2019). Herds with fewer than 50 cows were not considered in our instance generation procedure. After generating each producer's herd category, a value is randomly selected between the minimum and the maximum number of cows in that category (e.g., 50 and 99). This process continues until the total number of cows across all herds is adequate to produce the targeted annual volume of milk assuming each cow produces an average daily milk volume for a cow. Finally, we reduce the last producer's herd size if it causes the total volume of milk to be more than the target value.

Daily production volume – The next step is to generate each producer's exact daily production and ISC value. The average volume of daily produced milk by a cow is generated using a normal distribution. To determine the parameters of this distribution, mean and standard deviation, we use the data reported for 24 selected states in the United States in 2018 (United States Department of Agriculture, 2019). As shown in **Table 4**, an average of 1,951 lb milk was produced by one cow in each month, which is equal to 64.13 lb or 15.36 half-gallon per day. We use one-fourth of the range (i.e., $(65.9 - 62.3)/4$ lb) in the sample of the average daily milk over 12 months as an approximation of the distribution's standard deviation. Thus, the daily milk production of each cow follows a normal distribution with a mean of 64.13 lb (15.36 HGP) and a standard deviation of 0.98 lb (0.23 HGP).

Daily initial spore count values – To generate an ISC value for each producer's daily raw milk, we assign each producer to one of the five categories of raw milk. This means without introducing any new on-farm interventions, one producer consistently produces milk in one category; however, they may produce milk within the neighboring categories on some days. We now explain the raw milk categories.

We define five non-overlapping intervals as the five categories of raw milk. Previously, Masiello et al. (2014) and Buehler et al. (2018) have reported data regarding psychrotolerant spore formers in bulk tank milk across New York State collected between 2009 and 2010. According to these studies, the fitted distribution of the initial spore count in milk approximately follows a lognormal distribution with parameters mean -0.72 MPN/ml and standard deviation 0.99 MPN/ml. This distribution is equivalent to a lognormal distribution with parameters mean 2.56 MPN/HGP and standard deviation 0.99 MPN/HGP. We use the same distribution to generate the producers' initial spore count. Using this distribution, we define five non-overlapping intervals, each with a probability of 0.2 , as shown in **Figure 1**. Each interval represents one category of raw milk.

The details of these categories are presented in **Table 5**. The last column of the table shows the relative frequency (%) of each farm falling in each category based on data presented in Masiello et al. (2017), which includes sample data from 56 different farms in New York state. As an example, given a random producer, there is an 18% chance that it usually produces raw milk in category five. Note that the MPN/HGP values are integer values and not fractional in reality but our non-overlapping intervals need to cover all the continuous values since the model cannot round up final average spore counts that may be fractional. Therefore, we partitioned the intervals in a way that they contain all the intended spore levels. For example, in reality category two represents milk with 53–203 spores, but the interval for this category is $[53.5001, 203.4999]$. Also, note that the current categories of raw milk consider spore levels between -4 and 7 log MPN/HGP. These values were based on the existing data (Masiello et al., 2017); however, if applicable to a particular processor, the raw milk categories could include even higher contamination levels.

Masiello et al. (2017) reported spore count data for 10 farms with data collected for each month in a year. After categorizing the data based on our five spore count intervals, we calculate that farms produce milk in one main category and its first and second-hand neighboring categories with probability 70, 20, and 10%, respectively. This means producers do not always produce milk in one category and it is possible for them to produce better or worse quality milk on some days depending on many on-farm factors.

We now explain how daily spore counts are generated for each producer. All random numbers are generated based on the spore count distribution of lognormal $(2.56, 0.99)$ MPN/HGP adapted from Buehler et al. (2018). For each day and producer (e.g., producer p with $PC = 4$), with a probability of 70%, we keep generating values until it is within the PC_p category, which is four for producer p . With a probability of 20%, the generated value is within the neighboring categories, which are three and five for producer p . With the remaining 10% probability, the value should be within the second-hand neighboring categories, which is just category two for producer p .

Daily weighted average of initial spore counts – The weighted average of spore counts on day d is calculated using the following formula. In this formula, we calculate the weighted average of absolute spore counts in MPN/HGP and then translate it back to the logarithmic format.

$$ISC_d^{avg} = \log_{10} \left[\frac{1}{\sum_{p \in P} NP_{dp}^d} * \sum_{p \in P} NP_{dp}^d * 10^{ISC_{dp}^d} \right] \quad \forall d \in D \quad (33)$$

In rare cases, the total number of spores in all collected milk can be less than the total number of packages of milk that day. In such a case, we assume that ISC_d^{avg} is equal to one spore in HGP for $TP_d - TP_d^0$ of the packages and zero for the remaining ones.

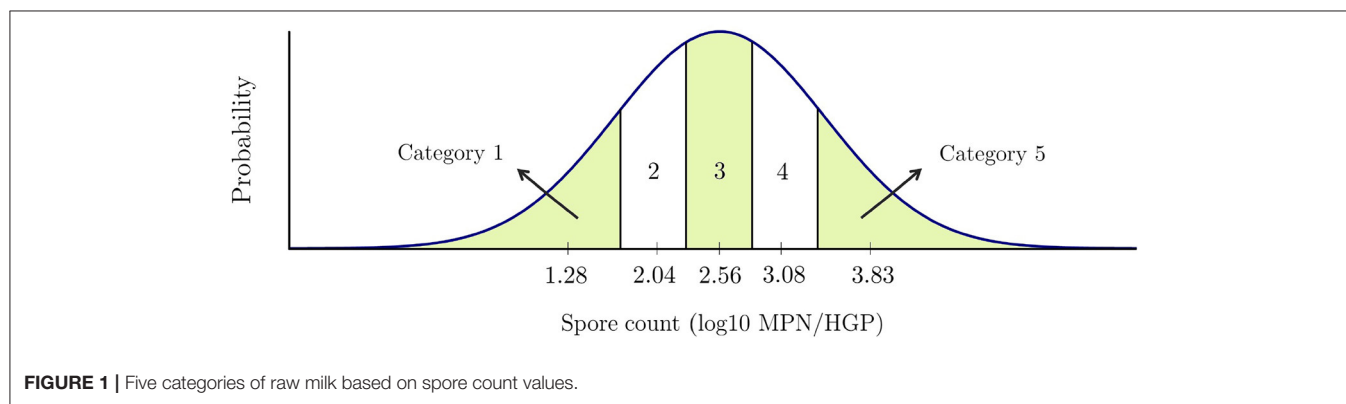
Parameters associated with MF and BF – The costs and spore reduction parameters associated with MF and BF are explained

TABLE 3 | Dairy cattle herd size by inventory and sales: 2017 (National Agricultural Statistics Service, 2019).

Herd size	50 to 99	100 to 199	200 to 499	500 to 999	1,000 to 2,499	2,500 to 4,999	5,000 and more
Number of farms	12,137	6,757	3,830	1,511	1,239	525	189
Relative Frequency (%)	46.3	25.8	14.6	5.8	4.7	2.0	0.7

TABLE 4 | Milk production for 24 selected states in the United States in 2018 (United States Department of Agriculture, 2019).

Month	Jan	Feb	Mar	Apr	May	Jun	Jul	Aug	Sep	Oct	Nov	Dec	Average
Monthly milk per cow (lb)	1,973	1,817	2,033	1,976	2,051	1,961	1,977	1,968	1,880	1,931	1,876	1,964	1,951
Average daily milk per cow (lb)	63.6	64.9	65.6	65.9	66.2	65.4	63.8	63.5	62.7	62.3	62.5	63.4	64.13

**FIGURE 1 |** Five categories of raw milk based on spore count values.**TABLE 5 |** Five categories of raw milk used for initial contamination data generation.

Category	Minimum value of spore count log10 MPN/HGP (MPN/HGP)	Maximum value of spore count log10 MPN/HGP (MPN/HGP)	Probability of a producer to be in this category
1	−4 (0.0001)	1.72836 (53.4999)	16%
2	1.72837 (53.5001)	2.30857 (203.4999)	20%
3	2.30858 (203.5001)	2.80990 (645.4999)	32%
4	2.80991 (9645.5001)	3.39217 (2466.9999)	14%
5	3.39218 (2467.0001)	7 (10000000)	18%

in the **Supplementary Material**. Note that all the costs associated with SRT units are translated into daily costs.

Daily budget – In the MSLOP, the processor has a fixed budget that can cover the costs of sample tests, premiums, and expenditures of SRTs' implementation and utilization. This budget can be provided by a few sources such as a possible existing budget for the current premium payments and the income they gain because of any extension in the shelf-life. Note that budgets for our case studies are solely provided by the first source and considering the profit that the processors might gain for any extension in the shelf-life is beyond the scope of this paper. We calculate the daily budget for different sizes of processors based on the data we obtained from our industry partners. The existing premium payment systems suggest that

processor pay \$2–\$3 for each 1000 lb of raw milk. We assumed small, medium, and large processors pay premiums up to \$3, \$2.5, \$2, respectively, for each 1000 lb of raw milk in a day (e.g., smaller processors may pay more because they have more personal relationships with their producers), but we appreciate that the relationship between processors size and premium payment may be different.

Premium/penalty systems – According to our experts, a spore test [e.g., test for aerobic bacterial spores (Frank et al., 2004)] of one raw milk sample costs \$25 in a laboratory; however, a contract lab charge is between \$10.75 and \$21 if asked to perform regular tests on multiple samples each week. Therefore, we assume each test's cost to be \$21, \$16, and \$11 if less than

10, between 11–20 and more than 21 weekly tests are requested, respectively.

On-farm intervention parameters – There are a variety of on-farm interventions that can result in supplying raw milk with a lower spore count. Producers with different milk quality can select from a variety of on-farm interventions to improve their milk's quality regardless of what category of milk they supply. In our models, we consider two different types of interventions that producers can apply in order to improve their raw milk quality. The first one includes interventions that start from day one and lasts until the intervention is ceased. We assume a reduction of $R_1^{PR} = 0.2 \log_{10}$ MPN/HGP for this intervention; examples of these interventions include (i) enhanced laundering of towels used in the milking parlor and (ii) training of milking parlor employees (Evanowski et al., 2020). The second one is a hypothetical repetitive intervention that gradually improves the milk quality by a small amount each year and continues reducing the spore counts by $R_2^{PR} = 0.05 \log_{10}$ MPN/HGP compared to the previous year. Note that for each of these two types, there are a variety of interventions from which producers with different milk quality can select. Even though high-quality milk producers may already be doing many of the on-farm interventions, due to the absence of data about their behavior and effectiveness of different interventions, we assume that they could implement additional strategies to further improve milk quality. This simplifying assumption should be tested when more data becomes available. Note that due to the limitation of all the units being in logarithmic values, in this model, we cannot have farm-specific values of reduction as it is impossible to calculate the final average spore levels by linear functions.

Given the on-farm interventions' impact and the differences between the spore levels of consecutive categories in **Table 5**, producers are able to improve their milk quality one category in the short run and two categories in the long run via on-farm interventions. In our model, we assume $\alpha = 0.7$ and $\beta = 0.3$ since intuitively it takes less time (e.g., 1–2 years) and effort for a producer to improve their raw milk to be in the next better category and remain there for a long time until they can reach the next category which for our purposes we assume can take up to 5 years. Note that when generating the data for the daily ISCs of each producer, the probability of the spore counts being in the producer's main category was equal to 0.7. That is also why the effort to reach the next category is 0.7 compared to 0.3 for the second next category. Also, in the long run, it is unlikely that producers would improve their milk more than two categories as it requires more than 1 \log_{10} MPN/HGP spore reduction and this would be challenging unless they had very high initial spore contamination levels. Thus, just the two next categories' premiums are the ones with which the producers are concerned.

Since \hat{PR} represents how much producers are motivated by the premium for just one HGP of milk, its value going to be small, so we need to scale its impact by multiplying it by a scaling factor (i.e., a_q). In order to estimate this value, we assume \hat{PR} to be exactly the same as the current average premiums; that is \$2–3 for 1000 lb or \$0.0083–0.0125 for an HGP. Considering

the middle range of \$0.01 for \hat{PR} , a_q has to be equal to 100, so that for each $\hat{PR} * a_q = 1$, one reduction of R_q^{PR} occurs. Thus, in our model, $a_q = 100$ for both of the on-farm interventions. We also set \hat{PR}^{max} to be 0.02 so that $\hat{PR} * a_q$ do not exceed two. This means the premium payments' impact has a limit (i.e., $\leq 2R_q^{PR}$ for intervention q) on the reductions resulted from the on-farm interventions. PR^{max} is also considered to be equal to 0.1, which means a premium for a CWT cannot exceed \$2.4. Based on the current premium/penalty system values \$2.4 is a fairly large upper bound for the premiums.

Generated instances – We present 24 generated instances (representing 24 processors) in **Table 6**. These instances mainly vary in parameters: (i) processor size, (ii) number of producers, and (iii) planning horizon. Among these 24 instances, there are eight cases each for small (i.e., S1–S8), medium (i.e., M1–M8), and large (i.e., L1–L8) processors. Note that the size of the problems are based on the annual lb of processed milk by the processor explained earlier in this section. For each of the three processor size categories, we selected two numbers as the annual lb of milk processed (i.e., 4M, 8M, 40M, 70M, 100M, and 150M) and generated instances for planning horizons of 5 and 10 years. Then, for each of the combinations, we generated two instances, one with a lower and one with a higher number of producers (e.g., instances M1 and M2 have three and nine producers, respectively).

The maximum penalty for these instances is considered to be \$0.6 per 100 lb of raw milk in category five. Finally, based on the number of producers and the daily volume of milk that needs to be processed, the daily budget and costs (e.g., test costs, MF costs) are determined, as shown in the remaining columns of the table. In the next section, the optimal solutions of the model for these instances are presented. All optimization problems were conducted on a 6-core 16 GB computer in Python using Gurobi 8.1.1. with a time-limit of one hour. Note that due to reasonable solving time of the problems with a standard solver (i.e., Gurobi), it was not deemed necessary to develop a new solution approach for this application paper.

2.3.2. Monte Carlo Model

In order to predict the shelf-life of packaged milk which is contaminated with a given level of spores, we first determine the category of milk for this level of spore contamination and then assume its shelf-life is equal to the shelf-life of the representative point of that category. To this end, we first calculate the shelf-life for the representative points of the five categories of raw milk, shown in **Figure 1**, by using a Monte Carlo simulation model in R software adapted from the model in Buehler et al. (2018). This model is further explained in the **Supplementary Material**. In our adaptation of the model by Buehler et al. (2018), the underlying Monte Carlo simulations are based on exactly the same parameters with the only exception that the initial contamination level of spore-formers was used as a set of fixed values shown in **Table 7** instead of a probability distribution. This change allowed us to reduce the number of iterations from 100,000

TABLE 6 | Instance data.

Instance number	Annual lb of processed milk (lb/yr)	Planning horizon (yr)	Number of producers	B (\$/day)	TC (\$)	FC^{MF} (\$/day)	VC^{MF} (¢/HGP)	FC^{BF1} (\$/day)	VC^{BF1} (¢/HGP)	FC^{BF2} (\$/day)	VC^{BF2} (¢/HGP)
S1	4M	5	1	33	21	344	0.013	95	0.039	95	0.039
S2	4M	5	2	33	21	344	0.013	95	0.039	95	0.039
S3	4M	10	1	33	21	344	0.013	95	0.039	95	0.039
S4	4M	10	2	33	21	344	0.013	95	0.039	95	0.039
S5	8M	5	1	66	21	344	0.013	95	0.039	95	0.039
S6	8M	5	3	66	21	344	0.013	95	0.039	95	0.039
S7	8M	10	1	66	21	344	0.013	95	0.039	95	0.039
S8	8M	10	3	66	21	344	0.013	95	0.039	95	0.039
M1	40M	5	3	274	21	344	0.013	95	0.039	110	0.029
M2	40M	5	9	274	21	344	0.013	95	0.039	110	0.029
M3	40M	10	5	274	21	344	0.013	95	0.039	110	0.029
M4	40M	10	9	274	21	344	0.013	95	0.039	110	0.029
M5	70M	5	5	479	21	619	0.010	110	0.029	120	0.019
M6	70M	5	8	479	21	619	0.010	110	0.029	120	0.019
M7	70M	10	6	479	21	619	0.010	110	0.029	120	0.019
M8	70M	10	10	479	21	619	0.010	110	0.029	120	0.019
L1	100M	5	3	548	21	619	0.010	110	0.029	163	0.013
L2	100M	5	11	548	16	619	0.010	110	0.029	163	0.013
L3	100M	10	7	548	21	619	0.010	110	0.029	163	0.013
L4	100M	10	14	548	16	619	0.010	110	0.029	163	0.013
L5	150M	5	8	822	21	619	0.010	120	0.019	163	0.013
L6	150M	5	17	822	16	619	0.010	120	0.019	163	0.013
L7	150M	10	9	822	21	619	0.010	120	0.019	163	0.013
L8	150M	10	24	822	11	619	0.010	120	0.019	163	0.013

to 50,000, while still being able to effectively sample the whole probability space (this was confirmed by obtaining the same predictions in simulations ran with five different random seeds).

For the five raw milk categories shown in **Figure 1**, we determine representative points whose cumulative distribution functions are equal to 0.1, 0.3, 0.5, 0.7, and 0.9. For example, category 2 is the interval [1.73, 2.31] with 2.04 as its representative point. Running our Monte Carlo model for each of the five representative points' values, the predicted shelf-lives are 26, 25, 24, 22, 20 days, respectively. After examining other values of ISCs with the simulation model, we notice considerable differences between shelf-lives of category one's values and the other categories. Since implementing SRTs will result in lower levels of spore counts in packaged milk compared to raw milk, we took a closer look at the category 1 and tried multiple values of ISCs other than its representative point. We break down category one into four subcategories making the total number of subcategories for packaged pasteurized fluid milk's bacterial counts equal to eight. **Table 7** presents the details of the eight categories and their assigned shelf-lives obtained from the Monte Carlo simulation model.

3. RESULTS

In this section, we present the results of the proposed models for the 24 case studies (instances), described in section 2.3, and sensitivity analysis for the main parameter of each model.

3.1. Computational Results of MSLOP

Table 8 shows the optimal solutions of the MSLOP model for the 24 instances. In columns 2-6, we show the percentages of annual milk volume in each category. These percentages help us better understand the relationship between the distribution of raw milk in different categories and the premium values in the optimal solutions. The details of the optimal solutions, the optimal objective values, and the solution times are presented in columns 8-16, 17, and 18, respectively. The solutions include whether or not the processors should implement any of the SRTs or pay premiums, and the premium they should pay for each category of raw milk. Note that a blank cell means the value of the corresponding variable is zero in the optimal solution. We also compute the optimal objective value assuming no intervention is implemented, which is shown in column 19. In the last column, the increases in the objective values when interventions are allowed are shown.

TABLE 7 | Eight categories of packaged milk used for shelf-life calculation.

Category	\bar{C}^{min} - log10 CFU/HGP (CFU/HGP)	\bar{C}^{max} - log10 CFU/HGP (CFU/HGP)	Representative point's bacterial count log10 CFU/HGP (CFU/HGP)	Shelf-life (day)
1	-10 (≥ 0)	-0.30111 (0.4999)	-4 (0.0001)	34
2	-0.30112 (0.5001)	0.17610 (1.4999)	0.0000 (1)	28
3	0.17611 (1.5001)	0.81291 (6.4999)	0.7282 (6)	27
4	0.81292 (6.5001)	1.72836 (53.4999)	1.4771 (30)	26
5	1.72837 (53.5001)	2.30857 (203.4999)	2.0414 (110)	25
6	2.30858 (203.5001)	2.80990 (645.4999)	2.5587 (362)	24
7	2.80991 (9645.5001)	3.39217 (2466.9999)	3.0777 (1196)	22
8	3.39218 (2467.0001)	7 (10000000)	3.8275 (6722)	20

Looking at the optimal solutions' details, it seems that the majority of the small processors do not have enough budget to implement any of the SRTs and they mainly take advantage of the premium/penalty system to improve their raw milk quality. Note that except for instance S7, all the small processors need to apply penalties for the least desirable milk. This means that the premium payments for categories 1-4 are sourced by the processors' available daily budgets and the income gained from the applied penalties. The only small processor that did not implement any of the interventions, including the premium/penalty system, is instance S7. In this instance, the optimal objective value does not change when we allow the implementation of the interventions. This is because the processor in instance S7 is already supplied by raw milk with good quality (i.e., 51 and 28% of its supplied raw milk volume is in categories 1 and 2, respectively). On the other hand, the processor in instance S8, which has the same budget, is supplied by producers whose milk is in categories with lower qualities (i.e., 53 and 24% of their supplied milk is in categories 5 and 4, respectively). This allows the processor to take advantage of the premium/penalty system. The gained income from the penalty application allows them to implement double-BF to improve the milk's shelf-life. Note that its best weighted average shelf-life is more than that of instance S7. This means the optimal strategies are highly dependent on the structure of the supplied raw milk's quality and can increase the average shelf-life up to 5.2. days.

Comparing different medium processors, we can infer that all the processors should take advantage of the premium/penalty system. However, whether or not they should implement SRTs varies amongst these processors. For example, the processors for instances M1, M2, M4, M5, and M7 need to implement MF or double-BF. The optimal weighted average shelf-lives of these five instances are between 28.3 and 31 days. Other medium-sized processors' optimal solutions suggest implementing both MF and double-BF so that they can reach higher shelf-life (i.e., 34 days). This means that the other five medium processors the budget (including the income obtained from the penalties) was restricting the average shelf-life.

In the larger instances, except for L3 and L4, the processors use the premium/penalty system, apply the maximum penalty, and implement MF and double-BF resulting in a maximum weighted average shelf-life of 34 days; however, premiums are different as

the quality of raw milk is different. In the two instances, L3 and L4, they just use MF which is still adequate for L4 to obtain the 34 days of shelf-life. This means that many of the larger processors either have a large budget or, if raw milk quality is poor, the resulting income from penalties may be used to implement both MF and double-BF.

Overall, the computational results suggest that optimal solutions for the small processors are mostly focused on the premium/penalty system rather than implementing SRTs due to their costly implementations; however, depending on their supplied milk's quality, penalizing the producers can allow them to implement SRTs, which will increase the maximum weighted average shelf-life. Medium processors' best solutions showed to be the most variable. This means that the optimal strategic decisions are highly dependent on the processors' specific situation, including raw milk quality and the processor's budget. The optimal solutions for the medium-sized processors show shelf-life increases between 5.1 and 13.3 days compared to the cases where no intervention is allowed. Larger processors showed to have the most similar results. Due to their high volumes of processed milk, which allow them to have a higher budget, and penalizing producers with undesirable quality of raw milk, which provide them with more income, most of them can reach the maximum possible weighted average shelf-life, which are 7.5–12. days more than when no intervention is allowed.

3.2. Computational Results of MPBOP

Table 9 shows the optimal solutions of the MPBOP model for the 24 instances. The MPBOP model varied when compared to the MSLOP model by targeted shelf-life which is the fixed value of 28 days for the MPBOP model. Note that all instances were solved in less than an hour except for L7 and L8; however, the final integer solution for those instances are included in the table.

To reach the shelf-life of 28 days, small processors require to allocate between \$94.0 and \$287.0 per day. Not all of them are required to use the premium/penalty system but they all need to use at least one of the SRTs. The objective values for the medium and large processors, varies between \$122.2–\$521.5 per day and \$0–\$489.8 per day, respectively. They are all required to use the premium/penalty system and at least one of the SRTs. An interesting case in **Table 9** is instance L5 which does not need to allocate any budget to extend its milk shelf-life to 28 days. Since

TABLE 8 | Computational results - MSLOP model.

Instance number	Raw milk lb in categories (%)					<i>B</i> (\$/day)	x^{MF}	x^{BF1}	x^{BF2}	x^{PR}	Premiums (¢/CWT)					Best OFV (day)	Running time (s)	OFV of NI ^a case (day)	Increase ^b (day)
	1	2	3	4	5						1	2	3	4	5				
S1	2	5	71	14	8	33				1	142				-60	24.8	3	23.8	1.0
S2	32	42	18	7	0	33				1	32					25.7	0	25.2	0.5
S3	2	7	70	14	8	33				1	36	36			-60	25.1	34	23.8	1.3
S4	29	19	16	31	5	33				1	26	26	26		-60	25.0	4	24.1	0.9
S5	5	65	12	17	0	66				1	44				-60	25.7	1	24.8	0.9
S6	1	6	42	41	10	66				1	214				-60	24.1	7	22.5	1.6
S7	51	28	22	0	0	66										25.8	0	25.8	0.0
S8	0	2	21	24	53	66			1	1	87				-60	26.2	186	21.0	5.2
M1	3	44	33	16	3	274			1	1	36				-60	31.0	17	24.1	6.9
M2	3	23	27	16	31	274	1			1	20				-60	28.3	60	21.5	6.8
M3	0	5	11	28	56	274	1		1	1	76	1	1		-60	34.0	102	20.7	13.3
M4	4	24	27	22	24	274	1			1	9				-60	28.8	1349	21.9	6.9
M5	2	13	30	46	9	479			1	1	105				-60	27.8	82	22.7	5.1
M6	5	11	9	16	59	479	1		1	1	19	6	6	6	-60	34.0	27	21.2	12.8
M7	7	13	47	12	20	479	1			1	3	3			-59	28.7	789	22.1	6.6
M8	3	6	25	36	30	479	1		1	1					-60	34.0	1465	21.1	12.9
L1	2	11	45	15	28	548	1		1	1	29	1			-60	34.0	33	21.9	12.1
L2	1	13	40	17	28	548	1		1	1	1				-60	34.0	234	21.4	12.6
L3	26	22	22	17	14	548	1			1	2	2	2	2	-60	30.4	706	22.9	7.5
L4	22	19	21	17	21	548	1			1	4	4	4	4	-60	34.0	2155	22.1	11.9
L5	1	3	17	15	63	822	1		1	1	203	5	5		-60	34.0	39	21.1	12.9
L6	2	21	32	29	16	822	1		1	1	13					34.0	57	21.8	12.2
L7	2	6	50	23	19	822	1		1	1	12	12			-60	34.0	31	21.6	12.4
L8	3	14	33	29	21	822	1		1	1	10				-60	34.0	1308	21.3	12.7

^aNI: no intervention is implemented.^bIncrease: the increase in the OFV (difference between columns 17 and 19).

they process a large volume of milk 63% of which is in category five, the money they gain through the penalties is enough for implementing SRTs.

Comparing the results between the two models, it is noticed that when maximizing the shelf-life, many of the medium and large processors use double-BF and never use single-BF while in MPBOP, single-BF is more popular, and double-BF is used mostly in smaller processing facilities. This is because the targeted shelf-life is 28 days and the processors do not demand the milk's shelf-life to be more; thus, they do not need to spend more on the second round of bactofugation to reach a lower level of spore counts. Another main difference between the two models is that premiums are paid less for categories 1-4 milk and in most of the cases, they are just used to penalize suppliers who produce milk in category five.

3.3. Sensitivity Analysis

In this subsection, we analyze the sensitivity of the two models to two important parameters. **Table 10** shows the sensitivity of the MSLOP model to parameter PR^{min} and **Table 11** shows the sensitivity of the MPBOP model to parameter SL^{min} .

We perform sensitivity analysis to examine the sensitivity of optimal solutions in MSLOP for the maximum allowable

penalty, PR^{min} , since the total acquired penalty is proportional to parameter PR^{min} and the volume of milk processed. The former can be changed by the managers at the processing facilities in the MSLOP model; therefore, it can alter the best strategies in the optimal solutions for different problem sizes. We solve five instances S6, S8, M2, L3, and L5, described in section 2.3, for different values of PR^{min} (see **Table 10**). The five instances are solved with maximum penalties of \$0, \$0.3, \$0.6, and \$0.9 per 100 lb, shown in the second column of the table. The details of the optimal solutions and the effects of the changes in PR^{min} on the optimal objective values are shown in columns 4-13 and 14, respectively. Note that the percentages of raw milk in category five (which incurs a penalty) for these instances are 10, 53, 31, 14, and 63% for instances S6, S8, M2, L3, and L5, respectively.

Comparing the results for small instance S6, we conclude that applying penalties has a very small impact (i.e., up to 0.1 days) on the maximum weighted average shelf-life. This is because only 10% of the milk is in category five. However, the results for the second small instance, S8, is different since the majority (i.e., 53%) of its supplied milk represents the lowest quality category. Applying penalties for this instance improves the objective value between 3.6 and 3.8 days. This means that even if the total volume

TABLE 9 | Computational results - MPBOP model.

Instance	Raw milk lb in categories (%)					SL^{min}	x^{MF}	x^{BF1}	x^{BF2}	x^{PR}	Premiums (¢/CWT)					Best OFV	Running	OFV of NI ^a	Increase ^b
number	1	2	3	4	5	(day)					1	2	3	4	5	(\$/day)	time (s)	case (day)	(day)
S1	2	5	71	14	8	28			1	1	24				–60	95.8	72	23.8	4.2
S2	32	42	18	7	0	28			1							94.0	36	25.2	2.8
S3	2	7	70	14	8	28			1	1					–60	94.8	487	23.8	4.2
S4	29	19	16	31	5	28			1							94.0	260	24.1	3.9
S5	5	65	12	17	0	28			1							96.1	28	24.8	3.2
S6	1	6	42	41	10	28			1	1	207				–60	154.5	114	22.5	5.5
S7	51	28	22	0	0	28		1								88.0	37	25.8	2.2
S8	0	2	21	24	53	28	1			1	118				–60	287.0	17.94	21.0	7
M1	3	44	33	16	3	28			1	1	1				–60	122.2	58	24.1	3.9
M2	3	23	27	16	31	28	1			1	11				–60	242.7	242	21.5	6.5
M3	0	5	11	28	56	28	1	1		1					–60	127.3	679	20.7	7.3
M4	4	24	27	22	24	28	1			1					–60	248.9	1515	21.9	6.1
M5	2	13	30	46	9	28	1			1					–60	521.5	169	22.7	5.3
M6	5	11	9	16	59	28	1	1		1					–60	262.0	171	21.2	6.8
M7	7	13	47	12	20	28	1			1					–60	443.5	695	22.1	5.9
M8	3	6	25	36	30	28	1	1		1					–60	456.3	1584	21.1	6.9
L1	2	11	45	15	28	28	1			1					–60	266.5	143	21.9	6.1
L2	1	13	40	17	28	28	1			1	23				–60	400.4	650	21.4	6.6
L3	26	22	22	17	14	28	1			1					–60	489.8	571	22.9	5.1
L4	22	19	21	17	21	28	1			1					–60	440.9	1143	22.1	5.9
L5	1	3	17	15	63	28	1	1		1					–60	0.0	69	21.1	6.9
L6	2	21	32	29	16	28	1			1	7				–60	390.4	776	21.8	6.2
L7	2	6	50	23	19	28	1			1					–60	381.2	3600 ^c	21.6	6.4
L8	3	14	33	29	21	28	1	1		1					–60	397.7	3600 ^c	21.3	6.7

^aNI: no intervention is implemented.^bIncrease: the intended increase in the OFV (difference between columns 7 and 19).^cGap between the upper and lower bounds = 100%.

of processed milk is relatively low, the quality of milk plays an important role in applying penalties.

The impact of the penalty parameter is more significant for the medium-sized processor, M2. The maximum weighted average shelf-life shows that the optimal objective value will suffer 1.5 (= 28.3 – 26.8) days if the original maximum allowable penalty is cut in half (i.e., \$0.6 to \$0.3) and 1.6 days if the penalty is not applied. In both of these cases, the optimal solutions suggest implementing double-BF instead of MF and paying higher premiums. On the other hand, increasing the penalty by \$0.3 per 100 lb only improves the objective value by 0.2 (= 28.5 – 28.3) days; this means applying more penalty does not always result in significant improvement in the shelf-life and the processors need to investigate the impacts of different levels of penalties with this model to decide what level of penalty works best for them without penalizing producers more than required.

We purposefully selected two different instances in categories of small and large processors from **Table 6** so that we have two small and two large instances with a smaller percentage of low milk quality (i.e., S6 and L3) and two with a larger percentage of milk with low-quality (i.e., S8 and L5). In contrast with the two small instances, we observe different changes in the objective

values for the two larger instances. L3, in which only 14% of milk in category five, benefits from applying penalties more than L5, which is supplied 63% by low-quality milk. Applying penalties for instance L5 can only increase the average shelf-life by 0.1 days whereas in L3, applying a small amount of penalty can improve the objective value by 2.8 days. This happens because the volume of milk processed by L5 is higher, hence they have assigned more budget to increase their shelf-life. The results for L5 show that it is not always the best action to penalize producers even when the majority of the supplied milk is in category five.

Overall, the sensitivity analysis of the maximum allowable penalty parameter shows that its impact is highly dependent on the quality of the supplied milk and the assigned budget by the processor which is relative to the total volume of processed milk.

In the MPBOP model, parameter SL^{min} , minimum shelf-life, defines the main limitation of the problem. Therefore, we perform sensitivity analysis for three instances, S6, M5, and L1, with three values of 26, 28, and 30 days for this parameter (see **Table 11**). The second column of the table shows the minimum shelf-life for each problem and the last column presents the difference in the objective value of each problem to that of the

TABLE 10 | MSLOP sensitivity to parameter PR^{min} .

Instance number	PR^{min} (\$/CWT)	B (¢/day)	x^{MF}	x^{BF1}	x^{BF2}	x^{PR}	PR_1 (¢/CWT)	PR_2 (¢/CWT)	PR_3 (¢/CWT)	PR_4 (¢/CWT)	PR_5 (¢/CWT)	OFV (day)	Diff ^a
S6	0	66				1	210					24.0	0.0
	-0.3	66				1	214				-30	24.0	0.0
	-0.6	66				1	214				-60	24.1	0.1
	-0.9	66				1	217				-90	24.1	0.1
S8	0	66				1	31	31	31	31		22.6	0.0
	-0.3	66			1	1	87				-30	26.2	3.6
	-0.6	66			1	1	87				-60	26.2	3.6
	-0.9	66			1	1	172				-90	26.4	3.8
M2	0	247				1	1	39				26.7	0.0
	-0.3	247				1	1	47			-30	26.8	0.1
	-0.6	247	1			1	20				-60	28.3	1.6
	-0.9	247	1			1	27				-90	28.5	1.8
L3	0	548				1	1	13	13	13		27.4	0.0
	-0.3	548	1			1	1	1	1	1	-30	30.2	2.8
	-0.6	548	1			1	2	2	2	2	-60	30.4	3.0
	-0.9	548	1			1	3	3	3	3	-90	30.5	3.1
L5	0	822				1	1	25				33.9	0.0
	-0.3	822	1			1	1	160			-30	34.0	0.1
	-0.6	822	1			1	1	203	5	5	-60	34.0	0.1
	-0.9	822	1			1	1	33	33	33	-60	34.0	0.1

^aDiff: the difference between the current OFV and the OFV when no penalty is applied.

TABLE 11 | MPBOP sensitivity to parameter SL^{min} .

Instance number	SL^{min} (day)	x^{MF}	x^{BF1}	x^{BF2}	x^{PR}	PR_1 (¢/CWT)	PR_2 (¢/CWT)	PR_3 (¢/CWT)	PR_4 (¢/CWT)	PR_5 (¢/CWT)	OFV (day)	Diff ^a
S6	26				1					-60	94.2	-60.3
	28				1	207				-60	154.5	0.0
	30	1				47				-60	316.4	161.9
M2	26				1	47				-60	27.4	-215.3
	28	1			1	20				-60	242.7	0.0
	30	1	1	1	1	27				-60	315.1	72.4
L1	26				1					-60	0.0	-266.5
	28	1			1					-60	266.5	0.0
	30	1		1	1					-60	384.5	118.0

^aDiff: the difference between the current OFV and the OFV when $SL^{min} = 28$.

problem where $SL^{min} = 28$. The rest of the table is similar to **Table 10**.

As seen in this table, 2 days difference in the targeted shelf-life can have a significant impact on the amount of required budget. This difference varies for different processors. For example, if the processor in instance S6 decides to have a 26-day shelf-life, then they can spend \$60.3 per day less compared to when they targeted 28 days of shelf-life. On the other hand, it will cost them an additional \$161.9 to increase the shelf-life by 2 days. Therefore, the MPBOP model provides dairy processors a tool by which they can determine the increase in costs when aiming for a higher shelf-life compared to their product's current shelf-life. Such information would allow them

to evaluate whether or not each day of shelf-life extension is profitable for them depending on their knowledge of how much additional income they can gain by each day of extension in the shelf-life.

3.4. Use of MSLOP and MPBOP Models Simultaneously

It should be noted that the models are meant to be used separately since they solve two different problems [i.e., when the processor has (i) a limited budget or (ii) a shelf-life threshold]. However, processors with limited budgets can also take advantage of both models simultaneously. In order to use both models, the

processor would first use the MSLOP model to reach the optimal value of shelf-life they can obtain with their limited budget. Then, they feed the obtained optimal shelf-life value (or a rounded down value) as an input value to MPBOP model and see if they can reach that shelf-life threshold with a lower value of budget. Running both models for problem instances S6, S8, M2, L3, and L5, we found that larger processors who typically have higher budget values can take advantage of this and optimize interventions to reach the same shelf-life with a reduced budget. Among the five instances, only processor L5 could benefit from running both models. Instead of spending a budget of \$822/day, processor L5 can spend \$672.2/day to reach the same value of shelf-life (i.e., 34 days).

4. DISCUSSION

In this study, we developed two models to facilitate decision-making for dairy processors. Specifically, the MSLOP model can be used to determine the maximum shelf-life that can be reached within a processor's defined budget (e.g., \$100/day), whereas the MPBOP can be used to assess the minimum cost of reaching a set shelf-life target (e.g., 21-day shelf-life). In total, 24 case studies, varying by (i) processor size (i.e., small, medium, or large) and its annual lb. of milk processed, (ii) number of producers and the quality of milk they supply to the processors with respect to contamination with spores of Psychrotolerant bacteria, (iii) processor's budget for shelf-life improvement, and (iv) planning horizon (i.e., 5 or 10 years), were evaluated for both the MSLOP model and the MPBOP model, respectively (Table 6). Overall, our findings showed that the optimal solutions across the case studies appear to differ by processor size and are determined by the quality of raw milk with which processors are supplied, giving rise to processor-specific optimal combinations of the proposed premium/penalty system and SRT interventions. As such, the developed models provide a novel tool that will aid processors in the optimization of their pasteurized fluid milk's shelf-life.

4.1. Optimal Combinations of the Proposed Novel Premium/Penalty System and SRT Interventions Are Processor-Specific

Fluid milk processors who aim to extend product shelf-life need evidence-based solutions that are optimal for their raw milk supply and processing characteristics. Our previous studies have shown nearly 50% of HTST pasteurized fluid milk spoils due to sporeforming bacteria (Alles et al., 2018; Reichler et al., 2018); however, the reasons for spoilage vary within a facility across time and among products (Murphy et al., 2021). Our study specifically addresses needs of processors whose product is primarily spoiled by psychrotolerant sporeforming bacteria (i.e., not dealing with spoilage issues due to post-pasteurization contamination). Optimal solutions differed considerably between the small, medium and large processors (referred to in our models as "instances"), and they were the most diverse across the medium-sized processors.

Notably, our findings demonstrate that premium/penalty systems are often beneficial for processors targeting shelf-life extension through the reduction of spores in their raw milk. However, the optimal system to implement will depend on a number of processor-specific factors (e.g., expected quality of the raw milk supply, volume of milk processed, and available budget). Based on our findings, we recommend that fluid milk processors seeking to extend shelf-life by reducing spore levels in raw milk, consider implementation of premium/penalty systems based on raw milk spore count. Given this novel finding, it is necessary to discuss the value and potential implications of implementing a premium/penalty system for both processors and producers.

Previous studies support that premiums and penalties are used as a tool to motivate producers (e.g., Sargeant et al., 1998; Valeeva et al., 2007; Nightingale et al., 2008). While there are examples of premium payment systems for low-spore raw milk (Visser et al., 2007a,b), the majority of studies evaluating aspects of quality-based premium payment programs for raw milk focus on somatic cell count (Sargeant et al., 1998; Nightingale et al., 2008; Botaro et al., 2013; Volpe et al., 2016). In practice, these systems may include only penalties for low-quality raw milk (Sargeant et al., 1998), only premiums for high-quality raw milk (Nightingale et al., 2008), or a combination of penalties and premiums (Botaro et al., 2013; Volpe et al., 2016). For example, Nightingale et al. (2008) evaluated the impact of a premium payment system implemented by a large United States milk cooperative, which paid producers a premium for supplying raw milk with a low somatic cell count (<100,000 cells/mL), and found that implementing premiums was effective in reducing mean somatic cell counts in overall raw milk supplied to the cooperative. Nightingale et al. (2008) also reported that only relatively high premium levels provided enough incentive for producers to lower somatic cell counts in their raw milk; thus, the authors recommended that a combined penalty and premium payment program would be most effective for motivating producers to strive toward reducing somatic cell counts in their raw milk. Considering our findings, the design of such a premium/penalty system based on spore levels in raw milk should be processor-specific. While penalties may provide motivation to producers, there also could be unforeseen consequences of such a system (e.g., potential for negative impact on producer-processor relationship), which should be considered. Importantly, our study showed that the impact of applying a penalty, as part of a premium/penalty system, will not always have a significant impact on shelf-life. Thus, prior to implementing a system that includes a penalty for low-quality raw milk, a processor should assess the potential impacts of different levels of penalties (e.g., using our MSLOP model) to decide the appropriate level of penalty that will benefit the processor while without penalizing producers more than is required. Overall, implementing a premium/penalty system may be relatively attainable especially for processors with restricted budgets below what is needed to implement an SRT. For an individual processor that considers implementing a premium/penalty system based on spore levels in their supplied raw milk, we recommend our models be used to assess the optimal design of this system to maximize the processor's

budget (using the MPBOP model) and/or to achieve a target shelf-life (using the MSLOP model). It should be noted that for such processors, we recommend baseline spore levels of the incoming raw milk be determined (e.g., to be used as an input for expected raw milk quality in our models), prior to implementation.

Installing, operating, and maintaining SRTs are expensive (e.g., the purchasing cost of a MF unit is \$1-2M); therefore, it can be challenging for processors to decide to implement an SRT in their facility. Our findings suggest that a processor aiming to greatly extend the shelf-life of their HTST fluid milk will need to invest in one or multiple SRTs in order to achieve the desired shelf-life. Again, it is important to emphasize that this finding only applies to processors with milk consistently spoiling due to sporeforming bacteria and not due to post-pasteurization contamination. In particular, for small processors, implementing a SRT is often not economically feasible and thus, providing a premium for the highest quality raw milk and/or a penalty for the lowest quality raw milk has been shown here a more affordable option in some cases. While not considered in our case studies, a processor may have reasons to invest in the SRT technologies that are not motivated by extension of their pasteurized milk shelf-life. For example, MF is used in cheese making to increase cheese yield and thus, increase profit (Papadatos et al., 2002). This means certain processors may already have a MF unit for other purposes. An advantage of our models is their capability of being customized for the processors who already implemented one of the SRTs. This means by changing the cost parameters and fixing the associated variables (e.g., $x^{MF} = 1$ if they already implemented MF), they can address and assess their specific processing situation.

4.2. The Developed Models Provide a Novel Tool for Processors to Optimize Shelf-Life of Pasteurized Fluid Milk

Our study provides two novel mixed-integer linear programming models that can be used as decision support tools for dairy processors to set economically rational shelf-life targets for their final products. Importantly, our two MILP models are capable of providing decision support for individual dairy processors by applying processor-specific parameters. Thus, managers can use our models to reach their optimal strategies in regards to maximizing the weighted average shelf-life depending on their available budget (MSLOP) or minimizing their budget depending on their targeted weighted average shelf-life (MPBOP).

In contrast to our study, most optimization models developed for perishable agri-foods lack the consideration of the shelf-life aspect. For example, Papadatos et al. (2002, 2003) developed non-linear optimization models to investigate how MF can be used to increase cheese yield and increase the revenue without considering its impact on the shelf-life. Regarding agri-food planning models, Ahumada and Villalobos (2009) suggest shelf-life is often excluded from planning models because shelf-life features complicate the problem. Yet, it is obvious that shelf-life

has major practical implications for the dairy industry and thus should be considered when developing models for perishable foods. As such, our models specifically focus on maximizing shelf-life that is directly influenced by microbial aspects of raw milk quality. It is well-established that a major cause of spoilage in many perishable foods is due to microorganisms. However, the majority of previous studies including optimization models targeting the shelf-life of dairy products (e.g., Lütke Entrup et al., 2005; Bilgen and Çelebi, 2013), such as studies focusing on how dairy products can gain the maximum profit by considering the operations scheduling, transportation, and distribution aspects of the milk supply chain, do not address the impact of microbial contamination on product shelf-life. For example, Lütke Entrup et al. (2005) developed a mathematical model that maximized the contribution margin considering a shelf-life-dependent pricing component in the yogurt supply chain, but did not address the impact of spoilage microorganisms on product shelf-life. Similarly, Bilgen and Çelebi (2013) optimized an integrated production scheduling and distribution planning for a yogurt supply chain and maximized the profit by taking into account the shelf-life-dependent pricing component and costs such as processing, storage, and transportation costs, but also did not consider the impact of microorganisms on product shelf-life. Thus, this paper presents a valuable foundational approach for studying optimization models for milk and other food supply chains in which microorganisms play a crucial role in diminishing the shelf-life and/quality of the food.

We acknowledge that there were limitations in defining the problem and parameterization of the models in this work. In particular, an intervention study is necessary to establish an understanding of the actual impact a premium/penalty system would have on the spore levels in raw milk at the processing level. Additionally, while the impact of individual MF and BF on spore levels in raw milk has been studied, the impact of combining MF and BF in a facility, needs to be investigated. It should be noted that the scope of our models was limited to the spore-forming bacteria in raw milk; however, our models could be adapted in the future to consider other spoilage microorganisms (e.g., whose source is contamination during processing). Also, due to the novelty of the proposed premium payment system, no suitable data were available for validation of that component of our optimization models. However, other components of our optimization models were based on synthesis of published data and models, including the Monte Carlo model that has been validated in Buehler et al. (2018). Additionally, as also mentioned in Section 2.3.2, our optimization models as presented in this study incorporated the output of predicted shelf-life of packaged milk from a Monte Carlo model (Buehler et al., 2018). The Monte Carlo model had limitations that, in turn, impacted our optimization models. Specifically, the Monte Carlo model had an assumption of constant storage temperature across the milk supply chain; version 2 of the Monte Carlo model, which is currently under development, will allow for modeling of temperature variation, which will in turn, allow for further development of our optimization models to include this feature. Finally, a more

comprehensive model should be developed to consider the monetary impact of extension in the shelf-life, by considering shrinkage caused by the SRT units (which was omitted here) and evaluating the overall Return on Investment for shelf-life extension.

5. CONCLUSION

In this paper we propose a new raw milk premium/penalty system structure based on levels of psychrotolerant spores in raw milk, a microbiological agent which limits the shelf-life of conventionally pasteurized fluid milk products. Our novel approach, which combines microbiology and operations research in the form of two mixed-integer linear programming models is aimed at addressing these shelf-life limitations from the dairy processors' perspective. Using our models, processors of various sizes, with unique processing parameters and distinct raw milk supplies, will be able to optimize their available budgets to obtain shelf-life goals. These decision support tools will ultimately allow processors to reach new markets, improve distribution efficiencies and provide consumers with long-lasting, high quality dairy products. The future development of a user-friendly interface will facilitate more widespread use of these models.

DATA AVAILABILITY STATEMENT

The raw data supporting the conclusions of this article will be made available by the authors, without undue reservation.

REFERENCES

- AhmadBeygi, S., Cohn, A., and Weir, M. (2009). An integer programming approach to generating airline crew pairings. *Comput. Oper. Res.* 36, 1284–1298. doi: 10.1016/j.cor.2008.02.001
- Ahumada, O., and Villalobos, J. R. (2009). Application of planning models in the agri-food supply chain: a review. *Eur. J. Oper. Res.* 196, 1–20. doi: 10.1016/j.ejor.2008.02.014
- Alexander, M. (1983). Most probable number method for microbial populations. *Methods Soil Anal. Chem. Microbiol. Propert.* 9, 815–820. doi: 10.2134/agronmonogr9.2.2ed.c39
- Alles, A. A., Wiedmann, M., and Martin, N. H. (2018). Rapid detection and characterization of postpasteurization contaminants in pasteurized fluid milk. *J. Dairy Sci.* 101, 7746–7756. doi: 10.3168/jds.2017-14216
- Apaiiah, R. K., and Hendrix, E. M. (2005). Design of a supply chain network for pea-based novel protein foods. *J. Food Eng.* 70, 383–391. doi: 10.1016/j.jfoodeng.2004.02.043
- Bilgen, B., and Çelebi, Y. (2013). Integrated production scheduling and distribution planning in dairy supply chain by hybrid modelling. *Ann. Oper. Res.* 211, 55–82. doi: 10.1007/s10479-013-1415-3
- Bishop, J., and White, C. (1986). Assessment of dairy product quality and potential shelf-life-a review. *J. Food Protect.* 49, 739–753. doi: 10.4315/0362-028X-49.9.739
- Botaro, B. G., Gameiro, A. H., and Santos, M. V. D. (2013). Quality based payment program and milk quality in dairy cooperatives of southern brazil: an econometric analysis. *Sci. Agricola* 70, 21–26. doi: 10.1590/S0103-90162013000100004

AUTHOR CONTRIBUTIONS

RI and MW supervised the project and with FE-A defined the objective of the article. FE-A and NM collected information for the optimization model. SM coded the Monte Carlo model. FE-A developed, coded, and analyzed the optimization model and drafted the manuscript. All authors participated in the interpretation of results.

FUNDING

The research reported in this publication was supported by the Foundation for Food and Agriculture Research under award number – Grant ID: CA18-SS-0000000206. The content of this publication is solely the responsibility of the authors and does not necessarily represent the official views of the Foundation for Food and Agriculture Research.

ACKNOWLEDGMENTS

Authors would like to thank Dr. Negin Enayaty Ahangar, Dr. Carmen Moraru, Dr. Aaron Adalja, Dr. Aljosa Trmcic, Mr. Michael Phillips, our industry partners, and SRT companies' experts for assisting with model development and data parameterization.

SUPPLEMENTARY MATERIAL

The Supplementary Material for this article can be found online at: <https://www.frontiersin.org/articles/10.3389/fsufs.2021.670029/full#supplementary-material>

- Buehler, A., Martin, N., Boor, K., and Wiedmann, M. (2018). Psychrotolerant spore-former growth characterization for the development of a dairy spoilage predictive model. *J. Dairy Sci.* 101, 6964–6981. doi: 10.3168/jds.2018-14501
- Buzby, J. C., Farah-Wells, H., and Hyman, J. (2014). *The Estimated Amount, Value, and Calories of Postharvest Food Losses at the Retail and Consumer Levels in the United States*. USDA-ERS Economic Information Bulletin, 121.
- Carey, N., Murphy, S., Zadoks, R., and Boor, K. (2005). Shelf lives of pasteurized fluid milk products in new york state: a ten-year study. *Food Protect. Trends* 25, 102–113. Available online at: <https://www.foodprotection.org/publications/food-protection-trends/archive/2005-02shelf-lives-of-pasteurized-fluidmilk-products-in-new-york-state-a-ten-year-study/>; <https://pubag.nal.usda.gov/catalog/3096923>
- Christiansson, A., Bertilsson, J., and Svensson, B. (1999). *Bacillus cereus* spores in raw milk: factors affecting the contamination of milk during the grazing period. *J. Dairy Sci.* 82, 305–314. doi: 10.3168/jds.S0022-0302(99)75237-9
- de Keizer, M., Akkerman, R., Grunow, M., Bloemhof, J. M., Haijema, R., and van der Vorst, J. G. (2017). Logistics network design for perishable products with heterogeneous quality decay. *Eur. J. Oper. Res.* 262, 535–549. doi: 10.1016/j.ejor.2017.03.049
- Doll, E. V., Scherer, S., and Wenning, M. (2017). Spoilage of microfiltered and pasteurized extended shelf life milk is mainly induced by psychrotolerant spore-forming bacteria that often originate from recontamination. *Front. Microbiol.* 8:135. doi: 10.3389/fmicb.2017.00135
- Enayaty-Ahangar, F., Rainwater, C. E., and Sharkey, T. C. (2019). A logic-based decomposition approach for multi-period network interdiction models. *Omega* 87, 71–85. doi: 10.1016/j.omega.2018.08.006
- Evanowski, R. L., Kent, D. J., Wiedmann, M., and Martin, N. H. (2020). Milking time hygiene interventions on dairy farms reduce spore counts

- in raw milk. *J. Dairy Sci.* 103, 4088–4099. doi: 10.3168/jds.2019-17499
- Ferrer, J.-C., Mac Cawley, A., Maturana, S., Toloza, S., and Vera, J. (2008). An optimization approach for scheduling wine grape harvest operations. *Int. J. Prod. Econ.* 112, 985–999. doi: 10.1016/j.ijpe.2007.05.020
- Frank, J., Yousef, A., Wehr, H., and Frank, J. (2004). *Standard Methods for the Examination of Dairy Product*. Washington, DC: American Public Health Association.
- Ghezavati, V., Hooshyar, S., and Tavakkoli-Moghaddam, R. (2017). A benders' decomposition algorithm for optimizing distribution of perishable products considering postharvest biological behavior in agri-food supply chain: a case study of tomato. *Central Eur. J. Oper. Res.* 25, 29–54. doi: 10.1007/s10100-015-0418-3
- Glen, J. (1986). A linear programming model for an integrated crop and intensive beef production enterprise. *J. Oper. Res. Soc.* 37, 487–494. doi: 10.1057/jors.1986.83
- Griep, E. R., Cheng, Y., and Moraru, C. I. (2018). Efficient removal of spores from skim milk using cold microfiltration: spore size and surface property considerations. *J. Dairy Sci.* 101, 9703–9713. doi: 10.3168/jds.2018-14888
- Guerra, A., Jonsson, G., Rasmussen, A., Nielsen, E. W., and Edelman, D. (1997). Low cross-flow velocity microfiltration of skim milk for removal of bacterial spores. *Int. Dairy J.* 7, 849–861. doi: 10.1016/S0958-6946(98)00009-0
- Hall-Phillips, A., and Shah, P. (2017). Uncertainty confusion and expiration date labels in the United States: a consumer perspective. *J. Retail. Consum. Serv.* 35, 118–126. doi: 10.1016/j.jretconser.2016.12.007
- Higgins, A. J. (2002). Australian sugar mills optimize harvester rosters to improve production. *Interfaces* 32, 15–25. doi: 10.1287/inte.32.3.15.41
- Huck, J. R., Woodcock, N. H., Ralyea, R. D., and Boor, K. J. (2007). Molecular subtyping and characterization of psychrotolerant endospore-forming bacteria in two new york state fluid milk processing systems. *J. Food Protect.* 70, 2354–2364. doi: 10.4315/0362-028X-70.10.2354
- Hurt, E., Adams, M., and Barbano, D. (2015). Microfiltration of skim milk and modified skim milk using a 0.1- μ m ceramic uniform transmembrane pressure system at temperatures of 50, 55, 60, and 65°C. *J. Dairy Sci.* 98, 765–780. doi: 10.3168/jds.2014-8775
- International Dairy Food Association (n.d.). *Pasteurization*. Available online at: <https://www.idfa.org/news-views/media-kits/milk/pasteurization> (accessed June 2020).
- Jabbarzare, Z., Zolfagharian, H., and Najafi, M. (2019). Dynamic interdiction networks with applications in illicit supply chains. *Omega* 96:102069. doi: 10.1016/j.omega.2019.05.005
- Jiao, Z., Higgins, A. J., and Prestwidge, D. B. (2005). An integrated statistical and optimisation approach to increasing sugar production within a mill region. *Comput. Electron. Agric.* 48, 170–181. doi: 10.1016/j.compag.2005.03.004
- Lemma, Y., Kitaw, D., and Gatew, G. (2014). Loss in perishable food supply chain: an optimization approach literature review. *Int. J. Sci. Eng. Res.* 5, 302–311. Available online at: <https://www.ijser.org/researchpaper/loss-in-perishable-food-supply-chain-an-optimization-approach-literaturereview.pdf>; <https://www.ijser.org/onlineResearchPaperViewer.aspx?Loss-in-Perishable-Food-Supply-Chain-An-Optimization-Approach-Literature-Review.pdf>
- Lütke Entrup, M., Günther, H.-O., Van Beek, P., Grunow, M., and Seiler, T. (2005). Mixed-integer linear programming approaches to shelf-life-integrated planning and scheduling in yoghurt production. *Int. J. Prod. Res.* 43, 5071–5100. doi: 10.1080/00207540500161068
- Martin, N., Carey, N., Murphy, S., Wiedmann, M., and Boor, K. (2012). A decade of improvement: New York state fluid milk quality. *J. Dairy Sci.* 95, 7384–7390. doi: 10.3168/jds.2012-5767
- Martin, N. H., Boor, K. J., and Wiedmann, M. (2018). Symposium review: effect of post-pasteurization contamination on fluid milk quality. *J. Dairy Sci.* 101, 861–870. doi: 10.3168/jds.2017-13339
- Martin, N. H., Kent, D. J., Evanowski, R. L., Hrobuchak, T. J. Z., and Wiedmann, M. (2019). Bacterial spore levels in bulk tank raw milk are influenced by environmental and cow hygiene factors. *J. Dairy Sci.* 102, 9689–9701. doi: 10.3168/jds.2019-16304
- Masiello, S., Kent, D., Martin, N., Schukken, Y., Wiedmann, M., and Boor, K. (2017). Longitudinal assessment of dairy farm management practices associated with the presence of psychrotolerant bacillales spores in bulk tank milk on 10 new york state dairy farms. *J. Dairy Sci.* 100, 8783–8795. doi: 10.3168/jds.2017-13139
- Masiello, S., Martin, N., Watters, R., Galton, D., Schukken, Y., Wiedmann, M., and Boor, K. (2014). Identification of dairy farm management practices associated with the presence of psychrotolerant sporeformers in bulk tank milk. *J. Dairy Sci.* 97, 4083–4096. doi: 10.3168/jds.2014-7938
- McDonald, C. M., and Karimi, I. A. (1997). Planning and scheduling of parallel semicontinuous processes. 1. production planning. *Indus. Eng. Chem. Res.* 36, 2691–2700. doi: 10.1021/ie960901+
- McKinnon, C. H., and Pettipher, G. L. (1983). A survey of sources of heat-resistant bacteria in milk with particular reference to psychrotrophic spore-forming bacteria. *J. Dairy Res.* 50, 163–170. doi: 10.1017/S0022029900022962
- Mehta, R. (1980). Milk processed at ultra-high-temperatures—a review. *J. Food Protect.* 43, 212–225. doi: 10.4315/0362-028X-43.3.212
- Muir, D. D. (1996). The shelf-life of dairy products: 1. factors influencing raw milk and fresh products. *Int. J. Dairy Technol.* 49, 24–32. doi: 10.1111/j.1471-0307.1996.tb02616.x
- Munch, D. M., Schmit, T. M., and Severson, R. M. (2020). *Differences in Milk Payment Structures by Cooperative and Independent Handlers: An Examination from New York State*. Ithaca, NY: Department of Applied Economics and Management, Cornell University. Available online at: https://dyson.cornell.edu/wp-content/uploads/sites/5/2020/06/WP_2020-03-Differences_in_Milk_Payment_VD.pdf
- Murphy, S. I., Reichler, S. J., Martin, N. H., Boor, K. J., & Wiedmann, M. (2021). Machine learning and advanced statistical modeling can identify key quality management practices that affect postpasteurization contamination of fluid milk. *J. Food Protect.* doi: 10.4315/JFP-20-431
- National Agricultural Statistics Service (2019). *Census 2017 report - National Agricultural Statistics*. Available online at: https://www.nass.usda.gov/Publications/AgCensus/2017/Full_Report/Volume_1,_Chapter_1_US/usv1.pdf
- Nightingale, C., Dhuyvetter, K., Mitchell, R., and Schukken, Y. (2008). Influence of variable milk quality premiums on observed milk quality. *J. Dairy Sci.* 91, 1236–1244. doi: 10.3168/jds.2007-0609
- Pafylas, I., Cheryan, M., Mehaia, M., and Saglam, N. (1996). Microfiltration of milk with ceramic membranes. *Food Res. Int.* 29, 141–146. doi: 10.1016/0963-9969(96)00007-5
- Papadatos, A., Berger, A., Pratt, J., and Barbano, D. (2002). A nonlinear programming optimization model to maximize net revenue in cheese manufacture. *J. Dairy Sci.* 85, 2768–2785. doi: 10.3168/jds.S0022-0302(02)74364-6
- Papadatos, A., Neocleous, M., Berger, A., and Barbano, D. (2003). Economic feasibility evaluation of microfiltration of milk prior to cheesemaking. *J. Dairy Sci.* 86, 1564–1577. doi: 10.3168/jds.S0022-0302(03)73742-4
- Ranieri, M., and Boor, K. (2009). Bacterial ecology of high-temperature, short-time pasteurized milk processed in the United States. *J. Dairy Sci.* 92, 4833–4840. doi: 10.3168/jds.2009-2181
- Reichler, S., Trmčić, A., Martin, N., Boor, K., and Wiedmann, M. (2018). *Pseudomonas fluorescens* group bacterial strains are responsible for repeat and sporadic postpasteurization contamination and reduced fluid milk shelf life. *J. Dairy Sci.* 101, 7780–7800. doi: 10.3168/jds.2018-14438
- Rysstad, G., and Kolstad, J. (2006). Extended shelf life milk—advances in technology. *Int. J. Dairy Technol.* 59, 85–96. doi: 10.1111/j.1471-0307.2006.00247.x
- Saenger, C., Qaim, M., Torero, M., and Viceisza, A. (2013). Contract farming and smallholder incentives to produce high quality: experimental evidence from the vietnamese dairy sector. *Agric. Econ.* 44, 297–308. doi: 10.1111/agec.12012
- Sargeant, J. M., Schukken, Y. H., and Leslie, K. E. (1998). Ontario bulk milk somatic cell count reduction program: progress and outlook. *J. Dairy Sci.* 81, 1545–1554. doi: 10.3168/jds.S0022-0302(98)75720-0
- Schroeter, C., Nicholson, C. F., and Meloy, M. G. (2016). Consumer valuation of organic and conventional milk: does shelf life matter? *J. Food Distrib. Res.* 47, 118–133. doi: 10.22004/ag.econ.250003. Available online at: <https://ageconsearch.umn.edu/record/250003/>
- Sheikh-Zadeh, A., and Rossetti, M. D. (2020). Classification methods for problem size reduction in spare part provisioning. *Int. J. Prod. Econ.* 219, 99–114. doi: 10.1016/j.ijpe.2019.05.011

- Stoecker, A., Seidmann, A., and Lloyd, G. (1985). A linear dynamic programming approach to irrigation system management with depleting groundwater. *Manage. Sci.* 31, 422–434. doi: 10.1287/mnsc.31.4.422
- U.S. Energy Information Administration (2019). *Electric Power Monthly with Data for November 2019*. Available online at: https://www.eia.gov/electricity/monthly/epm_table_grapher.php?t=epmt_5_3
- United States Department of Agriculture (1996). *Farmers' Use of Marketing and Production Contracts*. Available online at: https://www.ers.usda.gov/webdocs/publications/40764/18614_aer747a_1_.pdf?v=41063 (accessed November, 2020).
- United States Department of Agriculture (2014). *The Estimated Amount, Value, and Calories of Postharvest Food Losses at the Retail and Consumer Levels in the United States*. Available online at: https://www.ers.usda.gov/webdocs/publications/43833/43680_eib121.pdf
- United States Department of Agriculture (2019). *Milk Production*. Available online at: https://www.nass.usda.gov/Publications/Todays_Reports/reports/mkpr0819.pdf
- Valeeva, N., Lam, T., and Hogeveen, H. (2007). Motivation of dairy farmers to improve mastitis management. *J. Dairy Sci.* 90, 4466–4477. doi: 10.3168/jds.2007-0095
- Vissers, M., Driehuis, F., Te Giffel, M., De Jong, P., and Lankveld, J. (2007a). Minimizing the level of butyric acid bacteria spores in farm tank milk. *J. Dairy Sci.* 90, 3278–3285. doi: 10.3168/jds.2006-798
- Vissers, M., Te Giffel, M., Driehuis, F., De Jong, P., and Lankveld, J. (2007b). Minimizing the level of *Bacillus cereus* spores in farm tank milk. *J. Dairy Sci.* 90, 3286–3293. doi: 10.3168/jds.2006-873
- Volpe, R. J., Park, T. A., Dong, F., and Jensen, H. H. (2016). Somatic cell counts in dairy marketing: quantile regression for count data. *Eur. Rev. Agric. Econ.* 43, 331–358. doi: 10.1093/erae/jbv021
- Widodo, K. H., Nagasawa, H., Morizawa, K., and Ota, M. (2006). A periodical flowering-harvesting model for delivering agricultural fresh products. *Eur. J. Oper. Res.* 170, 24–43. doi: 10.1016/j.ejor.2004.05.024

Conflict of Interest: The authors declare that the research was conducted in the absence of any commercial or financial relationships that could be construed as a potential conflict of interest.

Copyright © 2021 Enayaty-Ahangar, Murphy, Martin, Wiedmann and Ivanek. This is an open-access article distributed under the terms of the Creative Commons Attribution License (CC BY). The use, distribution or reproduction in other forums is permitted, provided the original author(s) and the copyright owner(s) are credited and that the original publication in this journal is cited, in accordance with accepted academic practice. No use, distribution or reproduction is permitted which does not comply with these terms.



Smart and Active Food Packaging: Insights in Novel Food Packaging

Hamed Ahari* and Solmaz P. Soufiani

Department of Food Science and Technology, Science and Research Branch, Islamic Azad University, Tehran, Iran

OPEN ACCESS

Edited by:

Shalini Gaur Rudra,
Indian Agricultural Research Institute
(ICAR), India

Reviewed by:

Pradeep Kumar,
North Eastern Regional Institute
of Science and Technology, India
Amitava Mukherjee,
VIT University, India

*Correspondence:

Hamed Ahari
dr.h.ahari@gmail.com

Specialty section:

This article was submitted to
Food Microbiology,
a section of the journal
Frontiers in Microbiology

Received: 22 January 2021

Accepted: 05 May 2021

Published: 09 July 2021

Citation:

Ahari H and Soufiani SP (2021)
Smart and Active Food Packaging:
Insights in Novel Food Packaging.
Front. Microbiol. 12:657233.
doi: 10.3389/fmicb.2021.657233

The demand for more healthy foods with longer shelf life has been growing. Food packaging as one of the main aspects of food industries plays a vital role in meeting this demand. Integration of nanotechnology with food packaging systems (FPSs) revealed promising promotion in foods' shelf life by introducing novel FPSs. In this paper, common classification, functionalities, employed nanotechnologies, and the used biomaterials are discussed. According to our survey, FPSs are classified as active food packaging (AFP) and smart food packaging (SFP) systems. The functionality of both systems was manipulated by employing nanotechnologies, such as metal nanoparticles and nanoemulsions, and appropriate biomaterials like synthetic polymers and biomass-derived biomaterials. "Degradability and antibacterial" and "Indicating and scavenging" are the well-known functions for AFP and SFP, respectively. The main purpose is to make a multifunctional FPS to increase foods' shelf life and produce environmentally friendly and smart packaging without any hazard to human life.

Keywords: active food packaging, smart food packaging, biopolymers, shelf life, nanomaterial

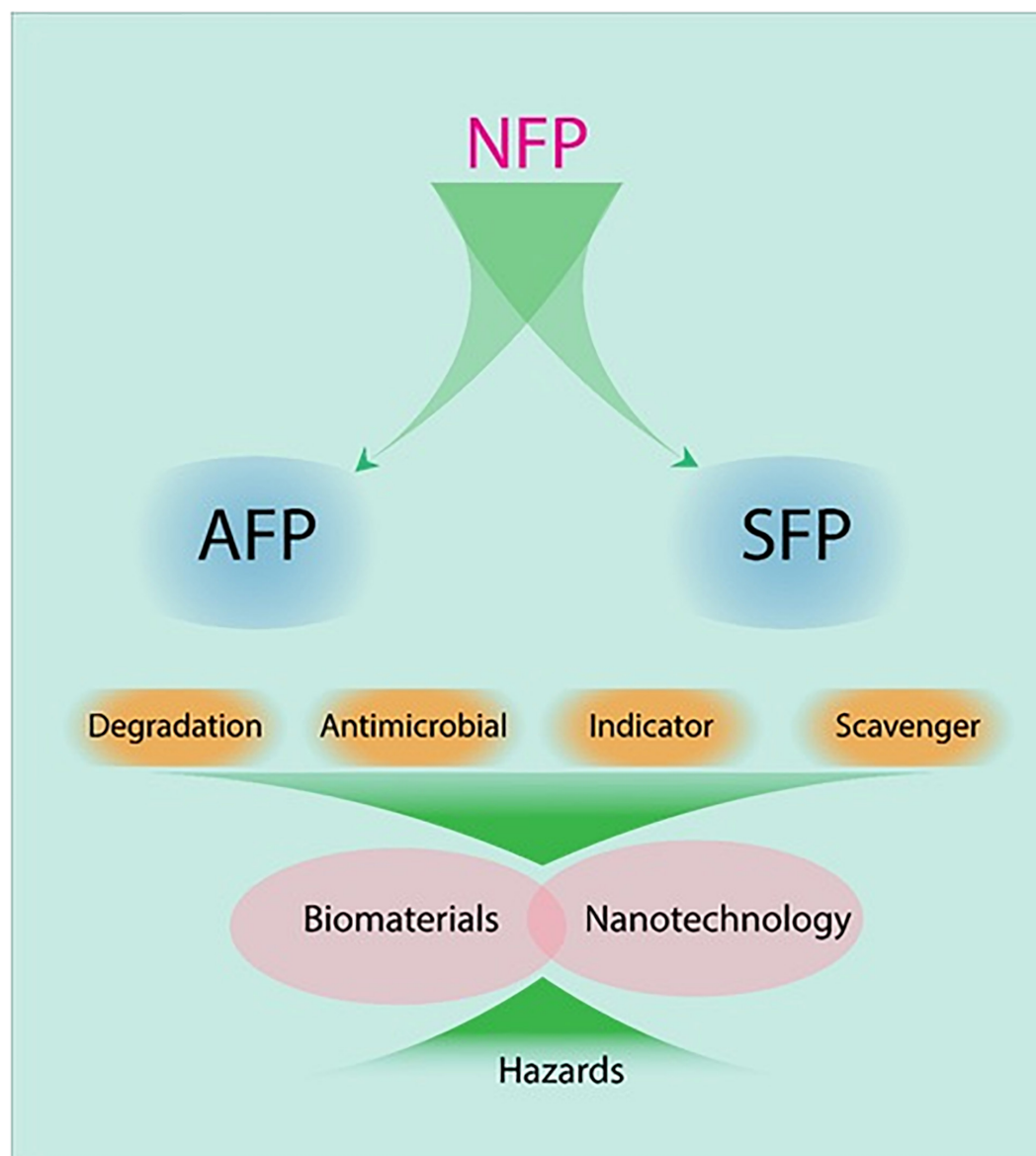
HIGHLIGHTS

- Novel food Packaging comprises Active and Smart food packaging.
- Nanotechnology plays a vital role in novel packaging systems.
- Food's shelf life is prolonged under Active packaging systems.
- Consumers can be informed about the quality of foods by smart packaging systems.
- Novel packaging systems may hazards human health.

INTRODUCTION

Basically, food packaging is one of the vital steps in the food industry, so that a suitable packaging not only attracts the customer's attention but also keeps the products at the highest possible level of nutrition and quality (Gupta and Dudeja, 2017). There are three levels of packaging, namely, primary packaging, secondary packaging, and tertiary packaging (Grönman et al., 2013). Primary packaging is the coating/film that directly encloses the food and communicates with the food. Primary packaging is the main layer affecting the quality of foods due to its direct contact with the materials. Secondary packaging covers the products packaged by the primary packaging. Tertiary packaging is the outer packaging employed for bulk handling, distribution, and storage. Despite these three layers of packaging, it is possible that food safety is not guaranteed (Muncke, 2014).

Transporting easily, protecting food quality, maintaining food integrity, keeping away from harmful particles and chemicals, and preventing bacterial growth and pests are the major benefits



GRAPHICAL ABSTRACT | Novel food packaging comprises several technologies.

of food packaging including primary, secondary, and tertiary packaging (Robertson, 2014). Packaging also gives consumers necessary information about the products via labeling. The name of products, the list of ingredients, the way of consumption, the price, and the expiry date are the main information reported by labeling (Roche, 2016).

Microbial spoilage and its metabolism and oxidation are the principal reasons for many food deterioration, such as bananas, tomatoes, pears, apples, mangoes, and kiwifruit, from production and transportation till storage and marketing (Petruzzi et al., 2017). Communication, protection, containment, and convenience are the most common features of traditional food packaging (TFP). TFP is a typical system providing just physical support and food protection against stimuli

and environments in the packaging process, distribution, transportation, and storage (Lloyd et al., 2019). In general, an effective TFP often helps preserve foods and is just a nonfunctional physical barrier against chemical, physical, and microbial damage (Robertson, 2019). It is also estimated that TFP generates tons of waste annually. However, due to the progress of technology and modern life, demands for a healthy and high-quality food product, easy transportation, and especially long shelf life are increasing; therefore, TFP systems are not able to meet the needs of the consumer, and hence, an appropriate alternative is necessary.

Considering primary packaging, it is required to develop novel food packaging (NFP) systems by employing different biomaterials and techniques, embedding sensors and indicators,

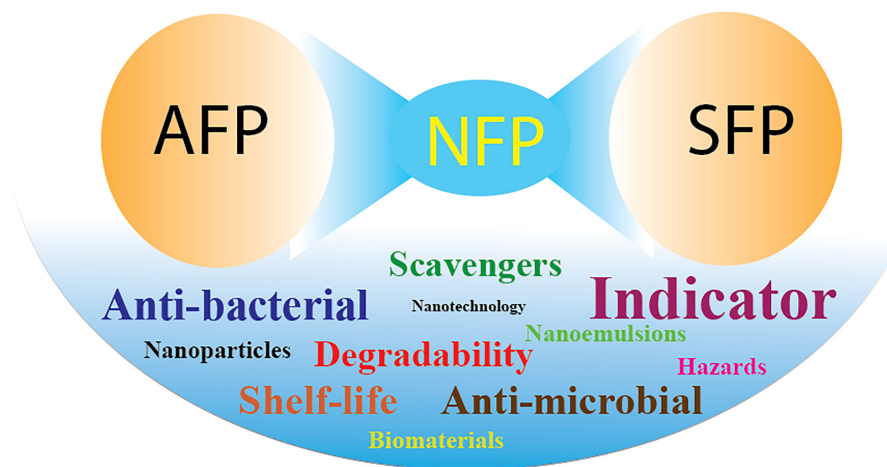


FIGURE 1 | New types of food packaging systems and their performances.

different functions, biodegradable materials, nanotechnology, essential oils, and plant extracts, while maintaining the quality and nutrition and improving the shelf life of food; the environmental effects of the package reduced food rationing (**Figure 1**; Zhang and Zhao, 2012; Liu et al., 2020; Zhang et al., 2021). The strengths of NFP, also known as active, smart, and green technologies, are the lack of inactivity and negative inactivity between packaging and food components, long-term performance, prevention of food spoilage, and enhancement of consumer health, and these can be considered as the ultimate goal in the future for food packaging technology (Lone et al., 2016).

As can be seen from **Figure 1**, there is a difference between smart food packaging (SFP) and active food packaging (AFP). SFP monitors the condition of packaged foods to provide information about their quality and nutrients, before consumption, while in AFP, there are some mechanisms to control microbial growth, moisture, and oxidation.

In general, SFP and AFP are two promising packaging systems in the food industry (**Table 1**). SFP allows the consumer to detect changes in food quality parameters over time due to the presence of certain substances in its matrix, which act as indicators. As can be seen in **Table 1**, packaging systems, depending on foods, can be designed as coating or films (thick or thin). Both of them can be engineered as AFP or SFP. Employing this system in FPS will increase food shelf-life by controlling microorganisms' growth, food freshness, appropriate color, desired smell, customer satisfaction, and so on.

As **Table 1** shows, several technologies including nanomaterials (Kaur et al., 2020), biomaterials (Asensio et al., 2020), nanoemulsion (Moghimi et al., 2017), microbiology (Jaworska et al., 2020), and food science can play a vital role in NFP. It is hypothesized that the role of these technologies and the way they perform in NFP are still of interest to scientists. Based on our survey, numerous studies considering new food packaging systems have been published. Giving scientists a comprehensive review of NFP would be beneficial. The current study was carried out to provide a comprehensive review about

the NFP systems including AFP and SFP by covering the main functions, employed biomaterial, and the role of nanotechnology and finally discussing the related hazards.

NFP SYSTEMS

Degradability of Food Packaging

Considering AFP/SFP, various functions and features are designed by scientists for new packaging (**Table 1**). For example, regarding environmental issues, leaving the residue of packaging in the environment causes pollution and hazards to human and animal life (Marsh and Bugusu, 2007). Food packaging utilizes various materials to protect foods, of which a high percentage are nondegradable and remain in the environment for years. Metal and glass as food containers are the most well-known and traditional materials in FPS (Marsh and Bugusu, 2007).

As can be inferred from **Table 1**, the presence of polymers, such as polystyrene, polyvinylchloride, polyethylene, polyethylene terephthalate, polypropylene, and polyamide, in food packaging systems provided more satisfaction to customers in the viewpoints of ease of use, appearance, and transparency (Stoica et al., 2018). Furthermore, these polymers showed good availability, lower price, good water vapor permeability, good mechanical properties (tensile strength and shear strength), and good gas barrier properties (oxygen and carbon dioxide) (Pawar and Purwar, 2013; Stoica et al., 2018). They can also be natural (e.g., gelatin-chitosan) or synthetic (e.g., polycaprolactone). In spite of this, contamination and environmental pollution issues still remain unsolved (Moore, 2008; Williams and Wikström, 2011).

"Environmentally friendly" is a new term defined in NPS. According to European law, biopolymers and bioplastics must be biodegradable, especially in terms of composting, so they can act as soil softeners and fertilizers. This issue has been indicated in **Table 1**. Many researchers have evaluated the biodegradability of the prepared packaging by burying it in soil (**Table 1**).

TABLE 1 | a short description of some NFP systems.

Food packaging system	Type of FPS AFP - SPF	Employed materials	Type of nanomaterial	Purpose	Results	References
Film	AFP	Polyvinyl Chloride	–	Degradation in soil in present of <i>Tenebrio molitor</i> larvae	<ul style="list-style-type: none"> • <i>T. molitor</i> larvae are capable of performing • broad depolymerization/biodegradation. 	Peng et al., 2020
Film	AFP	Chitosan, gelatin, polyethylene glycol	Ag NP	Biodegradation	<ul style="list-style-type: none"> • The shelf life of the fruit extended for additional two weeks. • Nano-Ag enhanced the mechanical properties and reduced transparency. • The film is appropriate for FPS. 	Kumar et al., 2018
Film	SFP	Poly lactide and polyhydroxybutyrate	Colorants	Color-based indicator	<ul style="list-style-type: none"> • Color changes depicted the life time of the materials. • changes in the samples color under due to UV, thermooxidation, and weathering • The system is biodegradable. 	Latos-Brozio and Masek, 2020
Film	SFP	Polyolefin elastomer (POE)	Potassium permanganate, nanoclay and nanosilica	Ethylene scavenger	<ul style="list-style-type: none"> • The film showed improvement in mechanical properties, larger Ethylene scavenging, and lower Water Vapor Permeability compared to the neat POE film. • Ethylene absorption efficacy enhanced at higher level of impregnated NP because of their higher potassium permanganate concentration. • The optimized film could extend the shelf life of bananas up to 15 days. 	Ebrahimi et al., 2021
Film	AFP	Polyhydroxybutyrate	Eugenol	Degradation in various soil type (agricultural, landfill and sandy)	<ul style="list-style-type: none"> • Films in agricultural soil showed a higher biodegradation due to high fungi load. • The phosphorus availability, soil acidity, moisture and crystallinity of polymer were critical factors in evaluation of the differences in biodegradation rates microbial growth. • Eugenol enhanced the polymer crystallinity and decreased the mechanical properties. 	Rech et al., 2020
Film	AFP	gelatin-chitosan	TiO ₂ -Ag NP	antimicrobial	<ul style="list-style-type: none"> • The addition TiO₂-Ag in the film enhanced the interaction between components and notably enhanced the water solubility. • When the concentration of TiO₂-Ag increased to 0.5%, the best antibacterial ability was observed. • The addition TiO₂-Ag to the film, decreased the tensile strength of the film. 	Lin et al., 2020
Film	AFP	Cellulose nanofiber	Carbon and Ag NP	Antimicrobial	<ul style="list-style-type: none"> • The film were evaluated against food pathogens, <i>S. aureus</i> and <i>E. coli</i>. • 140–450 ppm was the optimum concentration of Ag NP to inhibit the growth of <i>S. aureus</i> and <i>E. coli</i>. 	Sobhan et al., 2020
Film	SFP	Cellulose	TiO ₂ NP	Oxygen-scavenger	<ul style="list-style-type: none"> • The film could scavenge oxygen at the rate of 0.017 cm³ O₂ h⁻¹ cm⁻² during 24 h. 	Mills et al., 2006
Film	SFP	Gluten	chlorophyll/ polypyrrole	Conductivity and color indicator	<ul style="list-style-type: none"> • Adding chlorophyll and polypyrrole increased the opacity and tensile strength of films. • Chlorophyll did not affect the antibacterial property against <i>E.coli</i> while polypyrrole did vice versa. • The film can be employed as SFP because of changes in its conductivity and color during storage. 	Chavoshizadeh et al., 2020
Film	SFP	Cellulose/chitosan	Carrot anthocyanin	pH-responsive indicator	<ul style="list-style-type: none"> • The water solubility and swelling enhanced by addition of carrot anthocyanin into the film. • The pH indicator depicted a clear color changes from pink to khaki at various pH values between 2–11. • Based on the stability tests, the pH indicator showed an acceptable color stability within storage for one month at 20°C. • The addition of carrot anthocyanin showed no effect on the super-molecular and chemical structure of the films. 	Ebrahimi Tirtashi et al., 2019

(Continued)

TABLE 1 | Continued

Food packaging system	Type of FPS AFP - SPF	Employed materials	Type of nanomaterial	Purpose	Results	References
Film	AFP	Hydroxyethyl cellulose	ZnO NP	Antimicrobial	<ul style="list-style-type: none"> • The film stopped <i>S. aureus</i> and <i>E. coli</i> bacteria growth. • ZnO addition improved the mechanical properties of the films. 	El Fawal et al., 2020
Coating	SFP	Chitosan	ZnO NP	Antimicrobial	<ul style="list-style-type: none"> • ZnO NP at $\geq 0.0125\%$ stopped <i>E. coli</i> growth at 37°C or 10. • The coating notably decreased <i>E. coli</i> population on white cheese at 4°C or 10. • The coating increased white cheese color but didn't affect a_w. 	Al-Nabulsi et al., 2020
Film	SFP	low density polyethylene (LDPE)	curcumin	A hydrophobic ammonia sensor	<ul style="list-style-type: none"> • The LDPE-curcumin composite film was sensitive to ammonia • The film depicted light yellow to light brown color changes during the storage time in case of beef storage at 4 °C. • Color changes means enhancement in TVB-N contents of the meat samples. 	Zhai et al., 2020
Coating	AFP	Polyethylene	Carvacrol	Antimicrobial	<ul style="list-style-type: none"> • The coating decreased the bacterial growth on packaged chicken surfaces. • coated surfaces showed low bacterial attachment. 	Alkan Tas et al., 2019
Coating	SFP	–	PdCl ₂ –CuSO ₄ , carbon powder	Ethylene scavenger	<ul style="list-style-type: none"> • CuSO₄ and PdCl₂ addition enhanced ethylene removal efficacy. • Ethylene scavenging capacity of the film can be regenerated. • The film could inhibit ethylene production and increased the shelf life of broccoli. 	Cao et al., 2015
Film	SFP	LDPE, HDPE and PP	Carvacrol	Microbial activity-based indicator	<ul style="list-style-type: none"> • Employing several film layers • Prediction of the expected shelf life during food storage. 	Vilas et al., 2020
Film	SFP	EMCO and ATCO	sodium carbonate,	Oxygen and carbon dioxide	<ul style="list-style-type: none"> • Color seemed better in all treated strawberries. • Scavenging oxygen and carbon dioxide increased the shelf life of strawberries. • The use of these scavengers depicted slowed consumption of oxygen and carbon dioxide accumulation. 	Aday et al., 2011
Film	SFP	cellulose	Iridescence (as a color)	color humidity indicator	<ul style="list-style-type: none"> • When the film was exposed to the water or high relative humidity, a shift in the film's color observed from blue-green (dry state) to red-orange (wet state). • The art of color change depends on the film thickness (40 m: 1–3 min). 	Zhang et al., 2013

However, some natural plastics based on natural monomers may lose their biodegradability through chemical modification of the polymerization process. Materials that ensure not only the nutrition and maintenance of the product (from production to consumption) but also their release into the environment do not pose a risk to the environment and decompose over time and, as one of the primary goals in the SFP and AFP, were taken into consideration (Siracusa et al., 2008).

There are a variety of biomaterials which are classified according to their source. (i) Natural polymers have attracted

the attention of scientists due to their natural source and higher-degradability features. Chitosan, polysaccharide, starch, alginate, and gelatins are examples of these biomaterials which are nontoxic and environmentally friendly (Malhotra et al., 2015). (ii) Biomaterials generated by the activity of microorganisms such as bacterial cellulose, polyhydroxybutyrate (PHB), and xanthan are suitable for various medical and industrial applications (Rehm, 2010). (iii) Synthetic products are derived from natural sources of biomass and oil (biopolyester or lactic acid) or from a polymerization process and renewable monomers such as

polyethylene terephthalate (PET) (Ali et al., 2006; Hacker et al., 2019). Basically, using the current petroleum-based polymers such as PET and polyamide in FPS is still the only way of packaging production (Ferreira et al., 2016; Mishra, 2018; Bumbudsanpharoke and Ko, 2019). Plastic waste is a global problem, and the doubling of global plastic production over the next decade is expected to have a major adverse effect on the environment due to its lack of environmental degradability (GreenFacts, 2020).

Many plastics are mixtures of synthetic components such as polymers and additives to improve the functional properties of the final product and expand the scope of application. In this regard, numerous studies have been conducted to produce new packaging with the aim of shortening the residence time in the environment using renewable resources and biodegradable materials. Along with biodegradability, there are other properties which must be considered and fulfilled. Biodegradable packaging from biopolymers requires some water solubility to promote degradability. However, at the same time, hydrophilic property decreases mechanical and barrier properties. This contradiction has also encouraged the development of some NFP systems. These features are important to modify and control the barrier and mechanical properties which are related to the polymeric packaging material structure (Boyle et al., 2019).

In a research done by Goudarzi and Shahabi-Ghahfarrokhi (2018), a photodegradable bio-nanocomposite starch/TiO₂ was produced as a food packaging material using photochemical-based reactions. The prepared film showed good degradability under UV exposure and reduction in the mechanical and barrier properties. It was reported that UV rays lowered the hydrophobicity of the films and that enhanced duration of exposure negatively reduced Young's modulus and tensile strength. Degradation behavior in water/in soil/on the earth is one of the main characteristics of food packaging materials. Addition of nano-silica to biopolymeric films such as polyvinyl alcohol/liquefied ball-milled chitin showed good degradation in soil (**Figure 2A**; Zhang J. et al., 2020). Employing alkali hydrolysis and microbial/bacterial attack during burial in soil is a common phenomenon which needs to be evaluated too (Arvanitoyannis et al., 1994). The mechanism of biodegradation of the matrix may be covered in three stages: first, the microorganisms grow on the surface of the matrix, then the microorganisms use the matrix material as a source for growth, and finally, destruction of the matrix occurs (**Figure 2B**; Tharanathan, 2003). Factors such as nutrients, soil temperature, oxygen, pH, and salinity affect the activity and survival of microorganisms (**Figure 2C**; Rech et al., 2020). The temperature of agricultural soil is reported to be in the range of 18–37°C; for the landfill, the temperature ranged from 18 to 41°C; and finally, the sandy soil showed temperatures between 19 and 34°C. This temperature is close to the optimum temperature for the growth of fungi (22–30°C) and mesophilic bacteria (25–40°C). Soil properties including humidity, phosphorus content, potassium content, and pH were also checked during the biodegradation process. As can be seen in **Figure 2C**, the PHB films, incorporated with different concentrations of eugenol as an antimicrobial compound, buried in the agricultural soil presented a faster

degradation rate than in the other soil types. It was reported that the presence of eugenol did not affect the biodegradation behavior of the films. The high soil moisture content also makes PHB less crystalline and contributes to the increase of the bacterial population (Rech et al., 2020). The bacterial activity is higher in moister environments (Zhang et al., 2016). Overall, the greater the soil fertility, the greater the soil microbial biomass (Rech et al., 2020).

Using natural sources instead of the synthesis materials has been of interest to scientists (Siracusa et al., 2008). Some polymers like celluloses microfibers (CMFs) are hydrophilic in nature, and this property probably helps microorganisms such as fungi and bacteria to penetrate into the matrix using water as an internal environment. It was reported that fungi attack the CMF loaded on the surface of the ethylene/vinyl acetate (EVA) film (**Figure 2B**; Sonia and Dasan, 2013). This process weakens the polymer matrix and increases hydrophilicity, permeability of the film, and the surface volume ratio. As another example, chitosan exhibited high potential in biodegradable FPS due to its biocompatibility and biodegradability features. The naturally sourced polymers have shown interesting functional features after combination with other materials (Priyadarshi and Rhim, 2020). For instance, the electrospun PVA/chitosan nanocomposite showed good biodegradability along with antimicrobial properties (Pandey et al., 2020). Similar results were reported in a previous study by Yu et al. (2018). In another study, it was reported that the chitosan-based film containing Chinese chive showed a good biodegradability behavior (47.36%) (Riaz et al., 2020). Adding xylan and carvacrol to the chitosan-based films improved both biodegradability and antibacterial activity (Kamdem et al., 2019).

Regarding biodegradable films employed in food packaging, water resistance is a vital property, because in some cases, the packaging will be in contact with humidity and water during the food storage, and due to the high water activity, the packaging's function will be disrupted. In films made only of polymers (e.g., chitosan, starch, and sodium alginate), higher values for solubility in water at room temperature have been reported, such as solubility rates of 76 and 21% for the chitosan and starch, respectively. It was reported that with the mixture of both polymers without any synthetic polymer (F127 0%), the prepared film showed a solubility of 42% (Fonseca-García et al., 2021), while with the addition of pluronic F127 to the blend of the chitosan–starch, a significant reduction (39%) in the water solubility of the films was reported, which decreased to only 3% when the concentration of pluronic F127 was 5% (Fonseca-García et al., 2021).

In a research, the role of glycerol (as plasticizer) content in modifying the solubility of the material was examined. Thereby, 25% glycerol was added to the starch. The results showed a water solubility lower than that of starch films, and the addition of 30% glycerol resulted in a film with a water solubility of 32% (Loredo et al., 2018). The addition of plasticizers, such as polyols (glycerol), plays an important role in disrupting the interactions between the molecular chains of polymers and weakening them, as well as in increasing the free volume between the chains, for which the reason is the highly hydrophilic nature of the emollient

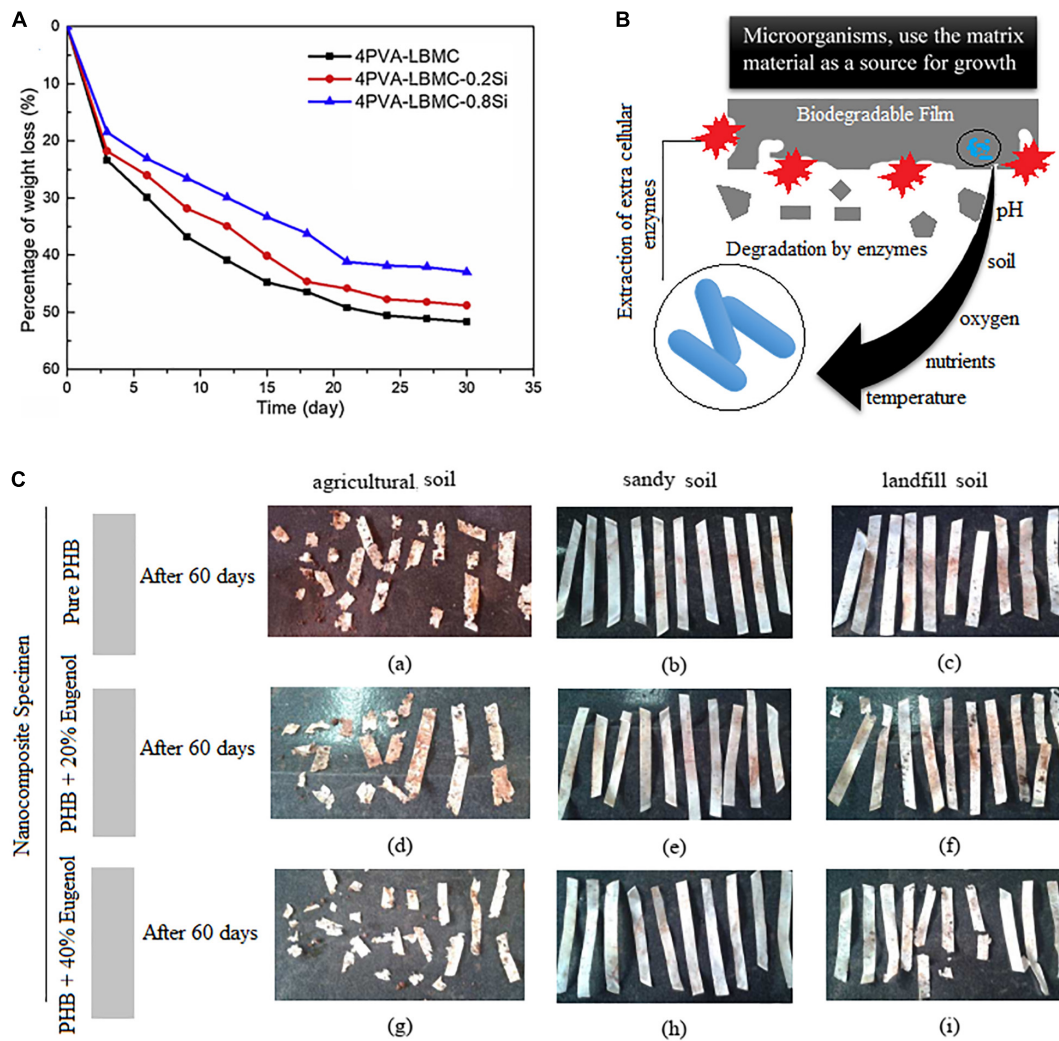


FIGURE 2 | (A) Biodegradation of the blend films in the soil [reproduced with permission from Zhang J. et al. (2020)]. **(B)** The mechanism of biodegradation of the film matrix. **(C)** Pure polyhydroxybutyrate (PHB) films containing eugenol after 60 days of biodegradation. (a–c) Pure PHB. (d–f) PHB films containing 20% of eugenol. (g–i) PHB films containing 40% of eugenol [reproduced with permission from Rech et al. (2020)].

(Sanyang et al., 2015). This enhances the water molecule diffusion into the matrix of films and, finally, increases their solubility.

It has been reported that promoting the mechanical properties of FPS may negatively affect their degradability. However, the mechanical properties of packaging films can be improved by adding a biodegradable synthetic polymer to them (Gómez-Aldapa et al., 2020). Although the prepared polymer is not totally biodegradable, the combination of chitosan with synthetic polymers can otherwise lead to the destruction of nondegradable plastics. Polyvinyl alcohol (PVA), as a nontoxic and water-soluble polymer, is one of the most commonly employed synthetic polymers combined with chitosan. The prepared films not only depicted a highly improved mechanical properties but also promoted barrier performances toward oxygen and water (Giannakas et al., 2020).

One of the techniques to predict the biodegradation properties of the FPS is a mechanical test. Degradation over time will

negatively affect the mechanical properties. In a research, the effect of biodegradation on the mechanical properties of the hydrogel (made of PVP:carboxymethyl cellulose (CMC) (20:80)) was assessed for 8 weeks (Figure 3A; Roy et al., 2012). The tensile strength values of the prepared films were more or less increased with time of biodegradation, and the highest values were revealed after 7 weeks, but during 14 days, the E-modulus gradually reduced because of degradation and enhanced after that. The following reasons were hypothesized for this behavior: modulus E values were initially low due to slow degradation of the polymer film and then increased slowly due to the penetration of microbial growth into the hydrogel film (Figure 3B; Roy et al., 2012). As a packaging substance, it is expected that hydrogel films exhibit higher elongation before break. The hydrogel films should be flexible, not brittle. The dried PVP–CMC films before degradation revealed 10% of strain at break, but as the biodegradation process lasted, the values of strain

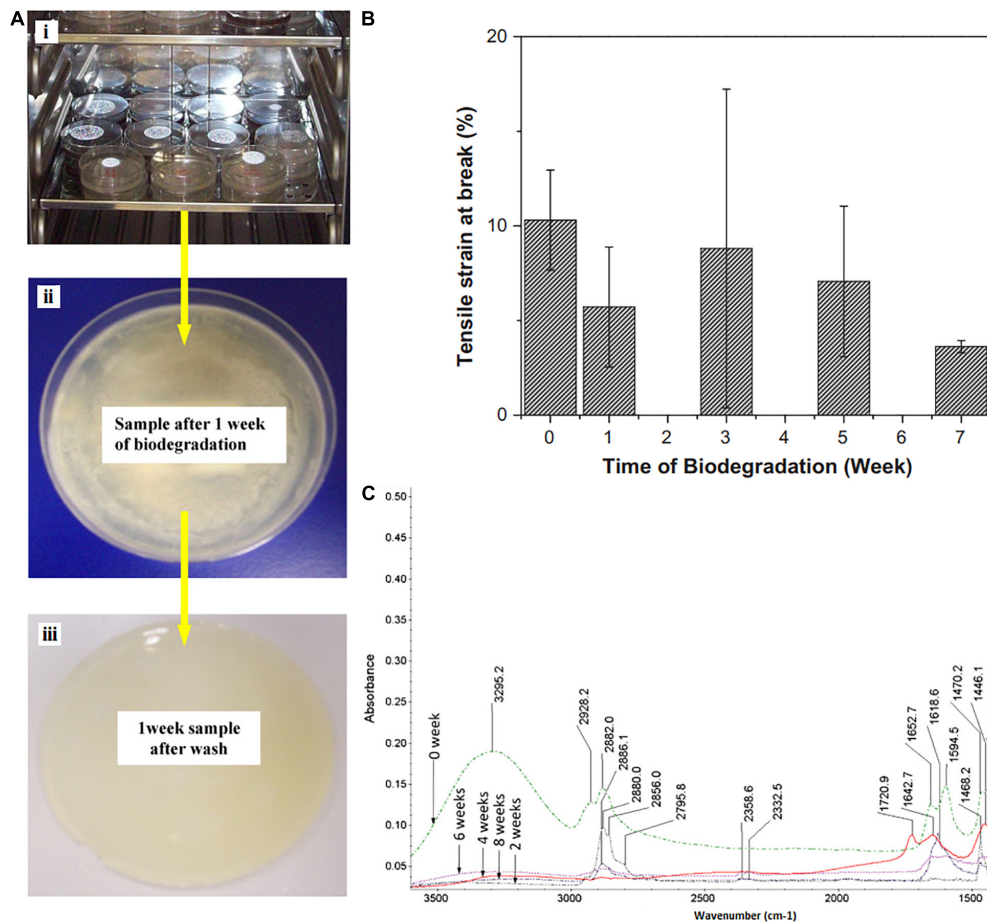


FIGURE 3 | (A) Optical view for biodegradation behavior of PVP-CMC films during the biodegradation process in liquid kept inside an incubator at 30°C (i) plates with films in liquid environment inside, (ii) an image of microbial growth on film, and (iii) an image of the film after removing the biodegradation conditions. **(B)** Tensile strain (at break) of dried PVP-CMC films before and after biodegradation. **(C)** FTIR of PVP-CMC films in dry state, before after biodegradation [reproduced with permission from Roy et al. (2012)].

at break reduces noticeably, and after 7 weeks of degradation phenomenon, the films depicted strain at break of about 4%. This may be due to the reaction of extracellular enzymes secreted by microorganisms in the liquid degradation medium with the PVP-CMC hydrogel and the change or breakage of the pseudo crosslinking bonding structure of hydrogels, which causes a reduction in the values of tensile strain at break (Roy et al., 2012). **Figure 3C** illustrates the FTIR spectra of PVP-CMC hydrogel for various periods (2, 4, 6, and 8 weeks) of biodegradation. As the degradation began, the peak intensities decreased noticeably. The broad peak at 3,295 cm⁻¹ totally disappeared for all the samples during 2–8 weeks (Roy et al., 2012). These significant changes in height and the presence of peaks could be the reason for the decomposition of the hydrogel through some interactions that resulted in a change in their chemical structure leading to biodegradation of PVP-CMC hydrogel films.

In the production of AFP, consideration of environmental conditions can be effective in the process of degradability of packaging coatings. In this regard, the researchers found that the biodegradation time of packaging coatings [e.g., poly(lactic acid)

(PLA)] in the environment can be variable and long depending on environmental conditions. Therefore, in order to solve this problem, the addition of organic matter from renewable sources, such as lignin, was suggested, because it can reduce the time of biological degradation. Based on the results, lignin is a suitable choice to accelerate the biological degradation of PLA in garden soil (da Silva et al., 2019).

In conclusion, biodegradable packaging helps the environment remove waste materials left from food packaging. AFP has the high potential of decomposition in comparison with common packaging due to the employed biodegradable materials and embedded specific ingredients.

Antibacterial Function of Food Packaging

One of the most important food safety concerns in the world is foodborne illness caused by various microorganisms such as viruses, bacteria, and fungi. Some products, such as raw agricultural products, as a major part of food products (e.g.,

fruits), due to the lack of a way to increase their safety are contaminated by foodborne pathogens (Oliver et al., 2005; Heredia and García, 2018).

Antibacterial property is another vital application in NFP (Table 1). Preventing the growth of microorganisms and consequently food spoilage is one of the main goals of NFP. Increasing consumer demand for organic and healthy foods has led to the use of new technologies for food packaging and storage. Thereby, AFP proved its potential in FPS. Based on AFP, new packaging contains natural antimicrobial agents or is made of antibacterial substrates (Aziz and Karboune, 2018). As can be seen in Table 1 and also based on the published reports regarding antimicrobial properties of different agents, numerous studies have been published about the efficacy of various potent agents against numerous species of both Gram-negative and Gram-positive bacteria, including *Staphylococcus epidermidis*, *Escherichia coli*, *Pseudomonas aeruginosa*, *Staphylococcus aureus*, *Enterococcus faecalis*, and *Vibrio cholera* (Aymonier et al., 2002; Baker et al., 2005; Panáček et al., 2006; Lok et al., 2007; Ahari et al., 2008; Zanjani et al., 2014; Ydollahi et al., 2016; Lotfi et al., 2019; Marrez et al., 2019). AFP is a new candidate for increasing the shelf life and quality of food products (Table 1). According to the “Results” section in Table 1, the efficacy and performance of AFP have been promoted through the nanoencapsulation technique, in which nanoparticles loaded with antimicrobial agents are embedded in the packaging structure, leading to enhancement in food quality during storage (Bahrami et al., 2020).

Incorporation of natural antimicrobial-loaded nanocarriers (metal oxide, essential oil, herbal extracts, etc.) is the most effective way to create AFP in food packaging systems, which has become feasible by employing nanoencapsulated antimicrobials in coating or film structures, instead of interpolation of antibacterial agents (Valdés et al., 2015; Ydollahi et al., 2016; Garcia et al., 2018; Pisoschi et al., 2018; Ju et al., 2019). This approach was further able to make many benefits including release control, protection against environmental stresses, and solubility improvement and natural antimicrobial absorption in AFP, which are the main achievements in overcoming the obstacles of using natural antimicrobials in food packaging (Bahrami et al., 2020).

To promote AFP with the aim of antibacterial power, coating the package with antibacterial agents has been of interest to scientists. The prepared coatings (made of polysaccharide) on paper surface can act as an impressive carrier for interpolation of antibacterial agents. This approach was able further to make the paper materials more practical in AFP (Nechita, 2017). In a research done by He et al. (2021), carboxymethyl cellulose (CMC) film coated with AgNPs was synthesized to promote antibacterial and barrier properties. They reported that CMC-coated paper without AgNPs and the uncoated paper showed no antibacterial activity and no inhibition zone. Contrariwise, CMC paper coated with CNC/AgNPs (cellulose nanocrystals (CNC)) revealed the antibacterial efficacy against *S. aureus* and *E. coli* depending on CNC@AgNPs and the presence of AgNPs. The inhibition power of the coating-based AFP may change against different types of microorganism like species of bacteria. Thereby, it is important to choose the right

antibacterial agents according to the food type. For instance, it was found that *E. coli* showed good resistance against the CMC/CNC@AgNPs-coated papers compared with *S. aureus* (Table 2). To synthesize the more efficient AFP, it is important to analyze the structural difference in the cell wall of Gram-negative bacteria and Gram-positive bacteria (Wu et al., 2018). In a similar research, a new nanocomposite has been synthesized using cellulose acetate and AgNPs as antibacterial-based AFP for food safety (Marrez et al., 2019). Based on the minimum inhibitory concentration (MIC) and minimum bactericidal concentration (MBC) results, the new film revealed distinct antibacterial behavior (efficacy) against various types of bacteria, including *S. aureus*, *Bacillus cereus*, *Salmonella typhi*, *E. coli*, *Klebsiella pneumonia*, with high activity and two strains of *Pseudomonas* spp. with low activity.

To promote antibacterial-based AFP, apart from AgNPs, other nanoparticles including TiO₂, CuO, ZnO, nanoemulsions, and nanoclay showed their potential as antibacterial and antimicrobial agents (Table 1). For instance, TiO₂-Ag-loaded fish gelatin-chitosan (FG-CH) antibacterial composite was synthesized for food packaging purposes (Lin et al., 2020). FG-CH revealed no antibacterial effect, the reason for which was attributed to the limited antibacterial performance of chitosan at natural pH. After the addition of TiO₂-AgNP (at the concentration of 0.5%), the film could gain antibacterial ability. These NPs could enhance the UV barrier capability of the film too (Figure 4A). AFP also showed their potential in preventing the coliform bacteria growth during food storage. By employing ZnONP and integration with polymeric films such as low-density polyethylene (LDPE)-based nanocomposite, the coliform bacterial growth was significantly delayed while the neat LDPE could not prevent bacteria (Shankar et al., 2019). In this study, the authors also used grapefruit seed extract (GSE) along with ZnONP to promote antibacterial effects in AFP; thereby, it was reported that the release of flavonoids, which are polyphenolic in structure, might be the reason for the antimicrobial activity of GSE. According to previous studies, flavonoids can diffuse into bacterial membranes and then react with cellular proteins or cytoplasm to destroy bacteria (Corrales et al., 2009; Wang and Rhim, 2016). Generally, the antimicrobial and antibacterial performance of nanoparticles in AFP has been hypothesized to be due to (i) nanoparticle contact with the cell wall of the microorganism directly which damages the bacterial cell, (ii)

TABLE 2 | Inhibition zone Diameter of coated and uncoated paper exposed to *E. coli* and *S. aureus* [Reproduced with permission from Wu et al. (2018)].

Samples	Inhibition zone diameter (mm) against:	
	<i>E. coli</i>	<i>S. aureus</i>
Uncoated	0	0
CMC	0	0
CMC/CNC@AgNPs 1%	1.23	2.6
CMC/CNC@AgNPs 3%	2.5	3.8
CMC/CNC@AgNPs 5%	3.3	4.7
CMC/CNC@AgNPs 7%	5.5	6.1

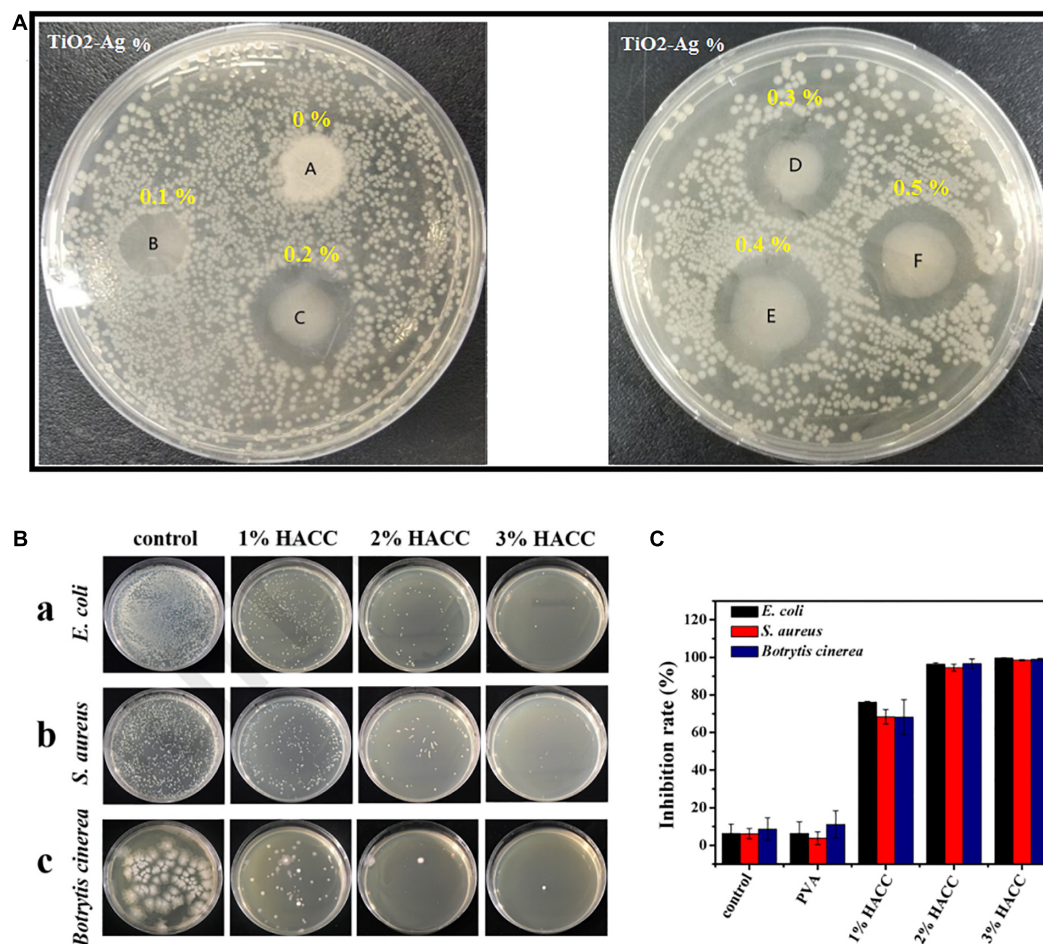


FIGURE 4 | (A) Inhibition zone test for fish gelatin-chitosan films containing different percentages of TiO₂-Ag against *E. coli* [reproduced with permission from Lin et al. (2020)]. **(B)** The antibacterial impact of the chitosan/polyvinyl alcohol (HACC/PVA) composite films: (a) *E. coli*, (b) *S. aureus*, and (c) *Botrytis cinerea*. **(C)** The inhibition rate of different coatings for *B. cinerea*, *S. aureus*, and *E. coli* [reproduced with permission from Min et al. (2020)].

interference with protein synthesis and the release of Zn²⁺ ions that participate with DNA replication, and (iii) generation of reactive oxygen species (ROS) which degrade bacterial cells (Shankar et al., 2019).

Scientists, to promote more reliable and safer antibacterial-based AFP, employed natural antibacterial agents such as essential oils (EOs) due to their potent antibacterial properties, low price, accessibility, and nontoxicity properties to enhance the shelf life of foods packed with biocompatible materials (Brobbe, 2017; Ju et al., 2019; Sharma et al., 2020a). If such additives were directly incorporated into the food system, a sudden reduction in the bacterial population will be seen, but it may change the smell and taste of food and also limit its long-term efficiency. Various biopolymers capable of holding EO have been employed in antibacterial-based AFP, in the forms of film and coating. It has been proved that embedding EO in the form of nanoparticles will result in better stability and efficacy compared with the free form (El Asbahani et al., 2015).

Regarding their antimicrobial potential, as well as metal nanoparticles, AFP efficacy may be different from different

sources, and no single specific mechanism has been proposed for the antimicrobial performance of EO. Antimicrobial potential depends on the concentration of EO, active ingredients, and the type of the microorganisms (Hyldgaard et al., 2012). It was also reported that EO can alter the physiochemical and biochemical aspects of the pathogen (Rao et al., 2019). Studies have shown that the cell wall of Gram-positive bacteria is more sensitive than that of Gram-negative bacteria and is mainly made of peptidoglycan. This makes their walls permeable to hydrophobic compounds such as EOs (Nazzaro et al., 2013).

Another type of antibacterial-based AFP is based on the antibacterial properties of the base material for film or coating production. For instance, chitosan is known as the only natural polysaccharide that shows noticeable antimicrobial activity against a range of microorganisms (Oyervides-Muñoz et al., 2017). Its antimicrobial activity is related to its cationic nature, concentration, deacetylation, exposure time, and organism. The right mechanism of chitosan antimicrobial performance is still unclear. The utilization of natural chitosan was restricted owing to its insolubility in

water and antibacterial valency (Oyervides-Muñoz et al., 2017). In another study, as shown in **Figure 4B**, the ammonium chitosan/polyvinyl alcohol (HACC/PVA) composite coatings revealed significant antibacterial activity for three types of bacteria, while many bacterial colonies were reported in the control groups. Furthermore, the antibacterial efficacy was promoted by enhancement in HACC content (Min et al., 2020) (**Figure 4C**).

Indicators of Food Freshness and Spoilage

NFP is looking for new packaging systems to help customers diagnose product quality and spoilage. So far, many studies have been performed to produce packaging systems with the ability to detect corruption. In 20th-century developments in FPS such as packages loaded with oxygen scavengers and antimicrobial agents, new precedents have been established for expanding food shelf-life by protecting them from external environmental conditions.

On the other hand, it would be interesting if consumers realize the quality, nutrition, or spoilage of foods during their shopping without help from specialists. Additionally, if the sellers could easily assess the quality of their products and remove any rotten food from the shelves, the quality of the people's food basket would increase, and SFP would reveal its potential in fulfilling this approach.

Temperature is a vital factor in distinguishing the shelf life of a food product. One of the strategies for FPS for informing the customer about the status of the product is time temperature indicators (TTIs) (**Figure 5A**; Gao et al., 2020). These systems are in the form of color dots that exhibit color changes due to temperature changes. These systems are mostly used in products that require specific temperature conditions for storage or consumption (Wang et al., 2015).

In some cases, a product should not be heated above a certain temperature (for example, in a microwave); otherwise, the materials and ingredients of the product will be damaged. In such a case, the color point at the desired temperature indicates a specific color and warns the consumer not to increase the temperature (Aadil et al., 2019). As another example, such a system can be used for some beverage products such as juices. Some products must be stored or consumed at the refrigerator temperature. For the color dot, a special color is considered at the refrigerator temperature, and if the temperature decreases or increases, the color change warns the consumer that the product temperature is not suitable (Aadil et al., 2019). It is very important that color changes be proportional with the real condition of food. For instance, based on **Figure 5B**, the boundary between color changes is limited, and there is a likelihood of wrong detection. Biological responses depend on biological mechanisms such as spores, microorganisms, or enzymes during specific periods and temperatures (Pavelková, 2013). The Fresh-Check proposed by Lifeline Technologies is another example of a TTI. Its mechanism follows a polymerization reaction and leads to a color change in the indication area. TTIs for spoilage products looks dark in the center, and a clear center means the food is fresh.

If the center color matches the color of the outer ring, the product must be consumed soon (Endoza et al., 2004).

Deviations in temperature can cause microorganisms to grow or survive in the food, resulting in spoilage of the product. In general, TTIs or time temperature integrators are simple, inexpensive gadgets attached to the package (Gao et al., 2020). Three types can be distinguished: critical temperature indicators, which show if temperature exceeds proper limits; secondly, partial history indicators, which indicate if a product has been subjected to temperature that causes a change in product quality; thirdly, a full history indicator which records the complete temperature profile along the food supply chain (O'Grady and Kerry, 2008).

The consumer label is another system in SFP. It is a partial-history indicator that provide information about the history of product's quality based on color changes during storage condition that are different than the recommended storage (e.g., temperature) and will also inform if the product is not consumable anymore (Chen et al., 2019). One of the commercial labels is TimestripsTM, which monitors how long a kind of food has been open or has been in use (Food Lable Timestrip, 2020).

There is another type of SFP which is a pH-based system. In a packaged food product, due to the spoilage of the food, the pH level in the product increases or decreases over time, which can be detected by suitable pH sensors. pH sensors change color when exposed to an acidic or alkaline environment, which is a key element of these sensors (Kuswandi and Nurfawaidi, 2017). There are various metabolites which result in pH changes during food storage including glucose (based on glucose oxidases activity), lactic acid (based on lactate oxidase and peroxidase activities), carbon dioxide, oxygen, biogenic amines (based on amine oxidases or transglutaminase), and microorganisms. To design pH-based indicators, it is necessary to put the indicator inside the packaging to sense pH changes. The pH-based indicators perform based on color changes as well as TTIs (O'Grady and Kerry, 2008). In this regard, a pH-sensitive color is entrapped within a polymeric network inside the indicator; the acidic liquid diffuses within the network and reacts with the dye; and, consequently, the color changes. The food spoilage (especially fish and meat) correlates with bacterial growth patterns; hence, color changes indicate bacterial growth (Chen et al., 2019).

Considering fruits and vegetables, during ripening, aromas are released by fruits. The novel colorimetric indicators sense the aromas and show various changes in color, whose range depicts the process of ripening (Bordbar et al., 2018). By monitoring the color of the sensor, consumers realize which fruit is at the preferred ripeness. RipesenseTM is known as a commercial indicator with the same protocol (Nanotechnology Products Database, 2020).

Another type of indicators is gas based, which senses the indoor atmosphere of packaging (Weston et al., 2020). During the storage time, some metabolites including CO₂, H₂S, O₂, ethylene, and volatile compounds like ammonia, amines, and ethanol appear in the headspace of the packaging (Mills, 2009; Lang and Hübert, 2011; Koskela et al., 2015; Saliu and Pergola, 2017). These metabolites can be employed as a quality-indicating index for spoilage monitoring by employing an indicator within

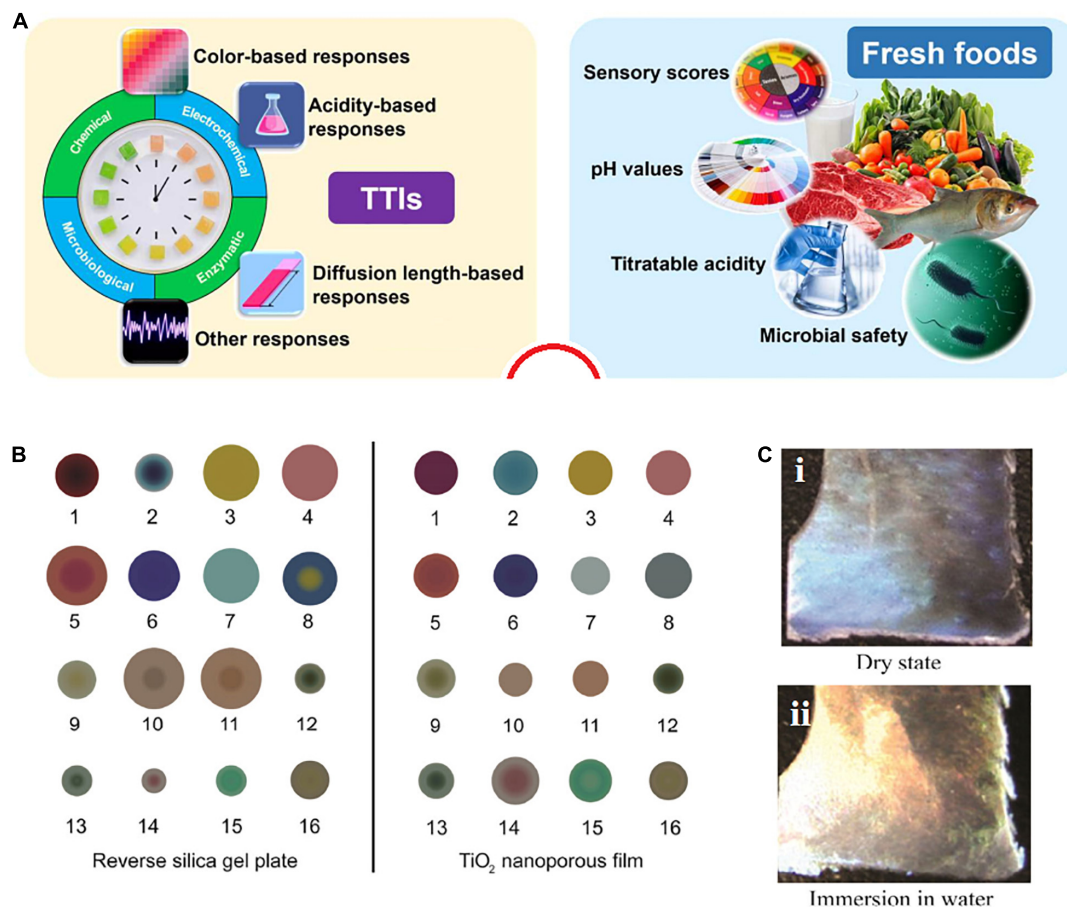


FIGURE 5 | (A) Employed parameters for designing TTIs (left) and indexes for informing about the conditions (right) [reproduced with permission from Gao et al. (2020)]. **(B)** A colorimetric sensor based on the TiO_2 (right) and reverse gel silica plate films (left) [reproduced with permission from Xiao-wei et al. (2016)]. **(C)** Color changes of CNC film: (i) dry film, (ii) after immersing in water [reproduced with permission from El Asbahani et al. (2015)].

the packaging system (Mohammadian et al., 2020). Not only do majority of these indicators identify the carbon dioxide and oxygen concentrations (Meng et al., 2014), but water vapor, ethanol, hydrogen sulfide, and other gases are also checked (Fang et al., 2017). A sensor is sensitive and reacts to (gas) changes inside the packaging atmosphere, while an actual indicator detects the quality status. The condition in the atmosphere inside the packaging is based on the food activities, such as chemical reactions or enzymatic actions (e.g., microorganisms generate gases, and the gases transmit through the packaging), and, on the other hand, on the package nature and the storage condition like humidity (Figure 5C).

As the expiration time of different products lasts from days to years, it is important that the SFP keeps its quality at a higher level till the last day of consumption and provide reliable information during storage in the refrigerator or freezer, at normal ambient or even elevated temperatures.

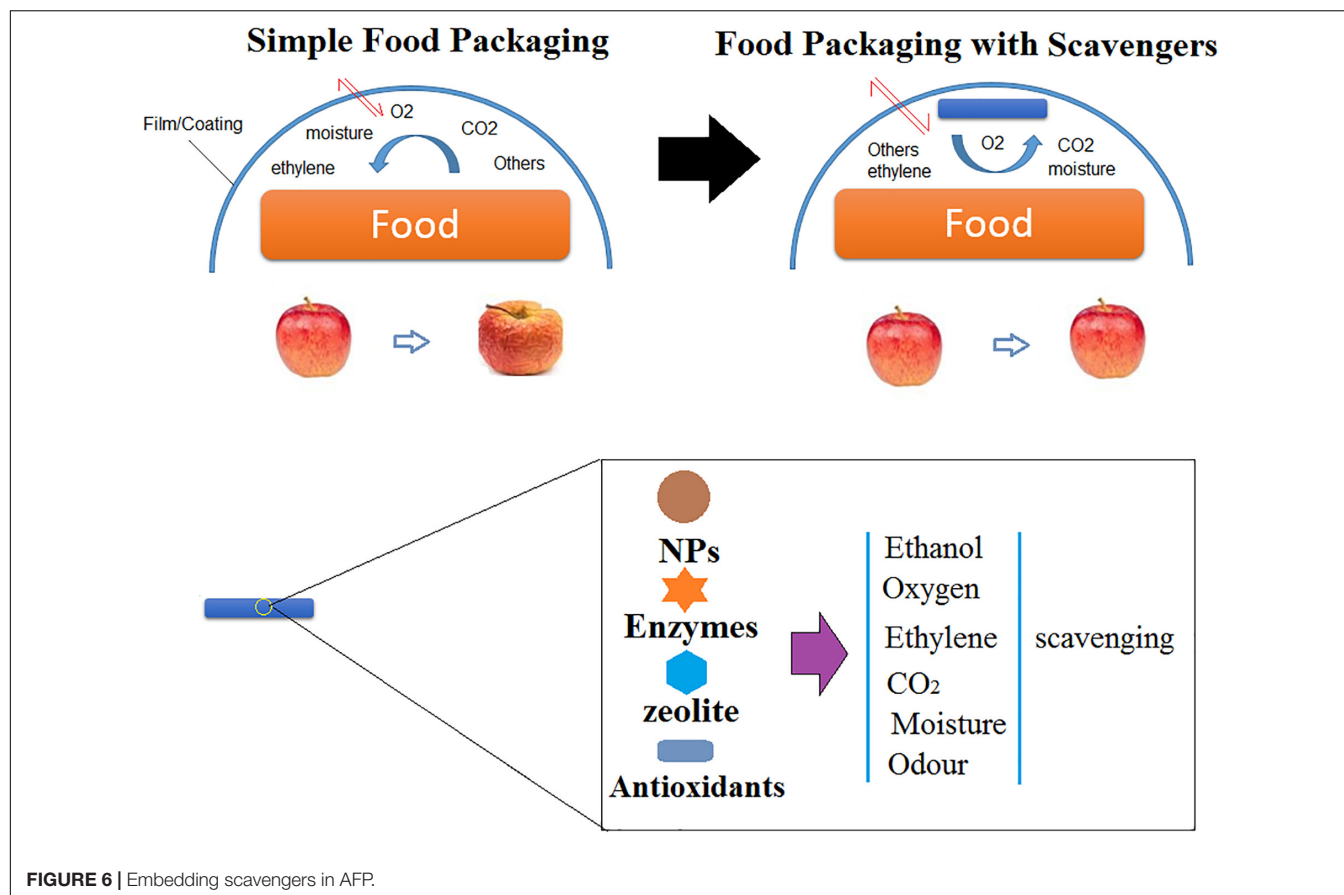
Scavengers in Food Packaging

NFP includes additives that are capable of absorbing or scavenging carbon, oxygen, dioxide, ethylene, moisture,

odor, and flavor taints; releasing carbon dioxide, oxygen, ethanol, sorbates, antioxidants, and other preservatives and antimicrobials; and maintaining and controlling temperature (Figure 6; Biji et al., 2015).

Apart from microbial growth, lipid oxidation is the vital reason for spoilage of various types of foods, including meats, fish, nuts, sauces, milk powders, and oils. It results in a loss of both nutritional and sensorial quality of foods and may even cause the formation of toxic aldehydes. Vacuum packaging is a technique to avoid oxygen accumulation in food packages (Narasimha Rao and Sachindra, 2002). There are some new approaches that are commonly employed to prevent lipid oxidation of packaged foods. In this technique, packaging is under modified atmospheres or direct addition of antioxidants in which the presence of oxygen is limited (Gómez-Estaca et al., 2014). AFPs have been engineered to prevent food spoilage by embedding applicable agents within the packaging (film/coating).

Considering AFP containing oxygen scavengers are able to remove the remaining oxygen in packages, there is a high possibility of affecting the color, taste, and odor of the food and enhancing aerobic bacterial growth before consumption. Various



commercialized scavengers that take away the relict oxygen (or other gases) from the packaging are accessible in the form of plastic films, sachets, labels, bottle crowns, and plastic trays (Cichello, 2015). Oxygen scavenging (OS) can employ various mechanisms such as oxidation of iron powder (Miltz and Perry, 2005; Byun et al., 2011). Iron powder sachets are known as the most employed OS agent for commercial purposes. They function based on the criteria of oxidation in the presence of Lewis acids (e.g., FeCl₃ and AlCl₃) or moisture (Cruz et al., 2006). In this case, iron powder is embedded within polymer films for AFP purposes. It should be considered that the type of the employed polymer affects the potential OS capacity of iron. The reason turns back to differences in the permeability and barrier properties of different polymeric films (Khalaj et al., 2016).

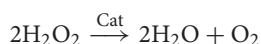
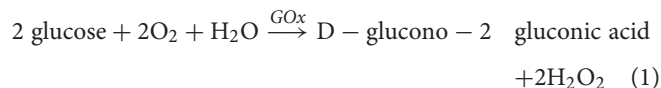
Other metals including platinum, cobalt, and palladium also revealed OS properties (Cherpinski et al., 2018). It was reported that these metals reinforce the oxygen reaction in the presence of low concentrations of hydrogen, leading to an oxygen level reduction by two orders of magnitude (Yu et al., 2004). Similar to that of iron, their OS efficacy alters with the change in oxygen permeability capacity of the polymers. For instance, different OS efficacy rates for Pd (10% w/w) have been obtained for different polymers. In the case of coating made of palladium + polymer, the oxygen reduced from 1 to 0.28% in 91 min (Pd + silicone rubber), 0.15% in 200 min (Pd + nitrocellulose), 0.31% in 123 min (Pd + polyvinyl butyral),

0.17% in 75 min (Pd + polyurethane), and 0.3% in 60 min (Pd + ethyl cellulose).

The technique of OS comprises stimulation of an inorganic or organic compound embedded in the polymer structure by UV radiation (Dey and Neogi, 2019). 2-Vinylanthraquinone and 2-methylhydroquinone are two organic compounds that when exposed to UV radiation act as oxygen scavengers. An OS system containing triphenylphosphine, 2-methylhydroquinone, and ethyl cellulose decreased oxygen level (from 14.6 to 0.07 vol% every 25.3 h) in the headspace of the container. The triphenylphosphine scavenged the hydrogen peroxide formed during the process (Rooney, 2002).

Unsaturated hydrocarbon-based OS systems are potent candidates for dried foods, but the main problem is the formation of by-products such as ketones, aldehydes, or organic acids which may affect food quality. Organic acids (ascorbic and gallic acids) (Lo Scalzo, 2008), photosensitive dyes (Nie and Xiao, 2020), and enzymes (Hitzman, 1983) are other mechanisms for OS but with lower capacity. Ascorbic acid and α -tocopherol with OS rates of 11.9 and 0.21 cm³ of O₂ day⁻¹ g⁻¹, respectively, are highly compatible for AFP (Byun et al., 2011; Rodríguez et al., 2020), but both need to be stimulated by UV, light, heat, or transition metals, which entails higher expenses as compared to nano-iron-based scavengers. Besides, they show low efficacy in oxygen scavenging in high moisture content and avoid lipid oxidation because to inhibit lipid oxidation, 98% oxygen scavenging must

be obtained (Johnson et al., 2016). The enzyme function of OS is based on reactions with a specific substance. Catalase (Cat) along with glucose oxidase (GOx) are the most commonly employed enzymes for OS in AFP (Gaikwad et al., 2018). According to Eq. 1, to aim for a good OS, it is mandatory that glucose exists in the scavenger formulation or in the food.



Embedding clay in the polymeric matrix results in enhancement in OS activity. In this regard, clay prevents glucose pre-oxidation. Besides, the presence of clay in the film matrix increases the porosity of the films, which leads to an increase in surface area and thus an increase in OS capacity (Johansson et al., 2011).

Moisture is another factor which must be controlled in FPS. In this case, moisture scavenging (MS) operatives such as silica gel, natural clays, calcium chloride, calcium oxide, and molecular sieves have been developed to act as OS systems to control residual or excess moisture in packages, thereby preventing or delaying foggy film formation and microbial growth (Ozdemir and Floros, 2004).

To decrease the perishable fruit maturation which happens by the presence of ethylene during a short time, ethylene scavenging (ES) factors are often employed (Gaikwad et al., 2019). The most employed ES agents are based on potassium permanganate; then dispersed minerals like zeolite, pumice, and active carbon; and finally, metal catalysts like palladium with charcoal (Álvarez-Hernández et al., 2019).

Carbon dioxide is another factor which needs to be controlled for increasing food shelf life. Carbon dioxide scavenging (CS) agents, including zeolites and calcium hydroxide, are mostly employed to remove CO₂ gas generated from microbial growth, degradation mechanisms, and respiration. CO₂ releasers such as food acids and sodium bicarbonate decrease the microbial growth and the respiration rate of vegetables (Lee, 2016). Different synthetic antioxidants including organophosphates and polyphenols and natural antioxidants like spices and herbs are embedded in the packaging to delay or prevent the negative effects of oxidation and thermal degradation (Lee, 2016). To sum up, scavenging-based AFP, such as NFP, is a potent candidate to reduce lipid oxidation and food spoilage in packaged foods (Gómez-Estaca et al., 2014).

BIOMATERIALS FOR NFP

Since 50 years ago, plastic has been widely used in the production of packaging materials due to its ease of production, storage, and transportation. With the development and progress of the food industries, there is a great demand for packaging materials based on petroleum products such as PVC, PET, polystyrene (PS), polypropylene (PP), and polyamide (PA) for use in this industry (Ebnesajjad, 2012). Despite their advantages,

these plastic products have caused serious environmental problems due to their nondegradability in the environment (Rhein and Schmid, 2020).

The advent of biopolymers is a good solution to improve the environmental problems caused by plastics, because they are biodegradable despite imitating the properties of plastics and only remain in the environment for a short time. Biopolymers are divided into three categories based on the source of production (Table 3; Gupta and Dudeja, 2017) polymers extracted from biomass (Grönman et al., 2013), those synthesized from biomass-derived monomers, and (Muncke, 2014) those produced from microorganisms (Mangaraj et al., 2014; Naveena and Sharma, 2020). Considering applications in the food industry, these bio-based materials are particularly applicable in three main areas in FPS: food coating, food packaging, and edible films. NFPs basically employ biomaterials from the category above for professional purposes.

In order to use these materials, it is necessary to produce them in a specific form (polymeric films). There are various film-forming methods for biopolymers, including the melt mixing method, solution casting method, thermal pressure method, electrospinning method, and extrusion blown film method. The quality of polymers can be described as various properties such as physical, thermal, mechanical, and barrier properties. With increased awareness on sustainability, packaging industries around the globe are looking for biopolymers as a replacement for synthetic polymer. Biopolymers may be defined as the polymers that are biodegradable by the enzymatic action of microbes. In the last two decades, a lot of research has been done on biopolymers for food packaging applications (Fabra et al., 2014).

The employment of edible packaging (EP), as a thin layer covering the food surface, drew much attention from scientists and industries (food and beverage). EP has the ability to remove the issues associated with plastic packaging systems. EP showed several targets including moisture loss restriction, gas permeability management, quality of microbial activity (e.g., chitosan, which acts against microbes), gradual release of flavors, and maintenance of the structural integrity of the product in the food (Jeevahan and Chandrasekaran, 2019). However, the sources of biopolymers used for NFP are also important.

Group 1: Polymers directly derived, removed, or extracted from biomass showed reliable results in FPS. Cellulose, starch, and proteins such as casein and gluten, as certain polysaccharides, are a few of the commonly used biomaterials. However, all of them are inherently hydrophilic and crystalline, causing problems during processing. In case of moist foods, their performances revealed poor results, whereas due to their excellent gas barrier properties, they are a good candidate for FPS (Azeredo et al., 2014). This type of biomaterials is useful for expanding the shelf life.

Other extracted materials from biomass resources, like polysaccharides (e.g., chitosan), proteins (e.g., zein), and lipids (e.g., waxes), also showed excellent potential as aroma and gas barriers in FPS. Chitosan has depicted significant potential as an antimicrobial biomaterial to keep foods from different microorganisms (Wang H. et al., 2017; Mohamed et al., 2020). In a research, pork sausages were covered by chitosan film, resulting

TABLE 3 | Three category of bio-based polymers.

Bio-based Polymers				
Polymers extracted from biomass			Polymers synthesized from bio-derived monomers	Polymers produced from microorganisms
Polysaccharides	Proteins	Lipid	Poly lactate	Bacterial compounds
Starch	Animal	Waxes	Poly lactic acid	Cellulose
Chitosan	Casein	Oils	Polycaprolactan	Xanthan
Chitin	Whey	Fats		Culanpullulan
Potato	Collagen			
Corn	Gelatin			
Wheat				
Rice				
Other derivative				
Cellulose	Plant			
Cotton	Zein			
Wood	Soy			
Other derivative	Gluten			
Gums				
Guar				
Locust bean				
Alginate				
Carrageenan				
Pectin				

in oxidative and color stability improvement (Siripatrawan and Noipha, 2012). Previous studies focusing on AFP have assessed the antimicrobial efficacy of chitosan when combined with other polymers, such as starch (Haghighi et al., 2020). Green plants such as rice, wheat, corn, and potatoes are the most common and new ingredients employed to produce starch biopolymers. It was reported that when chitosan is combined with tapioca starch, greater antimicrobial effectiveness was observed (Vásconez et al., 2009). Starch due to its low cost and availability is known as the most preferred biopolymer. Cellulose, with potent mechanical features and being made of glucose units, is a polar polymer. The configuration of the polymer chain in a different way from that seen in starch provides an opportunity to strengthen this polymer due to the formation of strong hydrogen bonds (Chen et al., 2014).

The main disadvantages of these kinds of materials are the inherently high adversity and problem of processing them in common and conventional equipment (Zhao et al., 2019). For instance, although starch is known as a biodegradable biopolymer that can be synthesized in large quantities with low cost, can be easily handled, and can form films for FPS with low oxygen permeability, the main challenge of native starch is that it is fragile and hydrophilic. This weakness fails them in NFP. These issues restrict its different applications like its employment for plastic bags and food packaging manufacturing (Weber et al., 2002). To overcome this drawback and improve its flexibility and ease of processing, various plasticizers like glycerol, glycol, and sorbitol are utilized to make the starch into a thermoplastic starch (TPS) using heat and extrusion processes (Abdorrezza et al., 2011; Isotton et al., 2015; Mikkonen et al., 2015). In the case of microencapsulation and nanoencapsulation in NFP, these biomaterials showed their potential too. For

instance, encapsulation of probiotics, antioxidants, and bioactive ingredients help NFP to act as an AFP. Each of these ingredients, due to their chemical structure and surface charge, needs specific biomaterials to be encapsulated with. The most widely employed material for probiotic encapsulation is alginate, which can be employed alone or combined with other biomaterials like chitosan (Chandramouli et al., 2004).

Another disadvantage of polysaccharides and proteins is their very potent water sensitivity generated by their hydrophilic nature (Chivrac et al., 2009). This leads to a powerful plasticization resulting in oxygen barrier properties being spoiled as the water sorption and relative humidity in the matrix of materials increase (Laufer et al., 2013). The low water resistance of proteins and polysaccharides restricts their usage in FPS. It would be extremely advantageous to decrease the water sensitivity of polysaccharides and proteins and to improve the gas barrier properties and total functionalities of thermoplastic biopolyesters to promote their properties in APS (Laufer et al., 2013). Proteins, based on their origin, comprise two categories, namely, plant proteins (e.g., gluten, soy, potato, zein, and pea) and animal proteins (e.g., casein, collagen, whey, and keratin) (Ahmadzadeh and Khaneghah, 2019). Proteins, due to their functionalities, are suitable to be modified to make a polymer. Protein-based polymers (except keratin) are sensitive to moisture. This sensitivity can be overcome by lamination or blending with chitin (as the second abundant polysaccharide). Chitin is abundant in marine invertebrates like crabs, shellfish, shrimps, insects, and some yeasts and fungi. Chitosan and chitin are eco-friendly, nontoxic, water-insoluble, and biodegradable polymers, with no antigenic features; besides, they show good biocompatibility (Priyadarshi and Rhim, 2020). Lipid compounds such as wax and glycerides are mostly employed to

provide hydrophobicity in FPS (coating/films). They impressively prevent water vapor diffusion within edible films. This ability will help FPS to prevent the growth of microorganisms and food spoilage as a feature of AFP. The functional characteristics of FPS containing lipids are efficiently influenced by lipid properties including the physical state, saturation degree, structure, chain length, the crystal morphology, and distribution. Isolated soy protein-based films are moisture sensitive, which can be modified by the incorporation of stearic acid (SA) in a proportion of 25% (Lodha and Netravali, 2005; Han Y. et al., 2018). It has been recently revealed that incorporation of soy protein with K-carrageenan, glycerol, or gellan gum is effective in creating edible and biodegradable soy protein-based FPS.

Group 2: Synthesized polymeric materials are produced by classical polymerization techniques like aliphatic polyesters, aliphatic aromatic copolymers, aliphatic copolymer, polylactide using renewable bio-based monomers including PLA, and oil-based monomers such as poly-caprolactones (PCL). PLA is a good and well-known example of polymers and can be created into injection mold objects, blown film, and coating. PLA is popular in FPS due to its supreme transparency and relatively noticeable water resistance. In a study, PLA in combination with PCL, loaded with carvacrol and thymol oil, could show antioxidant activity as an AFP (Lukic et al., 2020). In another research, PLA films were functionalized to transfer cinnamaldehyde as an AFP (Villegas et al., 2019). The main challenge for these biomaterials is to promote their thermal and barrier properties; thereby, they act like PET. PLA can be used as laminates (barrier film) or homomaterials for FPS. However, it is not pliable, and it is also sensitive to rupture. PCL as another one of the most employed polymers in FPS is a hydrophobic aliphatic polyester which can be produced by chemical reactions from either renewable resources like polysaccharides or petroleum. PCL with a low viscosity is a biodegradable, thermoplastic, and biocompatible polymer, which has a low glass transition temperature. Besides, it can easily be utilized with common melt processing equipment (Cabedo et al., 2006; Woodruff and Hutmacher, 2010; Rešček et al., 2015). PCL in NFP depicted an antimicrobial character, inhibition or quenching potential, spoilage prevention, pathogenic microorganism removal, and at same time being environmentally friendly (Pina et al., 2020). There are other synthesized biopolymers that showed similar potential in NFP. Poly(vinyl alcohol) (PVA) has been another polymer suitable for food packaging. The films or coating prepared by PVA showed that it can be a good candidate in transferring antibacterial agents while controlling moisture, oxidation, and sensory properties (Bhat et al., 2021). poly(lactide)/poly(butylene adipate-co-terephthalate) (Sharma et al., 2020b), poly(methyl methacrylate) (Lin et al., 2019), and poly(*L*-glutamic) acid-poly(*L*-lysine) (Karimi et al., 2020) are some more examples that are employed in NFP due to their ability to provide antibacterial activities, to control nanoparticle migration, and to have good mechanical behavior and biodegradability.

Isocyanates and polyol are utilized to synthesize films/coating suitable for FPS. Polyol can be generated from edible oils,

and isocyanate can exclusively be generated from petroleum-based feedstock (Dong et al., 2020). Diversified synthesis and working on the parameters can give various biomaterials different characteristics.

Group 3: Polymers which are synthesized by genetically modified bacteria or microorganisms showed their potential in FPS. Different types of microorganisms such as *Bacillus*, *Alcaligenes*, *Rhizobium*, *Halobacterium*, and *Azotobacter* produce large amounts of renewable and biodegradable materials. These substances are collected by bacteria as an energy source and a store of carbon. Bacterial cellulose (BC) and polyhydroxyalkanoates (PHAs) are two of the main polymers which are synthesized by microorganisms and are highly used in FPS (Ivonkovic et al., 2017). PHAs as hydrophobic polyesters may have various properties and characteristics related to monomer building blocks, which lead to a variety of PHA types. The most important PHAs are PHB and the copolymers poly(3-hydroxybutyrate-co-3-hydroxyvalerate) (PHBV) and poly(3-hydroxybutyrate-co-3-hydroxyhexanoate) (PHBHHx) (Gouvêa et al., 2018). PHBV, as well as other biomaterials, showed its potential in NFP by carrying nanoclay functionalized by oregano EO. It showed better oxygen barrier properties with higher antimicrobial activity (da Costa et al., 2020). PHA may be a rigid, brittle, or rubber-like polymer depending on the carbon source and the bacterial type (Sharif et al., 2020). Copolymerization is one of the techniques to improve physical-mechanical properties of PHAs as well as other techniques such as blending. This behavior makes it a good candidate for various purposes in NFP proportional to the food type. BC has been employed for a number of distinct applications, specifically in the biomedical area. Although there are several noticeable applications of BC in FPS, only a few studies reported on this area, the reason for which, as a limiting factor, is the expensive process of BC production (Azeredo et al., 2019). BC in combination with chitosan could act as a biodegradable film for active packaging materials (Xu et al., 2021). Based on the results, the prepared film depicted the best antioxidant activity. In a research, it was reported that more than 50% of pure BC film goes through degradation in 3 days and 100% after 7 days in the soil (Zahan et al., 2020). Interestingly, *Bacillus* sp. and *Rhizopus* sp. were identified as the bacteria responsible for BC degradation.

In case of coating foods, under direct coating, the main goal is immobilization of the polymer directly on the food surface to provide adequate protection (due to containing active substances) from environmental hazards like microbes. Also, the coating can alter the gas permeability coefficients of the fruits and vegetables, thereby altering their respiration rate and shelf life. These coatings are environmentally friendly, biodegradable, and, in most cases, edible. Overall, three types of coating methods have been explored: spread coating, spray coating, and dip coating.

NANOTECHNOLOGY AS NFP MATERIAL

Subsequent generation of materials employed in NFP is presumably bio-nanocomposites. Expansion of bio-nanocomposites is a direction to develop original and inventive

biomaterials in the area of NFP. Nowadays, numerous nanoscale substances (metal nanoparticles, polymeric nanoparticles, nanoemulsion, nanoclay, and so on) are candidates in food packaging systems including AFP and SFP. Incorporation of nanotechnology with FPS enhances the viability and stability of susceptible active compounds and promotes the essential packaging functions—preservation and protection, containment, communications and marketing, and the efficacy of FPS.

On one hand, nutritional features of packaged foods can be promoted by utilizing nanoscale additives and nutrients and delivery systems for bioactive compounds (Silvestre et al., 2011). On the other hand, to enhance food shelf life and prevent spoilage, different functional agents like antimicrobials, antioxidants, colorants, anti-browning agents, and enzymes can be employed in FPS in the nano dimension by embedding them into the polymeric matrix or coating them on the surface (Kanmani and Rhim, 2014; Alfei et al., 2020).

One of the main aims in NFP is improving the packaging properties including film/coating flexibility, gas barrier properties (e.g., carbon dioxide, moisture, oxygen, and emission of ethanol and flavors) (Mei and Wang, 2020), and temperature/moisture stability (Kraśniewska et al., 2020). Employing diverse NPs in FPS is an option to boost these improvements. Thereby, integration of FPS and NPs has developed various polymeric nanocomposites and polymeric nanomaterials (Alfei et al., 2020). These nanomaterials may be employed alone or along with other NPs for FPS development. In this case, to promote and maintain texture, flavor, and color; reduce corruption; prevent adulteration; and enhance stability during storage, diverse nanofillers can be used including nanoclay, silicate, carbon nanotubes, graphene, metal NPs and their oxides, nanocellulose, and EO-based nanoemulsions (Carbone et al., 2016; Han C. et al., 2018; Biswas et al., 2019; Espitia et al., 2019; Emamhadi et al., 2020). NFP with the help of NPs has also more active properties such as biocatalysts and antibacterial actions (Kim et al., 2020). In order to make optimal use of NPs, they must be obtained completely homogeneously in the polymer matrix because the degree of homogeneous dispersion of NPs in the polymer matrix alters the relaxation of the polymer chains and molecular mobility, subsequently affecting mechanical properties and thermal resistance. Also, NPs also provided an interesting potential for NFP by which they are planned to act as gas scavengers, sensors, and condition indicator (food and environment surrounding) or can also serve as a protector against fraudulent imitation (Ding et al., 2020). As previously mentioned, there are numerous NPs which are employed in NFP [this topic has been nicely reviewed by Alfei et al. (2020)].

Nanoclay NP in NFP

One of the most employed NPs is nanoclays that are aluminum silicate made of fine-grained minerals with a natural structure in sheet-like geometry. Nanoclay for NFP is utilized in the polymer formation as nanocomposites due to its high stability and benignity, convenient process ability, low cost, and good availability. Montmorillonite (MMT) is a clay nanomaterial emanating from volcanic or rocks ash, which is extensively employed in nanocomposites (Bai et al., 2020). When nanoclay

is embedded in a polymer matrix, they oppose the penetration of gases and other materials. Nanoclay NPs showed their potential in improving barrier properties and minimizing gas and small-molecule transmission between food and the outside packaging environment, which shows improvement in diffusion and solubility coefficients (Horst et al., 2020).

AgNPs in NFP

AgNPs as an inorganic metal oxide are industrially produced by mechanochemical or physical vapor methods (Casey, 2006). The use of AgNPs in NFP has recently attracted much attention. AgNPs possess the most impressive antibacterial properties against a wide range of microorganisms such as yeasts, bacteria, viruses, and fungi (Moadab et al., 2011; Martínez-Abad et al., 2012). Besides shelf life enhancement, AgNPs cause no change in food physical characteristics (Ahari, 2017). Numerous studies reported about the potential of AgNPs in NFP for orange juice and beverage (Emamifar et al., 2010), bread (Sattari et al., 2010), fish and meat (Umaraw et al., 2020), and fruits and vegetables (Ijaz et al., 2020). AgNPs showed improved potential when combined with other nanoparticles such as ZnO and CuO.

ZnONP in NFP

The application of ZnO nanoparticles increased in safe food packaging due to their antimicrobial activities, UV blocking, and being cheaper than AgNPs (Emamifar et al., 2010). By integrating ZnONPs with polymeric FPS, characteristics such as mechanical strength, blockade properties, and durability can be noticeably improved (Espitia et al., 2012). It was reported that the uniformly dispersed ZnONPs within the PLA matrix effectively adjusted the diffusion of penetrant molecules (e.g., CO₂ and O₂). The reason was increasing the tortuosity of the diffusive route (Vasile et al., 2017). Similar results were reported by Sossio Cimmino. They also reported the high potential of ZnONPs in preventing *E. coli* growth (Marra et al., 2016). As previously mentioned, the proposed mechanisms for microbial growth prevention by NPs comprise cell respiration, cell wall disruption, and interaction with thiol groups of DNA and sulfhydryl or phosphorous, proteins and enzymes, and ROS (Kanmani and Rhim, 2014). For example, generated ROS due to NPs causes disruption of the cell membrane, damaging the DNA and mitochondria and interrupting transmembrane electron transport in the cell (Garcia et al., 2018).

TiO₂NP in NFP

TiO₂, CuO, and AlOx, as well as ZnO, AgNPs, and silica, are also employed in FPS. These NPs (in the form of being blended with or coated on the diverse biological and synthetic polymers) are generally employed as photocatalysts with antimicrobial and EE properties and can also improve mechanical properties (e.g., tensile strength) and gas barrier and UV barrier properties of the FPS (Xing et al., 2012; Bumbudsanpharoke et al., 2015). There are several reports that bond formation between TiO₂NPs and the polymer prevents the interaction of water molecules with the polymeric chains by blocking the number of sites in the polymer chains (Siripatrawan and Kaewklin, 2018; Anvar et al., 2019). It was also found in studies that addition of TiO₂NP to the

polymeric films increased the tensile strength and elongation at break (Xing et al., 2012).

SiO₂NP in NFP

Modification of nano-SiO₂ with ethylene/vinyl acetate and mixed with polypropylene (PP) showed tensile strength enhancement and gas permeability improvement. Compared to the pure nanocomposite, addition of SiO₂ resulted in less ink solvent adsorption, which can be important in the case of laminated food packaging as the PP layer is used for printing (Li et al., 2016). SiO₂ also showed its potential in adjusting the barrier properties of coated nanocomposites. For example, this process increased the gas barrier properties up to 70% compared with the pure PLA films while keeping its physical properties (e.g., remaining transparent) (Bang and Kim, 2012). In addition, silicon is one of the most widely used nanoparticles in the fight against Gram-positive and Gram-negative bacteria and fungi. Its antimicrobial effect in a variety of food packaging coatings has been proven in recent studies (Al-Tayyar et al., 2020; Hajizadeh et al., 2020).

AlOxNP in NFP

Aluminum oxide (AlOx), as well as the previous NPs, has revealed high potential in FPS in the viewpoint of barrier properties. PLA-Al₂O₃-coated board paper, compared with the double-coated PLA film with a layer of Al₂O₃ and a layer of alginate-chitosan, substantially increased the water, oxygen, and aroma barrier properties (Hirvikorpi et al., 2011). In another study, it was reported that coating of PET with aluminum oxide could also promote the barrier properties, which could become a potent substitute to the common metallized retortable packaging (Struller et al., 2014).

SnO₂NP in NFP

Nanocrystalline stannic oxide (SnO₂) showed its potential in indicator-based NFP. SnO₂ has the potential to indicate oxygen because a dye photo-reduction can change the film's color depending on oxygen exposure. This system would be beneficial to approving the effectiveness of vacuum or nitrogen packaging. There are other NPs with similar performances but different efficacies [nicely reviewed by Jildeh and Matouq (2020)]. There are more reports about the antibacterial feature of SnO₂NP. Amininezhad and his colleagues reported that SnO₂NPs depict notable antibacterial activity against both Gram-positive and Gram-negative bacteria (Amininezhad et al., 2015). It was also reported that they had higher activity against *E. coli* than against *S. aureus*. In another study, scientists showed the antifungal properties of SnO₂ activity against *Candida albicans* (Fakhri et al., 2015).

Nanoemulsion in NFP

Other types of nanosystems such as nanoemulsion showed high functionality in NFP. Nanoemulsions possess nanosized droplets. This colloidal systems, due to the small size of the droplets, are kinetically stable, and their formulation comprises two immiscible liquids (water and oil) and an emulsifier [nicely reviewed by Salome Amarachi et al. (2014)]. The structure and

composition of this system can be engineered for the loading, encapsulation, and fruitful delivery of antimicrobial, oxygen scavenging, antibacterial, antioxidant, and flavoring and coloring agents (Salem and Ezzat, 2018). Based on the literature survey, the thermal, mechanical, barrier, and sensory properties are the most studied topics in nanoemulsion-incorporated NFP. In nanoemulsions, plant EO and oil compounds are employed as dispersed phases which are revealed to be useful antibacterial agents with an anti-plasticizing role in NFP (Du et al., 2008; Ahari and Massoud, 2020). The incorporation of EO into NFP caused higher water vapor permeability values and gas permeability in packages that possess low water barrier properties (Dammak et al., 2017). Furthermore, nanoemulsion-based NFP depicted remarkable antimicrobial activity when one of the components of the nanoemulsion is a biologically active agent. For instance, scientists reported that methylcellulose-based packaging films incorporated with oregano or clove bud EO enhanced the shelf life of sliced bread (Otoni et al., 2014). Salvia-Trujillo et al. (2015) expanded sodium alginate-based edible coatings loaded with lemongrass EO-based nanoemulsions to preserve freshly cut Fuji apples. In another study, thyme EO nanoemulsions showed their antibacterial effect on fish as a component of AFP systems, resulting in bacterial cell membrane rupture (Ozogul et al., 2020). Alexandre et al. (2016) integrated ginger EO with gelatin for food packaging application. The final film showed good antioxidant activity. Employing the nanoemulsion of saffron showed good antibacterial features in food packaging systems. The results of Ahari and his colleagues, as a patent, depicted high potential of saffron nanoemulsion in NFP (Hamed et al., 2021). *Thymus daenensis* EO embedded in hydroxypropyl methyl cellulose edible films could improve antibacterial activity and physical and mechanical properties (Moghimi et al., 2017). In addition, employing nanoemulsion enhanced the bioactivity and caused reduction in the impact on organoleptic characteristics.

Pickering emulsions are another new method in the field of nanoemulsions that has attracted a lot of attention in the field of food science (Chen et al., 2020). Unlike conventional nanoemulsions and emulsions, stabilization of Pickering emulsions is made by solid particles, which can be irreversibly absorbed at the oil-water interface and form a dense film (made of solid particles) to prevent droplet accumulation. Compared to conventional emulsions, Pickering emulsions have the advantages of less usage of emulsifiers, biocompatibility, higher safety, higher stability, reduction of droplet aggregation, and uniform droplet size distribution. Different types of solid particles include chitosan (Lim et al., 2020), starch (Zhu, 2019), cellulose (Liu et al., 2019), whey protein (Zhang Y. et al., 2020), zein (Zhu et al., 2019), soy protein (Ju et al., 2020), fat crystals (Wang Q. et al., 2017), and hydroxyapatite (Rodriguez et al., 2019) [nicely reviewed by Chen et al. (2020)]. Food-grade Pickering emulsions have significant applications in food packaging. For example, stabilized starch nanocrystal Pickering emulsions have been used to produce starch nanocrystalline nanocomposites, which are employed to produce active packaging coatings with better optical and mechanical quality (Zhu, 2019). A similar study was done by Almasi et al. using WPI-inulin complexes for stabilizing. The

final film showed good mechanical behavior (Almasi et al., 2020). In another research, Pickering emulsions were prepared using encapsulated hesperidin and then stabilized by chitosan nanoparticles. The obtained Pickering emulsions were integrated with gelatin to produce films/coatings with good flexibility while having strong antioxidant activity (Dammak et al., 2019).

Based on the results, an impressive antimicrobial behavior of the nanoemulsion-based coating was observed against *E. coli* compared to the control group. To sum up, scientists utilized different types of nanomaterials to promote NFP to aim in SFP and AFP (Nasiri et al., 2019).

HAZARDS OF NANOTECHNOLOGY IN NFP

Although the nano-based SFP and AFP under the category of NFP benefit from novel systems including nanoemulsions and nanoparticles, various reports have revealed many uncertainties still remaining about these systems, such as their interest for bioaccumulation, migration to food matrix, toxicity of the biomaterials, and human health risks. On one hand, scientists try to synthesize NFP, and on the other hand, many of them are worried about the consequences. Several commercialized forms of nano-based NFP in the form of composite or coating containing inorganic materials are employed in FPS. Some of them contain AgNPs, CuNPs, TiO₂NPs, and other metal NPs as the main agent for preventing microorganism activity (Brobbe, 2017; Aziz and Karboune, 2018; Bahrami et al., 2020). Numerous studies have reported about the possible migration of nanomaterial from FPS to foodstuff (Song et al., 2011; Ahari and Lahijani, 2021). There is still a debate among researchers about the extent to which migration is negligible and safe (Bumbudsanpharoke and Ko, 2015). A group of scientists have indicated that nanoparticles such as AgNPs have the capacity to damage human cells. This damage may happen by rectifying the function of the mitochondria, producing (ROS), and enhancing membrane permeability (Song et al., 2011). Scientists have reported that time and temperature are effective in nanoparticle migration. For example, it has been assessed that as time and temperature increased, AgNP migration slightly enhanced in 3% (w/v) acetic acid before reaching a steady state (Song et al., 2011). In a similar research, it has been reported that generally, the level of NP migration is significantly enhanced by temperature and time in all food-simulating solutions (Huang et al., 2011).

The conceivable mechanism considered for the NP migration phenomenon comprises two steps. First, the initial release is considered to be from the encapsulated NPs located on the specimen surface layers. Then, the further release of NPs is accomplished by the geminate-sorption process, embedding, and diffusion. Along with metal NPs, the migration of other types of nanomaterials like nanoclay, nanoemulsion, and microcrystalline cellulose has been monitored. Various polymeric nanocomposites (e.g., PE, PLA, and LLDPE) are integrated with one type of nanomaterials (e.g., nanoclay, silver, copper, or iron) with purposes of SFP and AFP. When they went into contact with real foods or food simulants, NP migration could not be neglected,

although different results have been reported. It means that choosing materials with the least migration capacity is a criterion in NFP (Huang et al., 2011).

Apart from nanoparticles, monomer migration has been reported and confirmed as a hazard in NFP. In this case, Pilevar et al. (2019) reported about the migration of styrene monomer (SM) from packaging made of polystyrene into foods. Based on the results, the characteristics of polystyrene packaging material in the viewpoint of their residual SM level and the storage conditions of foods can greatly affect SM migration. Also, food characteristics such as pH, moisture, and fat content can dramatically affect SM migration. Scientists showed their report to prevent or lower SM migration; for instance, in a research, organoclay and zinc oxide nanoparticles (ZnONPs) were employed for the control and optimization of the SM migration into food simulants. It has been concluded that these NPs reduced SM migration but not completely. As another concern about the entrance of NFP to human life, migration of chlorinated paraffins (CP) is one of the main hazards. Wang et al. (2019) reported the migration of CP from plastic food packaging into food simulants. In different types of NFP, multilayer material food packaging (20 multilayer) employed in FPS is generally manufactured with a polyurethane adhesive layer in its structure, which may include cyclic ester oligomers as hazard migrants in FPS (Ubeda et al., 2020). The results showed the migration of cyclic ester oligomers into stimulants.

Consequently, there are studies which report about the migration of active agents (like nanoparticles) in NFP (SFP and AFP), which means there is still a need for sufficient toxicological data about the safety assessments of NFP. Thereby, more research is mandatory to promote NFP and ensure that NFP does not cause hazard to human life.

CONCLUSION AND THE FUTURE PROSPECTIVE

The aim of this review was to discuss the NFP systems including AFP and SFP talking about their main functions, features, and components. NFP could show high potential in functions like antibacterial function, degradation, indication, and scavenging. These functions can be designed or controlled depending on the food type. Surprisingly, to the knowledge of the authors, AFP systems showed significant progress in shelf life enhancement by controlling the microorganism growth, relative humidity, oxygen level, barrier properties, and humidity. Employing different kinds of biomaterials, nanoparticles, nanoemulsions, and different carriers improved these functions. Making SFP has been another brilliant progress in NPS. It would be interesting if the consumer is aware of the product quality during their shopping without any aid from an expert. The embedded indicators and sensors can react against different environmental changes in the food matrix or inside the packaging such as pH, humidity, and temperature. Embedding sensors and indicators in FPS can alert the consumer about the food quality by a range of colors. Regarding environment issues, biodegradable packaging materials can notably decrease the packaging residual

in the environment. Reaching a smart packaging that is environmentally friendly and with high mechanical quality, no toxicity, and low cost still needs more studies. It seems that the industry of packaging is going to experience a revolution in FPS.

In spite of the remarkable advantages of NFP and the employment of various technologies, scientists still warn about the side effects and hazards of the employed changes in FPS. There is still a gap between the ideal food packaging system and the current situation. Addition of nanoparticles as a remedy to fight against microorganisms, prevent their growth, act as an indicator of quality and spoilage, and act as a gas scavenger improved the quality of FPS, while there are evidences that it increases the likelihood of nanoparticle migration from the packaging to the food matrix. Importantly, the embedded sensors or indicators in SFP should guarantee their accuracy and validity

each time from packaging until consumption. They should not be sensitive to other parameters like environmental conditions (temperature, humidity, pressure, and so on). In general, the results of some studies still recommend more research to guarantee the future of NFP.

In conclusion, there has been a promising progress in FPS, and people will experience a healthier life than before, but it is important to carry out adequate studies to reach a more reliable FPS. This progress should not affect the final cost of products.

AUTHOR CONTRIBUTIONS

Both authors announce the equal contribution in literature review and the manuscript preparation.

REFERENCES

- Aadil, R. M., Roobab, U., Maan, A. A., and Madni, G. M. (2019). "Effect of heat on food properties," in *Encyclopedia of Food Chemistry*, eds L. Melton, F. Shahidi, and P. Varelis (Oxford: Academic Press), 70–75. doi: 10.1016/b978-0-08-100596-5.21660-0
- Abdorrezza, M. N., Cheng, L., and Karim, A. (2011). Effects of plasticizers on thermal properties and heat sealability of sago starch films. *Food Hydrocoll.* 25, 56–60. doi: 10.1016/j.foodhyd.2010.05.005
- Aday, M. S., Caner, C., and Rahvali, F. (2011). Effect of oxygen and carbon dioxide absorbers on strawberry quality. *Postharvest Biol. Technol.* 62, 179–187. doi: 10.1016/j.postharvbio.2011.05.002
- Ahari, H. (2017). The use of innovative nano emulsions and nano-silver composites packaging for anti-bacterial properties: an article review. *Iran. J. Aquat. Anim. Health* 3, 61–73. doi: 10.18869/acadpub.ijaah.3.1.61
- Ahari, H., Dastmalchi, F., Ghezelloo, Y., Paykan, R., Fotovat, M., and Rahmanny, J. (2008). The application of silver nano-particles to the reduction of bacterial contamination in poultry and animal production. *Food Manuf. Effic.* 2, 49–53. doi: 10.1616/1750-2683.0028
- Ahari, H., and Lahijani, L. K. (2021). Migration of silver and copper nanoparticles from food coating. *Coatings* 11:380. doi: 10.3390/coatings11040380
- Ahari, H., and Massoud, R. (2020). The effect of cuminum essential oil on rheological properties and shelf life of probiotic yoghurt. *J. Nutr. Food Security* 5, 296–305.
- Ahmadzadeh, S., and Khaneghah, A. M. (2019). "Role of green polymers in food packaging," in *Encyclopedia of Renewable and Sustainable Materials*, eds S. Hashmi, and I. A. Choudhury (Amsterdam: Elsevier).
- Alexandre, E. M. C., Lourenço, R. V., Bittante, A. M. Q. B., Moraes, I. C. F., and Sobral, P.JdA (2016). Gelatin-based films reinforced with montmorillonite and activated with nanoemulsion of ginger essential oil for food packaging applications. *Food Packag. Shelf Life* 10, 87–96. doi: 10.1016/j.fpsl.2016.10.004
- Alfei, S., Marengo, B., and Zuccari, G. (2020). Nanotechnology application in food packaging: a plethora of opportunities versus pending risks assessment and public concerns. *Food Res. Int.* 137:109664. doi: 10.1016/j.foodres.2020.109664
- Ali, I., Marenduzzo, D., and Yeomans, J. M. (2006). Polymer packaging and ejection in viral capsids: shape matters. *Phys. Rev. Lett.* 96:208102.
- Alkan Tas, B., Sehiti, E., Erdinc Tas, C., Unal, S., Cebeci, F. C., Menceloglu, Y. Z., et al. (2019). Carvacrol loaded halloysite coatings for antimicrobial food packaging applications. *Food Packag. Shelf Life* 20:100300. doi: 10.1016/j.fpsl.2019.01.004
- Almasi, H., Azizi, S., and Amjadi, S. (2020). Development and characterization of pectin films activated by nanoemulsion and Pickering emulsion stabilized marjoram (*Origanum majorana* L.) essential oil. *Food Hydrocoll.* 99:105338. doi: 10.1016/j.foodhyd.2019.105338
- Al-Nabulsi, A., Osaili, T., Sawalha, A., Olaimat, A. N., Albiss, B. A., Mehyar, G., et al. (2020). Antimicrobial activity of chitosan coating containing ZnO nanoparticles against *E. coli* O157:H7 on the surface of white brined cheese. *Int. J. Food Microbiol.* 334:108838. doi: 10.1016/j.ijfoodmicro.2020.108838
- Al-Tayyar, N. A., Youssef, A. M., and Al-Hindi, R. R. (2020). Antimicrobial packaging efficiency of ZnO-SiO₂ nanocomposites infused into PVA/CS film for enhancing the shelf life of food products. *Food Packag. Shelf Life* 25:100523. doi: 10.1016/j.fpsl.2020.100523
- Álvarez-Hernández, M. H., Martínez-Hernández, G. B., Avalos-Belmontes, F., Castillo-Campohermoso, M. A., Contreras-Esquivel, J. C., and Artés-Hernández, F. (2019). Potassium permanganate-based ethylene scavengers for fresh horticultural produce as an active packaging. *Food Eng. Rev.* 11, 159–183. doi: 10.1007/s12393-019-09193-0
- Amininezhad, S., Rezvani, A., Amouheidari, M., Amininejad, S., and Rakhshani, S. (2015). The antibacterial activity of SnO₂ nanoparticles against *Escherichia coli* and *Staphylococcus aureus*. *Zahedan J. Res. Med. Sci.* 17:e1053.
- Anvar, A., Haghighat Kajavi, S., Ahari, H., Sharifan, A., Motalebi, A., Kakoolaki, S., et al. (2019). Evaluation of the antibacterial effects of Ag-TiO₂ nanoparticles and optimization of its migration to sturgeon caviar (Beluga). *Iran. J. Fish. Sci.* 18, 954–967.
- Arvanitoyannis, I., Nikolaou, E., and Yamamoto, N. (1994). Novel biodegradable copolyamides based on adipic acid, bis(p-aminocyclohexyl)methane and several α -amino acids: synthesis, characterization and study of their degradability for food packaging applications: 4. *Polymer* 35, 4678–4689. doi: 10.1016/0032-3861(94)90821-4
- Asensio, E., Montaños, L., and Nerin, C. (2020). Migration of volatile compounds from natural biomaterials and their safety evaluation as food contact materials. *Food Chem. Toxicol.* 142:111457. doi: 10.1016/j.fct.2020.111457
- Aymonier, C., Schlotterbeck, U., Antonietti, L., Zacharias, P., Thomann, R., Tiller, J. C., et al. (2002). Hybrids of silver nanoparticles with amphiphilic hyperbranched macromolecules exhibiting antimicrobial properties. *Chem. Commun.* 8, 3018–3019. doi: 10.1039/b208575e
- Azeredo, H., Barud, H., Farinas, C., Vasconcellos, V., and Claro, A. (2019). Bacterial cellulose as a raw material for food and food packaging applications. *Front. Sustain. Food Syst.* 3:7. doi: 10.3389/fsufs.2019.00007
- Azeredo, H., Rosa, M., Sá, M., Filho, M., and Waldron, K. (2014). "The use of biomass for packaging films and coatings," in *Advances in Biorefineries: Biomass and Waste Supply Chain Exploitation*, Vol. 1, ed. K. Waldron (Cambridge: Woodhead Publishing), 819–874. doi: 10.1533/9780857097385.2.819
- Aziz, M., and Karboune, S. (2018). Natural antimicrobial/antioxidant agents in meat and poultry products as well as fruits and vegetables: a review. *Crit. Rev. Food Sci. Nutr.* 58, 486–511.
- Bahrami, A., Delshadi, R., Assadpour, E., Jafari, S. M., and Williams, L. (2020). Antimicrobial-loaded nanocarriers for food packaging applications. *Adv. Coll. Interface Sci.* 278:102140. doi: 10.1016/j.cis.2020.102140
- Bai, C., Ke, Y., Hu, X., Xing, L., Zhao, Y., Lu, S., et al. (2020). Preparation and properties of amphiphilic hydrophobically associative polymer/montmorillonite nanocomposites. *R. Soc. Open Sci.* 7:200199.
- Baker, C., Pradhan, A., Pakstis, L., Pochan, D. J., and Shah, S. I. (2005). Synthesis and antibacterial properties of silver nanoparticles. *J. Nanosci. Nanotechnol.* 5, 244–249.

- Bang, G., and Kim, S. W. (2012). Biodegradable poly (lactic acid)-based hybrid coating materials for food packaging films with gas barrier properties. *J. Ind. Eng. Chem.* 18, 1063–1068. doi: 10.1016/j.jiec.2011.12.004
- Bhat, V. G., Narasagoudar, S. S., Masti, S. P., Chougale, R. B., and Shanbhag, Y. (2021). Hydroxy citric acid cross-linked chitosan/guar gum/poly(vinyl alcohol) active films for food packaging applications. *Int. J. Biol. Macromol.* 177, 166–175. doi: 10.1016/j.ijbiomac.2021.02.109
- Biji, K. B., Ravishankar, C. N., Mohan, C. O., and Srinivasa Gopal, T. K. (2015). Smart packaging systems for food applications: a review. *J. Food Sci. Technol.* 52, 6125–6135.
- Biswas, M. C., Tiimob, B. J., Abdela, W., Jeelani, S., and Rangari, V. K. (2019). Nano silica-carbon-silver ternary hybrid induced antimicrobial composite films for food packaging application. *Food Packag. Shelf Life* 19, 104–113. doi: 10.1016/j.fpsl.2018.12.003
- Bordbar, M. M., Tashkhourian, J., and Hemmateenejad, B. (2018). Qualitative and quantitative analysis of toxic materials in adulterated fruit pickle samples by a colorimetric sensor array. *Sens. Actuators B Chem.* 257, 783–791. doi: 10.1016/j.snb.2017.11.010
- Boyle, K. K., Kuo, F.-C., Horcajada, J. P., Hughes, H., Cavagnaro, L., Marculescu, C., et al. (2019). General assembly, treatment, antimicrobials: proceedings of international consensus on orthopedic infections. *J. Arthroplasty* 34, S225–S237.
- Brobbe, K. J. (2017). Efficacy of natural plant extracts in antimicrobial packaging systems. *J. Appl. Packag. Res.* 9:6.
- Bumbudsanpharoke, N., Choi, J., and Ko, S. (2015). Applications of nanomaterials in food packaging. *J. Nanosci. Nanotechnol.* 15, 6357–6372.
- Bumbudsanpharoke, N., and Ko, S. (2015). Nano-food packaging: an overview of market, migration research, and safety regulations. *J. Food Sci.* 80, R910–R923.
- Bumbudsanpharoke, N., and Ko, S. (2019). Nanoclays in food and beverage packaging. *J. Nanomater.* 2019:8927167.
- Byun, Y., Darby, D., Cooksey, K., Dawson, P., and Whiteside, S. (2011). Development of oxygen scavenging system containing a natural free radical scavenger and a transition metal. *Food Chem.* 124, 615–619. doi: 10.1016/j.foodchem.2010.06.084
- Cabedo, L., Luis Feijoo, J., Pilar Villanueva, M., Lagarón, J. M., and Giménez, E. (2006). Optimization of biodegradable nanocomposites based on aPLA/PCL blends for food packaging applications. *Macromol. Symp.* 233, 191–197. doi: 10.1002/masy.200690017
- Cao, J., Li, X., Wu, K., Jiang, W., and Qu, G. (2015). Preparation of a novel PdCl₂-CuSO₄-based ethylene scavenger supported by acidified activated carbon powder and its effects on quality and ethylene metabolism of broccoli during shelf-life. *Postharvest Biol. Technol.* 99, 50–57. doi: 10.1016/j.postharvbio.2014.07.017
- Carbone, M., Donia, D. T., Sabbatella, G., and Antiochia, R. (2016). Silver nanoparticles in polymeric matrices for fresh food packaging. *J. King Saud Univ. Sci.* 28, 273–279. doi: 10.1016/j.jksus.2016.05.004
- Casey, P. (2006). “Nanoparticle technologies and applications,” in *Nanostructure Control of Materials*, eds R. H. J. Hannink, and A. J. Hill (Amsterdam: Elsevier), 1–31. doi: 10.1533/9781845691189.1
- Chandramouli, V., Kailasapathy, K., Peiris, P., and Jones, M. (2004). An improved method of microencapsulation and its evaluation to protect *Lactobacillus* spp. in simulated gastric conditions. *J. Microbiol. Methods* 56, 27–35. doi: 10.1016/j.mimet.2003.09.002
- Chavoshizadeh, S., Pirs, S., and Mohtarami, F. (2020). Conducting/smart color film based on wheat gluten/chlorophyll/polypyrrole nanocomposite. *Food Packag. Shelf Life* 24:100501. doi: 10.1016/j.fpsl.2020.100501
- Chen, G., Zhang, B., Zhao, J., and Chen, H. (2014). Development and characterization of food packaging film from cellulose sulfate. *Food Hydrocoll.* 35, 476–483. doi: 10.1016/j.foodhyd.2013.07.003
- Chen, H.-Z., Zhang, M., Bhandari, B., and Yang, C.-H. (2019). Development of a novel colorimetric food package label for monitoring lean pork freshness. *LWT* 99, 43–49. doi: 10.1016/j.lwt.2018.09.048
- Chen, L., Ao, F., Ge, X., and Shen, W. (2020). Food-grade Pickering emulsions: preparation, stabilization and applications. *Molecules* 25:3202. doi: 10.3390/molecules25143202
- Cherpinski, A., Gozutok, M., Sasmazel, H. T., Torres-Giner, S., and Lagaron, J. M. (2018). Electrospun oxygen scavenging films of poly (3-hydroxybutyrate) containing palladium nanoparticles for active packaging applications. *Nanomaterials* 8:469. doi: 10.3390/nano8070469
- Chivrac, F., Pollet, E., and Avérous, L. (2009). Progress in nano-biocomposites based on polysaccharides and nanoclays. *Mater. Sci. Eng. R Rep.* 67, 1–17. doi: 10.1016/j.mser.2009.09.002
- Cichello, S. A. (2015). Oxygen absorbers in food preservation: a review. *J. Food Sci. Technol.* 52, 1889–1895. doi: 10.1007/s13197-014-1265-2
- Corrales, M., Han, J., and Tauscher, B. (2009). Antimicrobial properties of grape seed extracts and their effectiveness after incorporation into pea starch films. *Int. J. Food Sci. Technol.* 44, 425–433. doi: 10.1111/j.1365-2621.2008.01790.x
- Cruz, R. S., Soares, N. F. F., and de Andrade, N. J. (2006). Evaluation of oxygen absorber on antimicrobial preservation of lasagna-type fresh pasta under vacuum packed. *Ciênc. Agrotecnol.* 30, 1135–1138. doi: 10.1590/s1413-70542006000600015
- da Costa, R. C., Daitx, T. S., Mauler, R. S., da Silva, N. M., Miotto, M., Crespo, J. S., et al. (2020). Poly(hydroxybutyrate-co-hydroxyvalerate)-based nanocomposites for antimicrobial active food packaging containing oregano essential oil. *Food Packag. Shelf Life* 26:100602. doi: 10.1016/j.fpsl.2020.100602
- da Silva, T. F., Menezes, F., Montagna, L. S., Lemes, A. P., and Passador, F. R. (2019). Effect of lignin as accelerator of the biodegradation process of poly(lactic acid)/lignin composites. *Mater. Sci. Eng. B* 251:114441. doi: 10.1016/j.mseb.2019.114441
- Dammak, I., de Carvalho, R. A., Trindade, C. S. F., Lourenço, R. V., and do Amaral Sobral, P. J. (2017). Properties of active gelatin films incorporated with rutin-loaded nanoemulsions. *Int. J. Biol. Macromol.* 98, 39–49. doi: 10.1016/j.ijbiomac.2017.01.094
- Dammak, I., Lourenço, R. V., and do Amaral Sobral, P. J. (2019). Active gelatin films incorporated with Pickering emulsions encapsulating hesperidin: preparation and physicochemical characterization. *J. Food Eng.* 240, 9–20. doi: 10.1016/j.jfoodeng.2018.07.002
- Dey, A., and Neogi, S. (2019). Oxygen scavengers for food packaging applications: a review. *Trends Food Sci. Technol.* 90, 26–34. doi: 10.1016/j.tifs.2019.05.013
- Ding, L., Li, X., Hu, L., Zhang, Y., Jiang, Y., Mao, Z., et al. (2020). A naked-eye detection polyvinyl alcohol/cellulose-based pH sensor for intelligent packaging. *Carbohydr. Polym.* 233:115859. doi: 10.1016/j.carbpol.2020.115859
- Dong, H., He, J., Xiao, K., and Li, C. (2020). Temperature-sensitive polyurethane (TSPU) film incorporated with carvacrol and cinnamyl aldehyde: antimicrobial activity, sustained release kinetics and potential use as food packaging for Cantonese-style moon cake. *Int. J. Food Sci. Technol.* 55, 293–302. doi: 10.1111/ijfs.14276
- Du, W.-X., Olsen, C. W., Avena-Bustillos, R. J., Mchugh, T. H., Levin, C. E., and Friedman, M. (2008). Storage stability and antibacterial activity against *Escherichia coli* O157: H7 of carvacrol in edible apple films made by two different casting methods. *J. Agric. Food Chem.* 56, 3082–3088. doi: 10.1021/jf703629s
- Ebnesajjad, S. (2012). *Plastic Films in Food Packaging: Materials, Technology and Applications*. Oxford: William Andrew.
- Ebrahimi, A., Zabihzadeh Khajavi, M., Mortazavian, A. M., Asilian-Mahabadi, H., Rafiee, S., Farhoodi, M., et al. (2021). Preparation of novel nano-based films impregnated by potassium permanganate as ethylene scavengers: an optimization study. *Polym. Test.* 93:106934. doi: 10.1016/j.polymertesting.2020.106934
- Ebrahimi Tirtashi, F., Moradi, M., Tajik, H., Forough, M., Ezati, P., and Kuswandi, B. (2019). Cellulose/chitosan pH-responsive indicator incorporated with carrot anthocyanins for intelligent food packaging. *Int. J. Biol. Macromol.* 136, 920–926. doi: 10.1016/j.ijbiomac.2019.06.148
- El Asbahani, A., Miladi, K., Badri, W., Sala, M., Addi, E. A., Casabianca, H., et al. (2015). Essential oils: from extraction to encapsulation. *Int. J. Pharm.* 483, 220–243.
- El Fawal, G., Hong, H., Song, X., Wu, J., Sun, M., He, C., et al. (2020). Fabrication of antimicrobial films based on hydroxyethylcellulose and ZnO for food packaging application. *Food Packag. Shelf Life* 23:100462. doi: 10.1016/j.fpsl.2020.100462
- Emamhadi, M. A., Sarafraz, M., Akbari, M., Fakhri, Y., Linh, N. T. T., and Khaneghah, A. M. (2020). Nanomaterials for food packaging applications: a systematic review. *Food Chem. Toxicol.* 146:111825.
- Emamifar, A., Kadivar, M., Shahedi, M., and Soleimani-Zad, S. (2010). Evaluation of nanocomposite packaging containing Ag and ZnO on shelf life

- of fresh orange juice. *Innov. Food Sci. Emerg. Technol.* 11, 742–748. doi: 10.1016/j.ifset.2010.06.003
- Endoza, T. F. M., Welt, B. A., Otwell, S., Teixeira, A. A., Kristonsson, H., and Balaban, M. O. (2004). Kinetic parameter estimation of time-temperature integrators intended for use with packaged fresh seafood. *J. Food Sci.* 69, FMS90–FMS96.
- Espitia, P. J., Fuenmayor, C. A., and Otoni, C. G. (2019). Nanoemulsions: synthesis, characterization, and application in bio-based active food packaging. *Compr. Rev. Food Sci. Food Saf.* 18, 264–285. doi: 10.1111/1541-4337.12405
- Espitia, P. J. P., Soares, N. F. F., Coimbra, J. S. R., de Andrade, N. J., Cruz, R. S., and Medeiros, E. A. A. (2012). Zinc oxide nanoparticles: synthesis, antimicrobial activity and food packaging applications. *Food Bioprocess Technol.* 5, 1447–1464. doi: 10.1007/s11947-012-0797-6
- Fabra, M. J., López-Rubio, A., and Lagaron, J. M. (2014). “15 - Biopolymers for food packaging applications,” in *Smart Polymers and their Applications*, eds M. R. Aguilar, and J. San Román (Cambridge: Woodhead Publishing), 476–509. doi: 10.1533/9780857097026.2.476
- Fakhri, A., Behrouz, S., and Pourmand, M. (2015). Synthesis, photocatalytic and antimicrobial properties of SnO₂, SnS₂ and SnO₂/SnS₂ nanostructure. *J. Photochem. Photobiol. B Biol.* 149, 45–50. doi: 10.1016/j.jphotobiol.2015.05.017
- Fang, Z., Zhao, Y., Warner, R. D., and Johnson, S. K. (2017). Active and intelligent packaging in meat industry. *Trends Food Sci. Technol.* 61, 60–71. doi: 10.1016/j.tifs.2017.01.002
- Ferreira, A. R., Alves, V. D., and Coelho, I. M. (2016). Polysaccharide-based membranes in food packaging applications. *Membranes* 6:22. doi: 10.3390/membranes6020022
- Fonseca-García, A., Jiménez-Regalado, E. J., and Aguirre-Loredo, R. Y. (2021). Preparation of a novel biodegradable packaging film based on corn starch-chitosan and poloxamers. *Carbohydr. Polym.* 251:117009. doi: 10.1016/j.carbpol.2020.117009
- Food Lable Timestrip (2020). *Food Industry*. Available online at: <https://timestrip.com/industries/food/> (accessed November 29, 2020).
- Gaikwad, K., Singh, S., and Lee, Y. S. (2018). Oxygen scavenging films in food packaging. *Environ. Chem. Lett.* 16, 523–538. doi: 10.1007/s10311-018-0705-z
- Gaikwad, K., Singh, S., and Negi, Y. (2019). Ethylene scavengers for active packaging of fresh food produce. *Environ. Chem. Lett.* 18, 269–284. doi: 10.1007/s10311-019-00938-1
- Gao, T., Tian, Y., Zhu, Z., and Sun, D.-W. (2020). Modelling, responses and applications of time-temperature indicators (TTIs) in monitoring fresh food quality. *Trends Food Sci. Technol.* 99, 311–322. doi: 10.1016/j.tifs.2020.02.019
- García, C. V., Shin, G. H., and Kim, J. T. (2018). Metal oxide-based nanocomposites in food packaging: applications, migration, and regulations. *Trends Food Sci. Technol.* 82, 21–31. doi: 10.1016/j.tifs.2018.09.021
- Giannakas, A., Stathopoulou, P., Tsiamis, G., and Salmas, C. (2020). The effect of different preparation methods on the development of chitosan/thyme oil/montmorillonite nanocomposite active packaging films. *J. Food Process. Preserv.* 44:e14327.
- Gómez-Aldapa, C. A., Velazquez, G., Gutierrez, M. C., Rangel-Vargas, E., Castro-Rosas, J., and Aguirre-Loredo, R. Y. (2020). Effect of polyvinyl alcohol on the physicochemical properties of biodegradable starch films. *Mater. Chem. Phys.* 239:122027. doi: 10.1016/j.matchemphys.2019.122027
- Gómez-Estaca, J., López-de-Dicastillo, C., Hernández-Muñoz, P., Catalá, R., and Gava, R. (2014). Advances in antioxidant active food packaging. *Trends Food Sci. Technol.* 35, 42–51. doi: 10.1016/j.tifs.2013.10.008
- Goudarzi, V., and Shahabi-Ghahfarrokhi, I. (2018). Photo-producible and photo-degradable starch/TiO₂ bionanocomposite as a food packaging material: development and characterization. *Int. J. Biol. Macromol.* 106, 661–669. doi: 10.1016/j.ijbiomac.2017.08.058
- Gouvêa, R. F., Del Aguila, E. M., Paschoalin, V. M. F., and Andrade, C. T. (2018). Extruded hybrids based on poly(3-hydroxybutyrate-co-3-hydroxyvalerate) and reduced graphene oxide composite for active food packaging. *Food Packag. Shelf Life* 16, 77–85. doi: 10.1016/j.fpsl.2018.02.002
- GreenFacts (2020). Available online at: <https://www.greenfacts.org/en/digests/food-lifestyle.htm>
- Grönman, K., Soukka, R., Järvi-Kääriäinen, T., Katajajuuri, J. M., Kuisma, M., Koivupuro, H. K., et al. (2013). Framework for sustainable food packaging design. *Packag. Technol. Sci.* 26, 187–200.
- Gupta, R. K., and Dudeja, P. (2017). “Chapter 46 - Food packaging,” in *Food Safety in the 21st Century*, eds R. K. Gupta, P. Dudeja, and M. Singh (San Diego, CA: Academic Press), 547–553.
- Hacker, M. C., Kriehoff, J., and Mikos, A. G. (2019). “Chapter 33 - Synthetic polymers,” in *Principles of Regenerative Medicine*, 3rd Edn. eds A. Atala, R. Lanza, A. G. Mikos, and R. Nerem (Boston, MA: Academic Press), 559–590.
- Haghighi, H., Licciardello, F., Fava, P., Siesler, H. W., and Pulvirenti, A. (2020). Recent advances on chitosan-based films for sustainable food packaging applications. *Food Packag. Shelf Life* 26:100551. doi: 10.1016/j.fpsl.2020.100551
- Hajizadeh, H., Peighambari, S. J., Peighambari, S. H., and Peressini, D. (2020). Physical, mechanical, and antibacterial characteristics of bio-nanocomposite films loaded with Ag-modified SiO₂ and TiO₂ nanoparticles. *J. Food Sci.* 85, 1193–1202. doi: 10.1111/1750-3841.15079
- Hamed, A., AmirAli, A., Mahdi, R., Sara Allahyari, B., and Moradi, S. (2021). *Formulation of Saffron and A Method of Preparation Thereof Iran. USA Patent, Virginia*.
- Han, C., Zhao, A., Varughese, E., and Sahle-Demessie, E. (2018). Evaluating weathering of food packaging polyethylene-nano-clay composites: release of nanoparticles and their impacts. *NanoImpact* 9, 61–71. doi: 10.1016/j.nimpact.2017.10.005
- Han, Y., Yu, M., and Wang, L. (2018). Soy protein isolate nanocomposites reinforced with nanocellulose isolated from licorice residue: water sensitivity and mechanical strength. *Ind. Crops Prod.* 117, 252–259. doi: 10.1016/j.indcrop.2018.02.028
- He, Y., Li, H., Fei, X., and Peng, L. (2021). Carboxymethyl cellulose/cellulose nanocrystals immobilized silver nanoparticles as an effective coating to improve barrier and antibacterial properties of paper for food packaging applications. *Carbohydr. Polym.* 252:117156. doi: 10.1016/j.carbpol.2020.117156
- Heredia, N., and García, S. (2018). Animals as sources of food-borne pathogens: a review. *Anim. Nutr.* 4, 250–255. doi: 10.1016/j.aninu.2018.04.006
- Hirvikorpi, T., Vähä-Nissi, M., Harlin, A., Salomäki, M., Areva, S., Korhonen, J. T., et al. (2011). Enhanced water vapor barrier properties for biopolymer films by polyelectrolyte multilayer and atomic layer deposited Al₂O₃ double-coating. *Appl. Surf. Sci.* 257, 9451–9454. doi: 10.1016/j.apsusc.2011.06.031
- Hitzman, D. O. (1983). *Oxygen Scavenging with Enzymes*. Google Patents US5977212A. Bartlesville, OK: Phillips Petroleum Company.
- Horst, J. D., De Andrade, P. P., Duvoisin, C. A., and Vieira, R. D. (2020). Fabrication of conductive filaments for 3D-printing: polymer nanocomposites. *Biointerface Res. Appl. Chem.* 10, 6577–6586. doi: 10.33263/briac106.65776586
- Huang, Y., Chen, S., Bing, X., Gao, C., Wang, T., and Yuan, B. (2011). Nanosilver migrated into food-simulating solutions from commercially available food fresh containers. *Packag. Technol. Sci.* 24, 291–297. doi: 10.1002/pts.938
- Hyldegaard, M., Mygind, T., and Meyer, R. L. (2012). Essential oils in food preservation: mode of action, synergies, and interactions with food matrix components. *Front. Microbiol.* 3:12. doi: 10.3389/fmicb.2012.00012
- Ijaz, M., Zafar, M., Afsheen, S., and Iqbal, T. (2020). A review on Ag-nanostructures for enhancement in shelf time of fruits. *J. Inorg. Organomet. Polym. Mater.* 30, 1475–1482. doi: 10.1007/s10904-020-01504-x
- Isotton, F., Bernardo, G., Baldasso, C., Rosa, L., and Zeni, M. (2015). The plasticizer effect on preparation and properties of etherified corn starches films. *Ind. Crops Prod.* 76, 717–724. doi: 10.1016/j.indcrop.2015.04.005
- Ivonkovic, A., Zeljko, K., Talic, S., and Lasic, M. (2017). Biodegradable packaging in the food industry. *J. Food Saf. Food Qual.* 68, 26–38.
- Jaworska, G., Sidor, A., Pycia, K., Jaworska-Tomczyk, K., and Surówka, K. (2020). Packaging method and storage temperature affects microbiological quality and content of biogenic amines in *Agaricus bisporus* fruiting bodies. *Food Biosci.* 37:100736. doi: 10.1016/j.fbio.2020.100736
- Jeevahan, J., and Chandrasekaran, M. (2019). Nanoedible films for food packaging: a review. *J. Mater. Sci.* 54, 12290–12318. doi: 10.1007/s10853-019-03742-y
- Jildeh, N. B., and Matouq, M. (2020). Nanotechnology in packing materials for food and drug stuff opportunities. *J. Environ. Chem. Eng.* 8:104338. doi: 10.1016/j.jece.2020.104338

- Johansson, K., Jönsson, L. J., and Järnström, L. (2011). Coating: oxygen scavenging enzymes in coatings – effect of coating procedures on enzyme activity. *Nord. Pulp Pap. Res. J.* 26, 197–204. doi: 10.3183/npprj-2011-26-02-p197-204
- Johnson, D., Gisder, J., Lew, L., Goddard, J., and Decker, E. (2016). Is oxygen reduction a viable antioxidant strategy for oil-in-water emulsions? *Eur. J. Lipid Sci. Technol.* 119:1600285. doi: 10.1002/ejlt.201600285
- Ju, J., Chen, X., Xie, Y., Yu, H., Guo, Y., Cheng, Y., et al. (2019). Application of essential oil as a sustained release preparation in food packaging. *Trends Food Sci. Technol.* 92, 22–32. doi: 10.1016/j.tifs.2019.08.005
- Ju, M., Zhu, G., Huang, G., Shen, X., Zhang, Y., Jiang, L., et al. (2020). A novel Pickering emulsion produced using soy protein-anthocyanin complex nanoparticles. *Food Hydrocoll.* 99:105329. doi: 10.1016/j.foodhyd.2019.105329
- Kamdern, D. P., Shen, Z., Nabinejad, O., and Shu, Z. (2019). Development of biodegradable composite chitosan-based films incorporated with xylan and carvacrol for food packaging application. *Food Packag. Shelf Life* 21:100344. doi: 10.1016/j.fpsl.2019.100344
- Kanmani, P., and Rhim, J.-W. (2014). *Nano and Nanocomposite Antimicrobial Materials for Food Packaging Applications*. London: Future Medicine.
- Karimi, M., Yazdi, F. T., Mortazavi, S. A., Shahabi-Ghahfarrokhi, I., and Chamani, J. (2020). Development of active antimicrobial poly (l-glutamic) acid-poly (l-lysine) packaging material to protect probiotic bacterium. *Polym. Test.* 83:106338. doi: 10.1016/j.polymertesting.2020.106338
- Kaur, J., Sood, K., Bhardwaj, N., Arya, S. K., and Khatri, M. (2020). Nanomaterial loaded chitosan nanocomposite films for antimicrobial food packaging. *Mater. Today Proc.* 28, 1904–1909. doi: 10.1016/j.matpr.2020.05.309
- Khalaj, M.-J., Ahmadi, H., Lesankhosh, R., and Khalaj, G. (2016). Study of physical and mechanical properties of polypropylene nanocomposites for food packaging application: nano-clay modified with iron nanoparticles. *Trends Food Sci. Technol.* 51, 41–48. doi: 10.1016/j.tifs.2016.03.007
- Kim, I., Viswanathan, K., Kasi, G., Thanakkasaranee, S., Sadeghi, K., and Seo, J. (2020). ZnO nanostructures in active antibacterial food packaging: preparation methods, antimicrobial mechanisms, safety issues, future prospects, and challenges. *Food Rev. Int.* 1–29. doi: 10.1080/87559129.2020.1737709
- Koskela, J., Sarfraz, J., Ihalainen, P., Määtänen, A., Pulkkinen, P., Tenhu, H., et al. (2015). Monitoring the quality of raw poultry by detecting hydrogen sulfide with printed sensors. *Sens. Actuators B Chem.* 218, 89–96. doi: 10.1016/j.snb.2015.04.093
- Kraśniewska, K., Galus, S., and Gniewosz, M. (2020). Biopolymers-based materials containing silver nanoparticles as active packaging for food applications—a review. *Int. J. Mol. Sci.* 21:698. doi: 10.3390/ijms21030698
- Kumar, S., Shukla, A., Baul, P. P., Mitra, A., and Halder, D. (2018). Biodegradable hybrid nanocomposites of chitosan/gelatin and silver nanoparticles for active food packaging applications. *Food Packag. Shelf Life* 16, 178–184. doi: 10.1016/j.fpsl.2018.03.008
- Kuswandi, B., and Nurfawaidi, A. (2017). On-package dual sensors label based on pH indicators for real-time monitoring of beef freshness. *Food Control* 82, 91–100. doi: 10.1016/j.foodcont.2017.06.028
- Lang, C., and Hübert, T. (2011). A colour ripeness indicator for apples. *Food Bioprocess Technol.* 5, 3244–3249. doi: 10.1007/s11947-011-0694-4
- Latos-Brozio, M., and Masek, A. (2020). The application of natural food colorants as indicator substances in intelligent biodegradable packaging materials. *Food Chem. Toxicol.* 135:110975. doi: 10.1016/j.fct.2019.110975
- Laufer, G., Kirkland, C., Cain, A. A., and Grunlan, J. C. (2013). Oxygen barrier of multilayer thin films comprised of polysaccharides and clay. *Carbohydr. Polym.* 95, 299–302. doi: 10.1016/j.carbpol.2013.02.048
- Lee, D. S. (2016). Carbon dioxide absorbers for food packaging applications. *Trends Food Sci. Technol.* 57, 146–155. doi: 10.1016/j.tifs.2016.09.014
- Li, D., Zhang, J., Xu, W., and Fu, Y. (2016). Effect of SiO₂/EVA on the mechanical properties, permeability, and residual solvent of polypropylene packaging films. *Polym. Compos.* 37, 101–107. doi: 10.1002/pc.23159
- Lim, H.-P., Ho, K.-W., Singh, C. K. S., Ooi, C.-W., Tey, B.-T., and Chan, E.-S. (2020). Pickering emulsion hydrogel as a promising food delivery system: synergistic effects of chitosan Pickering emulsifier and alginate matrix on hydrogel stability and emulsion delivery. *Food Hydrocoll.* 103:105659. doi: 10.1016/j.foodhyd.2020.105659
- Lin, D., Yang, Y., Wang, J., Yan, W., Wu, Z., Chen, H., et al. (2020). Preparation and characterization of TiO₂-Ag loaded fish gelatin-chitosan antibacterial composite film for food packaging. *Int. J. Biol. Macromol.* 154, 123–133. doi: 10.1016/j.ijbiomac.2020.03.070
- Lin, W., Ni, Y., and Pang, J. (2019). Microfluidic spinning of poly (methyl methacrylate)/konjac glucomannan active food packaging films based on hydrophilic/hydrophobic strategy. *Carbohydr. Polym.* 222:114986. doi: 10.1016/j.carbpol.2019.114986
- Liu, G., Agostinho, F., Duan, H., Song, G., Wang, X., Giannetti, B. F., et al. (2020). Environmental impacts characterization of packaging waste generated by urban food delivery services. A big-data analysis in Jing-Jin-Ji region (China). *Waste Manag.* 117, 157–169. doi: 10.1016/j.wasman.2020.07.028
- Liu, S., Zhu, Y., Wu, Y., Lue, A., and Zhang, C. (2019). Hydrophobic modification of regenerated cellulose microparticles with enhanced emulsifying capacity for O/W Pickering emulsion. *Cellulose* 26, 6215–6228. doi: 10.1007/s10570-019-02538-2
- Lloyd, K., Miroso, M., and Birch, J. (2019). “Active and intelligent packaging,” in *Encyclopedia of Food Chemistry*, eds L. Melton, F. Shahidi, and P. Varela (Oxford: Academic Press), 177–182.
- Lo Scalzo, R. (2008). Organic acids influence on DPPH scavenging by ascorbic acid. *Food Chem.* 107, 40–43. doi: 10.1016/j.foodchem.2007.07.070
- Lodha, P., and Netravali, A. N. (2005). Thermal and mechanical properties of environment-friendly ‘green’ plastics from stearic acid modified-soy protein isolate. *Ind. Crops Prod.* 21, 49–64. doi: 10.1016/j.indcrop.2003.12.006
- Lok, C.-N., Ho, C.-M., Chen, R., He, Q.-Y., Yu, W.-Y., Sun, H., et al. (2007). Silver nanoparticles: partial oxidation and antibacterial activities. *JBIC J. Biol. Inorg. Chem.* 12, 527–534. doi: 10.1007/s00775-007-0208-z
- Lone, A., Anany, H., Hakeem, M., Aguis, L., Avdjian, A.-C., Bouget, M., et al. (2016). Development of prototypes of bioactive packaging materials based on immobilized bacteriophages for control of growth of bacterial pathogens in foods. *Int. J. Food Microbiol.* 217, 49–58. doi: 10.1016/j.ijfoodmicro.2015.10.011
- Loredo, Y., Velazquez, G., Gutierrez, M., Castro-Rosas, J., Rangel Vargas, E., and Gomez-Aldapa, C. (2018). Effect of airflow presence during the manufacturing of biodegradable films from polymers with different structural conformation. *Food Packag. Shelf Life* 17, 162–170. doi: 10.1016/j.fpsl.2018.06.007
- Lotfi, S., Ahari, H., and Sahraeyan, R. (2019). The effect of silver nanocomposite packaging based on melt mixing and sol-gel methods on shelf life extension of fresh chicken stored at 4 °C. *J. Food Saf.* 39:e12625. doi: 10.1111/jfs.12625
- Lukic, I., Vulic, J., and Ivanovic, J. (2020). Antioxidant activity of PLA/PCL films loaded with thymol and/or carvacrol using scCO₂ for active food packaging. *Food Packag. Shelf Life* 26:100578. doi: 10.1016/j.fpsl.2020.100578
- Malhotra, B., Keshwani, A., and Kharkwal, H. (2015). Natural polymer based cling films for food packaging. *Int. J. Pharm. Pharm. Sci.* 7, 10–18.
- Mangaraj, S., Goswami, T. K., and Panda, D. (2014). Modeling of gas transmission properties of polymeric films used for MA packaging of fruits. *J. Food Sci. Technol.* 52, 5456–5469. doi: 10.1007/s13197-014-1682-2
- Marra, A., Silvestre, C., Duraccio, D., and Cimmino, S. (2016). Polylactic acid/zinc oxide biocomposite films for food packaging application. *Int. J. Biol. Macromol.* 88, 254–262. doi: 10.1016/j.ijbiomac.2016.03.039
- Marrez, D. A., Abdelhamid, A. E., and Darwesh, O. M. (2019). Eco-friendly cellulose acetate green synthesized silver nano-composite as antibacterial packaging system for food safety. *Food Packag. Shelf Life* 20:100302. doi: 10.1016/j.fpsl.2019.100302
- Marsh, K., and Bugusu, B. (2007). Food packaging—roles, materials, and environmental issues. *J. Food Sci.* 72, R39–R55.
- Martinez-Abad, A., Lagaron, J. M., and Ocio, M. J. (2012). Development and characterization of silver-based antimicrobial ethylene-vinyl alcohol copolymer (EVOH) films for food-packaging applications. *J. Agric. Food Chem.* 60, 5350–5359. doi: 10.1021/jf300334z
- Mei, L., and Wang, Q. (2020). Advances in using nanotechnology structuring approaches for improving food packaging. *Annu. Rev. Food Sci. Technol.* 11, 339–364. doi: 10.1146/annurev-food-032519-051804
- Meng, X., Kim, S., Puligundla, P., and Ko, S. (2014). Carbon dioxide and oxygen gas sensors-possible application for monitoring quality, freshness, and safety of agricultural and food products with emphasis on importance of analytical signals and their transformation. *J. Korean Soc. Appl. Biol. Chem.* 57, 723–733. doi: 10.1007/s13765-014-4180-3
- Mikkonen, K. S., Laine, C., Kontro, I., Talja, R. A., Serimaa, R., and Tenkanen, M. (2015). Combination of internal and external plasticization

- of hydroxypropylated birch xylan tailors the properties of sustainable barrier films. *Eur. Polym. J.* 66, 307–318. doi: 10.1016/j.eurpolymj.2015.02.034
- Mills, A. (2009). “Oxygen indicators in food packaging,” in *Sensors for Environment, Health and Security*, ed. M. I. Baraton (Dordrecht: Springer Netherlands).
- Mills, A., Doyle, G., Peiro, A. M., and Durrant, J. (2006). Demonstration of a novel, flexible, photocatalytic oxygen-scavenging polymer film. *J. Photochem. Photobiol. A Chem.* 177, 328–331. doi: 10.1016/j.jphotochem.2005.06.001
- Miltz, J., and Perry, M. (2005). Evaluation of the performance of Iron-based oxygen scavengers, with comments on their optimal applications. *Packag. Technol. Sci.* 18, 21–27. doi: 10.1002/pts.671
- Min, T., Zhu, Z., Sun, X., Yuan, Z., Zha, J., and Wen, Y. (2020). Highly efficient antifogging and antibacterial food packaging film fabricated by novel quaternary ammonium chitosan composite. *Food Chem.* 308:125682. doi: 10.1016/j.foodchem.2019.125682
- Mishra, M. (2018). *Encyclopedia of Polymer Applications, 3 Volume Set*. Boca Raton, FL: CRC Press.
- Moadab, S., Ahari, H., Shahbazzadeh, D., Motalebi, A. A., Anvar, A. A., Rahmania, J., et al. (2011). Toxicity study of nanosilver (Nanocid®) on osteoblast cancer cell line. *Int. Nano Lett.* 1, 11–16.
- Moghim, R., Aliahmadi, A., and Rafati, H. (2017). Antibacterial hydroxypropyl methyl cellulose edible films containing nanoemulsions of *Thymus daenensis* essential oil for food packaging. *Carbohydr. Polym.* 175, 241–248. doi: 10.1016/j.carbpol.2017.07.086
- Mohamed, S. A. A., El-Sakhawy, M., and El-Sakhawy, M. A.-M. (2020). Polysaccharides, protein and lipid -based natural edible films in food packaging: a review. *Carbohydr. Polym.* 238:116178. doi: 10.1016/j.carbpol.2020.116178
- Mohammadian, E., Alizadeh-Sani, M., and Jafari, S. M. (2020). Smart monitoring of gas/temperature changes within food packaging based on natural colorants. *Compr. Rev. Food Sci. Food Saf.* 19, 2885–2931. doi: 10.1111/1541-4337.12635
- Moore, C. J. (2008). Synthetic polymers in the marine environment: a rapidly increasing, long-term threat. *Environ. Res.* 108, 131–139. doi: 10.1016/j.envres.2008.07.025
- Muncke, J. (2014). “Hazards of food contact material: food packaging contaminants,” in *Encyclopedia of Food Safety*, ed. Y. Motarjemi (Waltham, MA: Academic Press), 430–437. doi: 10.1016/b978-0-12-378612-8.00218-3
- Nanotechnology Products Database (2020). *RipeSense*. Available online at: <https://product.statnano.com/product/6730/ripesense> (accessed November 11, 2020).
- Narasimha Rao, D., and Sachindra, N. M. (2002). Modified atmosphere and vacuum packaging of meat and poultry products. *Food Rev. Int.* 18, 263–293. doi: 10.1081/fri-120016206
- Nasiri, M., Sharifan, A., Ahari, H., Anvar, A. A., and Kakooolaki, S. (2019). Food-grade nanoemulsions and their fabrication methods to increase shelf life. *Food Health* 2, 37–45.
- Naveena, B., and Sharma, A. (2020). Review on properties of bio plastics for packaging applications and its advantages. *Int. J. Curr. Microbiol. Appl. Sci.* 9, 1428–1432. doi: 10.20546/ijcmas.2020.905.163
- Nazzaro, F., Fratianni, F., De Martino, L., Coppola, R., and De Feo, V. (2013). Effect of essential oils on pathogenic bacteria. *Pharmaceuticals* 6, 1451–1474. doi: 10.3390/ph6121451
- Nechita, P. (2017). Active-antimicrobial coatings based on silver nanoparticles and natural polymers for paper packaging functionalization. *Nord. Pulp Pap. Res. J.* 32, 452–458. doi: 10.3183/npprj-2017-32-03-p452-458
- Nie, G., and Xiao, L. (2020). New insight into wastewater treatment by activation of sulfite with photosensitive organic dyes under visible light irradiation. *Chem. Eng. J.* 389:123446. doi: 10.1016/j.cej.2019.123446
- O’Grady, M. N., and Kerry, J. P. (2008). “Smart packaging technologies and their application in conventional meat packaging systems,” in *Meat Biotechnology*, ed. F. Toldrá (New York, NY: Springer New York), 425–451. doi: 10.1007/978-0-387-79382-5_19
- Oliver, S. P., Jayarao, B. M., and Almeida, R. A. (2005). Foodborne pathogens in milk and the dairy farm environment: food safety and public health implications. *Foodborne Pathog. Dis.* 2, 115–129. doi: 10.1089/fpd.2005.2.115
- Otoni, C. G., Pontes, S. F., Medeiros, E. A., and Soares, N. F. (2014). Edible films from methylcellulose and nanoemulsions of clove bud (*Syzygium aromaticum*) and oregano (*Origanum vulgare*) essential oils as shelf life extenders for sliced bread. *J. Agric. Food Chem.* 62, 5214–5219. doi: 10.1021/jf501055f
- Oyervides-Muñoz, E., Pollet, E., Ulrich, G., de Jesús Sosa-Santillán, G., and Avérous, L. (2017). Original method for synthesis of chitosan-based antimicrobial agent by quaternary ammonium grafting. *Carbohydr. Polym.* 157, 1922–1932. doi: 10.1016/j.carbpol.2016.11.081
- Ozdemir, M., and Floros, J. D. (2004). Active food packaging technologies. *Crit. Rev. Food Sci. Nutr.* 44, 185–193.
- Ozogul, Y., Kuley Boğa, E., Akyol, I., Durmus, M., Ucar, Y., Regenstein, J. M., et al. (2020). Antimicrobial activity of thyme essential oil nanoemulsions on spoilage bacteria of fish and food-borne pathogens. *Food Biosci.* 36:100635. doi: 10.1016/j.fbio.2020.100635
- Panáček, A., Kvittek, L., Pucek, R., Kolář, M., Večeřová, R., Pizúrová, N., et al. (2006). Silver colloid nanoparticles: synthesis, characterization, and their antibacterial activity. *J. Phys. Chem. B* 110, 16248–16253.
- Pandey, V. K., Upadhyay, S. N., Niranjan, K., and Mishra, P. K. (2020). Antimicrobial biodegradable chitosan-based composite nano-layers for food packaging. *Int. J. Biol. Macromol.* 157, 212–219. doi: 10.1016/j.ijbiomac.2020.04.149
- Pavelková, A. (2013). Time temperature indicators as devices intelligent packaging. *Acta Univ. Agric. Silviculturae Mendelianae Brunensis* 61, 245–251. doi: 10.1118/actaun201361010245
- Pawar, P., and Purwar, A. H. (2013). Biodegradable polymers in food packaging. *Am. J. Eng. Res.* 2, 151–164.
- Peng, B.-Y., Chen, Z., Chen, J., Yu, H., Zhou, X., Criddle, C. S., et al. (2020). Biodegradation of Polyvinyl Chloride (PVC) in *Tenebrio molitor* (Coleoptera: Tenebrionidae) larvae. *Environ. Int.* 145:106106. doi: 10.1016/j.envint.2020.106106
- Petruzzi, L., Corbo, M. R., Sinigaglia, M., and Bevilacqua, A. (2017). “Chapter 1 - Microbial spoilage of foods: fundamentals,” in *The Microbiological Quality of Food*, eds A. Bevilacqua, M. R. Corbo, and M. Sinigaglia (Sawston: Woodhead Publishing), 1–21.
- Pilevar, Z., Bahrami, A., Beikzadeh, S., Hosseini, H., and Jafari, S. M. (2019). Migration of styrene monomer from polystyrene packaging materials into foods: characterization and safety evaluation. *Trends Food Sci. Technol.* 91, 248–261. doi: 10.1016/j.tifs.2019.07.020
- Pina, H. V., de Farias, A. J. A., Barbosa, F. C., William de Lima Souza, J., de Sousa Barros, A. B., Batista Cardoso, M. J., et al. (2020). Microbiological and cytotoxic perspectives of active PCL/ZnO film for food packaging. *Mater. Res. Express* 7:025312. doi: 10.1088/2053-1591/ab7569
- Pisoschi, A. M., Pop, A., Georgescu, C., Turcuș, V., Olah, N. K., and Mathe, E. (2018). An overview of natural antimicrobials role in food. *Eur. J. Med. Chem.* 143, 922–935. doi: 10.1016/j.ejmech.2017.11.095
- Priyadarshi, R., and Rhim, J.-W. (2020). Chitosan-based biodegradable functional films for food packaging applications. *Innov. Food Sci. Emerg. Technol.* 62:102346. doi: 10.1016/j.ifset.2020.102346
- Rao, J., Chen, B., and McClements, D. J. (2019). Improving the efficacy of essential oils as antimicrobials in foods: mechanisms of action. *Annu. Rev. Food Sci. Technol.* 10, 365–387. doi: 10.1146/annurev-food-032818-121727
- Rech, C. R., da Silva Brabes, K. C., Bagnara e Silva, B. E., Bittencourt, P. R. S., Koschevic, M. T., da Silveira, T. F. S., et al. (2020). Biodegradation of polyhydroxybutyrate films incorporated with eugenol in different soil types. *Case Stud. Chem. Environ. Eng.* 2:100014. doi: 10.1016/j.csee.2020.100014
- Rehm, B. (2010). Bacterial polymers: biosynthesis, modifications and applications. *Nat. Rev. Microbiol.* 8, 578–592. doi: 10.1038/nrmicro2354
- Rešček, A., Kratočil Krehula, L., Katančić, Z., and Hrnjak-Murgić, Z. (2015). Active bilayer PE/PCL films for food packaging modified with zinc oxide and casein. *Croat. Chem. Acta* 88, 461–473. doi: 10.5562/cca2768
- Rhein, S., and Schmid, M. (2020). Consumers’ awareness of plastic packaging: more than just environmental concerns. *Resour. Conserv. Recycl.* 162:105063. doi: 10.1016/j.resconrec.2020.105063
- Riaz, A., Lagnika, C., Luo, H., Dai, Z., Nie, M., Hashim, M. M., et al. (2020). Chitosan-based biodegradable active food packaging film containing Chinese chive (*Allium tuberosum*) root extract for food application. *Int. J. Biol. Macromol.* 150, 595–604. doi: 10.1016/j.ijbiomac.2020.02.078
- Robertson, G. L. (2014). “Food packaging,” in *Encyclopedia of Agriculture and Food Systems*, ed. N. K. van Alfen (Oxford: Academic Press), 232–249.
- Robertson, G. L. (2019). “Packaging and food and beverage shelf life,” in *Reference Module in Food Science. Woodhead Publishing Series in Food Science, Technology and Nutrition*, (Amsterdam: Elsevier).

- Roche, K. A. (2016). "Food labeling: applications," in *Encyclopedia of Food and Health*, eds B. Caballero, P. M. Finglas, and F. Toldrá (Oxford: Academic Press), 49–55. doi: 10.1016/b978-0-12-384947-2.00785-6
- Rodríguez, G. M., Sibaja, J. C., Espitia, P. J., and Otoni, C. G. (2020). Antioxidant active packaging based on papaya edible films incorporated with *Moringa oleifera* and ascorbic acid for food preservation. *Food Hydrocoll.* 103:105630. doi: 10.1016/j.foodhyd.2019.105630
- Rodríguez, K., Villalta, M., Marin, E., Briceno, M., Leon, G., and Montero, M. (2019). Physical characteristics of nano-Hydroxyapatite Pickering-emulsions and their adjuvant activity on the antibody response towards the *Bothrops asper* snake venom. *Mater. Sci. Eng. C* 100, 23–29. doi: 10.1016/j.msec.2019.02.088
- Rooney, M. L. (2002). *U.S. Patent 6,346,200. USA Patent, Virginia Oxygen Scavengers Independent of Transition Metal Catalysts.*
- Roy, N., Saha, N., Kitano, T., and Saha, P. (2012). Biodegradation of PVP-CMC hydrogel film: a useful food packaging material. *Carbohydr. Polym.* 89, 346–353. doi: 10.1016/j.carbpol.2012.03.008
- Salem, M., and Ezzat, S. (2018). "Nanoemulsions in food industry," in *Some New Aspects of Colloidal Systems in Foods*, ed. J. M. Milani (London: InechOpen).
- Saliu, F., and Pergola, R. (2017). Carbon dioxide colorimetric indicators for food packaging application: applicability of anthocyanin and poly-lysine mixtures. *Sens. Actuators B Chem.* 258, 1117–1124. doi: 10.1016/j.snb.2017.12.007
- Salome Amarachi, C., Kenchukwu, F., and Attama, A. (2014). "Nanoemulsions — advances in formulation, characterization and applications in drug delivery," in *Application of Nanotechnology in Drug Delivery*, ed. A. D. Sezer (London: InTechOpen), 76–126.
- Salvia-Trujillo, L., Rojas-Grau, M. A., Soliva-Fortuny, R., and Martín-Belloso, O. (2015). Use of antimicrobial nanoemulsions as edible coatings: impact on safety and quality attributes of fresh-cut Fuji apples. *Postharvest Biol. Technol.* 105, 8–16. doi: 10.1016/j.postharvbio.2015.03.009
- Sanyang, M., Sapuan, S., Jawaid, M., Ishak, M., and Sahari, J. (2015). Effect of plasticizer type and concentration on physical properties of biodegradable films based on sugar palm (*Arenga pinnata*) starch for food packaging. *J. Food Sci. Technol.* 53, 326–336. doi: 10.1007/s13197-015-2009-7
- Sattari, M., Minaee, S., Azizi, M., and Afshari, H. (2010). Effects of nanofilms packaging on organoleptic and microbial properties of bread. *Iran. J. Nutr. Sci. Food Technol.* 4, 65–74.
- Shankar, S., Bang, Y.-J., and Rhim, J.-W. (2019). Antibacterial LDPE/GSE/Mel/ZnONP composite film-coated wrapping paper for convenience food packaging application. *Food Packag. Shelf Life* 22:100421. doi: 10.1016/j.fpsl.2019.100421
- Sharif, F., Muhammad, N., and Zafar, T. (2020). "Cellulose based biomaterials: benefits and challenges," in *Biofibers and Biopolymers for Biocomposites: Synthesis, Characterization and Properties*, eds A. Khan, S. Mavinkere Rangappa, S. Siengchin, and A. M. Asiri (Cham: Springer International Publishing), 229–246. doi: 10.1007/978-3-030-40301-0_11
- Sharma, S., Barkauskaite, S., Jaiswal, A. K., and Jaiswal, S. (2020a). Essential oils as additives in active food packaging. *Food Chem.* 343:128403. doi: 10.1016/j.foodchem.2020.128403
- Sharma, S., Jaiswal, A. K., Duffy, B., and Jaiswal, S. (2020b). Ferulic acid incorporated active films based on poly(lactide) /poly(butylene adipate-co-terephthalate) blend for food packaging. *Food Packag. Shelf Life* 24:100491. doi: 10.1016/j.fpsl.2020.100491
- Silvestre, C., Duraccio, D., and Cimmino, S. (2011). Food packaging based on polymer nanomaterials. *Prog. Polym. Sci.* 36, 1766–1782. doi: 10.1016/j.progpolymsci.2011.02.003
- Siracusa, V., Rocculi, P., Romani, S., and Dalla Rosa, M. (2008). Biodegradable polymers for food packaging: a review. *Trends Food Sci. Technol.* 19, 634–643.
- Siripatrawan, U., and Kaewklin, P. (2018). Fabrication and characterization of chitosan-titanium dioxide nanocomposite film as ethylene scavenging and antimicrobial active food packaging. *Food Hydrocoll.* 84, 125–134. doi: 10.1016/j.foodhyd.2018.04.049
- Siripatrawan, U., and Noipha, S. (2012). Active film from chitosan incorporating green tea extract for shelf life extension of pork sausages. *Food Hydrocoll.* 27, 102–108. doi: 10.1016/j.foodhyd.2011.08.011
- Sobhan, A., Muthukumarappan, K., Wei, L., Van Den Top, T., and Zhou, R. (2020). Development of an activated carbon-based nanocomposite film with antibacterial property for smart food packaging. *Mater. Today Commun.* 23:101124. doi: 10.1016/j.mtcomm.2020.101124
- Song, H., Li, B., Lin, Q.-B., Wu, H.-J., and Chen, Y. (2011). Migration of silver from nanosilver-polyethylene composite packaging into food simulants. *Food Addit. Contam. Part A* 28, 1758–1762.
- Sonia, A., and Dasan, P. (2013). Celluloses microfibers (CMF)/poly (ethylene-co-vinyl acetate) (EVA) composites for food packaging applications: a study based on barrier and biodegradation behavior. *J. Food Eng.* 118, 78–89. doi: 10.1016/j.jfoodeng.2013.03.020
- Stoica, M., Dima, C., and Alexe, P. (2018). "Eco-friendly nanocomposites from bacterial cellulose and biopolyesters as a sustainable alternative for plastic food packaging," in *Food Packaging and Preservation Techniques Applications and Technology*, eds A. D. Galaz, and D. S. Bailey (New York, NY: Nova Science Publisher), 113–127.
- Struller, C., Kelly, P., and Copeland, N. (2014). Aluminum oxide barrier coatings on polymer films for food packaging applications. *Surf. Coat. Technol.* 241, 130–137. doi: 10.1016/j.surfcoat.2013.08.011
- Tharanathan, R. N. (2003). Biodegradable films and composite coatings: past, present and future. *Trends Food Sci. Technol.* 14, 71–78. doi: 10.1016/s0924-2244(02)00280-7
- Ubeda, S., Aznar, M., Rosenmai, A. K., Vinggaard, A. M., and Nerin, C. (2020). Migration studies and toxicity evaluation of cyclic polyesters oligomers from food packaging adhesives. *Food Chem.* 311:125918. doi: 10.1016/j.foodchem.2019.125918
- Umaraw, P., Munekata, P. E. S., Verma, A. K., Barba, F. J., Singh, V. P., Kumar, P., et al. (2020). Edible films/coating with tailored properties for active packaging of meat, fish and derived products. *Trends Food Sci. Technol.* 98, 10–24. doi: 10.1016/j.tifs.2020.01.032
- Valdés, A., Mellinas, A., Ramos, M., Burgos, N., Jiménez, A., and Garrigós, M. C. (2015). Use of herbs, spices and their bioactive compounds in active food packaging. *RSC Adv.* 5, 40324–40335. doi: 10.1039/c4ra17286h
- Vásconez, M., Flores, S., Campos, C., Alvarado, J., and Gerschenson, L. (2009). Antimicrobial activity and physical properties of chitosan-tapioca starch based edible films and coatings. *Food Res. Int.* 42, 762–769. doi: 10.1016/j.foodres.2009.02.026
- Vasile, C., Răpă, M., Ștefan, M., Stan, M., Macavei, S., Darie-Niță, R., et al. (2017). New PLA/ZnO: Cu/Ag bionanocomposites for food packaging. *Express Polym. Lett.* 11, 531–544. doi: 10.3144/expresspolymlett.2017.51
- Vilas, C., Mauricio-Iglesias, M., and García, M. R. (2020). Model-based design of smart active packaging systems with antimicrobial activity. *Food Packag. Shelf Life* 24:100446. doi: 10.1016/j.fpsl.2019.100446
- Villegas, C., Arrieta, M. P., Rojas, A., Torres, A., Faba, S., Toledo, M. J., et al. (2019). PLA/organoclay bionanocomposites impregnated with thymol and cinnamaldehyde by supercritical impregnation for active and sustainable food packaging. *Compos. B Eng.* 176:107336. doi: 10.1016/j.compositesb.2019.107336
- Wang, C., Gao, W., Liang, Y., Jiang, Y., Wang, Y., Zhang, Q., et al. (2019). Migration of chlorinated paraffins from plastic food packaging into food simulants: concentrations and differences in congener profiles. *Chemosphere* 225, 557–564. doi: 10.1016/j.chemosphere.2019.03.039
- Wang, H., Qian, J., and Ding, F. (2017). Emerging chitosan-based films for food packaging applications. *J. Agric. Food Chem.* 66, 395–413. doi: 10.1021/acs.jafc.7b04528
- Wang, L.-F., and Rhim, J.-W. (2016). Grapefruit seed extract incorporated antimicrobial LDPE and PLA films: effect of type of polymer matrix. *LWT* 74, 338–345. doi: 10.1016/j.lwt.2016.07.066
- Wang, Q., Huang, J., Hu, C., Xia, N., Li, T., and Xia, Q. (2017). Stabilization of a non-aqueous self-double-emulsifying delivery system of rutin by fat crystals and nonionic surfactants: preparation and bioavailability study. *Food Funct.* 8, 2512–2522. doi: 10.1039/c7fo00439g
- Wang, S., Liu, X., Yang, M., Zhang, Y., Xiang, K., and Tang, R. (2015). Review of time temperature indicators as quality monitors in food packaging. *Packag. Technol. Sci.* 28, 839–867. doi: 10.1002/pts.2148
- Weber, C., Haugaard, V., Festeren, R., and Bertelsen, G. (2002). Production and applications of biobased packaging materials for the food industry. *Food Addit. Contam.* 19, 172–177. doi: 10.1080/02652030110087483
- Weston, M., Phan, M. A. T., Arcot, J., and Chandrawati, R. (2020). Anthocyanin-based sensors derived from food waste as an active use-by date indicator for milk. *Food Chem.* 326:127017. doi: 10.1016/j.foodchem.2020.127017

- Williams, H., and Wikström, F. (2011). Environmental impact of packaging and food losses in a life cycle perspective: a comparative analysis of five food items. *J. Clean. Prod.* 19, 43–48. doi: 10.1016/j.jclepro.2010.08.008
- Woodruff, M. A., and Huttmacher, D. W. (2010). The return of a forgotten polymer—polycaprolactone in the 21st century. *Prog. Polym. Sci.* 35, 1217–1256. doi: 10.1016/j.progpolymsci.2010.04.002
- Wu, Z., Huang, X., Li, Y.-C., Xiao, H., and Wang, X. (2018). Novel chitosan films with laponite immobilized Ag nanoparticles for active food packaging. *Carbohydr. Polym.* 199, 210–218. doi: 10.1016/j.carbpol.2018.07.030
- Xiao-wei, H., Zhi-hua, L., Xiao-bo, Z., Ji-yong, S., Han-ping, M., Jie-wen, Z., et al. (2016). Detection of meat-borne trimethylamine based on nanoporous colorimetric sensor arrays. *Food Chem.* 197(Pt A), 930–936. doi: 10.1016/j.foodchem.2015.11.041
- Xing, Y., Li, X., Zhang, L., Xu, Q., Che, Z., Li, W., et al. (2012). Effect of TiO₂ nanoparticles on the antibacterial and physical properties of polyethylene-based film. *Prog. Organ. Coat.* 73, 219–224. doi: 10.1016/j.porgcoat.2011.11.005
- Xu, Y., Liu, X., Jiang, Q., Yu, D., Xu, Y., Wang, B., et al. (2021). Development and properties of bacterial cellulose, curcumin, and chitosan composite biodegradable films for active packaging materials. *Carbohydr. Polym.* 260:117778. doi: 10.1016/j.carbpol.2021.117778
- Ydollahi, M., Ahari, H., and Anvar, A. A. (2016). Antibacterial activity of silver-nanoparticles against *Staphylococcus aureus*. *Afr. J. Microbiol. Res.* 10, 850–855. doi: 10.5897/ajmr2016.7908
- Yu, J., Liu, R. Y. F., Poon, B., Nazarenko, S., Koloski, T., Vargo, T., et al. (2004). Polymers with palladium nanoparticles as active membrane materials. *J. Appl. Polym. Sci.* 92, 749–756. doi: 10.1002/app.20013
- Yu, Z., Li, B., Chu, J., and Zhang, P. (2018). Silica in situ enhanced PVA/chitosan biodegradable films for food packages. *Carbohydr. Polym.* 184, 214–220. doi: 10.1016/j.carbpol.2017.12.043
- Zahan, K. A., Azizul, N. M., Mustapha, M., Tong, W. Y., Abdul Rahman, M. S., and Sahuri, I. S. (2020). Application of bacterial cellulose film as a biodegradable and antimicrobial packaging material. *Mater. Today Proc.* 31, 83–88. doi: 10.1016/j.matpr.2020.01.201
- Zanjani, M. K., Mohammadi, N., Ahari, H., Tarzi, B. G., and Bakhoda, H. (2014). Effect of microencapsulation with chitosan coating on survival of *Lactobacillus casei* and *Bifidobacterium bifidum* in ice cream. *Iran. J. Nutr. Sci. Food Technol.* 8, 125–134.
- Zhai, X., Wang, X., Zhang, J., Yang, Z., Sun, Y., Li, Z., et al. (2020). Extruded low density polyethylene-curcumin film: a hydrophobic ammonia sensor for intelligent food packaging. *Food Packag. Shelf Life* 26:100595. doi: 10.1016/j.fpsl.2020.100595
- Zhang, G., and Zhao, Z. (2012). Green packaging management of logistics enterprises. *Phys. Procedia* 24, 900–905. doi: 10.1016/j.phpro.2012.02.135
- Zhang, J., Xu, W.-R., Zhang, Y.-C., Han, X.-D., Chen, C., and Chen, A. (2020). In situ generated silica reinforced polyvinyl alcohol/liquefied chitin biodegradable films for food packaging. *Carbohydr. Polym.* 238:116182. doi: 10.1016/j.carbpol.2020.116182
- Zhang, Q., Wu, J., Yang, F., Lei, Y., Zhang, Q., and Cheng, X. (2016). Alterations in soil microbial community composition and biomass following agricultural land use change. *Sci. Rep.* 6:36587.
- Zhang, X., Liu, X., Yang, C., Xi, T., Zhao, J., Liu, L., et al. (2021). New strategy to delay food spoilage: application of new food contact material with antibacterial function. *J. Mater. Sci. Technol.* 70, 59–66. doi: 10.1016/j.jmst.2020.08.045
- Zhang, Y., Liang, S., Zhang, J., Chi, Y., Tian, B., Li, L., et al. (2020). Preparation of whey protein isolate nanofibrils by microwave heating and its application as carriers of lipophilic bioactive substances. *LWT* 125:109213. doi: 10.1016/j.lwt.2020.109213
- Zhang, Y. P., Chodavarapu, V. P., Kirk, A. G., and Andrews, M. P. (2013). Structured color humidity indicator from reversible pitch tuning in self-assembled nanocrystalline cellulose films. *Sens. Actuators B Chem.* 176, 692–697. doi: 10.1016/j.snb.2012.09.100
- Zhao, G., Lyu, X., Lee, J., Cui, X., and Chen, W.-N. (2019). Biodegradable and transparent cellulose film prepared eco-friendly from durian rind for packaging application. *Food Packag. Shelf Life* 21:100345. doi: 10.1016/j.fpsl.2019.100345
- Zhu, F. (2019). Starch based Pickering emulsions: fabrication, properties, and applications. *Trends Food Sci. Technol.* 85, 129–137. doi: 10.1016/j.tifs.2019.01.012
- Zhu, Q., Lu, H., Zhu, J., Zhang, M., and Yin, L. (2019). Development and characterization of Pickering emulsion stabilized by zein/corn fiber gum (CFG) complex colloidal particles. *Food Hydrocoll.* 91, 204–213. doi: 10.1016/j.foodhyd.2019.01.029

Conflict of Interest: The authors declare that the research was conducted in the absence of any commercial or financial relationships that could be construed as a potential conflict of interest.

Copyright © 2021 Ahari and Soufiani. This is an open-access article distributed under the terms of the Creative Commons Attribution License (CC BY). The use, distribution or reproduction in other forums is permitted, provided the original author(s) and the copyright owner(s) are credited and that the original publication in this journal is cited, in accordance with accepted academic practice. No use, distribution or reproduction is permitted which does not comply with these terms.



Antimicrobial Properties of Food Nanopackaging: A New Focus on Foodborne Pathogens

Amir Ali Anvar¹, Hamed Ahari^{2*} and Maryam Ataee¹

¹ Department of Food Hygiene, Science and Research Branch, Islamic Azad University, Tehran, Iran, ² Department of Food Science and Technology, Science and Research Branch, Islamic Azad University, Tehran, Iran

OPEN ACCESS

Edited by:

Anindya Chanda,
Mycologics LLC, United States

Reviewed by:

Judith Maria Braganca,
Birla Institute of Technology
and Science, India
Suresh Babu Naidu Krishna,
Durban University of Technology,
South Africa

*Correspondence:

Hamed Ahari
dr.h.ahari@gmail.com

Specialty section:

This article was submitted to
Food Microbiology,
a section of the journal
Frontiers in Microbiology

Received: 03 April 2021

Accepted: 21 June 2021

Published: 12 July 2021

Citation:

Anvar AA, Ahari H and Ataee M
(2021) Antimicrobial Properties
of Food Nanopackaging: A New
Focus on Foodborne Pathogens.
Front. Microbiol. 12:690706.
doi: 10.3389/fmicb.2021.690706

Food products contaminated by foodborne pathogens (bacteria, parasites, and viruses) cause foodborne diseases. Today, great efforts are being allocated to the development of novel and effective agents against food pathogenic microorganisms. These efforts even might have a possible future effect in coronavirus disease 2019 (COVID-19) pandemic. Nanotechnology introduces a novel food packaging technology that creates and uses nanomaterials with novel physiochemical and antimicrobial properties. It could utilize preservatives and antimicrobials to extend the food shelf life within the package. Utilizing the antimicrobial nanomaterials into food packaging compounds typically involves incorporation of antimicrobial inorganic nanoparticles such as metals [Silver (Ag), Copper (Cu), Gold (Au)], and metal oxides [Titanium dioxide (TiO₂), Silicon oxide (SiO₂), Zinc oxide (ZnO)]. Alternatively, intelligent food packaging has been explored for recognition of spoilage and pathogenic microorganisms. This review paper focused on antimicrobial aspects of nanopackaging and presented an overview of antibacterial properties of inorganic nanoparticles. This article also provides information on food safety during COVID-19 pandemic.

Keywords: food packaging, nanoparticles, foodborne pathogens, antimicrobial, COVID-19

INTRODUCTION

Foods or beverages contaminated by foodborne pathogens (bacteria, parasites, and viruses) cause foodborne diseases that are generally classified into foodborne infection and foodborne intoxication. Foodborne infection occurs when a pathogen is ingested with food and establishes and multiplies itself in the human host. Foodborne intoxication occurs when a toxigenic pathogen establishes itself in a food and produces a toxin, which is then ingested by the human host (Bintsis, 2017). World Health Organization (WHO) reports also indicate foodborne diarrheal diseases cause 550 million cases and 230,000 deaths worldwide a year (WHO, 2015). The overall rate of foodborne diseases outbreak leads to a great concern about the infectious food products; therefore great efforts are being allocated to the development of novel and effective agents against food pathogenic microorganisms. These efforts might have a possible future effect in more critical conditions, such as pandemic diseases like influenza viruses, Severe Acute Respiratory Syndrome (SARS), and its newer form, SARS-CoV-2 (corona virus disease 2019, COVID-19).

When considering foods safety, the original source of the food, the microbiological quality of the raw food, the microbiological quality of the processed food, and subsequently the packaging, storage, and distribution are all important. Packaging alone has become a separate area for extensive

research into the prevention of foodborne illnesses. Food packaging is universally used to preserve the food quality and to extend the shelf life. Proper packaging could protect food products from microbial damage or from any other type of environmental contamination while a poor quality food packaging increases food waste and foodborne illnesses. Traditional food packages are passive barriers which can only delay the adverse effects of environmental contamination (Brody et al., 2008). In fact the key safety objective for traditional packaging materials is to be inert as possible in contact with food (Biji et al., 2015).

Today, the development of non-conventional packaging is becoming a key research field. The next generation of food packaging can play an important role in reducing the risk of pathogen contamination and extending the shelf-life of foods. Application of nanotechnology presents novel opportunities for exploring the bactericidal effect of nanomaterials with a marked bioactivity (Singh et al., 2017). Nanotechnology is the study and use of matter and structures sized from 1 to 100 nm (the word “nano” means 10^{-9} or one billionth of something) (Sujithra and Manikkandan, 2019).

Nanotechnology introduce a novel food packaging technology for the food industry (Dasgupta et al., 2015). The term nanopackaging comes from this combination of nanotechnology and food packaging shows a direct application of nanotechnology in food science. Nano-sciences create and use nanomaterials with novel physiochemical properties that offer many new opportunities for food industries (Gupta et al., 2016; Singh et al., 2017). More potent food coloring, flavoring, nutritional additives, and antibacterial ingredients for food packaging are the new opportunities for food industries.

Utilizing the antimicrobial nanomaterials into food packaging compounds typically involves incorporation of antimicrobial inorganic nanoparticles (NPs) (Rhim and Ng, 2007). Materials in the nanoscale range with a higher surface-to-volume ratio can attach more copies of microorganism, which confers greater efficiency (Luo and Stutzenberger, 2008). The antimicrobial nanomaterials are especially interesting because of their barrier properties and desirable structural integrity leads to decrease the spoilage and pathogenic microorganism growth (Rhim and Ng, 2007). In antimicrobial films, nanomaterials can be employed as growth inhibitors, killing agents, or even antibiotic carriers. Several studies show the biological effectiveness of inorganic NPs with a strong antibacterial activity in low concentrations (Jafarzadeh et al., 2020). The typical inorganic NPs used for food packaging are silver nanoparticles (AgNPs) that are popular for its excellent toxicity to many microorganisms, with low volatility and high-temperature stability (Shahbazzadeh et al., 2009; Ahari et al., 2020; Kavakebi et al., 2021). The most common method for AgNPs preparation is chemical reduction. The reduction of silver ions in aqueous solution leads to the formation of silver atoms and aggregation into colloidal clusters. These clusters form the Ag particles with nanometer dimensions. Smaller AgNPs have larger surface area to interact with microbial cells that results in better bactericidal efficiency (Azeredo, 2009). Other antimicrobial NPs which have been applied in food packaging are titanium dioxide

NPs (TiO_2 NPs). TiO_2 NPs have a photocatalytic activity that creates the polyunsaturated phospholipids peroxidation in the microbial cell membranes. This property has been applied to inactivate several foodborne pathogens (Chorianopoulos et al., 2011). Combining TiO_2 with metal increases its photocatalytic bacterial inactivation. The combination of $\text{TiO}_2/\text{AgNPs}$ has been used in several studies (Barani et al., 2018; Lotfi et al., 2019). In addition to AgNPs and TiO_2 NPs, there are a wide range of nanomaterials introduced to the food industries. Due to the fundamental differences in structural and physicochemical properties, each nanomaterial has different applications in the food nanopackaging. Many informative studies have addressed the practical applications of various nanomaterials in the food packaging industry. However, the number of studies focusing on the application of nanopackaging technology in food microbiology is limited. Despite the antimicrobial effectiveness aspects of nanopackaging, it is important to stress the nanomaterial interactions with food ingredients and possible alterations of food quality ranged from sensory features to safety aspects (Ahari and Lahijani, 2021). This largely depends on the nanomaterial doses and concentrations used in fabrication of nanopackages. Optimizing the right dose and concentration that leads to controlled release of nanoparticle can preserve antimicrobial properties without any alteration in the food quality and safety.

The goals of this study are to focus on antimicrobial aspects of nanopackaging. Here, we present an overview of antibacterial properties of inorganic NPs and highlight their specific effectiveness. Finally, the toxicity of inorganic NPs and their possible danger to human health are discussed.

FOODBORNE PATHOGENS

Foodborne pathogenic microorganisms are a branch of food microbes that may not alter the appearance, taste, and quality of products, but they can contaminate foods and cause foodborne illnesses. Therefore, the food safety could not be assessed based on product appearance alone. According to the Centers for Disease Control and Prevention (CDC), every year, 48 million people get sick in the United States from a foodborne illness, 128,000 are hospitalized, and 3,000 die. **Table 1** presents the list of foodborne pathogens involved in foodborne diseases.

Based on the inherent function of the pathogens, foodborne diseases are classified into “intoxication,” “toxicoinfection,” and “infection.” Intoxication occurs when water or a food product contaminated by pathogenic toxin is ingested. The symptoms of this class appear very quickly. *Staphylococcus aureus*, *Clostridium botulinum*, and *Bacillus cereus* are the most important pathogens cause food intoxication. “Toxicoinfection” results when an ingested pathogen produces a toxin inside the host body. The symptoms of this type are diarrhea and occasional vomiting. *Clostridium perfringens*, *Escherichia coli*, and *Vibrio cholera* are the examples of this class. “Foodborne infection” occurs when an invasive pathogen is ingested. *Salmonella enterica*, *Campylobacter jejuni*, *Escherichia coli* (E. coli O157:H7), *Shigella* sp., *Yersinia enterocolitica*, and *Listeria monocytogenes* are the

most important bacteria involved in the foodborne infections (Bhunia, 2018).

Campylobacter sp. mostly associated with raw or undercooked poultry while *Salmonella* sp. mostly found in meat, poultry, and eggs. *Shigella* sp., and *Escherichia coli* mostly found in meat and unpasteurized milk. *Clostridium botulinum* often found in improperly home-canned foods. *Clostridium perfringens*, *Yersinia*, *Vibrio* sp., *Staphylococcus aureus*, *Bacillus* sp., and *Listeria* are found in uncooked meats, vegetables, unpasteurized milk, and soft cheese (Safavieh et al., 2015).

Toxoplasma gondii, *Cryptosporidium parvum*, *Cyclospora cayetanensis*, *Giardia intestinalis*, *Taenia solium*, *Trichinella spiralis*, and Norovirus, hepatitis A virus, and Rotavirus are the most marked parasites and viruses which cause foodborne diseases (Table 1; Bhunia, 2018).

COVID-19

COVID-19 is an infectious disease caused by SARS-CoV-2 which is manifested by symptoms ranging from mild influenza to severe pneumonia and acute respiratory distress syndrome (Petrosillo et al., 2020). COVID-19 is an enveloped single-stranded RNA virus that its outbreak had become a pandemic in 2020 (Asselah et al., 2021). The beginning of the SARS-CoV-2 outbreak has been attributed to the seafood market in Wuhan, Hubei, China (Chan et al., 2020). According to the WHO, the main route for COVID-19 transmission is respiratory droplets generated by coughing, sneezing, speaking, and breathing of an infected person (Tang et al., 2020). There is no evidence suggesting food is transmission route for COVID-19. The Food and Drug Administration (FDA) (U.S. Food and Drug Administration [FDA], 2020) and CDC emphasize that the risk of infection by the COVID-19 from food

products, and food packaging is thought to be very low. Up to now, no cases of COVID-19 have been reported where infection was thought to have occurred by consuming and touching food or food packaging.

Previous studies on coronaviruses family indicated that these viruses can persist in the environment for a long time and may be transmitted through the package surfaces (Geller et al., 2012). Currently, the proposed route for the possible transmission of SARS-CoV-2 through food is the consumption of infected animal foods or the consumption of cross-contaminated foods (Olaimat et al., 1854).

To date, no studies have investigated the survival of SARS-CoV-2 in various foods and food packaging. Therefore, it is not possible to comment at this time on the potential survival of SARS-CoV-2 in food products.

The COVID-19 virus can live on inanimate objects for 72 h (van Doremalen et al., 2020). If the respiratory secretions of a person with corona are secreted onto a food product, it may become a virus carrier. Contact with these food carriers can cause the virus to enter the respiratory system. Since each food product travels a long distance from farm to fork, and along this route they may be contaminated with infectious droplets, regular hand washing and the proper use of sanitizers, and disinfectants are recommended (Olaimat et al., 1854). Besides, the use of online food delivery is advised to create a physical distance between customers and sales staff (U.S. Food and Drug Administration [FDA], 2020). It is also recommended to use cooked foods because coronaviruses do not survive in high temperatures. Raw foods should be washed first and then frozen; because the virus can survive up to 2 years at freezing temperatures (Olaimat et al., 1854).

Food nanopackaging can be a promising approach to maintaining food health against SARS-CoV-2. However, the number of studies that have been done on this subject can be summarized as one where it reported that coatings or films containing copper, silver and zinc NPs have the ability to fight the virus (Sportelli and Izzi, 2020). Antiviral potency of NPs is an open field of research that needs to be fully addressed.

TABLE 1 | Types of food pathogens.

Microorganism		
Foodborne bacteria	Foodborne parasites	Foodborne viruses
<i>Aeromonas hydrophila</i>	<i>Cryptosporidium parvum</i>	Astrovirus
<i>Bacillus anthracis</i>	<i>Cyclospora cayetanensis</i>	Avian influenza
<i>Bacillus cereus</i>	<i>Cystoisospora belli</i>	Hepatitis A virus
<i>Brucella</i> sp.	<i>Entamoeba histolytica</i>	Hepatitis E virus
<i>Campylobacter</i> sp.	<i>Giardia intestinalis</i>	Norovirus
<i>Clostridium botulinum</i>	<i>Helminths</i>	Rotavirus
<i>Clostridium perfringens</i>	<i>Taenia solium/saginata</i>	
<i>Cronobacter sakazakii</i>	<i>Toxoplasma gondii</i>	
<i>Escherichia coli</i>	<i>Trematodes</i>	
<i>Escherichia coli</i> O157:H7	<i>Trichinella spiralis</i>	
<i>Listeria monocytogenes</i>		
<i>Mycobacterium paratuberculosis</i>		
<i>Salmonella</i> sp.		
<i>Shigella</i> sp.		
<i>Staphylococcus aureus</i>		
<i>Vibrio</i> sp.		
<i>Yersinia enterocolitica</i>		

ANTIMICROBIAL NANOPACKAGING

Types of Antimicrobial Nanopackaging

Nanopackaging can be divided into three main categories (Figure 1); (i) Improved packaging: These packages contain NPs and are resistant to temperature and humidity; (ii) Active packaging: Packages containing preservatives such as inorganic NPs that can interact directly with food and provide antimicrobial properties; (iii) Intelligent/smart packaging: Packages that are designed for sensing biochemical or microbial changes and specific pathogen developing in the food.

The basic goal of improved packaging is to increase the mechanical and physical properties of the packages. Various nanocomposites are manufactured for various food products such as beverages and oils to reduce the oxygen and carbon dioxide permeation for up to 80–90%. One of the most popular NPs used in improved packaging is nanoclay. Nanoclay

TABLE 2 | Some of the most important nanopacking articles from 2018 to February 2021.

Nanocomposite	Nanoparticle concentration (method)*	Tested foodborne pathogens	Types of food**	Effect	References
Gelatin/Cellulose nanofibers/ZnONPs/ and or Selenium NPs	Different concentrations (Casting method)	<i>E. coli</i> , <i>L. monocytogenes</i> , <i>P. fluorescens</i> , <i>S. aureus</i>	–	A stronger antibacterial effect of ZnONPs compared with SeNPs. The bacterial susceptibility to the antibacterial films was as follows: <i>L. monocytogenes</i> > <i>E. coli</i> > <i>S. aureus</i> > <i>P. fluorescens</i>	Ahmadi et al., 2021
Plasticized polylactide/Polyethylene glycol/Ag-Cu NPs/Cinnamon essential oil	4% Ag-Cu NPs with 50% Cinnamon essential oil (Compression-molding method)	<i>C. jejuni</i> , <i>L. monocytogenes</i> , <i>S. Typhimurium</i>	Chicken meat	Maximum antibacterial action during 21 days at the refrigerated condition	Ahmed et al., 2018
Low-density polyethylene/AgNPs/TiO ₂ NPs	0, 1, 3, and 5% of AgNPs (Melt mixing and sol-gel methods)	<i>A. niger</i> , <i>C. albicans</i> , <i>E. coli</i> , <i>S. aureus</i>	Pikeperch filets	Effectiveness against all examined bacteria in 3% of AgNPs	Barani et al., 2018
Low-density polyethylene/AgNPs	1.50, 3.75, 7.50, 15.00, 30.00, 60.00, and 75.00 µg/ml of AgNPs	<i>Apple-isolated Penicillium expansum</i> , <i>E. coli</i> , <i>Enterococcus faecalis</i> , <i>Salmonella enterica</i> subsp. <i>enterica</i> serovar <i>Typhimurium</i> , and <i>S. aureus</i>	–	Antimicrobial effects against all the microorganisms studied, although more notably for fungi and gram-negative bacteria than the gram-positive bacteria	Brito et al., 2020
Cellulose/AgNPs	0.005, 0.01, 0.02, 0.04, and 0.08 g of AgNPs (Using N,N-dimethylacetamide as a reducing agent in the presence of PVP-K30)	<i>E. coli</i> and <i>S. aureus</i>	–	Remarkable antibacterial activities. The sterilization effect of produced film with 0.04 g of AgNPs against both bacteria exceeds 99.9%	Chen et al., 2020
Low-density polyethylene/AgNPs + CuNPs/TiO ₂ NPs	0.1, 0.3, 0.5, 1, 3, and 5% of AgNPs + CuNPs (Melt mixing masterbatch method)	<i>E. coli</i> and <i>L. monocytogenes</i>	Nile Tilapia fish	a film containing 2.5% of AgNPs and 2.5% of CuNPs had the most significant antimicrobial effect on the Nile Tilapia fish	Efatian et al., 2021
Carboxymethyl cellulose/Cellulose nanocrystal-AgNPs	1, 3, 5, and 7% of AgNPs	<i>E. coli</i> and <i>S. aureus</i>	Strawberries	The best antibacterial activities against the two bacterial strains Better maintenance of strawberries quality compared with unpackaged strawberries and extending the shelf-life of strawberries to 7 days	He et al., 2021
Chitosan/Nigella sativa extract-AgNPs	0.1% w/v, 0.2% w/v, 0.3% w/v of AgNPs	<i>B. subtilis</i> , <i>E. coli</i> , <i>P. aeruginosa</i> , <i>S. aureus</i>	–	A good antibacterial activity against gram-negative bacteria compared to the gram-positive bacteria For both gram-positive and gram-negative bacteria, antibacterial activity significantly influenced by the AgNPs concentration	Kadam et al., 2019
Chitosan-TiO ₂ NPs/Red apple pomace extract	10% TiO ₂ NPs	<i>E. coli</i> and <i>S. aureus</i>	–	More effective antimicrobial activities against <i>S. aureus</i> than <i>E. coli</i>	Lan et al., 2021
Carboxymethyl cellulose/Glycerol/Dioscorea opposita mucilage from Chinese yam/ZnONPs	"CMC to DOM weight ratio" of approximately 1:1, 2.0 g ZnONPs (Casting method)	<i>E. coli</i> , <i>S. aureus</i>	–	Antibacterial effects against both <i>E. coli</i> and <i>S. aureus</i>	Li et al., 2021
Low-density polyethylene/AgNPs/TiO ₂ NP and Low-density polyethylene/nanoclay/TiO ₂ NPs	0.1, 0.3, 0.5, 1, 3, and 5% of AgNPs or nanoclay (Melt mixing and sol-gel methods)	<i>E. coli</i> , <i>S. aureus</i>	Chicken meat	Greatest antimicrobial effect on gram-positive and gram-negative bacteria for films containing 5% silver and 5% titanium dioxide nanoparticles	Lotfi et al., 2019
Polyvinyl alcohol/Boiled rice starch/AgNPs	6.8 µg/mg AgNPs (Photo-assisted method)	<i>S. aureus</i> and <i>S. typhimurium</i>	–	Stronger antibacterial activity against <i>S. typhimurium</i> than <i>S. aureus</i>	Mathew et al., 2019
Cellulose/CuNPs	5, 25, 125, and 250 mM (Simple casting ethanol regeneration method)	<i>E. coli</i> and <i>Bacillus</i> sp.	–	Remarkable biocidal activity against <i>E. coli</i> in 250 mM concentration	Muthulakshmi et al., 2019
Poly (3-hydroxybutyrate-co-3-hydroxyvalerate)/Biogenic SiO ₂ NPs	Different concentrations (Solution casting method)	<i>E. coli</i> and <i>S. aureus</i>	–	Progressively improvement of antibacterial activity of nanocomposites upon increasing SiO ₂ NPs concentration	Ojha and Das, 2020

(Continued)

TABLE 2 | Continued

Nanocomposite	Nanoparticle concentration (method)*	Tested foodborne pathogens	Types of food**	Effect	References
Poly lactic acid/Oligomeric lactic acid/Chitosan-AgNPs	0.5 wt%, 1 wt%, 3 wt%, 5 wt% of AgNPs (Facile and green synthesis method)	<i>E. coli</i> , <i>S. aureus</i>	-	Antimicrobial activities against the both bacteria. However, the low content of chitosan-AgNPs was not effective against <i>E. coli</i> but was against <i>S. aureus</i> bacteria	Sonseca et al., 2019
Carrageenan/Laponite on the oxygen plasma surface modified polypropylene film/AgNPs	20 µg/ml AgNPs (Green synthesis method from the <i>Digitalis purpurea</i> plant)	<i>E. coli</i> and <i>S. aureus</i>	-	The excellent antimicrobial activity against the both bacteria	Vishnuvarthanan and Rajeswari, 2019
Chitosan/ZnONPs/Gallic acid	30, 50, and 70 mg of ZnONPs (Facile green method using solution casting technique)	<i>B. subtilis</i> and <i>E. coli</i>	-	Antimicrobial activities against both bacterial strains	Yadav et al., 2021
Cellulose nanofibril/AgNPs	50–1,000 µg/ml of AgNPs (Reduction method using NaBH ₄)	<i>E. coli</i> O157:H7, <i>L. monocytogenes</i>	-	Greater inhibitory effect on the growth of <i>E. coli</i> O157:H7 than on <i>L. monocytogenes</i>	Yu et al., 2019
Poly(lactic acid)/3-(4'-epoxyethyl-benzyl)-5,5-dimethylhydantoin/SiO ₂ NPs	1, 3, 5, 7, and 9% of SiO ₂ NPs	<i>E. coli</i> and <i>S. aureus</i>	-	Strong antibacterial activities against both bacterial strains	Zhao et al., 2020

*The nanocomposite fabrication method referred to it directly by the authors was mentioned in the parentheses.

**In addition to routine microbiological tests, some studies have tested the antibacterial properties of fabricated nanocomposites in the packaging of various foods. The type of food studied is listed in this column.

in situ by physical and chemical reduction methods. Hybrid materials produced by ultraviolet light and heat were effective against pathogenic microorganisms (mesophiles as well as lactic acid bacteria) on chicken exudates (Fernández et al., 2009). The chitosan silver oxide nanocomposite film showed excellent antibacterial performance against *E. coli*, *B. subtilis*, *P. aeruginosa*, and *S. aureus* microorganisms. This nanocomposite may be used to package foods that are highly sensitive to microbial growth or directly as a surface coating on perishable fruits and vegetables (Tripathi et al., 2011). Different concentrations of AgNPs to reduce total microbial count, mold, and coliform counts in nuts were also reported (Tavakoli et al., 2017). Silver-montmorillonite (Ag-MMT) NPs have also been considered to increase the fresh-cut carrots shelf life up to more than 2 months (Costa et al., 2012). Several studies have investigated the antimicrobial effects of nanosilver in combination with low density polyethylene (LDPE). Becaro et al. (2015) have reported the antibacterial effect of films containing silver NPs embedded in silica or titanium dioxide and were mixed with LDPE. Their films showed antimicrobial properties against *S. aureus* and *E. coli*, presenting better activity against *S. aureus* (Becaro et al., 2015). Lower concentrations of AgNPs incorporated in LDPE had antibacterial performance against mesophilic aerobic and coliforms in fresh-cut carrots packaged. Ascorbic acid content of fresh-cut carrots was also maintained (Becaro et al., 2016). A recent study reported that LDPE/AgNP films had a greater effect on gram-negative bacteria and fungi than gram-positive bacteria (Brito et al., 2020). Additional, antimicrobial properties of nanocomposites of carrageenan/AgNPs/Laponite was demonstrated against the both gram-negative *E. coli* and gram-positive *S. aureus* (Vishnuvarthanan and Rajeswari, 2019). It is well documented that AgNPs have strong antibacterial activity toward gram-negative than gram-positive bacteria (Shankar and Rhim, 2015; Orsuwan et al., 2016). Mathew et al. (2019) observed that both polyvinyl alcohol/AgNPs and polyvinyl alcohol/starch from the boiled red rice/sAgNPs films had stronger antibacterial activity against *S. typhimurium* than *S. aureus*. The difference in the cell wall structure of gram-negative and gram-positive bacteria causes this difference. In fact, the cell wall peptidoglycan layer in gram-positive bacteria makes it difficult for silver NPs to penetrate (Shankar and Rhim, 2017).

Copper Nanoparticles

Copper NPs are considered to be an antimicrobial agent for medicine and food. The potential biocidal activity of copper is low; however, copper NPs are preferred to silver NPs because of lower cost, easier mixing with polymers, and relatively more physicochemical characteristics.

Copper shows an excellent antimicrobial activity against a wide range of microorganisms. Three different methods including disc diffusion test, minimum inhibitory concentration (MIC) and minimum bactericidal concentration (MBC) have been used by Ruparelia et al. (2008) to study the effects of CuNPs against *E. coli*. This study showed that copper NPs have great promise as antimicrobial agent against *E. coli*, *B. subtilis*, and *S. aureus*. Cárdenas et al. (2009) tested the antimicrobial activity of colloidal CuNPs/chitosan composite film against

S. aureus and *Salmonella enterica* serovar *Typhimurium*. They showed the composite film was effective in alteration of cell wall and reduction of microbial concentration in the liquid culture for both bacteria tested (Càrdenas et al., 2009). Copper NPs synthesized using different types of copper salts had antimicrobial activity against *L. monocytogenes* as a gram-positive, and *E. coli* as a gram-negative foodborne pathogens (Shankar and Rhim, 2014). The antifungal activity as well as the antimicrobial activity against *Saccharomyces cerevisiae* has been illustrated in cellulose films containing copper oxide NPs (Llorens et al., 2012). Regardless of the type of microorganism in CuNPs bioactivity experiments, Cu-nano-antimicrobials proved to kill or inhibit the microorganism growth. Laser-generated CuNPs embedded in a biodegradable polymer matrix (polylactic acid) possess good antibacterial activity against *Pseudomonas* sp. (Longano et al., 2012). Polylactic acid films activated by CuNPs showed good antibacterial activity for fresh dairy products (Conte et al., 2013).

Gold Nanoparticles

Gold NPs have a great antimicrobial activity against several ranges of microorganisms depend upon their size and shape (Lima et al., 2013). Therefore, the biofilms containing gold NPs are very promising to be used as active food packaging for the extension of the food shelf life. Lima et al. (2013) showed that 5 nm AuNPs eliminated 90–95% of *E. coli* and *Salmonella typhi* colonies at short times. Active biofilms of quinoa (*Chenopodium quinoa*, W.) starch exhibited strong antibacterial activity against *E. coli* and *S. aureus* foodborne pathogens with inhibition percentages of 99 and 98%, respectively (Pagno et al., 2015). Gold NPs probably affect respiratory-chain enzymes which leading to cell death (Zawrah and Abd El-Moez, 2011). AuNPs in combination with bacteriocin had increased antimicrobial activity against four food spoiling organism of *Micrococcus luteus*, *Bacillus cereus*, *S. aureus*, and *E. coli* (Thirumurugan et al., 2013).

Titanium Dioxide Nanoparticles

Titanium dioxide is a photocatalytic agent used to inactivate a wide range of microorganisms. It is probably able to kill many microorganisms due to its strong oxidizing power and the production of free hydroxyl radicals in near-UV light (Chorianopoulos et al., 2011). The photocatalytic activity of TiO₂ has been used to purify contaminated water (Chaleshtori et al., 2009). Bodaghi et al. (2013) prepared a TiO₂ nanocomposite thin film by the extrusion method. They observed that when the film was exposed to UVA light, *Pseudomonas* sp., *R. mucilaginosa* and mesophilic bacteria were inactivated in saline and pear solution (Bodaghi et al., 2013). The antimicrobial activity of the TiO₂ nanoparticle-coated films has been found at various concentrations (0–0.11 g/100 ml organic solvent) under fluorescent and ultraviolet light (Othman et al., 2014). TiO₂NPs in gelatin-based films also showed excellent antimicrobial activity against *S. aureus* and *E. coli* (Nassiri and MohammadiNafchi, 2013). According to the Gumiero et al. (2013) study, the high-density polyethylene + CaCO₃ + TiO₂ composite matrix was able to provide a greater maintenance of the original cheese structure due to the inhibition of lactic acid bacteria and coliforms. Compared to the TiO₂ nanoparticle-incorporated film,

a hydrothermally synthesized sodium alginate film containing functional Au-TiO₂ nanocomposites improved the antimicrobial activity by 60 and 50% against *S. aureus* and *E. coli*, respectively (Tang et al., 2018). TiO₂-ZnO-MgO mixed oxide nanomaterials is another type of TiO₂ nano-alloy that has shown good antibacterial properties against *E. coli*, *Salmonella paratyphi*, *S. aureus*, and *L. monocytogenes* (Anaya-Esparza et al., 2019). Ansari et al. (2020) studied the synthesis of electrospun TiO₂ nanofibers, and showed TiO₂ nanofibers were more active against gram-negative *P. aeruginosa* cells than gram-positive *S. aureus*. They also demonstrated that TiO₂ nanofibers inhibited biofilm formation of methicillin-resistant *S. aureus* and *P. aeruginosa* in a dose-dependent manner (Ansari et al., 2020). In a recent study, nanosized TiO₂ and red apple pomace utilized as a potential extraction source to develop an intelligent chitosan-based film for packaging of the freshness of salmon filets. It was showed that this film had a synergistic enhancement of the antimicrobial activity as well as antioxidant property and pH responsive color-changing indicator (Lan et al., 2021).

Silicon Dioxide Nanoparticles

Silicon dioxide (SiO₂, silica) NPs possess several advantages such as high strength, thermal stability, high abundance, and low cost used in active polymer-inorganic composite materials (Hou et al., 2019). Recently, the antimicrobial activities of the gellan gum-sodium carboxymethyl cellulose (GC)-SiO₂ and GC-SiO₂-octadecyldimethyl-(3-trimethoxysilylpropyl)- ammonium chloride (ODDMAC) nanocomposites were tested against *S. aureus*, *Bacillus cereus*, *Cronobacter sakazakii*, *Salmonella enterica*, *Salmonella typhimurium*, and *E. coli*. The results indicate that the GC-SiO₂-ODDMAC film had a broad spectrum of antimicrobial activities for both gram-positive and gram-negative pathogens (Rukmanikrishnan et al., 2020). In another study, the nano-SiOx/chitosan complex coating film was applied for improving the tomatoes shelf life and preservation of tomatoes quality. The developed nano film slowed moisture loss, gas exchange, and respiration rates. It also limited bacterial growth, and prevented the increase of malondialdehyde and total polyphenol content. The novel nano-SiOx/chitosan complex film has been proposed for packaging the postharvested tomatoes (Zhu et al., 2019).

Zinc Oxide Nanoparticles

Zinc oxide is one of the generally recognized as safe (GRAS) material listed by the FDA (Espitia et al., 2012). Recently, a chitosan and zinc oxide NPs loaded gallic-acid films has been proposed for active food packaging for black grape, apple, mango fruits, tomato etc. (Yadav et al., 2021). For extending the shelf life of guava fruits, Kalia et al. (2021) fabricated a chitosan-based nanocomposite film containing CuO and ZnO NPs synthesized from the nettle leaf extract. The antioxidant and antimicrobial activity of biologically synthesized NPs was in order of CuONPs > ZnONPs > nettle extract (Kalia et al., 2021). Foodborne pathogens including *E. coli* O157:H7 can easily grow in white brined cheese. The chitosan and chitosan-ZnONPs coating reduced the initial numbers of *E. coli* O157:H7 in white brined cheese (Al-Nabulsi et al., 2020). Further, functionalized

absorbing pads containing ZnONPs have also been successfully applied for controlling *C. jejuni* in raw chicken meat, where the reduced *C. jejuni* count to an undetectable level by immobilized ZnONPs was reported (Hakeem et al., 2020).

Intelligent Packaging

Intelligent food packaging is a packaging structure that utilize the internal molecules or external conditions of the packed food as information to warn of any changes in the environment of the packages (Drago et al., 2020). Microbiological and chemical tests are regularly carried out on food products, but there is not adequate control after delivery to the supermarket. This unfilled space can be charged with intelligent packaging (Ghaani et al., 2016). Intelligent packaging can be used as a detection method for recognition of spoilage and pathogenic microorganisms. The intelligent packaging can provide information about both the food product status and the environment surrounding it (Vanderroost et al., 2014). They can be equipped with nanosensors classified as freshness indicators, time-temperature indicators, moisture indicators, optical oxygen sensors, optochemical CO₂ indicators, toxins indicators, ph contaminants indicators, and spoilage and pathogens indicators (Alfei et al., 2020). Most of these sensors or indicators are based on colorimetric methods. Natural dyes such as anthocyanins, curcumin, chlorophyll, and b-carotene found in many fruits and vegetables as well as synthetic dyes based on azo-compounds can be used as sensors in the packaging materials. Enzymatic processes that are capable to catalyze color chemical reactions are good candidate as sensors in intelligent packaging (Halonen et al., 2020). Currently, the selective interaction between antibody and antigen is one of the explored strategies used for intelligent packaging to identify microorganisms. The methods are based on antibodies conjugated with NPs, such as quantum dots (QDs). QDs are nanomaterials made from inorganic semiconductors and possess specific intrinsic characteristics. QDs are a promising class of fluorescent labels for biological detection because they can absorb wide and continuous wavelengths spectra and produce narrow fluorescence emission spectra depending on their size and composition (Valizadeh et al., 2012). QDs conjugated with antibodies are mainly employed due to their specific characteristics for detection of bacteria (Mihindukulasuriya and Lim, 2014). Mohamadi et al. (2017) presented a method to detect distribution of *E. coli* labeled with CdSe-QDs both on an agar nutrient and ground fish substrates. They showed that *E. coli* growth on food products can be easily monitored by CdSe-QDs (Mohamadi et al., 2017). Wang et al. (2011) developed a multiplex immunoassay by integrating magnetic nanobeads (MNBs) for immunoseparation with QDs as fluorescent labels for detection of *Salmonella Typhimurium*, *E. coli* O157:H7, and *L. monocytogenes*, in food products. Their presented multiplex immunoassay method detected simultaneously all three pathogens at levels of 20–50 CFU/ml or lower in food samples (Wang et al., 2011). Recently, a peptide-mediated immunomagnetic separation technique and an immunofluorescence quantum dot technique have been presented for detection of *E. coli* O157:H7, *S. aureus*, and *V. parahaemolyticus*. The method is able to detect three

kinds of foodborne pathogens at the same time (Wang et al., 2020). Researchers have recently developed a bacteria-detecting device to detect *L. monocytogenes* in opened food packages. These devices use strips on which gold or palladium nanoparticle-labeled antibodies detect the presence of bacteria (Yousefi et al., 2019).

From the above reports, it can be concluded that the development of new nanomaterials and devices are potential options for producing intelligent labels that can detect pathogens and toxins in food matrix. More future studies need to be done to establish this technique in food antimicrobial nanopackaging application.

Toxicological Aspects

Comprehensive information regarding the interface between NPs and the human body, particularly in relation to possible NPs hazards to human health must be obtained. NPs incorporated to the nano-packed food products may enter into the body through inhalation, ingestion or cutaneous exposure (Maisanaba et al., 2015). NPs are not soluble in biological fluids, so if they enter the bloodstream, they accumulate in organelles. A very few studies have investigated possible toxicity of NPs combined with food packages. A migration of low molecular mass constituents of nanopackaging to food products is a matter of high concern, both for researchers and consumers. The migration of NPs to food matrix mainly relies on the concentration and particle size of them and composition of food. The migration of metal NPs into the food matrix depends on temperature and acidity (Huang et al., 2015). Few studies points out toward the genotoxicity and carcinogenicity of NPs. Aschberger et al. (2011) observed that toxicity of nanosilver and nano TiO₂ can be present in high doses. ZnONPs even at low concentrations may possess a genotoxic potential in human epidermal cells which could be mediated through lipid peroxidation and oxidative stress (Sharma et al., 2009). NPs increase surface to volume ratio which leads to more interaction with biomolecules and create adverse biological responses. It is reported that cationic NPs may be quite toxic than neutral or anionic ones due to their high affinity toward the negatively charged biomolecules (Love et al., 2012). NPs may have adverse effects on circulation, especially affecting microcirculation. If NPs enter the circulatory system, they may affect the blood vessel lining or function and promote blood clot formation or may be associated with cardiovascular effects (Dimitrijevic et al., 2015).

In several *in vitro* studies, genotoxic, cytotoxic, and even carcinogenic aspects of AgNPs were evaluated. It has been observed that the exposure of normal human lung fibroblast cells (IMR-90) and human glioblastoma cells (U251) to 6–20 nm AgNPs disrupted the mitochondrial respiratory chain leading to ROS production and interruption of ATP synthesis. It also induced DNA damage and G2/M phase cell cycle arrest (AshaRani et al., 2009). Proliferating human intestinal cells (Caco-2 cell line) exposure to peptide-coated silver NPs induced ROS production and decreasing adherence capacity (Böhmert et al., 2012). It has been reported that AgNPs were internalized into the cytoplasm of Caco-2 cells and depolarized the mitochondrial membrane potential. In addition, AgNPs

depleted the total intracellular glutathione level, induced the activation of Nrf2 (a stress-responsive gene), and increased the expression of heme oxygenase-1 (HO-1) (Aueviriyavit et al., 2014). It concluded that AgNPs induced acute cytotoxicity and cellular responses via the activation of Nrf2/HO-1 signaling pathway in Caco-2 cells (Aueviriyavit et al., 2014). In another study, Miranda et al. (2017) investigated the toxicological interactions of AgNPs (size = 1–2 nm; zeta potential = –23 mV) in human hepatoma HepG2 cells. The co-exposure to AgNPs and metals potentiated cell death mainly by necrosis (Miranda et al., 2017). The synthesized green silver NPs may induce cytotoxicity and cause DNA damage and apoptosis. Bin-Jumah et al. (2020) showed that higher concentrations of green AgNPs reduced cell viability. They also demonstrated following a higher concentration exposure of green AgNPs, count of apoptotic and necrotic cells was increased. These kinds of AgNPs induced more ROS in the HuH-7 cells than in the CHANG cells (Bin-Jumah et al., 2020). Recently, it was reported that AgNPs altered morphology of freshly isolated circulating human peripheral blood mononuclear cells (hPBMC). They induced apoptosis and cell death in a dose- and time-dependent manner (Vuković et al., 2020).

CuNPs have been associated with cytotoxicity mediated through oxidative stress-dependent pathways. Recently, Fahmy et al. (2020) have reported that Cu/CuO NPs suppressed proliferation and viability of normal and carcinoma lung cells. Treatment of both cell types with Cu/CuO NPs resulted in the generation of a state of oxidative stress (Fahmy et al., 2020). In another study, the toxic potentials of CuONPs were evaluated in the two types of human cell lines (HepG2 hepatocarcinoma and Caco-2 colorectal adenocarcinoma). CuONPs were found to cause cytotoxicity, genotoxicity, and oxidative and apoptotic effects in both cell lines (Abudayyak et al., 2020).

AuNPs cytotoxicity was also evaluated in human erythrocytes, murine fibroblasts (NIH3T3), human cervix carcinoma cells (HeLa), and melanoma cells (B16F10) recently. It seems that the physicochemical properties and concentration of AuNPs and also cell type were limiting factors for the cytotoxic effect of AuNPs (Vechia et al., 2020). It has also been found that greatest concentrations of Ag and Ag-Au bimetallic NPs were toxic to both H4IIE-luc (rat hepatoma) and HuTu-80 (human intestinal) cells but AuNPs were not toxic alone. This study suggests that the toxic potency of Ag-Au bimetallic NPs is greater than AuNPs (Botha et al., 2019). However, Enea et al. (2020) showed that the 13 nm AuNPs are toxic to a cell line derived from normal human kidney (HK-2).

According to the studies using TiO₂ anatase NPs, TiO₂NPs are cytotoxic or genotoxic. When inhalation is a major route for entrance of nano TiO₂ into the human body, the most important adverse effect of TiO₂NPs in experimental models is pulmonary inflammatory responses and lung cancers (Shi et al., 2013). As reported by Koenen et al. (2010), TiO₂NPs at 10 µg/ml and above, can go through the epithelial lining by transcytosis. TiO₂ could penetrate into and through the cells without disrupting junctional complexes. Low concentrations of TiO₂ do not disrupt epithelial integrity and cell death (Koenen et al., 2010). It seems that low doses of nano TiO₂ are non-toxic.

According to the study conducted by Tarantini et al. (2015) silica NPs penetrate into the cytoplasm but not the nucleus of the human intestinal Caco-2 cell line and have toxic effects in the cells. They proposed that genotoxic effects of silica NPs are likely to be mediated through oxidative stress rather than a direct interaction with the DNA (Tarantini et al., 2015). It has been reported that silica NPs with 100 µg/ml concentration and 24-h exposure are safe for GES-1 and Caco-2 cells. However, at a higher concentration and longer exposure period, they arrest cell cycle and inhibit the cell growth (Yang et al., 2014). In contrast to the above reports, Schübbe et al. (2012) study showed neither cytotoxic nor genotoxic effects were detected for either 32 or 83 nm fluorescent silica NPs.

A significant inhibition of Caco-2 cell viability exposed to ZnONPs (3, 6, and 12 mM) for a 24-h exposure has been reported. Alteration in cell shape, abnormal nuclear structure, membrane blebbing, and cytoplasmic deterioration were the observed changes (Mao et al., 2016). In another study, treatment of rats with 50 and 100 mg/kg ZnONPs induced significantly intestinal injury, while treatment with 5 mg/kg ZnONPs normalized intestinal functions and structure. The authors concluded that ZnONPs have synergistic effects on liver enzyme, oxidative stress, apoptosis, inflammation, morphological changes and cell toxicity (Abbasi-Oshaghi et al., 2018). Caco-2 cells could be protected from ZnONP exposure by myricetin through modulating the apoptosis-ER stress pathway. In fact, co-exposure to myricetin and ZnONPs led to a significantly reduced ratio of cleaved caspase-3/pro-caspase-3 compared with the exposure to ZnONPs (Wu et al., 2019).

From the above reports, it can be concluded that there is no definite answer to the question of whether NPs are toxic. Studies have reported that NPs characteristics including shape, size, size distribution, structure, composition, surface functionality, porosity, surface area, surface charge, agglomeration, concentration, and solubility are all important in the toxicity of NPs (McCracken et al., 2016). For evaluation of NPs toxicity, biological and pathological effects of NPs should be determined by a number of variables, including NPs physiochemical properties, concentration, dose, exposure route, and duration. It seems that the size of NPs, the dose and the exposure time have a great effect on their toxicity. Current data are based on *in vitro* cell culture studies and/or *in vivo* animal model experiments. The potential and power of these models for predicting the NPs toxicity in humans is debated. Great care must be taken in using existing models to investigate and understand the biological and pathophysiological mechanisms of NPs toxicity. Full risk evaluations for various routes of exposure to different types of NPs are required.

CONCLUSION

Consumption of foods contaminated with foodborne microorganisms leads to foodborne diseases. The need to avoid foodborne pathogens contamination has led to the development of new preservative methods and innovative packaging. Antimicrobial packaging can play an important role

in reducing the risk of pathogen contamination, and improving the quality and shelf life of foods. This review underlines the capability of active and intelligent packages as antimicrobial agents against foodborne pathogens. Large numbers of scientific studies have demonstrated that active and intelligent packaging has many advantages in terms of food safety. Nanomaterials can provide new antimicrobials with wide spectrum of activity and improve durability and shelf life of food products. It is predicted that nanotechnology and nanopackaging could become part of the food industry and change the packaging process and fabrication in the coming years forward. However, a gap still exists, where the toxicity of NPs and their safe applications is controversial. The safety issues and environmental impact should be concerned before releasing the NPs to the market

in order to guarantee the human's health. Given the many benefits of nanopackaging in preserving foods, increasing the shelf-life, and preventing humans from foodborne illnesses, more focused research in the area of optimization of variables caused NPs toxicity must be carried out. A successful participation and collaboration between research activities and industry will promote the antimicrobial nanopackaging technologies.

AUTHOR CONTRIBUTIONS

MA assisted in compilation and proper editing of this review. All authors contributed to the article and approved the submitted version.

REFERENCES

- Abbasi-Oshaghi, E., Mirzaei, F., and Mirzaei, A. (2018). Effects of ZnO nanoparticles on intestinal function and structure in normal/high fat diet-fed rats and Caco-2 cells. *Nanomedicine* 13, 2791–2816. doi: 10.2217/nnm-2018-0202
- Abudayyak, M., Guzel, E., and Özhan, G. (2020). Cupric oxide nanoparticles induce cellular toxicity in liver and intestine cell lines. *Adv. Pharm. Bull.* 10, 213–220. doi: 10.34172/apb.2020.025
- Ahari, H., Amanolah Nejad, Z., Magharehei, M. A., and Paidari, S. (2020). Increasing Shelf Life of *Penaeus semisulcatus* in NanoSilver coatings based on titanium dioxide. *J. Food Technol. Nutr.* 17, 91–98.
- Ahari, H., and Lahijani, L. K. (2021). Migration of silver and copper nanoparticles from food coating. *Coatings* 11:380. doi: 10.3390/coatings11040380
- Ahmadi, A., Ahmadi, P., Sani, M. A., Ehsani, A., and Ghanbarzadeh, B. (2021). Functional biocompatible nanocomposite films consisting of selenium and zinc oxide nanoparticles embedded in gelatin/cellulose nanofiber matrices. *Int. J. Biol. Macromol.* 175, 87–97. doi: 10.1016/j.ijbiomac.2021.01.135
- Ahmed, J., Arfat, Y. A., Bher, A., Mulla, M., Jacob, H., and Auras, R. (2018). Active chicken meat packaging based on polylactide films and bimetallic Ag-Cu Nanoparticles and Essential Oil. *J. Food Sci.* 83, 1299–1310. doi: 10.1111/1750-3841.14121
- Alfei, S., Marengo, B., and Zuccari, G. (2020). Nanotechnology application in food packaging: a plethora of opportunities versus pending risks assessment and public concerns. *Food Res. Int.* 137:109664. doi: 10.1016/j.foodres.2020.109664
- Al-Nabulsi, A., Osaili, T., Sawalha, A., Olaimat, A. N., Albiss, B. A., Mehyar, G., et al. (2020). Antimicrobial activity of chitosan coating containing ZnO nanoparticles against *E. coli* O157:H7 on the surface of white brined cheese. *Int. J. Food Microbiol.* 334:108838. doi: 10.1016/j.ijfoodmicro.2020.108838
- Anaya-Esparza, L. M., Montalvo-González, E., González-Silva, N., Méndez-Robles, M. D., Romero-Toledo, R., Yahia, E. M., et al. (2019). Synthesis and characterization of TiO₂-ZnO-MgO mixed oxide and their antibacterial activity. *Materials* 12:698. doi: 10.3390/ma12050698
- Ansari, M. A., Albetran, H. M., Alheshibri, M. H., Timoumi, A., Algarou, N. A., Akhtar, S., et al. (2020). Synthesis of Electrospun TiO₂ nanofibers and characterization of their antibacterial and antibiofilm potential against gram-positive and gram-negative bacteria. *Antibiotics* 9:572. doi: 10.3390/antibiotics9090572
- Aschberger, K., Micheletti, C., Sokull-Klüttgen, B., and Christensen, F. M. (2011). Analysis of currently available data for characterising the risk of engineered nanomaterials to the environment and human health—lessons learned from four case studies. *Environ. Int.* 37, 1143–1156. doi: 10.1016/j.envint.2011.02.005
- AshaRani, P. V., Low Kah Mun, G., Hande, M. P., and Valiyaveetil, S. (2009). Cytotoxicity and genotoxicity of silver nanoparticles in human cells. *ACS Nano* 3, 279–290. doi: 10.1021/nn800596w
- Asselah, T., Durantel, D., Pasmant, E., Lau, G., and Schinazi, R. F. (2021). COVID-19: discovery, diagnostics and drug development. *J. Hepatol.* 74, 168–184. doi: 10.1016/j.jhep.2020.09.031
- Aueviriavit, S., Phummiratch, D., and Maniratanachote, R. (2014). Mechanistic study on the biological effects of silver and gold nanoparticles in Caco-2 cells—induction of the Nrf2/HO-1 pathway by high concentrations of silver nanoparticles. *Toxicol. Lett.* 224, 73–83. doi: 10.1016/j.toxlet.2013.09.020
- Azeredo, H. M. C. D. (2009). Nanocomposites for food packaging applications. *Food Res. Int.* 42, 1240–1253.
- Barani, S., Ahari, H., and Bazgir, S. (2018). Increasing the shelf life of pikeperch (*Sander lucioperca*) filets affected by low-density polyethylene/Ag/TiO₂ 2 nanocomposites experimentally produced by sol-gel and melt-mixing methods. *Int. J. Food Prop.* 21, 1923–1936. doi: 10.1080/10942912.2018.1508162
- Becaro, A. A., Puti, F. C., Correa, D. S., Paris, E. C., Marconcini, J. M., and Ferreira, M. D. (2015). Polyethylene films containing silver Nanoparticles for applications in food packaging: characterization of Physico-chemical and antimicrobial properties. *J. Nanosci. Nanotechnol.* 15, 2148–2156. doi: 10.1166/jnn.2015.9721
- Becaro, A. A., Puti, F. C., Panosso, A. R., Gern, J. C., Brandão, H. M., Correa, D. S., et al. (2016). Postharvest quality of fresh-cut carrots packaged in plastic films containing silver nanoparticles. *Food Bioprocess Technol.* 9, 637–649. doi: 10.1007/s11947-015-1656-z
- Bhunia, A. K. (2018). “Introduction to foodborne pathogens,” in *Foodborne Microbial Pathogens. Food Science Text Series*, (New York, NY: Springer). Available online at: https://link.springer.com/chapter/10.1007/978-1-4939-7349-1_1
- Biji, K. B., Ravishankar, C. N., Mohan, C. O., and Srinivasa Gopal, T. K. (2015). Smart packaging systems for food applications: a review. *J. Food Sci. Technol.* 52, 6125–6135.
- Bikiaris, D. N., and Triantafyllidis, K. S. (2013). HDPE/Cu-nanofiber nanocomposites with enhanced antibacterial and oxygen barrier properties appropriate for food packaging applications. *Mater. Lett.* 93, 1–4. doi: 10.1016/j.matlet.2012.10.128
- Bin-Jumah, M., Al-Abdan, M., Albasher, G., and Alarifi, S. (2020). Effects of green silver nanoparticles on apoptosis and oxidative stress in normal and cancerous human hepatic cells *in vitro*. *Int. J. Nanomed.* 15, 1537–1548. doi: 10.2147/ijn.s239861
- Bintsis, T. (2017). Foodborne pathogens. *AIMS Microbiol.* 3, 529–563.
- Bodaghi, H., Mostofi, Y., Oromiehie, A., Zamani, Z., Ghanbarzadeh, B., Costa, C., et al. (2013). Evaluation of the photocatalytic antimicrobial effects of a TiO₂ nanocomposite food packaging film by *in vitro* and *in vivo* tests. *LWT Food Sci. Technol.* 50, 702–706. doi: 10.1016/j.lwt.2012.07.027
- Böhmert, L., Niemann, B., Thünemann, A. F., and Lampen, A. (2012). Cytotoxicity of peptide-coated silver nanoparticles on the human intestinal cell line Caco-2. *Arch. Toxicol.* 86, 1107–1115. doi: 10.1007/s00204-012-0840-4
- Botha, T. L., Elemike, E. E., Horn, S., Onwudiwe, D. C., Giesy, J. P., and Wepener, V. (2019). Cytotoxicity of Ag, Au and Ag-Au bimetallic nanoparticles prepared using golden rod (*Solidago canadensis*) plant extract. *Sci. Rep.* 9:4169.
- Brito, S. D. C., Bresolin, J. D., Sivieri, K., and Ferreira, M. D. (2020). Low-density polyethylene films incorporated with silver nanoparticles to promote antimicrobial efficiency in food packaging. *Food Sci. Technol. Int.* 26, 353–366. doi: 10.1177/10822013219894202

- Brody, A., Bugusu, B., Han, J. H., Sand, C. K., and Mchugh, T. (2008). Innovative food packaging solutions. *J. Food Sci.* 73, 1750–1754. doi: 10.1111/j.1365-2656.2008.01111.x
- Cárdenas, G., Díaz, J. V., Meléndez, M. F., Cruzat, C. C., and García Cancino, A. (2009). Colloidal Cu nanoparticles/chitosan composite film obtained by microwave heating for food packaging applications. *Polym. Bull.* 62, 511–524. doi: 10.1007/s00289-008-0031-x
- Chaleshtori, M. Z., Masud, S. M. S., and Saupe, G. B. (2009). Using new porous nanocomposites for photocatalytic water decontamination. *MRS Online Proc. Libr.* 1145:436.
- Chan, J. F.-W., Yuan, S., Kok, K.-H., To, K. K.-W., Chu, H., Yang, J., et al. (2020). A familial cluster of pneumonia associated with the 2019 novel coronavirus indicating person-to-person transmission: a study of a family cluster. *Lancet* 395, 514–523. doi: 10.1016/s0140-6736(20)30154-9
- Chen, Q. Y., Xiao, S. L., Shi, S. Q., and Cai, L. P. (2020). A one-pot synthesis and characterization of antibacterial silver nanoparticle-cellulose film. *Polymers* 12:440. doi: 10.3390/polym12020440
- Chorianopoulos, N. G., Tsoukleris, D. S., Panagou, E. Z., Falaras, P., and Nychas, G. J. E. (2011). Use of titanium dioxide (TiO₂) photocatalysts as alternative means for *Listeria monocytogenes* biofilm disinfection in food processing. *Food Microbiol.* 28, 164–170. doi: 10.1016/j.fm.2010.07.025
- Conte, A., Longano, D., Costa, C., Ditaranto, N., Ancona, A., Cioffi, N., et al. (2013). A novel preservation technique applied to fiordilatte cheese. *Innov. Food Sci. Emerg. Technol.* 19, 158–165. doi: 10.1016/j.ifset.2013.04.010
- Costa, C., Conte, A., Buonocore, G. G., Lavorgna, M., and Del Nobile, M. A. (2012). Calcium-alginate coating loaded with silver-montmorillonite nanoparticles to prolong the shelf-life of fresh-cut carrots. *Food Res. Int.* 48, 164–169. doi: 10.1016/j.foodres.2012.03.001
- Dasgupta, N., Ranjan, S., Mundekkad, D., Chidambaram, R., Shanker, R., and Kumar, A. (2015). Nanotechnology in agro-food: from field to plate. *Food Res. Int.* 69, 381–400. doi: 10.1016/j.foodres.2015.01.005
- Dimitrijevic, M., Karabasil, N., Boskovic, M., Teodorovic, V., Vasilev, D., Djordjevic, V., et al. (2015). Safety aspects of nanotechnology applications in food packaging. *Procedia Food Sci.* 5, 57–60.
- Drago, E., Campardelli, R., Pettinato, M., and Perego, P. (2020). Innovations in smart packaging concepts for food: an extensive review. *Foods* 9:1628. doi: 10.3390/foods9111628
- Efatian, H., Ahari, H., Shahbazzadeh, D., Nowruzi, B., and Yousefi, S. (2021). Fabrication and characterization of LDPE/silver-copper/titanium dioxide nanocomposite films for application in Nile Tilapia (*Oreochromis niloticus*) packaging. *J. Food Meas. Charact.* 15, 2430–2439. doi: 10.1007/s11694-021-00836-7
- Enea, M., Pereira, E., de Almeida, M. P., Araújo, A. M., de Lourdes Bastos, M., and Carmo, H. (2020). Gold nanoparticles induce oxidative stress and apoptosis in human kidney cells. *Nanomaterials* 10:995. doi: 10.3390/nano10050995
- Espitia, P. J. P., Soares, N. D. F. F., Coimbra, J. S. D. R., de Andrade, N. J., Cruz, R. S., and Medeiros, E. A. A. (2012). Zinc oxide nanoparticles: synthesis, antimicrobial activity and food packaging applications. *Food Bioprocess Technol.* 5, 1447–1464. doi: 10.1007/s11947-012-0797-6
- Fahmy, H. M., Ebrahim, N. M., and Gaber, M. H. (2020). In-vitro evaluation of copper/copper oxide nanoparticles cytotoxicity and genotoxicity in normal and cancer lung cell lines. *J. Trace Elem. Med. Biol.* 60:126481. doi: 10.1016/j.jtemb.2020.126481
- Fernández, A., Soriano, E., López-Carballo, G., Picouet, P., Lloret, E., Gavara, R., et al. (2009). Preservation of aseptic conditions in absorbent pads by using silver nanotechnology. *Food Res. Int.* 42, 1105–1112. doi: 10.1016/j.foodres.2009.05.009
- Geller, C., Varbanov, M., and Duval, R. E. (2012). Human coronaviruses: insights into environmental resistance and its influence on the development of new antiseptic strategies. *Viruses* 4, 3044–3068. doi: 10.3390/v4113044
- Ghaani, M., Cozzolino, C. A., Castelli, G., and Farris, S. (2016). An overview of the intelligent packaging technologies in the food sector. *Trends Food Sci. Technol.* 51, 1–11. doi: 10.1016/j.tifs.2016.02.008
- Gumiero, M., Peressini, D., Pizzariello, A., Sensidoni, A., Iacumin, L., Comi, G., et al. (2013). Effect of TiO₂ photocatalytic activity in a HDPE-based food packaging on the structural and microbiological stability of a short-ripened cheese. *Food Chem.* 138, 1633–1640. doi: 10.1016/j.foodchem.2012.10.139
- Gupta, A., Eral, H. B., Hatton, T. A., and Doyle, P. S. (2016). Nanoemulsions: formation, properties and applications. *Soft Matter* 12, 2826–2841. doi: 10.1039/c5sm02958a
- Hakeem, M. J., Feng, J., Nilghaz, A., and Ma, L. (2020). Active packaging of immobilized zinc oxide nanoparticles controls *Campylobacter jejuni* in raw chicken meat. *Appl. Environ. Microbiol.* 86:e01195-20.
- Halonen, N., Pálvölgyi, P. S., Bassani, A., Fiorentini, C., Nair, R., Spigno, G., et al. (2020). Bio-based smart materials for food packaging and sensors – a review. *Front. Mater.* 7:82. doi: 10.3389/fmats.2020.00082
- He, Y., Li, H., Fei, X., and Peng, L. (2021). Carboxymethyl cellulose/cellulose nanocrystals immobilized silver nanoparticles as an effective coating to improve barrier and antibacterial properties of paper for food packaging applications. *Carbohydr. Polym.* 252:117156. doi: 10.1016/j.carbpol.2020.117156
- Hou, X., Xue, Z., Xiao, Y., Qin, Y., Zhang, G., Liu, H., et al. (2019). Effect of SiO₂ nanoparticle on the physical and chemical properties of eco-friendly agar/sodium alginate nanocomposite film. *Int. J. Biol. Macromol.* 125, 1289–1298. doi: 10.1016/j.ijbiomac.2018.09.109
- Huang, J.-Y., Weibiao, Z., and Xu, L. (2015). Safety assessment of nanocomposite for food packaging application. *Trends Food Sci. Technol.* 45, 187–199. doi: 10.1016/j.tifs.2015.07.002
- Jafarzadeh, S., Salehabadi, A., and Jafari, S. M. (2020). “10 - Metal nanoparticles as antimicrobial agents in food packaging,” in *Handbook of Food Nanotechnology*, ed. S. M. Jafari (Cambridge, MA: Academic Press), 379–414. doi: 10.1016/b978-0-12-815866-1.00010-8
- Kadam, D., Momin, B., Palamthodi, S., and Lele, S. S. (2019). Physicochemical and functional properties of chitosan-based nano-composite films incorporated with biogenic silver nanoparticles. *Carbohydr. Polym.* 211, 124–132. doi: 10.1016/j.carbpol.2019.02.005
- Kalia, A., Kaur, M., Shami, A., Jawandha, S. K., Alghuthaymi, M. A., Thakur, A., et al. (2021). Nettle-Leaf Extract Derived ZnO/CuO nanoparticle-biopolymer-based antioxidant and antimicrobial nanocomposite packaging films and their impact on extending the post-harvest shelf life of guava fruit. *Biomolecules* 11:224. doi: 10.3390/biom11020224
- Kavakebi, E., Anvar, A., Ahari, H., and Motalebi, A. (2021). Green biosynthesized *Satureja rechingeri* Jamzad-Ag/poly vinyl alcohol film: quality improvement of *Oncorhynchus mykiss* fillet during refrigerated storage. *Food Sci. Technol.* 41, 267–278. doi: 10.1590/fst.62720
- Kim, S. W., and Cha, S. H. (2014). Thermal, mechanical, and gas barrier properties of ethylene-Vinyl alcohol copolymer-based nanocomposites for food packaging films: effects of nanoclay loading. *J. Appl. Polym. Sci.* 131:40289.
- Koenenan, B. A., Zhang, Y., Westerhoff, P., Chen, Y., Crittenden, J. C., and Capco, D. G. (2010). Toxicity and cellular responses of intestinal cells exposed to titanium dioxide. *Cell Biol. Toxicol.* 26, 225–238. doi: 10.1007/s10565-009-9132-z
- Lan, W., Wang, S., Zhang, Z., Liang, X., Liu, X., and Zhang, J. (2021). Development of red apple pomace extract/chitosan-based films reinforced by TiO₂ nanoparticles as a multifunctional packaging material. *Int. J. Biol. Macromol.* 168, 105–115. doi: 10.1016/j.ijbiomac.2020.12.051
- Li, X., Ren, Z., Wang, R., Liu, L., Zhang, J., Ma, F., et al. (2021). Characterization and antibacterial activity of edible films based on carboxymethyl cellulose, *Dioscorea opposita* mucilage, glycerol and ZnO nanoparticles. *Food Chem.* 349:129208. doi: 10.1016/j.foodchem.2021.129208
- Lima, E., Guerra, R., Lara, V., and Guzmán, A. (2013). Gold nanoparticles as efficient antimicrobial agents for *Escherichia coli* and *Salmonella typhi*. *Chem. Cent. J.* 7:11.
- Llorens, A., Lloret, E., Picouet, P., and Fernandez, A. (2012). Study of the antifungal potential of novel cellulose/copper composites as absorbent materials for fruit juices. *Int. J. Food Microbiol.* 158, 113–119. doi: 10.1016/j.ijfoodmicro.2012.07.004
- Longano, D., Ditaranto, N., Cioffi, N., Di Niso, F., Sibillano, T., Ancona, A., et al. (2012). Analytical characterization of laser-generated copper nanoparticles for antibacterial composite food packaging. *Anal. Bioanal. Chem.* 403, 1179–1186. doi: 10.1007/s00216-011-5689-5
- Lotfi, S., Ahari, H., and Sahraeyan, R. (2019). The effect of silver nanocomposite packaging based on melt mixing and sol-gel methods on shelf life extension of fresh chicken stored at 4 °C. *J. Food Saf.* 39:e12644.

- Love, S. A., Maurer-Jones, M. A., Thompson, J. W., Lin, Y. S., and Haynes, C. L. (2012). Assessing nanoparticle toxicity. *Annu. Rev. Anal. Chem.* 5, 181–205. doi: 10.1146/annurev-anchem-062011-143134
- Luo, P. G., and Stutzenberger, F. J. (2008). Nanotechnology in the detection and control of microorganisms. *Adv. Appl. Microbiol.* 63, 145–181. doi: 10.1016/s0065-2164(07)00004-4
- Mahdi, S. S., Vadood, R., and Nourdahr, R. (2012). Study on the antimicrobial effect of nanosilver tray packaging of minced beef at refrigerator temperature. *Glob. Vet.* 9, 284–289.
- Maisanaba, S., Pichardo, S., Puerto, M., Gutiérrez-Praena, D., Cameán, A. M., and Jos, A. (2015). Toxicological evaluation of clay minerals and derived nanocomposites: a review. *Environ. Res.* 138, 233–254. doi: 10.1016/j.envres.2014.12.024
- Mao, X., Nguyen, T. H., Lin, M., and Mustapha, A. (2016). Engineered nanoparticles as potential food contaminants and their toxicity to Caco-2 Cells. *J. Food Sci.* 81, T2107–T2113.
- Mathew, S., Jayakumar, A., Kumar, V. P., Mathew, J., and Radhakrishnan, E. K. (2019). One-step synthesis of eco-friendly boiled rice starch blended polyvinyl alcohol bionanocomposite films decorated with in situ generated silver nanoparticles for food packaging purpose. *Int. J. Biol. Macromol.* 139, 475–485. doi: 10.1016/j.ijbiomac.2019.07.187
- McCracken, C., Dutta, P. K., and Waldman, W. J. (2016). Critical assessment of toxicological effects of ingested nanoparticles. *Environ. Sci. Nano* 3, 256–282. doi: 10.1039/c5en00242g
- Mihindukulasuriya, S. D. F., and Lim, L. T. (2014). Nanotechnology development in food packaging: a review. *Trends Food Sci. Technol.* 40, 149–167. doi: 10.1016/j.tifs.2014.09.009
- Miranda, R. R., Bezerra, A. G. Jr., Oliveira Ribeiro, C. A., Randi, M. A. F., Voigt, C. L., Skytte, L., et al. (2017). Toxicological interactions of silver nanoparticles and non-essential metals in human hepatocarcinoma cell line. *Toxicol. In Vitro* 40, 134–143. doi: 10.1016/j.tiv.2017.01.003
- Mohamadi, E., Moghaddasi, M., Farahbakhsh, A., and Kazemi, A. (2017). A quantum-dot-based fluoroassay for detection of food-borne pathogens. *J. Photochem. Photobiol. B Biol.* 174, 291–297. doi: 10.1016/j.jphotobiol.2017.08.005
- Mustafa, F., and Andreescu, S. (2020). Nanotechnology-based approaches for food sensing and packaging applications. *RSC Adv.* 10, 19309–19336. doi: 10.1039/d0ra01084g
- Muthulakshmi, L., Varada Rajalu, A., Kaliaraj, G. S., Siengchin, S., Parameswaranpillai, J., and Saraswathi, R. (2019). Preparation of cellulose/copper nanoparticles bionanocomposite films using a bioflocculant polymer as reducing agent for antibacterial and anticorrosion applications. *Comp. Part B Eng.* 175:107177. doi: 10.1016/j.compositesb.2019.107177
- Nassiri, R., and MohammadiNafchi, A. (2013). Antimicrobial and barrier properties of bovine gelatin films reinforced by Nano TiO₂. *J. Chem. Health Risks* 3, 12–28.
- Ojha, N., and Das, N. (2020). Fabrication and characterization of biodegradable PHBV/SiO₂ nanocomposite for thermo-mechanical and antibacterial applications in food packaging. *IET Nanobiotechnol.* 14, 785–795. doi: 10.1049/iet-nbt.2020.0066
- Olaimat, A. N., Shahbaz, H. M., Fatima, N., Munir, S., and Holley, R. A. (2015). Food safety during and after the Era of COVID-19 pandemic. *Front. Microbiol.* 11:1854. doi: 10.3389/fmicb.2020.01854
- Orsuwan, A., Shankar, S., Wang, L.-F., Sothornvit, R., and Rhim, J.-W. (2016). Preparation of antimicrobial agar/banana powder blend films reinforced with silver nanoparticles. *Food Hydrocoll.* 60, 476–485. doi: 10.1016/j.foodhyd.2016.04.017
- Othman, S. H., Abd Salam, N. R., Zainal, N., Kadir Basha, R., and Talib, R. A. (2014). Antimicrobial activity of TiO₂ nanoparticle-coated film for potential food packaging applications. *Int. J. Photoenergy* 2014:945930.
- Pagno, C. H., Costa, T. M. H., de Menezes, E. W., Benvenuti, E. V., Hertz, P. F., Matte, C. R., et al. (2015). Development of active biofilms of quinoa (*Chenopodium quinoa* W.) starch containing gold nanoparticles and evaluation of antimicrobial activity. *Food Chem.* 173, 755–762. doi: 10.1016/j.foodchem.2014.10.068
- Petrosillo, N., Viceconte, G., Ergonul, O., Ippolito, G., and Petersen, E. (2020). COVID-19, SARS and MERS: are they closely related? *Clin. Microbiol. Infect.* 26, 729–734. doi: 10.1016/j.cmi.2020.03.026
- Rhim, J. W., and Ng, P. K. (2007). Natural biopolymer-based nanocomposite films for packaging applications. *Crit. Rev. Food Sci. Nutr.* 47, 411–433. doi: 10.1080/10408390600846366
- Rukmanikrishnan, B., Jo, C., Choi, S., Ramalingam, S., and Lee, J. (2020). Flexible ternary combination of gellan gum, sodium carboxymethyl cellulose, and silicon dioxide nanocomposites fabricated by quaternary ammonium silane: rheological, thermal, and antimicrobial properties. *ACS Omega* 5, 28767–28775. doi: 10.1021/acsomega.0c04087
- Ruparelia, J. P., Chatterjee, A. K., Duttagupta, S. P., and Mukherji, S. (2008). Strain specificity in antimicrobial activity of silver and copper nanoparticles. *Acta Biomater.* 4, 707–716. doi: 10.1016/j.actbio.2007.11.006
- Safavieh, M., Nahar, S., Zourob, M., and Ahmed, M. U. (2015). “15 - Microfluidic biosensors for high throughput screening of pathogens in food,” in *High Throughput Screening for Food Safety Assessment*, eds A. K. Bhunia, M. S. Kim and C. R. Taitt (Cambridge: Woodhead Publishing), 327–357. doi: 10.1016/b978-0-85709-801-6.00015-0
- Schübbe, S., Schumann, C., Cavelius, C., Koch, M., Müller, T., and Kraegeloh, A. (2012). Size-dependent localization and quantitative evaluation of the intracellular migration of silica nanoparticles in Caco-2 Cells. *Chem. Mater.* 24, 914–923. doi: 10.1021/cm2018532
- Shahbazzadeh, D., Ahari, H., Rahimi, N., Dastmalchi, F., Soltani, M., Rahmanny, J., et al. (2009). The effects of Nanosilver (Nanocid®) on survival percentage of rainbow trout (*Oncorhynchus mykiss*). *Pak. J. Nutr.* 8, 1178–1179. doi: 10.3923/pjn.2009.1178.1179
- Shankar, S., and Rhim, J.-W. (2014). Effect of copper salts and reducing agents on characteristics and antimicrobial activity of copper nanoparticles. *Mater. Lett.* 132, 307–311. doi: 10.1016/j.matlet.2014.06.014
- Shankar, S., and Rhim, J.-W. (2015). Amino acid mediated synthesis of silver nanoparticles and preparation of antimicrobial agar/silver nanoparticles composite films. *Carbohydr. Polym.* 130, 353–363. doi: 10.1016/j.carbpol.2015.05.018
- Shankar, S., and Rhim, J.-W. (2017). Preparation and characterization of agar/lignin/silver nanoparticles composite films with ultraviolet light barrier and antibacterial properties. *Food Hydrocoll.* 71, 76–84. doi: 10.1016/j.foodhyd.2017.05.002
- Sharma, V., Shukla, R. K., Saxena, N., Parmar, D., Das, M., and Dhawan, A. (2009). DNA damaging potential of zinc oxide nanoparticles in human epidermal cells. *Toxicol. Lett.* 185, 211–218. doi: 10.1016/j.toxlet.2009.01.008
- Shi, H., Magaye, R., Castranova, V., and Zhao, J. (2013). Titanium dioxide nanoparticles: a review of current toxicological data. *Part Fibre Toxicol.* 10:15. doi: 10.1186/1743-8977-10-15
- Singh, T., Shukla, S., Kumar, P., Wahla, V., Bajpai, V. K., and Rather, I. A. (2017). Application of nanotechnology in food science: perception and overview. *Front. Microbiol.* 8:1501. doi: 10.3389/fmicb.2017.01501
- Sonseca, A., Madani, S., Rodríguez, G., Hevilla, V., Echeverría, C., and Fernández-García, M. (2019). Multifunctional PLA blends containing Chitosan mediated silver nanoparticles: thermal, mechanical, antibacterial, and degradation properties. *Nanomaterials* 10:22. doi: 10.3390/nano10010022
- Sportelli, M. C., and Izzi, M. (2020). Can Nanotechnology and Materials Science Help the Fight against SARS-CoV-2? *Nanomaterials* 10:802. doi: 10.3390/nano10040802
- Sujithra, S., and Manikkandan, T. R. (2019). Application of nanotechnology in packaging of foods: a review. *Int. J. ChemTech Res.* 12, 07–14. doi: 10.20902/ijctr.2019.120402
- Tang, D., Comish, P., and Kang, R. (2020). The hallmarks of COVID-19 disease. *PLoS Pathog.* 16:e1008536. doi: 10.1371/journal.ppat.1008536
- Tang, S., Wang, Z., Li, P., Li, W., Li, C., Wang, Y., et al. (2018). Degradable and photocatalytic antibacterial Au-TiO₂/sodium alginate nanocomposite films for active food packaging. *Nanomaterials* 8:930. doi: 10.3390/nano8110930
- Tarantini, A., Lancelot, R., Mourou, A., Lavault, M. T., Casterou, G., Jarry, G., et al. (2015). Toxicity, genotoxicity and proinflammatory effects of amorphous nanosilica in the human intestinal Caco-2 cell line. *Toxicol. In Vitro* 29, 398–407. doi: 10.1016/j.tiv.2014.10.023
- Tavakoli, H., Rastegar, H., Taherian, M., Samadi, M., and Rostami, H. (2017). The effect of nano-silver packaging in increasing the shelf life of nuts: an *in vitro* model. *Italian J. Food Saf.* 6:6874.

- Thirumurugan, A., Ramachandran, S., and Gowri, A. (2013). Combined effect of bacteriocin with gold nanoparticles against food spoiling bacteria - an approach for food packaging material preparation. *Int. Food Res. J.* 20, 1909–1912.
- Tripathi, S., Mehrotra, G. K., and Dutta, P. K. (2011). Chitosan–silver oxide nanocomposite film: preparation and antimicrobial activity. *Bull. Mater. Sci.* 34, 29–35. doi: 10.1007/s12034-011-0032-5
- U.S. Food and Drug Administration [FDA] (2020). *Food Safety and the Coronavirus Disease 2019 (COVID-19)*. White Oak Campus: FDA.
- Valizadeh, A., Mikaeili, H., Samiei, M., Farkhani, S. M., Zarghami, N., Kouhi, M., et al. (2012). Quantum dots: synthesis, bioapplications, and toxicity. *Nanoscale Res. Lett.* 7:480. doi: 10.1186/1556-276x-7-480
- van Doremalen, N., Bushmaker, T., and Morris, D. H. (2020). Aerosol and Surface Stability of SARS-CoV-2 as Compared with SARS-CoV-1. *N. Engl. J. Med.* 382, 1564–1567.
- Vanderroost, M., Ragaert, P., Devlieghere, F., and De Meulenaer, B. (2014). Intelligent food packaging: the next generation. *Trends Food Sci. Technol.* 39, 47–62. doi: 10.1016/j.tifs.2014.06.009
- Vechia, I. C. D., Steiner, B. T., Freitas, M. L., dos Santos Pedroso Fidelis, G., Galvani, N. C., Ronchi, J. M., et al. (2020). Comparative cytotoxic effect of citrate-capped gold nanoparticles with different sizes on noncancerous and cancerous cell lines. *J. Nanopart. Res.* 22:133.
- Vishnuvarthan, M., and Rajeswari, N. (2019). Preparation and characterization of carrageenan/silver nanoparticles/Laponite nanocomposite coating on oxygen plasma surface modified polypropylene for food packaging. *J. Food Sci. Technol.* 56, 2545–2552. doi: 10.1007/s13197-019-03735-4
- Vuković, B., Milić, M., Dobrošević, B., Milić, M., Ilić, K., Pavičić, I., et al. (2020). Surface stabilization affects toxicity of silver nanoparticles in human peripheral blood mononuclear cells. *Nanomaterials* 10:1390. doi: 10.3390/nano10071390
- Wang, D., Lian, F., Yao, S., Liu, Y., Wang, J., Song, X., et al. (2020). Simultaneous detection of three foodborne pathogens based on immunomagnetic nanoparticles and fluorescent quantum dots. *ACS Omega* 5, 23070–23080. doi: 10.1021/acsomega.0c02833
- Wang, H., Li, Y., Wang, A., and Slavik, M. (2011). Rapid, sensitive, and simultaneous detection of three foodborne pathogens using magnetic nanobead-based immunoseparation and quantum dot-based multiplex immunoassay. *J. Food Prot.* 74, 2039–2047. doi: 10.4315/0362-028x.jfp-11-144
- WHO (2015). *World Health Organization. Estimates of the Global Burden of Foodborne Diseases*. Available online at: <https://www.who.int/activities/estimating-the-burden-of-foodborne-diseases> (accessed March 13, 2020).
- Wu, C., Luo, Y., and Liu, L. (2019). Toxicity of combined exposure of ZnO nanoparticles (NPs) and myricetin to Caco-2 cells: changes of NP colloidal aspects, NP internalization and the apoptosis-endoplasmic reticulum stress pathway. *Toxicol. Res.* 8, 613–620. doi: 10.1039/c9tx00127a
- Yadav, S., Mehrotra, G. K., and Dutta, P. K. (2021). Chitosan based ZnO nanoparticles loaded gallic-acid films for active food packaging. *Food Chem.* 334:127605. doi: 10.1016/j.foodchem.2020.127605
- Yang, Y. X., Song, Z. M., Cheng, B., Xiang, K., Chen, X. X., Liu, J. H., et al. (2014). Evaluation of the toxicity of food additive silica nanoparticles on gastrointestinal cells. *J. Appl. Toxicol.* 34, 424–435. doi: 10.1002/jat.2962
- Yin, I. X., Zhang, J., Zhao, I. S., Mei, M. L., Li, Q., and Chu, C. H. (2020). The antibacterial mechanism of silver nanoparticles and its application in dentistry. *Int. J. Nanomed.* 15, 2555–2562. doi: 10.2147/ijn.s246764
- Yousefi, H., Su, H.-M., Imani, S. M., Alkhaldi, K. M., Filipe, C. D., and Didar, T. F. (2019). Intelligent food packaging: a review of smart sensing technologies for monitoring food quality. *ACS Sens.* 4, 808–821. doi: 10.1021/acssensors.9b00440
- Yu, Z., Wang, W., Kong, F., Lin, M., and Mustapha, A. (2019). Cellulose nanofibril/silver nanoparticle composite as an active food packaging system and its toxicity to human colon cells. *Int. J. Biol. Macromol.* 129, 887–894. doi: 10.1016/j.ijbiomac.2019.02.084
- Zawrah, M., and Abd El-Moez, S. (2011). Antimicrobial activities of gold nanoparticles against major foodborne pathogens. *Life Sci.* 8, 37–44.
- Zhao, Y., Wei, B., Wu, M., Zhang, H., Yao, J., Chen, X., et al. (2020). Preparation and characterization of antibacterial poly(lactic acid) nanocomposites with N-halamine modified silica. *Int. J. Biol. Macromol.* 155, 1468–1477. doi: 10.1016/j.ijbiomac.2019.11.125
- Zhu, Y., Li, D., Belwal, T., and Li, L. (2019). Effect of Nano-SiOx/Chitosan complex coating on the physicochemical characteristics and preservation performance of green tomato. *Molecules* 24:4552. doi: 10.3390/molecules24244552

Conflict of Interest: The authors declare that the research was conducted in the absence of any commercial or financial relationships that could be construed as a potential conflict of interest.

Copyright © 2021 Anvar, Ahari and Ataee. This is an open-access article distributed under the terms of the Creative Commons Attribution License (CC BY). The use, distribution or reproduction in other forums is permitted, provided the original author(s) and the copyright owner(s) are credited and that the original publication in this journal is cited, in accordance with accepted academic practice. No use, distribution or reproduction is permitted which does not comply with these terms.



***Bacillus cereus* in Packaging Material: Molecular and Phenotypical Diversity Revealed**

Paul Jakob Schmid, Stephanie Maitz and Clemens Kittinger*

Diagnostic and Research Institute of Hygiene, Microbiology and Environmental Medicine, Medical University of Graz, Graz, Austria

OPEN ACCESS

Edited by:

Anindya Chanda,
Mycologics LLC, United States

Reviewed by:

Ketan D. Patel,
University at Buffalo, United States
Catherine Mullié,
University of Picardie Jules Verne,
France

*Correspondence:

Clemens Kittinger
clemens.kittinger@medunigraz.at

Specialty section:

This article was submitted to
Food Microbiology,
a section of the journal
Frontiers in Microbiology

Received: 22 April 2021

Accepted: 21 June 2021

Published: 12 July 2021

Citation:

Schmid PJ, Maitz S and
Kittinger C (2021) *Bacillus cereus*
in Packaging Material: Molecular
and Phenotypical Diversity Revealed.
Front. Microbiol. 12:698974.
doi: 10.3389/fmicb.2021.698974

The *Bacillus cereus* group has been isolated from soils, water, plants and numerous food products. These species can produce a variety of toxins including several enterotoxins [non-hemolytic enterotoxin (Nhe), hemolysin BL (Hbl), cytotoxin K, and enterotoxin FM], the emetic toxin cereulide and insecticidal Bt toxins. This is the first study evaluating the presence of *B. cereus* in packaging material. Among 75 different isolates, four phylogenetic groups were detected (II, III, IV, and VI), of which the groups III and IV were the most abundant with 46.7 and 41.3%, respectively. One isolate was affiliated to psychrotolerant group VI. Growth experiments showed a mesophilic predominance. Based on PCR analysis, *nhe* genes were detectable in 100% of the isolates, while *hbl* genes were only found in 50.7%. The cereulide encoding gene was found in four out of 75 isolates, no isolate carried a crystal toxin gene. In total, thirteen different toxin gene profiles were identified. We showed that a variety of *B. cereus* group strains can be found in packaging material. Here, this variety lies in the presence of four phylogenetic groups, thirteen toxin gene profiles, and different growth temperatures. The results suggest that packaging material does not contain significant amounts of highly virulent strains, and the low number of cereulide producing strains is in accordance with other results.

Keywords: *Bacillus cereus*, phylogenetic affiliation, bacterial growth, toxins, packaging material

INTRODUCTION

The *Bacillus cereus* group, also called *Bacillus cereus sensu lato* (*B. cereus* s.l.) comprises at least eight different gram-positive, aerobic and endospore-forming species, including *B. cereus sensu stricto* (s.s.), *B. thuringiensis*, *B. anthracis*, *B. weihenstephanensis*, and *B. cytotoxicus* (Liu et al., 2015). They are ubiquitous and have been frequently reported in soil, sediments, water, and plants in a variety of natural environments (Von Stetten et al., 1999; Stenfors Arnesen et al., 2008; Brillard et al., 2015) as well as from fresh vegetables, rice, spices, raw meat and meat products, fish and seafood, dairy products and ready-to-eat foods (Konuma et al., 1988; Granum et al., 1993; Rahmati and Labbe, 2008; Samapundo et al., 2011; Carter et al., 2018; Fiedler et al., 2019; Yu et al., 2020). It has long been known, that packaging material may provide a reservoir for microorganisms (Välsänen et al., 1991) and regarding its widespread distribution, the occurrence of *B. cereus* group species in packaging material is more than obvious and has already been published (Suihko et al., 2004; Ekman et al., 2009). *B. cereus* is a causative agent for food spoilage and food poisoning. In particular, two types of gastrointestinal syndromes are associated to *B. cereus*, the diarrheal type caused by enterotoxins and the emetic type caused by the plasmid encoded toxin cereulide (Stenfors Arnesen et al., 2008).

There are numerous enterotoxins produced by species in the *B. cereus* group, of which hemolysin BL (Hbl), the non-hemolytic enterotoxin (Nhe), cytotoxin K (CytK) and enterotoxin FM (EntFM) are among the most investigated. Hbl is a three-component pore-forming complex encoded in the operon *hblDAC* leading to cytotoxic effects, necrosis and watery diarrhea (Beecher et al., 1995). Nhe is another three-component pore-forming toxin encoded in the operon *nheABC* and showed cytotoxic effects on different human cell lines (Jeßberger et al., 2014). For both, Hbl and Nhe, all three components are necessary for full toxin activity (Beecher et al., 1995; Lindbäck et al., 2010). CytK is a beta-barrel pore-forming toxin encoded by the gene *cytK* and resembles the beta-toxin of *Clostridium perfringens* (Lund et al., 2000). EntFM was identified in *B. cereus* s.s. and *B. thuringiensis* and is a putative cell wall peptidase important for virulence (Asano et al., 1997; Tran et al., 2010). The emetic toxin cereulide (*ces* gene cluster) is a small heat- and acid-stable dodecadeptide, which is synthesized by a non-ribosomal peptide synthetase (Ehling-Schulz et al., 2019). Research showed that enterotoxins are not limited to *B. cereus* s.s. but have been found in strains of *B. thuringiensis* (Ngamwongsatit et al., 2008), *B. weihenstephanensis* (Baron et al., 2007), *B. mycoides*, and *B. pseudomycoides* (Prüß et al., 1999). This is of relevance as former apathogenic species such as *B. thuringiensis* are also used as biopesticides through its plasmid encoded insecticidal crystal (Cry) or Bt toxin (Schnepf et al., 1998). This study aims to provide a comprehensive overview of *B. cereus* in packaging materials. For this purpose, 188 different samples were analyzed for the presence of *B. cereus*. In total, 75 isolates were selected for further characterization. All isolates were clustered into seven phylogenetic groups (I–VII) by partial *panC* sequencing according to Guinebretière et al. (2010) followed by maximum likelihood analysis. Furthermore, growth and hemolysis phenotypes were determined. The presence of enterotoxin genes was assessed by multiplex-PCR targeting *hblDAC*, *nheABC*, *cytK*, and *entFM*, and all isolates were tested for harboring the *ces* and *cryI*-type toxin genes. To our knowledge, this is the first study evaluating the presence of *B. cereus* in different samples of packaging material in terms of phylogeny, growth temperatures and toxin genes. Additionally, we aim to compare the results with previous data of environmental and food isolates to provide a better understanding of *B. cereus* occurring in the packaging industry.

MATERIALS AND METHODS

Samples

In this study, 188 samples of fiber-based packaging material were included. To provide a diverse view on packaging materials, the samples were manufactured in six different European packaging material facilities. All samples came from the food packaging sector reflecting primary and secondary food packaging with different applications (Table 1). The samples were taken under sterile conditions by instructed workers and wrapped in sterile aluminum foil to avoid contamination. Afterwards the samples were sent to the laboratory in sealed plastic bags.

TABLE 1 | Packaging material samples and corresponding applications.

Packaging material manufacturer	Number of samples	Food packaging applications
1	63	Dry, moist, fatty
2	5	Dry, moist, fatty
3	4	Dry, moist, fatty and non-fatty
4	5	Dry, reduced fat contact
5	15	Dry, fatty
6	96	Secondary food packaging
<i>n</i> = 188		

The samples were provided by six packaging material facilities. The packaging applications are according to the manufacturer's specifications.

Determination and Isolation of *B. cereus*

One gram of each sample was weighed and evenly homogenized with 99 ml of sterile buffered peptone water (Thermo Fisher Scientific, Waltham, United States) in sterile bags using a Bagmixer (Interscience, St. Nom la Bretèche, France). Afterwards, 0.5 ml of the sample suspension were transferred on Brilliance Bacillus cereus agar (Thermo Fisher Scientific) followed by incubation at 37°C for 48 h. Homogenized samples in buffered peptone water were additionally enriched at 37°C for 24°C and streaked again on Brilliance Bacillus cereus agar to detect low numbers of *B. cereus*. All samples were tested in duplicates. A total of 75 *B. cereus* group isolates with varying colony morphologies were isolated from 41 different samples and selected for further characterization. Those 41 samples were randomly selected representing four of the six sampling sites with the highest abundance of *B. cereus* (Table 2). On the selective agar, each colony with a differing morphology was picked. Clonal isolates were excluded after *panC* sequencing and toxin gene detection. The *B. cereus* group was confirmed by MALDI-TOF (VITEK® MS, bioMérieux Marcy-l'Étoile, France). Isolates were stored at –80°C for further experiments using the Microbank system (Pro-Lab Diagnostics, Richmond Hill, Canada).

Characterization of Growth and Hemolysis

All isolates were tested for growth at different temperatures (20, 37, 45, and 55°C) using the Bioscreen C growth monitoring system (Oy Growth Curves Ab Ltd., Helsinki, Finland). Isolates were grown on COL-S blood agar (Thermo Fisher Scientific) and colonies were suspended in sterile TSB (Thermo Fisher Scientific) to make a bacterial suspension equal to 0.5 McFarland standard. Afterwards, 2 µl of the suspension were incubated in 200 µl TSB for 72 h at the set temperature including continuous shaking. Measurement of the optical density at 600 nm (OD₆₀₀) was done automatically every 15 min. All isolates were tested in technical duplicates. Due to a limited range for low temperatures, growth at 5 to 7°C was tested by streaking isolates on COL-S agar plates and subsequent incubation in the refrigerator for 7 days. To assess hemolysis, isolates were streaked on COL-S and examined for beta-hemolysis after incubation at 30°C for 24 h.

TABLE 2 | *Bacillus cereus* in packaging materials from six different manufacturers.

Packaging material manufacturer	Samples with <i>B. cereus</i> detectable in the direct assessment	Samples with <i>B. cereus</i> detectable after enrichment	Number of <i>B. cereus</i> isolates for characterization
1	1/63 (1.6%)	36/63 (57.1%)	15
2	1/5 (20.0%)	4/5 (80.0%)	3
3	0/4	1/4 (25.0%)	–
4	0/5	4/5 (80.0%)	–
5	0/15	10/15 (66.7%)	5
6	94/96 (97.9%)	96/96 (100.0%)	55
	96/188 (51.1%)	152/188 (80.9%)	<i>n</i> = 75

Bacillus cereus was detected in a direct assessment and after enrichment on selective medium. A total of 75 isolates were collected from samples from four different origins for further characterization.

DNA Extraction

Isolates were grown in TSB at 30°C overnight and DNA was extracted using the innuPREP Bacteria DNA Kit (Analytik Jena, Jena, Germany). Successful extraction was verified by measuring the amount of extracted DNA using the Nanodrop2000 (Thermo Fisher Scientific). The DNA was stored in elution buffer at –20°C until needed.

Partial *panC* Sequencing

Partial *panC* gene was amplified using following primer sequences for groups I to VI according to Guinebretière et al. (2010): 5'-TYGGTTTTGTGCCAACRATGG-3' (forward degenerated primer) and 5'-CATAATCTACAGTGCCTTTTCG-3' (reverse primer). PCR was carried out in a Biometra Trio 48 thermocycler (Analytik Jena, Germany) in a final volume of 25 µl containing 1X NEB Q5 Reaction Buffer (New England Biolabs, Ltd, Ipswich, United States), 200 µM of each dNTP, 0.5 µM of each primer, 0.5 IU of NEB Q5 High Fidelity DNA Polymerase (New England Biolabs) and 1 µl DNA template. The temperature protocol included an initial denaturation at 98°C for 30 s followed by 30 cycles of 98°C for 10 s, 61°C for 30 s, 72°C for 30 s and a final extension at 72°C for 2 min. The INVISORB Spin DNA Extraction Kit (Invitex, Berlin, Germany) was used for DNA purification and products were sent to Eurofins Genomics Germany GmbH (Ebersberg, Germany) for sequencing using primer 5'-ATAATCTACAGTGCCTTTTCG-3' (Guinebretière et al., 2010). Sequence data analysis was done by uploading to an online algorithm¹ for assignment to groups I to VII (Guinebretière et al., 2010).

PCR Assays for Toxin Genes

Enterotoxin genes of the *B. cereus* group were tested using a multiplex PCR assay with specific primers for *hblD*, *hblA*, *hblC*, *nheA*, *nheB*, *nheC*, *cytK*, and *entFM* (Thaenthanee et al., 2005; Ngamwongsatit et al., 2008). The multiplex PCR was performed in a final volume of 25 µl containing 1X NEB Q5 Reaction Buffer (New England Biolabs), 400 µM of each dNTP, 0.2 µM (*nheABC*, *cytK*, and *entFM*), 0.4 µM (*hblDA*), and 4 µM (*hblC*) of primers, 0.5 IU of NEB Q5 High Fidelity DNA Polymerase (New England Biolabs Ltd, Ipswich, United States) and 1 µl DNA template.

¹<https://www.tools.symprevious.org/Bcereus/>

DNA templates were tested twice, undiluted and in 1:10 dilution to minimize amplification inhibition. The temperature protocol included an initial denaturation at 98°C for 2 min followed by 40 cycles of 98°C for 30 s, 58°C for 1.5 min, 72°C for 2 min and a final extension at 72°C for 5 min. *B. cereus* ATCC 14579 was used as positive control. *Ces*-gene PCR was carried out according to CSA Group Corporation (2018). PCR was performed in a final volume of 25 µl containing 1X NEB Q5 Reaction Buffer (New England Biolabs), 200 µM of each dNTP, 0.5 µM of each primer, 0.5 IU of NEB Q5 High Fidelity DNA Polymerase (New England Biolabs) and 1 µl DNA template. *B. cereus* DSM 4312 served as positive control for *ces*-PCR. The detection of *cryI*-type genes used primer sequences and PCR protocol previously described by Choo et al. (2007). *B. thuringiensis* ATCC 10792 served as positive control for *cryI*-type gene detection. Each PCR was carried out in a Biometra Trio 48 thermocycler (Analytik Jena). Amplicons were separated on 1.6% agarose gels using a 100 bp DNA molecular size standard (New England Biolabs) for enterotoxin multiplex PCR and *ces*-PCR and a 1 kb DNA molecular size standard for *cryI*-type PCR to estimate the size of the PCR products. Agarose gels were photographed using the AlphaImagerTM Imaging System (Biozym, Germany) and brightness and contrast were adjusted as necessary. All target genes for PCR were sent once to Eurofins Genomics Germany GmbH (Ebersberg, Germany) for sequencing to verify amplification specificity.

Data Analysis

All statistical data analyses were done in GraphPad Prism version 7.0.0 for Windows (GraphPad Software, San Diego, United States). Normality testing of the data was performed using the D'Agostino and Pearson omnibus normality test and the Shapiro–Wilk normality test, followed by the Wilcoxon matched-pairs signed rank test, a non-parametric test for differences in paired observations and the Kruskal–Wallis test, a non-parametric test for two or more independent medians. For the phylogenetic tree, sequences were first aligned using M-Coffee on the T-coffee server (Moretti et al., 2007) and followed by bootstrapping (100 bootstrap samples), maximum-likelihood analysis and consensus tree creation with the PHYLIP package (Felsenstein, 2005). SplitsTree was used for tree visualization (Huson and Bryant, 2006).

TABLE 3 | Phylogenetic affiliation of the isolates.

Phylogenetic group	No. of isolates (%)	Corresponding species ^a	Growth characteristics ^a
II	8 (10.7%)	<i>B. cereus</i> (8) <i>B. thuringiensis</i> (0)	Mesophilic/psychrotolerant 7–40°C
III	35 (46.7%)	<i>B. cereus</i> (35) <i>B. thuringiensis</i> (0) <i>B. anthracis</i> (0)	Mesophilic 15–45°C
IV	31 (41.3%)	<i>B. cereus</i> (31) <i>B. thuringiensis</i> (0)	Mesophilic 10–45°C
VI	1 (1.3%)	<i>B. weihenstephanensis</i> (1) <i>B. mycoides</i> (0) <i>B. thuringiensis</i> (0)	Psychrotolerant 5–37°C

^a species and growth characteristics according to Guinebretière et al. (2010). Further species classification within the phylogenetic groups was aimed using toxin gene PCR results (*cry-1* type toxin gene PCR for *B. thuringiensis*) and colony morphology (rhizoid growth for *B. mycoides*).

RESULTS

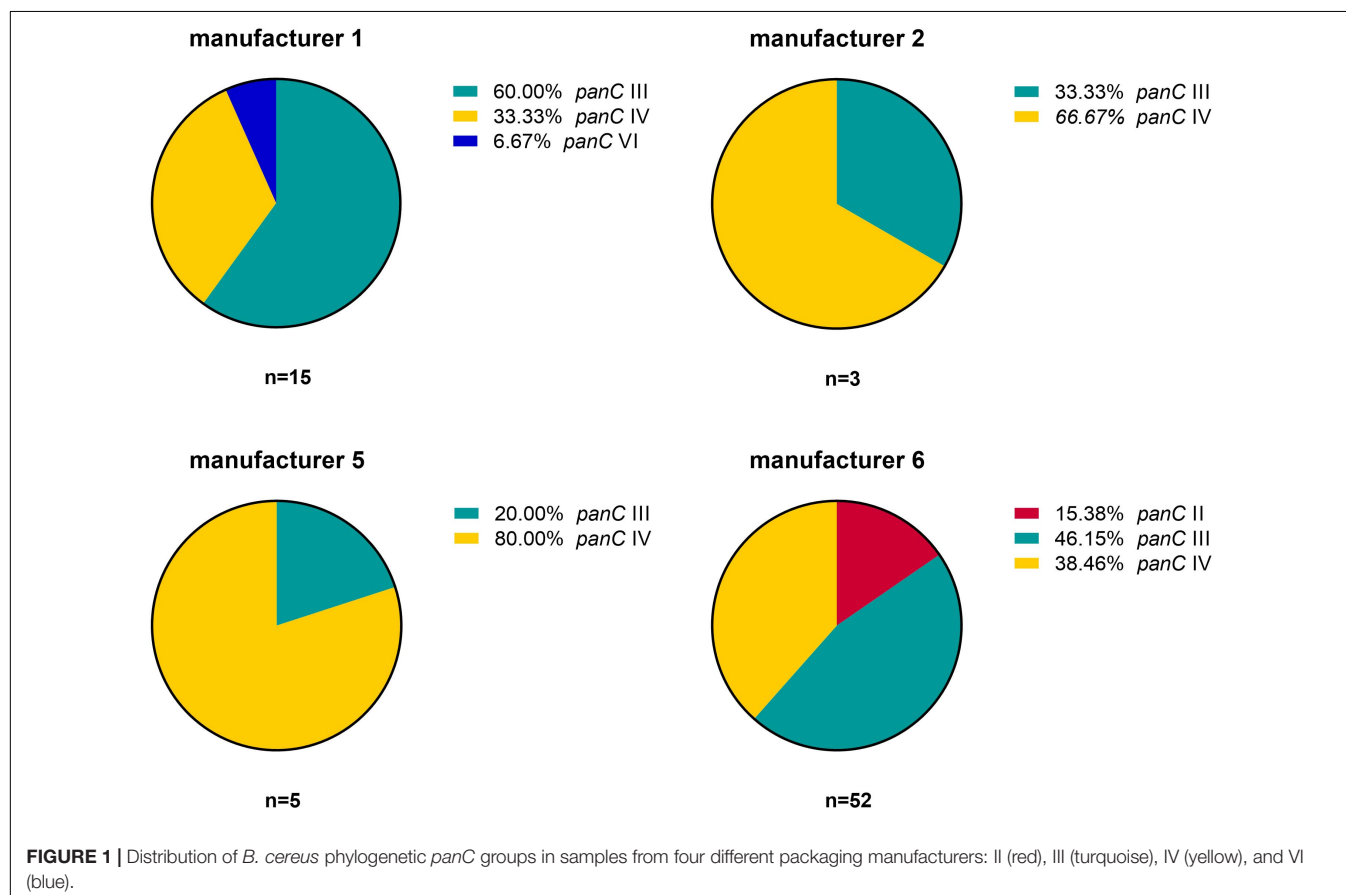
Determination of *B. cereus* in Packaging Material

Bacillus cereus was detected in 152 out of 188 packaging material samples (80.9%). In the direct assessment by plating 0.5 ml homogenized sample, however, *B. cereus* was detectable in only 96

samples (51.1%). In another 56 samples, we could detect *B. cereus* only after 24 h enrichment in buffered peptone water. The overall number of positive samples per manufacturer revealed an uneven distribution of *B. cereus* in packaging material samples (Table 2). We detected *B. cereus* in over 90% of the samples from manufacturer 6 in the direct assessment, but only at minimal rates in the samples from the manufacturers 1 to 5. The MALDI-TOF analysis confirmed all isolates selected for further characterization as members of the *B. cereus* group.

Affiliation to Phylogenetic *panC* Groups

Based on the sequence analysis of the partial *panC* gene, we were able to affiliate all 75 isolates to four phylogenetic *panC* groups (II, III, IV, and VI) as defined by Guinebretière et al. (2008). Among those, mesophilic *panC* groups III and IV were the most prevalent with 35 (46.7%) and 31 isolates (41.3%), respectively (Table 3), followed by eight isolates (10.7%) affiliated to *panC* group II. A single isolate (BC22) was found to be in phylogenetic group VI, which includes mainly psychrotolerant species of the *B. cereus* group. The distribution of the phylogenetic groups in samples from different manufacturers unveiled that the *panC* groups 3 and 4 formed the majority in the samples from all manufacturers (Figure 1). The *panC* group II was only found in samples from manufacturer 6, whereas the *panC* group VI was only detected in a single sample from manufacturer 1. Additionally, a phylogenetic tree based on bootstrap analysis

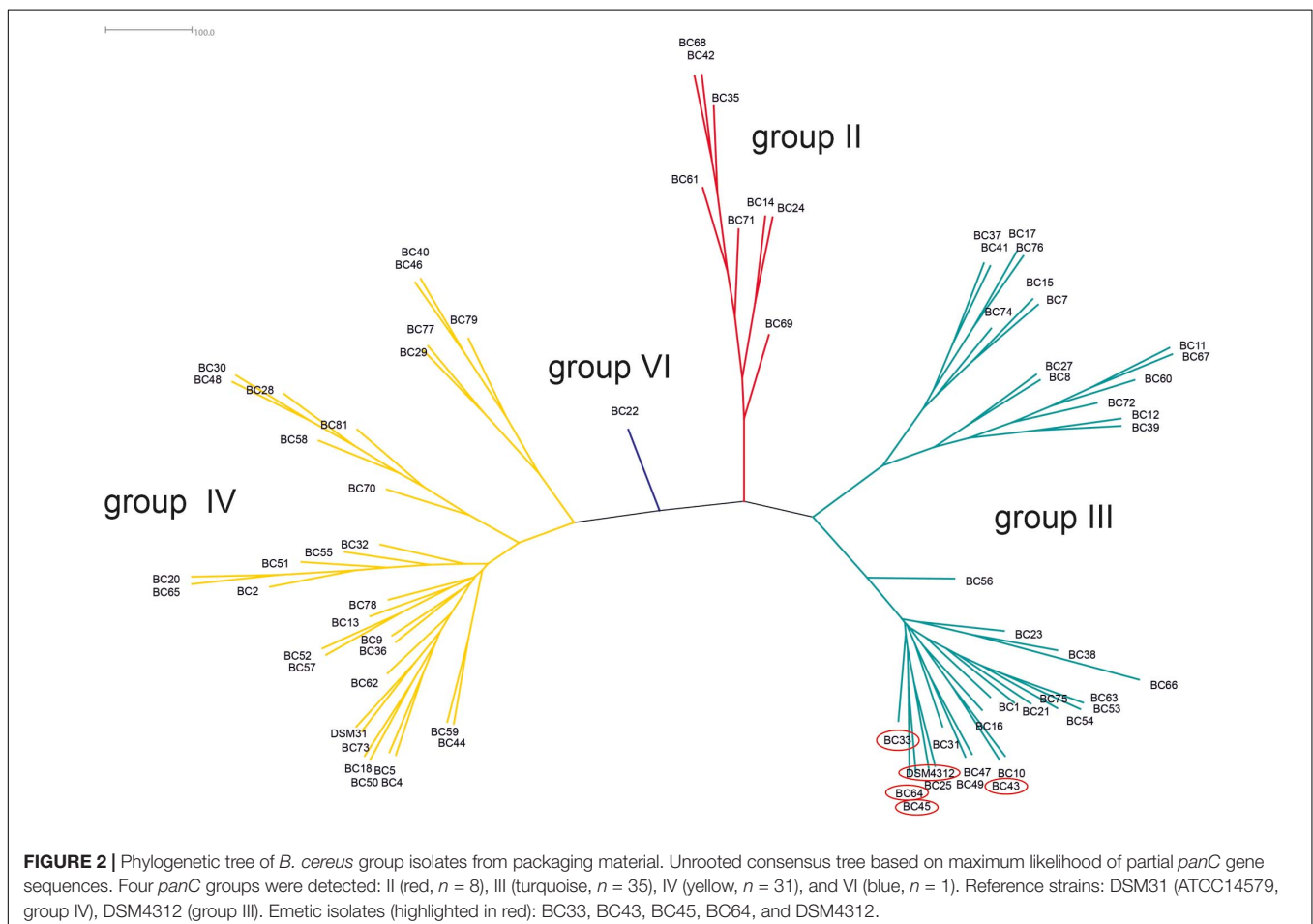


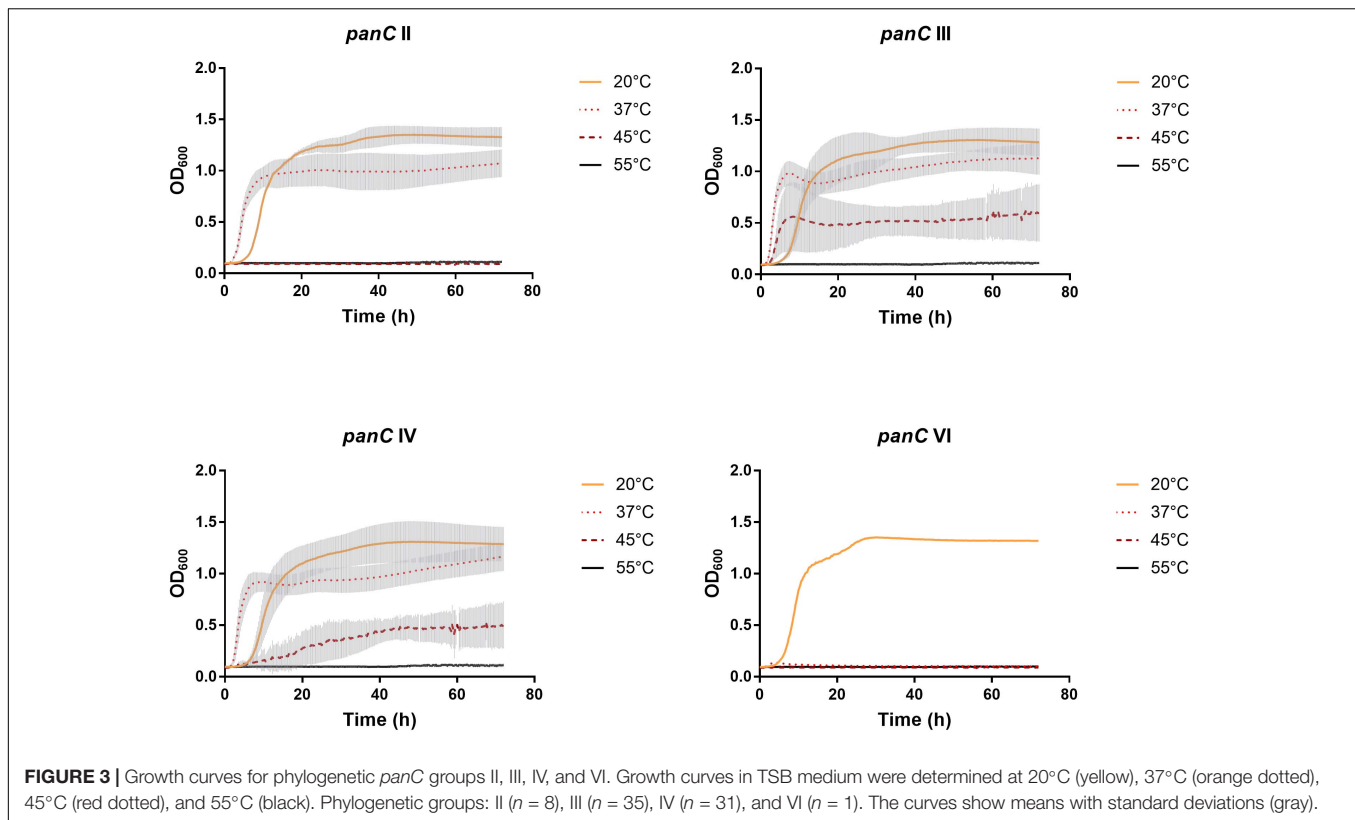
and maximum-likelihood shows concordant genetic clusters for each phylogenetic *panC* group determined (**Figure 2**). Here, *B. cereus* reference strains ATCC 14579 and DSM 4312 were included for group IV and III, respectively. Isolates possessing the emetic toxin cereulide were exclusively affiliated to group III and are phylogenetically close to reference strain DSM 4312. The phylogenetic tree revealed uniformly distributed isolates within group II, whereas group III and IV appear to be split into subgroups.

Growth and Hemolysis

After 72 h in the Bioscreen C, growth was detectable for all 75 isolates at 20°C (**Figure 3**) while isolates of mesophilic *panC* groups II, III and IV did grow at both temperatures, 20 and 37°C, the isolate affiliated to psychrotolerant *panC* group VI grew only at 20 but not at 37°C. At a temperature of 45°C, the number of growing isolates was reduced to 43 (58.7%) out of 75 and 34 of them (79.1%) were affiliated to group III. There was only one isolate of phylogenetic group III, which did not grow at 45°C. On the other side, only 9 out of 31 isolates (29.0%) belonging to *panC* group IV were able to grow at 45°C but only at a reduced rate (**Figure 3**). The isolates affiliated to groups II or VI were not able to grow at 45°C. In addition, no isolate could grow at 55°C. Screening for very low growth

temperatures was done using agar plates in the refrigerator (5 to 7°C) for 7 days. There was no isolate showing any visible growth on agar plates thus precluding growth of *B. cereus* from packaging materials in properly stored goods in the refrigerator. When comparing the growth curves at 37 and 45°C, especially isolates affiliated to group III showed curve shapes with a distinct decrease in biomass after initial exponential phase. We aimed to compare growth at 20°C with 37°C for isolates affiliated to mesophilic groups II, III, and IV and we revealed an overall increased growth rate at 37°C with an OD₆₀₀ slope of 0.0695 per 15 min compared to 0.0401 at 20°C. This implies a growth 1.7 times faster at 37°C within the exponential phase. The increased growth rate at 37°C could also be shown separately for these phylogenetic groups (**Figure 4**), with the difference between the slopes at 20 and 37°C being significantly more pronounced for groups III and IV than for group II. For the calculation, we selected those parts of the growth curves that had OD₆₀₀ values between 0.4 and 0.65 as representative of the exponential growth phase. Despite an increased growth rate at 37°C, incubation at 20°C resulted in overall higher amounts of biomass in group II, III, and IV compared to 37°C with a median difference of OD₆₀₀ = + 0.193 (74 isolates, Wilcoxon matched-pairs signed rank test, $p < 0.0001$). This could also be shown separately for averaged data of *panC* groups II, III, and IV, with median





differences in OD_{600} of +0.2727, +0.1945, and +0.2112 (each $p < 0.0001$), respectively. However, differences between the three phylogenetic groups are not significant (Kruskal–Wallis test, $p = 0.0643$). Furthermore, growth at 45°C was not only limited to 58.7% of the isolates, but also resulted in further decreasing amount of biomass compared to growth at 20 and 37°C (Kruskal–Wallis test, $p < 0.0001$; **Figure 5**). When grown on blood agar, there were 71 out of 75 isolates (94.7%) showing beta-hemolysis in different forms ranging from slight hemolytic activity to wide hemolytic halos of several millimeters, a tendency to certain phylogenetic groups was not observed, however. Four isolates (BC2, BC20, BC55, and BC65) did not cause beta-hemolysis and are located in close proximity to each other in the same phylogenetic sub-branch within *panC* group IV.

Toxin Gene Detection

The screening for enterotoxin genes (*hblDAC*, *nheABC*, *cytK*, and *entFM*) and the plasmid encoded toxin genes (*ces*, *cryI*-group genes) by a multiplex (**Figure 6**) and two singleplex PCR, respectively, revealed a broad heterogeneity of the isolates. While *hbl* genes were found in 38 out of 75 isolates (50.7%), the complete operon was detectable in only 33 isolates (44.0%). In five isolates bands for either *hblD*, *hblA*, or *hblC* were not detectable in the agarose gel. The *nhe* genes were found in all isolates, and in 68 out of 75 (90.7%) all three genes of the operon were detectable. Here, *nheC* but not *nheA* could be detected in some isolates and *vice-versa*. In addition, the *cytK* gene was present in 50 isolates (66.7%) and *entFM* gene was detected in all isolates.

Four isolates (5.3%) carried the *ces* gene, whereas none of the isolates carried a gene for *cryI* group crystal toxins. PCR products for each target gene were sequenced once and confirmed correct PCR amplification. In total, 13 different toxin gene profiles could be established (**Table 4**), which partially correspond to previously published toxin gene profiles of *B. cereus* s.l. isolates (Ehling-Schulz et al., 2006; Carter et al., 2018). Toxin profile E (*hbl*[−], *nhe*⁺, *cytK*⁺, *entFM*⁺, and *ces*[−]) was the most abundant with 23 isolates (30.7%), followed by profile A (*hbl*⁺, *nhe*⁺, *cytK*⁺, *entFM*⁺, and *ces*[−]) with 22 isolates (29.3%). Isolates possessing the *ces*-gene were negative for *hblDAC* and *cytK*. Furthermore, the emetic isolates were found in samples from manufacturers 1 and 6. Those four isolates not showing any hemolytic activity on blood agar were assigned to toxin profiles A (1) and E (3), thus questioning the actual role of individual enterotoxins in blood agar hemolysis.

DISCUSSION

Although *B. cereus* has been frequently isolated from numerous sources, its occurrence in packaging materials has been poorly investigated. We reported *B. cereus* in the majority of packaging material samples included in this study. Interestingly, samples from different manufacturing sites showed different loads of *B. cereus*, but it is unclear whether these results are attributable to differences in the production site environment (geographical location, raw materials, and process technology) or to specific properties of the packaging material itself. Nevertheless, the

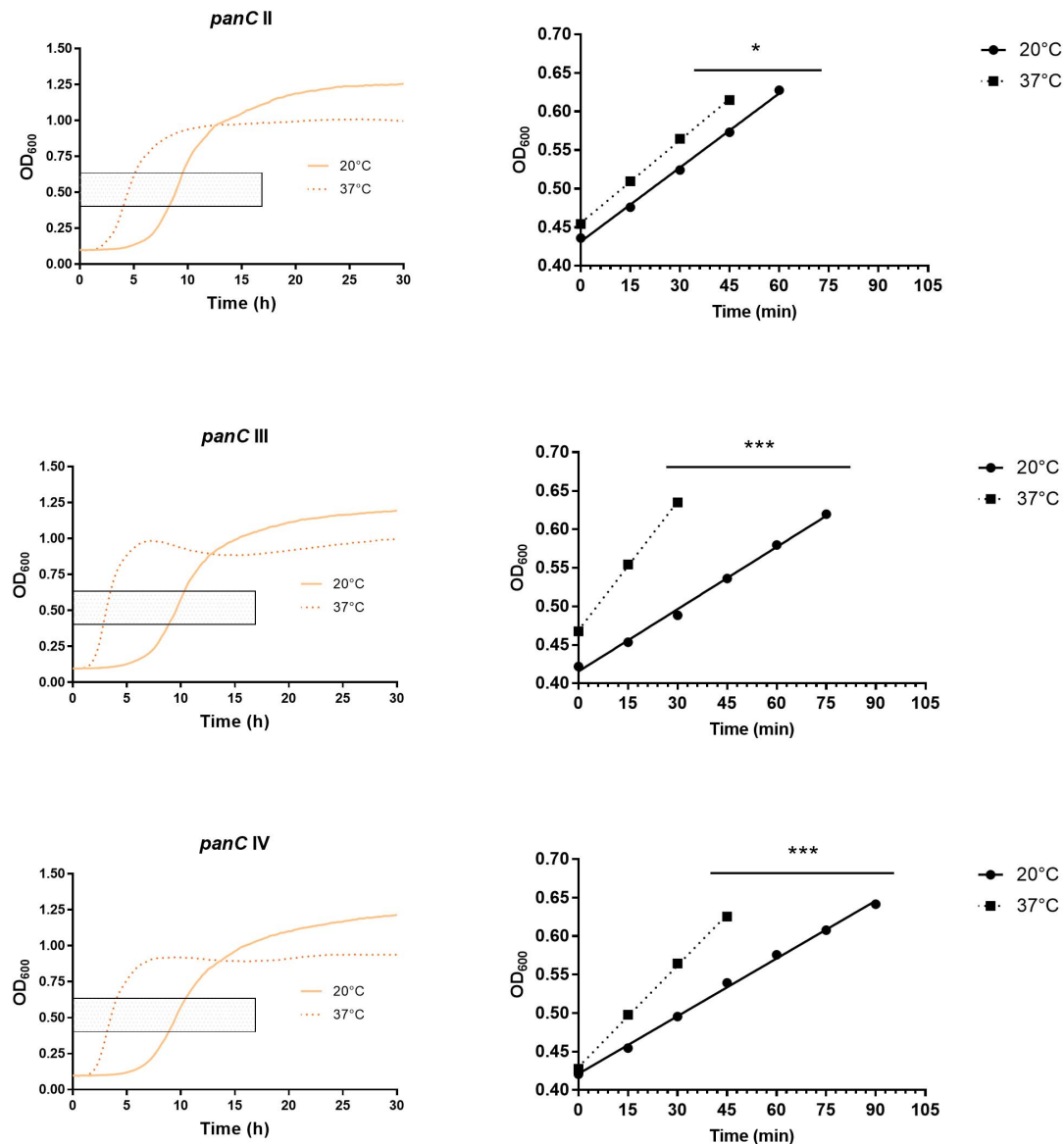
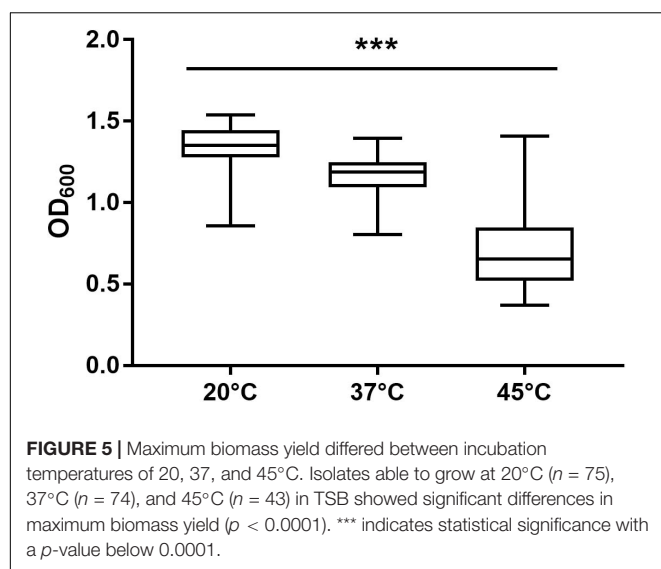


FIGURE 4 | Increased growth rates during exponential phase at 37°C compared to 20°C for phylogenetic *panC* groups II, III, and IV. Left: growth curves for 20°C (yellow) and 37°C (orange dotted). Exponential phase was defined for OD₆₀₀ values between 0.4 and 0.65 (gray box). Right: linear equations were modeled using OD₆₀₀ values between 0.4 and 0.65 for 20°C (dots) and 37°C (boxes). Slope differences were statistically significant for each phylogenetic group: II ($p = 0.0449$), III ($p < 0.0001$), and IV ($p < 0.0001$). * indicates statistical significance with a p -value below 0.05. *** indicates statistical significance with a p -value below 0.0001.

load of *B. cereus* appears to be significantly lower in primary packaging than in secondary packaging. The mere detection of *B. cereus* in packaging material is not surprising and has already been described several times. Suihko et al. (2004) isolated *B. cereus* from packaging materials in Finland and Pirttijarvi et al. (1999) found 16 different *B. cereus* ribotypes in packaging materials from four different countries in Europe and North America. The presence of *B. cereus* in packaging materials nevertheless appears to be negligible, because countless studies showed that *B. cereus* can be isolated from raw food such as fresh vegetables (Fiedler et al., 2019) as well as ready-to-eat meals (Kotzekidou, 2013; Yu et al., 2020). Furthermore,

a transfer of *B. thuringiensis* spores from food packaging to rice and chocolate was demonstrated only at very low rates (0.001 to 0.03%). We also aimed to characterize 75 different isolates from 41 packaging material samples. Although only isolates from the manufacturers with the highest abundance of *B. cereus* were investigated, our study provides the first solid overview of *B. cereus* in packaging materials and suggests that the results are transferable to other packaging manufacturers as well. Established differentiation schemes for the *B. cereus* group are either too unreliable like different colony morphologies and plasmid encoded toxin genes or often do not allow precise species identification, e.g., MALDI-TOF. Most MALDI-TOF



systems, like the one used in this study, are designed for clinical diagnostics and can therefore only assign species to the *B. cereus* group without more precise identification. This emphasizes the importance of molecular methods. Sequencing of the partial *panC* gene is a fast and reliable approach to cluster members of the *B. cereus* group into seven phylogenetic groups (Guinebretière et al., 2008). We found species affiliated to four different phylogenetic groups with mesophilic groups III and IV prevailing and groups with psychrotolerant tendency (II, VI) were the minority. Studies showed a predominance of group III isolates in powdered infant formula (Heini et al., 2018) and other food products (Amor et al., 2018) as well as stated

their role in food poisoning outbreaks (Glasset et al., 2016), followed by group IV. While members of groups III and IV were detected at equal frequencies in raw materials and processing environments of powdered infant formula (Zhuang et al., 2019), over half of all strains in a study on mostly environmental isolates from soil and animal feces belonged to group IV and all the food poisoning isolates to group III (Okutani et al., 2019). An epidemiologic and genetic survey revealed groups II, III, and IV in 23, 47, and 30% of patient and hospital environment strains, respectively, resembling the distribution in packaging material (Glasset et al., 2018). Therefore, the population of industrial products is likely to be between environmental and human-associated isolates, a conceivable hypothesis considering the presence of natural resources and humans in most industrial production fields. Due to the uneven distribution of the samples' origin, manufacturing sites 6 and 1 accounted for 69.3 and 20% of all isolates, respectively, it remains ambiguous if a distinct *panC* group predominates in a packaging material facility, but the results clearly suggest that the mesophilic *panC* groups III and IV prevail in all facilities. In addition to the seven major phylogenetic groups, Guinebretière et al. (2008) proposed 14 subgroups but an exact affiliation to subgroups was not made, although some subgroups are seen as particularly dangerous for food poisoning (Guinebretière et al., 2010). Surveillance of the *B. cereus* group in the food industry has become more important, since growth in stored food is a major cause of food spoilage and psychrotolerant strains that can grow at temperatures from 5 to 10°C are of particular concern. In this study, we did not find any isolate that showed visible growth on blood agar after 7 days in the refrigerator (5 to 7°C). This, together with the low frequency of isolates belonging to psychrotolerant groups and the limited transfer of bacterial spores from paper to food (Ekman et al., 2009), strongly suggests

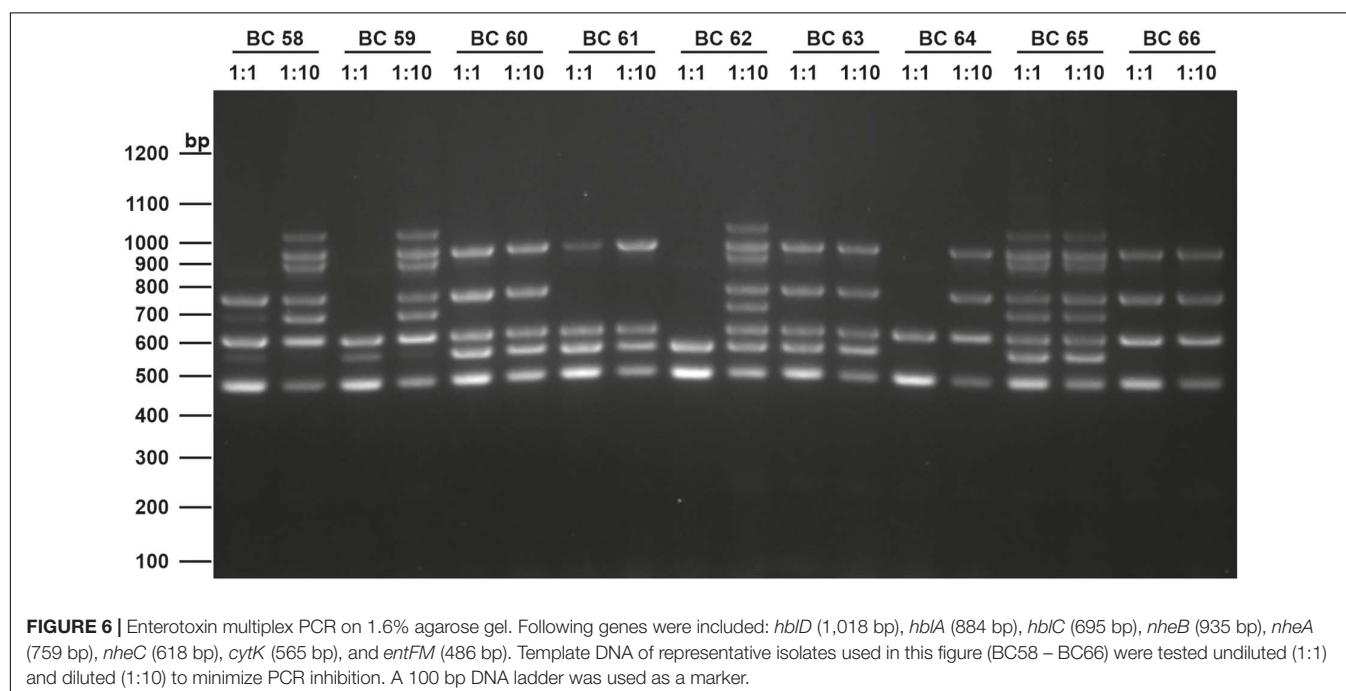


TABLE 4 | Toxin profiles of *B. cereus* group isolates.

Profile	Target gene										No. of samples
	<i>hblD</i>	<i>hblA</i>	<i>hblC</i>	<i>nheB</i>	<i>nheA</i>	<i>nheC</i>	<i>cytK</i>	<i>entFM</i>	<i>ces</i>	<i>cry1-type</i>	
A	(+)	(+)	(+)	(+)	(+)	(+)	(+)	(+)	(-)	(-)	22
B	(+)	(+)	(+)	(+)	(+)	(+)	(-)	(+)	(-)	(-)	7
C	(+)	(-)	(+)	(+)	(+)	(-)	(-)	(+)	(-)	(-)	1
D	(-)	(-)	(-)	(+)	(+)	(+)	(-)	(+)	(-)	(-)	8
E	(-)	(-)	(-)	(+)	(+)	(+)	(+)	(+)	(-)	(-)	23
F	(-)	(-)	(-)	(+)	(-)	(+)	(+)	(+)	(-)	(-)	2
G	(+)	(+)	(-)	(+)	(+)	(+)	(+)	(+)	(-)	(-)	1
H	(-)	(+)	(+)	(+)	(+)	(+)	(+)	(+)	(-)	(-)	1
I	(+)	(+)	(+)	(+)	(-)	(+)	(+)	(+)	(-)	(-)	1
J	(+)	(+)	(+)	(+)	(-)	(+)	(-)	(+)	(-)	(-)	3
K	(+)	(+)	(-)	(+)	(+)	(+)	(-)	(+)	(-)	(-)	1
L	(-)	(-)	(+)	(+)	(+)	(+)	(-)	(+)	(-)	(-)	1
M	(-)	(-)	(-)	(+)	(+)	(+)	(-)	(+)	(+)	(-)	4

n = 75

Thirteen different toxin profiles (A – M) were detected by multiplex PCR (enterotoxin genes) and two singleplex PCRs (*ces*, *cry1-type* genes). (+) indicates successful amplification.

that there is minimal risk for properly stored food. Nevertheless, more microbiological research on the interaction of packaging materials with packaged goods is needed, as literature in this field is scarce. To examine growth curves at different temperatures, we performed growth monitoring in the Bioscreen C for mesophilic and thermotolerant species and generally confirmed the growth characteristics previously associated with the phylogenetic *panC* groups (Guinebretière et al., 2008). Moreover, we showed for mesophilic isolates that growth rates in the exponential phase at 37°C are significantly increased compared to 20°C, which is, however, associated with an overall reduced maximum biomass. Higher temperatures may promote faster growth, and it has long been known that the optimal growth temperature is about 6°C below maximal growth temperature for many *Bacillus* species (Warth, 1978). Increased biomass at lower temperatures (10°C) has recently been shown for mesophilic food-associated bacteria, but only a single *B. cereus* isolate was tested (Seel et al., 2016). Our study can therefore support these results with a larger number of isolates. Limited biomass production at optimal growth temperatures may result from increased efforts to maintain cellular functions, as thermal instability of proteins appears to be a driving force in the adaption of life to different temperatures and habitats (Corkrey et al., 2012). Lower temperatures thus compensate detrimental effects in spite of challenging effects like reduced enzyme activity and low transcriptional and translational rates (D'Amico et al., 2006). The diversity within the *B. cereus* group is also reflected in their varying pathogenicity, which is mostly based on the production of several chromosomal or plasmid encoded toxins. Our results are generally in accordance with other findings of *B. cereus* group strains from various sources, where *nhe* genes were more prevalent than *hbl* genes (Guinebretière et al., 2002; Ngamwongsatit et al., 2008; Yu et al., 2020). This is supported by the phylogenetics of enterotoxins, which provided evidence, that gene deletion, duplications and horizontal gene transfer is likely for *hbl* genes, whereas *nhe* gene follow vertical inheritance

(Böhm et al., 2015). Nevertheless, some studies also showed *hbl* genes prevailing in food strains, thus no universal conclusion can be drawn. The CytK prevalence varies between different studies and generally matches with our findings. The actual role of EntFM in *B. cereus* remains still unclear, as it is not sufficiently understood whether it serves as an enterotoxin or as a cell wall peptidase (Asano et al., 1997; Tran et al., 2010). Overall, we discovered 13 different toxin profiles, some of which are consistent with previously published toxin gene profiles (Ehling-Schulz et al., 2006; Carter et al., 2018; Fiedler et al., 2019). The link between *panC* group and toxin genes has already been shown and could be confirmed by this study (Guinebretière et al., 2010). Although *panC* sequencing does not precisely distinguish the species within a phylogenetic group, combining the results with those from toxin PCRs can lead to species definitions that are more accurate. According to the literature, *B. thuringiensis* is defined by the presence of the plasmid encoded crystal toxins (Schnepf et al., 1998). Since we could not detect any isolate carrying this plasmid, we concluded that all isolates within groups II, III, and IV are likely *B. cereus sensu stricto* and not *B. thuringiensis*. In addition, the isolate affiliated to group VI is probably *B. weihenstephanensis* because it did not carry the crystal toxin plasmid and did not show rhizoid colony morphology typical for *B. mycoides*. Emetic strains were detected only at low rates in packaging materials and have been reported at comparable rates in food samples by other studies (Ehling-Schulz et al., 2006; Heini et al., 2018; Yu et al., 2020). The fact that emetic strains were isolated in samples from two manufacturers showed that they do not occur exclusively in one packaging type, but no link to manufacturing conditions or sample properties can be made due to lack of data. In accordance with other enterotoxin screenings, not all genes of the *hblDAC* and the *nheABC* operons were detectable for each isolate. While several other studies also indicated these strains to have individual toxin profiles, it is unlikely that this is caused by the absence of these genes, but rather by sequence polymorphisms that

prevent accurate primer annealing (Guinebretière et al., 2002). Consequently, PCR strategies that involve the detection of single genes have greater potential for false-negative results compared to multiplex assays that attempt to amplify each gene. Notwithstanding the phylogenetic affiliation is a simple approach to characterize isolates, toxin detection remains irreplaceable due to more and more reports of formerly less virulent *B. cereus* group species harboring enterotoxin genes (Prüß et al., 1999; Baron et al., 2007) as well as cereulide (Thorsen et al., 2006). Moreover, it has been suggested, that the *B. cereus* group only comprises lineages of the same species possessing different growth characteristics and virulence factors such as toxins encoded on plasmids (Helgason et al., 2000; Rasko et al., 2005). This indicates that several characteristics need to be taken into consideration to evaluate *B. cereus* group strains. This study shows that packaging material isolates share the same characteristics with strains from food or environmental sources and therefore packaging materials may not be a reservoir for particularly virulent strains.

DATA AVAILABILITY STATEMENT

The original contributions presented in the study are included in the article/supplementary material, further inquiries can be directed to the corresponding author/s.

REFERENCES

- Amor, M. G. B., Siala, M., Zayani, M., Grosset, N., Smaoui, S., Messadi-Akrout, F., et al. (2018). Isolation, identification, prevalence, and genetic diversity of *Bacillus cereus* group bacteria from different foodstuffs in Tunisia. *Front. Microbiol.* 9:447. doi: 10.3389/fmicb.2018.00447
- Asano, S. I., Nukumizu, Y., Bando, H., Iizuka, T., and Yamamoto, T. (1997). Cloning of novel enterotoxin genes from *Bacillus cereus* and *Bacillus thuringiensis*. *Appl. Environ. Microbiol.* 63, 1054–1057. doi: 10.1128/aem.63.3.1054-1057.1997
- Baron, F., Cochet, M. F., Grosset, N., Madec, M. N., Briandet, R., Dessaigne, S., et al. (2007). Isolation and characterization of a psychrotolerant toxin producer, *Bacillus weihenstephanensis*, in liquid egg products. *J. Food Prot.* 70, 2782–2791. doi: 10.4315/0362-028X-70.12.2782
- Beecher, D. J., Schoeni, J. L., and Lee Wong, A. C. (1995). Enterotoxic activity of hemolysin BL from *Bacillus cereus*. *Infect. Immun.* 63, 4423–4428. doi: 10.1128/iai.63.11.4423-4428.1995
- Böhm, M. E., Huptas, C., Krey, V. M., and Scherer, S. (2015). Massive horizontal gene transfer, strictly vertical inheritance and ancient duplications differentially shape the evolution of *Bacillus cereus* enterotoxin operons hbl, cytK and nhe. *BMC Evol. Biol.* 15:246. doi: 10.1186/s12862-015-0529-4
- Brillard, J., Dupont, C. M. S., Berge, O., Dargaignaratz, C., Oriol-Gagnier, S., Doussan, C., et al. (2015). The water cycle, a potential source of the bacterial pathogen *Bacillus cereus*. *Biomed. Res. Int.* 2015:356928. doi: 10.1155/2015/356928
- Carter, L., Chase, H. R., Giesecker, C. M., Hasbrouck, N. R., Stine, C. B., Khan, A., et al. (2018). Analysis of enterotoxigenic *Bacillus cereus* strains from dried foods using whole genome sequencing, multi-locus sequence analysis and toxin gene prevalence and distribution using endpoint PCR analysis. *Int. J. Food Microbiol.* 284, 31–39. doi: 10.1016/j.ijfoodmicro.2018.06.016
- Choo, E., Sung, S. J., Kyumson, K., Lee, K. G., Sunggi, H., and Ryu, S. (2007). Prevalence and genetic diversity of *Bacillus cereus* in dried red pepper in Korea. *J. Food Prot.* 70, 917–922. doi: 10.4315/0362-028X-70.4.917
- Corkrey, R., Olley, J., Ratkowsky, D., McMeekin, T., and Ross, T. (2012). Universality of thermodynamic constants governing biological growth rates. *PLoS One* 7:e32003. doi: 10.1371/journal.pone.0032003
- D'Amico, S., Collins, T., Marx, J. C., Feller, G., and Gerday, C. (2006). Psychrophilic microorganisms: challenges for life. *EMBO Rep.* 7, 385–389. doi: 10.1038/sj.embor.7400662
- Ehling-Schulz, M., Guinebretière, M. H., Monthán, A., Berge, O., Fricker, M., and Svensson, B. (2006). Toxin gene profiling of enterotoxic and emetic *Bacillus cereus*. *FEMS Microbiol. Lett.* 260, 232–240. doi: 10.1111/j.1574-6968.2006.00320.x
- Ehling-Schulz, M., Lereclus, D., and Koehler, T. M. (2019). The *Bacillus cereus* Group: *Bacillus* Species with Pathogenic Potential. *Microbiol. Spectr.* 7, 875–902. doi: 10.1128/microbiolspec.GPP3-0032-2018
- Ekman, J., Tsitko, I., Weber, A., Nielsen-Leroux, C., Lereclus, D., and Salkinoja-Salonen, M. (2009). Transfer of *Bacillus cereus* Spores from Packaging Paper into Food. *J. Food Prot.* 72, 2236–2242. doi: 10.4315/0362-028X-72.11.2236
- Felsenstein, J. (2005). *PHYMLIP (Phylogeny Inference Package) Version 3.6. Distributed by the Author*. Seattle: University of Washington.
- Fiedler, G., Schneider, C., Igbinosa, E. O., Kabisch, J., Brinks, E., Becker, B., et al. (2019). Antibiotics resistance and toxin profiles of *Bacillus cereus*-group isolates from fresh vegetables from German retail markets. *BMC Microbiol.* 19:250. doi: 10.1186/s12866-019-1632-2
- Glasset, B., Herbin, S., Granier, S. A., Cavalié, L., Lefeuvre, E., Guérin, C., et al. (2018). *Bacillus cereus*, a serious cause of nosocomial infections: epidemiologic and genetic survey. *PLoS One* 13:e0194346. doi: 10.1371/journal.pone.0194346
- Glasset, B., Herbin, S., Guillier, L., Cadel-Six, S., Vignaud, M., Grout, J., et al. (2016). *Bacillus cereus*-induced food-borne outbreaks in France, 2007 to 2014: epidemiology and genetic characterisation. *Eurosurveillance* 21:30413. doi: 10.2807/1560-7917.ES.2016.21.48.30413
- Granum, P. E., Brynestad, S., and Kramer, J. M. (1993). Analysis of enterotoxin production by *Bacillus cereus* from dairy products, food poisoning incidents and non-gastrointestinal infections. *Int. J. Food Microbiol.* 17, 269–279. doi: 10.1016/0168-1605(93)90197-0

AUTHOR CONTRIBUTIONS

PS: experimental design, data collection, analysis, and interpretation, and manuscript writing. SM: data collection and manuscript writing. CK: project supervision and manuscript writing. All authors have approved the final version to be published and agreed to be accountable for all aspects of the work in ensuring that questions related to the accuracy or integrity of any part of the work are appropriately investigated and resolved.

FUNDING

This work has been funded by the Christian Doppler Society, Austria (CD-Laboratory for Mass Transport through Paper). The financial support of the Austrian Federal Ministry for Digital and Economic Affairs and the National Foundation for Research, Technology and Development, Austria is acknowledged.

ACKNOWLEDGMENTS

We thank Daniela Toplitsch for technical and intellectual support.

- Guinebreti re, M. H., Broussolle, V., and Nguyen-The, C. (2002). Enterotoxigenic profiles of food-poisoning and food-borne *Bacillus cereus* strains. *J. Clin. Microbiol.* 40, 3053–3056. doi: 10.1128/JCM.40.8.3053-3056.2002
- Guinebreti re, M. H., Thompson, F. L., Sorokin, A., Normand, P., Dawyndt, P., Ehling-Schulz, M., et al. (2008). Ecological diversification in the *Bacillus cereus* Group. *Environ. Microbiol.* 10, 851–865. doi: 10.1111/j.1462-2920.2007.01495.x
- Guinebreti re, M. H., Velge, P., Couvert, O., Carlin, F., Debuyser, M. L., and Nguyen-The, C. (2010). Ability of *Bacillus cereus* group strains to cause food poisoning varies according to phylogenetic affiliation (groups I to VII) rather than species affiliation. *J. Clin. Microbiol.* 48, 3388–3391. doi: 10.1128/JCM.00921-10
- Heini, N., Stephan, R., Ehling-Schulz, M., and Johler, S. (2018). Characterization of *Bacillus cereus* group isolates from powdered food products. *Int. J. Food Microbiol.* 283, 59–64. doi: 10.1016/j.ijfoodmicro.2018.06.019
- Helgason, E.,  kstad, O. L. E. A., Cagant, D. A., Mock, L. E., Hegna, I. D. A., Johansen, H. A., et al. (2000). One Species on the Basis of Genetic Evidence. *Appl. Environ. Microbiol.* 66, 2627–2630. doi: 10.1128/AEM.66.6.2627-2630.2000.Updated
- Huson, D. H., and Bryant, D. (2006). Application of phylogenetic networks in evolutionary studies. *Mol. Biol. Evol.* 23, 254–267. doi: 10.1093/molbev/msj030
- CSA Group Corporation. (2018). *ISO 7932:2004/AMD 1:2018 Microbiology of food and animal feeding stuffs — Horizontal method for the enumeration of presumptive Bacillus cereus — Colony-count technique at 30 degrees C — Amendment 1: Inclusion of optional tests*. Canada: CSA Group Corporation.
- Je berger, N., Dietrich, R., Bock, S., Didier, A., and M rtlbauer, E. (2014). *Bacillus cereus* enterotoxins act as major virulence factors and exhibit distinct cytotoxicity to different human cell lines. *Toxicon* 77, 49–57. doi: 10.1016/j.toxicon.2013.10.028
- Konuma, H., Shinagawa, K., Tokumaru, M., Onoue, Y., Konno, S., Fujino, N., et al. (1988). Occurrence of *Bacillus cereus* in Meat Products, Raw Meat and Meat Product Additives. *J. Food Prot.* 51, 324–326. doi: 10.4315/0362-028x-51.4.324
- Kotzekidou, P. (2013). Microbiological examination of ready-to-eat foods and ready-to-bake frozen pastries from university canteens. *Food Microbiol.* 34, 337–343. doi: 10.1016/j.fm.2013.01.005
- Lindb ck, T., Hardy, S. P., Dietrich, R., S dring, M., Didier, A., Moravek, M., et al. (2010). Cytotoxicity of the *Bacillus cereus* Nhe enterotoxin requires specific binding order of its three exoprotein components. *Infect. Immun.* 78, 3813–3821. doi: 10.1128/IAI.00247-10
- Liu, Y., Lai, Q., G ker, M., Meier-Kolthoff, J. P., Wang, M., Sun, Y., et al. (2015). Genomic insights into the taxonomic status of the *Bacillus cereus* group. *Sci. Rep.* 5, 1–11. doi: 10.1038/srep14082
- Lund, T., De Buyser, M. L., and Granum, P. E. (2000). A new cytotoxin from *Bacillus cereus* that may cause necrotic enteritis. *Mol. Microbiol.* 38, 254–261. doi: 10.1046/j.1365-2958.2000.02147.x
- Moretti, S., Armougom, F., Wallace, I. M., Higgins, D. G., Jongeneel, C. V., and Notredame, C. (2007). The M-Coffee web server: a meta-method for computing multiple sequence alignments by combining alternative alignment methods. *Nucleic Acids Res.* 35, 645–648. doi: 10.1093/nar/gkm333
- Ngamwongsatit, P., Buasri, W., Pianariyanon, P., Pulsrikarn, C., Ohba, M., Assavanig, A., et al. (2008). Broad distribution of enterotoxin genes (hblCDA, nheABC, cytK, and entFM) among *Bacillus thuringiensis* and *Bacillus cereus* as shown by novel primers. *Int. J. Food Microbiol.* 121, 352–356. doi: 10.1016/j.ijfoodmicro.2007.11.013
- Okutani, A., Inoue, S., Noguchi, A., Kaku, Y., and Morikawa, S. (2019). Whole-genome sequence-based comparison and profiling of virulence-associated genes of *Bacillus cereus* group isolates from diverse sources in Japan. *BMC Microbiol.* 19:296. doi: 10.1186/s12866-019-1678-1
- Pirttij rvi, T. S. M., Andersson, M. A., Scoging, A. C., and Salkinoja-Salonen, M. S. (1999). Evaluation of methods for recognising strains of the *Bacillus cereus* group with food poisoning potential among industrial and environmental contaminants. *Syst. Appl. Microbiol.* 22, 133–144. doi: 10.1016/S0723-2020(99)80036-8
- Pr  , B. M., Dietrich, R., Nibler, B., M rtlbauer, E., and Scherer, S. (1999). The hemolytic enterotoxin HBL is broadly distributed among species of the *Bacillus cereus* group. *Appl. Environ. Microbiol.* 65, 5436–5442. doi: 10.1128/aem.65.12.5436-5442.1999
- Rahmati, T., and Labbe, R. (2008). Levels and toxigenicity of *Bacillus cereus* and *Clostridium perfringens* from retail seafood. *J. Food Prot.* 71, 1178–1185. doi: 10.4315/0362-028X-71.6.1178
- Rasko, D. A., Altherr, M. R., Han, C. S., and Ravel, J. (2005). Genomics of the *Bacillus cereus* group of organisms. *FEMS Microbiol. Rev.* 29, 303–329. doi: 10.1016/j.fmrre.2004.12.005
- Samapundo, S., Heyndrickx, M., Xhaferi, R., and Devlieghere, F. (2011). Incidence, diversity and toxin gene characteristics of *Bacillus cereus* group strains isolated from food products marketed in Belgium. *Int. J. Food Microbiol.* 150, 34–41. doi: 10.1016/j.ijfoodmicro.2011.07.013
- Schnepf, E., Crickmore, N., Van Rie, J., Lereclus, D., Baum, J., Feitelson, J., et al. (1998). *Bacillus thuringiensis* and Its Pesticidal Crystal Proteins. *Microbiol. Mol. Biol. Rev.* 62, 775–806. doi: 10.1128/mmbr.62.3.775-806.1998
- Seel, W., Derichs, J., and Lipski, A. (2016). Increased biomass production by mesophilic food-associated bacteria through lowering the growth temperature from 30 C to 10 C. *Appl. Environ. Microbiol.* 82, 3754–3764. doi: 10.1128/AEM.00211-16
- Stenfors Arnesen, L. P., F gerlund, A., and Granum, P. E. (2008). From soil to gut: *Bacillus cereus* and its food poisoning toxins. *FEMS Microbiol. Rev.* 32, 579–606. doi: 10.1111/j.1574-6976.2008.00112.x
- Suikko, M. L., Sinkko, H., Partanen, L., Mattila-Sandholm, T., Salkinoja-Salonen, M., and Raaska, L. (2004). Description of heterotrophic bacteria occurring in paper mills and paper products. *J. Appl. Microbiol.* 97, 1228–1235. doi: 10.1111/j.1365-2672.2004.02416.x
- Thaenthanee, S., Lee Wong, A. C., and Panbangred, W. (2005). Phenotypic and genotypic comparisons reveal a broad distribution and heterogeneity of hemolysin BL genes among *Bacillus cereus* isolates. *Int. J. Food Microbiol.* 105, 203–212. doi: 10.1016/j.ijfoodmicro.2005.04.003
- Thorsen, L., Hansen, B. M., Nielsen, K. F., Hendriksen, N. B., Phipps, R. K., and Budde, B. B. (2006). Characterization of emetic *Bacillus weihenstephanensis*, a new cereulide-producing bacterium. *Appl. Environ. Microbiol.* 72, 5118–5121. doi: 10.1128/AEM.00170-06
- Tran, S. L., Guillemet, E., Gohar, M., Lereclus, D., and Ramarao, N. (2010). CwpFM (EntFM) is a *Bacillus cereus* potential cell wall peptidase implicated in adhesion, biofilm formation, and virulence. *J. Bacteriol.* 192, 2638–2642. doi: 10.1128/JB.01315-09
- V ls nen, O. M., Mentu, J., and Salkinoja-Salonen, M. S. (1991). Bacteria in food packaging paper and board. *J. Appl. Bacteriol.* 71, 130–133. doi: 10.1111/j.1365-2672.1991.tb02967.x
- Von Stetten, F., Mayr, R., and Scherer, S. (1999). Climatic influence on mesophilic *Bacillus cereus* and psychrotolerant *Bacillus weihenstephanensis* populations in tropical, temperate and alpine soil. *Environ. Microbiol.* 1, 503–515. doi: 10.1046/j.1462-2920.1999.00070.x
- Warth, A. D. (1978). Relationship between the heat resistance of spores and the optimum and maximum growth temperatures of *Bacillus* species. *J. Bacteriol.* 134, 699–705. doi: 10.1128/jb.134.3.699-705.1978
- Yu, S., Yu, P., Wang, J., Li, C., Guo, H., Liu, C., et al. (2020). A Study on Prevalence and Characterization of *Bacillus cereus* in Ready-to-Eat Foods in China. *Front. Microbiol.* 10:3043. doi: 10.3389/fmicb.2019.03043
- Zhuang, K., Li, H., Zhang, Z., Wu, S., Zhang, Y., Fox, E. M., et al. (2019). Typing and evaluating heat resistance of *Bacillus cereus* sensu stricto isolated from the processing environment of powdered infant formula. *J. Dairy Sci.* 102, 7781–7793. doi: 10.3168/jds.2019-16392

Conflict of Interest: The authors declare that the research was conducted in the absence of any commercial or financial relationships that could be construed as a potential conflict of interest.

Copyright   2021 Schmid, Maitz and Kittinger. This is an open-access article distributed under the terms of the Creative Commons Attribution License (CC BY). The use, distribution or reproduction in other forums is permitted, provided the original author(s) and the copyright owner(s) are credited and that the original publication in this journal is cited, in accordance with accepted academic practice. No use, distribution or reproduction is permitted which does not comply with these terms.



Quantification of Viable *Brochothrix thermosphacta* in Cold-Smoked Salmon Using PMA/PMAXx-qPCR

Agnès Bouju-Albert, Sabrina Saltaji, Xavier Dousset, Hervé Prévost and Emmanuel Jaffrès*

UMR 1014, Secalim, INRAE, Oniris, Nantes, France

OPEN ACCESS

Edited by:

Santanu Basu,
Swedish University of Agricultural
Sciences, Sweden

Reviewed by:

Giulia Amagliani,
University of Urbino Carlo Bo, Italy
Anindya Chanda,
Mycologics LLC, United States

*Correspondence:

Emmanuel Jaffrès
emmanuel.jaffres@oniris-nantes.fr

Specialty section:

This article was submitted to
Food Microbiology,
a section of the journal
Frontiers in Microbiology

Received: 15 January 2021

Accepted: 17 June 2021

Published: 14 July 2021

Citation:

Bouju-Albert A, Saltaji S,
Dousset X, Prévost H and Jaffrès E
(2021) Quantification of Viable
Brochothrix thermosphacta
in Cold-Smoked Salmon Using
PMA/PMAXx-qPCR.
Front. Microbiol. 12:654178.
doi: 10.3389/fmicb.2021.654178

The aim of this study was to develop a rapid and accurate PMA-qPCR method to quantify viable *Brochothrix thermosphacta* in cold-smoked salmon. *B. thermosphacta* is one of the main food spoilage bacteria. Among seafood products, cold-smoked salmon is particularly impacted by *B. thermosphacta* spoilage. Specific and sensitive tools that detect and quantify this bacterium in food products are very useful. The culture method commonly used to quantify *B. thermosphacta* is time-consuming and can underestimate cells in a viable but not immediately culturable state. We designed a new PCR primer set from the single-copy *rpoC* gene. QPCR efficiency and specificity were compared with two other published primer sets targeting the *rpoC* and *rpoB* genes. The viability dyes PMA or PMAXx were combined with qPCR and compared with these primer sets on viable and dead *B. thermosphacta* cells in BHI broth and smoked salmon tissue homogenate (SSTH). The three primer sets displayed similar specificity and efficiency. The efficiency of new designed *rpoC* qPCR on viable *B. thermosphacta* cells in SSTH was 103.50%, with a linear determination coefficient (r^2) of 0.998 and a limit of detection of 4.04 log CFU/g. Using the three primer sets on viable cells, no significant difference was observed between cells treated or untreated with PMA or PMAXx. When dead cells were used, both viability dyes suppressed DNA amplification. Nevertheless, our results did not highlight any difference between PMAXx and PMA in their efficiency to discriminate viable from unviable *B. thermosphacta* cells in cold-smoked salmon. Thus, this study presents a rapid, specific and efficient *rpoC*-PMA-qPCR method validated in cold-smoked salmon to quantify viable *B. thermosphacta* in foods.

Keywords: viable, *Brochothrix thermosphacta*, spoilage, smoked salmon, PMA, PMAXx-based qPCR, *rpoC* gene

INTRODUCTION

Brochothrix thermosphacta is one of the main food spoilage bacteria, and can cause important economic losses in the food industry. This bacterium can produce off-odors leading to food waste, which moreover contributes to the ecological impact of food spoilage (Remenant et al., 2015; Illikoud et al., 2018a). In beef for example, *B. thermosphacta* can produce dairy – cheesy and

creamy – off-odors (Dainty and Mackey, 1992; Casaburi et al., 2014). Seafood products, whose consumption is constantly increasing worldwide, can also be spoiled by *B. thermosphacta*, such as cooked and peeled shrimp with the production of strong butter, buttermilk-like, sour, and nauseous off-odors (Mejlholm et al., 2005; Laursen et al., 2006; Jaffrès et al., 2011). In cold-smoked salmon, *B. thermosphacta* can also produce butter/plastic/rancid, blue-cheese, sour/pungent off-odors (Joffraud et al., 2001, 2006; Stohr et al., 2001). *B. thermosphacta* has been described as widely disseminated along the food chain, from the raw material to the final product and during storage until use by date. This bacterium has also been isolated from food processing plants (from floors, walls, machines, etc.) which constitute one of the main sources of food contamination during processing (Stackebrandt and Jones, 2006; Nychas et al., 2008).

In the field of microbiological analysis, the non-cultural molecular methods such as quantitative real-time PCR (qPCR) have become essential tools in the last decade to detect and quantify microorganisms, with high precision in complex microbiota, e.g., in food matrices or food processing plants (Kuchta et al., 2014; Franco-Duarte et al., 2019). Quantitative real-time PCR (qPCR) is specific and fast tool to detect and quantify microorganisms, in complex microbiota, e.g., in food matrices or food processing plants (Kuchta et al., 2014). The qPCR detects bacteria in a viable but not immediately culturable state (VBNC), which are underestimates when using culturable microbiological approaches (Postollec et al., 2011). Nevertheless, dead bacteria can be revealed and quantified by qPCR. The qPCR using viability dyes such as propidium monoazide (PMA-qPCR) has been developed. PMA used before DNA extraction can penetrate unviable/dead cells, bind to their DNA and subsequently inhibit the PCR amplification, ensuring a selective quantification of viable bacteria (Elizaquível et al., 2014). PMA-qPCR is largely used nowadays to efficiently detect and quantify viable bacteria in food, e.g., *Campylobacter* (Josefsen et al., 2010; Castro et al., 2018), *Listeria monocytogenes* (Pan and Breidt, 2007; Desneux et al., 2015), *Salmonella* (Liang et al., 2011; Fang et al., 2018), *Staphylococcus aureus* (Zhang et al., 2015; Dong et al., 2018), *Vibrio parahaemolyticus* (Zhu et al., 2012; Niu et al., 2018), *Escherichia coli* O157:H7 (Elizaquível et al., 2012; Zhou et al., 2017), *Photobacterium* (Macé et al., 2013), and *Brochothrix thermosphacta* (Pennacchia et al., 2009; Mamlouk et al., 2012). The choice of the targeted phylogenetic marker is determining when such molecular tools are used. The 16S ribosomal RNA gene, commonly used to identify bacterial species, presents biases because multiple copies of this gene are often present in bacterial genomes with possible sequence variations (e.g., genomes of *B. thermosphacta* strains can contain up to 9 copies of the 16S rRNA gene) (Paoli et al., 2017; Illikoud et al., 2018b). This can lead to mispriming affecting amplification efficiency or quantification reliability. The use of single-copy protein-coding genes such as *gyrB* (DNA gyrase subunit B) or *rpoB* and *rpoC* (RNA polymerase subunit B or C) for bacterial detection and quantification is an alternative to this limitation (Case et al., 2007; Macé et al., 2013; Fougy et al., 2016).

We designed a new *B. thermosphacta rpoC* gene primer set, and compared its PMA-qPCR efficiency with the efficiency of two previously published *rpoB* or *rpoC* gene primer sets. We compared the efficiency of PMA or PMAxx treatments and described a rapid assay to quantify viable *B. thermosphacta* using PMA-qPCR with the new *rpoC* primer set. The method was successfully used to quantify *B. thermosphacta* in artificially contaminated cold-smoked salmon. To our knowledge, this study is a first about the use of qPCR to quantify the spoilage bacterium *B. thermosphacta* in combination with the use of a viability dye (PMA or PMAxx) and the targeting of a single-copy gene (*rpoC* or *rpoB*).

MATERIALS AND METHODS

Bacterial Strains and *B. thermosphacta* Enumeration

A total of 26 strains belonging to 12 different bacterial species frequently isolated from various food products, notably cold-smoked salmon (CSS) or from a processing plant were used (Table 1). All strains were recovered from -80°C freezers on their appropriate agar media: Brain Heart Infusion agar (BHI) (VWR Chemicals Prolabo, France); BHI + 2% NaCl (Merck, France); de Man, Rogosa and Sharpe medium (MRS) (Biokar Diagnostics, France); Elliker broth (Biokar Diagnostics, France) supplemented with 1.5% agar (Biokar Diagnostics, France). Each strain was sub-cultured from the colonies on the plates in its corresponding broth and incubated at its optimal temperature growth for 24 to 48 h (Table 1) to obtain bacterial suspensions. *B. thermosphacta* DSM 20171 in pure culture was enumerated on BHI agar after 48 h incubation at 25°C . *B. thermosphacta* inoculated in smoked salmon tissue homogenate (SSTH) were enumerated on streptomycin tallous acetate actidione (STAA) agar supplemented with the STAA selective supplement (Oxoid, France), and incubated at 25°C for 48 h. Total viable counts in SSTH samples were estimated on plate count agar (PCA) (Biokar, France) supplemented with 2% NaCl (Merck, France) and incubated at 25°C for 72 h.

Preparation of the Smoked Salmon Tissue Homogenate

Cold-smoked salmon was provided by a French company. *B. thermosphacta* was not detected in it using standard culture method on STAA, with the STAA selective supplement, and the real-time PCR methods developed in this study. The smoked salmon tissue homogenate (SSTH) was prepared either from packaged smoked salmon slices preserved under vacuum at 4°C (leaving the factory) (SSTHf) or from smoked salmon fillets sent by the French company sampled just after the smoking stage of CSS production (SSTHs). A 20-g portion was aseptically weighed in a sterile stomacher plastic bag equipped with a 63- μm porosity filter (Interscience, France), and 80 mL of sterile water were added to obtain a 5-fold dilution. The sample was then homogenized for 2 min using a stomacher device (Masticator IUL, Spain). The bag-filtered samples were divided into aliquots

TABLE 1 | Bacterial strains used to assess the specificity of the qPCR primers.

Species	Strains	Isolated from	Incubation temperature (°C)	Growth medium ^a
<i>Brochothrix thermosphacta</i>	DSM 20171 ^T	Fresh pork sausage	25	BHI
<i>Brochothrix thermosphacta</i>	Oniris 19/R/663	Smoked salmon	25	BHI
<i>Brochothrix thermosphacta</i>	CD 340 (a)	Shrimp	25	BHI
<i>Brochothrix thermosphacta</i>	EBP 3084 (b)	Salmon	25	BHI
<i>Brochothrix thermosphacta</i>	TAP 125 (c)	Chicken	25	BHI
<i>Brochothrix thermosphacta</i>	EBP 3017 (b)	Cod	25	BHI
<i>Brochothrix campestris</i>	DSM 4712 ^T	Soil	25	BHI
<i>Carnobacterium maltaromaticum</i>	Oniris 19/R/671	Smoked salmon factory	30	Elliker
<i>Carnobacterium divergens</i>	NCDO 2763 ^T	Vacuum-packaged beef	30	Elliker
<i>Enterococcus faecalis</i>	ATCC 19433 ^T	Unknown	37	Elliker
<i>Enterococcus faecium</i>	CIP 54.33	Canned fish	37	Elliker
<i>Escherichia coli</i>	CIP 53.125	Human feces	37	BHI
<i>Companilactobacillus alimentarius</i>	DSM 20181	Marinated fish product	30	MRS
<i>Lactilactobacillus sakei subsp. sakei</i>	DSM 20017 ^T	Moto starter of sake	30	MRS
<i>Lactococcus piscium</i>	Oniris 19/R/684	Smoked salmon	25	Elliker
<i>Lactococcus raffinolactis</i>	Oniris MIP 2453	Unknown	25	Elliker
<i>Listeria monocytogenes</i>	DSM 12464 ^T	Poultry	37	BHI
<i>Listeria monocytogenes</i>	CIP 78.35	Spinal fluid	37	BHI
<i>Listeria grayi</i>	CIP 68.18 ^T	Feces of chinchilla	37	BHI
<i>Listeria innocua</i>	CIP 80.11 ^T	Brain of cow	37	BHI
<i>Photobacterium phosphoreum</i>	CIP 102511 ^T	Unknown	15	BHI 2% NaCl
<i>Pseudomonas fluorescens</i>	CIP 69.13 ^T	Pre-filter tanks	30	BHI
<i>Psychrobacter</i> sp.	Oniris 19/R/675	Smoked salmon factory	25	BHI 2% NaCl
<i>Serratia liquefaciens</i>	ATCC 27592 ^T	Milk	37	BHI
<i>Shewanella baltica</i>	Oniris 19/R/670	Smoked salmon factory	25	BHI 2% NaCl
<i>Staphylococcus epidermidis</i>	CIP 68.21	Unknown	37	BHI

DSM, Deutsche Sammlung von Mikroorganismen und Zellkulturen GmbH, Braunschweig, Germany; CIP, Centre de Ressources Biologiques de l'Institut Pasteur, Paris, France; NCDO, National Collection of Dairy Organisms, Shinfield, United Kingdom; ATCC, American Type Culture Collection, Manassas (VA) United States; Oniris, Secalim Bacterial Culture Collection, Nantes, France. ^T: Type Strain; BHI, Brain Heart Infusion agar (VWR Chemicals Prolabo, France); MRS, de Man Rogosa and Sharpe and Elliker media (Biokar Diagnostics, France). (a) Jaffrès et al. (2009), (b) Chaillou et al. (2015), (c) Illikoud et al. (2019).

in sterile vials, and then stored at -80°C until their inoculation by fresh bacterial cultures. In order to limit qPCR inhibition, 1% of bovine serum albumin (BSA) fraction V (Sigma-Aldrich, France) and 4% of polyvinylpyrrolidone (PVP) (Sigma-Aldrich, France) were added to SSTH before DNA extraction (Kreader, 1996; Furet et al., 2009; Schrader et al., 2012).

Viable and Dead Cell Preparation

The efficiency of the PMA and PMAxx treatments was assessed on *B. thermosphacta* DSM 20171 viable or dead cells in BHI broth or SSTH. The viable cells were obtained from a pre-culture in 10 mL of BHI broth at 25°C for 8 h, followed by a culture in 100 mL of BHI broth for 4 h, in order to obtain an 8 log CFU/mL exponential growth phase culture. The 100% viable cell culture in SSTH was produced as follows: 5 mL of the 8 log CFU/mL exponential growth phase BHI culture were centrifuged at $6,000 \times g$ for 2 min, the supernatant was discarded, and the cells were re-suspended in 5 mL of SSTH (with BSA and PVP). Dead cells were obtained by heating 5 microtubes containing 1 mL of the 8 log CFU/mL exponential growth phase in BHI culture at 90°C for 15 min in a water bath. The suspensions were pooled and centrifuged at $6,000 \times g$ for 2 min. The supernatant was discarded, and the cells were re-suspended in

5 mL of SSTH (with BSA and PVP). Cell viability was checked by plating on STAA agar.

PMA and PMAxx Treatments

PMAxxTM is a new and improved version of viability dye PMA (propidium monoazide) designed by Biotium (Biotium, Inc., Hayward, CA, United States). Like PMA, PMAxxTM is a photo-reactive dye that binds covalently to DNA with high affinity after photolysis with visible light. The PCR cannot amplify this modified DNA. PMA and PMAxxTM dyes are cell membrane-impermeants. PMAxxTM is described to be more effective than PMA to inhibit DNA PCR amplification of dead cell with injured cell membranes, and therefore provides best discrimination between live and dead bacteria (Han et al., 2018). Commercial PMA and PMAxx solutions (20 mM) (VWR, France) were diluted in pure sterile water to obtain 1.5 mM working solutions kept at -20°C in light-tight microtubes. The samples to be treated were separated in 4 sterile microtubes containing each 580 μL of bacterial cell suspensions in BHI or inoculated SSTH. Twenty microliters of PMA working solution were added in 2 microtubes and 20 μL of PMAxx working solution were added in the remaining 2 tubes (50 μM final concentration). The microtubes were placed in the dark at room temperature

for 10 min, and mixed occasionally for PMA/PMAXx to penetrate into the dead cells. To photoactivate PMA/PMAXx, the PMA-Lite™ LED Photolysis Device (Biotium) was used as recommended by the PMAXx™ manufacturer (Biotium). The PMA-Lite™ LED Photolysis Device is a thermally stable blue LED light source (LED power: 60 W, output wavelength: 465–475 nm) that provides even illumination to the sides and bottoms of all vials. The microtubes were exposed to blue light for 20 min, to ensure complete cross-linking to the available DNA (free DNA or DNA from unviable cells). The content of the 2 microtubes treated with PMA was pooled and 1 mL of the suspension was conserved for further DNA extraction. The same operation was realized for the microtubes treated with PMAXx. For each cell suspension tested in BHI or in SSTH, one milliliter of viable or dead cell suspension was not treated with PMA or PMAXx and used as an untreated control.

PMA and PMAXx treatments were tested on SSTHs in the presence of mixes of dead and viable *B. thermosphacta* cell suspensions. Several mix conditions were tested: (i) 5.65 log CFU/g of dead cells mixed with 4.70, 5.70, or 6.70 log CFU/g of viable cells, and (ii) 7.65 log CFU/g of dead cells mixed with 4.70, 5.70, or 6.70 log CFU/g of viable cells. The samples were treated or not with PMA and PMAXx, as mentioned above. Two controls were also included: (i) 5.70 or 7.70 log CFU/g of viable cells treated or not with PMA/PMAXx, and (ii) 5.70 or 7.70 log CFU/g of dead cells treated or not with PMA/PMAXx.

Extraction of Bacterial DNA

Genomic DNA extraction from bacterial cells cultured in BHI broth was performed using the Qiagen DNeasy Blood and Tissue kit (Qiagen, France). One milliliter of culture was centrifuged at $11,000 \times g$ for 10 min at 4°C (Biofuge Pimor, Heraeus). The supernatant was removed. Bacterial DNA extraction was conducted on cell pellets according to the manufacturer's instructions (Qiagen, France). A Qubit® 2.0 fluorometer using a Qubit® dsDNA BR Assay Kit (Life technologies, Thermo Fisher Scientific, France) was used to quantify the extracted DNA. Extracted DNAs were stored at –20°C until qPCR amplification.

For bacterial DNA extraction in SSTH, one milliliter of SSTH inoculated with *B. thermosphacta* cells was centrifuged at $11,000 \times g$ for 10 min at 4°C. The supernatant was removed, and the pellet was stored at –20°C until use. DNA extraction was performed with the DNeasy PowerFood Microbial kit (Qiagen, France). Briefly, this kit is designed to isolate high-quality genomic DNA from microorganisms hosted in food. The microbial cell pellet from food was thawed and re-suspended in 450 µL of MBL lysis buffer preheated at 55°C for 10 min. The suspension was transferred to PowerBead tubes, containing beads designed for mechanical microbial-cell lysis, and shaken horizontally for 30 s on a Vortex-Genie 2 device (Scientific industries, United States), then on a FastPrep-24 G at 6 m/s for 30 s (MP Biomedicals, France), for mechanical lysis. Each sample was centrifuged at $10,000 \times g$ for 1 min at room temperature. The supernatant was transferred to a microtube, and 100 µL of IRS solution were added. The microtube was incubated on crushed ice for 30 min. The next steps were performed as described in the Qiagen kit instruction manual. DNA samples were stored

at –20°C until use. DNA extracts were diluted 1/10 before the qPCR amplification.

Primer Design and Quantitative Real-Time PCR Assay

A new PCR primer set was designed to amplify a *rpoC* gene DNA fragment specific to *B. thermosphacta*, excluding other *Brochothrix* spp. (*B. campestris*) and closely related species such as *Listeria*. The *in silico* primer design was based on multiple alignment of the DNA-dependent RNA polymerase subunit (*rpoC*) gene sequences of *B. thermosphacta* and closely related species, available from the GenBank database (release 225.0). The *rpoC* sequences from *B. thermosphacta*, *B. campestris* and the most closely related bacterial species were aligned using the CLC DNA Workbench 6.5 (CLC bio, Aarhus, Denmark) and BioEdit sequence alignment software (Hall, 1999). Primer specificity was tested *in silico* using the basic local alignment search tool (BLAST) program [National Center for Biotechnology Information (NCBI)] and Primer BLAST (Ye et al., 2012) using Genbank release 225.0.

Two other previously described primer sets targeting the *rpoC* (Fougy et al., 2016) or *rpoB* (Illikoud et al., 2019) genes were also used (Table 2). AmplifX 2.0.7 software was used to evaluate the quality of the primers (Jullien, 2019). The annealing temperature was optimized using the temperature gradient test of the Bio-Rad CFX connect real-time PCR detection system (Bio-Rad, France).

Quantitative real-time PCR amplification was performed using the Sso Advanced universal SYBR Green supermix (Bio-Rad, France). The reaction was performed in a final volume of 12.5 µL containing 1 µM of each primer, 6.25 µL of 2 X Sso Advanced universal SYBR Green Supermix, 2.75 µL of water (molecular biology grade) and 3 µL of DNA extract. DNA concentrations were standardized at 1 ng/µL for the specificity test. The amplification reaction was conducted using a Bio-Rad CFX connect real-time PCR detection system (Bio-Rad, France). The cycling parameters were as follows: initial denaturation step at 95°C for 3 min, 39 cycles of 95°C for 15 s, and 60°C for 30 s. A melting curve from 65 to 95°C was determined after the last amplification cycle and at a temperature transition rate of 0.5°C/3 s. Quantification cycles (C_q) values were automatically obtained by the Biorad CFX Manager software program. All amplification reactions were run in triplicate in three independent assays.

Efficiency of the Quantitative Real-Time PCR

The efficiency of the qPCR was evaluated by using three different sample preparations. The first two were obtained from *B. thermosphacta* BHI culture: DNA was extracted from a 10-fold serial dilution range of *B. thermosphacta* BHI culture (7 to 2 log CFU/mL) (BHI culture extract), or from an 8 log CFU/mL of *B. thermosphacta* BHI suspension. This DNA extract was then serially diluted 10-fold, corresponding to 7 to 2 log CFU/mL (diluted DNA extract). The third sample preparation corresponded to DNA extracted from SSTHf inoculated with *B. thermosphacta* from 7 to 4 log CFU/mL. The *rpoC* and

TABLE 2 | Description of the three sets of qPCR primers.

Target gene	Primer pair	Primer sequences (5' - 3')	Amplicon size (bp)	Tm (°C)	References
<i>rpoC</i>	rpoC-126-F	ATACTGTACCAATGGTTGCTC	126	52	This study
	rpoC-126-R	CAACAGTGATAACATCAGTTAC			
<i>rpoC</i>	QSF03-BTH-F	GGACCAGAGGTTATCGAAACATTAAGT	151	56	Fougy et al. (2016)
	QSF03-BTH-R	TAATACCAGCAGCAGGAATTGCTT			
<i>rpoB</i>	rpoB-Fw1	GCGTGCATTAGGTTTCAGTACA	394	55	Illikoud et al. (2019)
	rpoB-Rev1	TCCAAGACCAGACTCTAATTGCT			

rpoB sequences were amplified using the three different species-specific primers used in this study in the qPCR conditions described above. The linear standard curves were generated by plotting the C_q values *versus* log CFU/mL to determine the analytical efficiency of the qPCR assay. The efficiency of the real-time PCR assay was calculated from the slope (m) of the standard curve according to equation $E = 10^{(-1/m)} - 1$. The qPCR was performed in three independent assays under the same conditions, using three replicates of each template concentration. The linearity of the standard curve was expressed as a coefficient of determination (r^2).

Limit of Detection (LOD)

The LOD was established in SSTHf for the two primer sets: rpoC-126-F/R (designed in this study) and rpoB-Fw1/Rev1. Ten replicates of 10-fold serial dilutions of *B. thermosphacta* inoculated in SSTHf from 7 to 1 log CFU/mL were prepared. DNA extracts from these inoculated samples were used as qPCR templates in triplicate. Each C_q datum corresponding to the amplification of a PCR product whose melting temperature corresponded to that of the studied gene was considered as a positive signal. The LOD was established by comparing the positive signals and the enumeration of cells on STAA agar and analyzed by a Probit model (Kralik and Ricchi, 2017) with R version 3.3.2 (2016-10-31) (The R Foundation for Statistical Computing). The *p*-value was fixed at 0.05 to detect the gene with 95% probability.

Statistical Analysis

The Shapiro-Wilk's test was used to check the normality of the data. Student's *t*-test or Wilcoxon's test were applied to determine differences between conditions tested (treated vs. untreated cultures, PMA vs. PMAxx treatments, differences of amplification between the 3 primer sets) on viable or dead *B. thermosphacta* cells in BHI broth or SSTH. Homoscedasticity was checked on the values of the standard curves obtained in SSTH using Levene's test. ANOVA was used to control the significant statistical differences between these standard curves. ANOVA, followed by Tukey's multiple comparison of means test was used to analyze the quantification of viable *B. thermosphacta* in cold-smoked salmon fillet sampled after the smoking step. The significant threshold of 5% was established for all the statistical tests. The tests were performed using R version 3.3.2 (2016-10-31) (The R Foundation for Statistical Computing) and the XLSTAT add-in software (version 2020) in Microsoft Excel software 2016.

RESULTS

Primer Design

A new PCR primer set was designed to amplify a fragment of the *B. thermosphacta* *rpoC* gene encoding a DNA-dependent RNA polymerase subunit. The *in silico* primers design was based on multiple alignment of *B. thermosphacta* *rpoC* gene sequences and on those of closely related species available from the GenBank database. Based on this analysis, a region of the *rpoC* gene was selected as a target of the primers design to specifically distinguish *B. thermosphacta* from other related bacterial species examined in this study. The forward primer rpoC-126-F (5'-ATACTGTACCAATGGTTGCTC-3') matched positions 3005 to 3025, and the reverse primer rpoC-126-R (5'-CAACAGTGATAACATCAGTTAC-3') matched positions 3109 to 3130 of the *B. thermosphacta* DSM 20171 type strain *rpoC* gene (accession number X89231), to amplify a specific 126-bp fragment. Two other previously described primer sets targeting the *rpoC* or *rpoB* genes were used. Firstly, the primers QSF03-BTH-F/QSF03-BTH-R targeting the *rpoC* gene (accession number X89231), with a specific 151-bp amplified fragment (Fougy et al., 2016). The forward primer matched positions 2494 to 2521, and the reverse primer matched positions 2621 to 2644 of the *B. thermosphacta* DSM 20171 type strain. Secondly, the primers rpoB-Fw1/Rev1 targeting a specific region of *B. thermosphacta* *rpoB* gene were used (Illikoud et al., 2019). The forward primer rpoB-Fw1 matched positions 609 to 630, and the reverse primer rpoB-Rev1 matched positions 980 to 1022 of the *B. thermosphacta* DSM 20171 type strain *rpoB* gene (Gene ID 29820965), with a specific 394-bp amplified fragment. We selected this later *rpoB* primer, amplifying a longer fragment, because the PCR inhibition effect by PMA can be dependent on the length of the amplification product (Martin et al., 2013).

In silico studies with BLAST program and Primer BLAST using Genbank release 225.0. demonstrated that the primers developed in the present study (rpoC-126-F/R) and those developed by Fougy et al. (2016) and Illikoud et al. (2019) were *B. thermosphacta*-specific. Furthermore, the quality assessment of the designed primers using AmplifX 2.0.7. software revealed no hairpin loop, dimer or duplex formation. The hybridization temperature of the primers was optimized using the temperature gradient test of the Bio-Rad CFX connect real-time PCR detection system (Bio-Rad, France). The 3 sets of primers were tested for qPCR specificity and efficiency.

Specificity of the qPCR Assay

The specificity of the qPCR assay was assessed by inclusivity and exclusivity tests using 26 different bacterial strains including six *B. thermosphacta* strains and 20 non-targeted strains frequently associated with *B. thermosphacta* in seafood products. DNAs were extracted from pure cultures in the appropriate growth conditions (Table 1). The specificity of the three primer sets was verified using the qPCR Cq values obtained with 3 ng of DNA template (Table 3). All the Cq values of the *B. thermosphacta* strains were lower than 16.76 ± 0.05 (rpoC QSF03-BTH-F/R, strain CD340). No amplification signal was observed for six non-targeted strains when the rpoB-Fw1/Rev1 primers were used. The lowest Cq value for a non-targeted strain was 29.48 ± 0.18 (*Staphylococcus epidermidis* CIP 68.21 with the rpoC-126-F/R primers); it was 12.72 Cq above the highest value of the targeted strains, and was considered as the unspecific detection threshold. The primers rpoC QSF03-BTH-F/R produced a single melting peak with Tm values of $81 \pm 0.50^\circ\text{C}$ while the rpoB-Fw1/Rev1 and the rpoC-126-F/R primers generated a single melting peak with a Tm value of $82 \pm 0.50^\circ\text{C}$.

This confirmed the high specificity levels of the three sets of primers. The three primer sets correctly identified all *B. thermosphacta* strains, including reference and food-isolate strains. As none of the tested sets gave specific amplification (<29.48 Cq) when DNA from non-targeted strains was used, the three sets were considered as species-specific by q-PCR.

qPCR Efficiency Using DNA Extracted From BHI Cultures

The qPCR efficiency of the three primer sets tested on BHI culture extracts and on diluted DNA extracts was calculated from the standard curves plotting the mean Cq values (three replicates) versus log CFU/mL (Table 4). The linear coefficient of determination (r^2) ranged from 0.990 (BHI culture extracts; rpoB-Fw1/Rev1) to 1 (diluted DNA extracts; rpoC-126-F/R). Using the primers rpoC-126-F/R (designed for this study), the efficiency levels were 97.45 and 92.58% for diluted DNA extracts and BHI culture extracts, respectively. Using the two other primer set, efficiency was lower and ranged from 89.46 to 92.80%.

TABLE 3 | Primer specificity (Cq values).

Strains	rpoC-126-F/R		QSF03-BTH-F/R		rpoB-Fw1/Rev1	
	Cq values ^a	Range of Tm	Cq values ^a	Range of Tm	Cq values ^a	Range of Tm
<i>Brochothrix thermosphacta</i> DSM 20171 ^T	15.32 ± 0.10	82–82.5	15.45 ± 0.06	81	14.67 ± 0.07	82
<i>Brochothrix thermosphacta</i> 19/R/663	14.42 ± 0.33	82–82.5	14.63 ± 0.05	81	13.94 ± 0.07	82
<i>Brochothrix thermosphacta</i> CD 340	16.43 ± 0.09	82–82.5	16.76 ± 0.05	81–81.5	16.43 ± 0.16	82–82.5
<i>Brochothrix thermosphacta</i> EBP 3084	15.26 ± 0.22	82–82.5	15.44 ± 0.04	81	14.60 ± 0.18	82
<i>Brochothrix thermosphacta</i> TAP 125	15.28 ± 0.18	82–82.5	15.44 ± 0.08	81	14.62 ± 0.14	82
<i>Brochothrix thermosphacta</i> EBP 3017	14.82 ± 0.21	82–82.5	14.93 ± 0.06	81	14.00 ± 0.22	82
<i>Brochothrix campestris</i> 4712 ^T	30.49 ± 0.23	81.5	31.03 ± 0.17	80.5–81	31.52 ± 0.30	82
<i>Carnobacterium maltaromaticum</i> 19/R/671	34.60 ± 0.48	79.5–81.5	36.04 ± 1.10	80.5–82	35.54*	NA
<i>Carnobacterium divergens</i> NCDO 2763 ^T	35.79 ± 0.47	78.5–82.5	35.43 ± 0.65	80–83.5	NA	NA
<i>Enterococcus faecalis</i> ATCC 19433 ^T	35.15 ± 0.68	79–81	35.02 ± 1.14	80.5–81	36.14 ± 1.39	81.5
<i>Enterococcus faecium</i> CIP 54.33	34.57 ± 0.79	80–81	34.37 ± 0.67	79.5–80.5	34.74 ± 1.35	80.5–81
<i>Escherichia coli</i> CIP 53.125	31.39 ± 0.60	87.5	36.88 ± 0.62	75.5–81	NA	NA
<i>Companilactobacillus alimentarius</i> DSM 20181	34.77 ± 1.09	73.5–81.5	36.14 ± 0.74	80.5–81	36.02 ± 0.76	82
<i>Latilactobacillus sakei</i> subsp. <i>sakei</i> DSM 20017 ^T	35.59 ± 0.63	79.5–81.5	36.12 ± 1.19	81–83.5	NA	NA
<i>Lactococcus piscium</i> 19/R/684	34.56 ± 0.92	79.5–82	35.46 ± 1.44	80.5–81.5	35.05 ± 0.84	82
<i>Lactococcus raffinolactis</i> Oniris MIP 2453	36.22 ± 0.10	79.5–80	NA	NA	NA	NA
<i>Listeria monocytogenes</i> DSM 12464 ^T	35.61 ± 0.66	79.5–83	34.12 ± 1.04	84–84.5	36.51 ± 0.99	82
<i>Listeria monocytogenes</i> CIP 78.35	35.37 ± 0.49	79.5–81.5	33.39 ± 1.20	84	35.53*	NA
<i>Listeria grayi</i> CIP 68.18 ^T	365.09 ± 0.22	81.5	35.01 ± 1.26	80.5–81	36.50 ± 0.46	82
<i>Listeria innocua</i> CIP 80.11 ^T	35.71 ± 0.62	79.5–83	36.32*	81	37.07*	76
<i>Photobacterium phosphoreum</i> CIP 102511 ^T	34.59 ± 1.05	81.5–83	35.31 ± 1.48	80.5–81	36.47 ± 0.79	82
<i>Pseudomonas fluorescens</i> CIP 69.13 ^T	34.35 ± 0.50	91	NA	NA	NA	NA
<i>Psychrobacter</i> sp. 19/R/675	35.09 ± 0.40	80.5–82.5	NA	NA	NA	NA
<i>Serratia liquefaciens</i> ATCC 27592 ^T	34.91 ± 0.30	82.5	NA	NA	NA	NA
<i>Shewanella baltica</i> 19/R/670	32.55 ± 0.38	82–87	NA	NA	NA	NA
<i>Staphylococcus epidermidis</i> CIP 68.21	29.48 ± 0.18	81.5–82	29.74 ± 0.22	80.5–81	29.98 ± 0.25	82
NTC	34.87 ± 1.99	72–83	38.58*	76.50	NA	NA

^aMean and standard deviation of three Cq values (obtained with 3 ng of DNA template). NTC, no template control; NA, no amplification. *no standard deviation calculated (only one Cq available).

TABLE 4 | qPCR efficiency.

	rpoC-126-F/R			QSF03-BTH-F/R			rpoB-Fw1/Rev1		
	Equation ^a y =	Efficiency (%)	r ²	Equation ^a y =	Efficiency (%)	r ²	Equation ^a y =	Efficiency (%)	r ²
BHI culture extracts	−3.5136x + 40.558	92.58	0.997	−3.5898x + 41.019	89.92	0.996	−3.5419x + 42.158	91.57	0.990
Diluted DNA extracts	−3.3845 + 40.947	97.45	1	−3.5074x + 41.542	92.80	0.998	−3.6035x + 41.882	89.46	0.995
Smoked salmon tissue homogenate	−3.2408x + 44.396	103.50	0.998	Not determined			−3.5789 + 46.805	90.29	0.998

^aequations derived from 3 replicates.

qPCR Efficiency and Limit of Detection Using DNA Extracted From Smoked Salmon Tissue Homogenates

The rpoC-126-F/R and rpoB-Fw1/Rev1 primer sets, showing the highest qPCR efficiency on BHI culture extracts, were chosen to evaluate efficiency on DNA extracted from SSTHf. DNA was extracted from SSTHf inoculated with *B. thermosphacta* DSM 20171 from 7 to 4 log CFU/mL (SSTHf extract). The efficiency of the qPCR amplification using rpoC-126-F/R and rpoB-Fw1/Rev1 (Table 4) was calculated from standard curves (data not shown) generated by plotting the mean Cq values from three replicates vs. log CFU/mL. When the rpoC-126-F/R primers (designed in this study) were used, an efficiency of 103.50% was obtained. Lower efficiency (90.29%) was calculated with the rpoB-Fw1/Rev1 primers. The linear coefficient of determination (r²) was 0.998 with both primer sets.

The limit of detection (LOD) was calculated using a Probit model (Kralik and Ricchi, 2017), only based on SSTHf. It was established at 3.34 log CFU/mL (2.20×10^3 CFU/mL) for the rpoC-126-F/R primers, corresponding to a load of 4.04 log CFU/g of salmon (1.10×10^4 CFU/g), with a 95% probability to detect the gene. For the rpoB-Fw1/Rev1 primers, the LOD was 3.15 log CFU/mL (1.41×10^3 CFU/mL), corresponding to a load of 3.85 log CFU/g of salmon (7.06×10^3 CFU/g).

PMA-qPCR Quantification of Viable *B. thermosphacta* in BHI Culture

To test the efficiency of the PMA and PMAXx treatments, viable or dead pure-culture *B. thermosphacta* cells were 10-fold serially diluted in BHI (7 to 3 log CFU/mL), and their DNA was extracted after PMA or PMAXx treatment. The qPCR assays using the three primer sets were used to quantify viable *B. thermosphacta*. The results were expressed in delta-Cq (i.e., differences in Cq values between PMA/PMAXx-treated cells/untreated dead cells on the one hand, and Cq values of untreated 100% viable cells on the other hand).

When viable cells were treated with PMA or PMAXx, the delta Cq values were low with the three primer sets (Supplementary Data 1). The minimum and maximum delta-Cq values were obtained with rpoB-Fw1/Rev1 (0.01 ± 0.46 vs. 1.34 ± 0.62 for 4 log CFU/mL of viable PMA-treated cells and 5 log CFU/mL of viable PMAXx-treated cells, respectively). These low delta-Cq values indicated no significant difference in the detection and quantification of *B. thermosphacta* between

viable untreated and dye-treated cells. These observations were statistically in accordance with Wilcoxon's test ($p > 0.4$). Moreover, there was no significant difference between the delta-Cq values following treatment with the two PMA and PMAXx dyes ($p > 0.16$) or between the three primer sets ($p > 0.18$).

When dead cells were used, delta Cq values were higher with PMA/PMAXx-treated cells than with untreated cells. The minimum delta-Cq values were obtained for the 6 log CFU/mL of dead PMA-treated cells with rpoC-126-F/R and rpoC QSF03-BTH-F/R (5.92 ± 0.82 and 5.92 ± 0.83 , respectively). The maximum delta-Cq value (8.57 ± 0.61) was obtained with rpoC QSF03-BTH-F/R for the 7 log CFU/mL of dead PMAXx-treated cells. Interestingly, we failed to calculate delta-Cq values for any cell concentration range when rpoB-Fw1/Rev1 was used with PMA/PMAXx-treated cells, indicating that the Cq values were either beyond the unspecific detection threshold (i.e., 29.48) or even none amplification signal was detected. Thus, there was no significant difference between the two rpoC primer sets, while there was a significant difference between the rpoC primer sets and the rpoB primer set ($p < 0.005$). Finally, there was no significant difference in delta-Cq values between the two PMA/PMAXx dyes ($p > 0.16$), similarly to viable cells.

Because the delta-Cq values obtained with the 2 sets of rpoC primers were similar and the efficiency of the rpoC-QSF03-BTH-F/R primers was lower, we decided to choose rpoC-126-F/R and rpoB-Fw1/Rev1 for further *B. thermosphacta* PMA-qPCR quantification in SSTH.

PMA-qPCR Quantification of Viable *B. thermosphacta* in Smoked Salmon Tissue Homogenates (SSTHf)

We used the rpoC-126-F/R and rpoB-Fw1/Rev1 primer sets to quantify viable *B. thermosphacta* in SSTHf by qPCR. Suspensions of *B. thermosphacta* viable or dead cells in SSTHf were 10-fold serially diluted in SSTHf (7 to 4 log CFU/mL), and their DNA was extracted after PMA or PMAXx treatment.

When viable cells were treated with PMA or PMAXx, delta Cq values were low with the two primer sets (Supplementary Data 1), and the highest value was obtained for 5 log CFU/mL of viable PMA-treated cells with the rpoC-126-F/R primer set (1.20 ± 0.41). The delta-Cq values of viable PMA/PMAXx-treated cells were not significantly different from those of untreated viable cells ($p > 0.05$). Moreover, as previously

shown in BHI broth, there was no significant difference in delta-Cq values between the two PMA/PMAXx dyes ($p > 0.28$) or between the two primer sets ($p > 0.36$). Interestingly, when dead cells were tested, none of the primer sets allowed determining delta-Cq on PMA- or PMAXx- treated cells because Cq values were beyond the detection limit. Therefore, no quantification was possible after dye treatment. When dead cells were not treated with the dyes, the difference between the Cq values of untreated dead cells vs. untreated viable cells was not significantly different ($p > 0.1$), even if the delta Cq ranged from 1.68 ± 0.77 to 2.66 ± 1.32 .

Quantification of Viable *B. thermosphacta* in Cold-Smoked Salmon Fillet Sampled After the Smoking Step (SSTHs)

The PMA and PMAXx treatments were tested on SSTHs in the presence of mixes of dead and viable *B. thermosphacta* cell suspensions. The ability of PMA/PMAXx-qPCR to discriminate viable cells from dead cells in the mixes was evaluated by establishing the relationship between Cq values obtained by qPCR (after PMA/PMAXx treatments or without treatment) and bacterial counts of untreated cells on STAA agar. The results are presented in **Figures 1A,B** and in **Supplementary Data 2**. ANOVA and the Tukey's multiple comparison of means were used to analyze the results. The significance level was set for p -values < 0.05 .

For both primer sets, the quantification of $5.70 \log \text{CFU/g}$ of PMA/PMAXx-treated viable cells was consistent with the quantification of untreated viable cells, with a non-significant difference ($p > 0.05$). Likewise, non-significant difference was observed between the quantification of $7.70 \log \text{CFU/g}$ of PMA/PMAXx-treated viable cells and the untreated viable cells with rpoB-Fw1/Rev1 but a significant difference was observed with the rpoC-126-F/R primers. As previously shown in SSTHf on 5.70 or $7.70 \log \text{CFU/g}$ of dead cells, quantification was only possible with untreated cells, whereas no quantification was possible once the cells were treated with PMA or PMAXx, suggesting that PMA and PMAXx inhibit dead cell DNA amplification.

In the mixes containing $5.65 \log \text{CFU/g}$ of dead cells and 4.70 or $5.70 \log \text{CFU/g}$ of viable cells, no significant difference was highlighted between PMA-treated and untreated cells using rpoB-Fw1/Rev1 but a significant difference was highlighted between PMAXx-treated and untreated cells. When rpoC-126-F/R was used, a significant difference was observed between PMA/PMAXx-treated and untreated cells in those mixes. No treatment-related difference was noticed in the mixes containing $5.65 \log \text{CFU/g}$ of dead cells and $6.70 \log \text{CFU/g}$ of viable cells with rpoB-Fw1/Rev1 whereas a significant difference was observed between PMAXx-treated and untreated cells with rpoC-126-F/R. In the mixes containing $7.65 \log \text{CFU/g}$ of dead cells and 4.70 , 5.70 , or $6.70 \log \text{CFU/g}$ of viable cells, the efficiency of PMA/PMAXx was more obvious: differences between treated and untreated cells were significant with both primer sets, and viable cells were preferentially amplified and quantified. This

shows again the good ability of PMA and PMAXx to inhibit DNA amplification from dead cells.

DISCUSSION

The detection and quantification of unviable cells is admittedly a question of molecular methods targeting the cell DNA directly without culturing steps. This requires methods that discriminate viable cells from unviable cells in biological samples such as food products (Kumar and Ghosh, 2019). In the field of food spoilage, *B. thermosphacta* is considered as one of the main bacteria, able to spoil many meat and seafood products whatever the packaging (i.e., under air, vacuum, or modified atmosphere) (Illikoud et al., 2018a). *B. thermosphacta* is even considered as ubiquitous along the food chain because it was also isolated from food factory surfaces (Nychas et al., 2008). Thus, it can be subjected to the environmental and food processing stresses likely to lead to unviable state, making it difficult to detect and quantify it from food products.

We developed an assay aimed at quantifying viable *B. thermosphacta* using viability dyes (PMA or PMAXx) and the targeting of a single-copy gene (*rpoC* or *rpoB*). After designing the primers *in silico*, we determined their specificity and compared it with that of two other single-copy gene primer sets from previous studies specifically designed to identify *B. thermosphacta* (Fougy et al., 2016; Illikoud et al., 2019). Using the real-time qPCR inclusivity and exclusivity tests, including DNA extracted and purified from 6 *B. thermosphacta* strains and 20 non-targeted closely related strains such as *B. campestris*, we demonstrated the specificity of the three primer sets, without misdetection or misquantification. The difference between targeted and untargeted strains was at least 12.72 Cq . The efficiency of the qPCR assays with the three primer sets was then assessed from the standard curves [$\text{Cq} = f(\text{CFU} (\log/\text{mL}))$]. The most efficient primer set to quantify *B. thermosphacta* from diluted DNA extracts and BHI culture extracts was rpoC-126-F/R, with satisfactory efficiency levels of 97.45% ($r^2 = 1$) and 92.58% ($r^2 = 0.997$), respectively.

We further investigated the efficiency of PMA and PMAXx treatments to quantify viable *B. thermosphacta* cells in BHI medium. As described in many previous studies (Zeng et al., 2016), our results showed that a viable dye treatment was clearly relevant to discriminate viable from unviable bacterial cells. The delta-Cq for dead *B. thermosphacta* cells was higher when PMA or PMAXx treatments were applied than it was for untreated cells, with a difference of at least 3.48 in the delta-Cq values between PMA-treated cells and untreated cells at $6 \log \text{CFU/mL}$ when rpoC QSF03-BTH-F/R was used. These results confirm that the number of amplification cycles is higher after dye treatment when it comes to detecting and quantifying dead *B. thermosphacta* cells rather than viable cells because the amount of amplifiable target DNA is very low when dead cells are treated with dyes. The most important effect of the two dye treatments was also obvious with the *rpoB* primer set: no delta-Cq values were calculable from dead treated cells, meaning that no amplification was possible in these conditions. In the absence of dye treatment, amplification

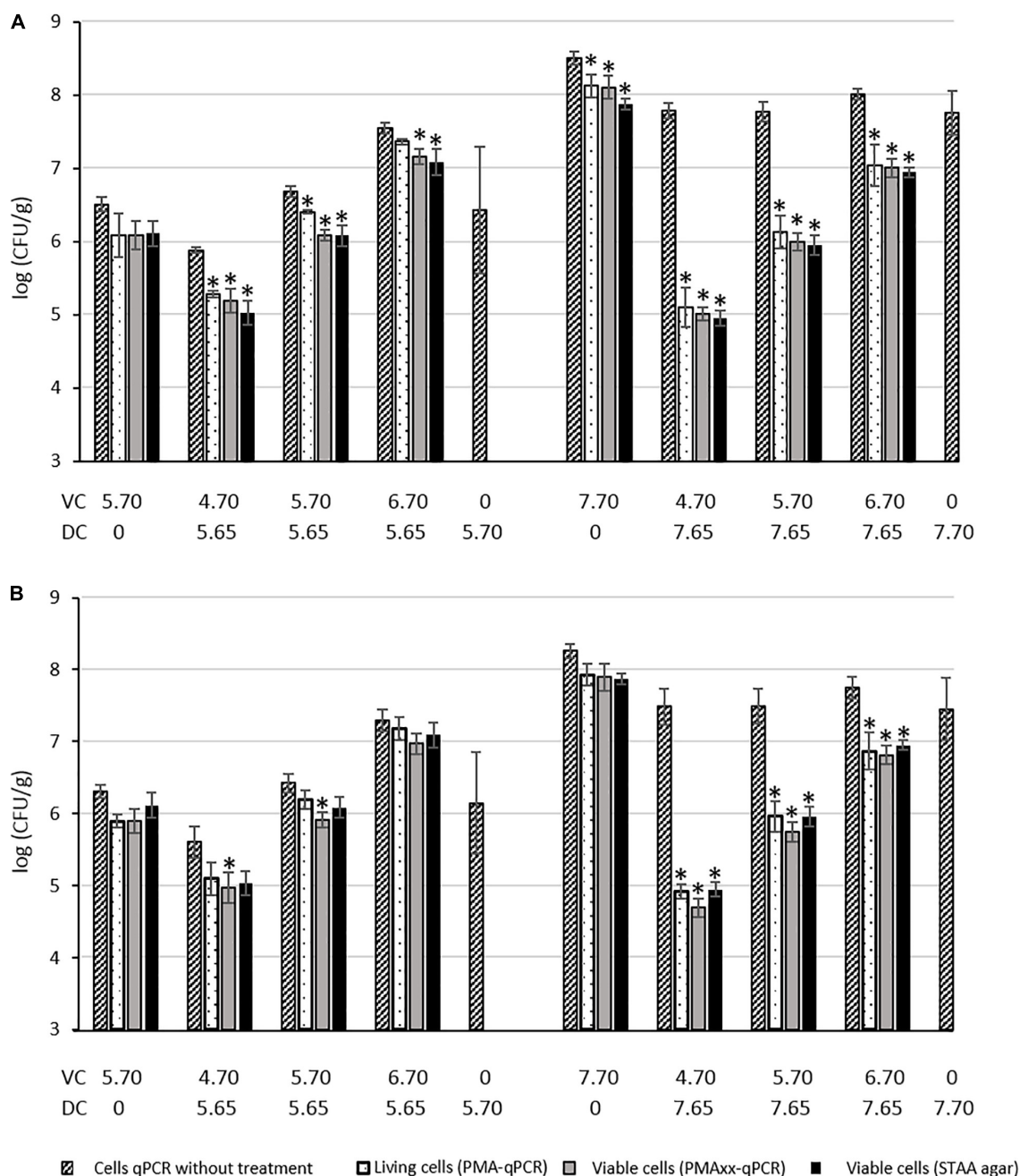


FIGURE 1 | Quantification of dead (DC) and viable (VC) *B. thermosphacta* cells mixed in smoked salmon tissue homogenate (SSTHs) with plating enumeration on STAA medium, and PMA or PMAxx qPCR using the rpoC-126F/R (A) or rpoB-Fw1/Rev1 (B) primer sets. Results expressed in log CFU/g. *significant difference between quantification results of untreated cells obtained by qPCR method and treated cells quantified by qPCR method or plating method.

was still detectable up to 4 log CFU/mL, with a low associated delta-Cq value (1.76 ± 0.70).

Regarding the two *rpoC* primer sets, they gave quite similar results on viable and dead cells. However, whatever the primer set, there was no significant difference between the PMA and PMAxx treatments, with similar delta-Cq values for the two conditions. Because the delta-Cq values obtained with both *rpoC* primer sets were quite similar and rpoC-126F/R was slightly

more efficient than rpoC-QSF03-BTH-F/R was, we only kept rpoC-126F/R for the further tests on SSTH.

The good efficiency of rpoC-126F/R was confirmed on smoked salmon tissue homogenate (SSTHf), with 103.50% ($r^2 = 0.998$), while rpoB-Fw1/Rev1 showed 90.29% ($r^2 = 0.998$) efficiency. We also determined the limit of detection (LOD) of the qPCR assays on SSTHf, but not on BHI, to be closest to a real food product. The LODs were established at 4.04 and 3.85

log CFU/g of smoked salmon for *rpoC*-126F/R and *rpoB*-Fw1/Rev1, respectively. We considered these LODs as relevant according to the food spoilage behavior of *B. thermosphacta*. In most of the reported cases of food spoilage, the amount of *B. thermosphacta* in the spoiled foods was above 7 log CFU/g when spoilage was perceived by sensory analysis panelists (Illikoud et al., 2018a). With our *rpoC* or *rpoB* qPCR assays, we detected the presence of *B. thermosphacta* around 3 log before spoilage perception. This could give smoked salmon producers the opportunity to redirect their matrices before spoilage by *B. thermosphacta* to other transformation processes with a strong stabilization step – e.g., pasteurization – to kill the spoilage agent and limit food losses. The results of the qPCR assays after PMA or PMAxx treatment of viable smoked salmon tissue homogenate were similar to those of viable cells cultured in BHI, with low delta-Cq values and no significant difference between the primer sets. Nevertheless, the effect of the dye treatments on dead cells was more obvious than it was on BHI-cultured cells because no delta-Cq value was calculable on treated dead cells for either primer set. Therefore, no amplification was possible with these primer sets after dye treatment of dead cells. By contrast, amplification was still detectable down to 4 log CFU/mL in untreated cells, with a low associated delta-Cq value (1.74 ± 0.52 and 2.66 ± 1.32 for the *rpoC* and *rpoB* primer sets, respectively).

The efficiency of PMA/PMAxx-qPCR to discriminate viable *B. thermosphacta* cells from dead cells was also confirmed on industrially processed cold-smoked salmon fillets after the smoking step (SSTHs). The DNA amplification of 5.70 or 7.70 log CFU/g of *B. thermosphacta* dead cells inoculated on SSTHs was inhibited by PMA and PMAxx, whereas qPCR amplification was consistently detectable in the absence of dye treatment. This efficiency was even more obvious in mixed viable/dead-cell conditions, with significantly different quantifications between the treated and the untreated cells with both primer sets. However, we did not find any significant difference between the two primer sets, except for the mixes containing 5.65 log CFU/g of dead cells + 4.70 or 5.70 log CFU/g of PMA/PMAxx-treated viable cells and 5.65 log CFU/g of dead cells + 6.70 log CFU/g of PMAxx-treated viable cells where *rpoC*-126F/R better discriminated between treated and untreated cells. Moreover, we did not find a better PCR inhibition by PMA or PMAxx with the longer *rpoB* amplicon (394 bp), as previously described by Martin et al. (2013), compared with the shorter *rpoC* amplicons (126 or 151 bp). Consequently, our results suggest using *rpoC*-126-F/R coupled with PMA or PMAxx treatment to specifically quantify *B. thermosphacta* with good efficiency and reliable discrimination between viable and dead cells in cold-smoked salmon samples.

In the last two decades, many studies have described the interest of molecular methods such as real-time quantitative PCR to detect and quantify a lot of bacterial species in food or other ecosystems instead of the classical culture methods (Postollec et al., 2011; Franco-Duarte et al., 2019), but also the usefulness of viability dyes such as EMA or PMA to discriminate viable cells from unviable or dead cells (Elizaquível et al., 2014; Zeng et al., 2016). Regarding *B. thermosphacta*,

only one study demonstrates the interest of PMA coupled with 16S rDNA-qPCR to detect and quantify this spoilage bacterium in cooked peeled shrimp (Mamlouk et al., 2012). These authors found a better LOD than ours (2.07 log CFU/g of cooked shrimp) with a similar efficiency of 105.3% ($r^2 = 0.999$). Nevertheless, their LOD was not determined from the food matrix, as it is in the present study, but from purified genomic *B. thermosphacta* DNA serially diluted 10-fold in sterile saline solution and subjected to real-time PCR amplification. Consequently, these conditions reduce the potential presence of PCR inhibitors likely present in food matrices and able to influence on qPCR efficiency, hence a shift of the LOD (Sidstedt et al., 2020).

The new viability dye PMAxx was developed recently. It improves the discrimination between viable and unviable cells (Randazzo et al., 2016). Few studies have been conducted with this new dye so far (Truchado et al., 2020) used it to detect and quantify VBNC *L. monocytogenes* cells in wash water from processed fruit and vegetables. It has also been used to quantify *L. monocytogenes* in chocolate liquor, corn flakes, and dry-roasted, shelled pistachios (Ly et al., 2020), quantify viable and non-viable *Salmonella* from a poultry environment (Zhang et al., 2020), quantify viable *Campylobacter* in raw milk (Wulsten et al., 2020), detect *Clavibacter michiganensis* in a viable but non-culturable state in tomato (Han et al., 2018), discriminate between viable and membrane-damaged cells of the plant pathogen *Xylella fastidiosa* (Sicard et al., 2019) or quantify VBNC *Vibrio parahaemolyticus* in raw shrimp (Cao et al., 2019). Among all these studies, three of them have compared this new dye with other available dyes, notably EMA or PMA. Two of them have demonstrated a higher suitability of PMAxx than PMA to quantify bacteria in food matrices (Han et al., 2018; Cao et al., 2019). By contrast, another study found PMA more suitable than EMA and PMAxx to detect and quantify viable bacterial cells (Wulsten et al., 2020). Other authors even reported the use of a combination of EMA and PMAxx to reduce the DNA signal from dead cells (with intact and damaged membranes) and viable cells with inactive membranes (Truchado et al., 2020). The use of the EMA-PMAxx combination yielded a more accurate estimation of viable *L. monocytogenes* cells. Our results did not allow us to clearly distinguish between PMAxx and PMA in their efficiency to discriminate viable *B. thermosphacta* cells from unviable ones in cold-smoked salmon: they gave similar results in most of the tested conditions.

In conclusion, we developed a rapid, specific and efficient *rpoC* PMA/PMAxx-qPCR method to detect and quantify *B. thermosphacta* in pure culture and in cold-smoked salmon samples, with efficient discrimination between viable and dead cells. This qPCR method specifically and quickly enumerates *B. thermosphacta* (within 3–4 h compared with 48 h for the STAA culture method). Moreover, this PMA/PMAxx-qPCR could be a relevant tool for smoked salmon producers to (i) quickly detect and quantify *B. thermosphacta* in their products early enough before spoilage is perceived and (ii) limit food losses. Finally, this *rpoC* PMA/PMAxx-qPCR method could be used to detect and quantify *B. thermosphacta* in other seafood products and even in other food matrices such as meat products.

DATA AVAILABILITY STATEMENT

The original contributions presented in the study are included in the article/**Supplementary Material**, further inquiries can be directed to the corresponding author/s.

AUTHOR CONTRIBUTIONS

AB-A, EJ, HP, and XD conceived and designed the experiments. AB-A contributed to reagents, materials, and analysis tools. AB-A and SS performed the experiments. AB-A, EJ, and HP wrote the manuscript. All authors analyzed the data, contributed to the article, and approved the submitted version.

REFERENCES

- Cao, X., Zhao, L., Zhang, J., Chen, X., Shi, L., Fang, X., et al. (2019). Detection of viable but nonculturable *Vibrio parahaemolyticus* in shrimp samples using improved real-time PCR and real-time LAMP methods. *Food Control* 103, 145–152. doi: 10.1016/j.foodcont.2019.04.003
- Casaburi, A., De Filippis, F., Villani, F., and Ercolini, D. (2014). Activities of strains of *Brochothrix thermosphacta* in vitro and in meat. *Food Res. Int.* 62, 366–374. doi: 10.1016/j.foodres.2014.03.019
- Case, R. J., Boucher, Y., Dahllof, I., Holmstrom, C., Doolittle, W. F., and Kjelleberg, S. (2007). Use of 16S rRNA and rpoB Genes as Molecular Markers for Microbial Ecology Studies. *Appl. Environ. Microbiol.* 73, 278–288. doi: 10.1128/AEM.01177-06
- Castro, A. G. S. A., Dorneles, E. M. S., Santos, E. L. S., Alves, T. M., Silva, G. R., Figueiredo, T. C., et al. (2018). Viability of *Campylobacter* spp. in frozen and chilled broiler carcasses according to real-time PCR with propidium monoazide pretreatment. *Poultry Sci.* 97, 1706–1711. doi: 10.3382/ps/pey020
- Chaillou, S., Chaulot-Talmon, A., Caekebeke, H., Cardinal, M., Christeans, S., Denis, C., et al. (2015). Origin and ecological selection of core and food-specific bacterial communities associated with meat and seafood spoilage. *ISME J.* 9, 1105–1118. doi: 10.1038/ismej.2014.202
- Dainty, R. H., and Mackey, B. M. (1992). The relationship between the phenotypic properties of bacteria from chill-stored meat and spoilage processes. *J. Appl. Bacteriol.* 73, 103s–114s. doi: 10.1111/j.1365-2672.1992.tb03630.x
- Desneux, J., Chemaly, M., and Pourcher, A.-M. (2015). Experimental design for the optimization of propidium monoazide treatment to quantify viable and non-viable bacteria in piggy effluents. *BMC Microbiol.* 15:505–506. doi: 10.1186/s12866-015-0505-6
- Dong, L., Liu, H., Meng, L., Xing, M., Wang, J., Wang, C., et al. (2018). Quantitative PCR coupled with sodium dodecyl sulfate and propidium monoazide for detection of viable *Staphylococcus aureus* in milk. *J. Dairy Sci.* 101, 4936–4943. doi: 10.3168/jds.2017-14087
- Elizaquivel, P., Aznar, R., and Sánchez, G. (2014). Recent developments in the use of viability dyes and quantitative PCR in the food microbiology field. *J. Appl. Microbiol.* 116, 1–13. doi: 10.1111/jam.12365
- Elizaquivel, P., Sánchez, G., Selma, M. V., and Aznar, R. (2012). Application of propidium monoazide-qPCR to evaluate the ultrasonic inactivation of *Escherichia coli* O157:H7 in fresh-cut vegetable wash water. *Food Microbiol.* 30, 316–320. doi: 10.1016/j.fm.2011.10.008
- Fang, J., Wu, Y., Qu, D., Ma, B., Yu, X., Zhang, M., et al. (2018). Propidium monoazide real-time loop-mediated isothermal amplification for specific visualization of viable *Salmonella* in food. *Lett. Appl. Microbiol.* 67, 79–88. doi: 10.1111/lam.12992
- Fougy, L., Desmonts, M.-H., Coeuret, G., Fassel, C., Hamon, E., Hézard, B., et al. (2016). Reducing Salt in Raw Pork Sausages Increases Spoilage and Correlates with Reduced Bacterial Diversity. *Appl. Environ. Microbiol.* 82, 3928–3939. doi: 10.1128/AEM.00323-16
- Franco-Duarte, R., Černáková, L., Kadam, S., Kaushik, K., Salehi, B., Bevilacqua, A., et al. (2019). Advances in Chemical and Biological Methods to Identify Microorganisms—From Past to Present. *Microorganisms* 7:microorganisms7050130. doi: 10.3390/microorganisms7050130

ACKNOWLEDGMENTS

We thank Vincent Gelamur and Julie Courtel from MerAlliance, Thai Union company, for the smoked salmon samples that were kindly provided. We thank the “Pays de la Loire” Region for financial support (Project Number n 2017-06930).

SUPPLEMENTARY MATERIAL

The Supplementary Material for this article can be found online at: <https://www.frontiersin.org/articles/10.3389/fmicb.2021.654178/full#supplementary-material>

- Furet, J.-P., Firmesse, O., Gourmelon, M., Bridonneau, C., Tap, J., Mondot, S., et al. (2009). Comparative assessment of human and farm animal faecal microbiota using real-time quantitative PCR. *FEMS Microbiol. Ecol.* 68, 351–362. doi: 10.1111/j.1574-6941.2009.00671.x
- Hall, T. A. (1999). BioEdit: A User-Friendly Biological Sequence Alignment Editor and Analysis Program for Windows 95/98/NT. *Nucleic Acids Symposium Ser.* 41, 95–98. doi: 10.14601/Phytopathol_Mediterr-14998u1.29
- Han, S., Jiang, N., Lv, Q., Kan, Y., Hao, J., Li, J., et al. (2018). Detection of *Clavibacter michiganensis* subsp. *michiganensis* in viable but nonculturable state from tomato seed using improved qPCR. *PLoS One* 13:e0196525. doi: 10.1371/journal.pone.0196525
- Illikoud, N., Jaffrès, E., and Zagorec, M. (2018a). “*Brochothrix thermosphacta*,” in *Reference Module in Life Sciences*, ed. B. D. Roitberg (Amsterdam: Elsevier), doi: 10.1016/B978-0-12-809633-8.12106-5
- Illikoud, N., Klopp, C., Roulet, A., Bouchez, O., Marsaud, N., Jaffrès, E., et al. (2018b). One complete and three draft genome sequences of four *Brochothrix thermosphacta* strains, CD 337, TAP 175, BSAS1 3 and EBP 3070. *Standards Genomic Sci.* 13:0333–z. doi: 10.1186/s40793-018-0333-z
- Illikoud, N., Rosso, A., Chauvet, R., Courcoux, P., Pilet, M.-F., Charrier, T., et al. (2019). Genotypic and phenotypic characterization of the food spoilage bacterium *Brochothrix thermosphacta*. *Food Microbiol.* 81, 22–31. doi: 10.1016/j.fm.2018.01.015
- Jaffrès, E., Lalanne, V., Macé, S., Cornet, J., Cardinal, M., Sérot, T., et al. (2011). Sensory characteristics of spoilage and volatile compounds associated with bacteria isolated from cooked and peeled tropical shrimps using SPME–GC–MS analysis. *Int. J. Food Microbiol.* 147, 195–202. doi: 10.1016/j.ijfoodmicro.2011.04.008
- Jaffrès, E., Sohler, D., Leroi, F., Pilet, M. F., Prévost, H., Joffraud, J. J., et al. (2009). Study of the bacterial ecosystem in tropical cooked and peeled shrimps using a polyphasic approach. *Int. J. Food Microbiol.* 131, 20–29. doi: 10.1016/j.ijfoodmicro.2008.05.017
- Joffraud, J. J., Leroi, F., Roy, C., and Berdagué, J. L. (2001). Characterisation of volatile compounds produced by bacteria isolated from the spoilage flora of cold-smoked salmon. *Int. J. Food Microbiol.* 66, 175–184. doi: 10.1016/S0168-1605(00)00532-8
- Joffraud, J.-J., Cardinal, M., Cornet, J., Chasles, J.-S., Léon, S., Gigout, F., et al. (2006). Effect of bacterial interactions on the spoilage of cold-smoked salmon. *Int. J. Food Microbiol.* 112, 51–61. doi: 10.1016/j.ijfoodmicro.2006.05.014
- Josefsen, M. H., Lofstrom, C., Hansen, T. B., Christensen, L. S., Olsen, J. E., and Hoorfar, J. (2010). Rapid Quantification of Viable *Campylobacter* Bacteria on Chicken Carcasses, Using Real-Time PCR and Propidium Monoazide Treatment, as a Tool for Quantitative Risk Assessment. *Appl. Environ. Microbiol.* 76, 5097–5104. doi: 10.1128/AEM.00411-10
- Julien, N. (2019). *Aix-Marseille Univ, CNRS. Marseille: INP, Inst Neurophysiopathol.*
- Kralik, P., and Ricchi, M. (2017). A Basic Guide to Real Time PCR in Microbial Diagnostics: Definitions, Parameters, and Everything. *Front. Microbiol.* 8:00108. doi: 10.3389/fmicb.2017.00108
- Kreader, C. A. (1996). Relief of amplification inhibition in PCR with bovine serum albumin or T4 gene 32 protein. *Appl. Environ. Microbiol.* 62, 1102–1106. doi: 10.1128/AEM.62.3.1102-1106.1996

- Kuchta, T., Knutsson, R., Fiore, A., Kudirkienė, E., Höhl, A., Horvatek Tomic, D., et al. (2014). A decade with nucleic acid-based microbiological methods in safety control of foods. *Lett. Appl. Microbiol.* 59, 263–271. doi: 10.1111/lam.12283
- Kumar, S. S., and Ghosh, A. R. (2019). Assessment of bacterial viability: a comprehensive review on recent advances and challenges. *Microbiology* 165, 593–610. doi: 10.1099/mic.0.000786
- Laursen, B. G., Leisner, J. J., and Dalgaard, P. (2006). *Carnobacterium* Species: Effect of Metabolic Activity and Interaction with *Brochothrix thermosphacta* on Sensory Characteristics of Modified Atmosphere Packed Shrimp. *J. Agric. Food Chem.* 54, 3604–3611. doi: 10.1021/jf053017f
- Liang, N., Dong, J., Luo, L., and Li, Y. (2011). Detection of Viable *Salmonella* in Lettuce by Propidium Monoazide Real-Time PCR. *J. Food Sci.* 76, M234–M237. doi: 10.1111/j.1750-3841.2011.02123.x
- Ly, V., Parreira, V. R., Sanchez-Maldonado, A. F., and Farber, J. M. (2020). Survival and Virulence of *Listeria monocytogenes* during Storage on Chocolate Liquor, Corn Flakes, and Dry-Roasted Shelled Pistachios at 4 and 23°C. *J. Food Prot.* 83, 1852–1862. doi: 10.4315/JFP-20-129
- Macé, S., Mamlouk, K., Chipchakova, S., Prévost, H., Joffraud, J.-J., Dalgaard, P., et al. (2013). Development of a Rapid Real-Time PCR Method as a Tool To Quantify Viable *Photobacterium phosphoreum* Bacteria in Salmon (*Salmo salar*) Steaks. *Appl. Environ. Microbiol.* 79, 2612–2619. doi: 10.1128/AEM.03677-12
- Mamlouk, K., Macé, S., Guilbaud, M., Jaffrès, E., Ferchichi, M., Prévost, H., et al. (2012). Quantification of viable *Brochothrix thermosphacta* in cooked shrimp and salmon by real-time PCR. *Food Microbiol.* 30, 173–179. doi: 10.1016/j.fm.2011.09.012
- Martin, B., Raurich, S., Garriga, M., and Aymerich, T. (2013). Effect of Amplicon Length in Propidium Monoazide Quantitative PCR for the Enumeration of Viable Cells of *Salmonella* in Cooked Ham. *Food Anal. Methods* 6, 683–690. doi: 10.1007/s12161-012-9460-0
- Mejlholm, O., Boknaes, N., and Dalgaard, P. (2005). Shelf life and safety aspects of chilled cooked and peeled shrimps (*Pandalus borealis*) in modified atmosphere packaging. *J. Appl. Microbiol.* 99, 66–76. doi: 10.1111/j.1365-2672.2005.02582.x
- Niu, B., Hong, B., Zhang, Z., Mu, L., Malakar, P. K., Liu, H., et al. (2018). A Novel qPCR Method for Simultaneous Detection and Quantification of Viable Pathogenic and Non-pathogenic *Vibrio parahaemolyticus* (tlh+, tdh+, and ureR+). *Front. Microbiol.* 9:01747. doi: 10.3389/fmicb.2018.01747
- Nychas, G.-J. E., Skandamis, P. N., Tassou, C. C., and Koutsoumanis, K. P. (2008). Meat spoilage during distribution. *Meat Sci.* 78, 77–89. doi: 10.1016/j.meatsci.2007.06.020
- Pan, Y., and Breidt, F. (2007). Enumeration of Viable *Listeria monocytogenes* Cells by Real-Time PCR with Propidium Monoazide and Ethidium Monoazide in the Presence of Dead Cells. *Appl. Environ. Microbiol.* 73, 8028–8031. doi: 10.1128/AEM.01198-07
- Paoli, G. C., Wijey, C., Nguyen, L.-H., Chen, C.-Y., Yan, X., and Irwin, P. L. (2017). Complete Genome Sequences of Two Strains of the Meat Spoilage Bacterium *Brochothrix thermosphacta* Isolated from Ground Chicken. *Genome Announcem.* 5, 1357–1317. doi: 10.1128/genomeA.01357-17
- Pennacchia, C., Ercolini, D., and Villani, F. (2009). Development of a Real-Time PCR assay for the specific detection of *Brochothrix thermosphacta* in fresh and spoiled raw meat. *Int. J. Food Microbiol.* 134, 230–236. doi: 10.1016/j.ijfoodmicro.2009.07.005
- Postollec, F., Falentin, H., Pavan, S., Combrisson, J., and Sohier, D. (2011). Recent advances in quantitative PCR (qPCR) applications in food microbiology. *Food Microbiol.* 28, 848–861. doi: 10.1016/j.fm.2011.02.008
- Randazzo, W., López-Gálvez, F., Allende, A., Aznar, R., and Sánchez, G. (2016). Evaluation of viability PCR performance for assessing norovirus infectivity in fresh-cut vegetables and irrigation water. *Int. J. Food Microbiol.* 229, 1–6. doi: 10.1016/j.ijfoodmicro.2016.04.010
- Remenant, B., Jaffrès, E., Dousset, X., Pilet, M.-F., and Zagorec, M. (2015). Bacterial spoilers of food: Behavior, fitness and functional properties. *Food Microbiol.* 45, 45–53. doi: 10.1016/j.fm.2014.03.009
- Schrader, C., Schielke, A., Ellerbroek, L., and Johne, R. (2012). PCR inhibitors - occurrence, properties and removal. *J. Appl. Microbiol.* 113, 1014–1026. doi: 10.1111/j.1365-2672.2012.05384.x
- Sicard, A., Merfa, M. V., Voeltz, M., Zeilinger, A. R., De La Fuente, L., and Almeida, R. P. P. (2019). Discriminating between viable and membrane-damaged cells of the plant pathogen *Xylella fastidiosa*. *PLoS One* 14:e0221119. doi: 10.1371/journal.pone.0221119
- Sidstedt, M., Rådström, P., and Hedman, J. (2020). PCR inhibition in qPCR, dPCR and MPS-mechanisms and solutions. *Anal. Bioanal. Chem.* 412, 2009–2023. doi: 10.1007/s00216-020-02490-2
- Stackebrandt, E., and Jones, D. (2006). “The Genus *Brochothrix*,” in *The Prokaryotes*, eds M. Dworkin, S. Falkow, E. Rosenberg, K.-H. Schleifer, and E. Stackebrandt (New York, NY: Springer), 477–491. doi: 10.1007/0-387-30744-3_12
- Stohr, V., Joffraud, J. J., Cardinal, M., and Leroi, F. (2001). Spoilage potential and sensory profile associated with bacteria isolated from cold-smoked salmon. *Food Res. Int.* 34, 797–806. doi: 10.1016/S0963-9969(01)00101-6
- Truchado, P., Gil, M. I., Larrosa, M., and Allende, A. (2020). Detection and Quantification Methods for Viable but Non-culturable (VBNC) Cells in Process Wash Water of Fresh-Cut Produce: Industrial Validation. *Front. Microbiol.* 11:673. doi: 10.3389/fmicb.2020.00673
- Wulsten, I. F., Galeev, A., and Stingl, K. (2020). Underestimated Survival of *Campylobacter* in Raw Milk Highlighted by Viability Real-Time PCR and Growth Recovery. *Front. Microbiol.* 11:1107. doi: 10.3389/fmicb.2020.01107
- Ye, J., Coulouris, G., Zaretskaya, I., Cutcutache, I., Rozen, S., and Madden, T. L. (2012). Primer-BLAST: a tool to design target-specific primers for polymerase chain reaction. *BMC Bioinform.* 13:134. doi: 10.1186/1471-2105-13-134
- Zeng, D., Chen, Z., Jiang, Y., Xue, F., and Li, B. (2016). Advances and Challenges in Viability Detection of Foodborne Pathogens. *Front. Microbiol.* 7:1833. doi: 10.3389/fmicb.2016.01833
- Zhang, J., Khan, S., and Chousalkar, K. K. (2020). Development of PMAXxTM-Based qPCR for the Quantification of Viable and Non-viable Load of *Salmonella* From Poultry Environment. *Front. Microbiol.* 11:581201. doi: 10.3389/fmicb.2020.581201
- Zhang, Z., Liu, W., Xu, H., Aguilar, Z. P., Shah, N. P., and Wei, H. (2015). Propidium monoazide combined with real-time PCR for selective detection of viable *Staphylococcus aureus* in milk powder and meat products. *J. Dairy Sci.* 98, 1625–1633. doi: 10.3168/jds.2014-8938
- Zhou, B., Liang, T., Zhan, Z., Liu, R., Li, F., and Xu, H. (2017). Rapid and simultaneous quantification of viable *Escherichia coli* O157:H7 and *Salmonella* spp. in milk through multiplex real-time PCR. *J. Dairy Sci.* 100, 8804–8813. doi: 10.3168/jds.2017-13362
- Zhu, R.-G., Li, T.-P., Jia, Y.-F., and Song, L.-F. (2012). Quantitative study of viable *Vibrio parahaemolyticus* cells in raw seafood using propidium monoazide in combination with quantitative PCR. *J. Microbiol. Methods* 90, 262–266. doi: 10.1016/j.mimet.2012.05.019

Conflict of Interest: The authors declare that the research was conducted in the absence of any commercial or financial relationships that could be construed as a potential conflict of interest.

Copyright © 2021 Bouju-Albert, Saltaji, Dousset, Prévost and Jaffrès. This is an open-access article distributed under the terms of the Creative Commons Attribution License (CC BY). The use, distribution or reproduction in other forums is permitted, provided the original author(s) and the copyright owner(s) are credited and that the original publication in this journal is cited, in accordance with accepted academic practice. No use, distribution or reproduction is permitted which does not comply with these terms.



Bruise Susceptibility and Impact on Quality Parameters of Pears During Storage

Pankaj B. Pathare* and Mai Al-Dairi

Department of Soils, Water and Agricultural Engineering, College of Agricultural and Marine Sciences, Sultan Qaboos University, Muscat, Oman

OPEN ACCESS

Edited by:

Anindya Chanda,
Mycologics LLC, United States

Reviewed by:

Joseph D. Eifert,
Virginia Tech, United States
Santanu Basu,
Swedish University of Agricultural
Sciences, Sweden

*Correspondence:

Pankaj B. Pathare
pankaj@squ.edu.om;
pbpathare@gmail.com

Specialty section:

This article was submitted to
Agro-Food Safety,
a section of the journal
Frontiers in Sustainable Food Systems

Received: 25 January 2021

Accepted: 30 June 2021

Published: 04 August 2021

Citation:

Pathare PB and Al-Dairi M (2021)
Bruise Susceptibility and Impact on
Quality Parameters of Pears During
Storage.
Front. Sustain. Food Syst. 5:658132.
doi: 10.3389/fsufs.2021.658132

Bruise damage is one of the mechanical injury problems that could appear in fresh produce during the post-harvest supply chain. The study investigated three main effects (drop impact level, storage temperature, and storage duration), which can expand the level of bruising and cause some quality changes that contribute to the damage of pear. Pear fruit samples were purchased from the market and delivered to the post-harvest laboratory. Each pear was impacted by a ball with a known mass at three different drop heights (20, 40, and 60 cm), stored at 22°C with 45 ± 5% RH and 10°C with 85 ± 5% RH for 14 days storage period. Bruise area (BA), bruise volume (BV), and bruise susceptibility (BS) were calculated. Different quality analyses were done like color, firmness, and total soluble solids (TSS). Analysis of variance (ANOVA), regression analysis, and pearson correlation coefficient were performed. With increasing drop height and temperature for 14 days storage, BA, BV, BS, lightness (L^*), yellowness (b^*), color saturation (Chroma), and total color difference increased. However, firmness was highly reduced (92.82%) due to the increase in drop height (60 cm), storage temperature (22°C), and storage duration (14 days). Color purity (Hue), redness (a^*), and TSS were not affected by drop height (impact level). A strong relationship with a strong linear regression (R^2) was found between BS and CIE L^* , a^* , and b^* color coordinates. A positive and strong correlation was also found between BS and CIEL*a*b* color parameters with a strong and negative correlation with firmness. Overall, this study can be considered as guideline for horticulture researchers and in fresh produce supply chain during post-harvest operations.

Keywords: bruising, color, firmness, drop height, pear, storage temperature

INTRODUCTION

Pear (*Pyrus* spp.) ranked second among the fruit produced and consumed in the world (Lipa et al., 2019). Pears are among the highly perishable agricultural products and have a lower storability compared to an apple, and at the same time, they are sensitive to inappropriate conditions during harvest, transport, and reloading. Impacts cause irreversible damage to the external and internal structure, consisting mostly in the mechanical deformation of both the fruit peel and the spatial deformation of flesh cells. The attractiveness of the pear is determined by the lack of mechanical defects on the fruit surface. As reviewed by Hussein et al. (2020b), bruising is the most common type

of mechanical damage that reduces fruit quality and causing considerable post-harvest losses. The presence of bruising and other types of mechanical damage (cuts, puncture, split, abrasion) causes significant economic loss of fresh produce due to downgrading or rejection of the appearance quality by the consumer. Besides, bruising can result in weight loss in fruit and vegetable and hence a decrease in their market value. So, minimizing the post-harvest losses and enhancing the storage potential are the major goals for growers.

Bruising is the most prevalent form of mechanical damage in many fruits, which is caused largely by excessive impact and/or compression forces concentrated on a small area of the fruit surface against a rigid body or fruit against fruit mainly involved during mechanical handling (Pathare and Al-Dairi, 2021). Furthermore, bruise damage modifies physiological and metabolic processes, leading to faster ripening, internal browning, and quality losses (Opara and Pathare, 2014; Costa et al., 2018; Hussein et al., 2019). Minor bruise damage on the “Galaxy” apple resulted in a decrease in firmness and fruit browning (Ergun, 2017). Similarly, bruising damage accelerated loss of firmness and the ratio of sugar to acid for Yali pears (Li et al., 2012). Bruising reduced firmness and weight loss of packaged kiwifruit after 10 days of storage (Xia et al., 2020). Decreased weight of the fruit and the unsightly shriveling lead to economic losses (Al-Dairi et al., 2021d). As one of the important quality attributes in fruit production, the fruit weight influences not only consumer preference but also the marketing of fresh fruit (Al-Dairi et al., 2021a). Impact bruising resulted in both the qualitative internal and minor external changes on fresh produce, including changes in citric acid content (Hussein et al., 2020b), soluble solid content, (Gao et al., 2021), respiration, and ethylene production (Xia et al., 2020).

Opara and Pathare (2014) highlighted the importance of bruise damage measurement or analysis in aiding interventions to inhibit quality changes. Recently, Hussein et al. (2020b) reported 40% weight loss of bruised pomegranate fruit during long cold storage. Bruising of fresh fruits during harvest and post-harvest processing is a major problem in the horticultural industry, particularly on fruit such as pears, which are highly sensitive to mechanical damage (Komarnicki et al., 2016). Damage is largely a result of the impact, particularly during sorting, grading, and packing operations. Based on our knowledge, the majority of the studies focused on the impact of bruising on pear and other fresh produce stored at one storage condition. However, the current study comprises the effect of different drop heights (20, 40, and 60 cm) and two storage temperature (10 and 22°C) for 14 days experimental period on pear quality changes. This can help to understand the mechanism of bruising and how to reduce it. Therefore, the objective of this study is to determine the extent of bruising [bruise area (BA), bruise volume (BV), and bruise susceptibility (BS)] and other quality attribute changes [color, firmness, and total soluble solids (TSS)] of pear as affected by drop impact levels, storage temperatures, and storage duration for 14 days. Besides, regression analyses between BS and the studied quality attributes during 14 days of storage were done.

MATERIALS AND METHODS

Pear Sample Preparation

Fresh pears *Pyrus communis*, variety “D’Anjou,” were purchased from the market (23°35′10.5″N latitudes and 58°12′07.0″E longitudes) and directly transported to the post-harvest laboratory at Sultan Qaboos University (23°35′25.1″N latitudes and 58°10′07.9″E longitudes), Sultanate of Oman. A total of 129 pears were selected based on their uniform color, shape, and surface condition (with no defects and blemishes or bruising). The average weight of each sample selected was 163.12 ± 4.26 g. Before bruising and storage study, the pear samples on the initial day (0 day) were tested for color, firmness, and TSS analysis.

Bruise Size Measurements of Pear Using Drop Test Method and Storage Conditions

Pear fruits were bruised using the drop test method described by Pathare and Al-Dairi (2021) (Figure 1). This technique includes a free fall of a steel ball of a known mass (110 g) through PVC hollow pipe into every individual pear from 20 cm (low), 40 cm (medium), and 60 cm (high) drop heights. The ball was fixed by hand after each drop to prevent multiple impacts into pears.

After the drop test, all bruised areas on pears were marked to simplify bruise recognition during measurements. To calculate the impact energy (E_i) resulted from drop impact, the equation used by Hussein et al. (2017) was performed as

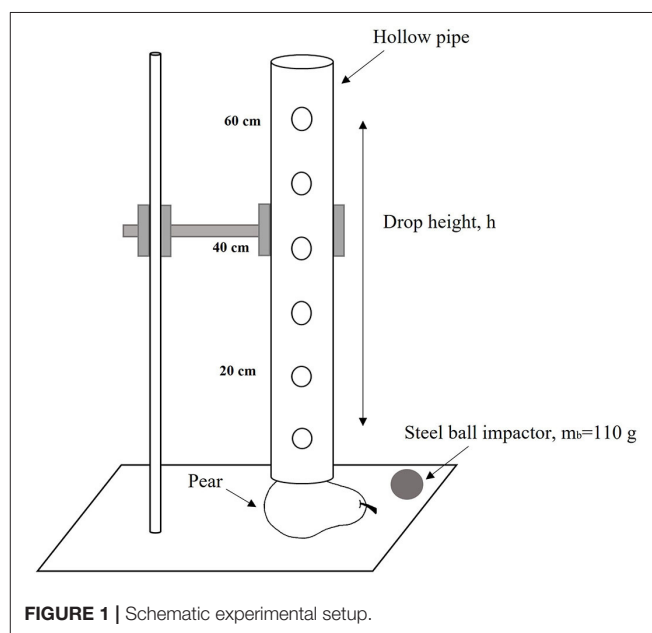


TABLE 1 | Experimental drop height and energy produced.

Drop height (cm)	Impact energy (J)
20	0.215
40	0.431
60	0.647

follows (Equation 1):

$$E_i = m_b \times g \times h \text{ (J)} \quad (1)$$

where m_b is the mass of dropped ball (110 g), g is the gravitational constant (9.81 m s^{-2}), and h is the drop height in cm. **Table 1** shows the impact energy generated from different drop impacts. To perform bruise measurements, pears were sliced from the middle of the marked Bruised area. Bruise sing was recognized by the presence of noticeably bruise tissue exist on the marked area of the pear. Digital caliper (Model: Mitutoyo, Mitutoyo Corp., Japan) was used to measure bruise diameter (d) like major and minor width (w_1 and w_2), respectively, and bruise depth (h_b) (**Figure 2**). Bruise size results were presented in the form of Bruise area (BA) (Equation 2), Bruise volume (BV) (Equation 3) (Opara and Pathare, 2014), and Bruise susceptibility (BS) (Equation 4) (Hussein et al., 2019).

$$BA = \frac{\pi}{4} \times w_1 w_2 \text{ (mm}^2\text{)} \quad (2)$$

$$BV = \frac{\pi d^2 h_b}{6} \text{ (m}^3\text{)} \quad (3)$$

$$BS = \frac{BV}{E_i} \text{ (m}^3\text{J}^{-1}\text{)} \quad (4)$$

The samples were divided and stored at 10°C ($85 \pm 5\%$ RH) and 22°C ($45 \pm 5\%$ RH) (65 pear samples per storage condition) at 2 days interval for 14 days to study bruise development and quality changes on pears like color, firmness (unbruised area), and Total soluble solids (TSS). Each storage condition consisted of three groups of different drop heights, where each of them consisted of seven subgroups for storage duration (temporal) assessment. The temperature meter (Model: TES 13604, TES Electrical Corp., Taiwan) was used for daily monitoring of temperature and relative humidity. Visual observations were taken to observe the incidence of bruising and other quality changes of pear.

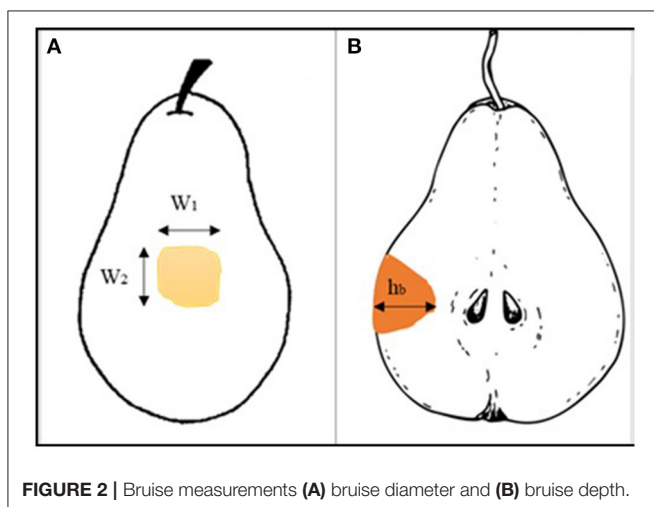


FIGURE 2 | Bruise measurements (A) bruise diameter and (B) bruise depth.

Pear Quality Response

Color

Pear fruit surface color was measured using a Colorimeter (Model: CR-310, Minolta, Japan), which was calibrated using a white plate ($L^* = 93.90$, $a^* = 3.13$, $b^* = 3.20$). Color measurements were conducted six times per sample (108 reading a day) for 14 days of analysis to obtain the changes of L^* (lightness-darkness), a^* (redness-greenness), and b^* (yellowness-blueness) subjected to different impact levels at 10 and 22°C . Total color differences (ΔE^*) (Equation 5), Chroma (Equation 6), and Hue (Equation 7) were also calculated using the equations explained by Pathare et al. (2013):

$$\Delta E^* = \sqrt{\Delta a^{*2} + \Delta b^{*2} + \Delta L^{*2}} \quad (5)$$

$$\text{Chroma} = \sqrt{a^{*2} + b^{*2}} \quad (6)$$

$$\text{Hue} = \tan^{-1} \left(\frac{b^*}{a^*} \right) \quad (7)$$

Firmness

Firmness was performed by penetrating the middle region of pear fruit by using a hand penetrometer (Model: FT 327, EFFEGI, Italy) at 2 days interval of the experiment and expressed in N by following the standard procedure of OECD (2018).

Total Soluble Solid

According to OECD (2018), TSS °Brix of pear was measured using a hand-held refractometer and was calibrated at 20°C . For each pear sample, two longitudinal slices were taken (from two opposite sides). Each slice was squeezed longitudinally to obtain a mixture of juice from all regions. From each group, 6 readings of TSS were taken (36 readings per day).

Statistical Analysis

To turn all statistical analysis, SPSS 20.0 (International Business Machine Corp., USA) software was performed. Three-way analysis of variance (ANOVA) was applied to investigate the effect of three independent variables (drop impact height, storage temperature, and storage duration) on several dependent variables (BA, BV, BS, color changes, firmness, and TSS properties). The significant differences were determined at $p < 0.05$, and the values of all properties are presented as average \pm standard deviation (S.D.). Regression analyses were performed to determine the relation between BS with color parameters (L^* , a^* , and b^*) and firmness. Pearson correlation coefficient was also performed to study the relationship between all resulted analyses.

RESULTS AND DISCUSSIONS

Bruise Measurements

Effect of Drop Height, Storage Temperature, and Storage Duration on BA, BV, and Impact Energy of Bruised Pears

Table 2 shows the values of BA (mean \pm Sd) and BV (mean \pm Sd) of selected pear fruits at different heights and storage temperatures for 14 days period. In this study, BA and BV of bruised pears were highly increased ($p < 0.05$) with the increase

TABLE 2 | Bruise area and bruise volume of pear fruits impacted with three drop heights levels at two storage conditions during 14 days of storage.

Bruising area and volume	Temp. Height (°C)	Storage days						
		2	4	6	8	10	12	14
Bruising area (mm ²)	10	95.7 ± 12	108.5 ± 10.8	113.2 ± 4.3	114.9 ± 9.8	115.0 ± 8.6	131.1 ± 21.9	132 ± 11
	40	130.3 ± 31.6	188.1 ± 25.6	189.8 ± 31.0	203.1 ± 59.3	209.8 ± 52.9	214.9 ± 40.6	219.8 ± 15.9
	60	140.6 ± 8.3	240.6 ± 49.6	242.0 ± 44.9	243.7 ± 19.3	244.0 ± 42.1	279.8 ± 34.3	283.1 ± 42.6
Bruising volume (m ³)	22	99.4 ± 6.8	109.2 ± 22.5	115.8 ± 14.5	135.2 ± 29.3	142.6 ± 7.8	152.9 ± 13.3	153.8 ± 22.4
	40	169.2 ± 26	172.0 ± 27.4	157.2 ± 6.8	202.9 ± 86.9	206.2 ± 28.7	213.4 ± 45.0	260.4 ± 152.2
	60	204.6 ± 51.5	260.6 ± 62.5	287.0 ± 25.2	295.2 ± 74.8	386.5 ± 185.6	411 ± 9 2.5	431.6 ± 34.3
	10	6.6 × 10 ⁻⁵ ± 1.9 × 10 ⁻⁴	8.8 × 10 ⁻⁵ ± 2.5 × 10 ⁻⁴	9.9 × 10 ⁻⁵ ± 9.4 × 10 ⁻⁵	1.0 × 10 ⁻⁴ ± 1.6 × 10 ⁻⁴	1.1 × 10 ⁻⁴ ± 1.5 × 10 ⁻⁴	1.6 × 10 ⁻⁴ ± 4.2 × 10 ⁻⁴	1.7 × 10 ⁻⁴ ± 5.8 × 10 ⁻⁴
	40	1.7 × 10 ⁻⁴ ± 7.5 × 10 ⁻⁴	4.0 × 10 ⁻⁴ ± 1.5 × 10 ⁻⁴	4.1 × 10 ⁻⁴ ± 1.2 × 10 ⁻⁴	4.9 × 10 ⁻⁴ ± 3.3 × 10 ⁻⁴	5.3 × 10 ⁻⁴ ± 2.4 × 10 ⁻⁴	5.7 × 10 ⁻⁴ ± 2.6 × 10 ⁻⁴	6.1 × 10 ⁻⁴ ± 1.2 × 10 ⁻³
	60	2.1 × 10 ⁻⁴ ± 2.2 × 10 ⁻³	6.9 × 10 ⁻⁴ ± 4.9 × 10 ⁻⁴	6.9 × 10 ⁻⁴ ± 2.7 × 10 ⁻⁴	8.9 × 10 ⁻⁴ ± 3.3 × 10 ⁻⁴	8.9 × 10 ⁻⁴ ± 3.8 × 10 ⁻⁴	1.2 × 10 ⁻³ ± 3.8 × 10 ⁻⁴	1.2 × 10 ⁻³ ± 4.3 × 10 ⁻⁴
	22	8.6 × 10 ⁻⁵ ± 5.3 × 10 ⁻³	1.1 × 10 ⁻⁴ ± 4.9 × 10 ⁻⁴	1.3 × 10 ⁻⁴ ± 4.3 × 10 ⁻⁴	2.1 × 10 ⁻⁴ ± 9.9 × 10 ⁻⁴	2.2 × 10 ⁻⁴ ± 4.6 × 10 ⁻⁴	2.6 × 10 ⁻⁴ ± 6.1 × 10 ⁻⁴	2.7 × 10 ⁻⁴ ± 4.7 × 10 ⁻⁴
	40	2.6 × 10 ⁻⁴ ± 8.6 × 10 ⁻⁴	2.9 × 10 ⁻⁴ ± 1.5 × 10 ⁻⁴	3.4 × 10 ⁻⁴ ± 4.6 × 10 ⁻⁴	5.1 × 10 ⁻⁴ ± 5.5 × 10 ⁻⁴	5.2 × 10 ⁻⁴ ± 1.6 × 10 ⁻⁴	5.7 × 10 ⁻⁴ ± 2.3 × 10 ⁻⁴	8.5 × 10 ⁻⁴ ± 1.1 × 10 ⁻³
	60	5.0 × 10 ⁻⁴ ± 2.1 × 10 ⁻⁴	9.2 × 10 ⁻⁴ ± 4.5 × 10 ⁻⁴	1.3 × 10 ⁻³ ± 4.5 × 10 ⁻⁴	1.4 × 10 ⁻³ ± 4.5 × 10 ⁻⁴	2.4 × 10 ⁻³ ± 2.5 × 10 ⁻³	2.8 × 10 ⁻³ ± 1.8 × 10 ⁻³	3.2 × 10 ⁻³ ± 6.5 × 10 ⁻⁴

The data were expressed in mean ± standard deviation. Error bars represent the standard deviation (S.D.) of the mean values ± S.D. of three readings of three replicates.

of all investigated factors like drop height, storage duration, and temperature condition. The highest drop height (60 cm, 0.647 J) increased the average value of BA from 140.6 mm² on day 2 and 243.7 mm² on day 8 to reach 283.1 mm² on day 14 on pears stored at 10°C. However, the BA was higher on pears stored at 22°C and impacted with the heights impact level (60 cm), where BA was 204.6 mm² on day 2 and 295.2 mm² on day 8 to reach 431.6 mm² on day 14 (Table 2). Same trends of results were shown on the BV of the pear fruits where high BV resulted on pear impacted with the steel ball from 60 cm height stored at ambient temperature condition followed by the one impacted from 40 and 20 cm heights at both storage conditions. In the current study, high storage temperature conditions and impact energy during storage time slightly increased BA and BV. The same findings were recorded in apples (Fadji et al., 2016) and pomegranate (Hussein et al., 2019). Shafie et al. (2017) also revealed that BV and BA were highly influenced by drop height. Similarly, Shafie et al. (2015) found an obvious tendency between BV and storage time, impact level, and storage temperature. Besides, Komarnicki et al. (2016) found that the maximum value of BV reached 15,000 mm³ (1.5 × 10⁻⁵ m³), which corresponded to impact from the height of 32.8 cm. However, Zarifneshat et al. (2010) recorded that high temperature can reduce BV/damage of apple.

Effect of Drop Height, Storage Temperature, and Storage Duration on BS of Pear Fruit

A statistical difference ($p < 0.05$) was found between BS and all other studied parameters such as drop height, storage temperature, and storage duration (Figure 3). The results showed that BS gradually increased with drop height at both storage temperature conditions throughout storage duration (14 days). The results also indicated that high storage temperature and drop height for 14 days storage can elevate the percentage of BS. Bruise susceptibility of pear fruit stored at 22°C reached the maximum value with $5.0 \times 10^{-3} \text{ m}^3 \text{ J}^{-1}$ for 60 cm drop height followed by 2.7×10^{-3} and $2.2 \times 10^{-3} \text{ m}^3 \text{ J}^{-1}$ for both 40 cm and 20 cm drop heights, respectively (Figure 3B). However, less BS was observed on bruised pears stored at 10°C, which was 1.9×10^{-3} , 1.4×10^{-3} , and $1.3 \times 10^{-3} \text{ m}^3 \text{ J}^{-1}$ for high, medium, and low drop heights, respectively, on the last day of storage (Figure 3A). Celik (2017) indicated higher BS as pear subjected to an impact from 1 m heights. High storage temperature can increase the occurrence of bruising in fresh produce as enzymes are still active resulting in cell wall degradation and stiffness (Ahmadi et al., 2010). Bugaud et al. (2014) recorded a less increment in BS of bananas stored at low temperature. Al-Dairi et al. (2021b) observed a higher percentage of bruise damage on tomatoes stored at room temperature. In contrast, Bollen (2005) observed no signs of bruising on dropped apple after storing at two different storage temperatures.

Pear Quality Response

Color

The measurements of CIE L^* , a^* , and b^* color coordinates were reported. In terms of storage days, the trend of all color values was similar in all treated pears. L^* value was varied

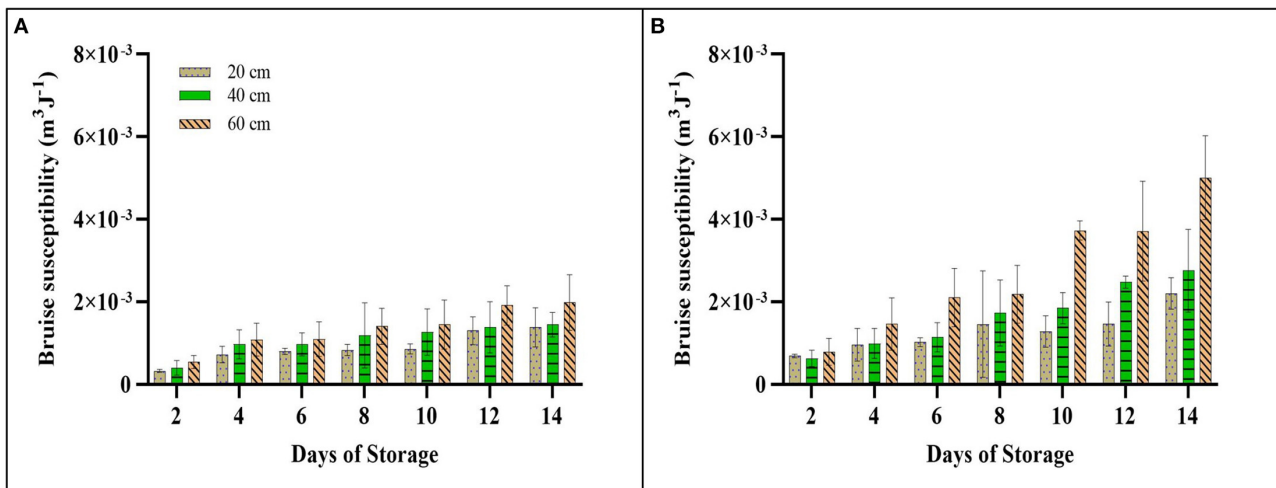


FIGURE 3 | Bruise susceptibility of pear impacted at different drop heights (20, 40, and 60 cm) during 14 days at (A) 10°C and (B) 22°C storage conditions. The data were expressed in mean \pm standard deviation. Error bars represent the standard deviation (S.D.) of the mean values \pm S.D. of three readings of three replicates.

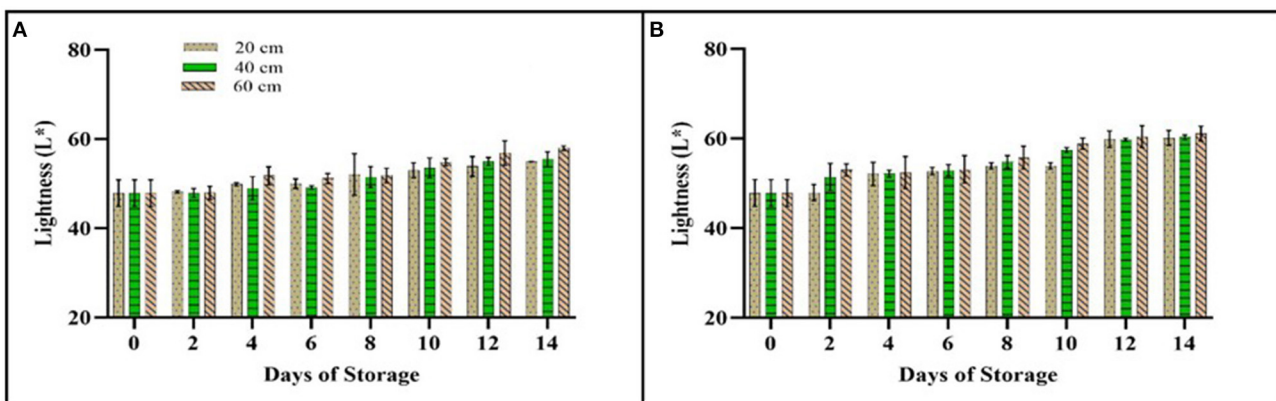


FIGURE 4 | L^* value of pear impacted at different drop heights (20, 40, and 60 cm) during 14 days at (A) 10°C and (B) 22°C storage conditions. The data were expressed in mean \pm standard deviation. Error bars represent the standard deviation (S.D.) of the mean values \pm S.D. of 18 readings per three replicates.

significantly ($p < 0.05$) with storage temperature, drop height, and storage duration. Alteration in lightness (L^* value) increased with the increase of drop height (impact energy), temperature condition, and days of storage (Figure 4). The L^* value of all bruised pears increased significantly, particularly, for 60 cm drop height bruised pears at 10 and 22°C, where the percentage of L^* increment reached 27.7% (Figure 4B) and 25.9% (Figure 4A) on the last day of storage, respectively. However, the lowest percentage of increment on L^* was observed for 20 cm drop height (24.7%) bruised pears stored at 10°C. This was due to the conversion of pear surface color from green to more yellow color. Moreover, the lightness L^* of bruised pears exposed to different impact energy levels (drop heights) at both storage conditions showed a strong relationship with the BS ($R^2_{20 \text{ cm}, 10^\circ \text{C}}: 0.8204$, $R^2_{40 \text{ cm}, 10^\circ \text{C}}: 0.7161$, $R^2_{60 \text{ cm}, 10^\circ \text{C}}: 0.9058$, $R^2_{20 \text{ cm}, 22^\circ \text{C}}: 0.9038$, $R^2_{40 \text{ cm}, 22^\circ \text{C}}: 0.8899$, $R^2_{60 \text{ cm}, 22^\circ \text{C}}: 0.9444$) (Figure 5).

The redness (a^*) increased in all treated samples. The a^* value was significantly differed ($p < 0.05$) with storage period and

storage temperature condition, while no statistical significance ($p > 0.05$) was observed in the a^* value of bruised pear with respect to drop height. Table 3 shows a rapid increase in a^* value on bruised pear stored at 22°C compared to bruised pears stored at 10°C after 14 days of storage. The highest change of a^* value was observed on bruised pears impacted with a steel ball from the medium height (40 cm) stored at 22°C, which increased from -9.66 on day 0 to reach 3.39 on day 14 followed by bruised pear impacted from low (20 cm) and high (60 cm) drop height that reached 3.38 and 3.02 , respectively. At 10°C storage condition, stored pears recorded less change in a^* , which altered from -9.66 to reach -0.03 , -0.49 , and 0.40 on the last day of storage for 20, 40, and 60 cm height bruised pears, respectively. Generally, a^* value was maintained on bruised pears stored at 10°C. The change of redness is attributed to green color loss on bruised pears during storage (Bodner and Scampicchio, 2020). Similarly, Gao et al. (2021) recorded no significant changes on the a^* value of impacted kiwifruit during storage. As observed, higher

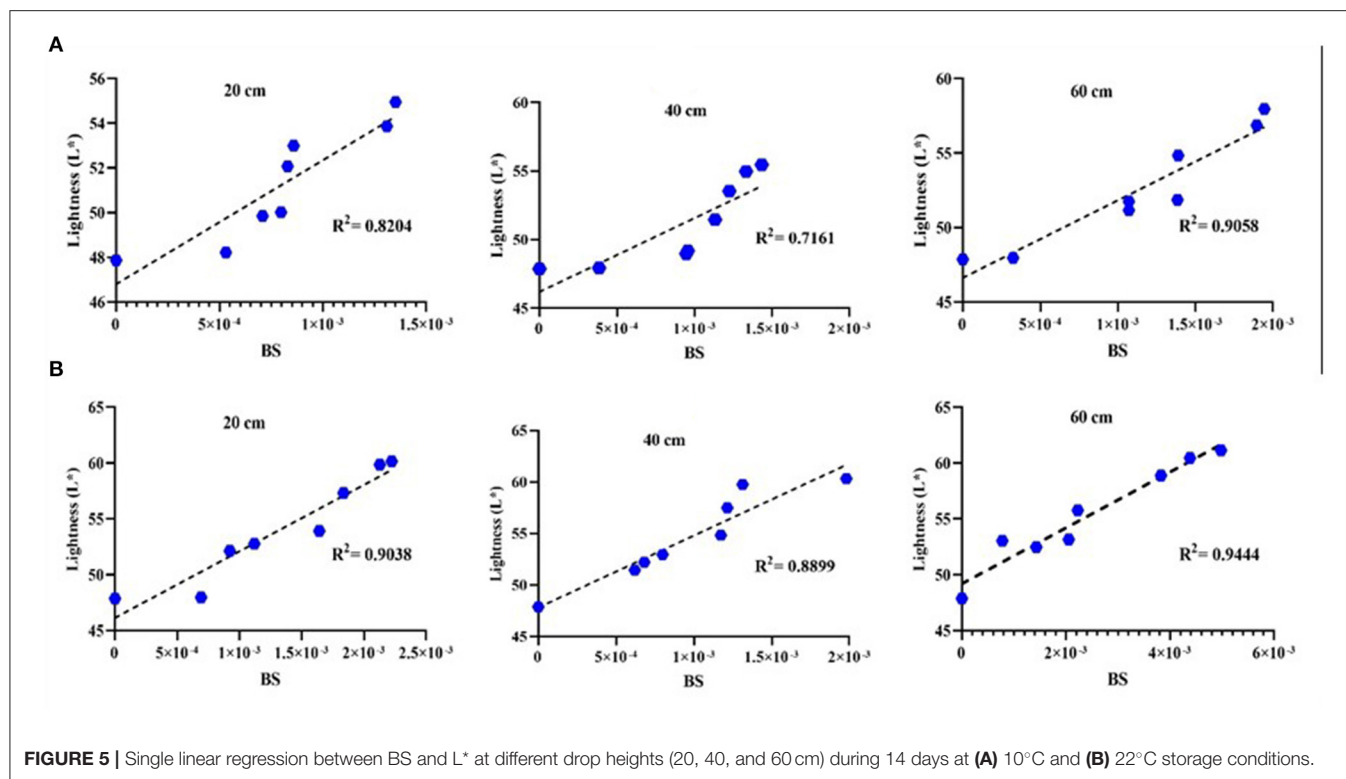


FIGURE 5 | Single linear regression between BS and L^* at different drop heights (20, 40, and 60 cm) during 14 days at **(A)** 10°C and **(B)** 22°C storage conditions.

TABLE 3 | a^* and hue values of pears impacted with three drop heights levels at two storage conditions during 14 days of storage.

Quality parameter	Storage temp. (°C)	Height (cm)	Storage days							
			0	2	4	6	8	10	12	14
a^*	10	20	-7.27 ± 1.19	-7.19 ± 0.37	-6.25 ± 0.96	-5.37 ± 1.35	-5.26 ± 1.00	-4.81 ± 1.08	-0.03 ± 1.05	
		40	-7.63 ± 0.30	-7.57 ± 0.40	-7.36 ± 1.32	-7.27 ± 1.48	-6.89 ± 1.15	-5.62 ± 2.97	-0.49 ± 0.63	
		60	-9.06 ± 0.83	-8.81 ± 0.93	-7.27 ± 0.80	-5.09 ± 2.21	-4.79 ± 0.25	-2.08 ± 1.63	-0.40 ± 1.92	
	22	20	-9.66 ± 0.88	-5.04 ± 2.30	-4.92 ± 1.07	-3.73 ± 0.14	-0.56 ± 0.92	1.09 ± 0.82	1.83 ± 0.77	3.38 ± 1.78
		40		-5.67 ± 0.86	-5.07 ± 0.63	-4.28 ± 1.09	-1.86 ± 1.98	0.03 ± 2.68	3.04 ± 1.02	3.39 ± 1.78
		60		-6.69 ± 0.53	-5.44 ± 0.95	-3.88 ± 1.31	-2.00 ± 1.85	0.22 ± 1.31	1.41 ± 1.79	3.02 ± 0.46
Hue	10	20	-1.35 ± 0.04	-1.36 ± 0.02	-1.39 ± 0.03	-1.41 ± 0.05	-1.42 ± 0.03	-1.45 ± 0.02	-1.57 ± 0.88	
		40	-1.33 ± 0.00	-1.34 ± 0.01	-1.34 ± 0.04	-1.35 ± 0.04	-1.38 ± 0.03	-1.42 ± 0.08	-0.51 ± 0.89	
		60	-1.31 ± 0.02	-1.31 ± 0.02	-1.36 ± 0.02	-1.42 ± 0.06	-1.45 ± 0.01	-0.82 ± 0.76	-0.52 ± 1.77	
	22	20	-1.3 ± 0.03	-1.23 ± 0.26	-1.43 ± 0.03	-1.47 ± 0.00	-0.33 ± 1.07	1.37 ± 0.30	1.35 ± 0.29	1.48 ± 0.05
		40		-1.40 ± 0.03	-1.42 ± 0.03	-1.45 ± 0.03	-0.99 ± 0.86	0.52 ± 1.74	1.49 ± 0.03	1.48 ± 0.05
		60		-1.38 ± 0.01	-1.42 ± 0.03	-1.46 ± 0.04	-1.51 ± 0.06	-0.18 ± 1.57	0.66 ± 1.47	1.50 ± 0.01

The data were expressed in mean ± standard deviation. Error bars represent the standard deviation (S.D.) of the mean values ± S.D. of 18 readings per three replicates.

BS indicated more redness (a^*) value per treatment as shown in **Figure 6**.

With storage time and temperature, an increasing trend in the color attribute of b^* was statistically ($p < 0.05$) observed. The impact of drop height on the b^* value of bruised pear fruit was also significant ($p < 0.05$). The b^* value was increasing gradually at both temperature conditions during storage (**Figure 7**). The results showed that the highest impact (60 cm 0.647 J) bruised pears provided the largest percentage of b^* increment (32.9%)

after 14 days of storage at room temperature (**Figure 7B**). This was followed by bruised pears subjected to an impact from 40 cm (0.4316 J) and 20 cm (0.215 J) drop heights, where the b^* value increased by 29.1 and 28.32%, respectively (**Figure 7B**). Storage at 10°C increased b^* value by 28 and 31.46% for low (20 cm) and high (60 cm) impact bruised pears, respectively (**Figure 7A**). Generally, the b^* value increased gradually during the whole 14 days due to the conversion of the green surface color of pear to yellow. As shown in **Figure 8**, b^* value of pear fruit increased with

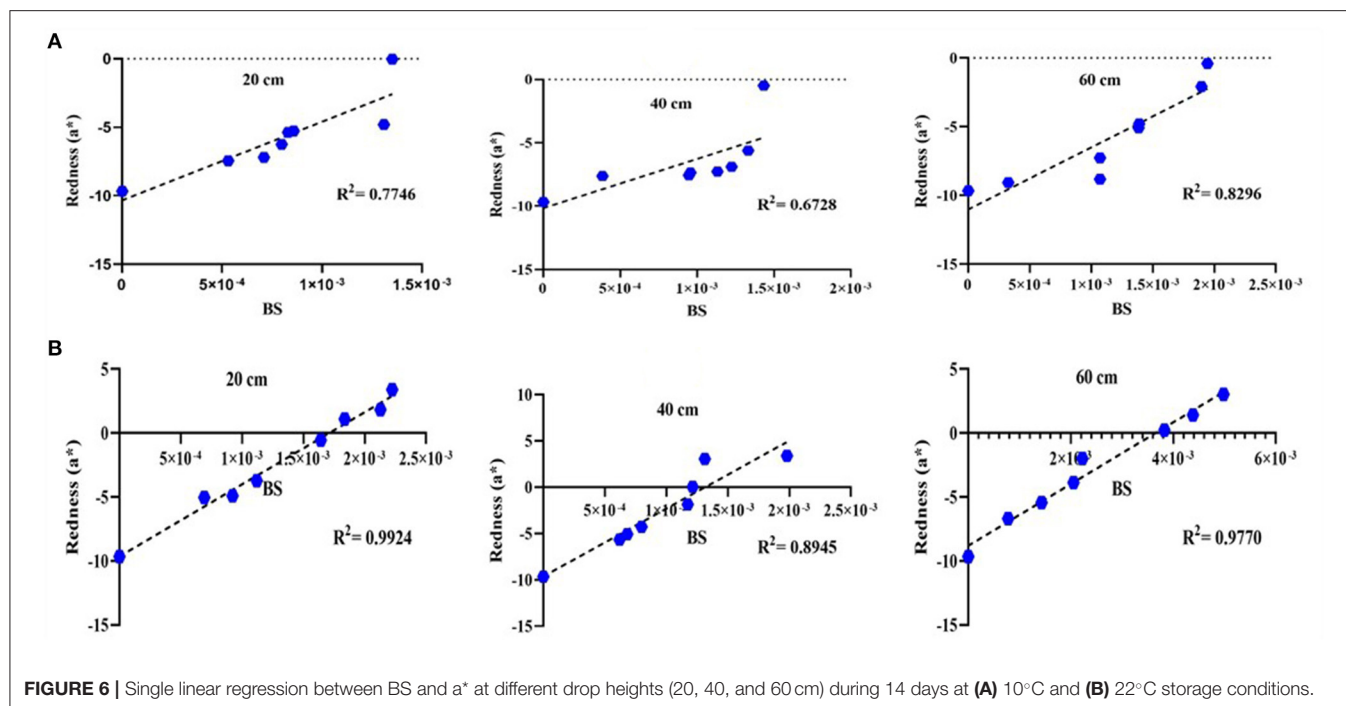


FIGURE 6 | Single linear regression between BS and a^* at different drop heights (20, 40, and 60 cm) during 14 days at **(A)** 10°C and **(B)** 22°C storage conditions.

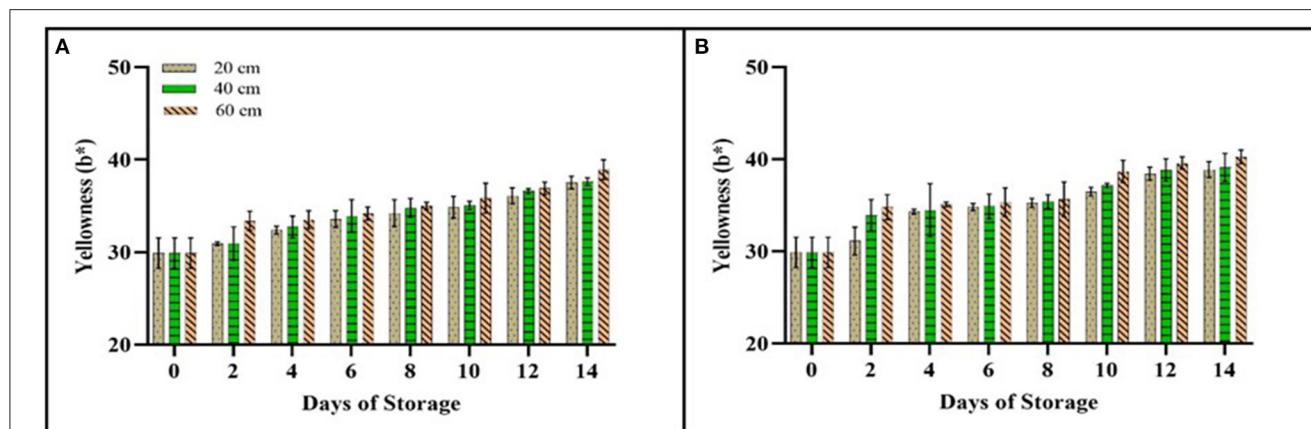


FIGURE 7 | b^* value of pear impacted at different drop heights (20, 40, and 60 cm) during 14 days at **(A)** 10°C and **(B)** 22°C storage conditions. The data were expressed in mean \pm standard deviation. Error bars represent the standard deviation (S.D.) of the mean values \pm S.D. of 18 readings per three replicates.

the increase on BS (R^2 20 cm, 10°C: 0.9034, R^2 40 cm, 10°C: 0.9173, R^2 60 cm, 10°C: 0.8795, R^2 20 cm, 22°C: 0.9087, R^2 40 cm, 22°C: 0.8822, R^2 60 cm, 22°C: 0.9105) (Figure 8).

Total color change (ΔE^*) was calculated to record the changes in bruised pear color difference (Figures 9A,B). Total color differences (ΔE^*) that increased significantly ($p < 0.05$) varied with drop height, storage temperature condition, and storage duration. The ΔE^* value was higher (21.23) in pear impacted at a drop height of 60 cm and stored at 22°C (Figure 9B), while the lowest value (17.12) was recorded in pear fruit stored at 10°C and impacted at a drop height of 20 cm (Figure 9A) during the whole days of the experiment. Bruising is one of the factors that cause fruit discoloration (Bodner and Scampicchio, 2020).

Pathare and Al-Dairi (2021) also observed the same findings where the total color change of tomato was highly affected by storage temperature and duration as well as drop impact. Bodner and Scampicchio (2020) recorded that the total color change value for bruised pear fruit was high, suggesting the effect of bruising in accelerating the ripening process. As reported by Al-Dairi and Pathare (2021), storage at ambient temperature can accelerate the color change of fresh produce than storage at 10°C. In this study, the difference between chroma and all studied factors (drop impact, storage condition, and storage duration) was generally significant ($p < 0.05$; Figures 9C,D). The highest drop height and storage at 22°C showed a great effect on chroma of bruised pear fruits (26.9%) followed by medium

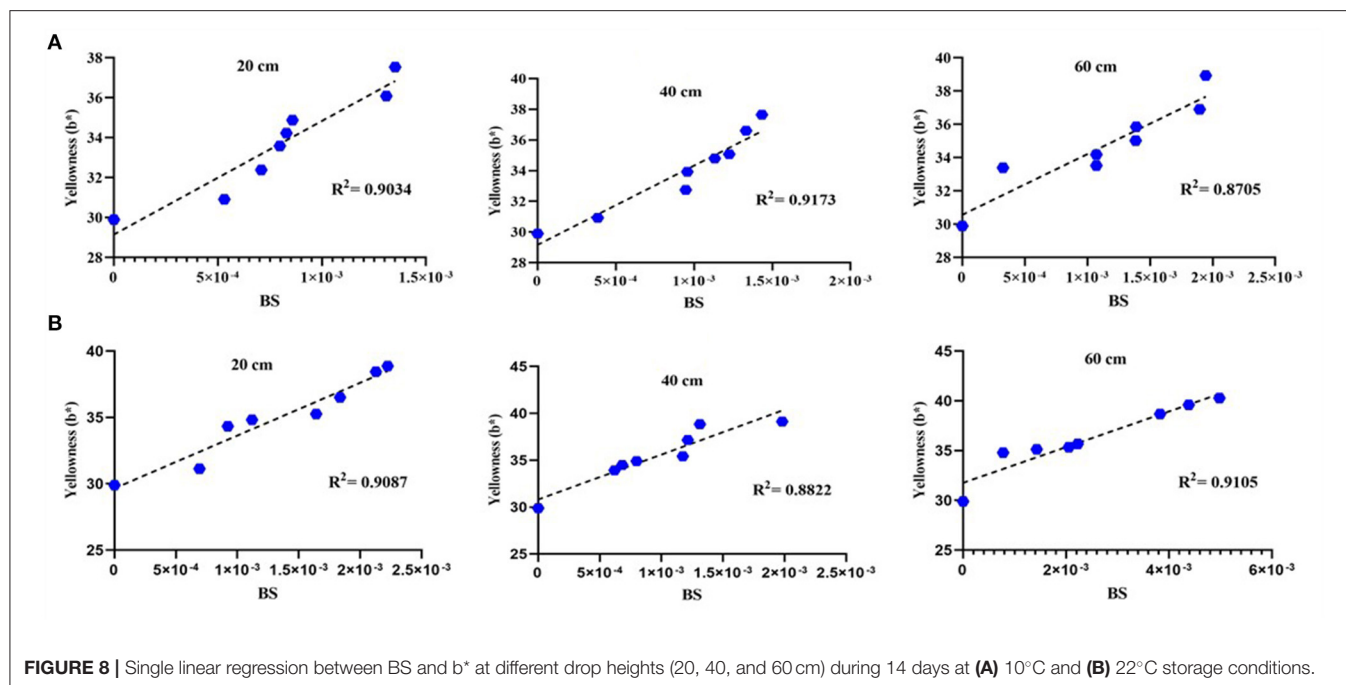


FIGURE 8 | Single linear regression between BS and b^* at different drop heights (20, 40, and 60 cm) during 14 days at **(A)** 10°C and **(B)** 22°C storage conditions.

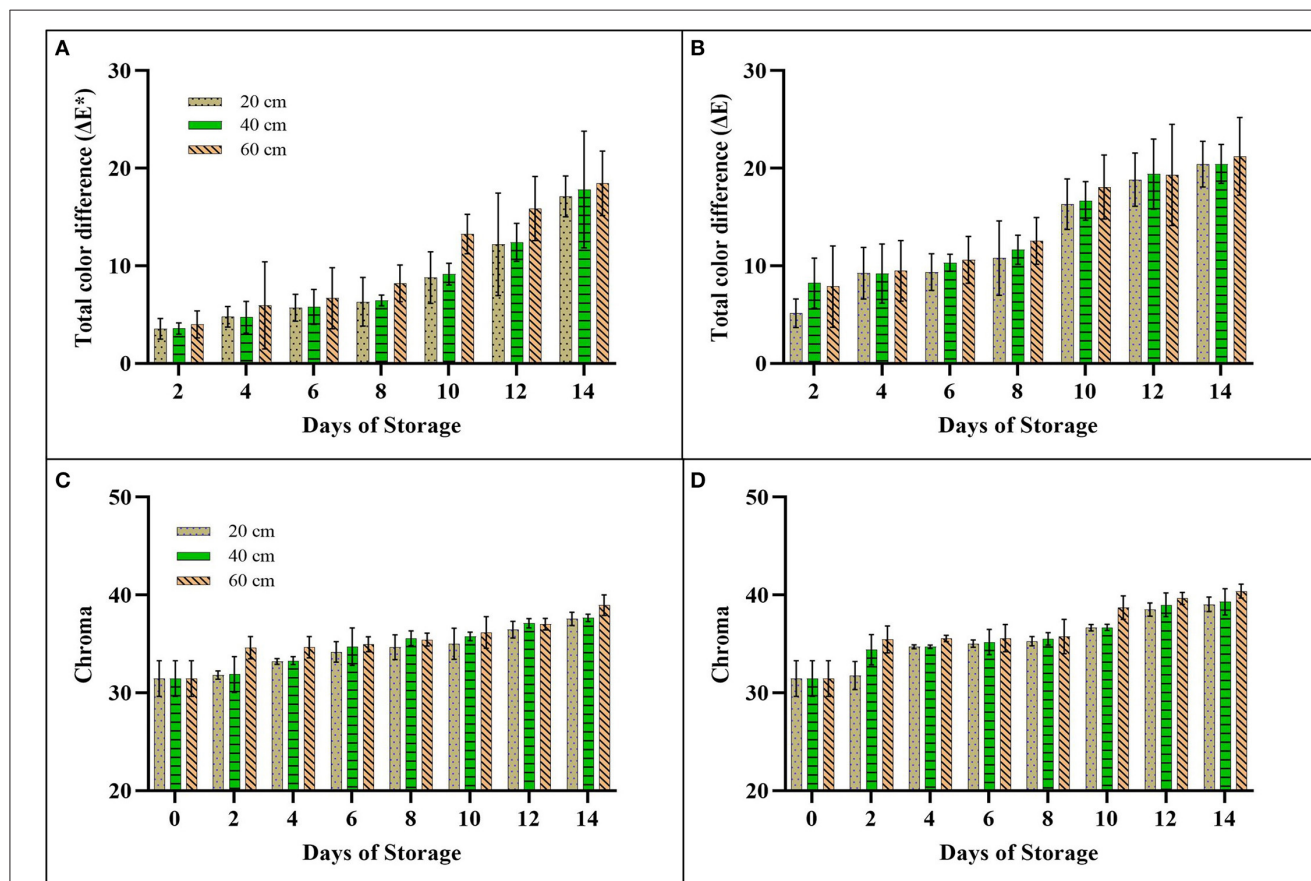


FIGURE 9 | Total color change (ΔE^*) and chroma of pear impacted at different drop heights (20, 40, and 60 cm) during 14 days at **(A,C)** 10°C and **(B,D)** 22°C storage conditions. The data were expressed in mean \pm standard deviation. Error bars represent the standard deviation (S.D.) of the mean values \pm S.D. of 18 readings per three replicates.

(23.5%) and low drop height impact (**Figure 9D**). Storage at 10°C showed less change with 19.4, 19.7, and 23.8% impacted at 20, 40, and 60 cm drop heights, respectively (**Figure 9C**). Regarding hue value (color purity), there was a significant ($p < 0.05$) influence of both storage duration and temperature with no pronounced significance ($p > 0.05$) with drop height (**Table 3**). This study showed that hue value was decreasing slowly at both storage temperature but then increased rapidly on day 10 at 22°C storage temperature to reach 1.50 and 1.48 on day 14 after it was -1.3 on day 0 for high and medium bruised fruit due to change of a^* value from $(-)$ to $(+)$ value during storage. Dobrzanski and Rybezynski (2002) recorded that color characteristics of bruised apples were significantly affected by bruise damage.

Firmness

Drop height, storage temperature, and storage duration statistically ($p < 0.05$) affect the firmness of bruised pear fruit (**Figure 10**). In this study, as drop height increased, the firmness of pear fruit tended to reduce by 89.2, 91.8, and 92.7% for low, medium, and high drop impact stored at 22°C, respectively. On the last day of storage, the firmness of pears stored at 10°C reduced by 80.4, 84.1, and 84.61% for low, medium, and high impact. The percentage of reduction can show that a high impact level can reduce the firm state of pear fruits in the last day of storage. Azadbakht et al. (2019) found that the firmness of pear was reduced with the increase of bruise and force level for the long storage

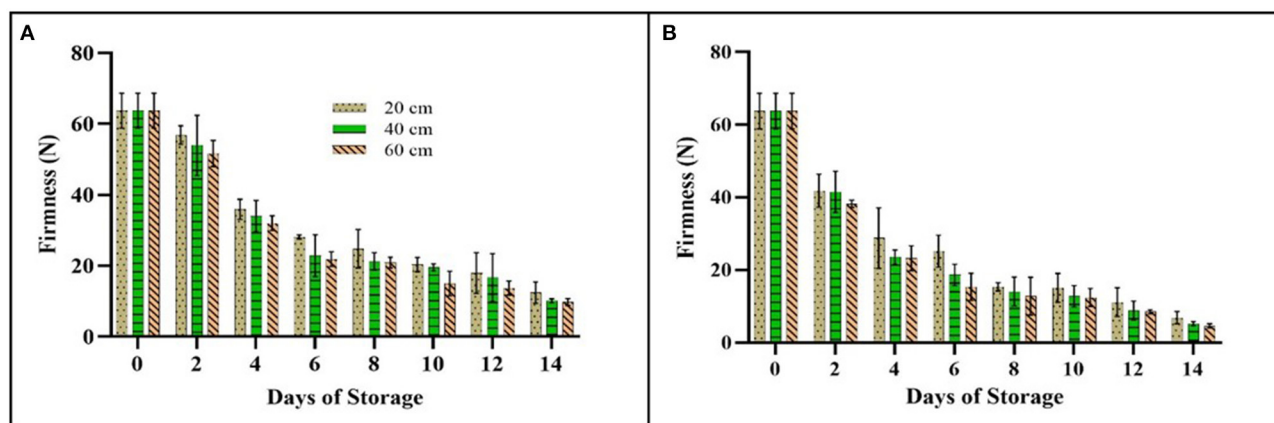


FIGURE 10 | Firmness (N) of pear impacted at different drop heights (20, 40, and 60 cm) during 14 days at **(A)** 10°C and **(B)** 22°C storage conditions. The data were expressed in mean \pm standard deviation. Error bars represent the standard deviation (S.D.) of the mean values \pm S.D. of six readings per three replicates.

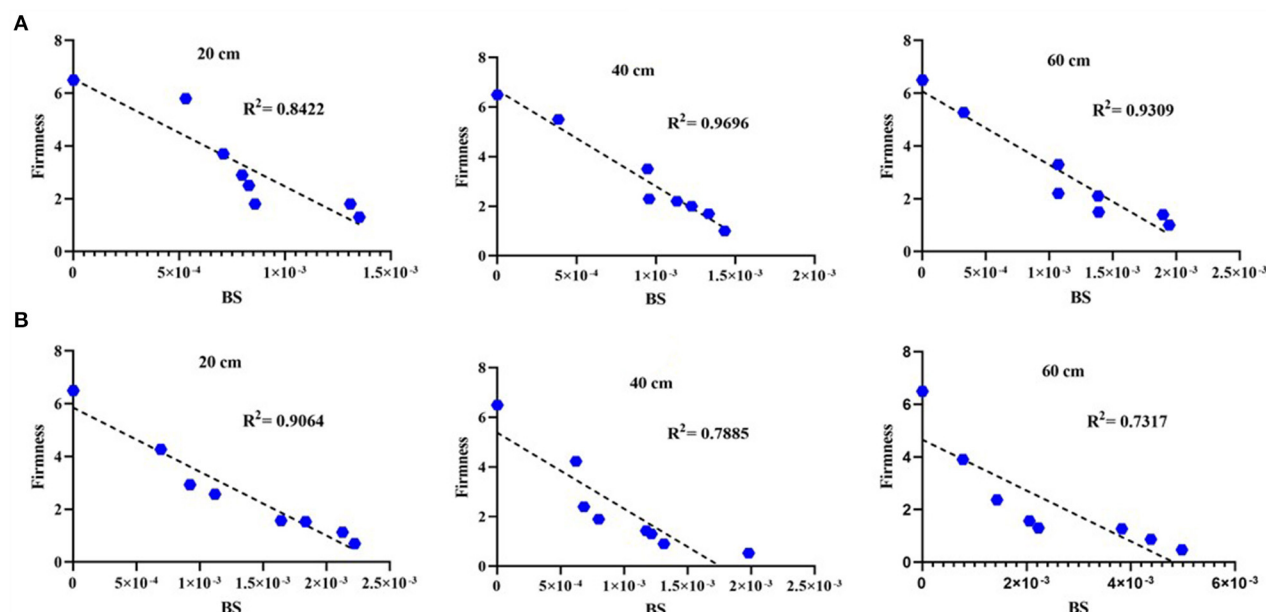


FIGURE 11 | Single linear regression between BS and firmness at different drop heights (20, 40, and 60 cm) during 14 days at **(A)** 10°C and **(B)** 22°C storage conditions.

TABLE 4 | Total soluble solids (TSS) value (°Brix) of pears impacted with three drop heights levels at two storage conditions during 14 days of storage.

Quality parameter	Storage temp. (°C)	Height (cm)	Storage days							
			0	2	4	6	8	10	12	14
TSS	10	20		13.97 ± 1.70	13.50 ± 1.32	14.00 ± 1.65	13.30 ± 0.52	12.50 ± 0.50	11.83 ± 0.76	13.30 ± 1.39
		40		12.17 ± 0.29	13.17 ± 0.76	14.40 ± 0.53	13.30 ± 0.61	11.90 ± 0.90	12.30 ± 1.13	14.27 ± 0.55
		60		13.17 ± 0.29	14.20 ± 0.61	13.37 ± 0.35	12.20 ± 8.49	13.50 ± 0.87	13.97 ± 1.00	14.80 ± 0.26
	22	20	12.13 ± 0.78	13.03 ± 0.06	13.10 ± 0.10	13.97 ± 0.90	14.43 ± 1.24	15.27 ± 0.46	15.10 ± 0.90	14.67 ± 0.40
		40		13.30 ± 0.06	13.33 ± 0.10	13.37 ± 0.90	14.60 ± 1.24	15.40 ± 0.46	15.10 ± 0.72	14.33 ± 0.40
		60		13.60 ± 0.52	13.83 ± 0.76	13.97 ± 0.95	14.63 ± 0.55	14.67 ± 1.50	14.90 ± 0.90	14.63 ± 0.46

The data were expressed in mean ± standard deviation. Error bars represent the standard deviation (S.D.) of the mean values ± S.D. of six readings per three replicates.

duration. Similar findings were reported on pomegranate (Hussein et al., 2020a) and apple (Van Zeebroeck et al., 2007). Also, Li et al. (2012) confirmed that bruising is another parameter that led to a decline in the firm state due to the increment of polygalacturonase activity included on pear. For storage time and temperature conditions, firmness was decreasing dramatically during the period of storage at both storage temperatures particularly at 22°C due to continued ripening of the pear. As stated by Zhou et al. (2007), firmness reduction was observed on pears at different storage temperature conditions and it was highly reduced at ambient temperature storage conditions, where the softening rate is increased. For 14 days storage at both storage condition, the firmness of bruised pears impacted at different drop height correlates strongly with BS ($R^2_{20\text{ cm}, 10^\circ\text{C}}: 0.8422$, $R^2_{40\text{ cm}, 10^\circ\text{C}}: 0.9696$, $R^2_{60\text{ cm}, 10^\circ\text{C}}: 0.9309$, $R^2_{20\text{ cm}, 22^\circ\text{C}}: 0.9064$, $R^2_{40\text{ cm}, 22^\circ\text{C}}: 0.7885$, $R^2_{60\text{ cm}, 22^\circ\text{C}}: 0.7317$) (Figure 11).

Total Soluble Solids

The statistics showed a significant ($p < 0.05$) effect of both temperature and storage duration on the TSS of pear fruit. At the same time, no interaction ($p > 0.05$) was found between the TSS of pear and drop height. TSS value was ranging between 12.13 and 15.40 °Brix on pear stored at 22°C compared to TSS value of pears stored at 10°C that was ranging between 12.13 and 14.80 °Brix (Table 4). The highest content of TSS was shown on day 10 of storage on pear impacted from medium (40 cm) drop height at 22°C. Also, there was a gradual decline and increase in TSS content of pear stored at 10°C (Table 4). The study agreed with the findings of Hussein et al. (2020b), who obtained no significant impact between TSS content and impact bruising in pomegranate. Montero et al. (2009) found that the TSS content of tangerines was highly reduced by impact bruise. Another finding was revealed by Maia et al. (2011) who reported that the total soluble content of bananas showed an increase after subjected to bruise damage. This was attributed to the conservation of starch to total soluble sugars during the ripening process under respiration resulted in high sugar content (Al-Dairi et al., 2021c; Gao et al., 2021), particularly at room temperature.

Pearson Correlation Coefficient

Table 5 presents the Pearson correlation coefficients between BS, color space values [L^* , a^* , b^* , total color change (ΔE^*),

chroma, and hue], firmness, and TSS on pear stored at 10 and 22°C and impacted by a steel ball from three drop heights. The results showed a positive correlation between L^* and BS ($p < 0.05$, $p < 0.001$) viz as BS in pear fruits increased, the pear surface became lighter. A positive and strong linear relationship was observed between L^* and a^* , b^* , total color difference, and chroma. All of these parameters increased gradually during storage time. However, a strong and negative correlation was found between all the previous color parameters and firmness. As firmness decreased, L^* , a^* , b^* , chroma, and total color difference increased. There was also a negative and a strong correlation between firmness and BS ($r = -0.91_{20\text{ cm}, 10^\circ\text{C}}: p < 0.001$, $r = -0.98_{40\text{ cm}, 10^\circ\text{C}}: p < 0.001$, $r = -0.96_{60\text{ cm}, 10^\circ\text{C}}: p < 0.001$, $r = -0.95_{20\text{ cm}, 22^\circ\text{C}}: p < 0.001$, $r = -0.88_{40\text{ cm}, 22^\circ\text{C}}: p < 0.001$, $r = -0.85_{60\text{ cm}, 22^\circ\text{C}}: p < 0.001$). Firmness of bruised pears impacted at different heights was correlated negatively with TSS at 22°C ($r = -0.92_{20\text{ cm}, 22^\circ\text{C}}: p < 0.001$, $r = -0.84_{40\text{ cm}, 22^\circ\text{C}}: p < 0.001$, $r = -0.96_{60\text{ cm}, 22^\circ\text{C}}: p < 0.001$), while there was no correlation between firmness and TSS of bruised pears stored at 10°C. The study showed a positive correlation between TSS of impacted pear stored at 22°C and BS ($r = 0.85_{20\text{ cm}, 22^\circ\text{C}}: p < 0.001$, $r = 0.78_{40\text{ cm}, 22^\circ\text{C}}: p < 0.05$, $r = 0.85_{60\text{ cm}, 22^\circ\text{C}}: p < 0.05$), with no pronounce correlation at 10°C storage condition. The same scenario was observed between hue and other quality analyses like L^* , b^* , chroma, total color change, and firmness at 10°C in contract to storage at 22°C.

CONCLUSIONS

Pear fruits impacted at the highest drop height and impact energy (60 cm 0.647 J) showed the highest increase in BA, BV, and BS. Storage temperature condition and storage duration had a great influence in increasing bruise damage. Rapid increase (L^* , a^* , b^* , total color change, and chroma) and reduction (firmness) were observed on pear stored at 22°C after it was subjected to an impact from 60 cm drop height for 14 days storage period. More color discoloration and ripening were observed on this treatment. Hue value and TSS were not affected by the drop height, but with storage temperature and storage duration. Storage at 10°C can retain the quality attributes of fresh produce that could be changed due to bruising.

TABLE 5 | Pearson correlation coefficients (r) ($n = 8$) between bruise susceptibility (BS), color space values [L^* , a^* , b^* , total color change (ΔE), chroma, and hue], firmness, and TSS on pear stored at 10 and 22°C and impacted by a steel ball from three drop heights.

Pear quality parameter	Drop height (cm)	Storage temp. (°C)	BS	L^*	a^*	b^*	ΔE	Hue	Chroma	TSS	Firmness
BS	20	10	1	0.884**	0.880**	0.950**	0.939**	0.418	0.940**	−0.029	−0.917**
		22	1	0.917**	0.996**	0.950**	0.962**	0.883**	0.932**	0.949**	−0.953**
	40	10	1	0.771*	0.710*	0.958**	0.831*	0.279	0.942**	412	−0.985**
		22	1	0.894**	0.946**	0.941**	0.941**	0.794*	0.936**	0.780*	−0.887**
	60	10	1	0.904**	0.911**	0.933**	0.938**	0.560	0.910**	0.641	−0.964**
		22	1	0.959**	0.988**	0.961**	0.976**	0.875**	0.964**	0.850**	−0.855**
L^*	20	10	0.884**	1	0.947**	0.951**	0.981**	0.695	0.962**	−0.246	−0.839**
		22	0.917**	1	0.909**	0.978**	0.972**	0.828*	0.973**	0.909**	−0.917**
	40	10	0.711*	1	0.919**	0.857**	0.968**	0.693	0.844**	0.316	−0.700
		22	0.894**	1	0.961**	0.958**	0.982**	0.922**	0.950**	0.865**	−0.830*
	60	10	0.904**	1	0.921**	0.897**	0.973**	0.645	0.868**	0.682	−0.852**
		22	0.959**	1	0.968**	0.971**	0.990**	0.820*	0.972**	0.893**	−0.832*
a^*	20	10	0.880**	0.947**	1	0.928**	0.962**	0.758*	0.922**	0.065	−0.836**
		22	0.996**	0.909**	1	0.940**	0.965**	0.878**	0.920**	0.944**	−0.954**
	40	10	0.710*	0.919**	1	0.816*	0.956**	0.838**	0.779*	0.511	−0.704
		22	0.946**	0.961**	1	0.986**	0.991**	0.893**	0.987**	0.874**	−0.895**
	60	10	0.911**	0.921**	1	0.941**	0.962**	0.740*	0.903**	0.552	−0.836**
		22	0.988**	0.968**	1	0.965**	0.987**	0.814*	0.959**	0.906**	−0.903**
b^*	20	10	0.950**	0.951**	0.928**	1	0.962**	0.513	0.996**	−0.152	−0.961**
		22	0.950**	0.978**	0.940**	1	0.979**	0.821*	0.994**	0.895**	−0.943**
	40	10	0.958**	0.857**	0.816*	1	0.931**	0.434	0.995**	0.415	−0.962**
		22	0.941**	0.958**	0.986**	1	0.992**	0.842**	0.990**	0.860**	−0.925**
	60	10	0.933**	0.897**	0.941**	1	0.973**	0.662	0.994**	0.705	−0.897**
		22	0.961**	0.971**	0.965**	1	0.990**	0.797*	0.996**	0.916**	−0.898**
ΔE	20	10	0.939**	0.981**	0.962**	0.962**	1	0.663	0.963**	−0.127	−0.864**
		22	0.962**	0.972**	0.965**	0.979**	1	0.862**	0.968**	0.924**	−0.943**
	40	10	0.831*	0.968**	0.956**	0.931**	1	0.669	0.909**	0.417	−0.822*
		22	0.941**	0.982**	0.991**	0.992**	1	0.889**	0.984**	0.878**	−0.887**
	60	10	0.938**	0.973**	0.962**	0.973**	1	0.685	0.953**	0.703	−0.888**
		22	0.976**	0.990**	0.987**	0.990**	1	0.809*	0.986**	0.921**	−0.894**
Hue	20	10	0.418	0.695	0.758*	0.513	0.663	1	0.533	0.121	−0.334
		22	0.883**	0.828*	0.878**	0.821*	0.862**	1	0.844**	0.837**	−0.720*
	40	10	0.279	0.693	0.838**	0.434	0.669	1	0.399	0.517	−0.299
		22	0.794*	0.922**	0.893**	0.842**	0.889**	1	0.884**	0.719*	−0.626
	60	10	0.560	0.645	0.740*	0.662	0.685	1	0.661	0.667	−0.384
		22	0.875**	0.820*	0.814*	0.797*	0.809*	1	0.841**	0.529	−0.529
Chroma	20	10	0.940**	0.962**	0.922**	0.996**	0.963**	0.533	1	−0.197	−0.947**
		22	0.932**	0.973**	0.920**	0.994**	0.968**	0.844**	1	0.864**	−0.902**
	40	10	0.942**	0.844**	0.779*	0.995**	0.909**	0.399	1	0.385	−0.956**
		22	0.936**	0.950**	0.987**	0.990**	0.984**	0.884**	1	0.806*	−0.881**
	60	10	0.910**	0.868**	0.903**	0.994**	0.953**	0.661	1	0.756*	−0.877**
		22	0.964**	0.972**	0.959**	0.996**	0.986**	0.841**	1	0.881**	−0.860**
TSS	20	10	−0.029	−0.246	0.065	−0.152	−0.127	0.121	−0.197	1	0.080
		22	0.859**	0.909**	0.944**	0.895**	0.924**	0.837**	0.864**	1	−0.922**
	40	10	0.412	0.316	0.511	0.415	0.417	0.517	0.385	1	−0.499
		22	0.780*	0.865**	0.874**	0.860**	0.878**	0.719*	0.806*	1	−0.842**
	60	10	0.641	0.682	0.552	0.705	0.703	0.667	0.756*	1	−0.584
		22	0.850**	0.893**	0.906**	0.916**	0.921**	0.529	0.881**	1	−0.963**
Firmness	20	10	−0.917**	−0.839**	−0.836**	−0.961**	−0.864**	−0.334	−0.947**	0.080	1
		22	−0.953**	−0.917**	−0.954**	−0.943**	−0.943**	−0.720*	−0.902**	−0.922**	1
	40	10	−0.985**	−0.700	−0.704	−0.962**	−0.822*	−0.299	−0.956**	−0.499	1
		22	−0.887**	−0.830*	−0.895**	−0.925**	−0.887**	−0.626	−0.881**	−0.842**	1
	60	10	−0.964**	−0.852**	−0.836**	−0.897**	−0.888**	−0.384	−0.877**	−0.584	1
		22	−0.855**	−0.832*	−0.903**	−0.898**	−0.894**	−0.529	−0.860**	−0.963**	1

Significant correlations of two-tailed tests are indicated: * $p < 0.05$; ** $p < 0.01$.

DATA AVAILABILITY STATEMENT

The raw data supporting the conclusions of this article will be made available by the authors, without undue reservation.

AUTHOR CONTRIBUTIONS

PP: conceptualization, formal analysis, writing—review and editing, funding acquisition, and supervision. MA-D: data curation, formal analysis, and writing—original draft.

REFERENCES

- Ahmadi, E., Ghassemzadeh, H. R., Sadeghi, M., Moghaddam, M., and Neshat, S. Z. (2010). The effect of impact and fruit properties on the bruising of peach. *J. Food Eng.* 97, 110–117. doi: 10.1016/j.jfoodeng.2009.09.024
- Al-Dairi, M., and Pathare, P. B. (2021). Kinetic modeling of quality changes of tomato during storage. *Agric. Eng. Int. CIGR J.* 23 183–193.
- Al-Dairi, M., Pathare, P. B., and Al-Mahdouri, A. (2021a). Effect of storage conditions on postharvest quality of tomatoes: a case study at market-level. *J. Agric. Marine Sci.* 26, 13–20. doi: 10.24200/jams.vol26iss1pp13-20
- Al-Dairi, M., Pathare, P. B., and Al-Mahdouri, A. (2021b). Impact of vibration on the quality of tomato produced by stimulated transport. In: *IOP Conference Series: Earth and Environmental Science*. Bristol: IOP Publishing. p. 012101.
- Al-Dairi, M., Pathare, P. B., and Al-Yahyai, R. (2021c). Chemical and nutritional quality changes of tomato during postharvest transportation and storage. *J. Saudi Soc. Agric. Sci.* In press. doi: 10.1016/j.jssas.2021.05.001
- Al-Dairi, M., Pathare, P. B., and Al-Yahyai, R. (2021d). Effect of postharvest transport and storage on color and firmness quality of tomato. *Horticulturae* 7:163. doi: 10.3390/horticulturae7070163
- Azadbakht, M., Mahmoodi, M. J., and Vahedi Torshizi, M. (2019). Effects of different loading forces and storage periods on the percentage of bruising and its relation with the qualitative properties of pear fruit. *Int. J. Horti. Sci. Technol.* 6, 177–188. doi: 10.22059/ijhst.2019.280000.290
- Bodner, M., and Scampicchio, M. (2020). Does bruising influence the volatile profile of pears? *Nutr. Food Sci.* ahead-of-print. doi: 10.1108/NFS-05-2020-0213
- Bollen, A. (2005). Major factors causing variation in bruise susceptibility of apples (*Malus domestica*) grown in New Zealand. *N Z J. Crop Horti. Sci.* 33, 201–210. doi: 10.1080/01140671.2005.9514351
- Bugaud, C., Ocrisse, G., Salmon, F., and Rinaldo, D. (2014). Bruise susceptibility of banana peel in relation to genotype and post-climacteric storage conditions. *Postharvest Bio. Technol.* 87, 113–119. doi: 10.1016/j.postharvbio.2013.08.009
- Celik, H. K. (2017). Determination of bruise susceptibility of pears (Ankara variety) to impact load by means of FEM-based explicit dynamics simulation. *Postharvest Bio. Technol.* 128, 83–97. doi: 10.1016/j.postharvbio.2017.01.015
- Costa, A. G., Braga, R. A., Jr., Boas, E. V. V., and Risso, M. (2018). Early prediction of internal bruising in potatoes by biospeckle laser technique. *African J. Agric. Res.* 13, 691–697. doi: 10.5897/AJAR2017.12959
- Dobrzanski, B., and Rybezynski, R. (2002). Colour change of apple as a result of storage, shelf-life, and bruising. *Int. Agrophysics.* 16, 261–268.
- Ergun, M. (2017). Physical, physiochemical and electrochemical responses of ‘Galaxy’ apples to mild bruising. *Eur. J. Horti. Sci.* 82, 244–250. doi: 10.17660/eJHS.2017/82.5.4
- Fadiji, T., Coetzee, C., Pathare, P., and Opara, U. L. (2016). Susceptibility to impact damage of apples inside ventilated corrugated paperboard packages: effects of package design. *Postharvest Bio. Technol.* 111, 286–296. doi: 10.1016/j.postharvbio.2015.09.023
- Gao, M., Guo, W., Huang, X., Du, R., and Zhu, X. (2021). Effect of pressing and impacting bruises on optical properties of kiwifruit flesh. *Postharvest Bio. Technol.* 172:111385. doi: 10.1016/j.postharvbio.2020.111385
- Hussein, Z., Fawole, O. A., and Opara, U. L. (2017). Investigating bruise susceptibility of pomegranate cultivars during postharvest handling. *Afr. J. Rural Devel.* 2, 33–39. doi: 10.22004/agecon.263298
- Hussein, Z., Fawole, O. A., and Opara, U. L. (2019). Bruise damage susceptibility of pomegranates (*Punica granatum*, L.) and impact on fruit physiological response during short term storage. *Sci. Horti.* 246, 664–674. doi: 10.1016/j.scienta.2018.11.026
- Hussein, Z., Fawole, O. A., and Opara, U. O. (2020a). Bruise damage of pomegranate during long-term cold storage: Susceptibility to bruising and changes in textural properties of fruit. *Intl. J. Fruit Sci.* 20, S211–S230. doi: 10.1080/15538362.2019.1709602
- Hussein, Z., Fawole, O. A., and Opara, U. O. (2020b). Effects of bruising and storage duration on physiological response and quality attributes of pomegranate fruit. *Sci. Horti.* 267:109306. doi: 10.1016/j.scienta.2020.109306
- Komarnicki, P., Stopa, R., Szyjczewicz, D., and Młotek, M. (2016). Evaluation of bruise resistance of pears to impact load. *Postharvest bio. Technol.* 114, 36–44. doi: 10.1016/j.postharvbio.2015.11.017
- Li, J., Yan, J., Cao, J., Zhao, Y., and Jiang, W. (2012). Preventing the wound-induced deterioration of Yali pears by chitosan coating treatments. *Food Sci. Technol. Int.* 18, 123–128. doi: 10.1177/1082013211414774
- Lipa, T., Szot, I., Dobrzański, B., Kaplan, M., and Baryła, P. (2019). Susceptibility of pear to bruising after harvest and storage. *Acta Agrophys.* 25, 485–499. doi: 10.31545/aagr/102717
- Maia, V. M., Salomão, L. C. C., Siqueira, D. L., Puschman, R., Mota Filho, V. J. G., and Cecon, P. R. (2011). Physical and metabolic alterations in “Prata Anã” banana induced by mechanical damage at room temperature. *Scientia Agricola* 68, 31–36. doi: 10.1590/S0103-90162011000100005
- Montero, C. R. S., Schwarz, L. L., Santos, L. C. D., Andreaza, C. S., Kechinski, C. P., and Bender, R. J. (2009). Postharvest mechanical damage affects fruit quality of ‘Montenegrina’ and ‘Rainha’ tangerines. *Pesquisa Agropecuária Brasileira* 44, 1636–1640. doi: 10.1590/S0100-204X2009001200011
- OECD (2018). *Guidelines on Objective Tests to Determine Quality of Fruit and Vegetables, Dry and Dried Produce*. Available online at: <https://www.oecd.org/agriculture/fruit-vegetables/publications/47288602.pdf> (accessed December 29, 2020).
- Opara, U. L., and Pathare, P. B. (2014). Bruise damage measurement and analysis of fresh horticultural produce—a review. *Postharvest Bio. Technol.* 91, 9–24. doi: 10.1016/j.postharvbio.2013.12.009
- Pathare, P. B., and Al-Dairi, M. (2021). Bruise damage and quality changes in impact-bruised, stored tomatoes. *horticulturae* 7, 113. doi: 10.3390/horticulturae7050113
- Pathare, P. B., Opara, U. L., and Al-Said, F. A. (2013). Colour measurement and analysis in fresh and processed foods: a review. *Food Bioprocess Technol.* 6, 36–60. doi: 10.1007/s11947-012-0867-9
- Shafie, M., Rajabipour, A., Castro-García, S., Jiménez-Jiménez, F., and Mobli, H. (2015). Effect of fruit properties on pomegranate bruising. *Int. J. Food Prop.* 18, 1837–1846. doi: 10.1080/10942912.2014.948188
- Shafie, M., Rajabipour, A., and Mobli, H. (2017). Determination of bruise incidence of pomegranate fruit under drop case. *Int. J. Fruit Sci.* 17, 296–309. doi: 10.1080/15538362.2017.1295416

- Van Zeebroeck, M., Darius, P., De Ketelaere, B., Ramon, H., and Tijskens, E. (2007). The effect of fruit factors on the bruise susceptibility of apples. *Postharvest Bio. Technol.* 46, 10–19. doi: 10.1016/j.postharvbio.2007.03.017
- Xia, M., Zhao, X., Wei, X., Guan, W., Wei, X., Xu, C., and Mao, L. (2020). Impact of packaging materials on bruise damage in kiwifruit during free drop test. *Acta Phys. Plantarum.* 42, 1–11. doi: 10.1007/s11738-020-03081-5
- Zarifneshat, S., Ghassemzadeh, H. R., Sadeghi, M., Abbaspour-Fard, M. H., Ahmadi, E., Javadi, A., and Shervani-Tabar, M. T. (2010). Effect of impact level and fruit properties on golden delicious apple bruising. *Am. J. Agric. Bio. Sci.* 5, 114–121. doi: 10.3844/ajabssp.2010.114.121
- Zhou, R., Su, S., Yan, L., and Li, Y. (2007). Effect of transport vibration levels on mechanical damage and physiological responses of huanghua pears (*Pyrus pyrifolia* Nakai, cv. Huanghua). *Postharvest Bio. Technol.* 46, 20–28. doi: 10.1016/j.postharvbio.2007.04.006

Conflict of Interest: The authors declare that the research was conducted in the absence of any commercial or financial relationships that could be construed as a potential conflict of interest.

Publisher's Note: All claims expressed in this article are solely those of the authors and do not necessarily represent those of their affiliated organizations, or those of the publisher, the editors and the reviewers. Any product that may be evaluated in this article, or claim that may be made by its manufacturer, is not guaranteed or endorsed by the publisher.

Copyright © 2021 Pathare and Al-Dairi. This is an open-access article distributed under the terms of the Creative Commons Attribution License (CC BY). The use, distribution or reproduction in other forums is permitted, provided the original author(s) and the copyright owner(s) are credited and that the original publication in this journal is cited, in accordance with accepted academic practice. No use, distribution or reproduction is permitted which does not comply with these terms.



Microbial Diversity and Non-volatile Metabolites Profile of Low-Temperature Sausage Stored at Room Temperature

Hongjiao Han, Mohan Li, Yanqi Peng, Zhenghan Zhang, Xiqing Yue* and Yan Zheng*

College of Food Science, Shenyang Agricultural University, Shenyang, China

OPEN ACCESS

Edited by:

Shalini Gaur Rudra,
Indian Agricultural Research Institute,
India

Reviewed by:

Aparna Banerjee,
Universidad Católica del Maule, Chile
Rajib Bandopadhyay,
University of Burdwan, India

*Correspondence:

Xiqing Yue
yxqsyau@126.com
Yan Zheng
zhengyan0403@163.com

Specialty section:

This article was submitted to
Food Microbiology,
a section of the journal
Frontiers in Microbiology

Received: 19 May 2021

Accepted: 05 August 2021

Published: 27 August 2021

Citation:

Han H, Li M, Peng Y, Zhang Z,
Yue X and Zheng Y (2021) Microbial
Diversity and Non-volatile Metabolites
Profile of Low-Temperature Sausage
Stored at Room Temperature.
Front. Microbiol. 12:711963.
doi: 10.3389/fmicb.2021.711963

Sausage is a highly perishable food with unique spoilage characteristics primarily because of its specific means of production. The quality of sausage during storage is determined by its microbial and metabolite changes. This study developed a preservative-free low-temperature sausage model and coated it with natural casing. We characterized the microbiota and non-volatile metabolites in the sausage after storage at 20°C for up to 12 days. *Bacillus velezensis* was the most prevalent species observed after 4 days. Lipids and lipid-like molecules, organoheterocyclic compounds, and organic acids and their derivatives were the primary non-volatile metabolites. The key non-volatile compounds were mainly involved in protein catabolism and β -lipid oxidation. These findings provide useful information for the optimization of sausage storage conditions.

Keywords: low-temperature sausage, sausage spoilage, bacterial communities, non-volatile metabolites, omics technology

INTRODUCTION

Low-temperature sausage is widely consumed throughout the world. The cooking process is centered on a temperature between 68 and 75°C, which retains the highest levels of quality and nutrition (Toldrá, 2017; Yang et al., 2020). However, low-temperature sausage is highly perishable because of incomplete sterilization and its natural casing (Salinas et al., 2014; Lv et al., 2021). To date, the general methods to reduce the spoilage and the maintain quality of meat products have been developed, such as the addition of preservatives (Pellissery et al., 2020), vacuum packaging, and chilled storage (Gammariello et al., 2015; Schumann and Schmid, 2018). Unfortunately, the unique appearance and quality of low-temperature sausage is detrimentally affected when stored under chilled conditions with vacuum packaging (Dong et al., 2020; Lv et al., 2021). In addition, many of these meat products are subjected to room temperature conditions and air-packaging when circulated among consumers, especially if the transportation and the cold chain are imperfect. Moreover, consumers often prefer natural, fresh, and minimally processed food with fewer additives (Pini et al., 2020). To meet these demands, our study developed a low-temperature sausage model without added preservatives that could be stored at room temperature without vacuum.

To improve the quality and safety of low-temperature sausage at room temperature, it is important to understand the changes that occur in the microbial succession within the product during storage. It has been reported that *Staphylococcus*, *Pseudomonas*, and *Acinetobacter* are the predominant bacteria contributing to the spoilage of meats at room temperature (Lv et al., 2021).

Apart from these reports, there is little information on the dominant spoilage-associated bacteria in low-temperature meat products stored at room temperature. In recent years, high-throughput sequencing (HTS) approaches based on the detection of microbial DNA have been successfully applied to the identification of microorganisms and microbial communities in meat and meat products, thus providing a better understanding of the microbial quality of meat products (Polka et al., 2015; Tian et al., 2017; Chen et al., 2020; Hu et al., 2020).

Additionally, the metabolic activities of spoilage-associated microorganisms lead to the accumulation of metabolites which promote the physical and chemical deterioration of meat products (Luong et al., 2020; Bekhit et al., 2021). Thus, there is a need to simultaneously investigate both microbial communities and metabolites during storage to comprehensively the quality evolution of meat products. Recently, metabolomics has been used for the analysis and monitoring of changes in non-volatile metabolites in stored and processed meat (Castro-Puyana et al., 2017). This strategy has been successfully applied to characterize non-volatile metabolites in various types of meat, including ovine meat (Subbaraj et al., 2016), chilled chicken (Wen et al., 2020), duck liver (Zhu et al., 2020), and duck (Wang et al., 2017). Therefore, the comprehensive understanding of non-volatile metabolites in low-temperature meat products could be explored by this strategy.

In this study, we investigated the changes in bacterial succession combined with physicochemical properties and non-metabolite changes of low-temperature sausage during storage at 20°C. Specifically, we aimed to investigate (i) the physicochemical changes in the sausage based on total viable counts, total volatile basic nitrogen (TVB-N), color, and pH, (ii) microbiota changes using 16S rDNA gene analysis, and (iii) the profiles of non-volatile metabolites in low-temperature sausage by untargeted LC-MS/MS-based metabolomics.

MATERIALS AND METHODS

Preparation of Low-Temperature Sausage

The low-temperature sausage were supplied by a local Chinese meat factory in Fuxin, Liaoning Province, China, and had been manufactured in accordance with Chinese food safety standards based on the method of Jin et al. (2017) with some modifications. A total of five independent batches were collected. The formulation included pork belly (95%, the ratio of fat to skin is about 3:1), salt (2.5%), starch (2%), sugar [0.4% (wt/wt)], and ice water (0.5–1.5%). The meats were minced in a grinder with an 8-mm plate and mixed with other supplementary material. Then, the mixture was stuffed into 30–35 mm diameter porcine natural casings, 10–12 cm long. Thereafter, the raw sausages were steamed at a temperature of 70–80°C for approximately 30 min until the internal temperature reached 74°C (Walton and McCarthy, 2007). When the steamed sausage had returned to room temperature, it was rapidly transferred to the laboratory within 2 h in a portable constant-temperature incubator (BX-10B, Kai Hang Instrument Co., Ltd., Changzhou, China). The

sausages were then packed under aseptic laboratory conditions into permeable polyethylene bags (200 × 300 mm) and stored in a constant temperature humidity chamber (LHS-50CL, Shanghai Yiheng Instruments Co., Ltd., Shanghai, China) at 20°C and humidity of 50 ± 5%. The sausages used for physicochemical, metabolites, and microbiological analysis were harvested at 0, 2, 4, 6, 8, 10, and 12 days during storage.

Physicochemical Analysis

Ten grams of sausage were ground to a puree in 90 ml deionized water according to the method of Chen et al. (2019) with some modifications. After multiple leaching and filtering in a stomacher (Pro-media, SH-2M) with a filter net, the pH of the supernatant was determined with a pH meter (PHS-3C pH Meters, Shanghai Kang Yi Instrument Co., Ltd., China).

The colors of the sausage samples were measured by a Minolta CM-2600d/2500d Chroma meter (Minolta Camera Co., Ltd., Osaka, Japan) using the standard white version for calibration before the measurement. Measurements were made perpendicular to the individual sample surface at 10 different positions. The measured areas on the sausage surface were randomly selected, sampling as much of the surface as possible and avoiding areas with obvious visual defects such as slime or exudate. The results were shown as lightness (L^*), redness (a^*), and yellowness (b^*) values.

The TVB-N content was measured according to the Chinese National Food Safety Standard method GB 5009.228-2016 [National Health and Family Planning Committee of China (NHFPCC), 2016]. Briefly, a 10 g sample was homogenized in 70 mL of distilled water for 30 min and then filtered. Then, 10 mL of the filtrate was transferred to a distillation tube. After adding 5 mL of magnesium oxide suspension (10 g/L), the distillation tube was connected to an automatic Kjeldahl (K1100, Hanon Instruments Co., Ltd., Jinan, China), according to the instructions. The distillate was collected using a boric acid solution (20g/L) and then titrated with hydrochloric acid standard titration solution. Finally, the TVB-N content was calculated as:

$$TVB-N \text{ (mg/100g)} = \frac{(V1 - V2) \times c \times 14}{m} \times 10$$

Where: V1 denotes the titration volume of the hydrochloric acid consumed by the sample (mL), V2 denotes the titration volume of the blank sample (mL), c denotes the actual concentration of hydrochloric acid (mol/L), and m denotes the sample weight (g).

Microbiological Analyses

Total Viable Counts

The total viable counts were determined as described by Li X. et al. (2019) with some modifications. Twenty-five grams of sausage sample were mixed with 225 mL sterile saline solution (NaCl, 8.5 g/L) and homogenized in the stomacher machine. Serial decimal dilutions were prepared, and 100 µl aliquots of the sample suspension were spread in triplicate on the Plate Count Agar (Beijing Aoboxing Bio-Tech Co., Ltd). The plates were incubated for 48 ± 2 h at 36 ± 1°C. The results were calculated and expressed as the means of log CFU/g.

Bacterial DNA Extraction and Sequencing

Total DNA was extracted using the CTAB method following an earlier reported method (Via and Falkinham, 1995; Brandfass and Karlovsky, 2008). The DNA purity was checked on 1% agarose gel electrophoresis, and the DNA concentration was measured using an ultraviolet spectrophotometer. The V3–V4 region of 16S ribosomal DNA was amplified using a pair of universal primers [341F(5'-CCTAYGGGRBGCASCAG-3'); 806R(5'-GGACTACNNGGTATCTAAT-3')] with the barcode. Sequencing libraries were generated using the Ion Plus Fragment Library Kit (Thermo Fisher Scientific, Inc., Waltham, MA, United States) following the manufacturer's recommendations. The library was then sequenced on an Ion S5TM XL platform, and 400 bp/600 bp single-end reads were generated.

Sequencing Analysis

Quality filtering was performed using Cutadapt software (Version 1.9.1) (Martin, 2011). The data were queried in the SILVA database (Quast et al., 2013) using the UCHIME algorithm (UCHIME Algorithm)¹ (Edgar et al., 2011) to check and remove chimeric sequences (Haas et al., 2011). Sequences with $\geq 97\%$ similarity were clustered into the operational taxonomic units (OTUs) by using UPARSE software (Version 7.0.1001) (Edgar, 2013). The SILVA database² was used based on the Mothur algorithm to annotate taxonomic information for each OTU representative sequence. Beta diversity on unweighted UniFrac was performed by QIIME software (Version 1.7) (Caporaso et al., 2010).

Analysis of Non-volatile Metabolites

Metabolite Extraction

Metabolites were extracted as described by Wen et al. (2020) with some modifications. Briefly, 100 mg of samples were individually ground with liquid nitrogen and homogenized in 80% methanol and 0.1% formic acid, following which the mixtures were stored in an ice bath for 5 min. The samples were then centrifuged at 15,000 rpm at 4°C for 5 min. A part of the supernatant was diluted with LC-MS-grade water to a final concentration containing 60% methanol. The samples were subsequently transferred into an Eppendorf tube with a 0.22 μm filter and were centrifuged at 15,000 $\times g$ at 4°C for 10 min. Finally, the filtrate was collected and stored for analysis. Equivalent metabolite extracts from each sausage sample were used for quality control (QC).

UHPLC-MS/MS Methods

Samples were analyzed using a Vanquish UHPLC system (Thermo Fisher Scientific) coupled with an Orbitrap Q Exactive HF-X mass spectrometer (Thermo Fisher Scientific). Metabolite extracts were separated on a Hypersil Gold column (100 \times 2.1 mm, 1.9 μm , 4°C, 0.2 mL/min). The eluents of the positive polarity mode consisted of eluent A (0.1% formic acid) and eluent B (methanol). The eluents of the negative polarity mode consisted of eluent A (5 mM ammonium acetate, pH 9.0) and eluent B (methanol). The solvent gradient was initially 2% B

(1.5 min) then 2% to 100% B (12 min), 100% B, (14 min), 100% to 2% B (14.1 min), and 2% B (16 min).

Raw MS Data Processing

The original data were converted by Compound Discoverer (Version 3.0, Thermo Fisher Scientific) to perform peak alignment, peak picking, and quantitation. The peak intensities were converted to the total spectral intensity. Then, the molecular formula was predicted according to the additive ions, molecular ion peaks, and fragment ions. Following that, the peaks were matched with the mzCloud³ and ChemSpider⁴ databases to obtain accurate qualitative and relative quantitative results.

Statistical Analysis

The data analysis was performed on the General Linear Model procedure of Statistix 8.1 software package (Analytical Software, St. Paul, MN, United States). Analysis of variance (ANOVA) with Tukey's multiple comparisons test was used at a significance level of $\alpha = 0.05$. The results were expressed as means \pm standard error of the mean. Principal component analysis (PCA) and partial least squares-discriminant (PLS-DA) were completed using R-3.5.3 software. The screening of differential metabolites depended on the variable importance in the projection (VIP) > 2 and $p < 0.05$.

RESULTS

Analysis of Physicochemical Properties

pH

The changes in pH values during the storage of the low-temperature sausage are listed in **Table 1**. Before storage, the initial pH of the sausage was 7.00 ± 0.01 which finally decreased to 6.20 after being stored for 12 days. At the early storage stage (0–4 days), the pH showed a slight decrease due to lower levels of acidic substances (Lv et al., 2021). As the numbers of aerobic bacteria increased (**Table 1**), glucose was degraded into organic acids (Dainty et al., 1989), creating an acidic environment, leading to a sharp and significant decreasing trend between 4 and 12 days ($p < 0.05$). Additionally, it was found that organic acids and their derivatives were the predominant differential metabolites, accounting for 45.31% of the total (shown in **Figure 1**), confirming the decreasing pH trend. This continuous decrease in pH has been previously demonstrated and is consistent with the findings of Benson et al. (2014) and Luong et al. (2020) in pork sausage.

Color

Color is both an effective criterion as well as an essential index to evaluate the appearance, quality, and freshness of meat products (Rubio et al., 2008). The values of L^* and b^* decreased continuously after 12 days' storage but there was no significant fluctuation at the beginning of storage (0–2 days) ($p > 0.05$). The L^* -value represents the color of the sausage surface and its

¹http://www.drive5.com/usearch/manual/uchime_algo.html

²<https://www.arb-silva.de/>

³<https://www.mzcloud.org/>

⁴<http://www.chemspider.com/>

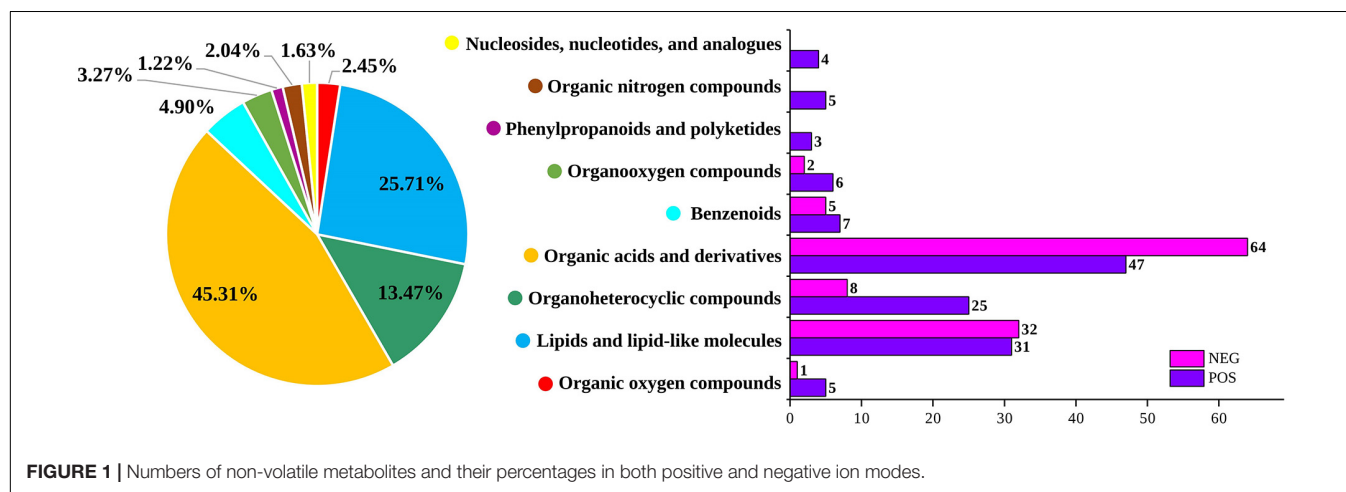
TABLE 1 | Total viable counts, pH, TVB-N, and color changes in low-temperature sausage during storage.

Physicochemical analyses	Storage times (days)						
	0	2	4	6	8	10	12
pH	7.00 ± 0.01 ^a	6.87 ± 0.01 ^a	6.78 ± 0.03 ^b	6.58 ± 0.02 ^c	6.37 ± 0.06 ^d	6.25 ± 0.04 ^e	6.20 ± 0.05 ^f
TVB-N (mg/100g)	6.54 ± 0.01 ^g	8.67 ± 0.05 ^f	13.43 ± 0.12 ^e	22.37 ± 0.40 ^d	25.92 ± 0.07 ^c	28.00 ± 0.02 ^b	35.48 ± 0.02 ^a
L*	51.83 ± 0.21 ^a	51.33 ± 0.17 ^a	50.98 ± 0.35 ^b	49.47 ± 0.29 ^c	48.52 ± 0.17 ^d	47.93 ± 0.33 ^e	47.19 ± 0.33 ^f
a*	18.21 ± 0.12 ^a	17.19 ± 0.17 ^b	15.15 ± 0.14 ^c	14.64 ± 0.14 ^d	10.72 ± 0.17 ^e	10.51 ± 0.24 ^e	9.32 ± 0.16 ^e
b*	9.19 ± 0.07 ^a	9.00 ± 0.11 ^a	8.32 ± 0.10 ^b	7.46 ± 0.11 ^c	7.24 ± 0.12 ^{cd}	6.83 ± 0.28 ^d	5.62 ± 0.20 ^e
(TVC)log CFU/g	2.25 ± 0.03 ^f	3.82 ± 0.04 ^e	6.82 ± 0.12 ^d	8.03 ± 0.10 ^c	8.70 ± 0.09 ^b	8.95 ± 0.10 ^{ab}	9.05 ± 0.10 ^a

Values are presented in the table as the mean ± standard deviation.

Means within the different superscript on a row indicate significant differences ($p < 0.05$).

The results were shown as lightness (L*), redness (a*), and yellowness (b*) values.

**FIGURE 1** | Numbers of non-volatile metabolites and their percentages in both positive and negative ion modes.

decrease may be responsible for moisture evaporation (Ferrini et al., 2012). The a^* -values decreased significantly ($p < 0.05$) until 6 days but did not change thereafter. The reduced a^* -values may be indicative of lipid oxidation (Yu et al., 2002). The changes in these color values indicated color deterioration in the spoiled samples.

TVB-N

The TVB-N value is one of the core indices to evaluate the freshness of meat products and represents the enzymatic and bacterial degradation of protein and non-protein nitrogenous substances (Chen et al., 2013). In this study, the TVB-N values increased slightly between 0 and 4 days and then increased rapidly after 6 days. Colby and Zatman (1973) reported that the accumulation of compounds contributing to the TVB-N is usually seen as a lag phase before an exponential growth period. Similarly, Tan et al. (2019) have also reported a lag phase in amine compounds in chicken meat stored at 20°C.

Microbiological Analyses

Total Viable Counts

Table 1 shows the counts of total aerobic bacteria at different storage times. The initial TVC of the fresh sausage started at 2.25 CFU/g and gradually increased to a maximum of 9.05 CFU/g at the end of the storage period. The TVC increased sharply from 0 to 4 days, possibly because there are sufficient nutrients to

ensure bacterial growth (Lv et al., 2021). However, the bacterial growth slowed between 6 and 12 days, which may have been due to an inhibition of growth in a low pH environment created by bacterial metabolism. Therefore, the observed constant decrease in pH was consistent with the gradual increase in bacterial growth seen between 4 and 12 days.

Microbial Community Structure

A total of 2,306, 140 high-quality bacterial sequences with an average length of 411 bp was chosen and classified into 8,487 OTUs with 97% similarity. A total of 20 phyla were identified, of which the top 10 are shown on the right side of Figure 2. To better illustrate the bacterial succession, the cluster tree analysis of the stored sausages is shown on the left side of Figure 2. The storage period was divided into three stages, with sausages stored between 0 and 2 days separated from those stored for longer periods. In the later storage period (4–12 days), there was a further separation of sausages stored between 4 and 6 days. These results suggest that the bacterial communities tended to be stable after 4 days, and few microorganisms became dominant (Li N. et al., 2019).

At the beginning of storage (0–2 days), Cyanobacteria and Proteobacteria were the most abundant phyla, accounting for 61.44% to 64.76%, and 22.52% to 15.05% of the total bacterial phyla, respectively. As reported, the initial microbial levels of meat products are strongly dependent on the

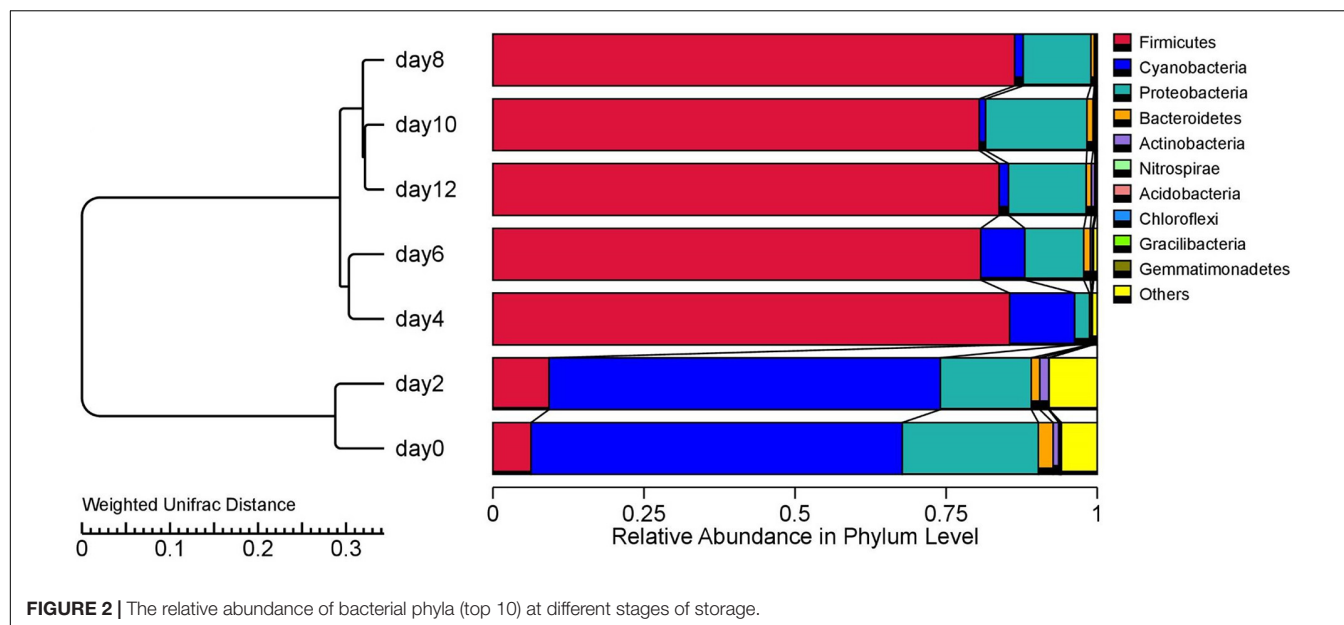


FIGURE 2 | The relative abundance of bacterial phyla (top 10) at different stages of storage.

processing environment (Stellato et al., 2016). Thus, the bacterial composition in the early storage period of this study may have been due to environmental issues such as meat handling and storage conditions. At 4 days, the relative abundance of Cyanobacteria and Proteobacteria decreased, while the Firmicutes increased to 85.5% of the total bacteria, and their relative abundance did not fluctuate significantly from the 6 days to the 12 days ($p > 0.05$). Similar changes in Firmicutes were observed during the storage of smoked bacon over 45 days (Li X. et al., 2019).

At the species level, an overview of the top 10 species is shown in **Figure 3**. It can be seen that the species composition underwent significant fluctuations. At 0 day, the predominant species were *Phaseolus vulgaris* (15.86%) and *Gleditsia sinensis* (9.52%). Although the TVC were low at the initial storage stage of 0–2 days as described above, the species proportions and abundance changed continuously. At 2 days, the dominant species was *P. vulgaris* (18.66%), while the abundance of *G. sinensis* had decreased to 1.75%. There were further changes until the composition of the microbial population gradually stabilized in the later storage stage (4–12 days). *Bacillus velezensis* was present throughout comprising more than 30% of the total population without significant fluctuation ($p > 0.05$), thus holding a relatively dominant position. As reported, *B. velezensis* was identified by Li et al. (2018) in the slaughter wastewater of a meat factory in Hunan Province, China, suggesting that the major microbial species associated with spoilage may have originated from the raw meat (Doulgeraki et al., 2012). Presumably, as a result of the mild heat treatment (68–75°C) used in this study, the microbes in the raw meat were not completely killed, allowing them to proliferate after the heat treatment. As *B. velezensis* became the predominant bacterial species from the fourth day to the end of storage suggested that *B. velezensis* was the dominant spoilage species in the sausage during the 20°C storage.

Non-volatile Metabolites Analysis

Principal Component Analysis of Non-volatile Metabolites

Using untargeted LC-MS/MS-based metabolomics, a total of 2,979 peaks (1,770 from the positive mode; 1,209 from the negative mode) were identified by the mzCloud and ChemSpider databases in low-temperature sausage. Among these, 845 (480 from the positive mode; 365 from the negative mode) metabolites were annotated by the Human Metabolome Database (HMDB)⁵ (Wishart et al., 2007). To obtain a comprehensive overview of the sausage samples, PCA analysis of non-volatile metabolites was performed and is shown in **Figure 4**. The present PCA model could detect 67.8% (PC1 57.84% and PC2 9.96%) and 68.87% (PC1 51.81% and PC2 17.06%) variation among the samples in both the positive and negative ion modes, respectively. Moreover, it also revealed the variation and similarity of the non-volatile metabolite compositions at different storage times. Thus, the 12-day storage period was clustered into three groups: 0–2, 4–6, and 8–12 days. The microbial community as described above showed a corresponding trend of change over the storage time.

Profiling of Differential Non-volatile Metabolites

As shown in **Figure 1**, 245 differential non-volatile metabolites were obtained based on VIP > 2 and $p < 0.05$. These non-volatile metabolites were assigned to nine classes of 92 compounds, including organic oxygen compounds, lipids and lipid-like molecules, organoheterocyclic compounds, organic acids and their derivatives, benzenoids, organooxygen compounds, phenylpropanoids and polyketides, organic nitrogen compounds, nucleosides, nucleotides, and analogs. The comprehensive list of 245 significant metabolites at different storage times is provided in the **Supplementary Tables 1–6**. Organic acids and their derivatives, lipids and lipid-like molecules, and

⁵<http://www.hmdb.ca/>

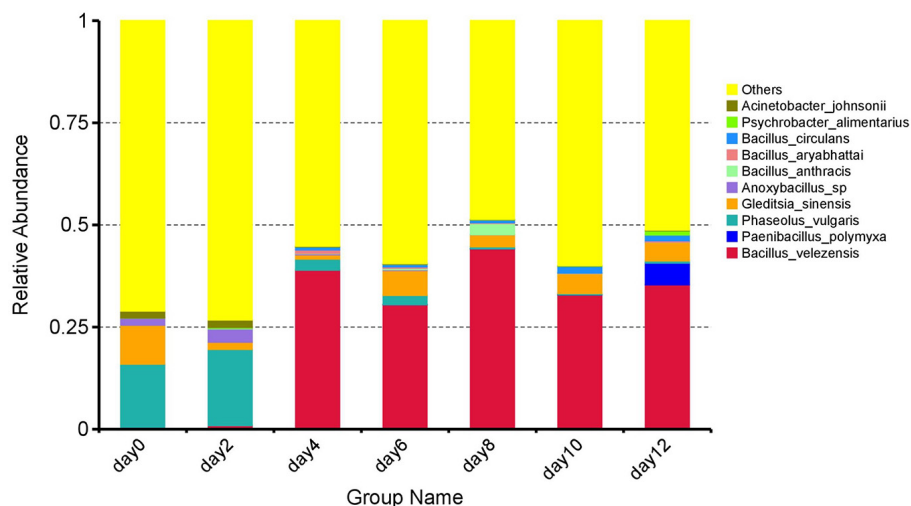


FIGURE 3 | The relative abundance of bacterial species (top 10) at different stages of storage.

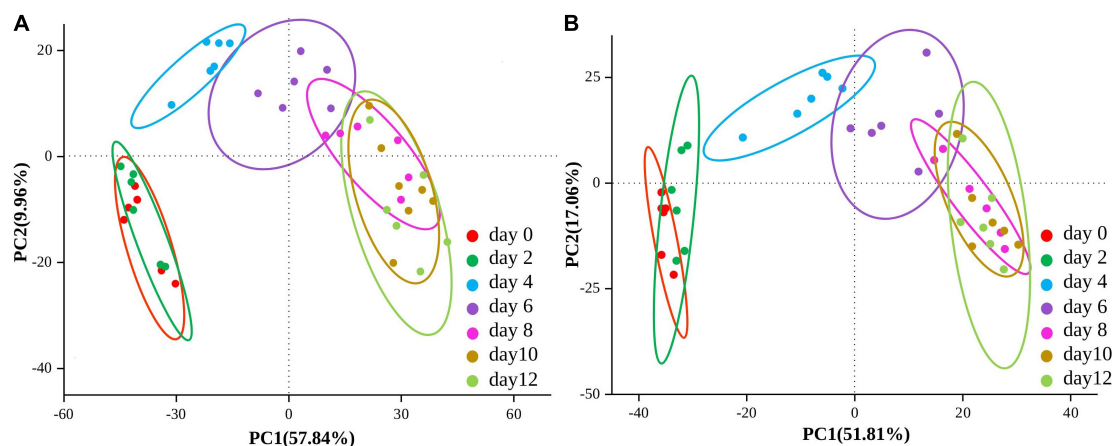


FIGURE 4 | Score plots of the principal component analysis (PCA) of both positive (A) and negative (B) ion mode of non-volatile metabolites at different stages of storage.

organoheterocyclic compounds were the major non-volatile metabolites identified in low-temperature sausage. **Figure 5** shows a visualization of relative content changes of non-volatile metabolites in the form of a heatmap.

During storage, microorganisms and endogenous enzymes degrade proteins in the sausage to various intermediate products, such as small peptides, tripeptides, dipeptides, and single amino acids, all of which greatly affect the quality of the meat product (Spaziani et al., 2009; Berardo et al., 2017; Hanagasaki and Asato, 2018). In this study, DL-serine, L-serine, N6-acetyl-L-lysine, pyridinolone, 4-guanidinobutyric acid, and capryloylglycine were found to be the primary free amino acids in low-temperature sausage during storage and were the main contributors to the differences between the groups. 4-guanidinobutyric acid and capryloylglycine are the degradation products of arginine and the glycine precursor, respectively. The relative contents of these compounds differed across the storage stages (**Figure 5**).

In addition, the decarboxylation of proteins or amino acids can result in the formation of biogenic amines, especially during relatively long storage periods (Lorenzo et al., 2017). As a typical biogenic amine in meat products, tyramine was identified in low-temperature sausage and was observed to increase over the storage time (**Figure 5**). A similar increase was previously reported in fermented sausage stored at $17 \pm 2^\circ\text{C}$ for 21 days (Bover-Cid et al., 2006). Another biogenic amine-related compound is formylkynurenine, formed during tryptophan degradation, was also a major contributor frequently observed in each group. Furthermore, various peptides containing Arg-His, Lys-Leu, Lys-Phe, Pro-Met, Tyr-Phe, Trp-Trp, Leu-enkephalin, and leucyltryptophan, also intermediate products of proteolysis, were identified. The peptide content was low between 0 and 2 days but increased rapidly thereafter.

In the current study, a total of nine acylcarnitines (ACs) were observed during the storage of the low-temperature sausage,

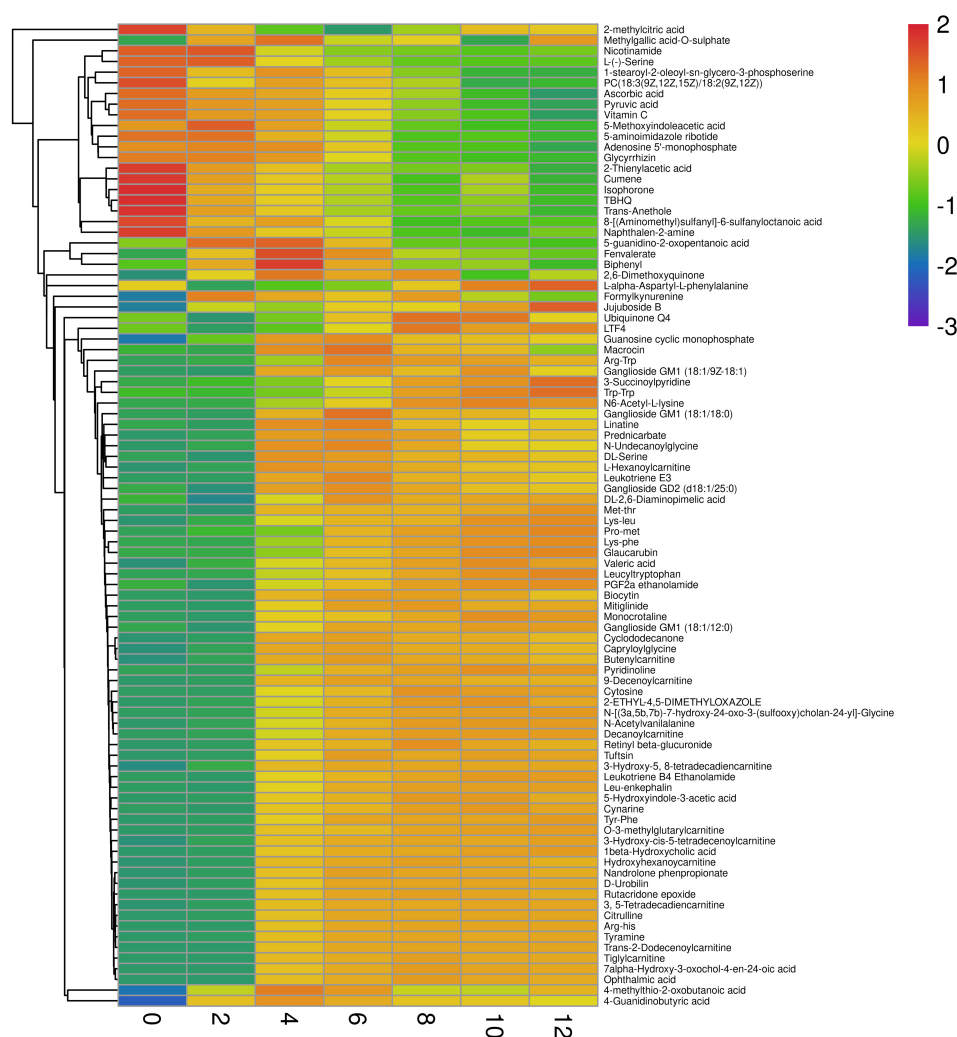


FIGURE 5 | Heatmap of individual non-volatile metabolites determined in both positive and negative ion modes. The scale with the range from -3 to 2 refers to the trend of peak area after logarithmic transformation. Red and blue color indicates the high and low content of different non-volatile metabolites, respectively.

namely, 3-hydroxy-cis-5-tetradecenylcarnitine, 3-hydroxy-5, 8-tetradecadienylcarnitine, O-3-methylglutarylarnitine, hexanoylcarnitine, 3, 5-tetradecadienylcarnitine, and hydroxyhexanoylcarnitine. As shown in **Figure 5**, only hexanoylcarnitine levels were high for the first 4 days, whereafter a decreasing trend was observed. Other ACs were abundant, and their concentrations increased steadily in the later storage period of 6–12 days (**Figure 5**).

To better analyze the relationship between the differential non-volatile metabolites during sausage storage, we investigated the biochemical processes responsible for their production (**Figure 6**). These processes included the metabolism of purine, tyrosine, and tryptophan, as well as nicotinate and nicotinamide and the biosynthesis of amino acids and β -lipid oxidation, all of which affected the changes in bacterial composition encouraging further growth and proliferation of the dominant microbial species. It appears from **Figure 6** that the majority of non-volatile metabolites were associated with amino acid and

bioamine metabolism. The presence of intermediate products from these pathways is usually indicative of proteolysis, and their accumulation contributes to the deterioration in meat quality (Hanagasaki and Asato, 2018; Wen et al., 2020). In addition, ACs are the principal products of β -lipid oxidation, suggesting a prominent role for β -lipid oxidation in the low-temperature sausage during storage.

DISCUSSION

In this study, the sausage samples were not only exposed to an open environment during production, marketing, and distribution but were also made without any preservatives. This type of perishable sausage model has rarely been reported. In the present study, *P. vulgaris* was abundant during the initial storage stage of 0–2 days, after which its abundance gradually decreased until 4 days and then dropped significantly,

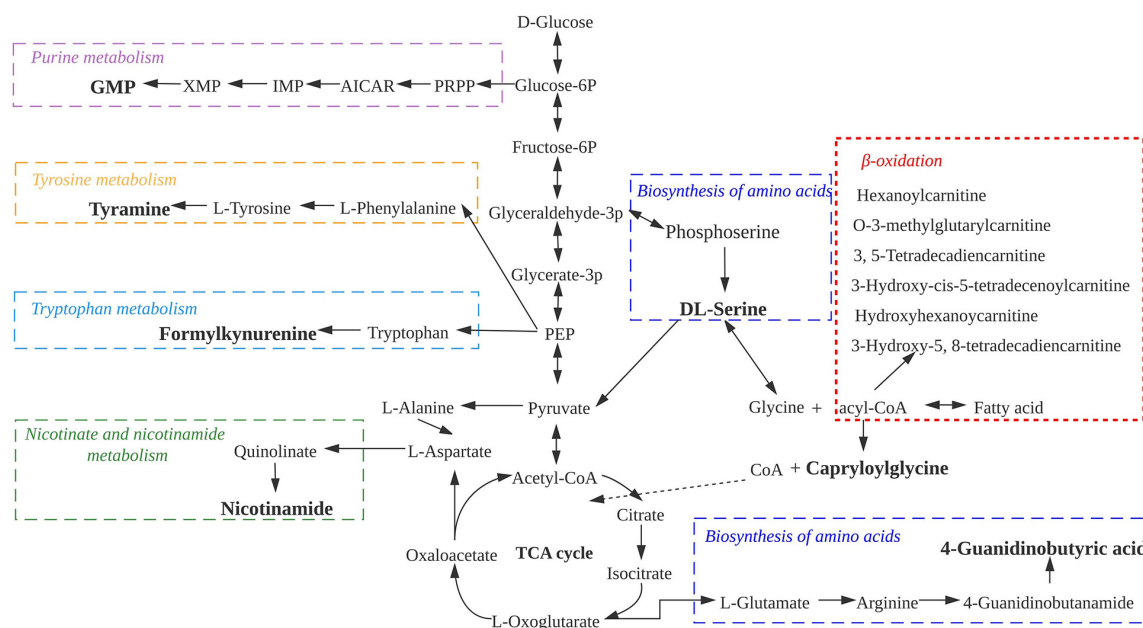


FIGURE 6 | Metabolic pathways of differential non-volatile metabolites in low-temperature sausage.

indicating that *P. vulgaris* was not a main contributor to sausage spoilage. This has not been previously reported. We speculate that the presence of *P. vulgaris* was understandable for the following reasons: firstly, it may have originated from contamination during the meat handling and processing, from non-sterile items such as processing surfaces and tools, or from microbiota in the meat itself (Doulgeraki et al., 2012; Ercolini et al., 2015; Hultman et al., 2015). Secondly, the excipients may have contained chloroplasts, and the plant chloroplast has a high sequence similarity to the 16S genes of bacteria (Sun et al., 2008; Hanshew et al., 2013). Its significant impact on analysis of data sets has also been acknowledged by Chelius and Triplett (2001). In addition, it is noteworthy that *Bacillus anthracis*, the etiological agent of the acute infectious disease anthrax, was identified by DNA sequencing. As shown in the **Supplementary Table 7**, except for 8 days, the relative abundance of *B. anthracis* over the remaining storage period remained constant with no significant change from 0.00% on 0 day. Thus, we speculate that this was a false positive based on *B. anthracis* has similarities with strains in *Bacillus* species (Rao et al., 2010). Moreover, accurate DNA-based detection of *B. anthracis* needs clean samples and is unable to detect toxins and other non-nucleic acid based samples (Rao et al., 2010; Zasada, 2020). Nevertheless, this suggests that retailers should pay attention to hygiene to ensure the safety of meat products, especially as other microorganisms such as *Bacillus circulans*, *Psychrobacter alimentarius*, and *Acinetobacter johnsonii*, are also commonly associated with food spoilage (Yucel et al., 2009; Li et al., 2014; Wang and Xie, 2020).

Notably, there was a large proportion of unassigned bacteria ("others") in the sausage microbial community (**Figure 3**). This could be attributed to the fact that the

sausage contained no preservatives and was also stored in the open at room temperature, leading to increased exposure to microorganisms and thus contamination. On the other hand, sausages manufactured in different settings, using different materials, processing technology, and workshops (e.g., different temperatures and humidity) will have unique, well-balanced microbial community structures and diversity. With this in mind, the microorganisms in the environment and within the food will eventually reach an equilibrium. In other words, microorganisms from both the raw materials and the environment contribute to the species composition during storage (Aquilanti et al., 2016; Liu et al., 2019). Based on the complex microbial components mentioned above, the TVC values remained constant until the end of storage, and no pathogens were detected during processing. This variability indicates the complexity and diversity of the microflora.

Regarding the non-volatile metabolites, the number of differential non-volatile metabolites increased and then decreased with prolonged storage time. This may be attributed to a similar change in bacterial succession (Lv et al., 2021). On the first 2 days, the bacterial counts were low with no apparent accumulation of non-volatile metabolites or only slight changes in their contents. After 4–6 days, when spoilage tends to become apparent, the dominant microorganisms in the meat also typically produce more metabolic by-products (Martin et al., 1998). At this stage, *B. velezensis* was predominant and increased sharply from 6 days. As has been reported, *B. velezensis* produces a number of enzymes that strongly promote organic matter decomposition (Li et al., 2018), resulting in the accumulation of organic substances such as sulfides and nitrogen (Samaei et al., 2013; Meng and Hao, 2017; Li et al., 2018). This would account for the large numbers of

non-volatile metabolites observed at this stage. After this, both the bacterial succession and the accumulation of non-volatile metabolites tend to be stabilize.

In particular, ACs showed sustained accumulation in low-temperature sausage during storage. Compared with 0 day, the fold-change (FC) increased by several hundred or even thousand during storage (**Supplementary Tables 1–6**), implying that ACs contributed significantly to the observed changes in non-volatile metabolites in the sausage during storage (Wen et al., 2020). ACs are also important intermediates of lipid β -oxidation, which is typically related to the odor or flavor of sausage meat products (Toldrá et al., 2014). In addition, aerobic conditions have been shown not only to promote β -lipid oxidation (Wen et al., 2019) but also to sustain biological processes (Yu et al., 2019). Wen et al. (2019) also found that β -lipid oxidation was the most common bacterial metabolic activity in dry sausage. Therefore, we infer that β -lipid oxidation may play an essential role in the spoilage of low-temperature sausage stored at room temperature. In addition, the observed increases in amino acid, peptide, and bioamine content are indicative of proteolysis (Zhao et al., 2016). In most cases, these proteolysis markers accumulated with the storage time, especially from 6 days up to 12 days with the majority plateauing at later stages indicating that protein catabolism was maintained at a high level throughout the storage period (Frank et al., 2020). Moreover, all the peptides detected in this study are either potentially volatile compounds or the precursors of such compounds, and all had a low molecular mass of <5,000 Da (Berardo et al., 2017). Therefore, the accumulation of these peptides not only reduced the meat quality but also produced undesirable odors.

Furthermore, it was difficult to establish a direct correlation between the microbial populations and metabolites because the non-volatile metabolites are derived from both the microorganisms and the sausage itself. Overall, this paper aimed to study the chemical spoilage of low-temperature sausage from the macroscopic perspective. To our knowledge, there have been no reports regarding the changes of non-volatile metabolites in sausage over a 12 days' storage period.

CONCLUSION

The dynamic changes in the bacterial communities and non-volatile metabolites of low-temperature sausage stored at 20°C for 12 days have been reported. The changes in the physical and chemical properties of the sausage verified the spoilage

process, shown by the decreases in pH, L^* , a^* , and b^* values, and the increases in TVB-N and TVC. Firmicutes dominated the bacterial communities in the later storage period. *B. velezensis* was the dominant core bacterium that acts as a spoilage indicator and is probably associated with compounds acting as spoilage indicators. Meanwhile, different non-volatile metabolites of lipids and lipid-like molecules, organoheterocyclic compounds, and organic acids and their derivatives were present in high concentrations at different storage stages. The key non-volatile molecules were mainly involved in protein catabolism and β -lipid oxidation. This work provides valuable information for the industrialization and standardization of low-temperature meat products. However, the volatile compounds which also affect the quality of sausage during storage have not been studied. Comprehensive metabolomic analysis under different storage conditions should be carried out in the future so that these results can improve the processing of low-temperature meat products.

DATA AVAILABILITY STATEMENT

The datasets presented in this study can be found in online repositories. The names of the repository/repositories and accession number(s) can be found below: NCBI BioProject PRJNA731615; MetaboLights MTBLS2871.

AUTHOR CONTRIBUTIONS

HH carried out the original draft, data curation, and data analyses. HH, ZZ, and YP performed the experiments. ML and YZ provided critical comments. HH, YZ, and XY conceived and designed the idea of the study. All authors reviewed and approved the final manuscript.

FUNDING

This work was supported by the National Key R&D Program of China (2018YFC1604302).

SUPPLEMENTARY MATERIAL

The Supplementary Material for this article can be found online at: <https://www.frontiersin.org/articles/10.3389/fmicb.2021.711963/full#supplementary-material>

REFERENCES

- Aquilanti, L., Garofalo, C., Osimani, A., and Clementi, F. (2016). Ecology of lactic acid bacteria and coagulase negative cocci in fermented dry sausages manufactured in Italy and other Mediterranean countries: an overview. *Int. Food Res. J.* 23, 429–445.
- Bekhit, A. E.-D. A., Holman, B. W. B., Giteru, S. G., and Hopkins, D. L. (2021). Total volatile basic nitrogen (TVB-N) and its role in meat spoilage: a review. *Trends Food Sci. Technol.* 109, 280–302. doi: 10.1016/j.tifs.2021.01.006
- Benson, A. K., David, J. R. D., Gilbreth, S. E., Smith, G., Nietfeldt, J., Legge, R., et al. (2014). Microbial successions are associated with changes in chemical profiles of a model refrigerated fresh pork sausage during an 80-day shelf life study. *Appl. Environ. Microbiol.* 80, 5178–5194. doi: 10.1128/aem.00774-14
- Berardo, A., Devreese, B., Maere, H. D., Stavropoulou, D. A., van Royen, G., Leroy, F., et al. (2017). Actin proteolysis during ripening of dry fermented sausages at different pH values. *Food Chem.* 221, 1322–1332. doi: 10.1016/j.foodchem.2016.11.023
- Bover-Cid, S., Miguelez-Arrizado, M., Moratalla, L., and Vidal-Carou, M. C. (2006). Freezing of meat raw materials affects tyramine and diamine

- accumulation in spontaneously fermented sausages. *Meat Sci.* 72, 62–68. doi: 10.1016/j.meatsci.2005.06.003
- Brandfass, C., and Karlovsky, P. (2008). Upscaled CTAB-based DNA extraction and real-time PCR assays for *Fusarium culmorum* and *F. graminearum* DNA in plant material with reduced sampling error. *Int. J. Mol. Sci.* 9, 2306–2321. doi: 10.3390/ijms9112306
- Caporaso, J. G., Kuczynski, J., Stombaugh, J., Bittinger, K., Bushman, F. D., Costello, E. K., et al. (2010). QIIME allows analysis of high-throughput community sequencing data. *Nat. Methods* 7, 335–336. doi: 10.1038/nmeth.f.303
- Castro-Puyana, M., Perez-Miguez, R., Montero, L., and Herrero, M. (2017). Application of mass spectrometry-based metabolomics approaches for food safety, quality and traceability. *TrAc Trends Anal. Chem.* 93, 102–118. doi: 10.1016/j.trac.2017.05.004
- Chelius, M. K., and Triplett, E. W. (2001). The diversity of archaea and bacteria in association with the roots of *Zea mays* L. *Microb. Ecol.* 41, 252–263. doi: 10.1007/s002480000087
- Chen, J., Hu, Y., Wen, R., Liu, Q., Chen, Q., and Kong, B. (2019). Effect of NaCl substitutes on the physical, microbial and sensory characteristics of Harbin dry sausage. *Meat Sci.* 156, 205–213. doi: 10.1016/j.meatsci.2019.05.035
- Chen, Q., Zhang, Y., Zhao, J., and Hui, Z. (2013). Nondestructive measurement of total volatile basic nitrogen (TVB-N) content in salted pork in jelly using a hyperspectral imaging technique combined with efficient hypercube processing algorithms. *Anal. Methods* 5, 63–82. doi: 10.1039/c3ay40436f
- Chen, X., Zhu, L., Liang, R., Mao, Y., Hopkins, D. L., Li, K., et al. (2020). Shelf-life and bacterial community dynamics of vacuum packaged beef during long-term super-chilled storage sourced from two Chinese abattoirs. *Food Res. Int.* 130:108937. doi: 10.1016/j.foodres.2019.108937
- Colby, J., and Zatman, L. J. (1973). Trimethylamine metabolism in obligate and facultative methylotrophs. *Biochem. J.* 132, 101–112. doi: 10.1042/bj1320101
- Dainty, R. H., Edwards, R. A., and Hibbard, C. M. (1989). Spoilage of vacuum-packed beef by *aclostridium* sp. *J. Sci. Food Agric.* 49, 473–486. doi: 10.1002/jsfa.2740490410
- Dong, C., Wang, B., Li, F., Zhong, Q., Xia, X., and Kong, B. (2020). Effects of edible chitosan coating on Harbin red sausage storage stability at room temperature. *Meat Sci.* 159:107919. doi: 10.1016/j.meatsci.2019.107919
- Doulgeraki, A. I., Ercolini, D., Villani, F., and Nychas, G.-J. E. (2012). Spoilage microbiota associated to the storage of raw meat in different conditions. *Int. J. Food Microbiol.* 157, 130–141. doi: 10.1016/j.ijfoodmicro.2012.05.020
- Edgar, R. C. (2013). UPARSE: highly accurate OTU sequences from microbial amplicon reads. *Nat. Methods* 10, 996–998. doi: 10.1038/nmeth.2604
- Edgar, R. C., Haas, B. J., Clemente, J. C., Quince, C., and Knight, R. (2011). UCHIME improves sensitivity and speed of chimera detection. *Bioinformatics* 27, 2194–2200. doi: 10.1093/bioinformatics/btr381
- Ercolini, D., Mancini, L., Stellato, G., Minervini, F., Di Cagno, R., De Angelis, M., et al. (2015). Relationships among house, rind and core microbiotas during manufacture of traditional Italian cheeses at the same dairy plant. *Food Microbiol.* 54, 115–126. doi: 10.1016/j.fm.2015.10.008
- Ferrini, G., Comaposada, J., Arnau, J., and Gou, P. (2012). Colour modification in a cured meat model dried by Quick-Dry-Slice process® and high pressure processed as a function of NaCl, KCl, K-lactate and water contents. *Innov. Food Sci. Emerg. Technol.* 13, 69–74. doi: 10.1016/j.ifset.2011.09.005
- Frank, D., Hughes, J., Piyasiri, U., Zhang, Y., Kaur, M., Li, Y., et al. (2020). Volatile and non-volatile metabolite changes in 140-day stored vacuum packaged chilled beef and potential shelf life markers. *Meat Sci.* 161:108016. doi: 10.1016/j.meatsci.2019.108016
- Gammariello, D., Incoronato, A. L., Conte, A., and DelNobile, N. A. (2015). Use of antimicrobial treatments and modified atmosphere to extend the shelf life of fresh sausages. *J. Food Process. Technol.* 6:456. doi: 10.4172/2157-7110.1000456
- Haas, B. J., Gevers, D., Earl, A. M., Feldgarden, M., Ward, D. V., Giannoukos, G., et al. (2011). Chimeric 16S rRNA sequence formation and detection in Sanger and 454-pyrosequenced PCR amplicons. *Genome Res.* 21, 494–504. doi: 10.1101/gr.112730.110
- Hanagasaki, T., and Asato, N. (2018). Changes in free amino acids and hardness in round of Okinawan delivered cow beef during dry- and wet-aging processes. *J. Anim. Sci. Technol.* 60:23. doi: 10.1186/s40781-018-0180-x
- Hanshew, A. S., Mason, C. J., Raffa, K. F., and Currie, C. R. (2013). Minimization of chloroplast contamination in 16S rRNA gene pyrosequencing of insect herbivore bacterial communities. *J. Microbiol. Methods* 95, 149–155. doi: 10.1016/j.mimet.2013.08.007
- Hu, Y., Zhang, L., Liu, Q., Wang, Y., Chen, Q., and Kong, B. (2020). The potential correlation between bacterial diversity and the characteristic volatile flavour of traditional dry sausages from Northeast China. *Food Microbiol.* 91:103505. doi: 10.1016/j.fm.2020.103505
- Hultman, J., Rahkila, R., Ali, J., Rousu, J., and Björkroth, K. (2015). meat processing plant microbiome and contamination patterns of cold-tolerant bacteria causing food safety and spoilage risks in the manufacture of vacuum-packaged cooked sausages. *Appl. Environ. Microbiol.* 81, 7088–7097. doi: 10.1128/AEM.02228-15
- Jin, S.-K., Yang, H.-S., and Choi, J.-S. (2017). Effect of *Gleditsia sinensis* lam. extract on physico-chemical properties of emulsion-type pork sausages. *Korean J. Food Sci. Anim. Resour.* 37, 274–287. doi: 10.5851/kosfa.2017.37.2.274
- Li, K., Lin, K., Li, Z., Zhang, Q., Song, F., Che, Z., et al. (2014). Spoilage and Pathogenic bacteria associated with spoilage process of sichuan pickle during the spontaneous fermentation. *Food Sci. Technol. Res.* 20, 899–904. doi: 10.3136/fstr.20.899
- Li, N., Zhang, Y., Wu, Q., Gu, Q., Chen, M., Zhang, Y., et al. (2019). High-throughput sequencing analysis of bacterial community composition and quality characteristics in refrigerated pork during storage. *Food Microbiol.* 83, 86–94. doi: 10.1016/j.fm.2019.04.013
- Li, W., Jia, M.-X., Deng, J., Wang, J.-H., Lin, Q.-L., Liu, C., et al. (2018). Isolation, genetic identification and degradation characteristics of COD-degrading bacterial strain in slaughter wastewater. *Saudi J. Biol. Sci.* 25, 1800–1805. doi: 10.1016/j.sjbs.2018.08.022
- Li, X., Li, C., Ye, H., Wang, Z., Wu, X., Han, Y., et al. (2019). Changes in the microbial communities in vacuum-packaged smoked bacon during storage. *Food Microbiol.* 77, 26–37. doi: 10.1016/j.fm.2018.08.007
- Liu, P., Wang, S., Zhang, H., Wang, H., and Kong, B. (2019). Influence of glycated nitrosohaemoglobin prepared from porcine blood cell on physicochemical properties, microbial growth and flavour formation of Harbin dry sausages. *Meat Sci.* 148, 96–104. doi: 10.1016/j.meatsci.2018.10.008
- Lorenzo, J. M., Munekata, P. E. S., and Domínguez, R. (2017). Role of autochthonous starter cultures in the reduction of biogenic amines in traditional meat products. *Curr. Opin. Food Sci.* 14, 61–65. doi: 10.1016/j.cofs.2017.01.009
- Luong, N.-D. M., Jeuge, S., Coroller, L., Feurer, C., Desmonts, M.-H., Moriceau, N., et al. (2020). Spoilage of fresh turkey and pork sausages: influence of potassium lactate and modified atmosphere packaging. *Food Res. Int.* 137:109501. doi: 10.1016/j.foodres.2020.109501
- Ly, Y., Yin, X., Wang, Y., Chen, Q., and Kong, B. (2021). The prediction of specific spoilage organisms in Harbin red sausage stored at room temperature by multivariate statistical analysis. *Food Control* 123:107701. doi: 10.1016/j.foodcont.2020.107701
- Martín, L., Antequera, T., Ruiz, J., Cava, R., Tejeda, J. F., and Córdoba, J. J. (1998). Influencia de las condiciones de elaboración sobre la proteólisis durante la maduración del jamón ibérico Influence of the processing conditions of Iberian ham on proteolysis during ripening. *Food Sci. Technol. Int.* 4, 17–22. doi: 10.1177/108201329800400103
- Martin, M. (2011). Cutadapt removes adapter sequences from high-throughput sequencing reads. *Embnet J.* 17:10. doi: 10.14806/ej.17.1.200
- Meng, Q., and Hao, J. (2017). Optimizing the application of *Bacillus velezensis* BAC03 in controlling the disease caused by *Streptomyces scabies*. *BioControl* 62, 535–544. doi: 10.1007/s10526-017-9799-7
- National Health and Family Planning Committee of China (NHFPC) (2016). *National Food Safety Standard Limitation of Total Volatile Basic Nitrogen in Food*. Available online at: <http://bz.cfsa.net.cn/staticPages/DB1B5954-5DFF-43FC-A3E8-FCF997E12E5B.html> (GB5009.228-2016).
- Pellissery, A. J., Vinayamohan, P. G., Amalaradjou, M. A. R., and Venkitanarayanan, K. (2020). “Chapter 17 - Spoilage bacteria and meat quality,” in *Meat Quality Analysis*, eds A. K. Biswas and P. K. Mandal (Cambridge, MA: Academic Press), 307–334.
- Pini, F., Aquilani, C., Giovannetti, L., Viti, C., and Pugliese, C. (2020). Characterization of the microbial community composition in Italian Cinta Senese sausages dry-fermented with natural extracts as alternatives to sodium nitrite. *Food Microbiol.* 89:103417. doi: 10.1016/j.fm.2020.103417
- Polka, J., Rebecchi, A., Pisacane, V., Morelli, L., and Puglisi, E. (2015). Bacterial diversity in typical Italian salami at different ripening stages as revealed by high-throughput sequencing of 16S rRNA amplicons. *Food Microbiol.* 46, 342–356. doi: 10.1016/j.fm.2014.08.023

- Quast, C., Pruesse, E., Yilmaz, P., Gerken, J., Schweer, T., Yarza, P., et al. (2013). The SILVA ribosomal RNA gene database project: improved data processing and web-based tools. *Nucleic Acids Res.* 41, D590–D596. doi: 10.1093/nar/gks1219
- Rao, S., Mohan, K., and Atreya, C. (2010). Detection technologies for *Bacillus anthracis*: prospects and challenges. *J. Microbiol. Methods* 82, 1–10. doi: 10.1016/j.mimet.2010.04.005
- Rubio, B., Martínez, B., García-Cachán, M. A. D., Rovira, J., and Jaime, I. (2008). Effect of the packaging method and the storage time on lipid oxidation and colour stability on dry fermented sausage salchichón manufactured with raw material with a high level of mono and polyunsaturated fatty acids. *Meat Sci.* 80, 1182–1187. doi: 10.1016/j.meatsci.2008.05.012
- Salinas, Y., Ros-Lis, J., Vivancos, J.-L., Martínez-Máñez, R., Marcos, M., Aucejo, S., et al. (2014). A novel colorimetric sensor array for monitoring fresh pork sausages spoilage. *Food Control* 35, 166–171. doi: 10.1016/j.foodcont.2013.06.043
- Samaei, M., Mortazavi, S., Bakhshi, B., and Jonidi Jafari, A. (2013). Isolation, genetic identification, and degradation characteristics of n-Hexadecane degrading bacteria from tropical areas in Iran. *Fresenius Environ. Bull.* 22, 1304–1312.
- Schumann, B., and Schmid, M. (2018). Packaging concepts for fresh and processed meat - recent progresses. *Innov. Food Sci. Emerg. Technol.* 47, 88–100. doi: 10.1016/j.ifset.2018.02.005
- Spaziani, M., Del Torre, M., and Stecchini, M. L. (2009). Changes of physicochemical, microbiological, and textural properties during ripening of Italian low-acid sausages. proteolysis, sensory and volatile profiles. *Meat Sci.* 81, 77–85. doi: 10.1016/j.meatsci.2008.06.017
- Stellato, G., La Stora, A., De Filippis, F., Borriello, G., Villani, F., and Ercolini, D. (2016). Overlap of spoilage-associated microbiota between meat and the meat processing environment in small-scale and large-scale retail distributions. *Appl. Environ. Microbiol.* 82, 4045–4054. doi: 10.1128/aem.00793-16
- Subbaraj, A. K., Kim, Y. H. B., Fraser, K., and Farouk, M. M. (2016). A hydrophilic interaction liquid chromatography-mass spectrometry (HILIC-MS) based metabolomics study on colour stability of ovine meat. *Meat Sci.* 117, 163–172. doi: 10.1016/j.meatsci.2016.02.028
- Sun, L., Qiu, F., Zhang, X., Dai, X., Dong, X., and Song, W. (2008). Endophytic bacterial diversity in rice (*Oryza sativa* L.) roots estimated by 16S rDNA sequence analysis. *Microb. Ecol.* 55, 415–424. doi: 10.1007/s00248-007-9287-1
- Tan, Z., Huang, Z., Lv, Y., Li, Y., and Chen, D. (2019). A gas fourier transform infrared spectroscopy methodology for the rapid and accurate discrimination of chicken spoilage through volatiles analysis. *Flavour Fragr. J.* 34, 271–279. doi: 10.1002/ffj.3500
- Tian, X., Wu, W., Yu, Q., Hou, M., Gao, F., Li, X., et al. (2017). Bacterial diversity analysis of pork longissimus lumborum following long term ohmic cooking and water bath cooking by amplicon sequencing of 16S rRNA gene. *Meat Sci.* 123, 97–104. doi: 10.1016/j.meatsci.2016.09.007
- Toldrá, F. (ed.). (2017). "The storage and preservation of meat: III—meating processing," in *Lawrie's Meat Science*, 8th Edn, Amsterdam: Elsevier Ltd., 265–296.
- Toldrá, F., Hui, Y. H., Astiasarán, I., Sebranek, J. G., and Talon, R. (2014). *Handbook of Fermented Meat and Poultry* (Toldrá/Handbook of Fermented Meat and Poultry) || Northern European Products. Chichester: Wiley.
- Via, L. E., and Falkinham, J. O. (1995). Comparison of methods for isolation of *Mycobacterium avium* complex DNA for use in PCR and RAPD fingerprinting. *J. Microbiol. Methods* 21, 151–161. doi: 10.1016/0167-7012(94)00045-9
- Walton, J., and McCarthy, M. (2007). New method for determining internal temperature of cooking meat via NMR spectroscopy. *J. Food Process Eng.* 22, 319–330. doi: 10.1111/j.1745-4530.1999.tb00488.x
- Wang, X. Y., and Xie, J. (2020). Quorum sensing system-regulated proteins affect the spoilage potential of co-cultured *acinetobacter johnsonii* and *pseudomonas fluorescens* from spoiled bigeye tuna (*Thunnus obesus*) as determined by proteomic analysis. *Front. Microbiol.* 11:940. doi: 10.3389/fmicb.2020.00940
- Wang, X., Fang, C., He, J., Dai, Q., and Fang, R. (2017). Comparison of the meat metabolite composition of Linwu and Pekin ducks using 600 MHz H-1 nuclear magnetic resonance spectroscopy. *Poult. Sci.* 96, 192–199. doi: 10.3382/ps/pew279
- Wen, D., Liu, Y., and Yu, Q. (2020). Metabolomic approach to measuring quality of chilled chicken meat during storage. *Poult. Sci.* 99, 2543–2554. doi: 10.1016/j.psj.2019.11.070
- Wen, R., Hu, Y., Zhang, L., Wang, Y., Chen, Q., and Kong, B. (2019). Effect of NaCl substitutes on lipid and protein oxidation and flavor development of Harbin dry sausage. *Meat Sci.* 156, 33–43. doi: 10.1016/j.meatsci.2019.05.011
- Wishart, D. S., Tzur, D., Knox, C., Eisner, R., Guo, A. C., Young, N., et al. (2007). HMDB: the human metabolome database. *Nucleic Acids Res.* 35, D521–D526. doi: 10.1093/nar/gkl923
- Yang, D., Jing, J., Zhang, Z., He, Z., Qin, F., Chen, J., et al. (2020). Accumulation of heterocyclic amines across low-temperature sausage processing stages as revealed by UPLC-MS/MS. *Food Res. Int.* 137:109668. doi: 10.1016/j.foodres.2020.109668
- Yu, L., Scanlin, L., Wilson, J., and Schmidt, G. (2002). Rosemary extracts as inhibitors of lipid oxidation and color change in cooked turkey products during refrigerated storage. *J. Food Sci.* 67, 582–585. doi: 10.1111/j.1365-2621.2002.tb10642.x
- Yu, Q., Tian, X., Shao, L., Li, X., and Dai, R. (2019). Targeted metabolomics to reveal muscle-specific energy metabolism between bovine longissimus lumborum and psoas major during early postmortem periods. *Meat Sci.* 156, 166–173. doi: 10.1016/j.meatsci.2019.05.029
- Yucel, N., Aslim, B., and Özdoğan, H. (2009). In Vitro antimicrobial effect of *satureja wiedemanniana* against *Bacillus* species isolated from raw meat samples. *J. Med. Food* 12, 919–923. doi: 10.1089/jmf.2008.0144
- Zasada, A. A. (2020). Detection and identification of *Bacillus anthracis*: from conventional to molecular microbiology methods. *Microorganisms* 8:125. doi: 10.3390/microorganisms8010125
- Zhao, C. J., Schieber, A., and Gänzle, M. G. (2016). Formation of taste-active amino acids, amino acid derivatives and peptides in food fermentations – a review. *Food Res. Int.* 89, 39–47. doi: 10.1016/j.foodres.2016.08.042
- Zhu, W., Liu, L., Yang, W., Wei, C., Geng, Z., and Chen, X. (2020). Comparative analysis of metabolites in liver of Muscovy duck at different egg-laying stages using nontargeted UPLC-MS based metabolomics. *J. Proteome Res.* 19, 3846–3855. doi: 10.1021/acs.jproteome.0c00414

Conflict of Interest: The authors declare that the research was conducted in the absence of any commercial or financial relationships that could be construed as a potential conflict of interest.

Publisher's Note: All claims expressed in this article are solely those of the authors and do not necessarily represent those of their affiliated organizations, or those of the publisher, the editors and the reviewers. Any product that may be evaluated in this article, or claim that may be made by its manufacturer, is not guaranteed or endorsed by the publisher.

Copyright © 2021 Han, Li, Peng, Zhang, Yue and Zheng. This is an open-access article distributed under the terms of the Creative Commons Attribution License (CC BY). The use, distribution or reproduction in other forums is permitted, provided the original author(s) and the copyright owner(s) are credited and that the original publication in this journal is cited, in accordance with accepted academic practice. No use, distribution or reproduction is permitted which does not comply with these terms.



Warehouse Storage Management of Wheat and Their Role in Food Security

Chandrasen Kumar¹, C. L. Ram¹, S. N. Jha² and R. K. Vishwakarma^{3*}

¹ Food Corporation of India, New Delhi, India, ² Agricultural Engineering Division, Indian Council of Agricultural Research, Pusa, New Delhi, India, ³ Indian Council of Agricultural Research-Central Institute of Post-Harvest Engineering and Technology, Ludhiana, India

OPEN ACCESS

Edited by:

Shalini Gaur Rudra,
Indian Agricultural Research
Institute, India

Reviewed by:

Francesco Facchini,
Politecnico di Bari, Italy
Kurt A. Rosentrater,
Iowa State University, United States

*Correspondence:

R. K. Vishwakarma
rkvciphet@gmail.com

Specialty section:

This article was submitted to
Sustainable Food Processing,
a section of the journal
Frontiers in Sustainable Food Systems

Received: 03 March 2021

Accepted: 06 July 2021

Published: 27 August 2021

Citation:

Kumar C, Ram CL, Jha SN and
Vishwakarma RK (2021) Warehouse
Storage Management of Wheat and
Their Role in Food Security.
Front. Sustain. Food Syst. 5:675626.
doi: 10.3389/fsufs.2021.675626

Silo storage is considered the best option for wheat storage. However, the storage losses in warehouse storage are also equivalent to silo storage of wheat when proper storage management practices are adopted and the Food Corporation of India (FCI) is the best example of a sustainable food storage system with only 0.3% storage losses in 3 years of wheat storage. The wheat procurement, storage, and distribution system of FCI is unique in the world and handles about 85 million tons of food grains annually by procuring from farmers at the guaranteed Minimum Support Price that meets certain quality standards. This article discusses the role of FCI in food security, warehouse storage management practice as a model, and storage loss level of wheat during storage.

Keywords: wheat, warehouse storage management, storage loss, food security, Food Corporation of India

INTRODUCTION

The post-harvest life and quality of agricultural produce depend mainly upon its quality at the time of harvest. However, after the harvest, several interrelated factors form complex interrelationships that may result in the deterioration of quality during storage. Although the harvest period of agricultural produce is relatively short, the demand for consumption extends throughout the year. Thus, the agricultural produce has to be stored safely using proper methods of preservation for consistent supply throughout the year. Cereals, as agricultural produce, occupy an important place in human food, as they are primary sources of energy to the majority of the global population. While farmers store cereals for the purpose of seed, feed, and their own consumption, marketing agencies and traders store them for economic gain. In many cases, Government agencies store food grains to ensure domestic food security, supply, and price stability in the market, and also to earn foreign exchange through export. Therefore, the dynamics of storage in terms of quality maintenance and losses form crucial components of economic and policy decisions. Storage losses are usually in the range of 1–2%, particularly in the developed countries, when grains are stored in well-managed silos with aeration and drying. However, it may be as high as 20–50% in the lesser developed countries, particularly in cover and plinth storage with poorly managed storage facilities (Jayas, 2012). The qualitative losses in wheat stored in jute bags may be as high as 6.6% and reduction of such loss can be brought down to 2% by storing in metal bins (Sinha and Sharma, 2004). Thus, savings of agricultural produce with proper storage is as good as additional production, which emphasizes the need for proper storage management (Jha et al., 2015). The factors responsible for storage losses are environmental, type of storage structure, duration, purpose of storage, treatment during storage, method of packaging and storing grains, etc. Environmental factors

mainly consist of temperature, relative humidity (RH), rainfall, exposure to direct sun, air velocity, etc. Besides, biological factors responsible for storage losses are moisture content, insects, pests, microorganisms, and rodents. Before storing wheat grain, it must be dried to a proper level of moisture content; otherwise many problems such as germination and loss of eating quality may occur (Gu et al., 2000; Ueno, 2003). Fluctuations in environmental factors, such as temperature, dampness, and longevity result in significant nutrient losses (Kumar and Singh, 1984). Prolonged storage with high seed moisture percentage also causes a reduction in germination, seedling vigor, accelerated seed aging, increased germination time, electrical conductivity, insect infestation, and eventually loss in seed weight (Mersal et al., 2006). Extreme dry environmental conditions during storage result in faster seed aging, reducing longevity and quality (Labuza, 1980). However, it has been observed that losses during storage in the warehouses are not as high as perceived in the literature, particularly when proper storage management practices are adopted. The best example of proper warehouse storage management practices of food grains, mainly for wheat and rice in developing countries can be said to be of the Food Corporation of India (FCI), which has bare minimum losses in long-duration storage of food grains. FCI handles about 3% of total world cereal production every year. Furthermore, food security in India is largely maintained by them through efficient handling and distribution of food grains. This chapter deliberates on storage management practices of wheat in FCI in their warehouse system and the extent of storage losses due to different factors based on a recent study.

FOOD CORPORATION OF INDIA AND ITS WHEAT STORAGE MANAGEMENT

In India, there are ~146.5 million farming families who own 157.8 million ha agricultural land with an average landholding of 1.08 ha in 2015–2016 (Directorate of Economics Statistics (DES) et al., 2020). However, only about 5.7% of farmers have ≥ 4 ha land and own 29.23% of total agricultural land leaving the rest of them with much smaller landholdings. Therefore, the sustainability of farmers becomes an important issue, particularly in the form of distress sale of the cereals produced as they have very little holding capacity and need quick money for their sustenance.

In order to safeguard such a large number of small and marginal farmers, procurement of staple cereals such as wheat at the minimum support price (MSP) is an important policy tool that involves large scale procurement dispersed in wheat producing states like Punjab, Haryana, Uttar Pradesh, Madhya Pradesh Himachal Pradesh, Uttarakhand, and Bihar. The procurement of wheat involves massive handling of small quantities from a large number of individuals, a mammoth task as it has to be completed during the limited period of 3 months of Rabi harvesting, i.e., from April to June. FCI with other supporting state agencies play a vital role in the procurement of wheat. They procure about 33% of total wheat

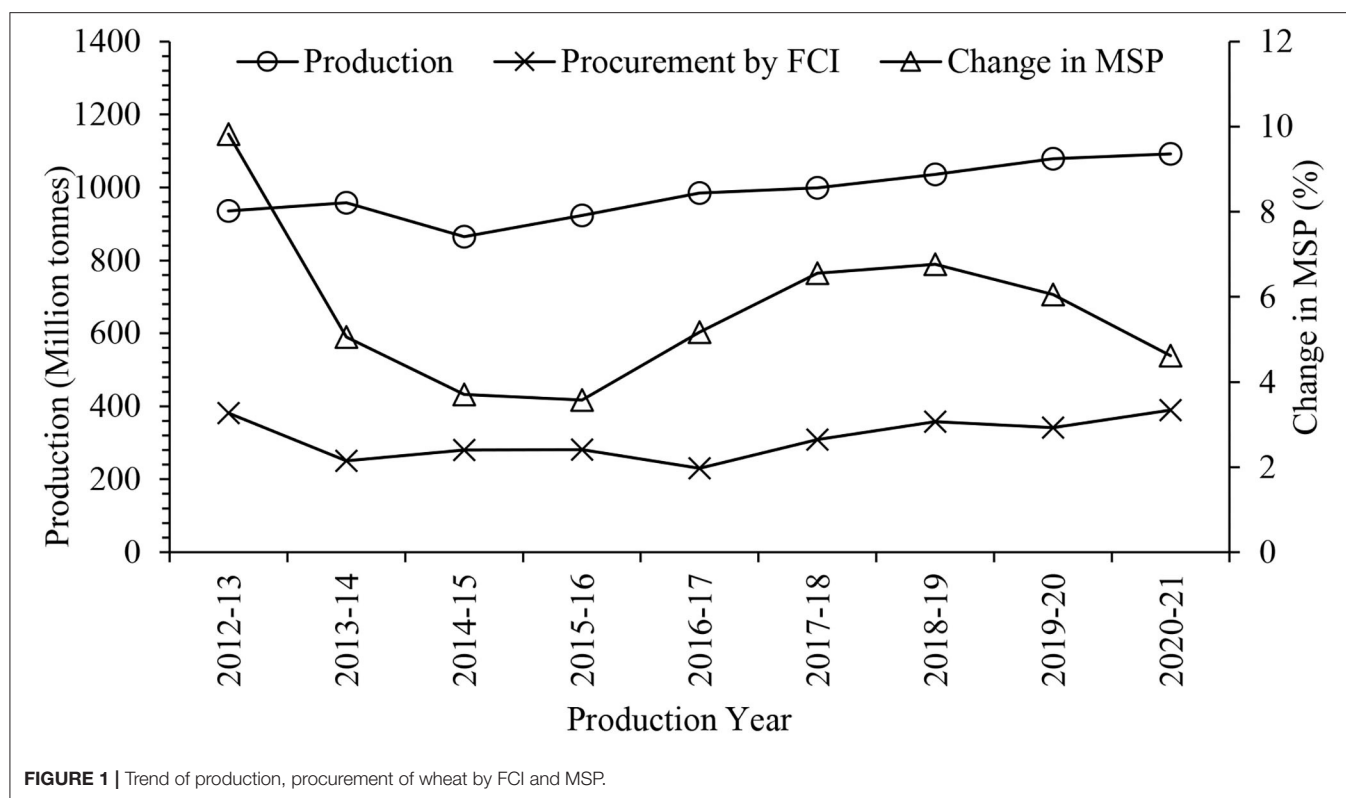
production in the country for the purpose of supporting farmers through minimum support price (MSP) to save them from distress sale, maintaining food security through the country-wide public distribution system (PDS), stocking reserves as a buffer to meet exigencies and to stabilize market prices through open sale of wheat in case of the steep rise of market prices.

FCI is the nodal agency for procurement, storage, transportation, and distribution of food grains, mainly wheat, rice, and some coarse grains. The storage system of FCI comprises of their owned warehouses, and hired warehouses of central warehousing corporation (CWC), state warehousing corporations (SWC), and privately owned warehouses for the storage of wheat. These agencies have a network of storage depots strategically located all over India. These depots have facility for short-term storage of wheat (<1 year), as well as longer-term storage (between 1 and 3 years). While short-term storage techniques developed by FCI with their experience is known as cover and plinth (CAP) storage system, the longer-term storage consists of covered warehouses and a small proportion in the silos. Such storage depots are located in almost all the states and union territories at more than 1,000 locations. Furthermore, FCI uses 2,085 warehouses and CAP systems for storage of cereals.

Under the contemporary socio-economic scenario, procurement has been showing an increasing trend and FCI along with allied state agencies have procured a record 85 million tons of food grains, i.e., wheat, rice, and coarse grains during the crop year 2019–2020. However, increasing procurement but almost constant off-take (distribution) of food grains under various schemes of the government has been pushing up the stock holding of the government leading to an increased average storage period of food grains. Average wheat procurement was about 36 million tons every year with an increasing trend. Furthermore, the MSP for wheat has been rising every year which had a positive impact on the production of wheat in subsequent years (Figure 1). As a result, the procurement of wheat in the central pool has also been increasing.

An important factor for the rise in stock holding is the ratio of off-take of procured wheat stock under various schemes run by the government of India to the total procured quantity during a given year. It may be seen that the procurement to off-take (O/P) ratio for wheat during the last decade has been declining and has been hovering around 0.80, which has resulted in stock built up of wheat. Under such a scenario the average storage period of stock becomes more than a year. This results in a higher cost of storage for every succeeding year resulting in increasing economic cost. In fact, a conservative estimate of 20% stock at the present level being held for another year would result in an additional cost of Rs 6,000 crores as storage cost.

However, the low off-take of wheat prior to 2020 has ensured enhanced supply of wheat to below poverty line families during the coronavirus disease of 2019 (COVID-19) pandemic lockdown free of cost and saved millions of people from food insecurity in India.



OPERATIONAL PROCEDURE FOR WHEAT PROCUREMENT AND DISTRIBUTION BY FCI

As per production, procurement, consumption, and storage period of wheat states and union territories can be segregated into three regions namely procuring regions, consuming regions, and transit regions. While wheat is procured mainly in surplus wheat-producing states, called procuring regions, the surplus is transported to consuming regions for distribution under National Food Security Act 2013 (NFSA) and other welfare schemes. So, while the storage period of wheat is longer in surplus and some of the consuming regions having adequate storage capacity, the period of storage is quite short in transit regions, mainly hill states with lower storage capacity. Important states under different categories are given in **Table 1**.

FCI procures wheat mainly from major wheat surplus states of Punjab, Haryana, Uttar Pradesh, Rajasthan, and Madhya Pradesh, which are termed wheat-procuring states. The procurement of wheat is done through a structured procedure from the grain markets in which farmers bring their produce for sale during the harvest season. The duration of procurement lasts 2–3 months after the harvest. The quality parameters applied during procurement are called fair average quality (FAQ) determined by the Government of India. Samples from wheat stock brought by farmers are tested for quality in the *mandi* after cleaning the stock of foreign matters. Once the stock passes the FAQ parameters, the same is weighed

TABLE 1 | Consuming, procuring, and transit regions defined by the FCI.

Commodity	Procuring regions	Consuming regions	Transit regions
Wheat (stored in covered godowns)	Punjab, Haryana, UP, MP, Rajasthan	Maharashtra, AP, Gujarat, Chhattisgarh, Kerala, Telangana, Karnataka, Tamil Nadu, WB, Odisha, Bihar, Jharkhand	North Eastern States, JandK, HP, Delhi, Uttarakhand
Wheat (stored in CAP)	Punjab, Haryana, UP, Rajasthan		

after packing into bags. The quantity of the wheat after weightment is acknowledged through necessary documentation and receipts for payment to farmers. Wheat packed into new jute sacks/gunnies of 50 kg capacity is transported to the warehouses for storage using hired trucks. Storage of such wheat in gunny bags is done in covered warehouses (godowns) through an arrangement called stacking of bags. One stack contains around 3,200–3,300 bags. A substantial amount of wheat is stored in CAP storage as the limited covered godowns are used for storing rice which cannot be stored in CAP. Besides, a small quantity of wheat is also stored in modern silos in bulk form. All the warehouses are equipped with a weighing facility to ensure accurately measurement of weight of stock during operations.

Procured wheat from surplus states is transported to all other remaining states (consuming regions) for distribution under National Food Security Act and other schemes. The major share of transportation is undertaken by railways apart from transportation by road to nearby places and hill states. After the transportation from surplus regions wheat is stored in stacks in the warehouses of consuming regions until the same is issued for consumption following the First-in-First-out (FIFO) principle. Thus, wheat operations involve storage in the warehouses across the country, i.e., procuring as well as consuming regions.

Storage Management

The average duration of storage of wheat is more than 1 year in the warehouses. In order to maintain the good health of the stored wheat in bags, aeration, fumigation, and spraying are undertaken at certain intervals to keep the wheat stock free from insects and pests. For this purpose, samples are taken with a specified procedure as explained below.

The sampling procedures and analysis methods prescribed by the Bureau of Indian Standards (BIS) incorporating IS: 14818 (2000), IS: 2813 (1995), and IS: 4333 Part I Part II (2002) for food grains in respect of moisture content, 1,000-grain weight, and loss due to insect infestation are followed. The sampling is done at the time of initial receipt, periodical quality, and moisture rebuilding inspection and issue of the stock after 100% weighment. The analysis of samples is done in the FCI/CWC Depots laboratories specially set up in most of the depots. The sampling time and analysis procedure followed by FCI are as below:

- a) **Moisture content measurement:** Measured at the time of stacking from the entire stack; fortnightly by taking samples from the periphery of the stacks; and at liquidation time by taking samples from the entire stack.
- b) **Quality parameters of stack, such as category of food grains (percentage of damaged, discolored, weevilled):** Fortnightly by taking samples from the periphery of stacks.
- c) **Level of infestation:** Monthly by taking samples from the periphery of stacks.
- d) **1,000-grain weight:** Monthly by taking samples from the periphery of stacks.
- e) **Incidences of rodents, birds, mites, monkey trouble during storage:** Monthly by visual observations.
- f) **Number of spray/fumigation applied with name of the chemicals used:** Prophylactic spray of malathion is done on the outer periphery of stacks fortnightly.
- g) **Recording of weight of spillage:** The spilled grains are collected after every 15 days and placed in a bag attached with each stack (called *palla* bag).
- h) **Incidence of pilferage, if any:** Depot officials report the information to authorized agency.
- i) **Microbial load in grain samples:** Quarterly basis, if suspected.
- j) **Mycotoxins:** Recorded only when suspected.

Causes of Storage Loss in Warehouses

Losses during storage are unavoidable due to biotic and abiotic factors and such losses are quantified on the basis of weight difference between intake and off-take. The loss during storage of wheat stacked in a warehouse may take place because of a decrease in grain moisture content, reduction in total weight owing to environmental conditions (high temperature and less relative humidity), operational factors (spillage, sampling, weighing system errors, measurement errors, etc.), and dry matter losses due to biotic factors (insects, pests, rodents, respiration of grains, mycotoxins, etc.). Wheat also exhibits gain in weight, mainly due to an increase in moisture content to the equilibrium moisture content (EMC).

Thus, sources of losses are environmental, operational, and biotic factors. However, owing to the fact that nature of all other operations including the control measures for losses due to biotic factors being standardized across all the warehouses, variation of losses mainly occur due to number of times of stacking and de-stacking of wheat bags, i.e., whether it has been stacked first time after procurement (as undertaken in procuring region) or stacked second time after transportation from the procuring region, as done in consuming regions, and change in moisture content. The operational factors such as number of times of stacking becomes important as it has been observed that moisture in the peripheral bags of a given stack is different as compared with the core bags when stored for more than a quarter.

The main causes of damage and spoilage of wheat which are constantly monitored by FCI are summarized in **Table 2**.

STORAGE STRUCTURES OF FCI AND OTHER AGENCIES

Cover and Plinth Storage

Cover and plinth storage also called CAP storage in FCI is a scientific storage system for storing wheat and paddy. Under the CAP system, the storage site is made at a higher elevation than adjoining ground and away from drainage, canals, and flood-prone area to prevent flooding of the area. Normally, the plinth is made with brick and mortar, which is at least 450 mm above the ground level. Antitermite treatment is given at the time of construction to avoid termite attacks. Stacking of bags is done on dunnage material, usually, wooden crates (frames), placed on a raised platform (plinth), and the stack of food grain bags are covered with 800–1,000-gauge-thick polyethylene sheets (**Figure 2**).

Dunnage is an important aspect of the storage of bagged food grain that helps in the proper aeration of the bottom layer of food grain bags and prevents it from getting damaged. It can be made from wooden planks in general, on which the bags are stacked. Polyethylene sheet alone or sandwiched between two layers of mats, bamboo mats, *ballies*, are also used as dunnage for short-term storage. These days, plastic crates have also come into use in place of wooden crates. Wooden dunnage is made using timber

TABLE 2 | Spoilage agents and cause of damages.

Parameters and spoilage agents	Possible damage and spoilage
Common structural issues like water entry, pest entry, harbor pests	Localized moisture gain, grain heating, risk of contamination, insect, and mold growth
Presence of dirt and debris in the food material	Shelter for pests; contaminate incoming stocks; difficulty in proper inspection for pest detection; and obstruction for effective pest control
Presence of infestation in the store prior to storage	It is the main threat to the stored commodity, and pest infestation takes place. Difficulties in fumigation due to poorly sealed storage areas. Results into damage of commodity
Improper cleaning and disinfection of stores	Risk of disease transmission to the stored grain
Moisture	
Higher initial moisture content of grain being stored	Chances of spoilage in cereals and oilseeds until dried to safe limits of 14.5 and 7.5% moisture contents, respectively
Change in grain moisture during storage	Grain moisture is associated with RH of the surrounding air. Spoilage due to insect and mold growth is possible.
Improper calibration of moisture measuring instruments	Poor calibration results in wrong information about moisture. Aeration is not done in time and spoilage takes place.
Control of moisture content, mites and molds	Surface layer moisture can increase or decrease due to environmental conditions and difficult to control. Moisture above 18% encourages mite's growth.
Moisture and market demands	Each food industry has specific demand, for example, the wheat industry may accept wheat up to 15% moisture, malt industry asks 13% with minimum germination of 98%
Drying	
Drying temperature	Drying at high temperature reduces the time and increases capacity but damages the quality of grains, especially protein and germination.
Controlling moisture content	Overdrying may cause damage to the grains whereas underdrying may lead to spoilage.
Improper cooling after drying	Storage of grains immediately after drying results in insects breeding.
Moisture content prior to drying	If grain moisture exceeds dryer limits, spoilage may occur before all material dries uniformly. The capacity of high-quality dryer is reduced by 15% for each 1% mc increase above 20%.
Temperature	
Storage temperature	Most of the insects die within a day at a temperature >40°C. Favorable temperature for rapid multiplication of most of the insects is 25–33°C whereas these do not breed below 15°C. However, grain weevils (<i>S. granaries</i>) breed at slow rate at 12°C. Suitable temperature for mycotoxin production varies between 15 and 25°C.
Grain heating due to biotic and abiotic factors	Changes in environmental temperature may cause moisture accumulation at the top or bottom of a bin. High moisture surfaces or damp pockets encourage mold growth, heating of grains, and sprouting. Insect infestation also generates heat and cause spoilage.
Improper airflow during aeration	Airflow of <10 m ³ /h/ton can cause improper cooling during aeration. Insect breeding rate may increase and spoilage is possible.
Insects	
Presence of field insects	Field insects like clover weevil can be present in freshly harvested grain, cause very low damage, and die quickly. Incorrect identification may cause spoilage.
Presence of primary storage pests (beetles and moths)	Primary insects intrude the grains from the previous stored grains and can breed even at low moisture and temperature conditions and damage takes place. Some species like grain weevil develop inside the grain and are difficult to detect at early stage.
Attack of secondary storage insects	These include fungus feeders, spider beetles, and booklice may enter in the bulk from nearby sources. These insects damage poorly managed or already infested grain only.
Presence of beneficial insects (predators of storage pests)	These may be present in the stores or on the grain. They are not very effective against harmful insects. Presence of beneficial insect also may be the reason for rejection of a grain lot.
Development of resistance in pests against pesticides	Resistance to pesticides can develop in some insects, for example, saw-toothed grain beetle and control is difficult. Resistance development reduces the effective life of treatments or requires more exposure time to control the insects.
Mites	
Identification and prevention problems	Mites cannot be distinguished from dust by the naked eye. These directly damage the grain by eating the germ or making holes in the oilseeds. Practically exclusion of mites is not possible from stores.
Presence of surface moisture	Mites build up at the moist surfaces. Storage at <13% moisture minimizes the risk of mites.
Control method of mites	A single control option is not sufficient. Combined conveying and cleaning kill 75–90% mites. However, the mites present inside the grain germ survive and grow again quickly, and it is a temporary measure.
Fungi	
Detection of mycotoxin produced and their level	Visible moldy grain suggests that mycotoxin production may have started. A few mite species feed on fungi and disguise indication of mold growth. Absence of visible mold growth is not a sign of freedom from mycotoxins.
Effect of physical treatment	Cooling grains is not sufficient for longer duration storage of damp grain. Storage fungi cannot grow at <14.5% moisture.

(Continued)

TABLE 2 | Continued

Parameters and spoilage agents	Possible damage and spoilage
Chemical treatments (only for animal feed)	Sodium hydroxide treated grains swell during storage and silo storage is not practical. This treatment is not for long-duration storage. Propionic acid-treated damp grains can be stored for short-duration storage.
Mycotoxin production	Mycotoxins produced by the fungi before harvest are stable and remain with grains during storage. Fungal growth produces mycotoxins when grain moisture is > 15%. Risk of fungal growth is higher when dried by spreading on the floor (near-ambient drying).
Rodents and birds	
Rats and mouse	A young rodent can enter in the stores from a gap of only 5 mm, damages structures, and contaminates food. The loss is more in the form of spillage and contamination.
Birds	Attack of birds causes direct losses. Food like spilled grain attracts the birds.
Other issues for oilseeds	
Drying to very low moisture at faster rate	Hard and brittle grains are formed. This may cause quality deterioration.
Slow rate of drying or cooling	Can encourage mold and mites growth and mycotoxin production may take place.
Non-availability of insecticide	Merchant grain beetle (<i>O. mercator</i>) and saw-toothed grain beetle (<i>O. surinamensis</i>) may grow to some extent in stored grains. No insecticides are available to control such mixed insect population.
Presence of immature seed in storage	It causes heating and rapid deterioration of mature seeds.
Issues of monitoring and management	
Pest monitoring issues	Invertebrate pests are very small and can be detected by careful examination only. Vertebrate pests are not noticed at several occasions. In case the rodents were observed in the past, their incidence may continue in next storage also. Insect traps in a store are not very effective in quantification of insect infestations. It shows population trends of insects only.



FIGURE 2 | A view of CAP storage.

planks in which the planks are one over the other and nailed. The lower member of dunnage is of $100 \times 50 \text{ mm}^2$ rectangular shape and 1 m long. In general, five planks at 362 mm distance from center to center are used. The upper member of dunnage is of $70 \times 50 \text{ mm}^2$ cross-section, 1.5 m long, and five planks are placed at 237 mm distance from center to center.



FIGURE 3 | Typical bag storage godown in India.

CAP storage system is used for short-term storage, usually less than a year. The need for CAP storage arises to store a high quantity of procured wheat and paddy, particularly immediately after the harvest period, at locations where covered storage capacity is not adequate, such as Punjab and Haryana.

A stack of $9.3 \times 9.3 \times 6.2$ m is generally preferred in CAP storage by FCI. The height of the stack may go up to 15 bags. The top of the stack is made in an inverted “V” shape for easy flow of rainwater after covering. A layer of bags filled with straw may be suitable in some areas to minimize the damage due to rain, birds, temperature, and condensation.

After placing the polyethylene cover, the stack is lashed with ropes in some regions where wind velocity is generally high. Plastic net-type covers on the polyethylene cover are more convenient to tie the stacks.

Aeration of the stack becomes important to control temperature and moisture. Lifting the plastic cover is a common method of aeration in the CAP system and the frequency of aeration is once a week in general when the sky is clear. Curative treatments, such as fumigation are also in practice in some places.

The main disadvantages of CAP are that the fumigation is not very effective if the covers are damaged at the time of fumigation, especially due to strong wind, birds, and continued exposure to sun and rains.

Bag Storage Godown/Warehouse

FCI mainly uses warehouses for the storage of bagged grains to safeguard them from environmental factors. While wheat and paddy can be temporarily stored in a CAP system, rice has to be compulsorily stored in a covered storage godown. Covered storage godown is a very common grain storage method in many developing countries. Any type of shaded structure or building, such as stone structure, brick wall, walls of corrugated sheet, mud and wattle, walls with or without plaster, earthen walls, floor of stone or cemented with a corrugated sheet, slab, or thatched roof can be used for stacking of bagged grains. However, FCI constructs the warehouses as per their own standards and specifications (**Figure 3**).

The warehouse system for bagged storage of food grains requires a huge number of labor for making stacks at the time of initial storage and braking stacks at the time of liquidating the food grain bags. Thus, it incurs a high operational cost, especially if the labor charges are high. Losses due to pest attacks, spillage during handling, and operational difficulties are limited when standardized protocols are followed properly. Seepage of water may occur in poorly constructed godown floors and ventilators and may increase the RH inside the warehouse. However, bagged storage systems need less capital investment and sophisticated aeration systems are not required for aeration and fumigation.

Requirements of Warehouses

The warehouse facility includes the structure, equipment for packaging of grains in bags, handling, ancillary facilities, quality evaluation equipment, and chemicals for pest control. The structures are constructed on a raised platform, well-drained locations, and away from flood-prone areas. The location of the warehouse should be at least 500 m away from waste management industries, such as bone-crushing mills, garbage

dumping areas, slaughterhouses, tanneries, hide curing units, sewage water treatment plants, etc. The structures near a carriage head or the main road are preferred. Typically, a godown or warehouse of FCI is made of the dimensions given in **Table 3**.

The major requirements of a warehouse are as follows:

- Suitable foundation depending upon the site conditions.
- Damp proof and rigid floor, which should be free from cracks and crevices.
- Plinth at 800 mm above the ground level for truck loading and 1,060 mm for the rail fed.
- Platform width of 1,830 mm for road head and 2,440 mm for rail fed.
- Slope of platform 1:40 (minimum).
- Longitudinal walls of brick or stone masonry up to 5.6 m height from the plinth level and 230 mm thick.
- Steel ventilators of opening $1,494 \times 594 \text{ mm}^2$ placed near the top on the longitudinal walls.
- Air inlets steel ventilator of $620 \times 620 \text{ mm}^2$ placed at 600 mm above the floor level.
- Suitable number of steel ventilators glazed with fixed wire mesh on the gable walls.
- Single span structural steel or tubular trusses for roof.

TABLE 3 | Bag storage godown/ warehouse capacities and their dimensions.

Godown type	Approximate capacity (tons)	Internal dimensions (m)		
		Length (m)	Width (m)	Height (m)
Small	1,120	100	12	7.5
	2,700	250	20	9
	5,400	500	34	12
	10,500	1,000	35.5	18
	28,510	2,500	97.19	14.48
Large	57,020	5,000	129.74	21.34

Note: for storage capacity above 2,500 tons, godowns are divided in suitable compartments.

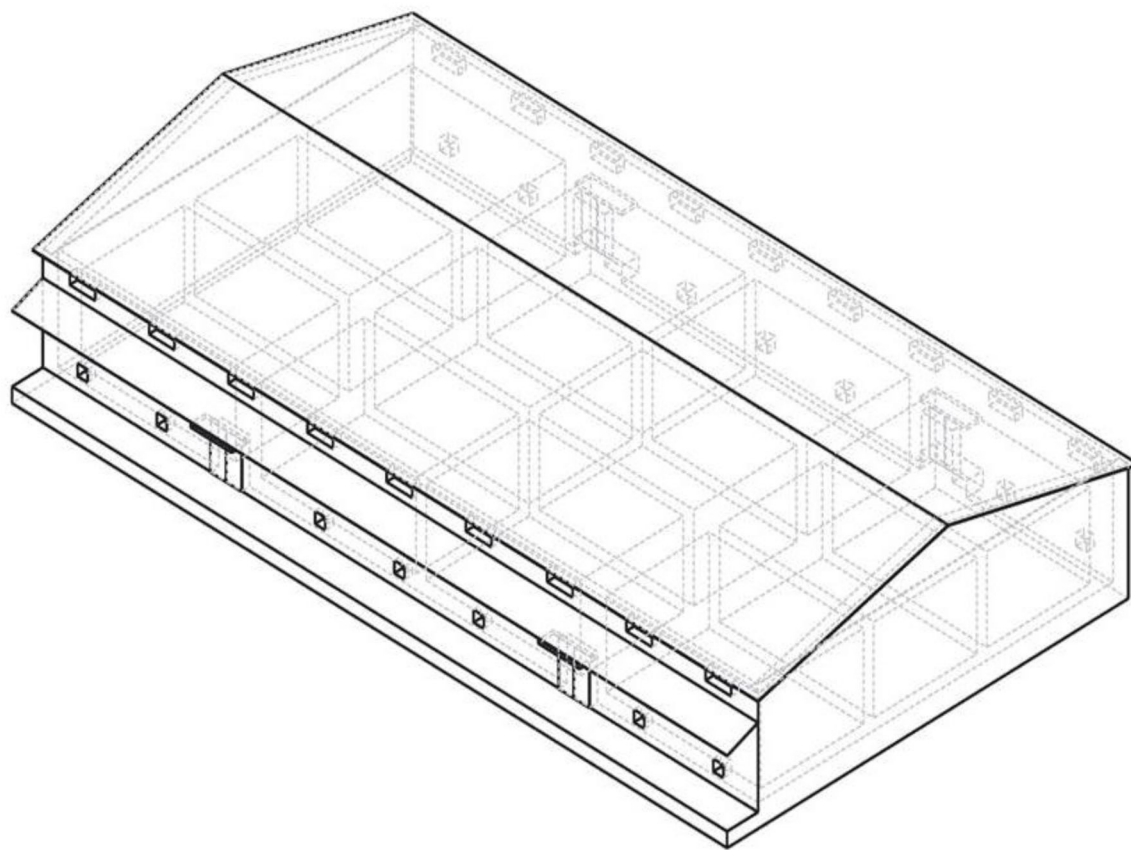


FIGURE 4 | A typical bag storage structure with stacking floor plan.

- Cantilever trusses are fixed on to RCC columns at 4,000 mm height.

Estimation of Space Requirement for Stacking of Bags

For movement of bags in a godown, a 3-m-wide gallery is kept along the width of the warehouse. A gangway of 2 m is kept along the length and in the center of the warehouse. For inspection of stacks, 1 m space around the entire stacking area should be kept. A typical stack arrangement in a godown is shown in **Figure 4**. A view of a typical stack inside an FCI godown is shown in **Figure 5**.

FCI has developed a protocol for wheat storage management in the warehouses. The protocol includes the methods of building a stack inside a warehouse, dunnage specifications, floor plan, prophylactic treatment procedures, fumigation treatment protocol, sampling procedure, and guidelines, dismantling process of the stacks, specifications for jute bags to be used, specifications for trucks to be used for transport, cleanliness, and hygiene protocol, warehouse ancillary equipment requirement, storage protocol for insecticides and chemicals, etc. All the operations are performed professionally by the trained manpower. Overall storage management practice of FCI may be used in any other country.

At present, FCI has a total storage capacity of 41.19 million tons. The warehouse storage capacity of FCI in 2020–2021 was 37.45 million tons (12.93 million tons owned by FCI and 24.52

million tons hired from other agencies and private warehouses). Furthermore, the silo storage capacity of FCI in the same period was 0.76 million tons, whereas storage under CAP is 3.32 million tons (2.57 million tons owned and 0.75 million tons hired). Thus, FCI stores the majority of procured cereals in warehouses (90.18%), whereas CAP storage is only 7.99% and silo storage is 1.83%. Therefore, warehouse management is the specialty of food grains storage by FCI in India.

ESTIMATES OF STORAGE LOSS DURING STORAGE OF WHEAT BY FCI IN WAREHOUSES

FCI defines gain/loss during storage of food grains in a warehouse as the change (increase/decrease) in weight after a certain period of storage. However, the quantitative loss of food grains is defined as the reduction in dry matter weight during storage. Losses such as quality deterioration, loss of food value, goodwill or reputation, seed vigor loss, etc., are not a part of the quantitative loss. The trends of storage losses observed by FCI in the last decade are shown in **Figure 6**.

It may be observed that the storage losses of wheat decreased continuously in the last decade and gain was observed after 2014–2015. However, the gain in weight was due to the increase in moisture content mainly in prolonged storage. As a matter of fact, the dry matter mass decreases with the storage period even when



FIGURE 5 | A view of bag storage in a warehouse.

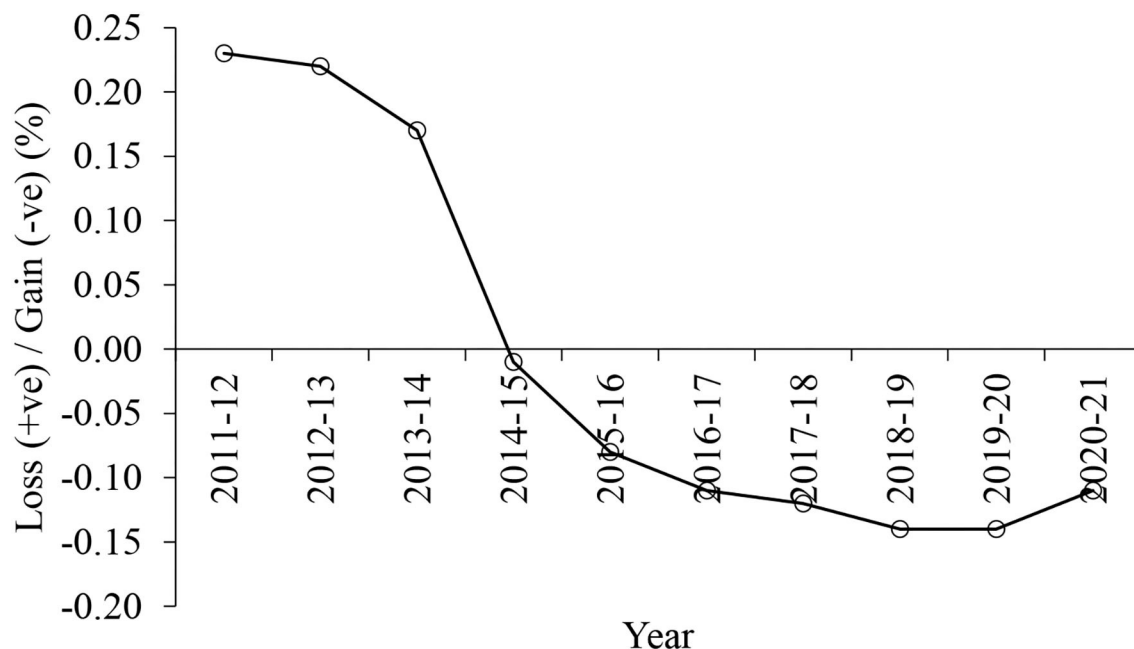


FIGURE 6 | Storage losses of wheat observed by FCI in warehouses.

external factors do not affect it. Therefore, a study on the extent of storage losses in wheat stored in the warehouses was conducted during 2013–2019.

Method of Study

A total of 30 depots of FCI were selected from different regions of the country. Multistage random sampling method was adopted to select stacks by taking depots as first-stage units, warehouse within each selected depot as second-stage units, a chamber in each of the selected warehouse as third-stage units, and stacks from each of selected chamber as fourth-stage units. At least two warehouses in each depot and two chambers in each warehouse were selected randomly for data collection. In one chamber, 12 wheat stacks were selected randomly for recording the losses. A set of four schedules were prepared for data collection. Altogether, 677 stacks of wheat (about 150 tons wheat in each stack having 3,000–3,200 bags) were taken in this study and continued for a storage period of 3 years. The stacks were built up, and initial parameters, such as weight, number of bags, moisture content, foreign matter, initial infestation level, broken grain, etc., were recorded. One stack from each chamber was liquidated randomly at 3 months interval, and their data were recorded including 100% weightage of the stack. After liquidation, the wheat was disposed of. All the norms and standards of storage management practices laid down by FCI were followed during the entire study. Samples were taken from each stack as described in section Storage Management. The observations on the physical parameters of the commodity were recorded fortnightly. Besides, environmental data inside the chamber were recorded on a daily basis and ambient environmental data of the locality were collected from the nearby meteorological station.

The sampling procedures and analysis methods prescribed by the Bureau of Indian Standards (BIS) incorporating IS: 14818 (2000), IS: 2813 (1995), and IS: 4333 Part I Part II (2002) for food grains in respect of moisture content, change in weight, 1,000-grain weight, and loss due to insect infestation were followed in this study.

Data Analysis

The data were analyzed using MS Excel. The estimation of losses was carried out at depot level initially and pooled at the zone level. The *t*-test (dependent samples or paired *t*-test) was conducted to compare the difference in mean values of moisture content, storage loss, etc. at the time of stacking and liquidation. Standard deviation, standard errors, and ANOVA were done using Statistica Version-6 software.

RESULTS AND DISCUSSION

Data collected in this study were scrutinized and matched with the records of depots as well as the hard copy records. The data, which were found unfit or could not get verified, were discarded. The remaining data were analyzed, and storage losses of wheat were estimated as discussed.

Change in Moisture Content of Wheat During Storage

The changes in moisture contents with storage periods are reported in Figure 7. The moisture contents of wheat at the time stacking in procuring region were $10.78 \pm 0.42\%$, which were significantly lower ($p < 0.05$) than the stacking moisture content in the consuming region ($11.34 \pm 0.13\%$). Wheat is procured

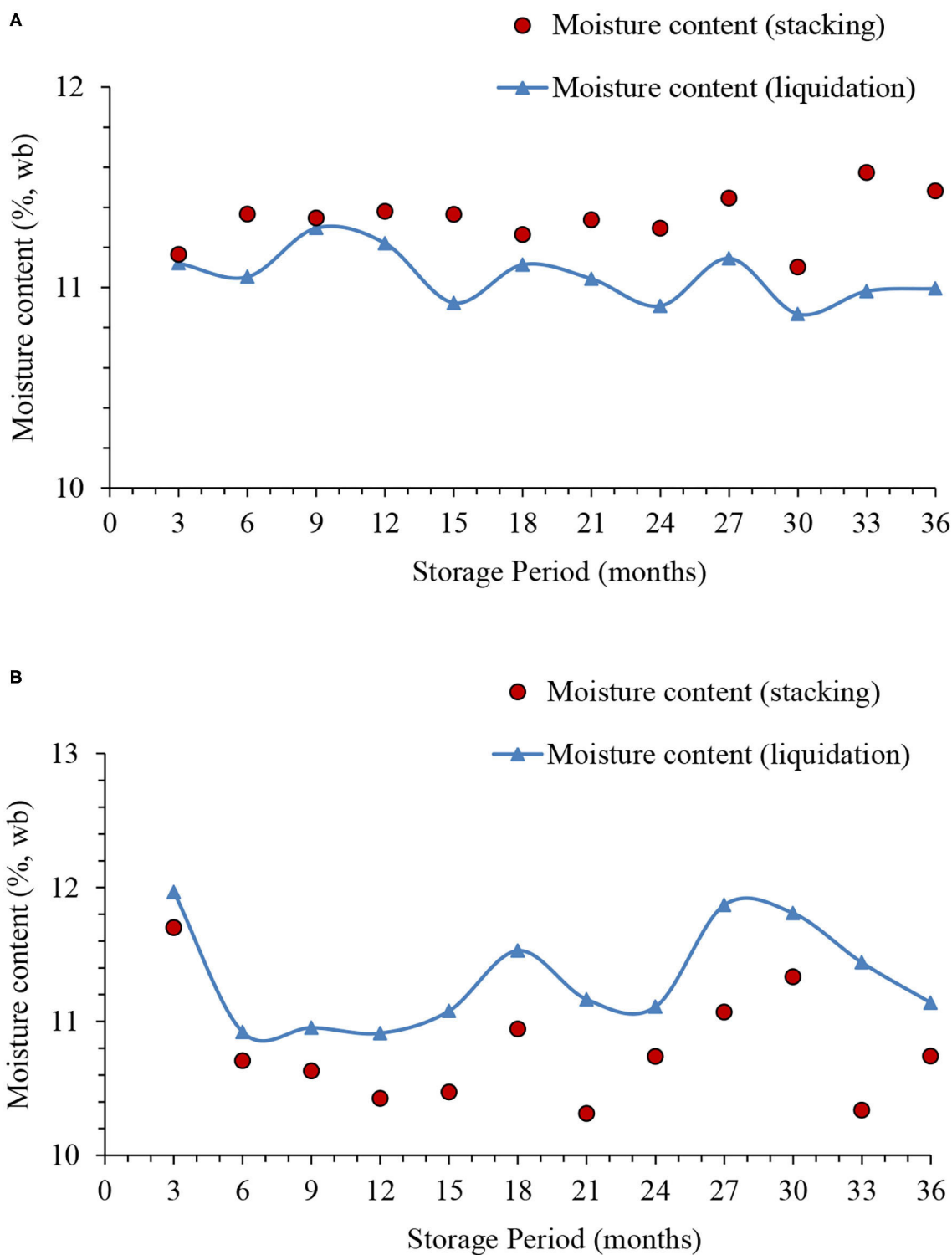
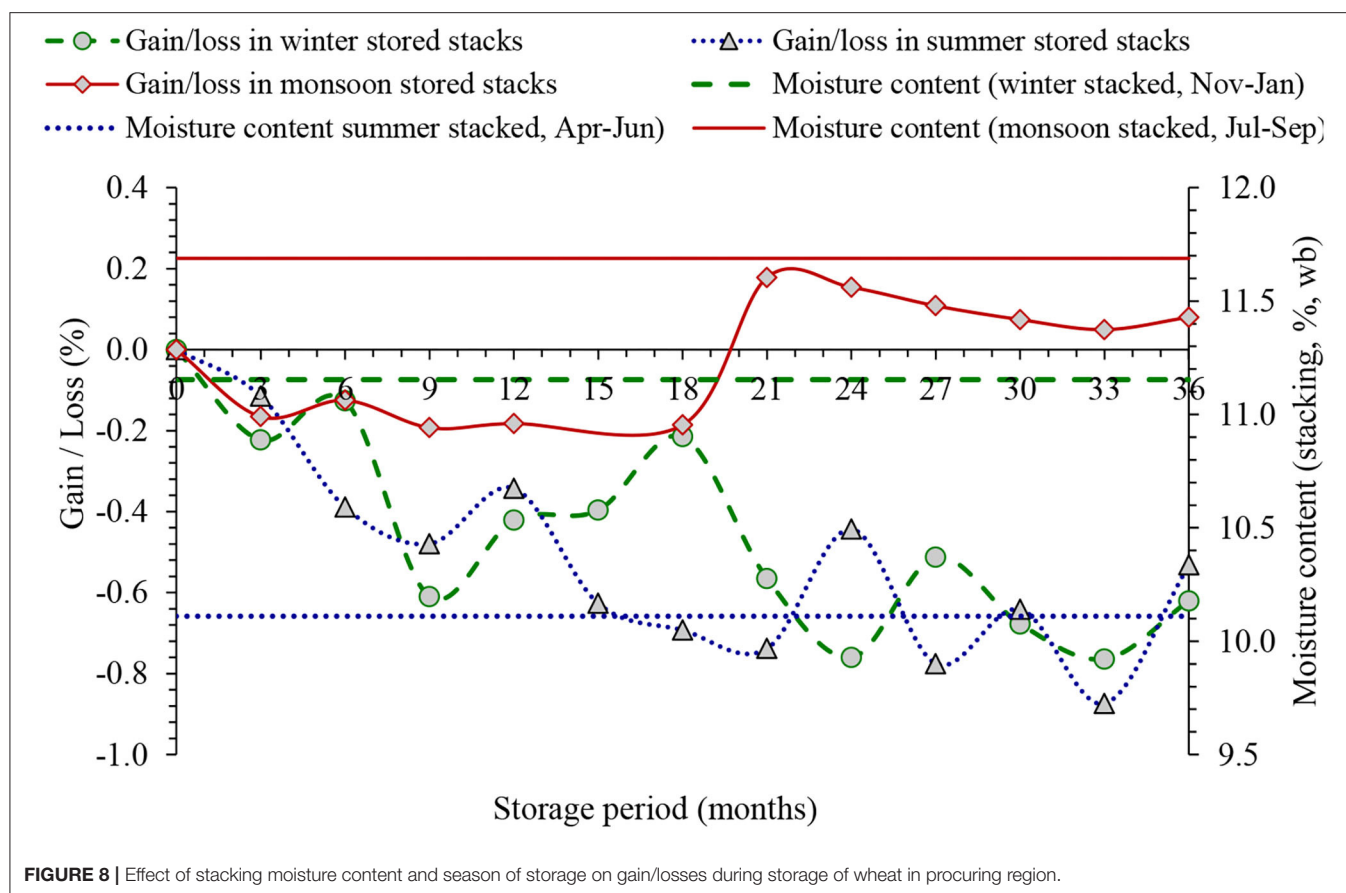


FIGURE 7 | Change in moisture content of wheat with storage period **(A)** consuming regions and **(B)** procuring regions.

in peak summer season in India and stacking procuring region was done in summer months and hence lower moisture content was expected in procuring region. Furthermore, the wheat was

transported from procuring region to the consuming regions in the monsoon season for further storage, and hence the wheat gained some moisture during storage in the procuring region.



The liquidation moisture content of wheat stored in consuming regions decreased significantly ($p < 0.5$) with the increase in storage period (Figure 7A) whereas it increased significantly ($p < 0.0.5$) in the procuring regions (Figure 7B). It may further be observed that the difference between stacking and liquidation moisture contents increased with the storage period and this difference varied according to the stacking moisture content in both regions. Thus, the wheat bags placed in the core of the stack gained/released moisture at a very slow rate and continuous alteration in environmental conditions of the warehouse affected the moisture of wheat in the periphery.

Wheat attained 11–11.50% moisture contents in both regions after 30–36 months of storage irrespective of the stacking moisture content. It indicated that the environmental conditions affected the rate of increase/decrease in moisture content. It may be inferred that the rate of gain/loss due to change in moisture content during storage is mainly dependent on the stacking moisture content.

Effect of Environmental Conditions on Weight Gain/Losses

A typical variation in weight gain/loss observed for the procuring region is shown in Figure 8, which explains the relationship between environmental conditions and moisture gain/losses. The

procuring region was the subtropical region of India where all seasons prevail in a year.

The stacking moisture content of wheat in winter, summer, and monsoon seasons were $11.15 \pm 0.43\%$, $10.11 \pm 0.28\%$, and $11.69 \pm 0.30\%$, respectively. The gains in weight of wheat were observed with increase in the storage periods only when storage was done in the summer and winter seasons when the moisture content was $\leq 11.15\%$. A slight gain in weight was also observed in monsoon-stored wheat up to 18 months storage and thereafter the weight loss was observed with an increase in storage period. It indicated that the moisture content of wheat might reduce in long-duration storage to attain equilibrium. Furthermore, the storage gain/losses increased with the increase in storage period irrespective of the season in which the wheat was stacked and liquidated. Thus, the weight gain/losses depended upon the moisture content at which stacking was done whereas the change in environmental conditions played a limited role.

Infestation Level and Its Contribution to the Loss

Weevilled grain percentages were significantly higher in consuming regions in comparison with the procuring regions and increased with the storage period. Procuring region has subtropical climatic conditions whereas the majority of the consuming region has humid climates or coastal regions of India

and hence the climatic conditions favored insect growth in the consuming region.

The infestation in food grains may cause loss of dry matter. However, such loss depends purely on the level of infestation. As per FCI norms, no insect per 500 g sample is considered “clear grain,” two insects per 500 g sample is considered “few infestation,” and more than two insects in 500 g sample is “heavy-infested grains.” The “heavy” infestation levels were observed in <2% of the stacks of consuming regions for the entire storage period whereas >74% stacks “clear” level of infestation during the entire storage period. Heavy infestations were observed in some specific locations of the consuming region where high rainfall was observed continuously for the longer duration and fumigation treatment failed repeatedly. In procuring region, the infestation level was clear in >80% stacks for the entire storage period. Curative measures were adopted immediately whenever >0 insect population was observed in any of the fortnightly sampling observations as per FCI norms. The insects do not cause any measurable loss in wheat when the insect population is three or less (Keskin and Ozkaya, 2015) for 1 month. The heavy infestation may cause dry matter loss of 0.03% in 1-month storage period in wheat (Keskin and Ozkaya, 2015).

Dry Matter Loss

No dry matter loss was observed in the consuming region up to 9 months of storage and highest loss of 0.12% was found after 18 months of storage due to heavy infestation in some specific depots. The dry matter loss in procuring region was up to 0.30% in 36 months of storage owing mainly due to spillage during heavy stock movement to the consuming regions.

Overall Gain/Loss in Consuming Region

The percentage changes in moisture of wheat were not consistent with storage period in consuming regions because the stacking moisture contents were different for stacks liquidated in different quarters as shown in **Figure 7A**. A reduction in dry matter weight of <0.18% was observed even after 36 months of storage whereas the net reduction in weight was up to 3% due to moisture decrease during long-term storage of wheat because the stacking was done at >11.5% moisture contents. The total loss during storage increased by the same level in addition to the decrease in moisture content in the same quarter. It may, therefore, be inferred that the total losses in consuming regions were contributed by the decrease in moisture content whereas dry matter loss due to biotic factors contributed up to 0.18% only.

The moisture content of wheat stored in procuring regions increased in all quarters of storage. The gain in moisture content in each quarter was consistent with the stacking moisture content shown in **Figure 7B**. When dry matter loss and gain in weight due to moisture content were put together, the total gain was consistent. The weevilled grains were 0.00–0.27% during the entire storage period. The dry matter loss up to 0.30% was observed and overall gain in weight of up to 1.25% were observed in the procuring regions.

From the study, it was evident that the final storage losses or gain were a function of moisture change and storage period. A longer period of storage shall always lead to higher net storage losses of wheat over a given period of time. However, the total dry

matter loss during storage of wheat for 3 years was not more than 0.3%, which showed that the warehouse storage of food grains is a fairly good practice when proper storage management practices are followed.

FCI AND FOOD SECURITY AND SUSTAINABILITY

FCI is the nodal agency to procure wheat from farmers at the MSP and distribution to the beneficiaries. The other agencies such as CWC, SWCs, and private godown owners hold the wheat on behalf of FCI until FCI transports the stock from surplus to deficient regions or issues for consumption under the National Food Security Act and other welfare schemes. The major responsibilities of FCI are procurement of wheat on MSP, storage, stock transportation, and allocation of wheat to the state governments. Whereas, the state governments identify the eligible families in their states for issuing Ration Cards and run Fair Price Shops (FPSs) through which the wheat is given to the poor families at subsidized rates. The government provides 35 kg wheat per family per month @ Rs. 2/kg to 23.7 million families (about 90 million persons) identified under Antyodaya Anna Yojana (AAY). Besides 703 million persons identified as Priority Households under AAY get 5 kg wheat/rice per person per month @ Rs. 2/kg for wheat and Rs. 3/kg for rice through the FPSs (Department of Food and Public Distribution, 2021). Furthermore, the government provided 5 kg wheat/rice per month free of cost to around 800 million persons in April–October 2020 and May–June 2021 as COVID-19 relief for poor, jobless, and migrant laborers. Thus, the buffer stock management of wheat by the FCI played a crucial role in managing the pandemic situation during 2019–2021 and ensuring no one will sleep without food in India.

The procurement system of FCI for wheat is open ended, i.e., the government guarantees to purchase any quantity of wheat from farmers at MSP, provided they meet the minimum prescribed quality standards. The MSP for wheat increased by 64.5%, i.e., from Rs. 1,170 in 2011–2012 to Rs. 1,925 in 2020–21. The FCI by its own and through state agencies purchased <35% of total wheat production prior to the year 2019–2020. However, during 2019–2020, the procurement increased to 43% of the total production as the COVID-19 relief package. Furthermore, in 2020–2021, the wheat procurement was more than 40% of total production as support to the farmers in COVID-19 situation. The role of FCI to meet any exigency has been visible in the COVID-19 pandemic during which The Government managed to provide food to all the population, particularly to the vulnerable population.

FCI operations of procurement, stack building, liquidation, transportation, distribution, etc. are helpful in providing employment opportunities, which may not be possible in the silo storage system. In the stack building or liquidation, a team of 14 persons works together. Each warehouse has eight teams on average and thus FCI provides employment to about 233 thousand persons annually besides FCI officials. Thus, the FCI not only ensures the food security of India but also provides employment to a large chunk of the population with efficient

storage management and related operations of food grains. FCI has developed a sound and efficient storage management practice for the storage of food grains in its long journey of existence for the last 56 years. This model may be replicated in many developing countries for food security and the creation of employment for the poor population.

Prior to 2013, the storage losses of food grains were $\geq 0.22\%$. However, with better follow up of storage management practices, after commencement of the study, the storage losses have declined steadily. Furthermore, after 2014–2015, the total quantity delivered by FCI for distribution was more than the quantity stored in the beginning because of weight gain due to an increase in moisture content during storage (Anonymous, 2018). Thus, the study on storage losses of wheat in FCI warehouses helped in improving the implementation of stock management practices in the warehouses.

CONCLUSION

Food Corporation of India is a unique agency in the world that procures, stores, and distributes more than 70 million tons of cereals annually. The storage of wheat is now mainly done in warehouses with $<0.3\%$ dry matter loss after 3 years of storage. Furthermore, the losses of wheat in warehouse

storage are not as high as perceived because the loss observed in this study was equivalent to the losses incurred in silo storage done in the developed world. Though this storage system demands huge recurring investment, it provides employment to a large number of rural populations. The warehouse storage management practices of FCI are exhaustive, practically applicable and sufficient to avoid the losses in long-duration storage when followed in a holistic manner. The storage losses of food grains have decreased substantially in FCI warehouses after the storage loss study commenced. Furthermore, the role of FCI food grain stock management was crucial in the COVID-19 pandemic due to which the Government of India managed to provide food to all the population, particularly to population below poverty line, jobless, and migrant laborers.

AUTHOR CONTRIBUTIONS

CK: FCI organization setup, operations, and management. CR: quality control in warehouse management, handling, and operational guidelines. SJ: storage loss study in FCI godowns. RV: planning of paper, editing, storage study, FCI operations, and storage practices. All authors contributed to the article and approved the submitted version.

REFERENCES

- Anonymous (2018). *FCI Handbook-Food Storage Operations Management*. Gurugram: Study Material, Institute of Food Security, 116.
- Department of Food and Public Distribution (2021). *Food Grain Bulletin*. Available online at: <https://dfpd.gov.in/writereaddata/Portal/Magazine/FBMar2021.pdf> (accessed July 1, 2021).
- Directorate of Economics and Statistics (DES), Department of Agriculture, Cooperation and Farmers Welfare, Ministry of Agriculture, Farmers Welfare. Government of India. (2020). *Agricultural Statistics at a Glance 2019*. Available online at: <https://eands.dacnet.nic.in/PDF/At%20a%20Glance%202019%20Eng.pdf> (accessed July 2, 2021).
- Gu, D., Sokhansanj, S., and Haghighi, K. (2000). Influence of floor air entry on grain moisture content, temperature, and bulk shrinkage during ambient air in-bin drying of wheat. *Canad. Agric. Eng.* 42, 185–193.
- IS: 14818 (2000). *Cereals and pulses and milled products- sampling of static batches*. New Delhi: Bureau of Indian Standards.
- IS: 2813 (1995). *Terminology for foodgrains*. New Delhi: Bureau of Indian Standards.
- IS: 4333 Part I and Part II. (2002). *Methods of analysis for foodgrains*. Bureau of Indian Standards. New Delhi: Manak Bhawan.
- Jayas, D. S. (2012). Storing grains for food security and sustainability. *Agric. Res.* 1, 21–24. doi: 10.1007/s40003-011-0004-4
- Jha, S. N., Vishwakarma, R. K., Ahmad, T., Rai, A., and Dixit, A. K. (2015). *Report on Assessment of Quantitative Harvest and Post-harvest Losses of Major Crops and Commodities in India*. Ludhiana: ICAR-All India Coordinated Research Project on Post-Harvest Technology.
- Keskin, S., and Ozkaya, H. (2015). Effect of storage and insect infestation on the technological properties of wheat. *J. Food* 13, 134–139. doi: 10.1080/19476337.2014.919962
- Kumar, R., and Singh, R. (1984). Levels of free sugars, intermediate metabolites and enzymes of sucrose-starch conversion in developing corn grains. *J. Agric. Food Chem.* 14, 231–235.
- Labuza, T. P. (1980). The effect of water activity on reaction kinetics of food deterioration. *Food Tech.* 34, 36–59.
- Mersal, I. F., El-Emam, A. A., and Amal, M. (2006). Effect of storage period, seed moisture content and insecticides treatment on wheat (*Triticum aestivum* L.) seed quality. *Annals Agric. Sci. Moshtohor.* 44, 111–124.
- Sinha, M. K., and Sharma, P. D. (2004). Storage performance of wheat in different storage structures. *J. Appl. Biol.* 14, 83–85.
- Ueno, K. (2003). Effects of desiccation and a change in temperature on germination of immature grains of wheat (*Triticum aestivum* L.). *Euphytica* 126, 107–113. doi: 10.1023/A:1019655218722

Conflict of Interest: CK and CLR were employed by company Food Corporation of India.

The remaining authors declare that the research was conducted in the absence of any commercial or financial relationships that could be construed as a potential conflict of interest.

Publisher's Note: All claims expressed in this article are solely those of the authors and do not necessarily represent those of their affiliated organizations, or those of the publisher, the editors and the reviewers. Any product that may be evaluated in this article, or claim that may be made by its manufacturer, is not guaranteed or endorsed by the publisher.

Copyright © 2021 Kumar, Ram, Jha and Vishwakarma. This is an open-access article distributed under the terms of the Creative Commons Attribution License (CC BY). The use, distribution or reproduction in other forums is permitted, provided the original author(s) and the copyright owner(s) are credited and that the original publication in this journal is cited, in accordance with accepted academic practice. No use, distribution or reproduction is permitted which does not comply with these terms.



Enabling Food Safety Entrepreneurship: Exploratory Case Studies From Nepal, Senegal, and Ethiopia

Yevheniia Varyvoda^{1*}, Thoric Cederstrom², Jenna Borberg² and Douglas Taren^{1,3}

¹ Mel and Enid Zuckerman College of Public Health, Health Promotion Sciences Department, The University of Arizona, Tucson, AZ, United States, ² Food Enterprise Solutions, Arlington, VA, United States, ³ School of Medicine, University of Colorado, Aurora, CO, United States

OPEN ACCESS

Edited by:

Shalini Gaur Rudra,
Indian Agricultural Research
Institute, India

Reviewed by:

Agnes Kilonzo-Nthenge,
Tennessee State University,
United States
Vikrant Dutta,
BioMérieux, United States

*Correspondence:

Yevheniia Varyvoda
varyvoda@email.arizona.edu

Specialty section:

This article was submitted to
Agro-Food Safety,
a section of the journal
Frontiers in Sustainable Food Systems

Received: 16 July 2021

Accepted: 30 August 2021

Published: 27 September 2021

Citation:

Varyvoda Y, Cederstrom T, Borberg J
and Taren D (2021) Enabling Food
Safety Entrepreneurship: Exploratory
Case Studies From Nepal, Senegal,
and Ethiopia.
Front. Sustain. Food Syst. 5:742908.
doi: 10.3389/fsufs.2021.742908

Today, formal and informal enterprises are increasingly contributing to the safety and nutritional ramifications of their food business activities. Enabling entrepreneurship in a sustainable manner means making profits, striving to prevent ingress of harmful substances, and increasing the efficiency of using local natural resources and thus mitigating food hazardous footprints. Using examples from Nepal, Senegal and Ethiopia, this review provides information on microbial and chemical contamination and food adulteration that lead to having unsafe food in the market and on factors that are limiting growing food businesses. Four examples for how to accelerate food safety entrepreneurship are presented that include safely diversifying markets with animal sourced foods, sustainably using neglected and underutilized animal sources, expanding, and integrating innovative technologies with traditional practice and using digital technology to improving monitoring and safety along the food supply chain.

Keywords: food, entrepreneurship, supply chain, safety, nutrition, market, system

INTRODUCTION

Access to safe and nutritious food is one of the most complex social and economic problems that has transparent frontiers and exists practically everywhere on the world map. The recent emergence of a “New Food Equation,” marked by food price hikes, dwindling natural resources, land grabbing activities, social unrest, the effects of climate change, and recent pandemic impact of COVID-19 is bringing onto the global food security and safety agenda a range of often interrelated sustainability concerns (Sonnino, 2016; Apostolopoulos et al., 2021). All these issues form a challenging environment in which food businesses operate but at the same time trigger the positive changes that can strengthen food safety systems. In particular, COVID-19 provided a boost to short supply chains in the agri-food sector and agri-food enterprises and those with new technologies and digital aspects at their core were privileged in competition. Agri-food enterprises relying on transportation for their inputs were limited in operations due to travel restrictions. Simultaneously, there was a forced change from fresh to dried agri-food products e.g., dried seafood (sardines, prawns), meat (beef jerky, goat meat), beans, lentils, and peas, fruits (bananas, mangos, pineapple), and vegetables (tomato, onion, okra) affecting agri-food entrepreneurial activities (Bene, 2020; Apostolopoulos et al., 2021; Belton et al., 2021; Nordhagen et al., 2021).

Following these conditions in prerequisites, for low- and middle-income countries (LMICs), the most promising trend in future foods depends to a large extent on food businesses awareness. Hence, the ability to expand the production of local foods and the need to employ indigenous and new technologies for food processing to produce safe, nutritious, and healthy products. Identifying and implementing technologies that reduce greenhouse gases and use of green technologies for transporting, processing and packaging that preserve the safety, quality, and nutritional value of food products provide an important avenue for building local and national economies. Among these novel technologies are the smart packaging systems based on natural food colorants for the monitoring of food quality and safety, digitalization of basic logistic processes realized through Internet-based solutions, light-emitting diode technology, smart moisture detection, and various other innovations to multiple health and environmental benefits along food supply chain (Alizadeh-Sani et al., 2020; Prasad et al., 2020; Chitrakar et al., 2021; Forcina and Falcone, 2021).

The rationale of this review is to understand the challenges food entrepreneurship is facing related to food safety and what kind of targeted interventions would be relevant to a particular country context. Diversity within country contexts will provide an opportunity to observe how ongoing or future food safety actions succeed or fail under a variety of circumstances.

By screening the existing drawbacks in food systems through the prospects of what food businesses can contribute in a given country context, stakeholders will be more capable in designing and implementing actionable and incentive-based recommendations for better food and nutrition safety practices. Effective food safety interventions should ensure that the size of the action is adjusted to the size of the problem, i.e., the level of effort is proportional to the significance of the expected impact. A number of recent reviews have found that diverse agricultural interventions have increased food production, but did not necessarily improve nutrition and “post-farm gate” methods that increase the availability, affordability, acceptability and consumption of nutritious foods also needed to support food safety for small formal and informal enterprises that often cannot comply with legislated criteria (Maestre et al., 2017).

Studies from Nepal, Senegal and Ethiopia were reviewed to identify key food safety issues and barriers to improving food safety practices and nutritional status of foods. These countries were selected because they have demonstrated potential to reshape their food safety systems that contribute to the sustainable development of the agri-food sector economy. Some of the significant signals that food safety and nutrition concepts are beginning to shape expectations and regulatory requirements in these countries include:

- Increased contributions to the large body of peer-reviewed materials and gray literature actualize and explore the problems of food safety and nutritional quality protection at the level of small- and medium businesses (Noort et al., 2016; Morse et al., 2018; Joardder and Masud, 2019; Nyarugwe et al., 2020).

- National governments of Nepal, Senegal and Ethiopia are exploring policy mechanisms to restore, maintain and evolve services around food safety (Grace, 2015; GFSP, 2018; Birke and Zawide, 2019; Uprety and Shivakoti, 2019; Forsido et al., 2020; Osti, 2020).
- A growing number of food entrepreneurs are ready to apply food safety best practices as pilot tests with a focus on business profits (Kussaga et al., 2014; Dongol et al., 2017; Dizon et al., 2019; Getachew and Christian, 2019; Ghimire and Koirala, 2019; Thapa et al., 2019; Bene, 2020).
- Trendsetting financial institutions have put into place requirements to consider food safety standards within financial due diligence processes (Van der Heijden et al., 1999; Kirezieva and Luning, 2017; Steier and Patel, 2017; FAO et al., 2020).

The following section illustrates existing and emerging drivers for food safety and include specific and sensitive insights that promote and inhibit growing sustainable food businesses.

UNSAFE FOOD AS PUBLIC HEALTH RISK

Historically dietary patterns in Nepal, Senegal, and Ethiopia are a mixture of plant and animal-sourced foods (ASFs) that are often minimally processed. As the population is increasing, especially with migration to urban areas, there is a modern trend to continuously expand food businesses to meet this shift in the size and location of the population. World projections modeled on the last 5 years of growth in urbanization, per capita income, and rates of income inequality anticipate that by 2040, 72% of all food will be processed to some degree, up from 58% today. Rural processed food consumption will grow from 43 to 50% and urban processed food consumption from 91 to 95% (IFTF, 2018). The distance between production and consumption spots are stretching and a number of developments which include changes in pre- and post-harvest practices are contributing to increased threats of biological, chemical and physical hazards on food safety.

Microbial contamination, chemical contamination, and food fraud are commonly reported public health risks related to food safety along the value chain in Nepal, Senegal, and Ethiopia. These challenges include, but not are limited to.

Microbial Contamination of Food

Failure to apply food safety strategies in every stage of the food supply chain, for example, bad feeding and watering practices, poor animal health, unhygienic production system, underdeveloped practice of packaging and labeling, poor infrastructure, informal market channels, poor marketing practices, and poor hygiene and sanitation lead to microbial contamination of foods. Moreover, fraudulent food processing practices such as adulteration, and selling of spoiled or expired foods are also causing microbial contamination (Dongol et al., 2017; Doutoum et al., 2018; Dhungel et al., 2019; Behera et al., 2020; Owusu-Kwarteng et al., 2020; Teferi, 2020; Teixeira et al., 2020). Numerous pathogenic microorganisms have been found in different food items along the value chain. The

following disease-causing bacteria were commonly reported in the target countries: *Salmonella* spp., *Escherichia coli*, *Klebsiella* spp., *Shigella* spp., *Citrobacter* spp., *Pseudomonas* spp., *Vibrio* spp., *Campylobacter* spp., *Listeria* spp., *Cryptosporidium*, *L. monocytogenes*, *Brucella* spp., *Coxiella burnetii*, *Proteus* spp., *Staphylococcus* spp., and *Bacillus cereus* (Hempfen et al., 2004; Dahal et al., 2010; Mersha et al., 2010; Kirk et al., 2014; Adugna et al., 2015; Abera et al., 2016; Atnafie et al., 2017; Markos et al., 2017; Mengistu et al., 2017; Bantawa et al., 2018; Dhungel et al., 2019; Kassahun and Wongiel, 2019; Keba et al., 2020; Kumar et al., 2020; Osti, 2020). The available sources indicate a trend toward increasing resistance rates among pathogens such as *Escherichia coli*, *Shigella* spp., *Salmonella* spp., and *Staphylococcus aureus* to commonly prescribed antibiotics, including ampicillin, amoxicillin, penicillin, tetracycline, and trimethoprim/sulfamethoxazole (Tesfaw et al., 2013; Dulo et al., 2015; Garedew et al., 2015; Ejo et al., 2016; Assefa and Bihon, 2018).

Chemical Contamination of Food

Food contamination with hazardous chemicals is one of the major public health concerns associated with the phases of food production, processing, packaging, transportation, and storage. Mycotoxins pose significant food safety challenges in the studied countries. In Ethiopia, aflatoxins, ochratoxin A (OTA), deoxynivalenol (DON), zearalenone (ZEN) and fumonisins (FUM) are considered to be widespread in major dietary and export-oriented crops (Ayelign and De Saeger, 2020). Getachew et al. (2018) reported the occurrence of 127 mycotoxins in maize grains collected from the major maize producing districts in Ethiopia. In the area of Southern Senegal a recent study found that 17 of 84 maize samples (20%) taken randomly from post-harvest cobs or shelled corn contained positive levels of aflatoxin (Bauchet et al., 2020). Studies of prevalence of aflatoxin contamination in Nepalese maize production have shown that the incidence in maize is high and average prevalence is about 50% (Pokhrel, 2016).

Among the hazardous chemicals commonly reported for grains, cereals, horticultural crops (mainly eggplants, tomatoes, chilis, lettuce, cabbage), fruits (banana), chicken eggs, pelagic fish, shrimps, dairy products are: heavy metals (like cadmium, zinc, iron, mercury, lead), pesticide residuals (like dicofol, chlorpyrifos, dimethoate, and λ -cyhalothrin), persistent organic pollutants [like lindane, hexachlorobenzene (HCB), cyclodienes (heptachlor and trans-nonachlor), DDT, dioxins, polychlorinated biphenyl (PCB)], organic compounds (like formalin, urea), and other chemical compounds (like bicarbonate, sodium hydroxide, sodium carbonate). In most cases, the concentration of chemicals has been found to exceed the tolerable limit for consumable food items (FAO, 2014; Thompson et al., 2017; Guy Bertrand, 2019). As an empiric example, a study of mercury, lead and cadmium contamination in fishery products from Senegal has detected mercury in 71% of the samples, cadmium in 60%, and lead in 58% of the samples. The greatest mercury contamination value (0.55 ppm) was found in cuttlefish during the 9-year study (Diouf et al., 2019). An investigation of pesticide residues in food indicated a 3-fold higher DDT residue concentration above the acceptable daily intake set by the WHO in human

mothers' and cows' milk samples. On top of the risk of pesticide residues in dairy products, other studies in Ethiopia also showed residues of organochlorine pesticides in cattle carcasses and honey samples (Negatu et al., 2021). In Nepal, due to over use and unsafe handling, the issue of pesticide use in agriculture farming is becoming a growing public health concern. Pesticide application is concentrated in relatively few provinces and is increasing by about 20% per year. Of the total pesticides imported in the country, more than 90% are used in vegetable farming (Kafle et al., 2021).

Food Authenticity Issue

The large number of food fraud incidents have impacted almost every stage of the food chain, and is identified as growing trend. Food fraud involves intentional or unintentional addition of useless, harmful, unnecessary chemical, physical, and biological agents to food which decreases the quality of food. It also includes removal of genuine components and processing foods in unhygienic way. The impacts of such incidents are far reaching, affecting not only consumers' trust to agri-food business and the reputation of the food supply chain but also present possible public health repercussions if a food fraud incident involves the addition of harmful substances or allergens. Chemicals [like metanil yellow, rhodamine, sudan red, calcium carbide, formalin, bicarbonate, sodium hydroxide (caustic soda), sodium carbonate, neutralizers, detergents]; items which are not the genuine component of foods (like starch, flour, water in milk, cow's fat and intestine in ghee, poisonous plant derivative); poor-quality products; and physical or inert agents (like clay, brick powder) are the commonest adulterants added mostly to dairy products, cereals, legumes, rice grains, edible oil, ghee, flour, and pepper (Sapkota and Phuyal, 2016; Gemechu et al., 2020; Thapa et al., 2020).

The case from Nepal illustrates that most of the times, the adulteration is intentional for raising profit, but it can be due to the lack of proper detecting technology and confusion regarding appropriate drug administration practices (Bhandari, 2020). Market inspection carried out in 2018 by the Department of Food Technology and Quality Control found that packaged milk sold in Kathmandu was adulterated with chemical contaminants such as washing soda and detergent chemicals. Harmful chemicals like bicarbonate, sodium hydroxide (caustic soda) and sodium carbonate were found in the 42 samples of packaged milk collected from 25 milk processing plants, which the firms had been using as neutralizer during storage. The deliberate mixing of milk with water, flour with gypsum, butter with banana, edible oil with poisonous plant derivative, and pepper with clay have been some of the reported cases in recent years in Ethiopia (Birke and Zawide, 2019).

Ways to ensure the quality and safety of food products is to guide priorities and to work with local food businesses to design actions to transform incentive-based business-to-business relationships within formal food and informal food networks.

The following actions for rebuilding the entrepreneurial partnership with agri-food business are consistent and applicable, albeit modified as needed for each explored country.

- Providing technical input on regulations and oversight for the implementation of food safety practices that improve local standards and meet export requirements.
- Provision of economic assistance to develop appropriate financial incentives. Governments and other financial institutions need to implement incentives for businesses to increase food safety practices. It is recognized that incentives may be more difficult for the informal and small businesses.
- Development and evaluation of food safety education materials and their impacts. A frequent finding is the need to educate all stakeholders. These stakeholders include consumers who need to link food safety with health; food producers who need to understand how food safety practices improve their return on investment; and policy makers who need to understand the intimate relationship between food safety, economic development, and public health.
- Development and dissemination of workshops and courses. Trainings need to focus on technical issues for implementing food safety practices and be directed to key personnel working in food businesses. Additionally, the trainings need to address the cost effectiveness of food safety practices.
- Provision of technical assistance and setting up collaborations. In order to have a successful scaling up of food safety practices, it is recognized that there needs to be collaboration among all stakeholders to implement and maintain these practices.

The success of such actions relies heavily on the understanding of food products, value chain functioning, consumer awareness of the value of nutrition and food safety, and expectations of agribusiness main actors.

FACTORS LIMITING GROWING FOOD BUSINESSES

Nepal, Senegal and Ethiopia are diverse countries in terms of geography, ethnicity and socioeconomic conditions. The market for food businesses in all three countries is strong due to an increase in population, an increase in demand for ASFs, a limited number of food-oriented businesses, and a large dependency on imported foods. Increasing local food businesses can enhance the income of small and medium size businesses and stimulate a slowly growing economy (Lake et al., 2015; Kwil et al., 2020). Small and medium size agri-food businesses now experience significant challenges from the local level all the way up to being engaged with international trade (Sautet, 2013; Deller et al., 2017). Unfortunately, food systems safety are decades behind in adopting technologies, standards, and business management tools due to various on-going weaknesses of the local market systems.

There are significant constraints to providing safe food with over 80% of food sold in informal markets that have restricted access to clean water, consistent power, and sanitary and waste disposal, and even social norms and beliefs (Haileselassie et al., 2020). Inroads to increasing food safety measures for food businesses in the informal sector especially need to address how they increase short and long-term revenue to balance the required risk adverse behaviors from this sector. At the same

time, the informal market participants can play a leading role in driving positive change through coordinated and co-shared food safety and quality responsibilities. For example, many people engaged in informal markets are highly knowledgeable about the indigenous methods of shelf-stable food safety which can be optimized and modernized to meet current market demands.

Meat and Dairy

Meat and dairy production are potential drivers of economic growth in Nepal. While several private companies operate in the dairy sector the lack of road access to urban areas has discouraged private investment in areas where the bulk of milk and meat are produced, preventing most producers from linking into value chains. Lack of access to affordable financing, credit, and information services have made it difficult for the private sector to establish and operate milking centers, processing plants, and other commercial operations (Sharma, 2017).

An example of a food safety specific influence relates to the production of safe and hygienic milk. This is especially the case for the dairy sector of Nepal (Kumar et al., 2017). In a survey of raw milk in Nepal, it was found that out of the 129 samples, 25% were positive for *E. coli*, 37.2% for *Salmonella* spp., 5.4% for *Shigella* spp., 7.7% for *Klebsiella* sp., 18.6% for *Citrobacter* spp., and 1.6% for *Pseudomonas* spp.. Air, feed, grass, soil, feces, and milking equipment were considered the primary sources. For a country with one of the worst child nutrition statistics in the world, safe, and hygienic milk production is critical (Dhungel et al., 2019).

The informal milk sector, which accounts for three quarters of Nepalese production, has a similar issue since it is sourced primarily from small and subsistence-level farmers. They produce primarily for household consumption and sell the excess into local markets for consumption as raw milk or for artisanal processing. Milk transacted through these channels is neither pasteurized nor labeled, and usually does not follow most of the good agricultural practices (GAP). In the small segment of branded dairy products, both pasteurization and labeling exist. Without pasteurization and adoption of GAP, the milk from the informal sector tends to be prone to adulterants such as water, benzoic and salicylic acid, detergents, urea, formalin, sugar, carbonates, and ammonium sulfate, partly due to pricing by fat content at the first point of sale (Thapa et al., 2020).

On average, a dairy farmer in Nepal has to incur an additional expenditure of Rs 2 (0.017 USD) per liter of milk production in order to follow food safety measures (FSM). Farmers are not very enthusiastic about fully complying with FSM since it involves incremental costs and the markets in Nepal often do not reward food safety. There are certain ways to address food business actors' initiatives around safety through public promotion (newspapers, websites, social media, banners); food safety recognition awards; favorable offers for testing, inspections and certification; consulting in standards design; customized business solutions, etc. In order to reach diverse audiences in terms of food safety recognition, digital communications should complement, not replace, traditional methods.

The results of a food safety consciousness study among the Nepalese smallholder dairy farmers revealed that an increase

in the food safety consciousness level by 1% increased the weekly milk expenditure, milk price paid, and weekly milk purchased by 1.37, 0.66, and 1.27%, respectively. Furthermore, an increase in food safety consciousness by 1% was associated with a 37% higher probability of selecting a modern milk outlet (Thapa et al., 2019).

The food entrepreneurs—mainly processors, traders, and retailers—lack the knowledge, adequate incentives, and understanding of how to prevent risks or mitigate impacts of food safety hazards. By incorporating food safety risk mitigation into their business operations, entrepreneurs can improve their competitiveness and overcome barriers of mistrust and negative perceptions about costs of actions to provide safer and more nutritious food to consumers. They also lack skills of setting and implementing certain food safety standards and procedures in a consistent and repeated manner for post-harvest loss minimization.

Eggs

Many technologies for reducing losses exist, but they are barely utilized and some of them have not yet been introduced in many LMICs. Examples include hermetic bags, heavy molded-plastic containers, and mobile processing units. These innovations have a small unit cost and are suited to individual use.

A study from Nepal by Martin Metzger states that the sustainability of small production Nepalese farmers is very important to egg production and consumption. For eggs to be transported without damage, egg trays or cartons are crucial, but for farmers to have access to egg cartons or trays, they need to be economical, available, and useable. Plastic egg trays cost more and because Nepal is a cost sensitive market, plastic egg trays are out of the price range. Therefore, pulp egg cartons are the safest, easiest to produce and most beneficial for Nepal.

Providing Nepalese farmers with egg cartons and trays can be achieved through two methods. The first method involves importing and distributing egg cartons or trays throughout Nepal. The more distribution centers that are set up, the shorter distance farmers would have to travel to get egg cartons and trays. The distribution center could become a new business for Nepalese entrepreneurs who want to help farmers by facilitating distribution of the egg cartons and trays. Multiple distribution centers could be independently owned and operated but linked to one larger distribution center that facilitates the importation of mass quantities of egg cartons and trays. By having one large distribution center supplying the smaller ones, it prevents price fixing and creates an equal price throughout Nepal. The second option is manufacturing egg cartons and trays in Nepal in either large or small-scale operations. There are many benefits to manufacturing egg cartons and trays in Nepal, but the main one is the direct boost to the local economy. Egg carton and tray production can be either a large or small-scale operation. There are no manual tools for making egg cartons or trays, so regardless of the system, it has to be in an industrial setting. With the goal of benefiting small production Nepalese farmers, the advantages and disadvantages of each solution have to be studied precisely.

Fish

Creating an infrastructure to expand food safety practices, in the aquaculture and fisheries in Senegal for fish destined for local markets, need to address the unsanitary handling of fish due to a lack of adequate cooling which is the greatest food safety issues for this sector (Doubouya et al., 2017; Lancker et al., 2019). Additionally, much of the production and harvest is undertaken by small-scale farmers and fishers who lack adequate resources to adopt safer food practices. Additionally, local markets lack the economic and regulatory drivers of food safety that export markets demand. In Senegal, like in many emerging economies, there is a lack of adequate processing infrastructure or electricity in landing sites and this contributes to significant food safety risks, post-harvest loss, and limits economic performance (Diop et al., 2019). Fish often lack icing or refrigeration from processing to final point-of-sale; and large quantities are processed using traditional techniques that can introduce harmful chemicals into products, such as polycyclic aromatic hydrocarbons (FES, 2000, 2021; Vergis et al., 2021). In Senegal, recent studies of the quality and safety issues in the minced sardinella filets production has shown that the sanitary conditions of the fish handling and preparation environment are poor: the floor is often sandy, dirty, or of damaged cement or tiles; lack of drainage facilities for wastewater; irregular and inadequate removal of solid wastes, absence of toilet facilities and potable water at some places. The operators were aware of these conditions and at least two thirds among them stated that they would have attracted many more customers and boosted their business if hygiene within their places was improved. Antidotally, the respondents recognized that the longest queue of customers in the market was for the kiosk owned by three women who applied comparatively better hygienic working practices, though their service was more expensive (Diei-Ouadi, 2005).

Small producers are unable to respond to the market-pull from country-level commercial producers, processors and traders. They lack assets, knowledge and understanding of values and culture of food safety management, organizational skills to consistently produce and process the nutrient rich food products in variety, quality, and volumes needed for local markets. Gross margin analysis on few dairy products sold by the private dairies in far-western Terai districts of Nepal revealed that selling curd, paneer, Khoa, and ice cream was two times, five times, and twenty times profitable, respectively than the selling standard milk (Bhandari, 2018). Moreover, there are underutilized indigenous food products in the studied countries that can be commercially produced and compliment food and nutrition security efforts. As an example, according to Aragaw et al. (2021) Ethiopia hosting hundreds of edible plants can fulfill nutritional demands of local people. Among the explored underutilized edible plant species in coffee agroforestry systems of Yayu, southwestern Ethiopia leafy vegetables, such as *Amaranthus graecizans*, *Portulaca oleracea*, and *Solanum nigrum*, have proved to be good sources of protein and minerals (Ca, Fe, and Zn). Other species were reported to be good sources of pro-vitamin A (*Rubus apetalus*) and vitamin C (*Syzygium guineense*), while at the same time contain relatively low amounts of antinutritional factors. It was found that the

nutritional values of the analyzed plants is comparable and sometimes higher than the ones of conventionally cultivated crops, e.g., *Portulaca oleracea* provides more dietary Iron than maize (Aragaw et al., 2021). The commercial potential of these plants lies in flourishing demand for superfoods with the nutritional, antioxidant, and antibacterial properties.

The study highlighted the fact that national governments are developing policy mechanism to restore, maintain and evolve services around food safety. In response to these efforts and due to local demands, most businesses practice food safety procedures but not always. Among the major on-going food safety challenges in Nepal, Senegal and Ethiopia are domination of informal markets that lack an enabling environment for implementing food safety practices, with significant constraints including restricted access to clean tap water, constant power supply, and waste disposal. Processors, traders, and retailers lack the knowledge of how to prevent risks or mitigate impacts of the food safety hazards. Further, they lack adequate incentives and a clear understanding of how modifying business operations can improve their competitiveness. This knowledge and understanding can help overcome barriers of mistrust and negative perceptions about costs of actions to provide safer and more nutritious food to consumers.

Growing agri-food business actors also lack skills of setting and implementing certain food safety standards and procedures in a consistent and repeated manner. More importantly, the surveillance systems and enforcement of regulations need to be strengthened and be more consistent to improve food safety. The most important motivational factor for food businesses to adopt safe food practices is improved product quality and factors related to consumers such as certification visible to the consumers and improved consumer preferences along with improved profits.

Overcoming the above-mentioned limitations in the emerging economies inherently necessitates active entrepreneurs' involvement into food safety procurement.

INSIGHTS TO FOOD SAFETY ENTREPRENEURSHIP ACCELERATION

The food industry provides various entrepreneurial opportunities along the food value chain and US and European agriculture investment activity has been on the rise in the area of converting and packaging in particular, followed by agriculture production and shipping and selling (Kuckertz et al., 2019). Hence, food safety interventions and business innovations are more likely to attract investors if they encompass initiatives along these steps in the value chain.

Examples of entrepreneurial opportunities for health and safe food market expansion include: superfood bites from indigenous nutrients-dense plant species, artificial intelligence and chemical sensing for food grading and sampling, antimicrobial food packaging based on local bio-based materials, processed premium exotic animal meat, and ancestral food promotion.

Four segmented pathways were identified for entrepreneurship acceleration based on safety, nutrition,

technology, and food that are present in these countries. The first pathway is to diversify markets with ASF. Second, food producers can improve their utilization of neglected and underutilized ASF. Third, growing food businesses require applying and integrating innovative technologies with locally scaled food practices. The fourth potential pathway is to introduce digital geotechnologies for on-going management that support growing food businesses.

Diversify Markets With ASF

From a health and environmental sustainability perspective, including ASFs can be an important source of nutrients that include its positive effects on plant diversity and on local economies. Expanding ASF requires producing feed, creating sustainable, and ethical practices for raising animals, and creating and marketing ASF products that utilize environmentally sound principles and address the double-burden of malnutrition that exists in LMICs.

For the countries studied, one of the most promising trends in future foods depends as much on entrepreneurs' awareness as it does on the ability to expand the production of local foods and the need to employ traditional and new technologies for ASF processing to produce sustainable, safe, nutritious, and healthy products (WorldBank, 1998; Godfray et al., 2010; Hodges et al., 2010; Asogwa et al., 2017; Dizon et al., 2019; Baldwin and Evans, 2020; Kuyu and Bereka, 2020). Identifying and implementing practices that reduce greenhouse gases and use green technologies for transporting, processing and packaging that preserve the safety, quality, and the nutritional value of food products provide an important avenue for building local and national economies. According to Kuyu and Bereka (2020) some of these practices include the use of botanical plants in the storage for post-harvest pest management, treatment the storage structure with hot pepper, tobacco dust, wood ash, sand, sawdust, neem seed powder, etc. (Kuyu and Bereka, 2020). Among the specific botanical plants, which have been documented as grain protectant in the storage, are the following: basil powder as insecticide against maize weevil (Mwangangi and Mutisya, 2013), *Eucalyptus tereticornis*, *Tagetes minuta*, and *Carica papaya* (Muzemu, 2013); cheese wood, lemon-scented gum, ginger, lime, mint, and tobacco (Longe, 2016); and ethanol extract of *Azadirachta indica* (*A. indica*), *Chenopodium ambrosioides*, *Melaleuca lanceolata*, and diatomaceous earth (Dekeba et al., 2016).

The financial considerations for developing ASF are significant. The market for ASF is driven by changes in the pattern of food consumption which are influenced by migration to urban centers, the growing desire of consumers to have tasteful, nutritious, and sustainable products. Combining traditional and new processing technologies can lead to a more diverse market that can enhance the nutrients that are provided by the consumption of ASF.

There is an urgent need to estimate the ability of entrepreneurs dealing with ASF in the production of new processed products and methods to supplement traditional ASF in terms of both nutritional quality and quantity. The use of different processing for ASF product development offer benefits such as oxidation stabilization, combining different food components and creating

higher nutritional equivalents of traditional food products, all of which increase the level of consumer acceptance and broadening consumer categories.

As an example, the rediscovery of a new generation of goat and sheep meat products as functional foods and eating quality is an exciting food research field, answering to the constant innovation requirements by the meat industry. Several possibilities exist to process sheep and goat meats to make them more diversified and appealing to the market. Methods such as dry aging, dry curing, high pressure processing, conventional cooking and fermentation have significantly expanded the types and varieties of foods available in markets. Nonetheless, there is a need to ensure that micronutrients such as iron, zinc and vitamin A are not lost during food processing. For example, up to 90% of vitamin A used in food fortification is absorbed, but 40% can be lost during food processing and storage. These losses are due to vitamin A sensitivity to light and oxygen, which positions packaging as key player in ensuring vitamin A availability. Food fortification could be expensive and demands high technological input, which may not be readily available for food entrepreneurs, but application of the best available packaging and storage practices can help tackling micronutrient deficiencies at business level (Ohanenye et al., 2021).

Teixeira et al. (2020) reported that starter cultures, spices, essential oils, and other additives in meat processing, sheep and goat products can be used as functional health-promoting foods and can also improve the shelf life, product color, and reduce the lipid and protein autoxidation. For example, qwanta, is a traditional air-dried meat product in Ethiopia, which is spiced and dried, with a shelf life of around 12 months that are commonly consumed and used in African countries as a complementary source of protein and support the nutritional status of populations at risk for undernutrition (Teixeira et al., 2020). So, development of ASFs with enhanced properties contribute to better utilization of by-products across the food supply chain, reduce the waste volumes, and improve nutrient composition of diets using locally available ingredients.

Retooling food processing techniques with market-driven food fortification for the improvement of the essential micronutrient contents of foods to enhance the nutritional and health benefits with minimal risk to health will open up new opportunities for entrepreneurs to produce functional food, enhance food safety, and to make them more diversified and appealing for consumers.

Capture the Potential of Neglected and Underutilized Animal-Sourced Food

Neglected and underutilized species (NUS) are useful species of plants, animals, fungi, insects, and fish, to which little attention is paid or which are largely overlooked by researchers, educators, breeders, extensionists, and policy makers. Some of these species have been domesticated by local communities, others are gathered from the wild, but their cultivation and wider use are constrained by the lack of awareness, poor investment in their development, and insufficient human and

institutional capacity, among other factors (Temu et al., 2016). While drawing extensively on promoting underutilized crops and trees, researchers also seeks to broaden the perspective to include other kinds of species, including animals and insects—neglected and underutilized animal-sourced food (NUASF) that can play a vital role to improve resilience of nutrition vulnerable communities (Borelli et al., 2020).

According to FAO, promising neglected and underutilized species (NUS) that are nutrient dense, climate resilient, economically viable, and locally available or adaptable have been prioritized as Future Smart Food and have a central role to play in the fight against hunger and malnutrition (FAO, 2018). While traditional foods of animal origin are often unaffordable in low-income households, various neglected products can offer an alternative source of macro and micronutrients, vitamins, protein, energy, and fiber. Globally it is estimated that there are over 12,000 edible species of plants and animals that are currently neglected and underutilized. Many of them are highly nutritious and some of them can withstand floods and droughts and therefore are useful for climate change adaptation. For instance, examples of NUSF used for food in Africa are rodents and insects like agave worms (*Hypopta agavis*) and Mopane worms (*Gonimbrasia belina*) (Kelemu et al., 2015).

Rodents are the most numerous and diverse group of mammals. In Africa, rodent species commonly utilized for meat include the cane rats (*Thryonomys swinderianus*), African giant pouched rats (*Cricetomys* spp.), porcupines and some species of rats and mice (*Mastomys natalensis*, *Arvicanthis niloticus*, and *Gerbilliscus* spp.). Guinea pigs (*Cavia porcellus*) are reared in cages for food in both urban and rural areas. However, much as utilization of rodent meat is widespread, this is an underutilized or neglected source of protein in the continent. To harness rodents as a major source of meat, there is need to encourage people to rear them in captivity, process, and package the meat for wider distribution to consumers. According to a study by Kasolo et al. (2018) three main rodent species *T. swinderianus*, *Cricetomys* spp., and *C. porcellus* have the potential of non-traditional farming animal.

A good scope exists to increase productivity and income for entrepreneurs that are experiencing significant challenges in the food market. Capacity building potential related to NUSFs is expected to empower local food systems by offering diverse food items, establishing new value chains, and processing methods that can reduce the economic risks associated with price and market for livestock production. As an example of species with underutilized livestock potential for growing entrepreneurs is water buffalo. The global population of water buffalo is ~194 million heads, an increase of 18 million over the last 10 years. These animals are important sources of milk and milk products, meat and meat products, horns, and skin and serve as an important source of farm power. Because of their adaptability to hot and humid climates, the water buffalo can positively address the challenges by climate change, increasing traditional livelihood, and support poverty alleviation, and food security (Minervino et al., 2020). Water buffalo can use lower quality and less digestible feeds and grazing options, making them easier to maintain on locally available roughages. The

water buffalo is considered an efficient converter of poor-quality forages into high quality milk and meat. In addition, they have advantages over cattle such as resistance to common bovine diseases, quality milk and meat products, and outstanding body weight gain (El Debaky et al., 2019). It is important to evolve species management based on ecologically sustainable ranching practices. It is especially important to focus on the fact that the loss of wildlife may threaten the food security of many marginalized areas since the farmer-forager communities that utilize these NUAFS are isolated from markets and depend on bushmeat as their primary protein source (Eves and Ruggiero, 2001).

The generalized drivers for commercialization of NUAFSs in high geographical, biological and agroecological diversity, strong traditional and indigenous knowledge, gradually increasing consumers' awareness about health and food quality, market potential for niche commodity, off-season production potential, increasing competitiveness against imports, incipient diversification in agriculture, growing climate-smart practices and technologies, and increasing focus on value chain development.

Apply Synergy of Innovative Technologies and Existing Practices

Innovations around food safety are being developed at an unprecedented rate, some of which could be deployed in the next decade (Barrett, 2020; Robert, 2020; Siegrist and Hartmann, 2020). For instance, plant-based packaging is "the already ready technology" that is available in many LMICs and the expansion and improvement in this approach could booster progress toward safer and more sustainable food system. Plant-based packaging for entrepreneurs is suggested to focus on local bioresources, incorporating socio-economic and cultural aspects. This is particularly applicable for businesses of many remote, marginal communities that have limited access to external production inputs.

According to Herrero et al. (2020), among the future technologies with transformation potential in packaging are: molecular printing, advanced sensors, artificial intelligence, big data, farm-to-fork virtual marketplaces, intelligent food packaging, Internet of Things deployment, nanotechnology, robotics, surface-enhanced Raman spectroscopy (SERS) sensors, smartphone food diagnostics, traceability technologies, biodegradable coatings, drying/stabilization tech, food safety tech, microorganisms coating, nanocomposites, sustainable processing technologies, personalized food, 3D printing, and the implementation of a circular economy (Herrero et al., 2020). All the above innovations improve food quality, nutrient retention for entrepreneurs (Stilgoe et al., 2013; Preston and Lehne, 2017). However, many of these state-of-the-art technologies are not present or easily accessible by small and medium size businesses in Nepal, Senegal, Ethiopia, and other LMICS.

There are a variety of indigenous plants that may be sustainably used as raw materials for the manufacture of plant-based packaging. In Nepal, the plant *Phanera vahlii* is

widely distributed in the forest area. The leaves are rich in various quercetin flavonoids and known to exhibit antimicrobial, antioxidant, anti-inflammatory, and antidiabetic effects. It is a common practice for small hotels and butcher shops in villages to use the leaves as packing material for cooked food, sweets, and meat. The cone-shaped leaf wraps are also used during the steam cooking of millet flour. The food wraps not only enhance the aroma of the steam cooked food but also extends their shelf life (Kora, 2019).

Another example is *Shorea robusta* (Sal in Nepali). Sal is one of the major commercial species of timber that is primarily used for construction purposes, fuel (cooking), and has been used for treating intestinal infections (Baral et al., 2020). It is a large, deciduous, highly regenerating, valued tree. The leaves are a rich source of various flavonoids and exhibit antiobesitic, anti-inflammatory, antinociceptive, antibacterial, antipyretic, analgesic, anthelmintic, alexiteric, and wound healing activities (Merish et al., 2014). The leaves have special properties such as water resistance, rigid structure, and color retention. There is a very high potential for making different types of plates and packaging from these leaves, they are extensively used for packing breakfast, meals, and groceries. The Nepalese commonly use these leaf plates on different occasions such as marriage parties, various local rituals, worship ceremonies, and festivals in both rural and urban areas. Since the raw material for this product is locally available in ample quantity, rural labor can be employed and there is no need for extensive capital investments to use it. Using the leaves to make leaf plates in different sizes and shapes can be done with manually operated machines and is a prospective enterprise for growing food businesses since most of these plates come to Nepal from India. Presently, three types of plates are being made by the rural women's groups. On average, it is estimated that there is ~50% after production costs. An analysis of the maximum margin obtained for producing these plates indicated that medium size plates (*tapari*) provided the greatest net income. It was also estimated that the value addition by mechanized pressing of raw Sal leaf plates could increase income by 96.40% and employment by 50 mandays/household/year (12.50%) (Islam et al., 2015). The growth of this industry is an example of the strong downstream impact growing food businesses can have on local economies.

The capacity building potential of plant-based packaging for entrepreneurs include the generation of employment opportunities for people living in and around the areas of plant diversity and business income generation by generous profit margins. The plant-based packaging industry can also support the production and use of locally available renewable resources. Supporting plant-based packaging may also lead to innovation and increase local technology that will grow the market for these products and continuously provide them throughout the year. These plant-based solutions can provide opportunities for retailers too and support ingredients to packaging, and help monetization of ecosystem services delivery. The economic incentives are then cycled back by the need to invest in growing agricultural production of plants to keep the industry sustainable.

Activity promotion related to the collection, processing, and sale of plant-products are prospective interventions for entrepreneurs contributing to food safety. The utilization of local plant material is cost-effective, labor-efficient, gender equal, environmentally friendly, time-tested, situation-specific, practical, and flexible. Implementing best practices and conducting training activity on the efficient use and management of local plant resources will contribute to a maintenance and evolution of safe and sustainable food system by traditional knowledge and practice.

Introduce Digital Geotechnologies for On-Going Management

Food safety information along the value chain is often diverse in terms of spatial scale (national, regional, local levels), how it is collected (data sources, data extraction methods), and presented since graphing and analyzing software and usually belongs to different stakeholders. There are also numerous agencies that have food safety information which are not always synchronized. These agencies include government agencies, research institutions, insurance companies, health care professionals, and industry. Moreover, in LMICs food system information is also considerably more variable, changing throughout diurnal and seasonal cycles. This heterogeneity of reporting data provides very little coordinated guidance to entrepreneurs and hinders effective transactions of food safety measures into practice. In order to provide efficient on-going management for food safety and nutrient retention, food businesses need consolidated information with quick access for decision-making for the prevention of food hazards and to prevent nutrients loss.

While reporting of food safety issues is limited, entrepreneurs need a reliable source of information about food hazard hotspots and business-related adverse events. Geographical Information Systems (GISs) can be an unraveling solution. GISs relates informational data to a geographic location and can be dynamically used to grow food businesses. GIS can help to aggregate, analyze, and present food safety data in a comprehensive and communicable way that are relevant to specific business purposes. At the level of food production, it can provide data on quantitative and qualitative post-harvest food losses for specific food group. GIS can also provide spatial correlations between business actors in the supply chain to improve profit margins and support safety standards by calculating more efficient delivery routes, identify the location of storage facilities and retail locations, and providing data for reports on performance metrics. This knowledge will also allow businesses to demonstrate compliance with regulatory requirements, evaluate trends, and make management decisions. Integrating digital geotechnologies offer the potential to triangulate multiple data sources, further improving knowledge and understanding of entrepreneurs' interactions with their food environment. Furthermore, the market-driven needs for implementation of standards ISO 22000:2018 Food safety management systems (ISO, 2018) may also be reinforced by GIS to generate and manage large amount of

data with regard to food safety. When it comes to the field of food safety, the GIS market is expected to grow in the coming years since rising investments by government organizations in GIS technologies and growing demand for enterprise GIS solutions (Merem et al., 2019; Tomita et al., 2020).

In terms of growing food businesses, GISs can be used for logistics and traceability to identify vulnerable areas in terms of monitoring and evaluating time and temperature within food safety procedures. GIS can also help build clusters and identify the best location for producers and food businesses. It can support the transportation of food and map optimized routes for delivery systems. At the consumer level, GIS can assess spatial accessibility by consumers to grocery stores selling fresh produce, to map dynamically the spatial distribution of fresh produce contamination and quantify its public health impact (Beni et al., 2011). The trend of utilizing GIS based traceability systems in food chains and networks is increasing, which facilitates to minimize the production and distribution of unsafe and low quality food products (Gölge and Türk, 2019).

According to Environmental Systems Research Institute (ESRI), businesses that have implemented GIS are benefiting from increased supply chain efficiencies through linear network functionality including reducing product storage times, better delivery routing and scheduling. These up-to-date asset management activities all work to strategically release investments and return profits faster. An example is the application of GIS that was used to analyze the route and optimal location of egg supply chain in south Chennai, India that led to identifying the need to add four new distribution centers reducing the traveling distance by 25 miles per day, resulting in a about 27% decrease in expenditures for distributors (Krishnaveni et al., 2017).

Although GIS solutions continue to evolve rapidly and large business operators are able to introduce them, it is expected that investment costs and lack of internal qualification keep many food business operators from adopting these solutions. The goal should be to make these systems scalable and available to smaller businesses so they can access these GIS tools to improve food safety and quality, achieve regulatory and certification requirements, and enhance overall business performance.

FINAL CONSIDERATIONS

The results of the limitations review offer deeper understanding of enabling food safety entrepreneurship along the supply chain. The proposed insights provide potential engagement of entrepreneurs along four different pathways to accelerate better access to safe and nutritious foods for populations. These insights have the capacity to: commercially benefit entrepreneurs' outcomes across various food landscape, promoting modern trends impacting food industry in 2020–2021; be matched and scaled in different political, financial, social, and environmental context; deliver impact to stakeholders across food systems, including processors, distributors, and consumers.

To intervene successfully there is a first step needed for businesses—clarification where opportunities lie for them.

The implication here is that if the local context in which businesses operate influences the food safety practices employed, intervention programs that acknowledge the influence, and consequences of local context may be more effective than those currently suggested.

AUTHOR CONTRIBUTIONS

YV and DT developed the study concept. YV, DT, TC, and JB conducted the study, including data collection, and analysis. DT and TC approved the final version for submission and agreed to be personally accountable for their contributions and for ensuring that questions related to the accuracy or integrity of any part of the work are appropriately investigated, resolved, and documented in the literature. All authors approved the final

version of the manuscript for submission and participated in the generation of study design.

FUNDING

This research was supported by the Feed the Future Business Drivers for Food Safety, which was funded by the United States Agency for International Development (USAID) under Cooperative Agreement No. 720BFS19CA00001 and implemented by Food Enterprise Solutions (FES).

ACKNOWLEDGMENTS

The concept for this paper was inspired by Russ Webster and Roberta Lauretti-Bernhard at Food Enterprise Solutions.

REFERENCES

- Abera, T., Legesse, Y., Mammed, B., and Urga, B. (2016). Bacteriological quality of raw camel milk along the market value chain in Fafen zone, Ethiopian Somali regional state. *BMC Res. Notes* 9:285. doi: 10.1186/s13104-016-2088-1
- Adugna, M., Asresie, A., Sciences, C., and Tabor, D. (2015). A review on microbiological quality of Ethiopian raw bovine milk. *Food Sci. Qual. Manag.* 35, 17–25. Available online at: <https://citeseerx.ist.psu.edu/viewdoc/download?doi=10.1.1.683.549&rep=rep1&type=pdf>
- Alizadeh-Sani, M., Mohammadian, E., Rhim, J.-W., and Jafari, S. M. (2020). pH-sensitive (halochromic) smart packaging films based on natural food colorants for the monitoring of food quality and safety. *Trends Food Sci. Technol.* 105, 93–144. doi: 10.1016/j.tifs.2020.08.014
- Apostolopoulos, N., Ratten, V., Petropoulos, D., Liargovas, P., and Anastasopoulou, E. (2021). Agri-food sector and entrepreneurship during the COVID-19 crisis: a systematic literature review and research agenda. *Strat. Change* 30, 159–167. doi: 10.1002/jsc.2400
- Aragaw, H. S., Nohr, D., and Callo-Concha, D. (2021). Nutritional potential of underutilized edible plant species in coffee agroforestry systems of Yayu, southwestern Ethiopia. *Agrofor. Syst.* 95, 1047–1059. doi: 10.1007/s10457-021-00626-6
- Asogwa, I. S., Okoye, J. I., and Oni, K. (2017). Promotion of indigenous food preservation and processing knowledge and the challenge of food security in Africa. *J. Food Secur.* 5, 75–87. doi: 10.12691/jfs-5-3-3
- Assefa, A., and Bihon, A. (2018). A systematic review and meta-analysis of prevalence of *Escherichia coli* in foods of animal origin in Ethiopia. *Heliyon* 4:e00716. doi: 10.1016/j.heliyon.2018.e00716
- Atnafie, B., Paulos, D., Abera, M., Tefera, G., Hailu, D., Kasaye, S., et al. (2017). Occurrence of *Escherichia coli* O157:H7 in cattle feces and contamination of carcass and various contact surfaces in abattoir and butcher shops of Hawassa, Ethiopia. *BMC Microbiol.* 17:24. doi: 10.1186/s12866-017-0938-1
- Ayelnig, A., and De Saeger, S. (2020). Mycotoxins in Ethiopia: current status, implications to food safety and mitigation strategies. *Food Control* 113:107163. doi: 10.1016/j.foodcont.2020.107163
- Baldwin, J., and Evans, E. W. (2020). Exploring novel technologies to enhance food safety training and research opportunities. *Food Protect. Trends* 40, 456–463. doi: 10.4315/1541-9576-40.6.456
- Bantawa, K., Rai, K., Subba Limbu, D., and Khanal, H. (2018). Food-borne bacterial pathogens in marketed raw meat of Dharan, eastern Nepal. *BMC Res. Notes* 11:618. doi: 10.1186/s13104-018-3722-x
- Baral, S., Neumann, M., Basnyat, B., Gauli, K., Gautam, S., Bhandari, S. K., et al. (2020). Form Factors of an economically valuable sal tree (*Shorea robusta*) of Nepal. *Forests* 11:754. doi: 10.3390/f11070754
- Barrett, C. B. (2020). Overcoming global food security challenges through science and solidarity. *Am. J. Agric. Econ.* 103, 422–447. doi: 10.1111/ajae.12160
- Bauchet, J., Prieto, S., and Ricker-Gilbert, J. (2020). Improved drying and storage practices that reduce aflatoxins in stored maize: experimental evidence from smallholders in senegal. *Am. J. Agric. Econ.* 103, 296–316. doi: 10.1111/ajae.12106
- Behera, S. S., El Sheikh, A. F., Hammami, R., and Kumar, A. (2020). Traditionally fermented pickles: How the microbial diversity associated with their nutritional and health benefits? *J. Funct. Foods* 70:103971. doi: 10.1016/j.jff.2020.103971
- Belton, B., Rosen, L., Middleton, L., Ghazali, S., Mamun, A.-A., Shieh, J., et al. (2021). COVID-19 impacts and adaptations in Asia and Africa's aquatic food value chains. *Mar. Policy* 129:104523. doi: 10.1016/j.marpol.2021.104523
- Bene, C. (2020). Resilience of local food systems and links to food security - a review of some important concepts in the context of COVID-19 and other shocks. *Food Secur.* 12, 1–18. doi: 10.1007/s12571-020-01076-1
- Beni, L. H., Villeneuve, S., LeBlanc, D. I., and Delaquis, P. (2011). A GIS-based approach in support of an assessment of food safety risks. *Transact. GIS* 15, 95–108. doi: 10.1111/j.1467-9671.2011.01264.x
- Bhandari, L. R. (2020). Impacts of food adulteration in Nepal. *Int. J. Appl. Res.* 6, 333–339. Available online at: <https://www.allresearchjournal.com/archives/2020/vol6issue9/PartE/6-6-60-703.pdf>
- Bhandari, T. (2018). Analysing dairy business value chains in far-western terai districts of Nepal. *J. Inst. Agric. Anim. Sci.* 33, 269–281. doi: 10.3126/jiaas.v33i0.20714
- Birke, W., and Zawide, F. (2019). Transforming research results in food safety to community actions: a call for action to advance food safety in Ethiopia. *Environ. Ecol. Res.* 7, 153–170. doi: 10.13189/eer.2019.070305
- Borelli, T., Hunter, D., Padulosi, S., Amaya, N., Meldrum, G., de Oliveira Beltrame, D. M., et al. (2020). Local solutions for sustainable food systems: the contribution of orphan crops and wild Edible species. *Agronomy* 10:231. doi: 10.3390/agronomy10020231
- Chitrakar, B., Zhang, M., and Bhandari, B. (2021). Improvement strategies of food supply chain through novel food processing technologies during COVID-19 pandemic. *Food Control* 125:108010. doi: 10.1016/j.foodcont.2021.108010
- Dahal, L. K., Karki, D. B. N., and Shah, R. (2010). Total bacterial counts of raw milk in eastern Terai of Nepal. *J. Agric. Environ.* 11, 46–50. doi: 10.3126/aej.v11i0.3651
- Dekeba, M., Yenenayet, B., and Waktole, S. (2016). Efficacy of ethanol extracted selected botanicals and diatomaceous earth against maize weevil, *Sitophilus zeamais* Motsch. (Coleoptera: Curculionidae) in the laboratory. *Pest Manag. J. Ethiopia* 19, 1–15. Available online at: https://www.researchgate.net/profile/Muluken-Goftishu/publication/315537001_Evaluation_of_Neem_Seed_and_Citrus_Peel_Powder_for_the_Management_of_Maize_Weevil_Sitophilus_zeamais_Motsch_Coleoptera_Curculionidae_in_Sorghum/links/59079aa20f7e9bc0d59a7d10/Evaluation-of-Neem-Seed-and-Citrus-Peel-

- Powder-for-the-Management-of-Maize-Weevil-Sitophilus-zeamais-Motsch-Coleoptera-Curculionidae-in-Sorghum.pdf
- Deller, S. C., Lamie, D., and Stickel, M. (2017). Local foods systems and community economic development. *Commun. Dev.* 48, 612–683. doi: 10.1080/15575330.2017.1373136
- Dhunge, D., Maskey, B., Bhattarai, G., and Shrestha, N. K. (2019). Hygienic quality of raw cows' milk at farm level in Dharan, Nepal. *J. Food Sci. Technol. Nepal* 11, 39–46. doi: 10.3126/jfstn.v11i0.29686
- Diei-Ouadi, Y. (2005). *Minced Sardinella Fillets in Fish-Landing and Marketing Sites in Senegal*. FAO Fisheries Circular. No. 999, Rome, FAO, 20.
- Diop, M. B., Fall, M., Konte, M. A., Montet, D., Maiga, A. S., and Guiro, A. T. (2019). Influence of salt and millet treatments during meat fish fermentation in Senegal. *J. Food Res.* 8:1–14. doi: 10.5539/jfr.v8n2p1
- Diouf, A., Fall, J., Diouf, A. S., Ndour, M. M., and Ndong, D. (2019). Evaluation of heavy metals contamination level (mercury, lead, cadmium) in fishery products exported from senegal. *J. Food Stud.* 8:49. doi: 10.5296/jfs.v8i1.15261
- Dizon, F., Josephson, A., and Raju, D. (2019). The nutrition sensitivity of food and agriculture in South Asia. *Policy Res. Work. Paper* 8766. doi: 10.1596/1813-9450-8766
- Dongol, P., Thapa, G., and Kumar, A. (2017). Adoption of milk safety measures and its impact on milk acceptance by buyers in Nepal. *Agric. Econ. Res. Rev.* 30:93. doi: 10.5958/0974-0279.2017.00008.8
- Doumbouya, A., Camara, O. T., Mamie, J., Intchama, J. F., Jarra, A., Ceesay, S., et al. (2017). Assessing the effectiveness of monitoring control and surveillance of illegal fishing: the case of West Africa. *Front. Mar. Sci.* 4:50. doi: 10.3389/fmars.2017.00050
- Doutoum, A. A., Tidjani, A., Doungous, D. M., Abba, H., Ndiaye, A., Faye, C., et al. (2018). Organoleptic, physical and microbiological characteristics of eggs consumed in Dakar (Senegal). *J. Food Stud.* 7:105. doi: 10.5296/jfs.v7i1.14023
- Dulo, F., Feleke, A., Szonyi, B., Fries, R., Baumann, M. P., and Grace, D. (2015). Isolation of multidrug-resistant *Escherichia coli* O157 from goats in the somali region of ethiopia: a cross-sectional, abattoir-based study. *PLoS ONE* 10:e0142905. doi: 10.1371/journal.pone.0142905
- Ejo, M., Garedew, L., Alebachew, Z., and Worku, W. (2016). Prevalence and antimicrobial resistance of *Salmonella* isolated from animal-origin food items in Gondar, Ethiopia. *Biomed Res. Int.* 2016:4290506. doi: 10.1155/2016/4290506
- El Debaky, H. A., Kutchy, N. A., Ul-Husna, A., Indriastuti, R., Akhter, S., Purwantara, B., et al. (2019). Review: potential of water buffalo in world agriculture: challenges and opportunities. *Appl. Anim. Sci.* 35, 255–268. doi: 10.15232/aas.2018-01810
- Eves, H., and Ruggiero, R. (2001). "Socio-economics and the Sustainability of Hunting in the Forest of Northern Congo (Brazzaville)," in *Hunting for Sustainability in Tropical Forest*, eds J. Robinson and E. Bennett (New York, NY: Columbia University Press), 427–454.
- FAO (2014). *Biosecurity Status of Food and Agriculture in Nepal*. Kathmandu, 106.
- FAO (2018). *Future Smart Food: Rediscovering Hidden Treasures of Neglected and Underutilized Species for Zero Hunger in Asia*. Bangkok, 36.
- FAO, IFAD, UNICEF, WFP, and WHO (2020). *The State of Food Security and Nutrition in the World 2020*. Transforming food systems for affordable healthy diets.
- FES (2000). *Water, Sanitation and Hygiene Conditions at Artisanal Seafood Processing Sites in Senegal*. Available online at: https://agrilinks.org/sites/default/files/media/file/WASH-Senegal-Technical-Note-24Nov2020_FINAL2_1.pdf (accessed February 15 2021).
- FES (2021). *Fish Smokers and Polycyclic Aromatic Hydrocarbon (PAH) Risks in Senegal*. Available online at: <https://agrilinks.org/sites/default/files/media/file/BD4FS-PAH-TLN-20210127.pdf> (accessed January 5 2021).
- Forcina, A., and Falcone, D. (2021). The role of Industry 4.0 enabling technologies for safety management: a systematic literature review. *Proced. Comput. Sci.* 180, 436–445. doi: 10.1016/j.procs.2021.01.260
- Forsido, S. F., Abddisa, F., Lemessa, F., Ejeta, T., Belew, D., Yadessa, G., et al. (2020). *COVID-19 Probable Impacts on Ethiopian Agriculture and Potential Mitigation and Adaptation Measures: No Food-No Health-No Life*. Jimma: Jimma University. doi: 10.13140/RG.2.2.29988.42888
- Garedew, L., Hagos, Z., Addis, Z., Tesfaye, R., and Zegeye, B. (2015). Prevalence and antimicrobial susceptibility patterns of *Salmonella* isolates in association with hygienic status from butcher shops in Gondar town, Ethiopia. *Antimicrob. Resist. Infect. Control* 4:21. doi: 10.1186/s13756-015-0062-7
- Gemechu, A. T., Tola, Y. B., Dejenie, T. K., Grace, D. R., Aleka, F. B., and Ejeta, T. T. (2020). Assessment of butter adulteration practices and associated food safety issues along the supply chain in traditional communities in the central highlands and Southwest Midlands of Ethiopia. *J. Food Prot.* 84, 885–895. doi: 10.4315/JFP-20-355
- Getachew, A., Chala, A., Hofgaard, I. S., Brurberg, M. B., Sulyok, M., and Tronsmo, A. M. (2018). Multimycotoxin and fungal analysis of maize grains from south and southwestern Ethiopia. *Food Addit Contam Part B Surveill* 11, 64–74. doi: 10.1080/19393210.2017.1408698
- Getachew, D., and Christian, M. (2019). *Building a Big Tent for Agricultural Transformation in Ethiopia*. Washington, DC: CSIS center for Strategic and International Studies. Available online at: https://csis-website-prod.s3.amazonaws.com/s3fs-public/publication/190423_Ethiopia_WEB.pdf
- GFSP (2018). *Food Safety in Africa. Past Endeavours and Future Directions*. Available online at: https://www.gfsp.org/sites/gfsp/files/public/GFSP%20Report_Food%20Safety%20in%20Africa-web.pdf/ (accessed February 25, 2021).
- Ghimire, S., and Koirala, B. (2019). Linkages among expatriates for agribusiness promotion in Nepal: present scenario. *Acta Sci. Agric.* 3, 169–176. doi: 10.31080/ASAG.2019.03.0585
- Godfray, H. C., Beddington, J. R., Crute, I. R., Haddad, L., Lawrence, D., Muir, J. F., et al. (2010). Food security: the challenge of feeding 9 billion people. *Science* 327, 812–818. doi: 10.1126/science.1185383
- Gölge, E., and Türk, T. (2019). A Geographical Information System (GIS) based traceability system suggestion for a pastry firm operating nationwide. *Cumhuriyet Sci. J.* 40, 245–252. doi: 10.17776/csj.352607
- Grace, D. (2015). Food safety in low and middle income countries. *Int. J. Environ. Res. Public Health* 12, 10490–10507. doi: 10.3390/ijerph120910490
- Guy Bertrand, P. (2019). "Uses and misuses of agricultural pesticides in africa: neglected public health threats for workers and population," in *Pesticides - Use and Misuse and Their Impact in the Environment*, eds L. Marcelo and S. Sonia (IntechOpen). doi: 10.5772/intechopen.84566
- Haileselassie, M., Redae, G., Berhe, G., Henry, C. J., Nickerson, M. T., Tyler, B., et al. (2020). Correction: why are animal source foods rarely consumed by 6-23 months old children in rural communities of Northern Ethiopia? A qualitative study. *PLoS ONE* 15:e0230527. doi: 10.1371/journal.pone.0230527
- Hempen, M., Unger, F. M., Seck, T., Niamy, V., and Münstermann, S. (2004). "The hygienic status of raw and sour milk from smallholder dairy farms and local markets and potential risk for public health in The Gambia, Senegal and Guinea," *Animal Health Research Working Paper* 3 (Banjul: International Trypanotolerance Centre), 54.
- Herrero, M., Thornton, P. K., Mason-D'Croz, D., Palmer, J., Benton, T. G., Bodirsky, B. L., et al. (2020). Innovation can accelerate the transition towards a sustainable food system. *Nature Food* 1, 266–272. doi: 10.1038/s43016-020-0074-1
- Hodges, R. J., Buzby, J. C., and Bennett, B. (2010). Postharvest losses and waste in developed and less developed countries: opportunities to improve resource use. *J. Agric. Sci.* 149, 37–45. doi: 10.1017/S0021859610000936
- IFTF (2018). *2018 Ten-Year Forecast Summit: Looking Back | Moving Forward*. Institute for the Future. Available online at: <https://www.iftf.org/2018tyf/> (accessed February 14, 2021).
- Islam, M. A., Quli, S. M. S., Sofi, P. A., Bhat, G. M., and Malik, A. R. (2015). Livelihood dependency of indigenous people on forest in Jharkhand, India. *Vegetos* 28, 106–118. doi: 10.5958/2229-4473.2015.00074.9
- ISO (2018). *ISO 22000:2018 Food Safety Management System*.
- Joardder, M. U. H., and Masud, M. H. (eds). (2019). "Foods and developing countries," in *Food Preservation in Developing Countries: Challenges and Solutions* (Switzerland AG: Springer), 1–22. doi: 10.1007/978-3-030-11530-2
- Kafle, S., Vaidya, A., Pradhan, B., Jørs, E., and Onta, S. (2021). Factors associated with practice of chemical pesticide use and acute poisoning experienced by farmers in Chitwan District, Nepal. *Int. J. Environ. Res. Public Health* 18:4194. doi: 10.3390/ijerph18084194
- Kasolo, W., Chemining'wa, G., and Temu, A. (2018). *Neglected and Underutilized Species (NUS) for Improved Food Security and Resilience to Climate Change*. Nairobi: ANAFE.

- Kassahun, M., and Wongiel, S. (2019). Food poisoning outbreak investigation in Dewachefa woreda, Oromia Zone, Amhara Region, Ethiopia, 2018. *BMC Res. Notes* 12:377. doi: 10.1186/s13104-019-4407-9
- Keba, A., Laura Rolon, M., Tamene, A., Dessie, K., Vipham, J., Kovac, J., et al. (2020). Review of the prevalence of foodborne pathogens in milk and dairy products in Ethiopia. *Int. Dairy J.* 109:104762. doi: 10.1016/j.idairyj.2020.104762
- Kelemu, S., Niassy, S., Torto, B., Fiaboe, K., Affognon, H., Tonnang, H., et al. (2015). African edible insects for food and feed: inventory, diversity, commonalities and contribution to food security. *J. Insects Food Feed* 1, 103–119. doi: 10.3920/JIFF2014.0016
- Kirezieva, K., and Luning, P. A. (2017). “The influence of context on food safety governance: Bridging the gap between policy and quality management,” in *Hybridization of Food Safety Governance, Chapter 8*, eds P. Verbruggen and T. Havinga (Edward Elgar Publishing), 156–180.
- Kirk, M., Ford, L., Glass, K., and Hall, G. (2014). Foodborne illness, Australia, circa 2000 and circa 2010. *Emerging Infect. Dis.* 20, 1857–1864. doi: 10.3201/eid2011.131315
- Kora, A. J. (2019). Leaves as dining plates, food wraps and food packing material: Importance of renewable resources in Indian culture. *Bull. Natl. Res. Centre* 43:205. doi: 10.1186/s42269-019-0231-6
- Krishnaveni, M., Patakamuri, S. K., and Rajeswari, A. (2017). Route and optimal location analysis of egg supplychain using geo-spatial technology. *J. Geomat.* 11. Available online at: <https://isgindia.org/wp-content/uploads/2017/04/007.pdf>
- Kuckertz, A., Hinderer, S., and Röhm, P. (2019). Entrepreneurship and entrepreneurial opportunities in the food value chain. *NPJ Sci. Food* 3:6. doi: 10.1038/s41538-019-0039-7
- Kumar, A., Thapa, G., Joshi, P. K., and Roy, D. (2017). Adoption of food safety measures among Nepalese producers: do smallholders benefit? *Food Policy* 70, 13–26. doi: 10.1016/j.foodpol.2017.05.002
- Kumar, A., Thapa, G., Mishra, A. K., and Joshi, P. K. (2020). Assessing food and nutrition security in Nepal: evidence from diet diversity and food expenditure patterns. *Food Sec.* 12, 327–354. doi: 10.1007/s12571-019-01004-y
- Kussaga, J. B., Jaxsens, L., Tiisekwa, B. P., and Luning, P. A. (2014). Food safety management systems performance in African food processing companies: a review of deficiencies and possible improvement strategies. *J. Sci. Food Agric.* 94, 2154–2169. doi: 10.1002/jsfa.6575
- Kuyu, C. G., and Bereka, T. Y. (2020). Review on contribution of indigenous food preparation and preservation techniques to attainment of food security in Ethiopian. *Food Sci. Nutr.* 8, 3–15. doi: 10.1002/fsn3.1274
- Kwil, I., Piwowar-Sulej, K., and Krzywonos, M. (2020). Local entrepreneurship in the context of food production: a review. *Sustainability* 12:424. doi: 10.3390/su12010424
- Lake, D., Sisson, L., and Jaskiewicz, L. (2015). Local food innovation in a world of wicked problems: the pitfalls and the potential. *J. Agric. Food Syst. Commun. Dev.* 5, 13–26. doi: 10.5304/jafscd.2015.053.002
- Lancker, K., Fricke, L., and Schmidt, J. O. (2019). Assessing the contribution of artisanal fisheries to food security: a bio-economic modeling approach. *Food Policy* 87:101740. doi: 10.1016/j.foodpol.2019.101740
- Longe, O. O. (2016). Insecticidal action of some plant powders on maize weevil [*Sitophilus zeamais* Curculionidae] affecting stored maize grains (*Zea mays*). *Int. J. Agric. Innov. Res.* 4, 784–788. Available online at: <https://ijair.org/index.php/issues?view=publication&task=show&id=698>
- Maestre, M., Poole, N., and Henson, S. (2017). Assessing food value chain pathways, linkages and impacts for better nutrition of vulnerable groups. *Food Policy* 68, 31–39. doi: 10.1016/j.foodpol.2016.12.007
- Markos, S., Belay, B., and Astatkie, T. (2017). Evaluation of egg quality traits of three indigenous chicken ecotypes kept under farmers’ management conditions. *Int. J. Poult. Sci.* 16, 180–188. doi: 10.3923/ijps.2017.180.188
- Mengistu, S., Abayneh, E., and Shiferaw, D. (2017). E. coli O157:H7 and Salmonella species: public health importance and microbial safety in beef at selected slaughter houses and retail shops in eastern Ethiopia. *J. Vet. Sci. Technol.* 8:468. doi: 10.4172/2157-7579.1000468
- Merem, E. C., Twumasi, Y., Wesley, J., Alsarari, M., Fageir, S., Crisler, M., et al. (2019). Regional assessment of the food security situation in west africa with GIS. *Food Public Health* 9, 60–77. doi: 10.5923/j.fph.20190902.04
- Merish, S., Tamizhamuthu, M., and Walter, T. M. (2014). Review of *Shorea robusta* with special reference to traditional Siddha medicine, research and reviews. *J. Pharmacoc. Phytochem.* 2, 5–13. Available online at: <https://www.rroij.com/open-access/review-of-shorea-robusta-with-special-reference-to-traditional-siddha-medicine-5-13.pdf>
- Mersha, G., Asrat, D., Zewde, B. M., and Kyule, M. (2010). Occurrence of *Escherichia coli* O157:H7 in faeces, skin and carcasses from sheep and goats in Ethiopia. *Lett. Appl. Microbiol.* 50, 71–76. doi: 10.1111/j.1472-765X.2009.02757.x
- Minervino, A. H. H., Zava, M., Vecchio, D., and Borghese, A. (2020). Bubalus bubalis: a short story. *Front. Vet. Sci.* 7:570413. doi: 10.3389/fvets.2020.570413
- Morse, T., Masuku, H., Rippon, S., and Kubwalo, H. (2018). Achieving an integrated approach to food safety and hygiene—meeting the sustainable development goals in sub-saharan Africa. *Sustainability* 10:2394. doi: 10.3390/su10072394
- Muzemu, S. (2013). Evaluation of *Eucalyptus tereticornis*, *Tagetes minuta* and *Carica papaya* as Stored Maize Grain Protectants against *Sitophilus zeamais* (Motsch.) (Coleoptera: Curculionidae). *Agric. For. Fisher.* 2, 196–201. doi: 10.11648/j.aff.20130205.13
- Mwangangi, B. M., and Mutisya, D. L. (2013). Performance of basil powder as insecticide against maize weevil, *Sitophilus Zeamais* (Coleoptera: Curculionidae). *Discour. J. Agric. Food Sci.* 1, 96–201. Available online at: http://www.resjournals.org/JAFS/PDF/2013/Dec/Mwangangi_and_Mutisya.pdf
- Negatu, B., Dugassa, S., and Mekonnen, Y. (2021). Environmental and health risks of pesticide use in Ethiopia. *J. Health Pollut.* 11:210601. doi: 10.5696/2156-9614-11.30.210601
- Noort, M. C., Reader, T. W., Shorrocks, S., and Kirwan, B. (2016). The relationship between national culture and safety culture: implications for international safety culture assessments. *J. Occup. Organ. Psychol.* 89, 515–538. doi: 10.1111/joop.12139
- Nordhagen, S., Igbeka, U., Rowlands, H., Shine, R. S., Heneghan, E., and Tench, J. (2021). COVID-19 and small enterprises in the food supply chain: early impacts and implications for longer-term food system resilience in low- and middle-income countries. *World Dev.* 141:105405. doi: 10.1016/j.worlddev.2021.105405
- Nyarugwe, S. P., Linnemann, A. R., Ren, Y., Bakker, E.-J., Kussaga, J. B., Watson, D., et al. (2020). An intercontinental analysis of food safety culture in view of food safety governance and national values. *Food Control* 111:107075. doi: 10.1016/j.foodcont.2019.107075
- Ohanenye, I. C., Emenike, C. U., Mensi, A., Medina-Godoy, S., Jin, J., Ahmed, T., et al. (2021). Food fortification technologies: influence on iron, zinc and vitamin A bioavailability and potential implications on micronutrient deficiency in sub-Saharan Africa. *Sci. Afr.* 11:e00667. doi: 10.1016/j.sciaf.2020.e00667
- Osti, N. P. (2020). Animal feed resources and their management in Nepal. *ACTA Sci. Agric.* 4, 2–14. doi: 10.31080/ASAG.2020.04.737
- Owusu-Kwarteng, J., Akabanda, F., Agyei, D., and Jespersen, L. (2020). Microbial safety of milk production and fermented dairy products in Africa. *Microorganisms* 8:752. doi: 10.3390/microorganisms8050752
- Pokhrel, P. (2016). Postharvest handling and prevalence of aflatoxin contamination in Nepalese Maize Produce. *J. Food Sci. Technol. Nepal* 9, 11–19. doi: 10.3126/jfstn.v9i0.16198
- Prasad, A., Du, L., Zubair, M., Subedi, S., Ullah, A., and Roopesh, M. S. (2020). Applications of Light-Emitting Diodes (LEDs) in food processing and water treatment. *Food Eng. Rev.* 12, 268–289. doi: 10.1007/s12393-020-09221-4
- Preston, F., and Lehne, J. A. (2017). *Wider Circle? The Circular Economy in Developing Countries*. Chatham House. Available online at: <https://www.chathamhouse.org/2017/12/wider-circle-circular-economy-developing-countries>
- Robert, H. (2020). Innovations in agriculture and food supply in response to the COVID-19 pandemic. *Mol. Plant* 13, 1095–1097. doi: 10.1016/j.molp.2020.07.011
- Sapkota, S., and Phuyal, R. (2016). An analysis of consumers awareness and their purchasing behavior for adulterated rice-grains in Nepal. *World Rev. Bus. Res.* 6, 98–119. Available online at: https://www.researchgate.net/publication/309290746_An_Analysis_of_Consumers_Awareness_and_Their_Purchasing_Behavior_for_Adulterated_Rice-Grains_in_Nepal/link/5808524508ae5ed04bfe83dc/download

- Sautet, F. (2013). Local and systemic entrepreneurship: solving the puzzle of entrepreneurship and economic development. *Entrep. Theor. Pract.* 37, 387–402. doi: 10.1111/j.1540-6520.2011.00469.x
- Sharma, B. (2017). Milk marketing and dairy value chain development in Nepal in relation with climate resilience effort in the present context. *Nepalese Vet. J.* 34, 144–151. doi: 10.3126/nvj.v34i0.22917
- Siegrist, M., and Hartmann, C. (2020). Consumer acceptance of novel food technologies. *Nat. Food* 1, 343–350. doi: 10.1038/s43016-020-0094-x
- Sonnino, R. (2016). The new geography of food security: exploring the potential of urban food strategies. *Geogr. J.* 182, 190–200. doi: 10.1111/geoj.12129
- Steier, G., and Patel, K. K. (2017). *International Food Law and Policy*. Springer International Publishing. doi: 10.1007/978-3-319-07542-6
- Stilgoe, J., Owen, R., and McNaghten, P. (2013). Developing a framework for responsible innovation. *Res. Policy* 42, 1568–1580. doi: 10.1016/j.respol.2013.05.008
- Teferi, S. C. (2020). A review on food hygiene knowledge, practice and food safety in Ethiopia. *Sci. J. Food. Sci. Nutr.* 6, 4–10. Available online at: <https://www.scireslit.com/Nutrition/SJFSN-ID27.pdf>
- Teixeira, A., Silva, S., Guedes, C., and Rodrigues, S. (2020). Sheep and goat meat processed products quality: a review. *Foods* 9:960. doi: 10.3390/foods9070960
- Temu, A., Rudebjer, P., Yaye, A. D., and Ochola, A. (2016). *Curriculum Guide on Neglected and Underutilized Species: Combating Hunger and Malnutrition with Novel Species*. Rome: African Network for Agriculture, Agroforestry and Natural Resources Education (ANAFE).
- Tesfaw, L., Taye, B., Alemu, S., Alemayehu, H., Sisay, Z., and Negussie, H. (2013). Prevalence and antimicrobial resistance profile of *Salmonella* isolates from dairy products in Addis Ababa, Ethiopia. *Afr. J. Microbiol. Res.* 7, 5046–5050. doi: 10.5897/AJMR2013.5635
- Thapa, G., Kumar, A., Roy, D., and Joshi, P. K. (2019). *Does Greater Food Safety Consciousness Benefit Smallholder Dairy Farmers? Evidence from Nepal*. The International Food Policy Research Institute.
- Thapa, G., Kumar, A., Roy, D., and Joshi, P. K. (2020). Food safety consciousness and consumers' milk purchasing behaviour: evidence from a developing country. *J. Agric. Appl. Econ.* 52, 503–526. doi: 10.1017/aae.2020.14
- Thompson, L. A., Darwish, W. S., Ikenaka, Y., Nakayama, S. M., Mizukawa, H., and Ishizuka, M. (2017). Organochlorine pesticide contamination of foods in Africa: incidence and public health significance. *J. Vet. Med. Sci.* 79, 751–764. doi: 10.1292/jvms.16-0214
- Tomita, A., Cuadros, D. F., Mabhaudhi, T., Sartorius, B., Ncama, B. P., Dangour, A. D., et al. (2020). Spatial clustering of food insecurity and its association with depression: a geospatial analysis of nationally representative South African data, 2008–2015. *Sci. Rep.* 10:13771. doi: 10.1038/s41598-020-70647-1
- Upreti, R., and Shivakoti, S. (2019). “Extension policies and reforms in Nepal: an analysis of challenges, constraints, and policy options,” in *Agricultural Extension Reforms in South Asia: Status, Challenges, and Policy Options*, eds S. Babu, and P. K. Joshi (Amsterdam: Academic Press; Elsevier Inc.), 61–77. doi: 10.1016/B978-0-12-818752-4.00004-7
- van der Heijden, K., Younes, M., Fishbein, L., and Miller, S. (eds.). (1999). *International Food Safety handbook: Science, International Regulation, and Control (1st edn.)*. Boca Raton, FL: Routledge. doi: 10.1201/9780203750346
- Vergis, J., Rawool, D. B., Singh Malik, S. V., and Barbuddhe, S. B. (2021). Food safety in fisheries: application of one health approach. *Indian J. Med. Res.* 153, 348–357. Available online at: <https://www.ijmr.org.in/article.asp?issn=0971-5916;year=2021;volume=153;issue=3;page=348;epage=357;aulast=Vergis>
- WorldBank (1998). *Indigenous Knowledge for Developmental Framework for Action*. Washington, DC: Knowledge Learning Center Africa Region.

Author Disclaimer: The views and opinions expressed in this paper are those of the authors and not necessarily the views and opinions of USAID or FES.

Conflict of Interest: The authors declare that the research was conducted in the absence of any commercial or financial relationships that could be construed as a potential conflict of interest.

Publisher's Note: All claims expressed in this article are solely those of the authors and do not necessarily represent those of their affiliated organizations, or those of the publisher, the editors and the reviewers. Any product that may be evaluated in this article, or claim that may be made by its manufacturer, is not guaranteed or endorsed by the publisher.

Copyright © 2021 Varyvoda, Cederstrom, Borberg and Taren. This is an open-access article distributed under the terms of the Creative Commons Attribution License (CC BY). The use, distribution or reproduction in other forums is permitted, provided the original author(s) and the copyright owner(s) are credited and that the original publication in this journal is cited, in accordance with accepted academic practice. No use, distribution or reproduction is permitted which does not comply with these terms.



Analysis of Microbial Diversity and Dynamics During Bacon Storage Inoculated With Potential Spoilage Bacteria by High-Throughput Sequencing

Xinfu Li¹, Qiang Xiong¹, Hui Zhou², Baocai Xu² and Yun Sun^{1*}

¹ College of Food Science and Light Industry, Nanjing Tech University, Nanjing, China, ² School of Food Science and Biology Engineering, Hefei University of Technology, Hefei, China

OPEN ACCESS

Edited by:

Anindya Chanda,
Mycologics LLC, United States

Reviewed by:

Clarita Olvera,
Universidad Nacional Autónoma
de México, Mexico
Muhammad Arslan,
University of Alberta, Canada

*Correspondence:

Yun Sun
yunsunny012@163.com

Specialty section:

This article was submitted to
Food Microbiology,
a section of the journal
Frontiers in Microbiology

Received: 23 May 2021

Accepted: 06 September 2021

Published: 28 September 2021

Citation:

Li X, Xiong Q, Zhou H, Xu B and
Sun Y (2021) Analysis of Microbial
Diversity and Dynamics During Bacon
Storage Inoculated With Potential
Spoilage Bacteria by
High-Throughput Sequencing.
Front. Microbiol. 12:713513.
doi: 10.3389/fmicb.2021.713513

Staphylococcus xylosus, *Leuconostoc mesenteroides*, *Carnobacterium maltaromaticum*, *Leuconostoc gelidum*, and *Serratia liquefaciens* were investigated for their roles in the spoilage of sterilized smoked bacon. These five strains, individually and in combination, were applied as starters on sliced bacon at 4–5 log₁₀ CFU/g using a hand-operated spraying bottle and stored for 45 days at 0–4°C. Dynamics, diversity, and succession of microbial community during storage of samples were studied by high-throughput sequencing (HTS) of the V3–V4 region of the 16S rRNA gene. A total of 367 bacterial genera belonging to 21 phyla were identified. Bacterial counts in all the inoculated specimens increased significantly within the first 15 days while the microbiota developed into more similar communities with increasing storage time. At the end of the storage time, the highest abundance of *Serratia* (96.46%) was found in samples inoculated with *S. liquefaciens*. Similarly, for samples inoculated with *C. maltaromaticum* and *L. mesenteroides*, a sharp increase in *Carnobacterium* and *Leuconostoc* abundance was observed as they reached a maximum relative abundance of 97.95 and 81.6%, respectively. Hence, these species were not only the predominant ones but could also have been the more competitive ones, potentially inhibiting the growth of other microorganisms. By analyzing the bacterial load of meat products using the SSO model, the relationships between the microbial communities involved in spoilage can be understood to assist further research.

Keywords: microbial diversity, bacon, spoilage bacteria, high-throughput sequencing, storage

INTRODUCTION

Bacon is widely consumed in Europe, North America, and some other parts of the world (Soladoye et al., 2015) but since they are highly susceptible to microbial contamination, thermal processing can be applied to reduce the bacterial load of meat products. However, some strains are still able to resist this heat-processing step (Li et al., 2021). For example, one report found that during refrigerated storage, microorganisms, such as *Leuconostoc carnosum* or *Weissella viridescens* survived, resulting in post-heat treatment recontamination and eventually, in spoilage

(Zagdoun et al., 2020). The spoilage of cooked and cured meat is generally considered to be the result of the growth and reproduction of microbes, such as *Leuconostoc* spp., *Lactobacillus* spp., *Enterobacteriaceae*, *Carnobacterium* spp., *Pseudomonas*, and *Brochothrix thermosphacta* (Borch et al., 1996; Korkeala and Björkroth, 1997; Samelis et al., 2000; Nychas et al., 2008) which, collectively, may be known as “specific/ephemeral spoilage microorganisms-S(E)SO,” as displayed in Table 1. Previous research indicates that these microorganisms dominate the meat matrix and produce spoilage-associated changes, such as slime, -odors, and other undesirable flavors (Nychas et al., 2008; Casaburi et al., 2015).

Different microbial taxa/species may be randomly developed during meat storage, thus influencing the type of spoilage development (Ercolini et al., 2009). This is because the spoilage process is a complex event involving biological activities which are likely to be different for different microorganisms. Moreover, details on the species involved in the spoilage of meat are still unclear and needs to be further assessed. Therefore, it is necessary to characterize these organisms, both at the species as well as the biotype levels, in order to better understand the spoilage process. Furthermore, SSOs contribute to spoilage despite having an initial low population (Säde, 2011). Hence, an appropriate method for describing and understanding their growth and activity, or even for evaluating their spoilage potential is also crucial (Pothakos et al., 2014a).

In this context, Pin et al. (1999) as well as McMeekin and Ross (1996) have suggested that the method involving the inoculation of sterile substrates with spoilage organisms provided a more accurate way for representing and predicting the growth of food spoilage organisms by comparing their growth rates. In fact, over the past few years, microbiological growth and spoilage potential of isolated bacterial species have been monitored using this SSO model (Mataragas et al., 2007). For example, many studies reported its application for fish products (Stohr et al., 2001; Macé et al., 2013; Wang et al., 2017), for processed meat containing beef (Leisner et al., 1995; De Filippis et al., 2013) or saveloy (Holm et al., 2013), and even for packaged meat products (Rahkila et al., 2012). Furthermore, this SSO model was also applied to evaluate the ability of some isolates [e.g., lactic acid bacteria (LAB)] to act as protective cultures for bio-preservation (Bredholt et al., 2001; Vermeiren et al., 2004; Alves et al., 2006). However, the microbiological studies reported in the above-mentioned studies were almost carried out using a culture-dependent approach (traditional microbial cultivation). This method can be rather unreliable when trying to provide accurate information about microbial communities in an ecosystem as only a small portion of the true microbial population can be cultivated. As an alternative, culture-independent methods, especially high-throughput sequencing (HTS), has been successfully applied in meat microbiology research to monitor the dynamic changes in microbial flora as this approach can provide more detailed information about the microbial communities compared with other molecular methods. However, to the best of our knowledge, as far as bacon is concerned, only few studies have been conducted so far. Therefore, it would be useful to apply this HTS technology to analyze the growth and activity of spoilage

microorganisms in bacon so that a deeper and more precise evaluation of its spoilage process can be made. This study enables us to understand the growth one taxa/species dominates the spoilage and is affected by the others.

In our previous study, *Staphylococcus xylosus*, *Carnobacterium maltaromaticum*, *Leuconostoc mesenteroides*, *Serratia liquefaciens*, and *Leuconostoc gelidum* were identified and considered responsible for the potential spoilage characteristics of bacon (Li et al., 2019). In this work, sterile bacon was inoculated with these five isolated organisms before investigating the bacon's bacterial diversity using HTS, in order to gain a deeper understanding of the dynamic nature of the microbial population during the spoilage process. Furthermore, changes in the physicochemical properties of the meat were also measured to evaluate how they were connected with the microbiota.

MATERIALS AND METHODS

Bacterial Strains and Sterile Samples

All strains used in this study were selected from the laboratory collection team, were previously isolated and identified from smoked bacon during refrigerated storage (Li et al., 2019), and maintained as frozen stocks at -80°C in a strain storage medium (Qingdao Hope Bio-Technology Co., Ltd., Qingdao, China). These strains belonged to the taxonomic groups: *S. xylosus*, *L. mesenteroides*, *C. maltaromaticum*, *L. gelidum*, *S. liquefaciens*, and combination of the above five strains at the same concentration could be stored in a sterile vial and mixed (Pm).

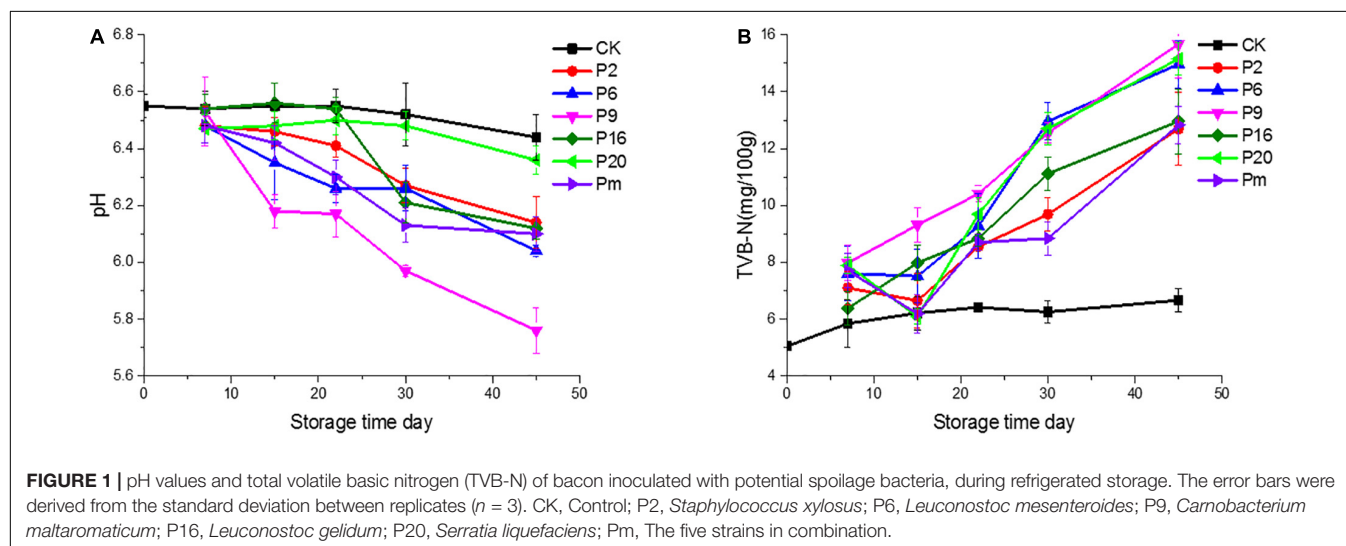
All vacuum-packaged bacon samples were prepared in a local western-style meat-processing company without use of preservatives. Specimens were approximately 200 mm long, 40 mm wide, and 2.5 mm thick, with eight or nine slices (around 200 g per bag). Sterile bacon was prepared to prevent any influence of bacterial impurities. To avoid the interference from natural microbiota, samples were immediately transferred in insulated boxes containing dry ice and thereafter sterilized by irradiation at a dose of 6 kGy (Dogbevi et al., 1999; Pothakos et al., 2015; Wang et al., 2017) using a ^{60}Co source at Hangyu (Hangyu Irradiation Technology Co., Ltd., Nanjing, China). The samples that had been irradiated were immediately transported back to the laboratory, and then stored for about 1 week at -80°C for inoculation.

Strain Culture, Sample Inoculation, and Packaging

The strains, deep-frozen before use, were reanimated, streaked by a single rolling magnetic bead driven by a magnet on the selective culture media from which the colonies were originally harvested by traditional microbiological methods, the cultures were recovered and incubated at the aforementioned temperature and time (Li et al., 2019). According to the previous method (Roig-Sagués and Eerola, 1997; Stavropoulou et al., 2018), growth of the precultures was verified twice during cultivation, then one standardized loopful of pure colonies was suspended in a tube of MRS broth, brain heart infusion (BHI) broth, and TSB (Tryptone Soya Broth, Oxoid) by

TABLE 1 | SSO/Dominant/Starter organism and the technique used in their determination in meat and meat products.

SSO/Dominant/Starter organism	Product	Technique	References
<i>Leuconostoc mesenteroides</i> , <i>Leuconostoc carnosum</i> , <i>Leuconostoc gelidum</i> , <i>Lactobacillus sakei</i>	Cooked ham, cooked meats, vacuum-packaged beef, bacon, beef	PFGE, culture-dependent, PCR, 16S rRNA sequencing	Korkeala and Björkroth, 1997; Björkroth et al., 1998; Samelis et al., 2000; Metaxopoulos et al., 2002; Hamasaki et al., 2003; Chenoll et al., 2007; Säde, 2011; Pothakos et al., 2014b; Pothakos et al., 2015; Comi et al., 2016; Li et al., 2019
<i>Carnobacterium maltaromaticum</i> , <i>Carnobacterium divergens</i>	Processed meat products, ham, bacon, fermented sausages, chicken	Culture-dependent, PCR, 16S rRNA sequencing	Leisner et al., 1995; Chenoll et al., 2007; Leisner et al., 2007; Casaburi et al., 2011
<i>Serratia liquefaciens</i> , <i>Rahnella aquatilis</i> , <i>Hafnia alvei</i>	Cooked/cured meat products, meat, minced meat, dry-cured ham	Culture-dependent, PCR, 16S rRNA sequencing	Lindberg et al., 1998; Gram et al., 1999; Doulgeraki et al., 2011; Belletti et al., 2013
<i>Staphylococcus xylosum</i>	Cured ham, fermented foods, sausage	Culture-dependent, PCR	Kotzekidou and Bloukas, 1996; Paarup et al., 1999; Leroy et al., 2006; Mah and Hwang, 2009; Ravyts et al., 2012



propagation at 30°C for 24 h. Thereafter, 0.1 mL was removed to another tube including the related broth supplemented and incubated at 30°C for 24 h anaerobically. The cell pellets were accumulated by centrifugation (4,000 rpm, 4°C, 10 min), then thrice-washed and resuspended in 50 mL of Ringer's solution (Oxoid), thereafter the cellular concentration was adjusted to approximately $6-7 \log_{10}$ CFU/mL as inoculum for the meat preparation. The five strains were added to a sterile vial and then stirred to homogenize the mixture to achieve the desired inoculation rate.

Before analysis, bacon specimens were thawed for 24 h at 0–4°C. A total of 108 samples were randomly divided into seven groups. Next, approximately equal volumes and concentrations of suspensions of strains were sprayed onto the surface of the six grouped samples by using a hand-operated spraying bottle: the initial contamination of the artificially bacon was between 4 and $5 \log_{10}$ CFU/g for all strains inoculated singly or in a

mix. The control group was treated by spraying sterile PBS without the addition of inoculum. The inoculation levels were selected according to previous studies of meat products (Bredholt et al., 2001; Alves et al., 2006). After inoculation, smoked bacon specimens were transferred to sterile plastic bags and vacuum-packaged in a sterile environment, then kept at 0–4°C for 45 days. The day upon which specimens were thawed and uninoculated was designated day 0. Analyses were carried out aseptically after 7, 15, 22, 30, and 45 days of storage, three packages from each treatment were randomly chosen at each time point.

Measurements of pH and Total Volatile Basic Nitrogen

The pH of bacon was monitored in triplicate by using S210 SevenCompact™ pH meter (Mettler-Toledo), and previously calibrated in standard solutions at pH 4.01 and 7.01 at room temperature. Total volatile basic nitrogen (TVB-N) was detected

TABLE 2 | Changes in viable counts of bacon inoculated with potential spoilage bacteria, during refrigerated storage after 45 days.

Colony and selective medium	Storage time (days)	Microbiological analysis (log ₁₀ CFU/g)						
		CK	P2	P6	P9	P16	P20	Pm
TVC (PCA 30°C)	0	ND	/	/	/	/	/	/
	7	ND	6.50 ± 0.66 ^d	6.41 ± 0.72 ^c	6.71 ± 0.47 ^c	6.31 ± 0.62 ^c	6.51 ± 0.44 ^d	6.94 ± 0.52 ^c
	15	ND	8.05 ± 0.37 ^c	8.21 ± 0.73 ^b	8.02 ± 0.58 ^b	8.17 ± 0.71 ^b	7.99 ± 0.66 ^c	8.09 ± 0.82 ^b
	22	ND	8.34 ± 0.84 ^{bc}	8.72 ± 0.96 ^{ab}	8.79 ± 0.85 ^{ab}	8.76 ± 0.65 ^a	8.37 ± 0.47 ^b	8.61 ± 1.24 ^{ab}
	30	ND	9.01 ± 1.13 ^a	8.91 ± 1.05 ^a	9.07 ± 1.21 ^a	8.64 ± 0.84 ^{ab}	8.66 ± 0.86 ^{ab}	8.97 ± 0.99 ^a
	45	ND	8.86 ± 0.99 ^b	8.64 ± 1.12 ^{ab}	8.74 ± 0.66 ^{ab}	8.34 ± 0.93 ^{ab}	8.78 ± 0.95 ^a	8.72 ± 0.85 ^{ab}
TVC (PCA 7°C)	0	ND	/	/	/	/	/	/
	7	ND	6.48 ± 1.20 ^d	6.52 ± 0.46 ^c	6.52 ± 0.48 ^c	6.72 ± 0.59 ^c	ND	6.22 ± 1.24 ^c
	15	ND	8.00 ± 0.42 ^c	8.04 ± 0.87 ^b	7.86 ± 0.67 ^b	7.55 ± 0.82 ^b	5.12 ± 0.47 ^c	7.74 ± 0.48 ^b
	22	ND	8.21 ± 0.77 ^b	8.27 ± 0.64 ^{ab}	8.38 ± 0.57 ^{ab}	8.62 ± 0.57 ^{ab}	6.35 ± 0.61 ^b	8.65 ± 1.08 ^a
	30	ND	8.83 ± 0.94 ^a	8.75 ± 0.95 ^a	8.67 ± 0.91 ^a	8.93 ± 1.25 ^a	6.16 ± 0.79 ^b	8.51 ± 1.22 ^{ab}
	45	ND	8.61 ± 0.88 ^{ab}	8.42 ± 0.58 ^{ab}	8.59 ± 0.86 ^{ab}	8.01 ± 0.76 ^{ab}	6.58 ± 0.92 ^a	8.62 ± 0.86 ^{ab}
LAB (MRS)	0	ND	/	/	/	/	/	/
	7	ND	ND	6.37 ± 0.77 ^c	ND	ND	ND	5.61 ± 0.51 ^e
	15	ND	4.15 ± 0.56 ^c	8.33 ± 0.59 ^b	5.20 ± 0.42 ^c	5.67 ± 0.47 ^c	ND	5.84 ± 0.63 ^d
	22	ND	3.17 ± 0.56 ^c	9.06 ± 1.36 ^a	8.05 ± 0.76 ^{ab}	7.89 ± 0.58 ^b	4.64 ± 0.39	6.85 ± 0.77 ^c
	30	ND	7.12 ± 0.58 ^b	8.88 ± 0.67 ^{ab}	8.42 ± 0.81 ^a	8.21 ± 0.67 ^a	5.75 ± 0.41	7.22 ± 0.68 ^b
	45	ND	7.79 ± 0.91 ^a	8.74 ± 0.85 ^b	7.89 ± 0.98 ^{ab}	8.20 ± 1.17 ^{ab}	5.39 ± 0.74	7.68 ± 0.49 ^a
Staphylococcaceae (BP)	0	ND	/	/	/	/	/	/
	7	ND	3.12 ± 0.55 ^e	ND	7.01 ± 0.82 ^c	5.43 ± 0.92 ^c	ND	5.87 ± 0.87 ^c
	15	ND	4.87 ± 0.63 ^d	ND	8.02 ± 0.86 ^b	6.92 ± 0.43 ^b	ND	7.89 ± 0.75 ^b
	22	ND	5.30 ± 1.12 ^c	ND	8.87 ± 1.34 ^{ab}	7.46 ± 0.66 ^{ab}	ND	8.46 ± 0.60 ^a
	30	ND	7.48 ± 0.58 ^b	ND	9.01 ± 0.68 ^a	7.75 ± 0.57 ^a	ND	7.84 ± 0.63 ^b
	45	ND	8.21 ± 0.58 ^a	ND	8.64 ± 1.24 ^{ab}	6.07 ± 0.85 ^{ab}	ND	8.24 ± 0.88 ^{ab}
Enterobacteriaceae (VRBGA)	0	ND	/	/	/	/	/	/
	7	ND	5.94 ± 0.41 ^d	ND	2.41 ± 0.35 ^d	5.27 ± 0.38 ^d	6.41 ± 0.74 ^d	4.47 ± 0.57 ^a
	15	ND	7.92 ± 0.87 ^c	4.53 ± 0.42 ^c	4.27 ± 0.48 ^{bc}	7.72 ± 0.57 ^b	7.39 ± 0.87 ^c	6.47 ± 0.86 ^a
	22	ND	8.32 ± 1.08 ^b	8.48 ± 1.05 ^b	4.65 ± 0.55 ^c	7.52 ± 1.30 ^c	8.22 ± 1.18 ^{ab}	7.24 ± 1.02 ^a
	30	ND	8.46 ± 0.94 ^a	8.57 ± 1.24 ^{ab}	6.92 ± 0.64 ^b	8.67 ± 0.71 ^a	8.16 ± 1.22 ^b	8.66 ± 1.42 ^a
	45	ND	8.62 ± 0.59 ^{ab}	8.28 ± 0.86 ^a	7.78 ± 0.97 ^a	8.28 ± 0.99 ^{ab}	8.49 ± 0.87 ^a	8.53 ± 1.04 ^a

Means with different letters within the same column indicate a significant difference at $P < 0.05$.

CK, control samples; P2, *Staphylococcus xylosum*; P6, *Leuconostoc mesenteroides*; P9, *Carnobacterium maltaromaticum*; P16, *Leuconostoc gelidum*; P20, *Serratia liquefaciens*; Pm, a mixture of these five strains.

by the Kjeldahl method with an automatic Kjeldahl nitrogen analyzer (Shanghai Xianjian Instrument Co., Ltd., China). The TVB-N value (mg/100 g bacon) was calculated according to the utilization of hydrochloric acid (0.01 mol/L).

Microbiological Analysis

For each sample, 25 g was homogenized aseptically in 225 mL cold Ringer's solution (Oxoid) for 2 min within a separate stomacher bag. Then the suspension was diluted (1:10) with sterile distilled water to acquire the final working dilution. After shaking, 0.1 mL of each dilution was spread on selective culture media: (i) total plate count (TPC) in Plate Count Agar (PCA) (OxoidTM), incubated at 30°C for

48 h, (ii) psychrophilic and psychrotrophic bacteria were also isolated in PCA at 7°C for 10 d, (iii) Violet Red Bile Glucose Agar (VRBGA) (Lang Bridge) for the cultivation of Enterobacteriaceae, incubated at 37°C for 36 h, (iv) LAB on de Man Rogosa and Sharpe (MRS) agar, incubated at 30°C for 48 h, and (v) Staphylococci were enumerated on Baird-Parker Agar (Lang Bridge), and incubated at 37°C for 48 h. The MRS and VRBGA agar plates were transported in 2.5-L anaerobic culture bags (Qingdao Hope Bio-Technology Co., Ltd., Shandong, China). The results are expressed as decimal logarithms of colony forming units per gram (log₁₀ CFU/g), and the method used in this study had a lower limit of detection of 2 log₁₀ CFU/g.

DNA Extraction, Pyrosequencing, and Data Analysis

Total DNA Extraction

The bacteria cells were analyzed following the method previously described by Li et al. (2019). The cells pellets were obtained and used to extract the total DNA according to the manufacturer's recommendations for use of the EZNA® bacterial DNA extraction kit (Omega Bio-tek, GA, United States). DNA quality and purity were determined through spectrophotometric quantification (NanoDrop Technologies, Wilmington, DE, United States).

Illumina High-Throughput Sequencing

Microbial diversity was determined by amplifying and sequencing the hypervariable region V3-V4 of the bacterial 16S rRNA gene, using primers containing barcodes and PCR conditions as previously reported (Polka et al., 2015; Li et al., 2019). All PCR amplification reaction mixtures were examined using 2.0% agarose gel electrophoresis with a loading buffer (containing SYBR green) and mixed in equidense ratios and purified using the GeneJET PCR Purification Kit (Thermo Fisher Scientific). HTS was conducted on the Illumina MiSeq (Illumina, United States) according to the manufacturer's specifications. Sequencing libraries were formed using an Ion Plus Fragment Library Kit 48 rxns (Thermo Fisher Scientific), following the manufacturer's protocol. The library quality was assessed by using a Qubit® 2.0 fluorometer (Thermo Fisher Scientific). The library was sequenced on an Ion S5™ XL platform and 400 bp/600 bp single-end reads were generated (Novogene Bioinformatics Technology Co., Ltd., Beijing, China). Raw data from a next-generation sequencing platform were submitted to the Sequence Read Archive of National Center for Biotechnology Information (NCBI), under BioProject ID PRJNA746727.

Bioinformatics and Data Analysis

Single-end reads were assigned based on their unique barcodes and truncated by removing the barcodes and primer sequences. Raw sequence reads were passed through quality filtering to obtain high-quality clean reads (Martin, 2011). Operational taxonomic units (OTUs) were assigned at 97% similarity levels using Uparse software (Edgar, 2013). Alpha-diversity and beta-diversity were calculated by QIIME software (Version 1.7.0), and the similarities were analyzed by non-metric multi-dimensional scaling (NMDS) using the R package vegan. OTUs were mapped to the SILVA database and classified according to phylum, class, order, family, and genus.

Statistical Analysis

The data pertaining to TVB-N, pH, and viable counts are presented as the mean \pm SD, and significant differences in mean values were compared by one-way analysis of variance (ANOVA) (Duncan's multiple range), with SPSS Statistics 20.0 software (SPSS Inc., Chicago, IL, United States), while $P < 0.05$ was considered statistically significant.

RESULTS AND DISCUSSION

pH and Total Volatile Basic Nitrogen

The trend in pH changed slightly during the first 7 days among the groups shown in **Figure 1**. Compared with the controls, the final pH decreased significantly ($P < 0.05$) at the end of the study on day 45, reached a relatively high 6.36 for *S. liquefaciens* group, and relatively low values of 5.74 and 6.06 for *C. maltaromaticum* and *L. mesenteroides* groups, respectively. The microbial activity may lead to a significant decrease of the pH of the samples (Comi et al., 2016). Additionally, different strain groups appeared in different downtrends, after 45 days of storage, it was found that the acidification in bacon inoculated by *C. maltaromaticum* and *L. mesenteroides* was lower ($P < 0.05$) than that measured in *S. liquefaciens* and other groups. This pH reduction may be attributed to the fact that LAB rapidly became the predominant microorganism, producing lactic acid which decreased the pH and antibacterial peptide concentration (bacteriocins) (Gram et al., 2002; Kuo and Chu, 2003; Wang et al., 2013). It was probably *S. liquefaciens*, as determined by its low ability to produce the metabolites, that was associated with this acidic pH. Furthermore, the low pH may inhibit bacterial growth but the degree of inhibition varies by species. Generally, LAB and *Enterobacteriaceae* show high acid resistance and are able to grow and survive at acidic pH (Houtsma et al., 1996; Pin and Baranyi, 1998), however, *Brochothrix thermosphacta* and other species cannot grow on meat, or cause spoilage of meat under acid conditions (low pH) (Sun and Holley, 2012; Mills et al., 2014).

As one of the important chemical indicators, the change of TVB-N values may be attributed to increased protein degradation by endogenous enzymes and bacteria (Huang et al., 2014). In this study, variable production of TVB-N was observed in the different bacterial groups and showed an increasing trend. As illustrated in **Figure 1**, the TVB-N values (15.68 and 15.16 mg/100 g, respectively) were increased significantly ($P < 0.05$) in samples inoculated with *C. maltaromaticum* and *S. liquefaciens*. The TVB-N was relatively low 12.69 for the *S. xylosum* group, while the control samples only reached 6.66. Thus we inferred whether *C. maltaromaticum* and *S. liquefaciens*, as active producers of TVB-N, had effective spoilage potential in a manner similar to descriptions of these strains as the main spoilage organisms in spoilage species (Stohr et al., 2001; Zhang et al., 2015).

Microbiological Analysis

Due to the different feed conditions of different bacteria, five different types of culture media that have been previously used to identify the level of microbial spoilage were used. As shown in **Table 2**, colonies were grown rapidly on selective culture media after incubation, and reached the lowest 7.99 log₁₀ CFU/g on PCA medium at 30°C on day 15 except for the control groups. In general, all tested strains showed good growth and survival during storage, there were significant differences at the 0.05 level in final bacterial populations. In inoculated samples, the total viable count (TVC) and LAB counts increased rapidly to about 8 log₁₀ CFU/g by day 15.

TABLE 3 | Alpha diversity estimation of the 16S rRNA gene libraries by sequencing on an Ion S5™ XL platform in bacon.

	Sample name	Total tags	OUTs	Shannon	Simpson	Chao1	ACE	Goods coverage
Day 0	CK.0d	71493 ± 14839	312 ± 10	5.878 ± 0.385	0.964 ± 0.011	324.383 ± 7.477	322.247 ± 8.397	0.999
	CK.7d	68496 ± 13865	321 ± 15	5.469 ± 0.123	0.933 ± 0.016	328.667 ± 27.319	324.478 ± 20.440	0.999
	P2.7d	64053 ± 15249	239 ± 30	4.646 ± 0.916	0.885 ± 0.073	257.667 ± 40.819	258.817 ± 39.047	0.998
	P6.7d	69774 ± 11907	210 ± 61	3.774 ± 1.309	0.759 ± 0.186	237.105 ± 62.780	238.501 ± 60.792	0.998
Day 7	P9.7d	80138 ± 43	204 ± 9	3.893 ± 0.520	0.785 ± 0.094	237.285 ± 3.592	233.512 ± 9.352	0.998
	P16.7d	77670 ± 4315	269 ± 51	5.516 ± 0.300	0.951 ± 0.011	284.552 ± 55.676	286.245 ± 51.688	0.998
	P20.7d	60857 ± 4449	264 ± 1	5.591 ± 0.301	0.957 ± 0.014	286.079 ± 18.371	287.616 ± 13.541	0.998
	Pm.7d	62284 ± 11974	223 ± 18	4.679 ± 1.139	0.867 ± 0.118	244.855 ± 15.973	242.537 ± 16.279	0.998
Day 15	CK.15d	79773 ± 685	301 ± 14	5.468 ± 0.527	0.939 ± 0.039	315.205 ± 12.794	310.881 ± 13.723	0.999
	P2.15d	61970 ± 13686	165 ± 137	3.563 ± 1.482	0.804 ± 0.110	210.937 ± 131.344	227.950 ± 114.921	0.998
	P6.15d	82203 ± 3496	107 ± 100	2.789 ± 1.574	0.704 ± 0.163	127.588 ± 103.329	130.114 ± 103.902	0.999
	P9.15d	80076 ± 65	46 ± 10	1.485 ± 0.933	0.430 ± 0.294	66.277 ± 8.910	70.344 ± 18.673	0.999
	P16.15d	80117 ± 104	114 ± 57	3.209 ± 0.526	0.811 ± 0.044	145.363 ± 59.737	151.362 ± 56.029	0.998
	P20.15d	80111 ± 59	205 ± 104	4.100 ± 1.870	0.869 ± 0.092	243.200 ± 76.977	249.795 ± 75.928	0.998
	Pm.15d	61511 ± 16295	63 ± 30	3.213 ± 0.226	0.857 ± 0.041	84.118 ± 41.677	91.340 ± 46.863	0.999
	CK.22d	73183 ± 12127	293 ± 17	5.616 ± 0.362	0.945 ± 0.027	293.666 ± 17.897	293.666 ± 17.897	1.000
Day 22	P2.22d	79485 ± 1554	47 ± 6	2.653 ± 0.347	0.754 ± 0.076	57.783 ± 11.145	66.961 ± 14.723	0.999
	P6.22d	78300 ± 3148	57 ± 18	2.786 ± 0.071	0.785 ± 0.009	71.444 ± 20.205	74.739 ± 12.082	0.999
	P9.22d	80132 ± 68	50 ± 5	2.452 ± 0.052	0.726 ± 0.022	73.174 ± 7.476	81.311 ± 13.151	0.999
	P16.22d	80163 ± 59	46 ± 3	2.778 ± 0.224	0.787 ± 0.036	68.714 ± 5.765	84.755 ± 14.827	0.999
	P20.22d	62869 ± 6208	99 ± 77	3.229 ± 0.911	0.840 ± 0.057	122.927 ± 85.611	127.332 ± 88.602	0.998
	Pm.22d	62525 ± 15307	40 ± 12	3.072 ± 0.443	0.834 ± 0.079	47.952 ± 14.375	53.788 ± 15.813	0.999
	CK.30d	72405 ± 13556	345 ± 20	5.902 ± 0.522	0.960 ± 0.024	363.222 ± 11.926	355.820 ± 10.079	0.999
Day 30	P2.30d	69744 ± 9827	39 ± 5	2.643 ± 0.231	0.756 ± 0.046	58.660 ± 5.395	74.742 ± 22.268	0.999
	P6.30d	74137 ± 5241	65 ± 12	2.859 ± 0.232	0.789 ± 0.040	92.825 ± 28.131	100.961 ± 35.978	0.999
	P9.30d	80127 ± 39	41 ± 5	2.598 ± 0.097	0.753 ± 0.032	60.322 ± 9.067	71.335 ± 17.811	0.999
	P16.30d	70178 ± 14083	47 ± 5	2.852 ± 0.034	0.812 ± 0.007	58.403 ± 2.984	65.936 ± 5.569	0.999
	P20.30d	58211 ± 6360	52 ± 27	2.739 ± 2.516	0.805 ± 0.013	78.322 ± 43.259	76.269 ± 32.442	0.999
	Pm.30d	60813 ± 16677	40 ± 14	3.183 ± 0.175	0.858 ± 0.025	54.166 ± 21.391	61.578 ± 27.871	0.999
	CK.45d	80115 ± 32	328 ± 6	5.711 ± 0.296	0.953 ± 0.013	346.329 ± 17.584	338.845 ± 9.457	0.999
Day 45	P2.45d	72141 ± 2356	42 ± 2	2.933 ± 0.112	0.810 ± 0.019	57.400 ± 12.770	63.965 ± 15.422	0.999
	P6.45d	76042 ± 7160	51 ± 2	2.883 ± 0.079	0.805 ± 0.014	76.375 ± 5.188	83.236 ± 6.265	0.999
	P9.45d	80108 ± 42.158	52 ± 6	2.145 ± 1.109	0.599 ± 0.329	91.277 ± 48.990	91.281 ± 33.496	0.999
	P16.45d	59889 ± 6463	66 ± 10	2.915 ± 0.137	0.819 ± 0.014	83.504 ± 10.886	87.552 ± 15.329	0.999
	P20.45d	64865 ± 7519	47 ± 11	2.548 ± 0.054	0.788 ± 0.009	65.441 ± 8.010	77.858 ± 13.622	0.999
	Pm.45d	60880 ± 16652	56 ± 4	3.309 ± 0.148	0.873 ± 0.018	95.923 ± 22.901	98.431 ± 13.871	0.999

CK, control samples; P2, *Staphylococcus xylosum*; P6, *Leuconostoc mesenteroides*; P9, *Carnobacterium maltaromaticum*; P16, *Leuconostoc gelidum*; P20, *Serratia liquefaciens*; Pm, a mixture of these five strains.

Microorganisms interacted with each other when the order of magnitude reached levels of approximately 7–9 log₁₀ CFU/g (Gram et al., 2002). In control samples, the microorganism populations were observed to be below the detection limit (2 log₁₀ CFU/g) after 45 days under refrigeration, which indicated that gamma irradiation was an efficient treatment when controlling the number of microorganisms and extending the shelf-life with no adverse changes or deterioration (O'bryan et al., 2008; Chen et al., 2016). Irradiated bacon was used as a suitable host material to simulate natural cooked meat of a substantially consistent nature. Sterile bacon was considered a suitable alternative model as an initial screening procedure. *Staphylococcaceae* populations inoculated with *L. mesenteroides* and *S. liquefaciens* at lower levels

(<2 log₁₀ CFU/g), indicated that the growth was significantly inhibited and suppressed.

Bacterial Richness and Diversity

After quality filtering and merging of paired reads, the total number of 7,752,153 effective sequences (tags) could be remained from 108 samples; sequence lengths were between 403 and 478 bp (Table 3). These effective sequences were clustered into 14,875 OTUs with 97% similarity level by using UPARSE algorithm embedded in Qiime. High Good's coverage at least 99.7% suggested that most of the bacteria OTUs in samples could be captured. The α-diversity indices including observed OTUs, Chao1, and Shannon diversity index were calculated and

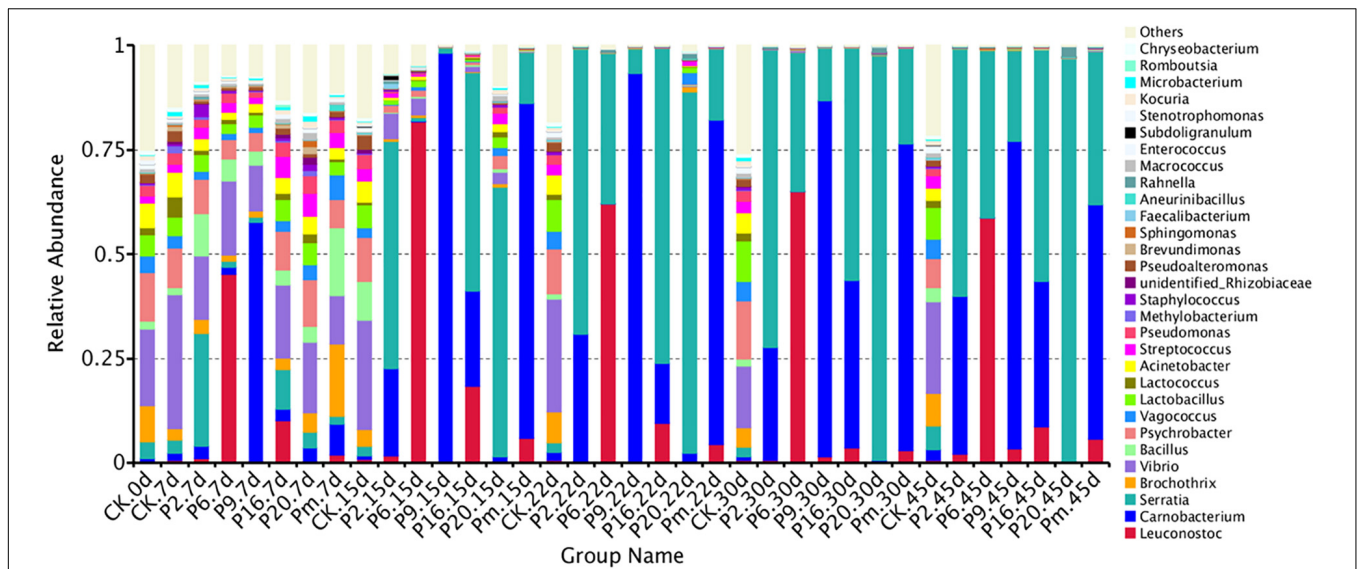


FIGURE 2 | Dynamics in relative abundance (%) of bacterial taxa at the phylum level in bacon inoculated with potential spoilage bacteria. Each bar represents the relative abundance of each group, below the top-30 abundances (at genus level) data were merged. CK, Control; P2, *Staphylococcus xylosum*; P6, *Leuconostoc mesenteroides*; P9, *Carnobacterium maltaromaticum*; P16, *Leuconostoc gelidum*; P20, *Serratia liquefaciens*; Pm, The five strains in combination.

shown as boxplots (**Supplementary Figure 1**). Shannon's index represents the species diversity, the observed OTUs and Chao1 index reflected species richness. According to **Supplementary Figure 1**, these three indices decreased over storage time, and much higher bacterial diversity in control samples and samples at initial stage were observed compared with the middle-late stages of storage after day 15. This behavior could directly show that the richness and diversity of microorganisms had been decreased and a subset of bacteria became dominant. High Good's coverage ($\geq 97.3\%$) indicated that the majority of microbial phylotypes were well-captured.

Composition of Bacterial Community

Bacterial community variations during bacon storage revealed by 16S rRNA gene and the mean relative abundance of microbial phyla are shown in **Supplementary Figure 2**. A total of 21 identified phyla were observed, and *Proteobacteria* and *Firmicutes* were the dominant phyla in the microbiota, representing 78.98–99.97% of the total catch. The proportion was associated with inoculation, for example, after inoculation with *S. liquefaciens*, *Proteobacteria* continuously increased and *Firmicutes* decreased, the highest *Firmicutes* level (99.97%) was reached at day 45, and also showed a much higher percentage (96.64%) at the genus level of *Serratia*. After inoculation with *C. maltaromaticum* (P9), after 45 days of storage, *Firmicutes* increased up to 98.43% on day 15, then decreased to 77.45% on day 15, while *Serratia* increased to 22.51% of the relative total abundance of *Proteobacteria*. The vast majority of the top 100 genera belong to the families *Firmicutes* and *Proteobacteria* (**Supplementary Figure 3**).

For a more detailed analysis, bacterial community dynamics at the genus level were studied, and a total of 367 bacteria identified were summarized in **Figure 2**. Control samples had the highest number of OTUs (**Table 3**) and the lowest loads

(those below the detection limit) throughout the storage period, implying more bacterial diversity and relative stability. As shown in **Figure 3A**, the main microbial groups were represented by *Vibrio* (23.38%), *Psychrobacter* (10.61%), *Lactobacillus* (6.67%), *Brochothrix* (5.88%), *Acinetobacter* (4.85%), *Serratia* (3.27%), *Bacillus* (3.17%), and *Pseudomonas* (2.54%). Similar microbial loads were frequently observed in processed meat products in the initial stage of storage (Chaillou et al., 2015; Quijada et al., 2018; Juárez-Castelán et al., 2019), indicating that these bacteria were primarily derived from raw meat and the processing unit (Borch et al., 1996; Hu et al., 2008; Chaillou et al., 2015). Therefore, these observations confirmed that irradiation could delay microbial growth and suppress final counts of spoilage microorganisms, extending the shelf-life stability of bacon.

Microbial communities evolved from day 7 to day 45 in bacon with inoculation during the storage process, where the microbial composition became less diverse and apparently more stable, with significantly decreased Chao 1 and Shannon diversity indices (**Table 3** and **Supplementary Figure 1**). Furthermore, *Serratia*, *Carnobacterium*, and *Leuconostoc* dominated at the end of the storage, suggesting that these members had strong survival rates and competitiveness.

The bacterial community of the various inoculations significantly differed from each other at the genus level. According to **Figure 3F**, a rapidly increased percentage of *Serratia* to 96.64% dominated the microbial population, after the samples were inoculated with *S. liquefaciens*, during 45 days of storage. Among the *Enterobacteriaceae* family, *Serratia* spp. are the most commonly found genus in meat products and often contribute to spoilage (Doulgeraki et al., 2011, 2012). *Serratia liquefaciens* was found in high numbers after refrigerated storage of packages of minced meat, such that they actually could spoil the product (Lindberg et al., 1998), and comprised

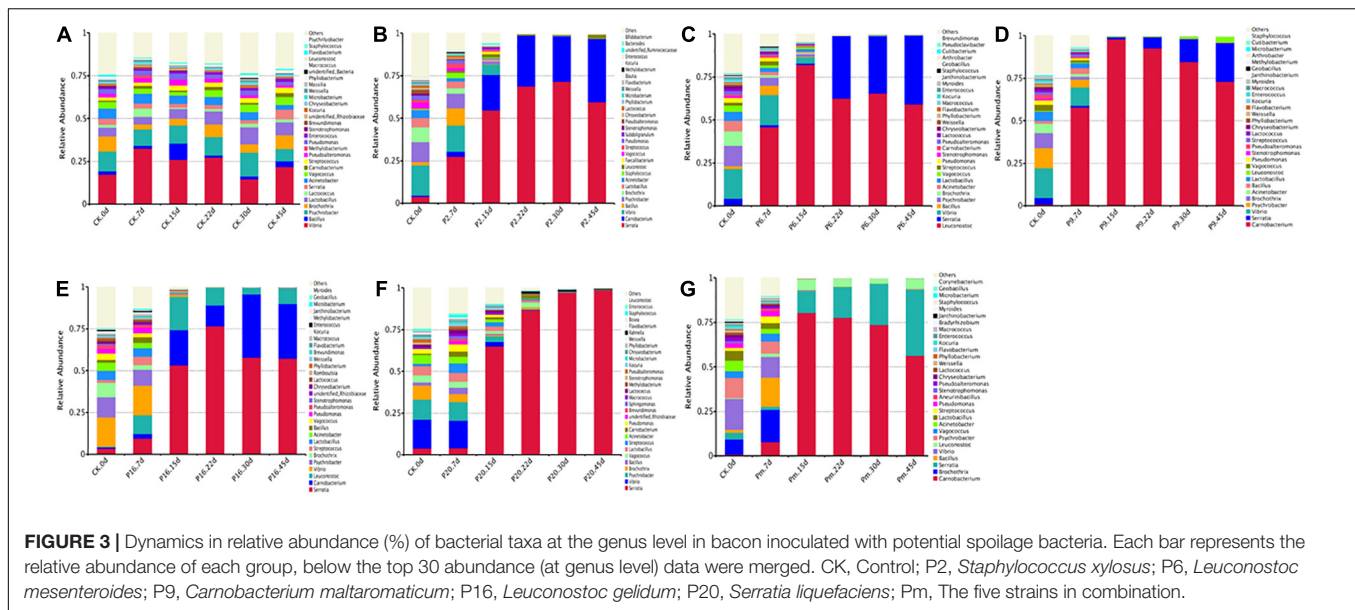


FIGURE 3 | Dynamics in relative abundance (%) of bacterial taxa at the genus level in bacon inoculated with potential spoilage bacteria. Each bar represents the relative abundance of each group, below the top 30 abundance (at genus level) data were merged. CK, Control; P2, *Staphylococcus xylosum*; P6, *Leuconostoc mesenteroides*; P9, *Carnobacterium maltaromaticum*; P16, *Leuconostoc gelidum*; P20, *Serratia liquefaciens*; Pm, The five strains in combination.

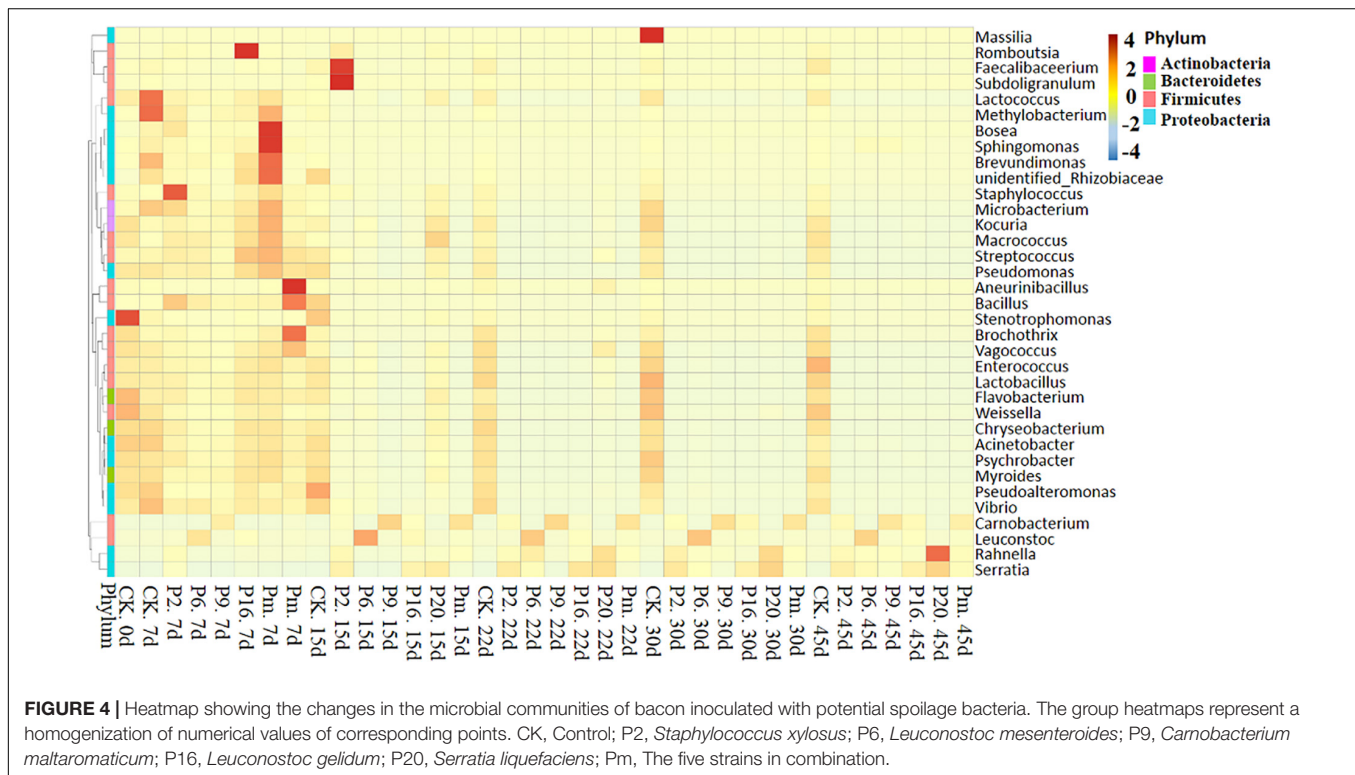


FIGURE 4 | Heatmap showing the changes in the microbial communities of bacon inoculated with potential spoilage bacteria. The group heatmaps represent a homogenization of numerical values of corresponding points. CK, Control; P2, *Staphylococcus xylosum*; P6, *Leuconostoc mesenteroides*; P9, *Carnobacterium maltaromaticum*; P16, *Leuconostoc gelidum*; P20, *Serratia liquefaciens*; Pm, The five strains in combination.

one of the most common species of *Enterobacteria* in spoiled hams (Paarup et al., 1999; Losantos et al., 2000), where they typically reached 5–7 log₁₀ CFU/g (Gram et al., 1999). In this study, **Figure 3C** illustrates that the *Serratia* populations grew rapidly and reached a peak to become dominant on day 15, then reached their stationary phase and suppressed the growth of other spoilage organisms. *Serratia* spp. may produce several antimicrobial metabolites, which have been characterized as strong N-acyl-homoserine lactone (AHL) producers in meat

(Bruhn et al., 2004). They may use quorum sensing to monitor their population density, synchronize their physiological functions, and socially interact with other bacteria (Van Houdt et al., 2007), thus we anticipated that once *Serratia* reached maximum abundance, it could make an important contribution to other spoilage-related bacteria.

The samples inoculated with *C. maltaromaticum* and *L. mesenteroides* underwent a more complex composting process of bacterial community succession. *Carnobacterium* and

Leuconostoc increased sharply after inoculation and reached a maximum relative abundance of 97.95 and 81.6% at day 15 (**Figures 3C,D**), respectively; however, the proportions thereof decreased to 73.60 and 58.67% at day 45, remaining in relatively high abundance and accompanied with a rapid increase of *Serratia*. *Carnobacterium maltaromaticum* inoculated with sterile sliced beef, then grew well and achieved maximum population after 2–8 weeks (Leisner et al., 1995). *Carnobacterium* spp. are ubiquitous psychrotrophic LAB that could grow in a wide variety of meat products at lower temperatures, and are commonly predominant members of the microflora, which may be conducive to rapid deterioration during storage (Leisner et al., 2007; Casaburi et al., 2011). *Carnobacteria* possessed the capability to produce antimicrobial peptides, bacteriocins, and wide spectrum action against pathogenic and spoilage bacteria (Leisner et al., 2007). *Leuconostoc mesenteroides* was the dominant species and consequently was responsible for the spoilage of commercial bacon (Comi et al., 2016). Morcilla de Burgos inoculated with *L. mesenteroides*, as a new species, grew more rapidly and influenced the signs of spoilage due to its more energy-efficient metabolism (Diez et al., 2009). Kotzekidou and Bloukas (1998) reported that inoculation of *Lactobacillus alimentarius* in vacuum-packed frankfurter-type sausage could increase LAB populations and suppress other saprophytic microorganisms.

Lactic acid bacteria produce various antimicrobial components, such as organic acids, hydrogen peroxide, ethanol, bacteriocins, and other substances (Holzapfel et al., 1995; Drosinos et al., 2006), one or more these metabolites refer to the inhibition of other undesirable bacteria, including spoilage microorganisms and pathogenic bacteria (Metaxopoulos et al., 2002; Drosinos et al., 2006). In this study, *Carnobacterium* and *Leuconostoc* reached maximum relative abundance on day 15, thereafter the suppression of *Serratia* by them was slowly alleviated (**Figures 3C,D**), which could be explained by the fact that the antimicrobial metabolites from lactic acid strains were ineffective as a mechanism of control.

The genera that presented the greatest abundances of samples inoculated with *S. xylosus* (P2) were *Serratia* (59.26%) and *Carnobacterium* (37.76%) on day 45 (**Figure 3B**), while the *Staphylococcus* was found at a very low level (0.01%). Similarly, the prevalent species were also *Serratia* (55.37%) and *Carnobacterium* (34.84%) inoculated with *L. gelidum* (P16), containing only a small proportion of *Leuconostoc* (8.7%) (**Figure 3E**). The bacterial load in the bacon product inoculated with *S. xylosus* and *L. gelidum*, increased initially, then decreased, indicating antimicrobial substances may be generated by the predominant *Serratia* and *Carnobacterium* (probably AHLs and bacteriocins). *Serratia* and *Carnobacterium* gradually outcompeted all other bacteria and became the dominant species with increasing storage time, which was consistent with the results from the viable counts. *Staphylococcus xylosus* and *L. gelidum* displayed a slower growth of the species and were deemed less competitive among microorganisms.

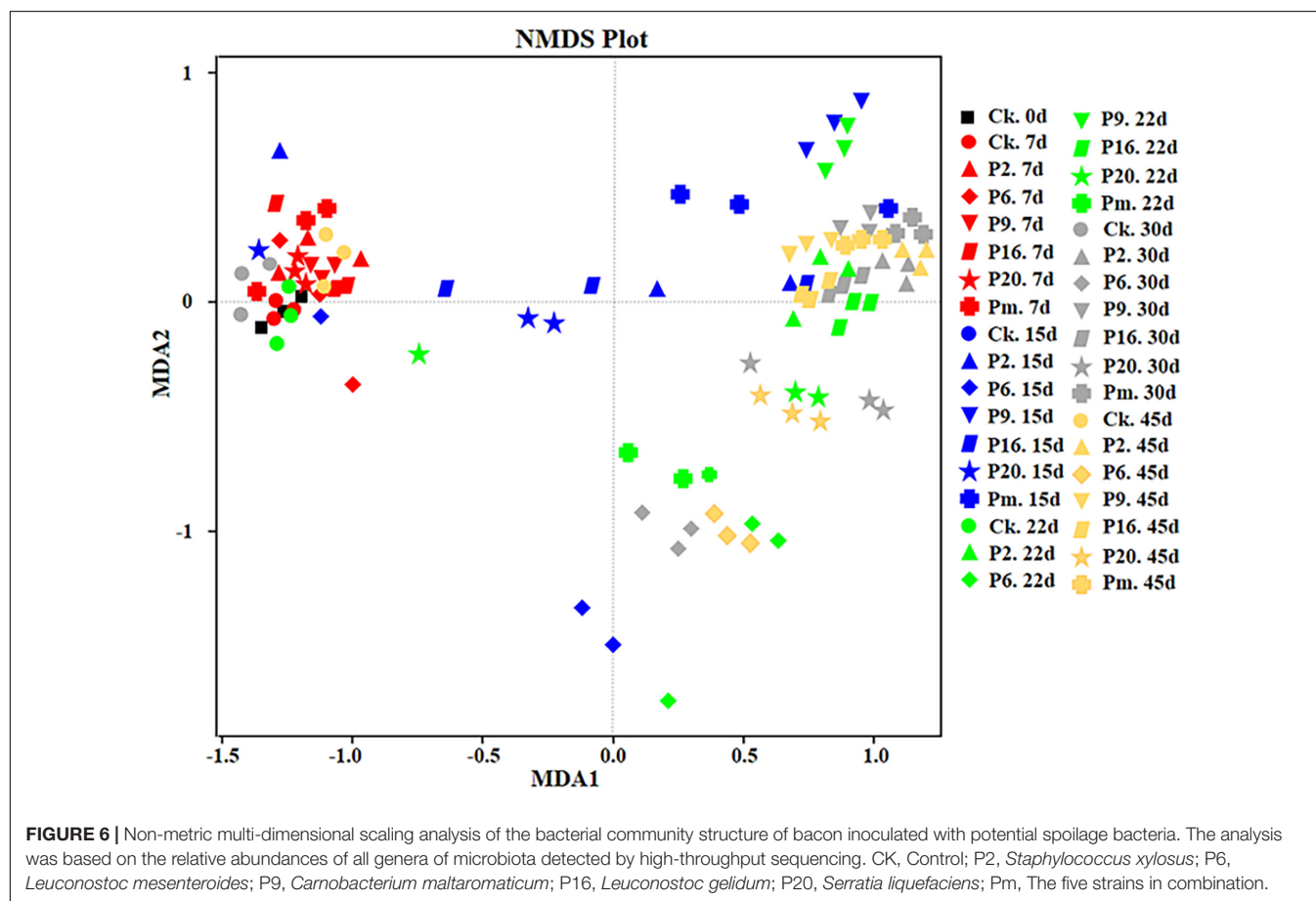
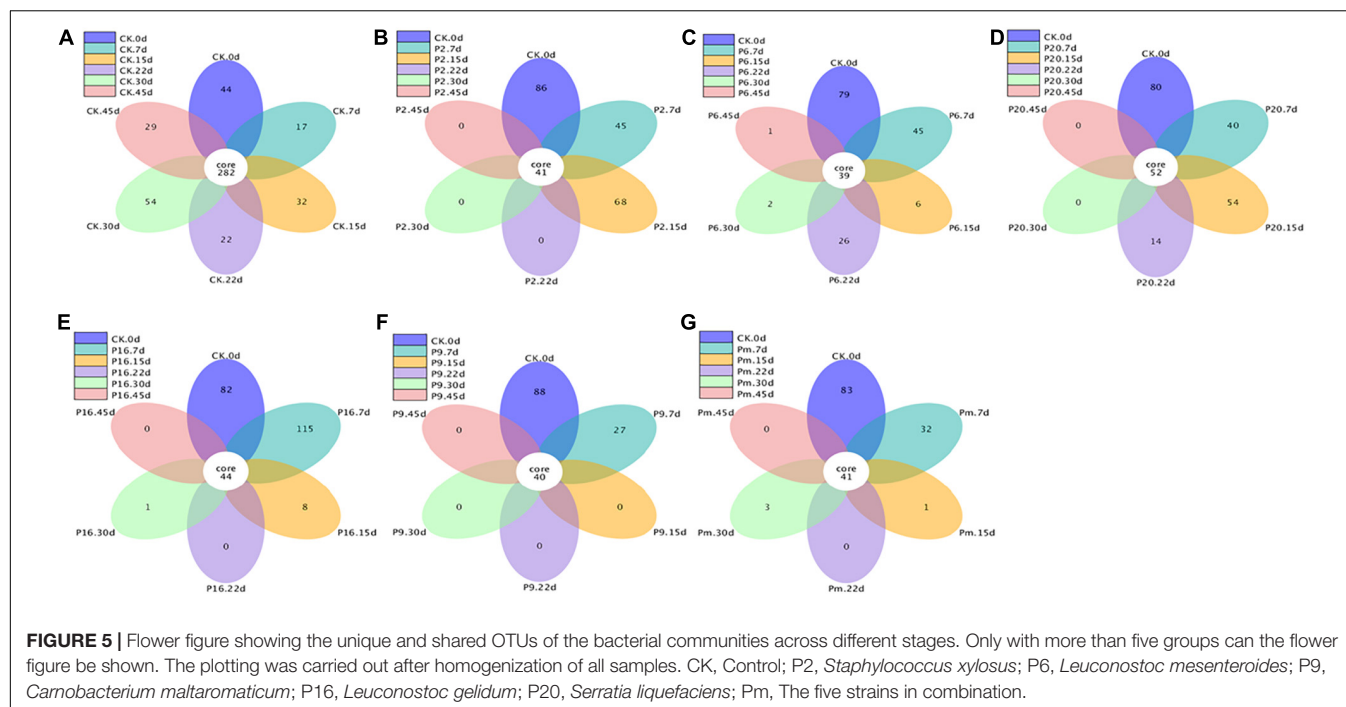
Carnobacteria had shown the ability to produce metabolites with antimicrobial activity (peptides and bacteriocins) and could inhibit spoilage bacteria, such as LAB and *Enterococcus*

(Leisner et al., 2007; Doulgeraki et al., 2012). Hydrogen peroxide and lactic acid are produced by a number of LAB (e.g., *Carnobacteria* spp. and *Leuconostoc* spp.), *Staphylococcus* spp. are more sensitive to these than most LAB, and would either be inhibited or destroyed (Holzapfel et al., 1995). *Leuconostoc gelidum* often prevail in chilled-stored, packaged, nutrient-rich, foods, such as cooked meats (Säde, 2011), however, *L. gelidum* cannot obtain energy from glycogen, proteinaceous substrates, lactate, or fatty acids, and its growth is thus inhibited. Additionally, *Carnobacterium* (56.16%) and *Serratia* (36.74%) grew rapidly and accounted for the most part of the microbial community in sterile bacon specimens inoculated with the five mixed strains (Pm) on day 45 (**Figure 3G**), and the proportion of *Leuconostoc* was only 5.73%. Referring to these results, the growth of *Leuconostoc* may also be inhibited by the strains of *Serratia* and *Carnobacterium*. Compared with the *Serratia*, the occurrence of *Carnobacterium* usually reported in meats and dairy products is most often ignored. Since MRS agar commonly used for LAB enumeration contained acetate it was efficient in terms of inhibiting *Carnobacterium* growth.

Microbial Diversity and Changes During Storage

To investigate the succession in microbial communities of bacon inoculated with spoilage bacteria during storage, heatmaps of bacteria at the genus level phylotypes were plotted (**Figure 4** and **Supplementary Figure 4**). Among the generated heatmaps, the redder color denotes higher relative abundances, and the greener color represents lower abundances. According to **Supplementary Figure 4**, a relatively high diversity was observed in control samples throughout the storage period, due to the low concentration of viable counts (**Table 2**), showing that they should form relatively stable compositions. At 7 days of storage after inoculation with spoilage bacteria, the microbial community composition differed among different groups and indicated less diversity in terms of trend. During the late storage period, *Serratia*, *Carnobacterium*, and *Leuconostoc* were clustered with the highest abundance in bacon inoculated with different bacterial strains, implying that the microbial communities became minimally diverse. Similar results were found by Nychas et al. (2008), who found the gradually stable microflora composition in the late stage of storage was generally the predominant bacteria. Additionally, the more abundant dominant bacterium, the less diverse the microbial community in the late storage stages, and the specimens inoculated with such strains evidently reduced the abundance of the reference microorganisms.

Similarities and differences among the groups were also analyzed using flower plots (**Figure 5**). According to **Figure 5**, for control samples, 282 groups (the largest percentage of all groups) were classified as core OTUs. Besides core OTUs, there were 44, 17, 32, 22, 54, and 29 unique OTUs on days 0, 7, 15, 22, 30, and 45, the number remained stable until the end of the storage period, indicating that the microbial composition changed slightly in control samples. In the inoculated groups, the core OTUs (39–42) were significantly lower than the control groups, and unique OTUs on days 7 and 15 were relatively large,



then very few were available, intimating that the bacterial community composition changed significantly. In conclusion, the microbiota changed toward simpler and similar communities with increasing storage time.

Additionally, non-metric multidimensional scaling (NMDS) analysis was performed to compare the differences and similarity of the community composition data (**Figure 6**). The figure shows joint-plot NMDS maps illustrating the bacterial community structure and the successive and dynamic changes prolonging the storage period. **Figure 6** demonstrates the continuing shifts (above plane to below plane) from the primary stable period (until day 7) to a late state (until day 45). The control groups and inoculated groups on day 7 showed similar microbiota forming one cluster, then scattered, which suggested that the similarity and differences were present among the groups and that the microbiota was affected by storage time.

Foods can support a complex microflora and interactions between different species of microorganisms. In this study, the inoculation decreased the levels of potential microorganisms and inhibited the growth of numerous organisms that correlate with meat spoilage. In general, high bacterial diversities were observed in the early stage of storage while *Serratia*, *Carnobacterium*, and *Leuconostoc* became the most abundant genera with prolonged storage. We can conclude only that the reason for the dominance is not exclusively their rapid growth; it cannot be that other elements acted as competing organisms since they were dominant. Gram (1993) found that the bacterial selection in the microflora of food products is the influence of microbial interactions.

In food ecosystems, the interactions between microbial growth and enzyme activities have been shown to cause various consequences such as: growth promotion, symbiotic relationships, growth inhibition, and competition (Gram et al., 2002; Andreevskaya et al., 2018). LAB-meat interactions have been studied frequently: in vacuum-packed and refrigerated meat products, it is reported that spoilage arises from the interaction among LAB (the dominant flora) and *Enterobacteriaceae*, *Pseudomonads*, *Brochothrix thermosphacta*, and other species (found in lower numbers) (Borch et al., 1996; Metaxopoulos et al., 2002; Bruhn et al., 2004). LAB could produce antimicrobial substances including organic acids and bacteriocins, which usually inhibit the growth of other microorganisms (Cleveland et al., 2001; Wang et al., 2016). *Leuconostoc mesenteroides* and *Lactobacillus curvatus* can produce bacteriocins and inhibit other spoilage microorganisms or even pathogens (Metaxopoulos et al., 2002). *Enterobacteriaceae*, notably *Serratia* spp. and *Hafnia alvei*, due to their ability to frequently become dominant in spoilage flora (Borch et al., 1996), were found to contribute to vacuum-packed meat spoilage through the quorum sensors (QS) systems (AHLs); however, AHL-producing *Hafnia alvei* might influence the spoilage in which other organisms participated with the spoilage process (Bruhn et al., 2004).

Bacterial interactions and competition have been extensively studied for the past few decades. A variety of interactions

(stimulation, delay, complete inhibition of growth, and no effects between them) could occur when lactic acid starters and probiotic bacteria were mixed (Vinderola et al., 2002). Co-culture studies can verify that interactions between *Lactobacillus sakei* 10A, *Lactobacillus sakei* LS5, and *Brochothrix thermosphacta* BT1 occurred in cooked meat (Vermeiren et al., 2006). Borch et al. (1996) found that sterilized beef inoculated with *Hafnia alvei* together with LAB, gave rise to unpleasant and unacceptable off-odors after 8 weeks, whereas no off-odors were detected with single *Hafnia alvei* culture. Inoculation with the three mixture of *Shewanella putrefaciens*, *Photobacterium phosphoreum*, and *Aeromonas* sp. in cold-smoked salmon cannot caused spoilage whereas co-inoculation of two bacteria *Brochothrix thermosphacta* and *Carnobacterium piscicola* was capable of producing off-odors (Joffraud et al., 2001). Morcilla de Burgos inoculated with *L. mesenteroides* and *W. viridescens*, both jointly and separately cultured, particular signs of spoilage increased compared to single-cell cultures (Diez et al., 2009). A number of these studies showed that the off-odor may originate from interactions among several bacteria. Microbial spoilage was caused by the growth and reproduction of a diversity of microorganisms, two or more microbial species exchange metabolites or nutrients to cause spoilage and disrupt product interactions (Gram et al., 2002). No single *S. liquefaciens* could be identified as the cause of spoilage, the growth and activity of bacteria usually contained a mixture of species/groups (Gram et al., 1999).

To develop novel preservation technologies and develop models for predictive microbiology, an insight into understanding of microbiota, and the dynamic changes and interactions during the refrigerated storage of meat products is of great importance, however, little information regarding possible interactions responsible for meat spoilage is available, so further research is needed.

CONCLUSION

In this study, the dynamic changes in bacterial community structures during the storage of bacon which had been previously inoculated with five potential spoilage bacteria, were evaluated. Using HTS, 21 phyla, and 367 bacteria genera were identified, with the control samples exhibiting the highest microbial diversity. Compared with the other groups, major microbiological and physicochemical changes appeared after 15 days, with the changes becoming gradually stable and less diverse bacterial communities appearing in the later stages of the storage period. *Serratia liquefaciens*, *C. maltaromaticum*, and *L. mesenteroides* were found to be more competitive species. The results from this study provide a basic understanding of the microbial composition and changes in the bacterial profile of bacon during the spoilage process. Although further investigations are needed to increase our understanding of the interactions between the microbial communities within the

spoilage environment, it is expected that this study will be of benefit to further improve the shelf-life of meat products.

All authors contributed to the article and approved the submitted version.

DATA AVAILABILITY STATEMENT

The datasets presented in this study can be found in online repositories. The names of the repository/repositories and accession number(s) can be found below: NCBI (accession: PRJNA746727).

AUTHOR CONTRIBUTIONS

YS and BX designed the experiments. XL carried out the experiments. QX analyzed the experimental results and assisted with the Illumina sequencing. HZ analyzed the sequencing data and developed the analysis tools. XL wrote the manuscript.

REFERENCES

- Alves, V., Martinez, R., Lavrador, M. A. S., and De Martinis, E. C. P. (2006). Antilisterial activity of lactic acid bacteria inoculated on cooked ham. *Meat Sci.* 74, 623–627. doi: 10.1016/j.meatsci.2006.05.012
- Andreevskaya, M., Jääskeläinen, E., Johansson, P., Ylinen, A., Paulin, L., Björkroth, J., et al. (2018). Food spoilage-associated *Leuconostoc*, *Lactococcus*, and *Lactobacillus* species display different survival strategies in response to competition. *Appl. Environ. Microbiol.* 84:e00554-18. doi: 10.1128/AEM.00554-18
- Belletti, N., Garriga, M., Aymerich, T., and Bover-Cid, S. (2013). Inactivation of *Serratia liquefaciens* on dry-cured ham by high pressure processing. *Food Microbiol.* 35, 34–37. doi: 10.1016/j.fm.2013.03.001
- Björkroth, K. J., Vandamme, P., and Korkeala, H. J. (1998). Identification and characterization of *Leuconostoc carnosum*, associated with production and spoilage of vacuum-packaged, sliced, cooked ham. *Appl. Environ. Microbiol.* 64, 3313–3319. doi: 10.1128/AEM.64.9.3313-3319.1998
- Borch, E., Kant-Muermans, M. L., and Blixt, Y. (1996). Bacterial spoilage of meat and cured meat products. *Int. J. Food Microbiol.* 33, 103–120. doi: 10.1016/0168-1605(96)01135-X
- Bredholt, S., Nesbakken, T., and Holck, A. (2001). Industrial application of an antilisterial strain of *Lactobacillus sakei* as a protective culture and its effect on the sensory acceptability of cooked, sliced, vacuum-packaged meats. *Int. J. Food Microbiol.* 66, 191–196. doi: 10.1016/S0168-1605(00)00519-5
- Bruhn, J. B., Christensen, A. B., Flodgaard, L. R., Nielsen, K. F., Larsen, T. O., Givskov, M., et al. (2004). Presence of acylated homoserine lactones (AHLs) and AHL-producing bacteria in meat and potential role of AHL in spoilage of meat. *Appl. Environ. Microbiol.* 70, 4293–4302. doi: 10.1128/AEM.70.7.4293-4302.2004
- Casaburi, A., Nasi, A., Ferrocino, I., Di Monaco, R., Mauriello, G., Villani, F., et al. (2011). Spoilage-related activity of *Carnobacterium maltaromaticum* strains in air-stored and vacuum-packed meat. *Appl. Environ. Microbiol.* 77, 7382–7393. doi: 10.1128/AEM.05304-11
- Casaburi, A., Piombino, P., Nychas, G. J., Villani, F., and Ercolini, D. (2015). Bacterial populations and the volatile associated to meat spoilage. *Food Microbiol.* 45, 83–102. doi: 10.1016/j.fm.2014.02.002
- Chaillou, S., Chaulot-Talmon, A., Caekebeke, H., Cardinal, M., Christies, S., Denis, C., et al. (2015). Origin and ecological selection of core and food-specific bacterial communities associated with meat and seafood spoilage. *ISME J.* 9, 1105–1118. doi: 10.1038/ismej.2014.202
- Chen, Q., Cao, M., Chen, H., Gao, P., Fu, Y., Liu, M., et al. (2016). Effects of gamma irradiation on microbial safety and quality of stir fry chicken dices with hot chili during storage. *Radiat. Phys. Chem.* 127, 122–126. doi: 10.1016/j.radphyschem.2016.06.022
- Chenoll, E., Macian, M. C., Elizaquivel, P., and Aznar, R. (2007). Lactic acid bacteria associated with vacuum-packed cooked meat product spoilage: population analysis by rDNA-based methods. *J. Appl. Microbiol.* 102, 498–508. doi: 10.1111/j.1365-2672.2006.03081.x
- Cleveland, J., Montville, T. J., Nes, I. F., and Chikindas, M. L. (2001). Bacteriocins: safe, natural antimicrobials for food preservation. *Int. J. Food Microbiol.* 71, 1–20. doi: 10.1016/S0168-1605(01)00560-8
- Comi, G., Andyanto, D., Manzano, M., and Iacumin, L. (2016). *Lactococcus lactis* and *Lactobacillus sakei* as bio-protective culture to eliminate *Leuconostoc mesenteroides* spoilage and improve the shelf life and sensorial characteristics of commercial cooked bacon. *Food Microbiol.* 58, 16–22. doi: 10.1016/j.fm.2016.03.001
- De Filippis, F., Pennacchia, C., Di Pasqua, R., Fiore, A., Fogliano, V., Villani, F., et al. (2013). Decarboxylase gene expression and cadaverine and putrescine production by *Serratia proteamaculans* in vitro and in beef. *Int. J. Food Microbiol.* 165, 332–338. doi: 10.1016/j.ijfoodmicro.2013.05.021
- Diez, A. M., Björkroth, J., Jaime, I., and Rovira, J. (2009). Microbial, sensory and volatile changes during the anaerobic cold storage of morcilla de Burgos previously inoculated with *Weissella viridescens* and *Leuconostoc mesenteroides*. *Int. J. Food Microbiol.* 131, 168–177. doi: 10.1016/j.ijfoodmicro.2009.02.019
- Dogbevi, M. K., Vachon, C., and Lacroix, M. (1999). Physicochemical and microbiological changes in irradiated fresh pork loins. *Meat Sci.* 51, 349–354. doi: 10.1016/S0309-1740(98)00133-8
- Doulgeraki, A. I., Ercolini, D., Villani, F., and Nychas, G. J. (2012). Spoilage microbiota associated to the storage of raw meat in different conditions. *Int. J. Food Microbiol.* 157, 130–141. doi: 10.1016/j.ijfoodmicro.2012.05.020
- Doulgeraki, A. I., Paramithiotis, S., and Nychas, G.-J. E. (2011). Characterization of the *Enterobacteriaceae* community that developed during storage of minced beef under aerobic or modified atmosphere packaging conditions. *Int. J. Food Microbiol.* 145, 77–83. doi: 10.1016/j.ijfoodmicro.2010.11.030
- Drosinos, E., Mataragas, M., and Metaxopoulos, J. (2006). Modeling of growth and bacteriocin production by *Leuconostoc mesenteroides* E131. *Meat Sci.* 74, 690–696. doi: 10.1016/j.meatsci.2006.05.022
- Edgar, R. C. (2013). UPARSE: highly accurate OTU sequences from microbial amplicon reads. *Nat. Methods* 10:996. doi: 10.1038/nmeth.2604
- Ercolini, D., Russo, F., Nasi, A., Ferranti, P., and Villani, F. J. A. (2009). Mesophilic and psychrotrophic bacteria from meat and their spoilage potential in vitro and in beef. *Appl. Environ. Microbiol.* 75, 1990–2001. doi: 10.1128/AEM.02762-08
- Gram, L. (1993). Inhibitory effect against pathogenic and spoilage bacteria of *Pseudomonas* strains isolated from spoiled and fresh fish. *Appl. Environ. Microbiol.* 59, 2197–2203. doi: 10.1128/aem.59.7.2197-2203.1993
- Gram, L., Christensen, A. B., Ravn, L., Molin, S., and Givskov, M. (1999). Production of acylated homoserine lactones by psychrotrophic members of the *Enterobacteriaceae* isolated from foods. *Appl. Environ. Microbiol.* 65, 3458–3463. doi: 10.1128/AEM.65.8.3458-3463.1999

FUNDING

This study was supported by the National Key Research and Development Programme of China (Grant No. 2016YFD0401501) and the Scientific Research Foundation for Introduced Talents of Nanjing Tech University.

SUPPLEMENTARY MATERIAL

The Supplementary Material for this article can be found online at: <https://www.frontiersin.org/articles/10.3389/fmicb.2021.713513/full#supplementary-material>

- Gram, L., Ravn, L., Rasch, M., Bruhn, J. B., Christensen, A. B., and Givskov, M. (2002). Food spoilage—interactions between food spoilage bacteria. *Int. J. Food Microbiol.* 78, 79–97. doi: 10.1016/S0168-1605(02)00233-7
- Hamasaki, Y., Ayaki, M., Fuchu, H., Sugiyama, M., and Morita, H. (2003). Behavior of psychrotrophic lactic acid bacteria isolated from spoiling cooked meat products. *Appl. Environ. Microbiol.* 69, 3668–3671. doi: 10.1128/AEM.69.6.3668-3671.2003
- Holm, E. S., Schäfer, A., Koch, A., and Petersen, M. A. (2013). Investigation of spoilage in saveloy samples inoculated with four potential spoilage bacteria. *Meat Sci.* 93, 687–695. doi: 10.1016/j.meatsci.2012.11.016
- Holzappel, W., Geisen, R., and Schillinger, U. (1995). Biological preservation of foods with reference to protective cultures, bacteriocins and food-grade enzymes. *Int. J. Food Microbiol.* 24, 343–362. doi: 10.1016/0168-1605(94)00036-6
- Houtsma, P. C., de Wit, J. C., and Rombouts, F. M. (1996). Minimum inhibitory concentration (MIC) of sodium lactate and sodium chloride for spoilage organisms and pathogens at different pH values and temperatures. *J. Food Protect.* 59, 1300–1304. doi: 10.4315/0362-028X-59.12.1300
- Hu, P., Xu, X., Zhou, G., Han, Y., Xu, B., and Liu, J. (2008). Study of the *Lactobacillus sakei* protective effect towards spoilage bacteria in vacuum packed cooked ham analyzed by PCR–DGGE. *Meat Sci.* 80, 462–469. doi: 10.1016/j.meatsci.2008.01.011
- Huang, L., Zhao, J., Chen, Q., and Zhang, Y. (2014). Nondestructive measurement of total volatile basic nitrogen (TVB-N) in pork meat by integrating near infrared spectroscopy, computer vision and electronic nose techniques. *Food Chem.* 145, 228–236. doi: 10.1016/j.foodchem.2013.06.073
- Joffraud, J., Leroi, F., Roy, C., and Berdague, J. (2001). Characterisation of volatile compounds produced by bacteria isolated from the spoilage flora of cold-smoked salmon. *Int. J. Food Microbiol.* 66, 175–184. doi: 10.1016/S0168-1605(00)00532-8
- Juárez-Castelán, C., García-Cano, I., Escobar-Zepeda, A., Azaola-Espinoza, A., Álvarez-Cisneros, Y., and Ponce-Alquicira, E. (2019). Evaluation of the bacterial diversity of Spanish-type chorizo during the ripening process using high-throughput sequencing and physicochemical characterization. *Meat Sci.* 150, 7–13. doi: 10.1016/j.meatsci.2018.09.001
- Korkeala, H. J., and Björkroth, K. J. (1997). Microbiological spoilage and contamination of vacuum-packaged cooked sausages. *J. Food Protect.* 60, 724–731. doi: 10.4315/0362-028X-60.6.724
- Kotzekidou, P., and Bloukas, J. (1996). Effect of protective cultures and packaging film permeability on shelf-life of sliced vacuum-packed cooked ham. *Meat Sci.* 42, 333–345. doi: 10.1016/0309-1740(95)00038-0
- Kotzekidou, P., and Bloukas, J. (1998). Microbial and sensory changes in vacuum-packed frankfurter-type sausage by *Lactobacillus alimentarius* and fate of inoculated *Salmonella enteritidis*. *Food Microbiol.* 15, 101–111. doi: 10.1006/fmic.1997.0138
- Kuo, C., and Chu, C. (2003). Quality characteristics of Chinese sausages made from PSE pork. *Meat Sci.* 64, 441–449. doi: 10.1016/S0309-1740(02)00213-9
- Leisner, J. J., Laursen, B. G., Prévost, H., Drider, D., and Dalgard, P. (2007). *Carnobacterium*: positive and negative effects in the environment and in foods. *FEMS Microbiol. Rev.* 31, 592–613. doi: 10.1111/j.1574-6976.2007.00080.x
- Leisner, J., Greer, G., Dilts, B., and Stiles, M. (1995). Effect of growth of selected lactic acid bacteria on storage life of beef stored under vacuum and in air. *Int. J. Food Microbiol.* 26, 231–243. doi: 10.1016/0168-1605(94)00133-Q
- Leroy, F., Verluyten, J., and De Vuyst, L. (2006). Functional meat starter cultures for improved sausage fermentation. *Int. J. Food Microbiol.* 106, 270–285. doi: 10.1016/j.ijfoodmicro.2005.06.027
- Li, X., Li, C., Ye, H., Wang, Z., Wu, X., Han, Y., et al. (2019). Changes in the microbial communities in vacuum-packaged smoked bacon during storage. *Food Microbiol.* 77, 26–37. doi: 10.1016/j.fm.2018.08.007
- Li, X., Xiong, Q., Xu, B., Wang, H., Zhou, H., and Sun, Y. (2021). (2021) Bacterial community dynamics during different stages of processing of smoked bacon using the 16S rRNA gene amplicon analysis. *Int. J. Food Microbiol.* 351:109076. doi: 10.1016/j.ijfoodmicro.2021.109076
- Lindberg, A.-M., Ljungh, Å., Ahrne, S., Löfdahl, S., and Molin, G. (1998). *Enterobacteriaceae* found in high numbers in fish, minced meat and pasteurised milk or cream and the presence of toxin encoding genes. *Int. J. Food Microbiol.* 39, 11–17. doi: 10.1016/S0168-1605(97)00104-9
- Losantos, A., Sanabria, C., Cornejo, I., and Carrascosa, A. (2000). Characterization of *Enterobacteriaceae* strains isolated from spoiled dry-cured hams. *Food Microbiol.* 17, 505–512. doi: 10.1006/fmic.2000.0350
- Macé, S., Joffraud, J. J., Cardinal, M., Malcheva, M., Cornet, J., Lalanne, V., et al. (2013). Evaluation of the spoilage potential of bacteria isolated from spoiled raw salmon (*Salmo salar*) fillets stored under modified atmosphere packaging. *Int. J. Food Microbiol.* 160, 227–238. doi: 10.1016/j.ijfoodmicro.2012.10.013
- Mah, J.-H., and Hwang, H.-J. (2009). Inhibition of biogenic amine formation in a salted and fermented anchovy by *Staphylococcus xylosus* as a protective culture. *Food Control* 20, 796–801. doi: 10.1016/j.foodcont.2008.10.005
- Martin, M. (2011). Cutadapt removes adapter sequences from high-throughput sequencing reads. *EMBnet J.* 17, 10–12. doi: 10.14806/ej.17.1.200
- Mataragas, M., Skandamis, P., Nychas, G.-J. E., and Drosinos, E. H. (2007). Modeling and predicting spoilage of cooked, cured meat products by multivariate analysis. *Meat Sci.* 77, 348–356. doi: 10.1016/j.meatsci.2007.03.023
- McMeekin, T. A., and Ross, T. (1996). Shelf life prediction: status and future possibilities. *Int. J. Food Microbiol.* 33, 65–83. doi: 10.1016/0168-1605(96)01138-5
- Metaxopoulos, J., Mataragas, M., and Drosinos, E. H. (2002). Microbial interaction in cooked cured meat products under vacuum or modified atmosphere at 4 °C. *J. Appl. Microbiol.* 93, 363–373. doi: 10.1046/j.1365-2672.2002.01701.x
- Mills, J., Donnison, A., and Brightwell, G. (2014). Factors affecting microbial spoilage and shelf-life of chilled vacuum-packed lamb transported to distant markets: a review. *Meat Sci.* 98, 71–80. doi: 10.1016/j.meatsci.2014.05.002
- Nychas, G. J., Skandamis, P. N., Tassou, C. C., and Koutsoumanis, K. P. (2008). Meat spoilage during distribution. *Meat Sci.* 78, 77–89. doi: 10.1016/j.meatsci.2007.06.020
- O'bryan, C. A., Crandall, P. G., Riche, S. C., and Olson, D. G. (2008). Impact of irradiation on the safety and quality of poultry and meat products: a review. *Crit. Rev. Food Sci.* 48, 442–457. doi: 10.1080/10408390701425698
- Paarup, T., Nieto, J. C., Peláez, C., and Reguera, J. I. (1999). Microbiological and physico-chemical characterisation of deep spoilage in Spanish dry-cured hams and characterisation of isolated *Enterobacteriaceae* with regard to salt and temperature tolerance. *Eur. Food Res. Technol.* 209, 366–371. doi: 10.1007/s002170050511
- Pin, C., and Baranyi, J. (1998). Predictive models as means to quantify the interactions of spoilage organisms. *Int. J. Food Microbiol.* 41, 59–72. doi: 10.1016/S0168-1605(98)00035-X
- Pin, C., Sutherland, J., and Baranyi, J. (1999). Validating predictive models of food spoilage organisms. *J. Appl. Microbiol.* 87, 491–499. doi: 10.1046/j.1365-2672.1999.00838.x
- Polka, J., Rebecchi, A., Pisacane, V., Morelli, L., and Puglisi, E. (2015). Bacterial diversity in typical Italian salami at different ripening stages as revealed by high-throughput sequencing of 16S rRNA amplicons. *Food Microbiol.* 46, 342–356.
- Pothakos, V., Devlieghere, F., Villani, F., Björkroth, J., and Ercolini, D. (2015). Lactic acid bacteria and their controversial role in fresh meat spoilage. *Meat Sci.* 109, 66–74. doi: 10.1016/j.meatsci.2015.04.014
- Pothakos, V., Nyambi, C., Zhang, B.-Y., Papastergiadis, A., De Meulenaer, B., and Devlieghere, F. (2014a). Spoilage potential of psychrotrophic lactic acid bacteria (LAB) species: *Leuconostoc gelidum* subsp. *gasicomitatum* and *Lactococcus piscium*, on sweet bell pepper (SBP) simulation medium under different gas compositions. *Int. J. Food. Microbiol.* 178, 120–129. doi: 10.1016/j.ijfoodmicro.2014.03.012
- Pothakos, V., Snauwaert, C., De Vos, P., Huys, G., and Devlieghere, F. (2014b). Psychrotrophic members of *Leuconostoc gasicomitatum*, *Leuconostoc gelidum* and *Lactococcus piscium* dominate at the end of shelf-life in packaged and chilled-stored food products in Belgium. *Food Microbiol.* 39, 61–67. doi: 10.1016/j.fm.2014.08.023
- Quijada, N. M., De Filippis, F., Sanz, J. J., del Camino Garcia-Fernandez, M., Rodríguez-Lázaro, D., Ercolini, D., et al. (2018). Different *Lactobacillus* populations dominate in “Chorizo de León” manufacturing performed in different production plants. *Food Microbiol.* 70, 94–102. doi: 10.1016/j.fm.2017.09.009
- Rahkila, R., Nieminen, T., Johansson, P., Säde, E., and Björkroth, J. (2012). Characterization and evaluation of the spoilage potential of *Lactococcus piscium* isolates from modified atmosphere packaged meat. *Int. J. Food Microbiol.* 156, 50–59. doi: 10.1016/j.ijfoodmicro.2012.02.022

- Ravyts, F., Vuyst, L. D., and Leroy, F. (2012). Bacterial diversity and functionalities in food fermentations. *Eng. Life Sci.* 12, 356–367. doi: 10.1002/elsc.201100119
- Roig-Sagués, A., and Eerola, S. (1997). Biogenic amines in meat inoculated with *Lactobacillus sake* starter strains and an amine-positive lactic acid bacterium. *Z. Lebensm. Unters. F. A* 205, 227–231. doi: 10.1007/s002170050156
- Säde, E. (2011). *Leuconostoc Spoilage of Refrigerated, Packaged Foods*. Academic Dissertation. Helsinki: University of Helsinki.
- Samelis, J., Kakouri, A., and Rementzis, J. (2000). Selective effect of the product type and the packaging conditions on the species of lactic acid bacteria dominating the spoilage microbial association of cooked meats at 4 °C. *Food Microbiol.* 17, 329–340. doi: 10.1006/fmic.1999.0316
- Soladoye, P., Shand, P., Aalhus, J., Gariépy, C., and Juárez, M. (2015). Pork belly quality, bacon properties and recent consumer trends. *Can. J. Anim. Sci.* 95, 325–340. doi: 10.4141/cjas-2014-121
- Stavropoulou, D. A., De Maere, H., Berardo, A., Janssens, B., Filippou, P., De Vuyst, L., et al. (2018). Pervasiveness of *Staphylococcus carnosus* over *Staphylococcus xylosum* is affected by the level of acidification within a conventional meat starter culture set-up. *Int. J. Food Microbiol.* 274, 60–66. doi: 10.1016/j.ijfoodmicro.2018.03.006
- Stohr, V., Joffraud, J., Cardinal, M., and Leroi, F. (2001). Spoilage potential and sensory profile associated with bacteria isolated from cold-smoked salmon. *Food Res. Int.* 34, 797–806. doi: 10.1016/S0963-9969(01)00101-6
- Sun, X., and Holley, R. (2012). Antimicrobial and antioxidative strategies to reduce pathogens and extend the shelf life of fresh red meats. *Compr. Rev. Food Sci.* 11, 340–354. doi: 10.1111/j.1541-4337.2012.00188.x
- Van Houdt, R., Givskov, M., and Michiels, C. W. (2007). Quorum sensing in *Serratia*. *FEMS Microbiol. Rev.* 31, 407–424. doi: 10.1111/j.1574-6976.2007.00071.x
- Vermeiren, L., Devlieghere, F., and Debevere, J. (2004). Evaluation of meat born lactic acid bacteria as protective cultures for the biopreservation of cooked meat products. *Int. J. Food Microbiol.* 96, 149–164. doi: 10.1016/j.ijfoodmicro.2004.03.016
- Vermeiren, L., Devlieghere, F., and Debevere, J. (2006). Co-culture experiments demonstrate the usefulness of *Lactobacillus sakei* 10A to prolong the shelf-life of a model cooked ham. *Int. J. Food Microbiol.* 108, 68–77. doi: 10.1016/j.ijfoodmicro.2005.11.001
- Vinderola, C. G., Mocchiutti, P., and Reinheimer, J. A. (2002). Interactions among lactic acid starter and probiotic bacteria used for fermented dairy products. *J. Dairy Sci.* 85, 721–729. doi: 10.3168/jds.S0022-0302(02)74129-5
- Wang, G.-Y., Wang, H.-H., Han, Y.-W., Xing, T., Ye, K.-P., Xu, X.-L., et al. (2017). Evaluation of the spoilage potential of bacteria isolated from chilled chicken *in vitro* and *in situ*. *Food Microbiol.* 63, 139–146. doi: 10.1016/j.fm.2016.11.015
- Wang, T., Zhao, L., Sun, Y., Ren, F., Chen, S., Zhang, H., et al. (2016). Changes in the microbiota of lamb packaged in a vacuum and in modified atmospheres during chilled storage analysed by high-throughput sequencing. *Meat Sci.* 121, 253–260. doi: 10.1016/j.meatsci.2016.06.021
- Wang, X., Ren, H., Liu, D., Zhu, W., and Wang, W. (2013). Effects of inoculating *Lactobacillus sakei* starter cultures on the microbiological quality and nitrite depletion of Chinese fermented sausages. *Food Control* 32, 591–596. doi: 10.1016/j.foodcont.2013.01.050
- Zagdoun, M., Coeuret, G., N'Dione, M., Champomier-Vergès, M.-C., and Chaillou, S. J. F. M. (2020). LARGE microbiota survey reveals HOW the microbial ecology of cooked ham is shaped by different processing steps. *Food Microbiol.* 91:103547. doi: 10.1016/j.fm.2020.10.3547
- Zhang, Y., Li, Q., Li, D., Liu, X., and Luo, Y. (2015). Changes in the microbial communities of air-packaged and vacuum-packaged common carp (*Cyprinus carpio*) stored at 4 °C. *Food Microbiol.* 52, 197–204. doi: 10.1016/j.fm.2015.08.003

Conflict of Interest: The authors declare that the research was conducted in the absence of any commercial or financial relationships that could be construed as a potential conflict of interest.

Publisher's Note: All claims expressed in this article are solely those of the authors and do not necessarily represent those of their affiliated organizations, or those of the publisher, the editors and the reviewers. Any product that may be evaluated in this article, or claim that may be made by its manufacturer, is not guaranteed or endorsed by the publisher.

Copyright © 2021 Li, Xiong, Zhou, Xu and Sun. This is an open-access article distributed under the terms of the Creative Commons Attribution License (CC BY). The use, distribution or reproduction in other forums is permitted, provided the original author(s) and the copyright owner(s) are credited and that the original publication in this journal is cited, in accordance with accepted academic practice. No use, distribution or reproduction is permitted which does not comply with these terms.



Mathematical Modeling of Total Volatile Basic Nitrogen and Microbial Biomass in Stored Rohu (*Labeo rohita*) Fish

Pramod K. Prabhakar^{1,2*}, Prem P. Srivastav^{2*}, Sant S. Pathak³ and Kalyan Das^{4*}

¹ Department of Food Science and Technology, National Institute of Food Technology, Entrepreneurship and Management, Sonapat, India, ² Department of Agricultural and Food Engineering, Indian Institute of Technology, Kharagpur, India,

³ Department of Electronics and Electrical Communication Engineering, Indian Institute of Technology, Kharagpur, India,

⁴ Department of Basics and Applied Sciences, National Institute of Food Technology, Entrepreneurship and Management, Sonapat, India

OPEN ACCESS

Edited by:

Shalini Gaur Rudra,
Indian Agricultural Research
Institute, India

Reviewed by:

Theofania Tsironi,
Agricultural University of
Athens, Greece
Eldho Varghese,
Central Marine Fisheries Research
Institute, India

*Correspondence:

Pramod K. Prabhakar
pramodkp@niftem.ac.in
Prem P. Srivastav
pps@agfe.iitkgp.ac.in
Kalyan Das
daskalyan27@gmail.com

Specialty section:

This article was submitted to
Agro-Food Safety,
a section of the journal
Frontiers in Sustainable Food Systems

Received: 18 February 2021

Accepted: 16 September 2021

Published: 20 October 2021

Citation:

Prabhakar PK, Srivastav PP,
Pathak SS and Das K (2021)
Mathematical Modeling of Total
Volatile Basic Nitrogen and Microbial
Biomass in Stored Rohu (*Labeo
rohita*) Fish.
Front. Sustain. Food Syst. 5:669473.
doi: 10.3389/fsufs.2021.669473

The paper deals with the dynamical behavior of fish volatiles and microbial growth in stored Rohu fish through mathematical modeling. Total volatile basic nitrogen (TVB-N) is formed in stored Rohu (*Labeo rohita*) fish due to some complicated biochemical activities. It considered the biomass populace of volatiles (TVB-N) and microorganisms in fish stored at two different temperatures, separately. The different models may be used to forecast TVB-N, microbial populace (total viable count; TVC), and various properties change during nourishment stockpiling coordination and diverse preparing tasks. Models might be dynamic, exact, hypothetical, and stochastic in nature. Various parameters are required to build up a model which can be utilized to foresee the freshness and timeframe of realistic usability of storage duration. The ecosystem is represented by algebraic equations involving volatile compounds and microbial populations separately. TVB-N and TVC of stored rohu fish was determined at an interval of 4 days for 24 days. The initial and final biomass of TVB-N was 4.57 (fresh sample), 19.88 (24 days at 5°C), and 7.10 mg/100 g (24th day at 0°C), respectively. The TVC values were found to be 2.29 (fresh sample), 9.5 (24 days at 5°C) and 8.1 log (cfu/g) (24 days at 0°C). Exponential, modified exponential, Howgate, and adapted Howgate models were considered for modeling the TVB-N formation, whereas logistic, modified logistic, Gompertz, and modified Gompertz model were taken forward for modeling the microbial biomass developed in stored rohu fish. The exponential model found be the best fit model fit model for TVB-N prediction in rohu fish stored at 0 and 5°C as it showed the highest R^2 (0.9796, 0.9887) the lowest χ^2 (0.2782, 0.3976), RMSE (0.52741, 0.6306) AIC (−7.3122, −4.8106), AICc (−0.5122, 1.9894) and BIC (−7.4204, −4.9188), respectively. The Gompertz model was found to be the best fit model for microbial biomass prediction in rohu fish stored at 5°C ($R^2 = 0.9947$, $\chi^2 = 0.0537$, AIC = −18.379, AICc = −6.3792 and BIC = −18.542), in contrast, both of the logistic and modified logistic models were the best suited at 0°C storage condition ($R^2 = 0.9919$, $\chi^2 = 0.0823$).

Keywords: empirical model, growth dynamics, microbial population, rohu (*Labeo rohita*), Total volatile basic nitrogen (TVBN)

INTRODUCTION

The increasing demand for fish is directly proportional to its nutritional values. Fish is an excellent food due to its high content of omega 3-fatty acids and proteins. Post-harvest fish losses (PHFL) are a major problem of concern that widely occurs across the world, resulting in less fish availability for the consumer due to which fish is either discarded or fetch a relatively low price due to deterioration in quality. PHFL starts after the death of fish when enzymatic, oxidative, and microbial-assisted physio-functional changes to begin to deteriorate the fish quality. Several factors like time, temperature and handling practices are the major factors that cause PHFL. Generally, raw food is initially contaminated with a wide variety of microorganisms during post-harvest handlings, but few of them can colonize, easily grow in food products, and spoil it. Different types of spoilage depend on the physical and chemical changes in the processing and packaging techniques of fish products (Gram and Huss, 1996). Specific and non-specific factors contribute to complex microbiological reactions and phenomena in seafood, leading to contamination before slaughtering and during product formation. The different intrinsic and extrinsic factors involving temperature, pH, and redox potential exert an electric effect on microbial growth, microbial inhibition, which decides the growth curve of microorganisms (Gram and Huss, 1996). Besides the factors pH, temperature, etc., other factors like the poikilothermic nature of the fish in the aquatic environment also influence the spoilage of the fish that can be dealt with in terms of high pH in the flesh of post-mortem fish and higher content of NPN (non-protein nitrogen). The presence of trimethylamine oxide (TMAO) as part of the NPN fraction after degradation during fish storage is generated as a volatile compound, i.e., trimethylamine (TMA). The volatile formation such as total volatile basic nitrogen (TVB-N) and TMA results from complex biochemical reactions such as microbiological and enzymatic etc. TVB-N, TMA, and other biogenic amines are the major chemical compounds which are used as a freshness index in fish (Tsironi and Petros, 2010; Prabhakar et al., 2019). As the amount of TMA increases, the TVB-N also increases rapidly; TMA is the compound responsible for starting and continuing this spoilage and fishy odor. During the bacterial growth in spoilage, bacteria establish themselves on the outer and inner surfaces of the live fish. Bacteria can easily grow over a wide range of temperatures due to this poikilothermic nature of fish. The main microorganisms present in temperate water where the fish interacts with are psychotropic Gram-negative, rod-shaped bacteria which have genera namely as *Pseudomonas*, *Moraxella*, *Acinetobacter*, *Shewanella*, *Flavobacterium*, *Vibrionaceae* and *Aeromonadaceae*, but many gram-positive organisms are also found in different proportions such as *Bacillus*, *Micrococcus*, *Clostridium*, *Lactobacillus* and *Corynebacterium*. The recent establishment of the specific spoilage organism (SSOs) concept has contributed significantly to understand seafood spoilage. The different SSOs such as *Shewanella putrefaciens* (Iced marine fish), *Pseudomonas* spp. (Iced freshwater fish), *Photobacterium phosphoreum* (CO₂-packed chilled fish) are found in different fish and fisheries products and may be single species. These

bacterial activities are also responsible for the breakdown of protein and other components of fish which results in the formation of biogenic amines such as trimethylamine (TMA), Dimethyl Amine (DMA), Ammonia (NH₃), and TVB-N. The TMA, DMA, and NH₃ are combined, known as TVB-N, which is considered a chemical indicator of further toxicity and spoilage. The amount of volatile formation is a function of fish species and variety (Whittle and Howgate, 2002). Marine species contain TMAO, which is a part of the NPN fraction and is present in all marine. Spoilage is influenced by TMAO, especially in anaerobic conditions. Spoilage bacteria utilize TMAO in anaerobic respiration, an electron acceptor at the terminal point, which results in the formation of trimethylamine (TMA) as an end product with off odor and bad flavor (Dalgaard et al., 1993; Broekaert et al., 2012). Bacteria are considered spoilage indicators as they are the sole precursor required for reducing TMAO to TMA. During cold storage and frozen cold chain of fishes, intrinsic enzyme activity induces dimethylamine (DMA) from TMAO with the same molar quantities of formaldehyde equivalents. Many white fishes have their freshness measured through this method. However, most industries and institutes go for direct microbial counts as the source of marking fish freshness and assessing shelf life. The microbial analysis that has been conventionally carried out for decades is time-consuming and quite inconvenient (Peleg, 2016). TMA, DMA, and TVB-N lead to the direct assessment of the freshness of fish. Consequently, here an attempt is made to use rapid and mathematical tools for evaluating fish freshness as a replacement of traditional microbial methods of analysis. The major parameters that affect the formation of volatiles (TMA and TVB-N) are the duration of storage and temperature (Heising et al., 2014a; Peleg et al., 2014; Peleg, 2016). Functional relations can easily be understood in terms of a mathematical model.

The various physical and chemical changes in the fish are also reflected in many characteristics such as color, texture, tenderness, and flavor. The color and appearance of muscles directly influence the value and acceptance of most fish species (Chouhan et al., 2015). Color is also considered an indicator of freshness, influencing consumers' purchase decisions (Chouhan et al., 2015). Visual assessment is an important parameter affecting the presentation of fish and fish products and a product is generally selected upon its appearance, especially its color. Storage duration at different temperatures causes oxygenation and oxidation of myoglobin which forms oxymyoglobin in fish tissue (Mancini and Hunt, 2005). Metmyoglobin and oxymyoglobin are also associated with changes in the color of the fish file. The conformational changes in the protein also impact the color change during iced and frozen storage of fish. The solubility of myofibrillar protein and sarcoplasmic protein is influenced by the storage duration and temperature (Mohan et al., 2006), which affects the visibility of Rohu. Degradation of muscle protein is a major problem associated with fish during storage (Mohan et al., 2006). These changes are brought either by enzymatic (endogenous/exogenous) or microbial-induced biochemical reactions during storage. These changes during fish storage play a vital role in the freshness assessment of the fish and fish products. Sensory rejection and sensory assessment based on

total viable count (TVC) values of fish being 5.74 and 4.66 log CFU/g for chilling and partial freezing, respectively.

This study considered the biomass population of volatiles coming under TVB-N and microbial load in rohu fish stored at different temperatures. The various models have been used to predict microbial population, enzyme inactivation, and different properties changes during food storage, logistics, and different processing operations. Models may be kinetic, empirical, theoretical, and stochastic in nature. A model to depict the freshness of fishes requires many different parameters under it (Baranyi and Roberts, 1994; Husain et al., 2016). The fish freshness indicators based on kinetic and mathematical modeling can also be applied to design and develop an efficient supply chain for fish and related fish products. There is a difference in the rate of biochemical reactions of frozen and unfrozen fishes. The modeling for this dependence of temperature can be performed in several ways, such as the Arrhenius model, which has wide application in understanding physicochemical and biochemical changes in the food system. The dynamics of food quality also change highly regarding the change in molecular arrangement (Gudmundsson and Kristbergsson, 2009). In case of packed cod filets, a mathematical model has been developed which reports the formation of Trimethylamine (Heising et al., 2014a). Application of trial-and-error method, using approximate and guessed calculations along with other factors is used every time for calculation of the exact value of TMA by using all these equations. This model has enormous potential, which can link the sensor data of TMA in fish to the real status of the freshness of fish (Heising et al., 2014a). Most of the developed models are either to determine microbial biomass or compounds generated in the food matrix. The present study aimed to exercise the multi-model approach for the mathematical analysis of the TVB-N and microbial biomass dynamics.

EXPERIMENTAL APPROACH AND METHODS

Fish Handling and Storage Conditions

Live Rohu samples were collected (irrespective of the sex ratio) from a local fish farm pond (near IIT Kharagpur, West Bengal, India) having same cultural practices and rearing environment and then collected sample were transported to the lab in polybag containing farm pond water. Fish were kept free from stress before stunning death. The fish were killed by percussive stunning (involves hitting the fish's head with a wooden) the head for sudden death on 0-day means starting day of storage (Abbas et al., 2005; Jain et al., 2007). Random sampling was done such that three fishes were taken from all the lots, and their average length and weights were further measured and found to be 29.53 ± 2.32 cm and 620 ± 30 g, respectively. Rohu samples were covered by a layer of aluminum foil and kept at different storage temperatures (5 ± 1 , $0 \pm 1^\circ\text{C}$) for the study. The fish sample was stored at the required temperature for the study in the refrigerator, which was domestic (Whirlpool, FF2D258C/2016, Gurugram, India), A deep freezer (Voltas,

205 CF Metal Top, Delhi, India), and a quick microprocessor freezer (REMI, RQFVM-205D, Vasai, India) for 24 days. A multi-probe thermocouple (digital thermometer) was used to ensure the consistency of the required set temperature in every case.

Total Volatile Basic Nitrogen (TVB-N)

The volatile compound, TVB-N were estimated by the method executed by Prabhakar et al. (2019) i.e., the Conway micro-diffusion method referred by FSSAI (2015) manual (Chouhan et al., 2015) with partial modification. However, some other routine methods may be used to check the TVB-N limit, such as the direct distillation method described by Conway, Antonacopoulos (1968) and the distillation of an extract deproteinized trichloroacetic acid reported by FAO/WHO through FAO/WHO (1968). As per FSSAI (2015) manual, 5 grams of fish muscle taken from stored fish was homogenized with 45 mL of distilled water. 5 ml of this homogenate were added with an equal volume of 10% trichloroacetic acid (TCA) (w/v) and then filtered through Whatman's filter paper no. 1. 1 ml of this extract and saturated potassium carbonate each was pipetted into the outer ring of the micro-diffusion unit containing 1 ml inner ring solution. Inner ring solution was prepared by mixing 2% boric acid (92 ml), 0.1% alcoholic bromocresol (4 ml), and 0.1% alcoholic methyl red (4 ml). The covered and sealed unit was rotated gently to mix the solutions of the outer ring. The unit was incubated for 180 mins at 37°C and cooled at room temperature. 0.02 N sulfuric acid was used for titration of the inner ring solution until it turned pink. Then, 1 ml of 10% trichloroacetic acid was taken for a blank test instead of sample extract. The same procedure was adopted for TMA-N determination as TVB-N, but 1 ml of formalin was added before adding potassium carbonate to the extract to react with ammonia, allowing only the TMA-N to diffuse over the unit. Each experiment was replicated three times for every storage condition, and the obtained TVB-N and TMA-N results were expressed in mg/100 g of sample. These TVB-N and TMA-N obtained data were used for its kinetic study.

Microbiological Analysis

In general, the number of spoilage bacteria (total bacterial count or specific bacterial) and level of some biochemical indexes (TVB-N) are used to evaluate the freshness of fish. However, as per Chouhan et al. (2015), Fan et al. (2008), and Prabhakar et al. (2020), the total viable count (TVC) was considered to be calculated to explore the microbiological quality of fish and fish products. Therefore, a microbiological quality analysis was done as per Downes and Ito (2001) with minor modification. 10 g of Rohu muscle was weighed aseptically into a sterile sample dish and homogenized with 90 ml of sterile physiological saline (0.854% NaCl) for 3 mins. using a sterile pipette, 1 ml of the supernatant was aseptically transferred into a 9 ml saline tube and mixed well-using vortex mixer. Similarly, further dilutions were prepared for the inoculation. 1 ml each of the appropriate dilutions was made and poured onto agar by spread plate technique. The plates were incubated for 48 h at 37°C in an

TABLE 1 | Empirical models consider for TVB-N and microbial biomass modeling.

Sr. no	Name of models	Model equation	TVB-N/microbial biomass	References
1	Exponential model	$C = C_0 e^{kt}$	TVB-N	Tsironi et al., 2009; Yao et al., 2011
2	Modified exponential model	$C = e^{k(t-d)} - 1 + C_0$		Howgate, 2010b
3	Howgate	$C = \frac{C_{\max} - C_{\min}}{1 + e^{k(t-d)}}$		Howgate, 2010b
4	Adapted Howgate	$C = \frac{C_{\max} - C_{\min}}{1 + e^{k(t-d)}} + C_{\min}$		Heising et al., 2014a
5	Logistic	$m = \frac{a}{1 + e^{-k(t-d)}}$	Microbial growth	Peleg and Corradini, 2011
6	Modified logistic	$m = \frac{a}{1 + b e^{-kt}}$		
7	Gompertz	$m = \frac{a}{e^{(e^{-k(t-d)})}}$		Giannuzzi et al., 1998
8	Modified Gompertz	$m = m_0 + \frac{a}{e^{e^{2.71828 \mu_{\max} \frac{t-1}{a}} + 1}}$		

inverted position. Total viable count (TVC) was enumerated and expressed as log₁₀ cfu/g of the sample. The experiment was conducted at an interval of 4 days.

$$\text{TVC} = \log_{10} \left[\frac{\text{Number of colony} \times \text{volume of sample taken (ml)}}{\text{dilution}} \right] \times \frac{1}{\text{weight of the sample (g)}} \quad (1)$$

Mathematical Modeling: Parameter Estimation and Statistical Analysis

Many biological reactions in fish, such as volatile formations (TVB-N, TMA-N, and other biogenic amines) and vitamins loss during isothermal storage and processing operation, probably follow fixed order of kinetics (Peleg, 2016). The formation of the TVB-N and microbial population in stored Rohu was modeled using different models (Table 1) that all set of algebraic equations (empirical and phenomenological models). In the present study, all analyses (TVB-N and microbial biomass) were done in triplicates, and readings were expressed as average values \pm SD. The biomass mass data (TVB-N and microbial population) were fitted to different models (Table 1) using non-linear regression analysis through the ORIGIN 2021 software (Origin Lab Corporation, Northampton, USA). The suitability and fitness of models were examined based on the coefficient of determination (R^2), chi-square (χ^2), and root mean square error (RMSE). However, secondary modeling, i.e., the Arrhenius model was not for the temperature sensitivity analysis of microbiological and chemical changes in the stored fish because the study has been made at only two temperatures.

$$R^2 = 1 - \frac{\sum_{i=1}^n (Y_{i,p} - Y_{i,e})^2}{\sum_{i=1}^n (Y_{i,p} - Y_e)^2} \quad (2)$$

$$\chi^2 = \sum_{i=1}^n \frac{(Y_{i,e} - Y_{i,p})^2}{Y_{i,p}} \quad (3)$$

$$\text{RMSE} = \sqrt{\frac{1}{n} \sum_{i=1}^n (Y_{i,e} - Y_{i,p})^2} \quad (4)$$

Where, n is the number of experiments; $Y_{i,e}$ is the experimental value of the i th experiment; $Y_{i,p}$ is the predicted value of

the n th experiment by model; and Y_e is the average value of experimentally determined values.

Along with the above statistical analysis, models were also discriminated using statistical analysis of the residuals and Akaike information criterion (AIC) and corrected Akaike information criterion (AIC_c), which were calculated from Equations 5, 6 (Van Boekel, 2009; Heising et al., 2014a). AICs is AIC with a correction for small sample sizes specially when the sample size is more than the number of model parameters. The lowest values of AIC and AICs are preferred for selecting the best fit model among all models.

$$\text{AIC} = n \ln \left(\frac{SS_r}{n} \right) + 2p \quad (5)$$

$$\text{AICc} = n \ln \left(\frac{SS_r}{n} \right) + 2(p+1) + 2(p+1) \left(\frac{p+2}{n-p} \right) \quad (6)$$

Where, SS_r is the residual sum of squares, n is the number of observations, and p is the number of parameters.

Bayesian information criterion (BIC) is also a criterion for model selection among a finite set of models. It penalizes the complexity of the model, which refers to the number of parameters in the model. The lowest value is preferred for the selection of the model. BIC can be calculated by using Equation 7.

$$\text{BIC} = n \ln \left(\frac{SS_r}{n} \right) + p \ln(n) \quad (7)$$

MATHEMATICAL MODELING: THEORETICAL STATUS, EXPERIMENTAL RESULTS AND DISCUSSION

Theoretical Status of Volatile Formation, Modeling and Parameterization

The results obtained in terms of TVB-N and microbial population from the storage study were used to consider existing empirical models (growth/kinetic) from literature (Table 1) to explore its suitability for TVB-N and Microbial biomass development. Thereafter, parameters were estimated and compared with other validated models from the literature, and the temperature effect was also explored. TVB-N formed

in fish during storage is due to some microbial metabolites responsible for off-flavors and off-odors (Cheng et al., 2015; Prabhakar et al., 2019). These metabolites may be TMA-N, ammonia, and DMA. The total volatile base-nitrogen (TVB-N) index combines these amines into a unique indicator used to assess the spoilage of fresh fish. In fact, the content of TVB-N is the only biochemical index presently included in EU regulations to discriminate fit from unfit fish in commerce or an official inspection. Neither TVB-N nor trimethylamine (TMA) content can be used as indexes of quality in the early stages of storage (Dalgaard et al., 1993; Howgate, 2010a). The Codex Alimentarius Committee (CAC) and FAO/WHO (1968) have recommended TVB-N as a regulatory compound for deciding the freshness of different fish species. TVB-N is also associated with the activity of endogenous enzymes (Kyrana et al., 1997; Varelziz et al., 1997). According to Connell (1990), spoiled fish exhibit a TVB-N level above 35 mg N/100 g. The formation of TVB-N is also the function of fish species. The European Commission (European Union Law 95/149/EC, 1995) has specified TVB-N limits for different species, such as 25 mg/100 g for *Sebastes* spp. (*Helicolenus dactylopterus*, *Sebastichthys capensis*), 30 mg/100 g for species belonging to the Pleuronectidae family (except halibut: *Hippoglossus* spp.), and 35 mg/100 g for *Salmo salar*. On the other hand, storage conditions (time and temperature) affect the shelf life and quality of fish (Fan et al., 2008) and can increase the formation of TVB-N, which is a significant cause of spoilage of Rohu fish (Mehta et al., 2014). According to Connell (1990), the permissible limit of the TMA-N level should be lower than 35 mg N/100 g, although this limit varies from species to species. Malle and Poumeyrol (1989) reported TMA-N values of 10–15 mg/100 g in aerobically stored fish and at a level of 30 mg TMA-N/100 g in packed cod. O'zogul et al. (2004) reported that the concentrations of TMA-N in numerous fatty fish never reached the limit of 5 mg TMA-N/100 g. However, the rejection limit in fish flesh is usually higher. Therefore, TMA-N formation in stored fish depends upon species, fish composition, storage temperature, duration, and local environmental composition. However, some studies have found significant correlations between TVB-N, TMA, and storage time (Baixas-Nogueras et al., 2001; Ruiz-Capillas and Moral, 2001). Storage conditions like temperature and duration influence the volatiles formation and other biochemical changes in fish caused by either microbial or enzymatic activities. Spoilage bacteria are selected primarily due to the physical and chemical conditions in the products; however, seafood spoilage involves the growth of the microorganism to a high number ($>10^6$ – 10^7 cfu/g) of antagonisms or symbiosis between the different groups of microorganisms may influence their growth and metabolism (Gram and Dalgaard, 2002).

The majority of quality and shelf-life models in the literature focus on the most probable prediction. There is a huge literature on fish spoilage, technological, economic, and safety implications, and a continuous attempt has been made to monitor the spoilage in quantitative terms. Microbial counts are probably the most direct method, which is generally exercised using a traditional technique that involves incubation. It is very time-consuming and logistically inconvenient (Peleg, 2016). A

mathematical tool can be applied to replace this direct method for rapid determination of microbial population, which predicts the shelf life (Heising et al., 2014a; Prabhakar et al., 2019). The various models (for TVB-N and microbial biomass) selected based on literature and the data pattern were analyzed for experimental data obtained in the present study. A variety of mathematical models has described microbial growth. Their properties and how well they fit and predict and predict experimental growth data are discussed by Peleg and Corradini (2011). Most of the empirical models are based on physical and biochemical principles of mass transport in stored fish. Adapted Howgate model uses a mathematical model framework for sensor response of intelligent packaging. Therefore, indicating that the modeling of TVB-N dynamics could be used to predict shelf life. For the volatile formation, a wide range of models starting from complete exponential to asymptotic behavior has been used to explain the dynamics (Van Boekel, 2008; Heising et al., 2014b; Garcia et al., 2017). Furthermore, models having asymptotic nature such as logistic, modified logistic, Gompertz, and modified Gompertz were found to be extensively used in the literature (Baranyi and Roberts, 1994; Giannuzzi et al., 1998). Based on this, these models were also considered for the present study with a hypothesis that asymptote is expected.

Modeling of TVB-N and Effect of Temperature on Model Parameters

The experimental TVB-N values during storage of Rohu fish at an interval of 4 days were modeled to find the best empirical models. The most common TMA-N or TVB-N formation model is usually an exponential model, i.e., Equation 8 (Tsironi et al., 2009; Tsironi and Petros, 2010; Yao et al., 2011; Garcia et al., 2017).

$$C = C_0 e^{kt} \quad (8)$$

Where, C stands for TVB-N content, k is the velocity of the reaction, and t describes the time elapsed since the fish arrived for the market (days). C_0 is the TVB-N content at $t = 0$, i.e., when the fish arrives to the storage. The experimental data of TVB-N were fitted to an exponential model (Equation 8). Model and statistical parameters were represented in **Table 2**. As per the fitted exponential model, the predicted initial concentration (C_0) of TVB-N was found to be closer to the sample stored at 5°C (5.69 ± 0.3102 mg/100 g) than 0°C (5.29 ± 0.2825 mg/100 g), which showed that it was independent of temperature. **Figure 1** showed the exponential model curve having coefficient of determination ($R^2 = 0.9887$ and 0.9796), Chi-square ($\chi^2 = 0.3976$ and 0.2782). The values of R^2 are quite high, and χ^2 are low, indicating its goodness of fit for the dynamical understanding of TVB-N under experimental conditions of the present study. The reaction rate, i.e., k -values, were 0.053 ± 0.003 and 0.042 ± 0.003 day⁻¹ for the TVB-N formation of the Rohu sample stored at 5°C and 0°C, respectively. k values indicated that lower storage temperature would have arrested the reaction, slowing the reaction velocity. **Figure 1** showed that there was a continuous increasing pattern of TVB-N formation throughout the storage period, irrespective of the demarcation of slow and

TABLE 2 | Model and statistical parameters of different empirical models for TVB-N formation in stored Rohu fish.

Parameters	Mathematical models				
	Temperature (°C)	Exponential model	Modified exponential model	Howgate model	Adapted howgate model
C_0	5	5.69 ± 0.3102	7.09 ± 0.9031		
	0	5.29 ± 0.2825	6.11464 ± 0.57414		
k	5	0.053 ± 0.003	0.11283 ± 0.00563	0.1394 ± 0.0486	0.14245 ± 0.04805
	0	0.042 ± 0.003	0.09483 ± 0.00536	0.0823 ± 0.0241	0.08677 ± 0.02523
d	5		4.94234E-15 ± 0	9.2161 ± 3.313	
	0		6.22189E-14 ± 0	14.0912 ± 7.6868	
C_{\max}	5			20 ± 3.6452	20 ± 3.47307
	0			19.99 ± 5.8026	18.94008 ± 4.86309
C_{\min}	5			9.9E-31 (~0)	4.11326E-57 (~0)
	0			9.9E-25 (~0)	3.9965E-29 (~0)
t_d	5			9.2161 ± 3.313	9.20794 ± 3.19474
	0			14.0912 ± 7.6868	12.64942 ± 6.56757
χ^2	5	0.3976	3.3328	2.16086	2.11961
	0	0.2782	1.2697	0.33722	0.36256
R^2	5	0.9887	0.9246	0.96338	0.96408
	0	0.9796	0.9255	0.98518	0.98406
Adj. R^2	5	0.9865	0.8870	0.92676	0.92816
	0	0.9755	0.8883	0.97036	0.96813
RMSE	5	0.6306	1.8256	1.46999	1.4593
	0	0.52741	1.1268	0.58071	0.60213
SSr	5	1.98825	13.33132	6.48259	6.38871
	0	1.3908	5.07898	1.01167	1.08767
AIC	5	-4.8106	10.5094	7.46247	7.36036
	0	-7.3122	3.7544	-5.5402	-5.0331
AICc	5	1.98941	22.5094	29.4625	29.3604
	0	-0.5122	15.7544	16.4598	16.9669
BICc	5	-4.9188	10.3472	7.24611	7.144
	0	-7.4204	3.59213	-5.7565	-5.2495

advanced spoilage, without reaching and explaining a maximum asymptote. Howgate (2010a), Heising et al. (2014b) critically pointed out that the critical drawback of the conventional model of TVB-N content is their inability to produce the initial dwell and the exponential behavior.

Heising et al. (2014b) postulated that the volatile formation in fish and fish products stored in ice or refrigerated conditions from the harvesting/catch often starts with a period in which the volatiles like TMA-N was not increased. It was followed by another phase with a rapid increase in the TMA-N concentration, followed by a third phase in which the volatile formation rate diminishes. The TVB-N is comprised of TMA-N, DMA-N, and NH_3 gas, and its formation is a function of enzymatic and bacterial actions influenced by storage conditions (Huss, 1995; Prabhakar et al., 2020). Nevertheless, the exponential model is sufficient enough to simulate the TVB-N formation in all phases and stages. Though the fitting of exponential mode is good, as attributed by R^2 and χ^2 values. Keeping these facts, another model, such as the modified exponential model (Equation 9), was considered for modeling the dynamics of TVB-N formation.

Moreover, this model was suggested by Howgate (2010b) for the TMA-N formation in fish stored on ice. The parameter “ d ” represents the dwell (days), and C_0 describes the TVB-N concentration at time $t = 0$. A logistic model, which is an advanced form of the exponential model, was found to have a good fit with the present TVB-N experiment values as ($R^2 = 0.9246$ and 0.9255), and chi-square ($\chi^2 = 3.3328$ and 1.2697) these statistical parameters showed less fit in comparison to exponential model (Equation 8).

Modified exponential model (Equation 9) attributed a dwell period of 4.94×10^{-15} days at 5°C , and a 6.22×10^{-14} day at 0°C , which was negligible, which can be understood through the logistic model curve (Figure 2), the corresponding k values were found to be 0.11283 ± 0.006 and $0.09483 \pm 0.005 \text{ day}^{-1}$. The present findings are in line with the trend of fishy odor formation in packed codfish filets at varied storage temperatures ($0, 5, 10, 15^\circ\text{C}$) which were reported by Heising et al. (2014a).

$$C = e^{k(t-d)} - 1 + C_0 \quad (9)$$

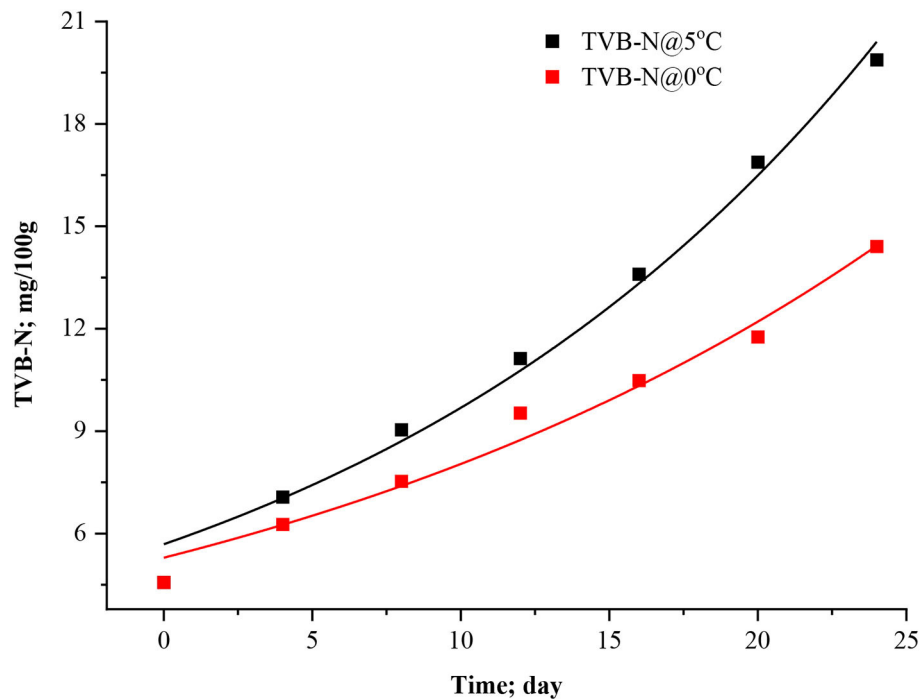


FIGURE 1 | Exponential model curve for TVB-N in stored Rohu fish.

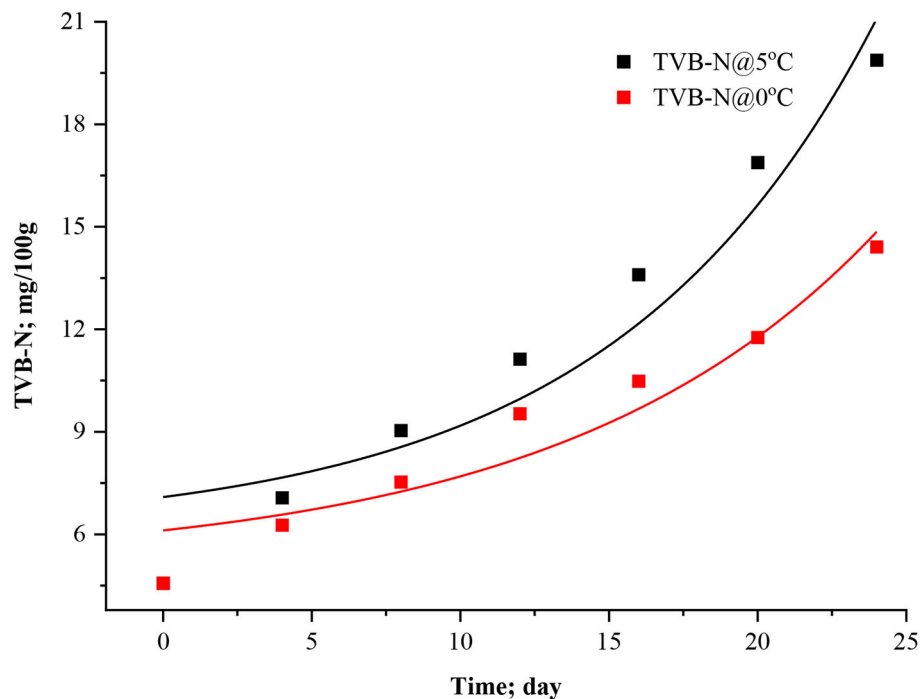


FIGURE 2 | Modified exponential model curve for TVB-N in stored Rohu fish.

It was inferred that this modified exponential model (Equation 9) doesn't include and describe a parameter for maximum concentration of TVB-N. Thus, the model increases

exponentially even under the advanced spoilage phase (Howgate, 2010b; Heising et al., 2014b). This equation only uses for the initial phase of volatile formation. For minimum and maximum

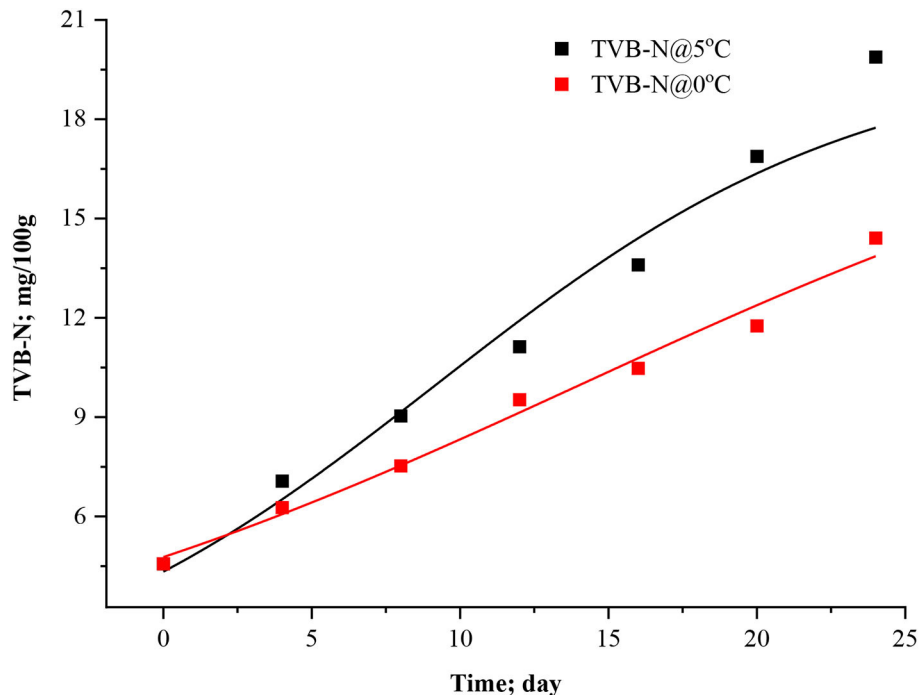


FIGURE 3 | Howgate model curve for TVB-N in stored Rohu fish.

asymptotic concepts, other models such as the Howgate (Equation 10) and adapted Howgate model (Equation 11) were considered for fitting analysis under present experimental conditions. The parameters C_{\max} represents upper asymptote concentration (mg TVB-N per 100 g fish muscle), C_{\min} lower asymptote concentration (mg TVB-N per 100 g fish). This equation gives the asymptote value of $C_{\max}-C_{\min}$ for a higher value of t . It will give a lower value of $C_{\text{TVB-N}}$ at the same time t and C_{\max} since the value of the numerator decreases with increasing C_{\min} . The data were modeled using Equations 10, 11 considering $C_{\min} > 0$, $k > 0$, $t_d > 0$, and $t > 0$; otherwise, it will make an unrealistic situation. The data of TVB-N under both storage conditions and the C_{\max} were parameterized for Howgate and adapted Howgate model as 20 ± 3.6452 and 20 ± 3.4707 mg/100 at 5°C which are very close to each other and, for 0°C , C_{\max} values were estimated to be 19.99 ± 5.8026 and 18.94 ± 4.8631 mg/100 g for the respective model.

$$C = \frac{C_{\max} - C_{\min}}{1 + e^{k(t_d - t)}} \quad (10)$$

$$C = \frac{C_{\max} - C_{\min}}{1 + e^{k(t_d - t)}} + C_{\min} \quad (11)$$

The points of inflection (t_d) ranged between 9.2161 ± 3.313 to 14.0912 ± 7.6868 days in the Howgate model (Equation 10), whereas it was ranged from 9.2079 ± 3.1947 to 12.6494 ± 6.5675 days for the adapted Howgate model (Equation 11). The estimated statistical parameters like R^2 ranged from 0.96338 to 0.98518 for the Howgate model. For the adapted Howgate model, R^2 values were found to be 0.9640 and 0.9840. The

k -values of the Howgate model were 0.1394 ± 0.0486 and $0.0823 \pm 0.0241 \text{ day}^{-1}$ whereas, for the adapted Howgate model, it was found 0.14245 ± 0.0450 and $0.08677 \pm 0.0252 \text{ day}^{-1}$. The graphical pattern of TVB-N formation in the model curve of Howgate and adapted Howgate model was present in **Figures 3, 4**. As a result, the exponential model was found to be the best fit model for predicting TVB-N biomass in rohu fish stored at 0°C and 5°C . The exponential model fitting showed R^2 (0.9796, 0.98887) Adj. R^2 (0.9755; 0.9865), the lowest χ^2 value (0.3976, 0.2782), RMSE (0.52741, 0.6306), AIC (−7.3122, −4.8106), AIC_c (−0.5122, 1.9894) and BIC (−7.4204, −4.9188) and thus this can be selected as the best fit model for TVB-N prediction in rohu fish stored at 0 and 5°C , respectively. After a complete interpretation, it was found that the TVB-N curve was not captured fully the whole storage phenomena, where it was hypothesized that an asymptote is expected. The asymptote model could be a better fit for this study, although no asymptote is observed.

Modeling of Microbial Growth and Effect of Temperature on Model Parameters

Predictive microbiology is now a possible alternative to traditional microbiological assessment of food safety and quality. Various environmental factors on the growth of microorganisms have since been quantified in laboratory media, and kinetic models have been developed (Dalgaard and Huss, 2020). However, for most fish products, the microorganisms responsible for spoilage are not known. Furthermore, the spoilage microflora is also likely to change when storage conditions (e.g., temperature

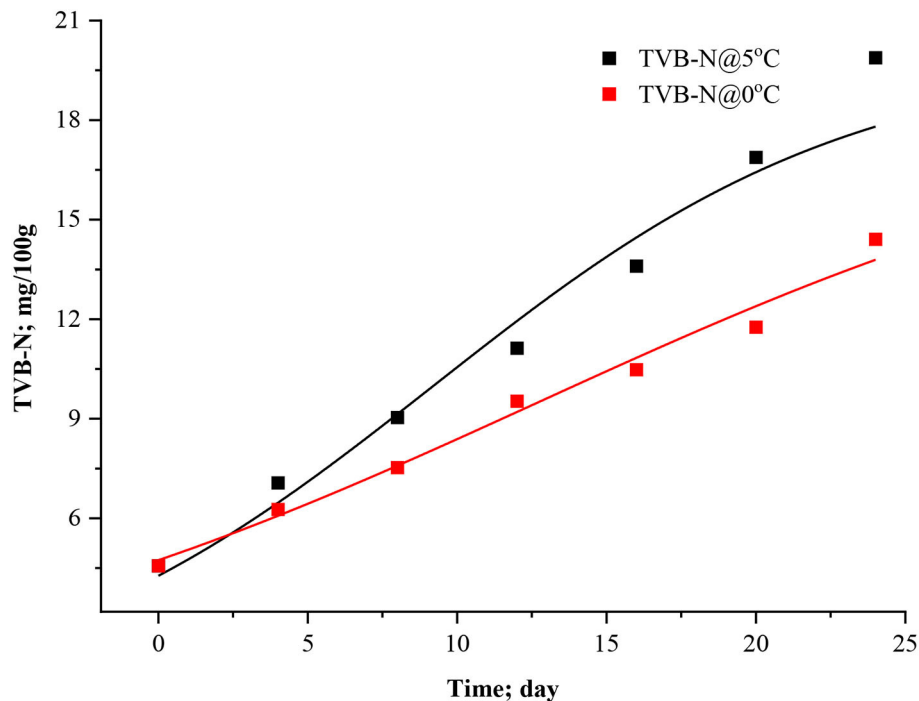


FIGURE 4 | Adapted Howgate model curve for TVB-N in stored Rohu fish.

and atmosphere) are changed over wide ranges. This dynamic nature of the microbial spoilage process indicates that specific spoilage organisms' spoilage domains must be determined before kinetic models can be developed. Sometimes, interpreting growth curves and growth parameters of non-specific microbial groups is always a complex undertaking since they represent the sum of growth curves of a mix of different microorganisms. Nevertheless, in the present study, specific spoilage bacteria were not determined; instead, total viable count (TVC) was calculated for dynamical analysis. At the first stage, three-parameter models (logistic, modified logistic, and Gompertz) and after that, four-parameter models such as modified Gompertz were fitted to microbial experimental data of stored Rohu. **Figures 5–8** represented the logistic, modified logistic, Gompertz, and modified Gompertz model curve. All the model equations are appended below:

The logistic model (Equation 12), initially proposed by Verhulst in the 18th centuries, is been a widely used model of organisms' growth dynamics in a finite resource habitat. It has opened the framework of more elaborative models like Baranyi and Roberts (1994) and others (Peleg et al., 2007). It represents the momentary growth rate of a microbial population in a virgin environment. There is a lot to explore about the habitat and resources. Thus, this study considered this model as a comparative mode and further exploitation of multi-parametric models as deemed fit to explore the microbial growth dynamics in stored rohu fish.

$$m = \frac{a}{1 + e^{-k(t-c)}} \quad (12)$$

Parameter "a" represents the difference of microbial biomass at lower and higher asymptote of Equation 12. The k is for growth rate, and c describes the carrying capacity of the biomass dynamics, and M is the microbial population after time t . Another modification like the modified logistic model is conceptualized by introducing another parameter like "b" ($b > 0$) depends upon temperature and other environmental factors; c without carrying capacity.

$$m = \frac{a}{1 + be^{-kt}} \quad (13)$$

A general Gompertz model expression (Equation 14) of three parameters was used to understand the microbial biomass during rohu fish storage as the Gompertz model and Baranyi and Roberts (1994) have been extensively used in the literature. The further extension of the Gompertz model in the form of modified Gompertz equation, as reported previously (Zwietering et al., 1991). Equation 15 represents the modified Gompertz model having some response factors such as lag phase duration (t_l) and maximal growth rate (μ_{\max}). This model has four parameters that can explain the storage conditions having an influence on the rohu fish.

$$m = \frac{a}{e^{(e^{-k(t-t_l)})}} \quad (14)$$

$$m = m_0 + \frac{a}{e^{\left[\left\{2.7182\mu_{\max} \frac{t-t_l}{a}\right\} + 1\right]}} \quad (15)$$

The data presented in **Table 3** imply the model and statistical parameters estimated after data fitting to different models

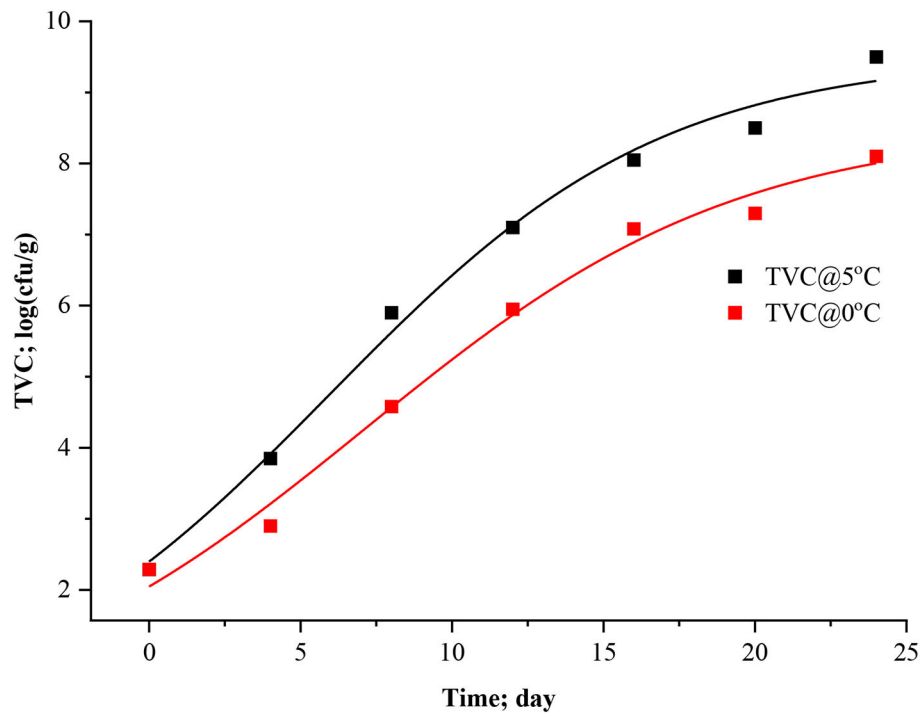


FIGURE 5 | Logistic model curve for TVC in in stored Rohu fish.

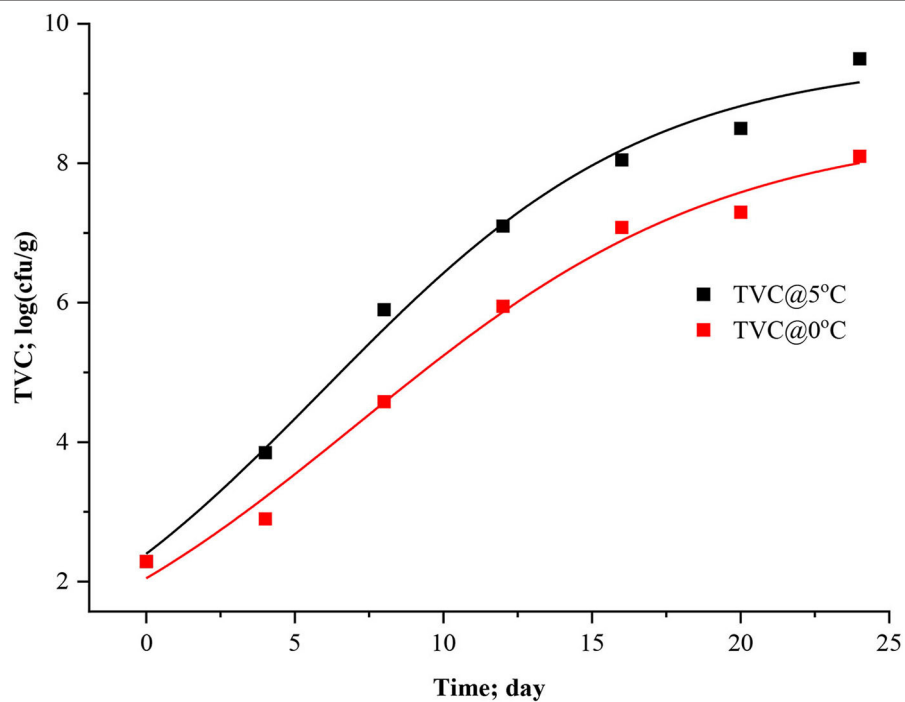


FIGURE 6 | Modified logistic model curve for TVC in stored Rohu fish.

(Equations 12, 13, 14, and 15). In light of this literature, discussion, and criticisms, all these models were considered curve fitting analysis to understand the dynamics of microbiological

assisted volatile formation to find the best fit model for predicting the freshness of stored Rohu fish under limited controlled refrigerated storage. The values range varied from $9.5031 \pm$

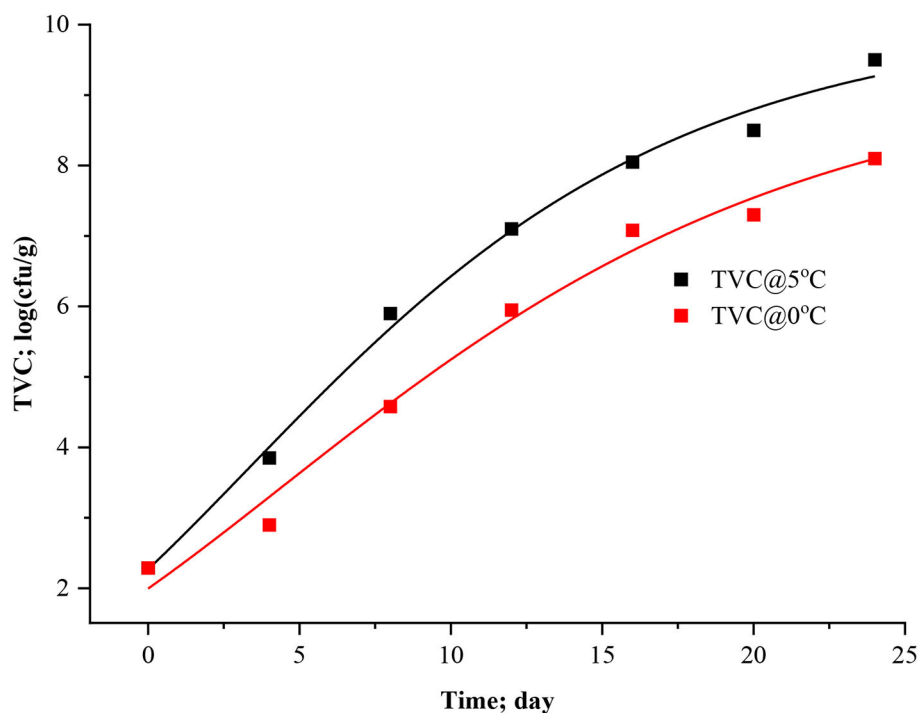


FIGURE 7 | Gompertz model curve for TVC in stored Rohu fish.

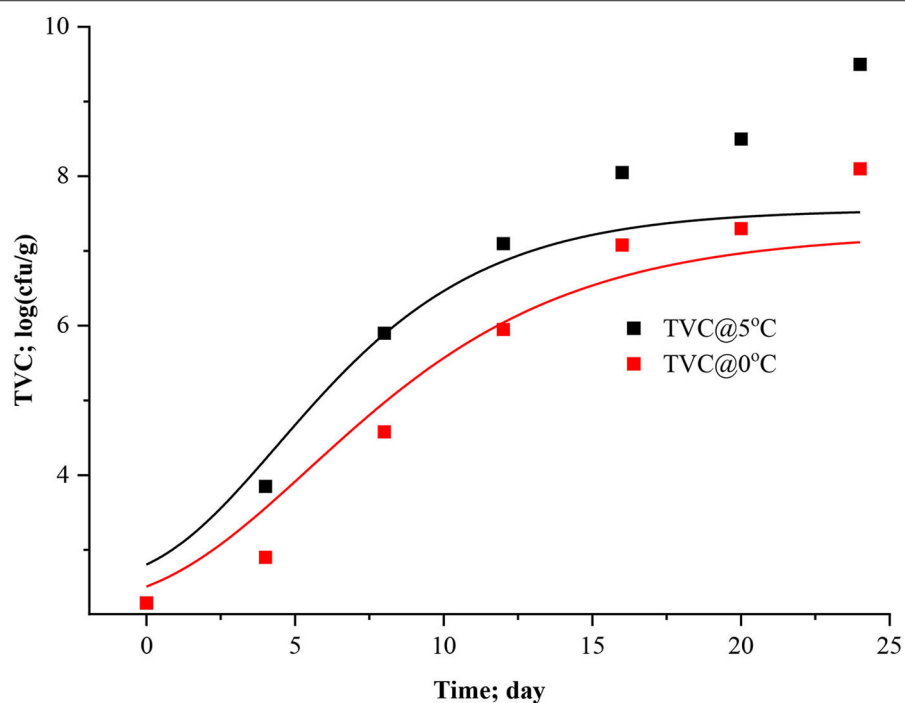


FIGURE 8 | Modified Gomperts model curve for TVC of Rohu fish stored.

0.3533 to 5.8469 ± 0.4564 , 9.5031 ± 0.3534 to 8.5469 ± 0.4564 , 10.0799 ± 0.4297 to 9.4356 ± 0.9688 and 5 ± 3.190 to 5 ± 2.455 for logistic and Gompertz and modified Gompertz model.

The Gompertz model's carrying capacity (c) was found to be ranged from 3.3349 ± 0.4799 and 4.4769 ± 1.2541 . The maximal growth rate (μ_{\max}) values were 0.4602 ± 0.41115 and 0.3631

TABLE 3 | Model and statistical parameters of different empirical models for microbial growth in stored Rohu fish.

Parameters	Mathematical models				
	Temperature (°C)	Logistic	Modified logistic	Gompertz	Modified gompertz
a	5	9.5031 ± 0.3533	9.5031 ± 0.3534	10.0799 ± 0.4297	5 ± 3.71903
	0	8.5469 ± 0.4564	8.5469 ± 0.4564	9.4356 ± 0.9688	5 ± 2.45512
b	5		2.9634 ± 0.3349		
	0		3.1264 ± 0.3688		
K	5	0.1822 ± 0.02119	0.1822 ± 0.0212	0.1197 ± 0.0137	
	0	0.15999 ± 0.0218	0.1599 ± 0.0218	0.0963 ± 0.0209	
m ₀	5				2.5550 ± 3.0840
	0				2.2439 ± 1.8525
μ _{max}	5				0.4602 ± 0.4115
	0				0.3631 ± 0.1772
t _l	5				0.4 ± 0.0231
	0				0.4 ± 0.0215
c	5	5.9623 ± 0.6361		3.3344 ± 0.4799	
	0	7.1246 ± 0.9393		4.4769 ± 1.2542	
χ ²	5	0.0823	0.0823	0.0537	2.0169
	0	0.0769	0.0769	0.1071	0.6329
R ²	5	0.9919	0.9919	0.9947	0.8518
	0	0.9899	0.9899	0.9859	0.9379
Adj. R ²	5	0.9879	0.9879	0.9921	0.7037
	0	0.9848	0.9848	0.9788	0.8758
RMSE	5	0.28683	0.2868	0.23187	1.42021
	0	0.2682	0.2682	0.31791	0.79556
SSr	5	0.32909	0.32909	0.21506	6.05096
	0	0.28772	0.28772	0.40427	1.89876
AIC	5	−15.401	−15.401	−18.379	6.98015
	0	−16.342	−16.342	−13.961	−1.133
AICc	5	−3.4013	−3.4013	−6.3792	28.9801
	0	−4.3417	−4.3417	−1.9611	20.867
BIC	5	−15.564	−15.564	−18.542	6.76379
	0	−16.504	−16.504	−14.123	−1.3493

± 0.1772 day^{−1} for the rohu samples stored at 5 and 0°C. The statistical parameters of model fitting ranged from 0.0823 to 0.0769, 0.0823–0.0769, 0.0537–0.1071 and 2.0169–0.6329 (χ²) and 0.9919–0.9899, 0.2291–0.9899, 0.9947–0.9859 and 0.8518–0.9379 (R²). From the analysis of model parameters, the Gompertz model was found to be the best fit model for microbial biomass prediction in rohu fish stored at 5°C (R² = 0.9947, χ² = 0.0537), having lowest AIC (−18.379), AIC_c (−6.3792), and BIC (−18.542). In contrast, both of logistic and modified logistic models were best suited at 0°C storage condition (R² = 0.9919, χ² = 0.0823, RMSE = 0.28683) as it showed the lowest AIC (−16.342), AIC_c (−3.4013) and BIC (−14.123) values. It has been evident from the literature that most researchers have modeled the microbial growth of specific species and strains. Antunes-Rohling et al. (2019) studied modeling of microbial growth in terms of different microbial groups such as Aerobic Mesophiles, Anaerobic Mesophiles, Aerobic Psychrotrophes, Anaerobic Psychrotrophes, Pseudomonas, Shewanella, Lactic Acid Bacteria, Enterobacteriaceae, Molds, and Yeasts. He examined these analyses in modified-atmosphere-packed hake (*Merluccius merluccius*) filets stored at different temperatures

ranging from 1–10°C. The present study's model curve and statistical parameters were found in line with Antunes-Rohling et al. (2019). Moreover, it is recommended to explore further growth modeling of a specific group of microorganisms under more range of storage temperatures. Overall, as a future study, it is recommended to go for higher no of data points (days of storage) to make the modeling process more robust and highly significant.

CONCLUDING REMARKS

In this study, mathematical models for the formation of TVB-N and microbial biomass were studied in order to predict the freshness of rohu fish stored under 0 and 5°C. The model fitting and its analysis was done along with the estimation of statistical and model parameters. Based on curve fitting statistical parameters, an exponential model was found the best fit model for predicting TVB-N biomass in rohu fish stored at 0 and 5°C. The exponential model fitting showed the highest R², the lowest χ², AIC, AIC_c, and BIC. The Gompertz model was found to be the best fit model for microbial biomass prediction in rohu

fish stored at 5°C. Whereas, logistic and modified models were best suited for 0°C storage conditions. The finding of this study can be helpful in the prediction of the freshness of rohu fish. In addition, it may help in designing and understanding cold chain logistics. It is to ponder that new research and technological development can make such measurement and mathematical analysis more accessible, faster, and non-destructive. These analyzed models under the present experimental conditions would produce a reliable statistic of the preliminary and initial conditions. However, TVB-N formation is the primary function of microbial and enzymatic actions. In the future, assuming no enzymatic conditions, a separate mechanistic model may be developed, which would predict TVB-N as a function of the microbial population.

DATA AVAILABILITY STATEMENT

The raw data supporting the conclusions of this article will be made available by the authors, without undue reservation.

REFERENCES

- Abbas, K. A., Mokhtar, A. S., Sapuan, S. M., and Mawlood, M. K. (2005). Quality deterioration of Malaysian patin fish during cold storage. *J. Food Agric. Environ.* 3, 88–91.
- Antonacopoulos, N. (1968). "Handbuch der Lebensmittelchemie," in *Bd III/2*, ed I. Acker (Berlin: Springer), 1493–1494.
- Antunes-Rohling, A., Artaiz, Á., Calero, S., Halaihel, N., Guillén, S., Raso, J., et al. (2019). Modelling microbial growth in modified-atmosphere-packed hake (*Merluccius merluccius*) fillets stored at different temperatures. *Food Res. Int.* 122, 506–516. doi: 10.1016/j.foodres.2019.05.018
- Baixas-Nogueras, S., Bover-Cid, S., Vidal-Carou, M. C., and Veciana-Nogues, M. T. (2001). Volatile and non-volatile amines in Mediterranean hake as function of their storage temperature. *J. Food Sci.* 66, 83–88. doi: 10.1111/j.1365-2621.2001.tb15586.x
- Baranyi, J., and Roberts, T. A. (1994). A dynamic approach to predicting bacterial growth in food. *Int. J. Food Microbiol.* 23, 277–294. doi: 10.1016/0168-1605(94)90157-0
- Broekaert, K., Nosedá, B., Heyndrickx, M., Vlaemynck, G., and Devlieghere, F. (2012). "The spoilage microbiota of ray (*Raja* sp.) during ice storage under different conditions: molecular identification and characterization of the spoilage potential," in *Molecular Identification of the Dominant Microbiota and Their Spoilage Potential of Crangon Crangon and Raja Sp.* (Ghent: Ghent University), 93–118.
- Cheng, J. H., Sun, D. W., Zeng, X. A., and Liu, D. (2015). Recent advances in methods and techniques for freshness quality determination and evaluation of fish and fish fillets: a review. *Crit. Rev. Food Sci. Nutr.* 55, 1012–1225. doi: 10.1080/10408398.2013.769934
- Chouhan, A., Kaur, B. P., and Rao, P. S. (2015). Effect of high-pressure processing and thermal treatment on quality of hilsa (*Tenualosailisha*) fillets during refrigerated storage. *Innov. Food Sci. Emerg. Tech.* 29, 151–160. doi: 10.1016/j.ifset.2015.03.016
- Connell, J. J. (1990). "Methods of assessing and selecting for quality," in *Control of Fish Quality*, 3rd Edn, ed J. J. Connell (Oxford: Fishing News Books), 122–150.
- Dalgaard, P., Gram, L., and Huss, H. H. (1993). Spoilage and shelf-life of cod fillets packed in vacuum or modified atmospheres. *Int. J. Food Microbiol.* 19, 283–294. doi: 10.1016/0168-1605(93)90020-H
- Dalgaard, P., and Huss, H. H. (2020). "Mathematical modeling used for evaluation and prediction of microbial fish spoilage," in *Seafood Safety, Processing, and Biotechnology*, eds F. Shahidi, Y. Jones, and D. D. Kitts (Boca Raton, FL: CRC Press), 73–89. doi: 10.1201/9781003075899-10
- Downes, F. P., and Ito, K. (2001). *Compendium of Methods for the Microbiological Examination of Foods*, 4th Edn. Washington, DC: American Public Health Association. doi: 10.2105/9780875531755
- European Union Law 95/149/EC. (1995). Available online at: <http://eur-lex.europa.eu/LexUriServ/LexUriServ.do?uri=CELEX:31995D0149:~en:NOT> (accessed January 24, 2021).
- Fan, W., Chi, Y., and Zhang, S. (2008). The use of a tea polyphenol dip to extend the shelf life of silver carp (*Hypophthalmichthys molitrix*) during storage in ice. *Food Chem.* 108, 148–153. doi: 10.1016/j.foodchem.2007.10.057
- FAO/WHO (1968). "Method for the determination of total volatile basic nitrogen (TVB) in fish muscle," *Proceedings of the Presented to the Codex Committee on Fish and Fishery Products*, 3rd session (Bergen). doi: 10.1055/s-0028-1105114
- FSSAI (2015). *Manual of Methods of Analysis of Foods: Meat and Meat Products and Fish and Fish Products. Lab Manual 6*. New Delhi: Food Safety and Standards Authority of India.
- García, M. R., Cabo, M. L., Herrera, J. R., Ramilo-Fernández, G., Alonso, A. A., and Balsa-Canto, E. (2017). Smart sensor to predict retail fresh fish quality under ice storage. *J. Food Eng.* 197, 87–97. doi: 10.1016/j.jfoodeng.2016.11.006
- Giannuzzi, L., Pinotti, A., and Zaritzky, N. (1998). Mathematical modelling of microbial growth in packaged refrigerated beef stored at different temperatures. *Int. J. Food Microbiol.* 39, 101–110. doi: 10.1016/S0168-1605(97)00127-X
- Gram, L., and Dalgaard, P. (2002). Fish spoilage bacteria—problems and solutions. *Curr. Opin. Biotech.* 13, 262–266. doi: 10.1016/S0958-1669(02)00309-9
- Gram, L., and Huss, H. H. (1996). Microbiological spoilage of fish and fish products. *Int. J. Food Microbiol.* 33, 121–137. doi: 10.1016/0168-1605(96)01134-8
- Gudmundsson, G., and Kristbergsson, K. (2009). Shelf-life prediction of chilled foods. *Pred. Model. Risk Assess.* 4, 101–119. doi: 10.1007/978-0-387-68776-6_6
- Heising, J. K., Bartels, P., Van Boekel, M. A. J. S., and Dekker, M. (2014b). Non-destructive sensing of the freshness of packed cod fish using conductivity and pH electrodes. *J. Food Eng.* 124:80e85. doi: 10.1016/j.jfoodeng.2013.10.008
- Heising, J. K., Van Boekel, M. A. J. S., and Dekker, M. (2014a). Mathematical models for the trimethylamine (TMA) formation on packed cod fish fillets at different temperatures. *Food Res. Int.* 56, 272–278. doi: 10.1016/j.foodres.2014.01.011
- Howgate, P. (2010a). A critical review of total volatile bases and trimethylamine as indices of freshness of fish. Formation of the bases, and application in quality assurance. *Elec. J. Env. Agricult. Food Chem.* 9(Pt 2), 29–57.
- Howgate, P. (2010b). A critical review of total volatile bases and trimethylamine as indices of freshness of fish. Determination. *Elec. J. Env. Agricult. Food Chem.* 9(Pt 1), 29–57.

ETHICS STATEMENT

Ethical review and approval was not required for this animal study, in accordance with the local legislation and institutional requirements.

AUTHOR CONTRIBUTIONS

PP: conceptualization, experimentation, data curation, analysis, and writing original draft. PS and SP: supervision, data analysis, and editing. KD: editing and analysis. All authors contributed to the article and approved the submitted version.

ACKNOWLEDGMENTS

The authors acknowledge the Agricultural and Food Engineering Dept., IIT Kharagpur, and Food Science and Technology Dept., NIFTEM, Kundli, India, for providing necessary assistance for accomplishing the work.

- Husain, R., Suparmo, H. E., and Hidayat, C. (2016). Kinetic oxidation of protein and fat in snapper (*Lutjanus* sp) fillet during storage. *AIP Conf. Proc.* 1755:050006. doi: 10.1063/1.4958489
- Huss, H. H. (ed.). (1995). *Quality and Quality Changes in Fresh Fish*, Vol. 348. Rome: FAO.
- Jain, D., Pathare, P. B., and Manikantan, M. R. (2007). Evaluation of texture parameters of Rohu fish (*Labeo rohita*) during iced storage. *J. Food Eng.* 81, 336–340. doi: 10.1016/j.jfoodeng.2006.11.006
- Kyranas, V. R., Lougovois, V. P., and Valsamis, D. S. (1997). Assessment of shelf life of maricultured gilthead sea bream (*Sparus aurata*) stored in ice. *Int. J. Food Sci. Tech.* 32, 339–347. doi: 10.1046/j.1365-2621.1997.00408.x
- Malle, P., and Poumeyrol, M. (1989). A new chemical criterion for the quality control of fish: trimethylamine/total volatile basic nitrogen (%). *J. Food Prot.* 52, 419–423. doi: 10.4315/0362-028X-52.6.419
- Mancini, R. A., and Hunt, M. (2005). Current research in meat color. *Meat Sci.* 71, 100–121. doi: 10.1016/j.meatsci.2005.03.003
- Mehta, N. K., Elavarasan, K., Reddy, A. M., and Shamasundar, B. A. (2014). Effect of ice storage on the functional properties of proteins from a few species of fresh water fish (Indian major carps) with special emphasis on gel forming ability. *J. Food Sci. Tech.* 51, 655–663. doi: 10.1007/s13197-011-0558-y
- Mohan, M., Ramachandran, D., and Sankar, T. V. (2006). Functional properties of Rohu (*Labeo rohita*) proteins during iced storage. *Food Res. Int.* 39, 847–854. doi: 10.1016/j.foodres.2006.04.003
- O'zogul, F., Polat, A., and O'zogul, Y. (2004). The effects of modified atmosphere packaging and vacuum packaging on chemical, sensory and microbiological changes of sardines (*Sardina pilchardus*). *Food Chem.* 85, 49–57. doi: 10.1016/j.foodchem.2003.05.006
- Peleg, M. (2016). A kinetic model and endpoints method for volatiles formation in stored fresh fish. *Food Res. Int.* 86, 156–161. doi: 10.1016/j.foodres.2016.06.004
- Peleg, M., and Corradini, M. G. (2011). Microbial growth curves: what the models tell us and what they cannot. *Crit. Rev. Food Sci. Nutr.* 51, 917–945. doi: 10.1080/10408398.2011.570463
- Peleg, M., Corradini, M. G., and Normand, M. D. (2007). The logistic (Verhulst) model for sigmoid microbial growth curves revisited. *Food Res. Int.* 40, 808–818. doi: 10.1016/j.foodres.2007.01.012
- Peleg, M., Mark, D. N., and Amy, D. K. (2014). Estimating thermal degradation kinetics parameters from the endpoints of non-isothermal heat processes or storage. *Food Res. Int.* 66, 313–324. doi: 10.1016/j.foodres.2014.10.003
- Prabhakar, P. K., Srivastav, P. P., and Pathak, S. S. (2019). Kinetics of total volatile basic nitrogen and trimethylamine formation in stored Rohu (*Labeo rohita*) fish. *J. Aquat. Food Prod. Technol.* 28, 452–464. doi: 10.1080/10498850.2019.1604598
- Prabhakar, P. K., Vatsa, S., Srivastav, P. P., and Pathak, S. S. (2020). A comprehensive review on freshness of fish and assessment: analytical methods and recent innovations. *Food Res. Int.* 133:109157. doi: 10.1016/j.foodres.2020.109157
- Ruiz-Capillas, C., and Moral, A. (2001). Correlation between biochemical and sensory quality indices in hake stored in ice. *Food Res. Int.* 34, 441–447. doi: 10.1016/S0963-9969(00)00189-7
- Tsironi, T., Dermesonlouoglou, E., Giannakourou, M., and Taoukis, P. (2009). Shelf-life modelling of frozen shrimp at variable temperature conditions. *LWT Food Sci. Technol.* 42:664e671. doi: 10.1016/j.lwt.2008.07.010
- Tsironi, T. N., and Petros, S. T. (2010). Modeling microbial spoilage and quality of gilthead seabream fillets: combined effect of osmotic pretreatment, modified atmosphere packaging, and nisin on shelf life. *J. Food Sci.* 75, 243–251. doi: 10.1111/j.1750-3841.2010.01574.x
- Van Boekel, M. A. J. S. (2008). Kinetic modeling of food quality: a critical review. *Comp. Rev. Food Sci. Tech.* 7, 144–158. doi: 10.1111/j.1541-4337.2007.00036.x
- Van Boekel, M. A. J. S. (2009). *Kinetic Modeling of Reactions in Foods*. Boca Raton, FL: CRC Press. doi: 10.1201/9781420017410
- Vareltzis, K., Koufidis, D., Gavrilidou, E., Papavergou, E., and Vasiliadou, S. (1997). Effectiveness of a natural Rosemary (*Rosmarinus officinalis*) extract on the stability of filleted and minced fish during frozen storage. *Z. Lebensm. Unters. Forsch.* 205, 93–96. doi: 10.1007/s002170050131
- Whittle, K. J., and Howgate, P. (2002). *Glossary of Fish Technology Terms*. Rome: Food and Agriculture Organization of the United Nations.
- Yao, L., Luo, Y., Sun, Y., and Shen, H. (2011). Establishment of kinetic models based on electrical conductivity and freshness indicators for the forecasting of crucian carp (*Carassius carassius*) freshness. *J. Food Eng.* 107:147e151. doi: 10.1016/j.jfoodeng.2011.06.034
- Zwietering, M. H., De Koos, J. T., Hasenack, B. E., De Witt, J. C., and Van't Riet, K. (1991). Modeling of bacterial growth as a function of temperature. *Appl. Environ. Microbiol.* 57, 1094–1101. doi: 10.1128/aem.57.4.1094-1101.1991

Conflict of Interest: The authors declare that the research was conducted in the absence of any commercial or financial relationships that could be construed as a potential conflict of interest.

Publisher's Note: All claims expressed in this article are solely those of the authors and do not necessarily represent those of their affiliated organizations, or those of the publisher, the editors and the reviewers. Any product that may be evaluated in this article, or claim that may be made by its manufacturer, is not guaranteed or endorsed by the publisher.

Copyright © 2021 Prabhakar, Srivastav, Pathak and Das. This is an open-access article distributed under the terms of the Creative Commons Attribution License (CC BY). The use, distribution or reproduction in other forums is permitted, provided the original author(s) and the copyright owner(s) are credited and that the original publication in this journal is cited, in accordance with accepted academic practice. No use, distribution or reproduction is permitted which does not comply with these terms.



Comparison of Physicochemical Changes and Water Migration of *Acinetobacter johnsonii*, *Shewanella putrefaciens*, and Cocultures From Spoiled Bigeye Tuna (*Thunnus obesus*) During Cold Storage

Xin-Yun Wang^{1,2,3,4} and Jing Xie^{1,2,3,4*}

¹ Shanghai Engineering Research Center of Aquatic Product Processing and Preservation, Shanghai, China, ² Shanghai Professional Technology Service Platform on Cold Chain Equipment Performance and Energy Saving Evaluation, Shanghai, China, ³ National Experimental Teaching Demonstration Center for Food Science and Engineering Shanghai Ocean University, Shanghai, China, ⁴ College of Food Science and Technology, Shanghai Ocean University, Shanghai, China

OPEN ACCESS

Edited by:

Santanu Basu,
Swedish University of Agricultural
Sciences, Sweden

Reviewed by:

Eduardo Esteves,
University of Algarve, Portugal
Anindya Chanda,
Mycologics LLC, United States

*Correspondence:

Jing Xie
jxie@shou.edu.cn

Specialty section:

This article was submitted to
Food Microbiology,
a section of the journal
Frontiers in Microbiology

Received: 18 June 2021

Accepted: 11 October 2021

Published: 29 October 2021

Citation:

Wang X-Y and Xie J (2021)
Comparison of Physicochemical
Changes and Water Migration
of *Acinetobacter johnsonii*,
Shewanella putrefaciens,
and Cocultures From Spoiled Bigeye
Tuna (*Thunnus obesus*) During Cold
Storage. *Front. Microbiol.* 12:727333.
doi: 10.3389/fmicb.2021.727333

This study investigates the physicochemical changes and water migration of *Acinetobacter johnsonii* (A), *Shewanella putrefaciens* (S), and cocultured *A. johnsonii* and *S. putrefaciens* (AS) inoculated into bigeye tuna during cold storage. The physicochemical indexes [fluorescence ratio (FR), total volatile base nitrogen (TVB-N), thiobarbituric acid (TBA), trimethylamine (TMA), peroxide value (POV), and pH] of bigeye tuna increased cold storage. A significant decrease in trapped water was found in the AS samples, and direct monitoring of the water dynamics was provided by low-field nuclear magnetic resonance. Samples inoculated with *A. johnsonii* and *S. putrefaciens* also induced the degradation of myofibrillar proteins and weakness of some Z-lines and M-lines. Higher values of physicochemical indexes and water dynamics were shown in the coculture of *S. putrefaciens* and *A. johnsonii* than in the other groups. Therefore, this paper reveals that the coculture of *A. johnsonii* and *S. putrefaciens* resulted in a bigeye tuna that was more easily spoiled when compared to the single culture. This study provides insight into the spoilage potential of *A. johnsonii* and *S. putrefaciens* during cold storage, which further assists in the application of appropriate technologies to keep the freshness of aquatic foods.

Keywords: Bigeye tuna (*Thunnus obesus*), spoilage potential, *Acinetobacter johnsonii*, *Shewanella putrefaciens*, muscle microstructure, bigeye tuna

INTRODUCTION

Bigeye tuna (*Thunnus obesus*) is one of the most abundant abyssal pelagic fish species throughout the world. As the demand for bigeye tuna increased, bigeye tuna have gained much attention for their high nutritional value (Wang and Xie, 2019; Andrews et al., 2020). It is well known that bigeye tuna is known for its high-quality source of animal protein and low fat. Bigeye tuna spoilage is

influenced by high water content and microbial activities (Wang and Xie, 2020a). Through low-field nuclear magnetic resonance (LF-NMR) analyses, the water migration and content of bigeye tuna were non-invasively and accurately monitored during cold storage (Sun et al., 2019; Wang and Xie, 2019). T_2 transverse relaxation time was correlated with physicochemical parameters, such as water-holding capacity, TCA-soluble peptide, hardness, chewiness, TVB-N and K -value (Wang and Xie, 2019). This correlation was developed to estimate the quality of surf clams (Wang et al., 2020a), sea cucumbers (Tan et al., 2018), vegetables, fruit (Sun et al., 2019), and beef (Cheng et al., 2019). All the results indicate that LF-NMR is an effective method to monitor water migration and predict quality changes of food during cold storage. Due to the water loss and storage temperature used, fish quality deterioration is generally related to structural changes in muscle that are also induced by lipid oxidation, protein degradation, and proteolysis (Mousakhani-Ganjeh et al., 2016; Sobieszczkańska et al., 2020). The quality deterioration of bigeye tuna results in reduced texture, and nutritional value contributes to harmful components that may even cause health issues for humans. To keep aquatic food fresh, cold storage is a convenient and effective method that can slow microorganism growth and endogenous enzyme activity to prevent aquatic food quality deterioration.

Although cold storage retards the growth of microorganisms, many bacteria can grow and generate spoilage metabolites, which cause pollution of aquatic products called specific spoilage organisms (SSOs) during storage. *Shewanella* spp. and *Acinetobacter* spp. are well-known gram-negative bacteria and have been isolated from aquatic food during cold storage (Odeyemi et al., 2018; Parlapani et al., 2019). These microorganisms were the main contributors of TVB-N, putrefactive flavor, trimethylamine, amines, and proteolysis in aquatic food (Li et al., 2019). Hence, bacterial metabolism plays a key role in evaluating the quality of aquatic food. Many research on aquatic food quality during cold storage has mainly focused on the spoilage potential of *Shewanella* spp. (e.g., Yan and Xie, 2020), *Acinetobacter* spp. (e.g., Carvalho et al., 2016), respectively. Many bacteria were raised during the early stage of cold storage, while *Shewanella* spp. and *Acinetobacter* spp. tended to become the major SSO during the early stage of cold storage. Previous studies have shown that *S. putrefaciens* has been found to dominate the SSO of aquatic food, such as bigeye tuna (Wang and Xie, 2019) and yellowfin tuna (Susanto et al., 2011) stored at 4°C, which can produce high levels of alcohols, aldehydes, 1-octen-3-ol, esters, alkanes, nitrogen and sulfur, causing strong off-odors. Meanwhile, *S. putrefaciens* can form biofilms that cause the sticky surface of aquatic products and are capable of producing H_2S (Yan and Xie, 2020). Therefore, the growth of *S. putrefaciens* as an aquatic food spoilage marker is necessary to limit the shelf life at low storage temperatures. In a previous study we demonstrated that *A. johnsonii* was isolated and identified as an SSO from bigeye tuna. We found that the TVB-N, TMA, and pH values to evaluate the spoilage potential of *A. johnsonii* increased as storage time increased (Wang and Xie,

2020b). Moreover, some lipid contents changed dramatically by culturing *A. johnsonii*, which directly accelerated the quality deterioration of bigeye tuna by lipid metabolites (Wang and Xie, 2020a). However, the effect of interactions between the growth and metabolism of two bacteria in aquatic food spoilage has been neglected.

Therefore, this study was conducted to further provide information about the interactions between *A. johnsonii* and *S. putrefaciens* on the quality deterioration of bigeye tuna during cold storage. Bacterial growth, physicochemical indexes, lipid oxidation [thiobarbituric acid (TBA), peroxide value (POV), fluorescence ratio (FR)], protein degradation (proteolytic activities, myofibril protein changes), water dynamics, and muscle structural changes were investigated. Furthermore, the spoilage mechanism of the cocultured *A. johnsonii* and *S. putrefaciens* was elucidated, providing novel insights into the aquatic food spoilage mechanism and inhibiting microbial growth to enhance the quality of aquatic foods for future research.

MATERIALS AND METHODS

Bacterial Strains and Reagents

Bigeye tuna steaks (Zhejiang Fenghui Ocean Fishing Company Ltd., China) were stored at 4°C until spoilage. Twenty-five grams of spoiled bigeye tuna was aseptically collected, mixed with 225 mL of sterile 0.85% NaCl solution and homogenized for 1 min. A 0.1 mL suitable dilution was spread on the surface of plate count agar and incubated at 30°C for 72 h. The two species (*A. johnsonii* and *S. putrefaciens*) were identified by 16S rRNA gene sequences and a VITEK® 2 CompactA system (BIOMÉRIEUX, France) and stored at -80°C. *A. johnsonii* (accession number CP070866) and *S. putrefaciens* (accession number CP070865) were thawed and cultured in tryptose soya broth at 30°C overnight until the maximal concentration (10^8 CFU/mL) was reached. The coculture was defined as a mixture of equal amounts (v/v) of *S. putrefaciens* and *A. johnsonii*.

Sterile Fish Juice and Sterile Fish Block Preparation

The preparation of sterile fish juice from the back muscle of bigeye tuna (2 kg) was modified from Jia et al. (2020). Bigeye tuna filets were minced, and distilled water was added to mixed muscle at a ratio of 1:1 (water: fish, w/w). The mixture was boiled for 5 min and filtered after cooling. Then, the filtrate was centrifuged at 4200 r/min for 30 min, and the supernatant was obtained. Each liter of fish juice was supplemented with 1.6 g of trimethylamine oxide, 40 mg of L-cysteine and 40 mg of L-methionine. The supernatant was collected and autoclaved at 121°C for 15 min. A 0.1 mL bacterial suspension was aseptically pipetted into 200 mL of sterile fish juice. The sterile fish juice was stored at 4°C. The fish juice was used for microbiological growth analysis, TVB-N, TMA, pH, TBA, POV, FR, and proteolytic activity analyses.

Sterile fish blocks were prepared from bigeye tuna according to the procedure of Wang and Xie (2020b). Sterile fish blocks were used to determine T_2 transverse relaxation time, water holding capacity (WHC), and muscle microstructure (scanning electron microscopy and transmission electron microscopy) analyses.

The samples were divided into groups according to the method of Niu et al. (2018); Jia et al. (2020), and Wang and Xie (2020b): (a) A control was prepared by adding sterile water into bigeye tuna blocks/juice supplemented with sterile water, (b) *A. johnsonii* suspensions were independently inoculated into sterile fish blocks/juice with an inoculation level of approximately 5 log (CFU/mL), (c) *S. putrefaciens* suspensions were independently inoculated into sterile fish blocks/juice with an inoculation level of approximately 5 log (CFU/mL), and (d) *A. johnsonii* and *S. putrefaciens* suspensions were mixed at a ratio of 1:1 and then inoculated on bigeye tuna blocks/juice with an initial bacterial level of 5 log (CFU/mL).

Microbiological Growth Analysis

The TVC of bigeye tuna was measured each day. The TVC was determined according to a previously described method (Wang et al., 2017). The results were expressed as colony-forming units in log CFU/mL.

Physicochemical Indexes

pH, Total Volatile Base Nitrogen, Trimethylamine, Water Holding Capacity Value

The determination of the pH value was performed according to Chen et al. (2019). A tuna sample (5.0 g) was added to 50 mL of distilled water in a stomacher to homogenize at 8000 r/min. Then, the sample was maintained at 4°C for 30 min to obtain a supernatant. The pH of the tuna was evaluated by inserting a pH electrode (Cyberscan Model 510; Eutech Instruments Pvt. Ltd., Singapore).

The determination of the TVB-N value was performed according to Li et al. (2019). TVB-N value expressed as TVB-N mg/100 mL bigeye tuna juice. The determination of the TMA value was performed according to Li et al. (2019). TMA value expressed as mg N/100 mL bigeye tuna juice. TVB-N value and TMA value were measured by an automatic Kjeldahl instrument (UDK159;VELP SCIENTIFICA, Italy).

The WHC value was determined according to Fidalgo et al. (2020) with some modifications. A previous 2 g of bigeye tuna block (W_a) was wrapped in two filter papers and centrifuged (3,000 × g, 10 min, 4°C). After centrifugation, the surface water was drained and weighed again (W_b). WHC value was calculated using the following formula:

$$\text{WHC}(\%) = (1 - (W_a - W_b)/W_a) \times 100\%$$

Lipid Oxidation of Bigeye Tuna

Thiobarbituric Acid, Peroxide Value, Fluorescence Ratio Indexes

The determination of the TBA value was performed according to Fidalgo et al. (2020). The TBA value was measured at 532 nm and expressed as mg malonaldehyde/kg muscle sample. The TBA value was calculated using the following formula:

$$\text{TBA}(\text{mg malonaldehyde/kg}) = A_{532} \times 7.8$$

where A_{532} is the absorbance at 532 nm.

The POV value of the bigeye tuna was measured according to the AOCS method (2003). The POV value was expressed as meq oxygen/kg.

The FR of the bigeye tuna assay at 393/463 nm and 327/415 nm was measured according to Nian et al. (2020). FR results were obtained from the following formula:

$$\text{FR} = \text{RF}_{393/463 \text{ nm}}/\text{RF}_{327/415 \text{ nm}}.$$

Protein Degradation

Proteolytic Activity

Proteolytic activity was spectroscopically quantified using azocasein as the substrate (Zhu et al., 2015). The samples were centrifuged (12,000 g, 10 min, 4°C) and 100 μL of supernatant was added 500 μL of PBS (50 mmol/L, pH 7.2, Sangon Biotech Co., Ltd., China) and 100 μL of azocasein substrate solution (15 g/L in 50 mmol/L PBS, pH 7.2) to incubate at 37°C for 30 min. The reaction was stopped by an equal volume of 0.5 mol/L trichloroacetic acid standing at room temperature for 30 min. Then, the mixture was centrifuged (12,000 g, 5 min, 4°C) to obtain the supernatant and 1 mol/L NaOH were mixed, and the absorbance at 366 nm with a multiplate reader (Synergy 2, BioTek, Winooski, VT, United States).

Water Dynamics

The T_2 transverse relaxation time of the bigeye tuna was determined by LF-NMR and Carr-Purcell-Meiboom-Gill pulse sequences according to the method of Wang and Xie (2019). NMR measurements were carried out with a Meso MR23-060HeI MRI system (Niumag Electric Corporation, Shanghai, China) with a time delay between the 90° and 180° pulses (τ -value) of 300 μs. The four groups of bigeye tuna were directly used for T_2 transverse relaxation times of 0, 3, and 6 days.

Sodium Dodecyl Sulfate-Polyacrylamide Gel Electrophoresis

Myofibrillar proteins were extracted according to the method of Wang and Xie (2019). The myofibrillar proteins (obtained supernatant) of bigeye tuna were used for Sodium Dodecyl Sulfate-Polyacrylamide Gel Electrophoresis (SDS-PAGE) for 0, 2, 4, and 6 days of storage. Six microliters of each myofibrillar protein sample was loaded in a sample well for SDS-PAGE

analysis. The gels were stained with 0.1% (w/v) Coomassie Brilliant Blue R-250 in 50% (v/v) methanol for 0.5 h and destaining solution (acetic acid: methanol: water, 3 V: V:6 V) until the bands appeared to be clear.

Muscle Microstructure

Scanning Electron Microscope

Bigeye tuna samples for SEM were prepared as described previously by Deng et al. (2019). The bigeye tuna samples were prefixed with 2.5% (v/v) glutaraldehyde at 4°C overnight. Longitudinal sections of freeze-dried bigeye tuna samples were prepared for extreme-resolution analytical field emission (Tescan Mira 3 XH, Tescan, Czech Republic).

Transmission Electron Microscopy

Bigeye tuna samples for TEM were prepared according to the method described by Bao et al. (2020) with some modifications. Bigeye tuna muscle was cut into small strips (5 mm × 3 mm × 2 mm), and precooled 2.5% glutaraldehyde solid was retained overnight. The samples were fixed with osmium oxide for 2 h and subjected to 30, 50, 70, 80, 90, and 95% ethanol gradient dehydration. Thin sections (70 nm) were stained with uranyl acetate and lead citrate using a JEM-2100 transmission electron microscope (JEOL Co., Ltd, Tokyo, Japan) operating at 200 kV.

Statistical Analysis

The data for TVC, TVB-N, TMA, pH, WHC, TBA, FR, POV, proteolytic activity and T₂ transverse relaxation time were plotted using OriginPro 2020b software (Microcal, United States). All analyses were conducted with three replicates. Two-way analysis of variance and Duncan's test significant difference test using SPSS (IBM Statistical Package for the Social Sciences Ver. 22.0 software, Armonk, NY, United States) and were used to find significant differences at a level of $P < 0.05$.

RESULTS AND DISCUSSION

Changes in Microbiological Growth

Figure 1A shows the microbiological growth of bigeye tuna inoculated with a single SSO and two SSOs throughout the 6-day storage period during cold storage. The initial log TVC values of *A. johnsonii*, *S. putrefaciens* and *A. johnsonii* + *S. putrefaciens* on bigeye tuna were 5.01, 5.22, and 5.02 lg CFU/mL, respectively. The TVC of bigeye tuna showed a significant increase ($P < 0.05$) during cold storage, especially for the group inoculated with *A. johnsonii* + *S. putrefaciens* (from 5.22 to 9.34 lg CFU/mL), while the CK was below 5.0 lg CFU/mL throughout the 6-day storage period and always increased slowly. The *A. johnsonii* group achieved a maximum TVC level and showed a relatively quicker growth rate than the *S. putrefaciens* group during cold storage, suggesting that low temperature was better for *A. johnsonii* to proliferate (Wang and Xie, 2020a). Compared to CK, the TVC of *A. johnsonii* + *S. putrefaciens* group increased significantly, and coculturing was probably one of the key factors accelerating bacterial growth. These results were also similar

to previous works that the changes in TVC of the co-culture group significantly increased in refrigerated cooked shrimp (Niu et al., 2018).

Changes in pH, Total Volatile Base Nitrogen, Trimethylamine, Water Holding Capacity

At the beginning of storage, the pH value of bigeye tuna in the CK, A, S, and AS groups decreased, changing from 6.06 to 5.76, 5.89, 5.86, and 5.93, respectively (**Figure 1B**). This decreasing trend in pH was observed due to the strong ability of *A. johnsonii* and *S. putrefaciens* to breakdown ATP (Zhou et al., 2019). The pH value of the AS group was significantly higher ($P < 0.05$) than that of the other groups on day 6. This suggested that coculturing *A. johnsonii* and *S. putrefaciens* was more susceptible to bacterial growth at a high pH caused by the production of more alkaline metabolites in coculturing *A. johnsonii* and *S. putrefaciens* (Aghaei et al., 2020; Wang and Xie, 2020a). As the storage time continued to increase, the pH value increased from neutral to the alkaline range, indicating that amines and histamine were produced and autolytic activity occurred during cold storage (Don et al., 2018).

The TVB-N value was utilized to evaluate the freshness of aquatic foods. As shown in **Figure 1C**, the initial TVB-N value was 9.76 mg/100 mL (day 0) and progressively increased to 18.03 (CK), 25.59 (A group), 24.49 (S group), and 26.12 mg/100 mL (AS group) ($p < 0.05$) after 6 days of storage. Compared to the TVB-N values of the CK, the A, S, and AS groups were all higher than 20 mg/100 mL at day 4, during which the TVB-N values of these three groups reached 21.13, 20.64, and 22.37 mg/100 mL ($P < 0.05$), respectively, which is a higher value than the fresh acceptability for aquatic foods (20 mg/100 mL) (Sharifian et al., 2011). The results showed a sudden increase in the inoculated AS group when bacterial spoilage commenced with the leaching of ammonia.

The spoilage potential and volatile metabolite production among the isolates, muscle protein degradation, reduction of TMAO to TMA and production of off odor (sulfide) due to the presence of proteolytic activity were investigated. The initial TMA value was 0.63 mg/100 mL and increased storage time (**Figure 1D**). The value of TMA was significantly increased ($P < 0.05$) with an increase in CK, A, S, AS groups from 0.63 to 5.33, 16.29, 13.23, 18.15 mg/100 mL, respectively. Similar results showed that increased cold storage time led to an increase in the TMA value of tuna (Wang and Xie, 2020a). In addition, the results showed that coculturing *A. johnsonii* and *S. putrefaciens* isolated from bigeye tuna resulted in higher TMAO reduction activity. The increase in TMA value might suggest the storage process, which plays in a major role in protein degradation of bigeye tuna causing the strong ability of spoilage potential (Wang and Xie, 2019).

Changes in WHC in four groups are shown in **Figure 1E**. The initial WHC value was 84.07% and showed a continuous decline with increasing storage time. At day 6, the WHC value significantly decreased to 71.34, 68.60, 69.61, 67.60% in the CK, A, S, and AS groups, respectively. The WHC of the AS group

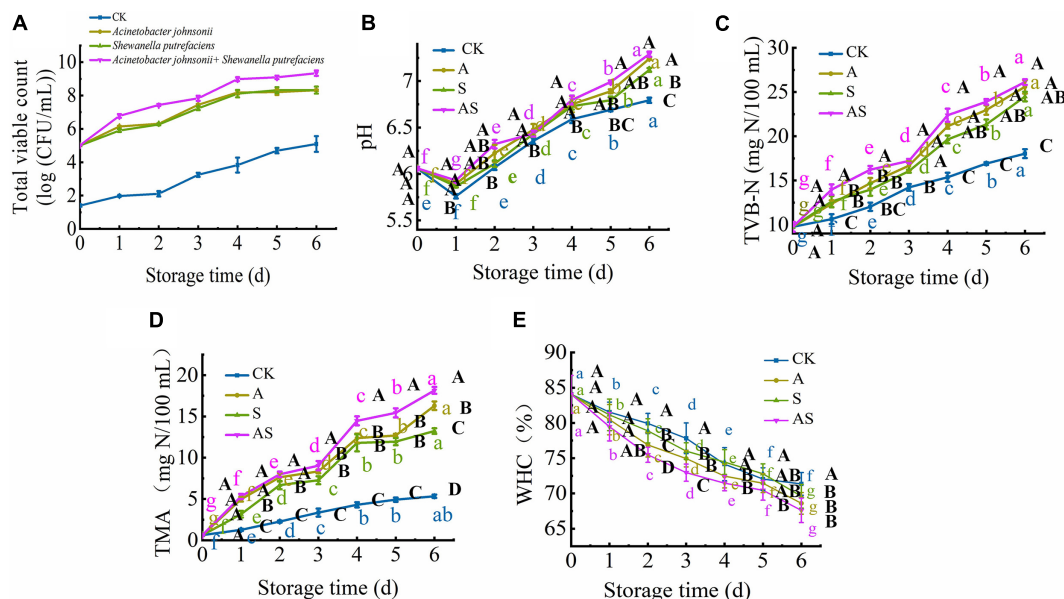


FIGURE 1 | Changes in the total viable count (TVC) (A), pH (B), total volatile base nitrogen (TVB-N) (C), trimethylamine (TMA) (D) and water holding capacity (WHC) (E) in bigeye tuna with different bacterial groups stored at 4°C for 6 days (each point is the mean value of three determinations). Different capital letters denote significant differences ($P < 0.05$) among bacterial groups at the same storage time. Different lowercase letters denote significant differences ($P < 0.05$) among the different storage times per treatment groups.

was always lower than those of the other treatment groups. This is probably because spoilage bacteria activities destroyed muscle tissue integrity during cold storage, leading to water loss of muscle (Tan et al., 2018), which was in good agreement with the results of this study (Figure 2).

Changes in Lipid Oxidation of Bigeye Tuna

Changes in Thiobarbituric Acid, Peroxide Value, FR Indexes

The TBA value is the major index for evaluating the degree of lipid oxidation, reflecting the quality of aquatic foods. The TBA value of the four groups showed a time-dependent increase during the 6 days of storage (Figure 3A). Based on the results of Le et al. (2020), the TBA value was also intensely low due to the very low lipid content in tuna, ranging between 0.24 and 1.76 mg/kg tuna juice over the 6 days of cold storage, although there was a significant increase ($p < 0.05$) at day 0. As the storage time reached day 6, the TBA value of the AS group was increased to 1.76 mg/kg and was higher than that of the other groups, indicating that co-culturing *A. johnsonii* and *S. putrefaciens* produced a large number of aldehydes and ketones by lipid automatic oxidation and hydrolysis, causing the quality deterioration of fish (Chen et al., 2019).

POV, an index of the number of hydroperoxides, evaluates the degree of lipid oxidation at the primary level of aquatic products (Cropotova et al., 2019). Figure 3B shows that the POV dramatically increased with increasing storage time. Moreover, the initial POV value was 10.15 meq/kg and increased to 30.36, 33.67, 32.67, 35.96 meq/kg on the 6th day for the CK, A, S

and AS groups, respectively. This result suggested that lipid oxidation products were continuously formed and decomposed into secondary oxidation products, leading to quality spoilage (Wang et al., 2020b). Lipid oxidative degradation of tuna in coculturing *A. johnsonii* and *S. putrefaciens* could accelerate the formation of secondary oxidation products.

Complex formation as a result of the interaction between oxidized lipids and biological amino constituents (mainly proteins, peptides, free amino acids, and phospholipids) was measured by fluorescence, including primary and secondary oxidation products of lipid oxidation. As shown in Figure 3C, there was a continuous increase in the FR value during cold storage. The FR value of the AS group was always higher than that of the other groups. FR was significantly increased after storage for 6 days compared to CK. The results suggested that co-culturing *A. johnsonii* and *S. putrefaciens* expedited lipid oxidation to acquire fluorescent growth due to exposing a variety of aldehydes, which also resulted in bacterial spoilage of tuna.

Changes in Water Dynamics

T_2 transverse relaxation has proven to be a precise technique to quantify the changes in water distribution and dynamics of aquatic foods during cold storage and thus helps to explain how these changes are estimated to aquatic food quality using LF-NMR (Wang et al., 2017, 2020a). The T_2 transverse relaxation is also displayed in Figure 3E. It is noteworthy that four main fractions can be defined as T_{2b} , T_{21} , T_{22} , and T_{23} , which were considered strongly bound water (0.1~1 ms), weakly bound water (1~10 ms), trapped water (10~100 ms), and free water

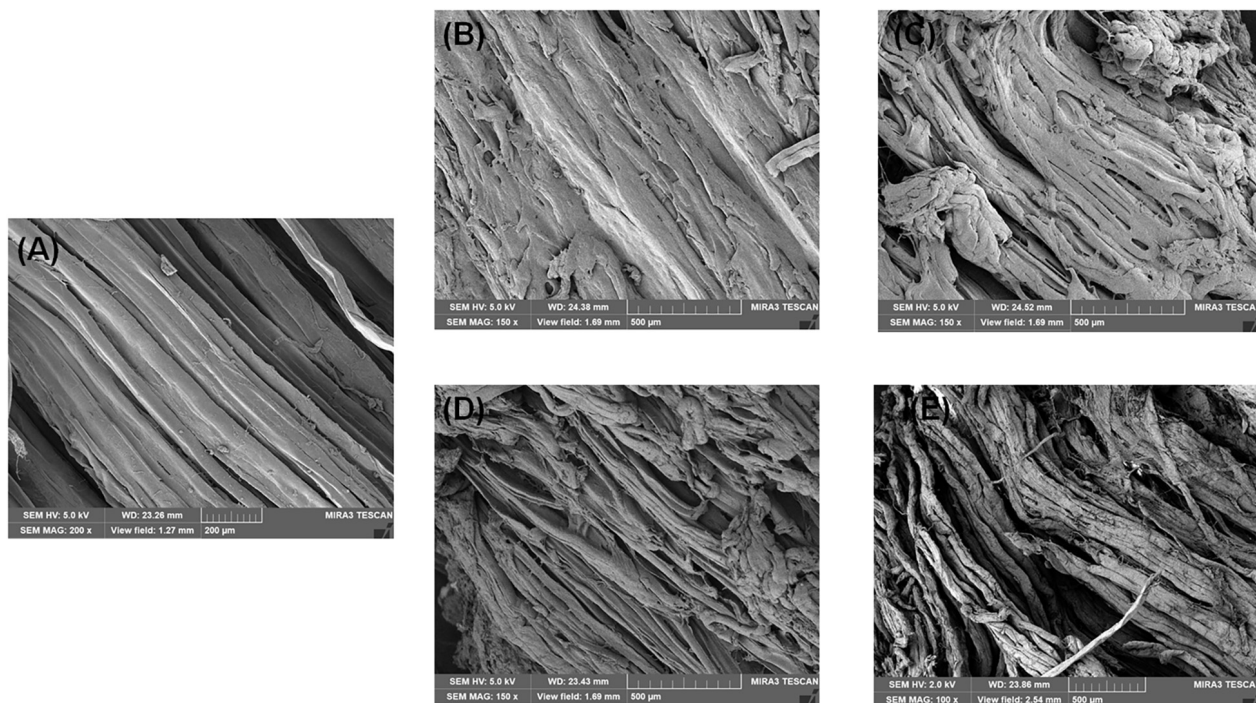


FIGURE 2 | Scanning electron microscopy (SEM) photographs of bigeye tuna muscle stored at 4°C for 0 day (A), stored at 4°C in the control group for 6 days (B), stored at 4°C in the A group for 6 days (C), stored at 4°C in the S group for 6 days (D), and stored at 4°C in the AS group for 6 days (E).

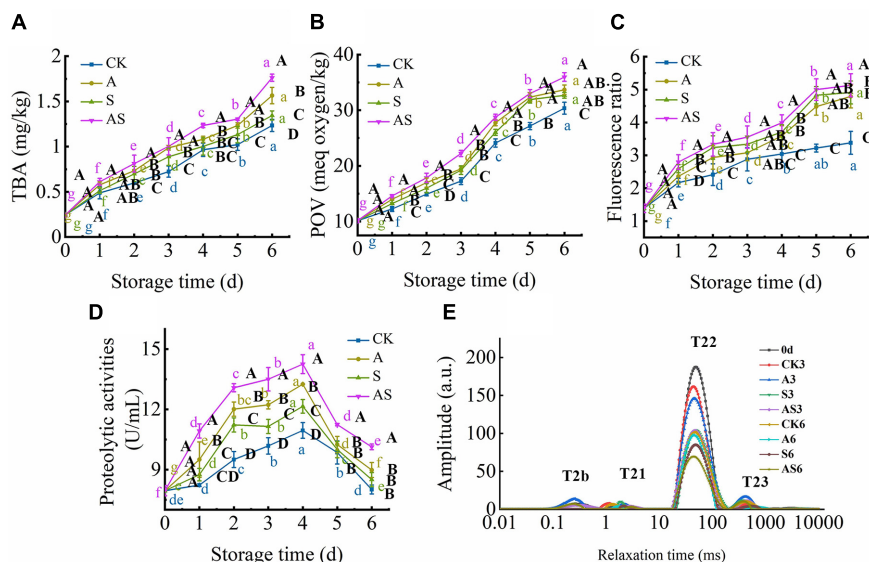


FIGURE 3 | Changes in thiobarbituric acid (TBA) (A), peroxide value (POV) (B), fluorescence ratio (FR) (C), proteolytic activities (D) and T_2 transverse relaxation time (E) in bigeye tuna with different bacterial groups stored at 4°C for 6 days (each point is the mean value of three determinations). Different capital letters denote significant differences ($P < 0.05$) among bacterial groups at the same storage time. Different lowercase letters denote significant differences ($P < 0.05$) among the different storage times per treatment groups.

(100~1,000 ms), respectively, which reflected the states of spin-lattice relaxation/spin-spin relaxation inside the bigeye tuna during cold storage (Wang et al., 2020a). The peaks of T_{2b} and T_{21} changed little with storage time in the four groups,

indicating that strongly bound water and weakly bound water were strongly related to protein macromolecules, which was in general agreement with Wang and Xie (2019). The distinct decreases in trapped water in the four groups provided a more

direct visualization of the water dynamics in bigeye tuna during cold storage. The peak of T_{21} was much higher in CK than in the treated groups, possibly due to the higher WHC in CK to maintain the void volume of the bigeye tuna muscle sample, resulting in water molecules on the muscle that was attached in water during cold storage. Specifically, trapped water showed a significant declining trend in the AS group for 6 days. These results suggested that coculturing *A. johnsonii* and *S. putrefaciens* had an effect on enzyme activity and degradation of the structure of myofibrillar proteins that proteolysis of aquatic food proteins to liberate peptides and enhanced the bioactivity of the protein, causing trapped water within the myofibrillar proteins to be lost. However, the peak of T_{23} increased due to water molecules moving to free water (Figure 3E). This result was proven to rupture the inside myofibrillar lattice membrane, resulting in the mobility of free water being enhanced by bacterial activity.

Changes in Protein Degradation of Bigeye Tuna

Changes in Proteolytic Activity

Proteolytic activity in the bacterium is examined in the presence of exogenous autoinducers, which play a key role in protein degradation and decomposition of protein into small peptides to evaluate the contribution to quality changes (Wang and Xie, 2020c). Proteolytic activity first significantly increased and then decreased (Figure 3D). A similar study showed that cold storage inhibited *A. johnsonii* and *S. putrefaciens* growth to produce protease, while protein was degraded, causing protease activity to increase as storage time increased (Wang and Xie, 2020c). At the end of storage time, small peptides were almost no longer sufficient, causing the proteolytic activity to decrease.

Changes in Sodium Dodecyl Sulfate-Polyacrylamide Gel Electrophoresis

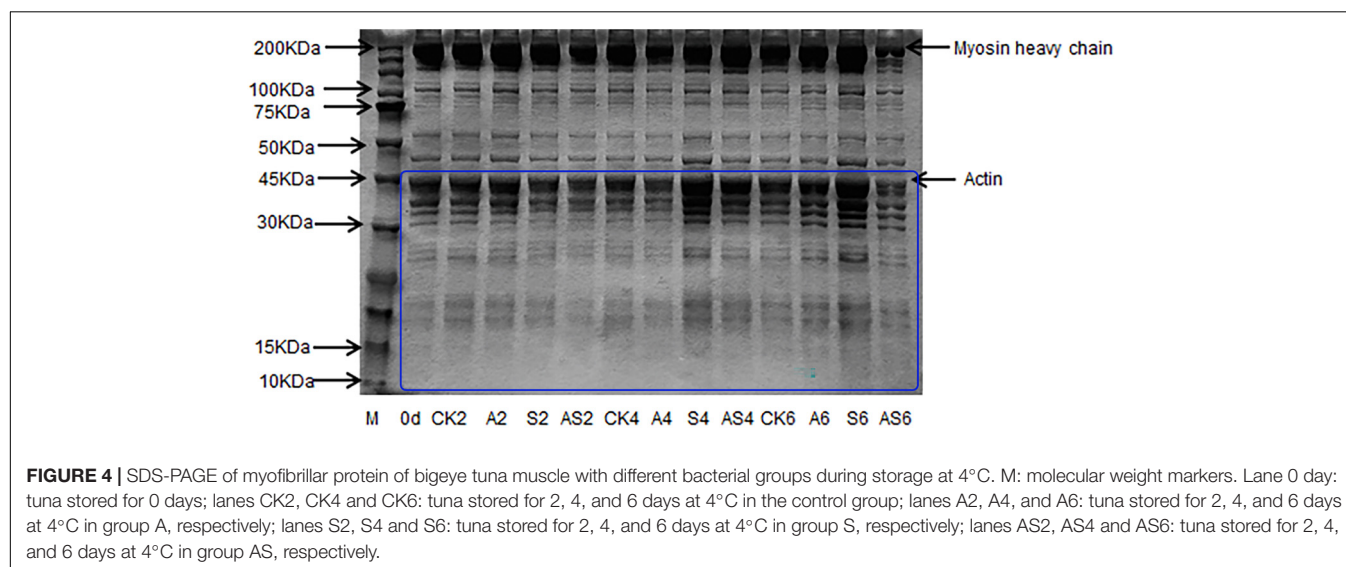
Changes in myofibrillar protein in the four groups are shown in Figure 4. In the CK, A, S, AS groups, there was apparent

myofibrillar protein breakdown as storage time increased. The intensity of the myosin heavy chain (MHC) of the bigeye tuna was reduced with the concomitant appearance of low molecular-weight fractions in gel following 4 days of storage. A similar result reported that the intensity of MHC in aquatic foods was slightly decreased during cold storage, as described by Wang and Xie (2019). The SDS-PAGE results showed a significant change in the 10–45 kDa AS group; conversely, neither myosin nor actin in the CK group was apparent during storage. These results indicated that low temperature has little effect on protein degradation. One band of approximately 45 kDa became weak in the AS group after preservation for 6 days. Interestingly, the band at 45 kDa in the S group always showed remarkably high intensity. Notable actin muscle content was observed in myofibrillar proteins from the S group. Many degradations of the bands slightly below 50 kDa were found in the AS group, which indicated that myofibrillar proteins gradually faded, including tropomyosin and actin alpha skeletal muscle, due to the microbial activity of coculturing *A. johnsonii* and *S. putrefaciens*, which produced some water-soluble small molecule protein degradation (Cropotova et al., 2019).

Microstructure Analysis

Scanning Electron Microscopy Changes in Muscle Tissues

The SEM images of the bigeye tuna muscle fiber sections are shown in Figure 2. On day 0, well-organized fibers with no damage or rupture of bigeye tuna were observed (Figure 2A). Storage for 6 days for bigeye tuna samples (Figures 2B–E) induced varying degrees of cracks inside the muscle fiber sections. As storage time increased, the muscle myofibril structure was disrupted and disordered due to protein degradation by proteolytic activity and water loss (Bao et al., 2020), which was in accordance with the previous work for Figures 3D,E. For samples stored at 6 days in the AS group (Figure 2E), there was visible deterioration of muscle fibers. These evolutions of myofibril



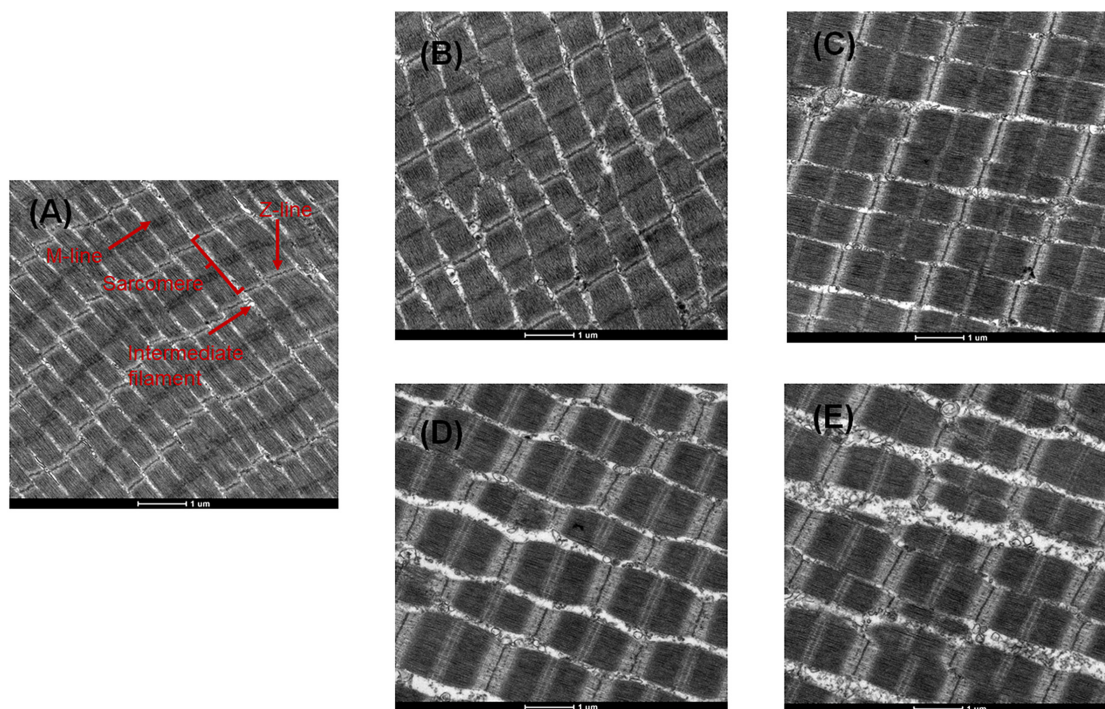


FIGURE 5 | Transmission electron microscopy (TEM) photographs of bigeye tuna muscle stored at 4°C for 0 day **(A)**, stored at 4°C in the control group for 6 days **(B)**, stored at 4°C in the A group for 6 days **(C)**, stored at 4°C in the S group for 6 days **(D)**, and stored at 4°C in the AS group for 6 days **(E)**.

structure might be due to the coculturing of *A. johnsonii* and *S. putrefaciens*, which verified that excess microorganism load could cause the gap between myofibril tissue with large changes in texture or high dehydration of the muscle fibers (Fidalgo et al., 2020). Meanwhile, the muscle fiber changes of the two SSOs in inoculated bigeye tuna samples could also influence the water-holding capacity. Therefore, the SEM results seemingly confirm the results of the T_2 transverse relaxation time; these disordered arrangements and numerous ruptures of fibers caused water dynamics.

Transmission Electron Microscopy Changes Myofibrils Muscle

TEM images of myofibril structural changes from bigeye tuna are shown in **Figure 5**. On day 0, well-organized muscle filaments, cytoskeletons, Z-lines, M-lines, I bands, and A bands were observed. With the extension of storage time, the cytoskeleton showed minor changes between 0 and 6 days in CK, while inter-myofibrillar spaces generally expanded, which was similar to the myofibrilla changes in black carp during cold storage (Bao et al., 2020). After 6 days, A, S, AS samples showed significantly destroyed membranes, and some Z-lines and M-lines were weakened and degraded (**Figures 5B–E**). Moreover, the increased space to the breakdown of intermyofibrillar links was generally complex and larger in the AS group than in the other groups. For the AS sample stored at 4°C for 6 days, inoculation of myofibrillar proteins with *A. johnsonii* and *S. putrefaciens* caused obvious ultrastructural changes in myofibrils, which were mainly

characterized in the thin I band near the Z-lines. The results indicated that *A. johnsonii* and *S. putrefaciens* had synergistic effects to accelerate the breakage of the sarcoplasmic reticulum and severe degradation of protein structures, evidenced by near the Z-line and discontinuous Z-disk.

CONCLUSION

The bacterial growth, physicochemical indexes, lipid oxidation, protein degradation, water dynamics and muscle structural changes of sterile bigeye tuna flesh/juice inoculated with *A. johnsonii* (A) and *S. putrefaciens* (S) and coculture with *A. johnsonii*, and *S. putrefaciens* (AS) were investigated. As storage time increased, AS group grew faster than the other groups and had the highest values of TBA, POV, and FR, indicating that coculture with *A. johnsonii* and *S. putrefaciens* had stronger corruption-inducing lipid oxidation. The results showed that the decreases in T_{21} (trapped water) and protein degradation in the AS group during cold storage can be visualized by LF-NMR and SDS-PAGE, respectively. Based on SEM and TEM analysis, microstructural changes in samples inoculated with *A. johnsonii* and *S. putrefaciens* were accompanied by the degradation of myofibrillar proteins (Z-line, M-line, sarcoplasmic reticulum) and the deterioration of muscle fibers during cold storage. These spoilage indexes were observed in lipid oxidation, protein degradation and water loss in bigeye tuna. This study provides an understanding of the spoilage mechanism of coculturing SSOs to help estimate aquatic food quality and shelf-life extension.

DATA AVAILABILITY STATEMENT

The original contributions presented in the study are included in the article/supplementary material, further inquiries can be directed to the corresponding author/s.

AUTHOR CONTRIBUTIONS

X-YW: writing—original draft, data curation, methodology, investigation, and formal analysis. JX: validation, review and editing, project administration, and funding acquisition.

REFERENCES

- Aghaei, Z., Ghorani, B., Emadzadeh, B., Kadjhodaee, R., and Tucker, N. (2020). Protein-based halochromic electrospun nanosensor for monitoring trout fish freshness. *Food Control*. 111:107065. doi: 10.1016/j.foodcont.2019.107065
- Andrews, A. H., Pacocco, A., Allman, R., Falterman, B. J., Lang, E. T., and Golet, W. (2020). Age validation of yellowfin (*Thunnus albacares*) and bigeye (*Thunnus obesus*) tuna of the northwestern Atlantic Ocean. *Can. J. Fish. Aquat. Sci.* 77, 637–643. doi: 10.1139/cjfas-2019-0328
- Bao, Y., Wang, K., Yang, H., Regenstein, J. M., Ertbjerg, P., and Zhou, P. (2020). Protein degradation of black carp (*Mylopharyngodon piceus*) muscle during cold storage. *Food Chem.* 308:125576. doi: 10.1016/j.foodchem.2019.125576
- Carvalho, A., Ferreira, V., Silva, J., and Teixeira, P. (2016). Enrichment of *Acinetobacter* spp. from food samples. *Food Microbiol.* 55, 123–127. doi: 10.1016/j.fm.2015.11.002
- Chen, H., Wang, M., Yang, C., Wan, X., Ding, H. H., Shi, Y., et al. (2019). Bacterial spoilage profiles in the gills of Pacific oysters (*Crassostrea gigas*) and Eastern oysters (*C. virginica*) during refrigerated storage. *Food Microbiol.* 82, 209–217. doi: 10.1016/j.fm.2019.02.008
- Cheng, S., Wang, X., Li, R., Yang, H., Wang, H., Wang, H., et al. (2019). Influence of multiple freeze-thaw cycles on quality characteristics of beef semimembranous muscle: with emphasis on water status and distribution by LF-NMR and MRI. *Meat Sci.* 147, 44–52. doi: 10.1016/j.meatsci.2018.08.020
- Cropotova, J., Mozuraityte, R., Standal, I. B., and Rustad, T. (2019). Assessment of lipid oxidation in Atlantic mackerel (*Scomber scombrus*) subjected to different antioxidant and sous-vide cooking treatments by conventional and fluorescence microscopy methods. *Food Control* 104, 1–8. doi: 10.1016/j.foodcont.2019.04.016
- Deng, S., Choto Lutema, P., Gwekwe, B., Li, Y., Akida, J. S., Pang, Z., et al. (2019). Bitter peptides increase engulf of phagocytes *in vitro* and inhibit oxidation of myofibrillar protein in peeled shrimp (*Litopenaeus vannamei*) during chilled storage. *Aquac. Rep.* 15:100234. doi: 10.1016/j.aqrep.2019.100234
- Don, S., Xavier, K. A. M., Devi, S. T., Nayak, B. B., and Kannuchamy, N. (2018). Identification of potential spoilage bacteria in farmed shrimp (*Litopenaeus vannamei*): application of Relative Rate of Spoilage models in shelf life-prediction. *Lwt. Food Sci. Technol.* 97, 295–301. doi: 10.1016/j.lwt.2018.07.006
- Fidalgo, L. G., Simões, M. M., Casal, S., Lopes-da-Silva, J. A., Carta, A. M. S., Delgadillo, I., et al. (2020). Physicochemical parameters, lipids stability, and volatiles profile of vacuum-packaged fresh Atlantic salmon (*Salmo salar*) loins preserved by hyperbaric storage at 10° C. *Food Res. Int.* 127:108740.
- Jia, S., Hong, H., Yang, Q., Liu, X., Zhuang, S., Li, Y., et al. (2020). TMT-based proteomic analysis of the fish-borne spoiler *Pseudomonas psychrophila* subjected to chitosan oligosaccharides in fish juice system. *Food Microbiol.* 90:103494. doi: 10.1016/j.fm.2020.103494
- Le, T., Takahashi, K., Okazaki, E., and Osako, K. (2020). Mitigation of lipid oxidation in tuna oil using gelatin pouches derived from horse mackerel (*Trachurus japonicus*) scales and incorporating phenolic compounds. *LWT* 128:109533. doi: 10.1016/j.lwt.2020.109533
- Li, Y., Huang, J., Yuan, C., Ding, T., Chen, S., and Hu, Y. (2019). Developing a new spoilage potential algorithm and identifying spoilage volatiles in small yellow croaker (*Larimichthys polyactis*) under vacuum packaging condition. *LWT* 106, 209–217. doi: 10.1016/j.lwt.2019.02.075
- Mousakhani-Ganjeh, A., Hamdami, N., and Soltanizadeh, N. (2016). Effect of high voltage electrostatic field thawing on the lipid oxidation of frozen tuna fish (*Thunnus albacares*). *Innov. Food Sci. Emerg. Technol.* 36, 42–47. doi: 10.1016/j.ifset.2016.05.017
- Nian, L., Cao, A., and Cai, L. (2020). Investigation of the antifreeze mechanism and effect on quality characteristics of largemouth bass (*Micropterus salmoides*) during FT cycles by hAFP. *Food Chem.* 325:126918. doi: 10.1016/j.foodchem.2020.126918
- Niu, B., Mu, L., Xiao, L., Zhang, Z., Malakar, P. K., Liu, H., et al. (2018). Reduction of infection risk mediated by co-culturing *Vibrio parahaemolyticus* and *Listeria monocytogenes* in refrigerated cooked shrimp. *J. Sci. Food Agr.* 98, 4454–4461. doi: 10.1002/jsfa.8969
- Odeyemi, O. A., Burke, C. M., Bolch, C. J., and Stanley, R. (2018). Evaluation of spoilage potential and volatile metabolites production by *Shewanella baltica* isolated from modified atmosphere packaged live mussels. *Food Res. Int.* 103, 415–425. doi: 10.1016/j.foodres.2017.10.068
- Parlapani, F., Michailidou, S., Anagnostopoulos, D., Koromilas, S., Kios, K., Pasentsis, K., et al. (2019). Bacterial communities and potential spoilage markers of whole blue crab (*Callinectes sapidus*) stored under commercial simulated conditions. *Food Microbiol.* 82, 325–333. doi: 10.1016/j.fm.2019.03.011
- Sharifian, S., Alizadeh, E., Mortazavi, M. S., and Shahriari Moghadam, M. (2011). Effects of refrigerated storage on the microstructure and quality of Grouper (*Epinephelus coioides*) filets. *J. Food Sci. Tech.* 51, 929–935. doi: 10.1007/s13197-011-0589-4
- Sobieszkańska, N., Myszk, K., Szwengiel, A., Majcher, M., Grygier, A., and Wolko, Ł. (2020). Tarragon essential oil as a source of bioactive compounds with anti-quorum sensing and anti-proteolytic activity against *Pseudomonas* spp. isolated from fish—*in vitro*, *in silico* and *in situ* approaches. *Int. J. Food Microbiol.* 331:108732.
- Sun, Q., Zhang, M., and Yang, P. (2019). Combination of LF-NMR and BP-ANN to monitor water states of typical fruits and vegetables during microwave vacuum drying. *LWT* 116:108548. doi: 10.1016/j.lwt.2019.108548
- Susanto, E., Agustini, T. W., Ritanto, E. P., Dewi, E. N., and Swastawati, F. (2011). Changes in oxidation and reduction potential (Eh) and pH of tropical fish during storage. *J. Coast. Res.* 14, 223–234.
- Tan, M., Lin, Z., Zu, Y., Zhu, B., and Cheng, S. (2018). Effect of multiple freeze-thaw cycles on the quality of instant sea cucumber: emphatically on water status of by LF-NMR and MRI. *Food Res. Int.* 109, 65–71. doi: 10.1016/j.foodres.2018.04.029
- Wang, S., Lin, R., Cheng, S., and Tan, M. (2020a). Water dynamics changes and protein denaturation in surf clam evaluated by two-dimensional LF-NMR T1-T2 relaxation technique during heating process. *Food Chem.* 320:126622. doi: 10.1016/j.foodchem.2020.126622
- Wang, Y., Liu, Y., Ma, L., Li, H., Wang, Z., Xu, J., et al. (2020b). The oxidation mechanism of phospholipids in Antarctic krill oil promoted by metal ions. *Food Chem.* 333:127448. doi: 10.1016/j.foodchem.2020.127448

Both authors contributed to the article and approved the submitted version.

FUNDING

This research was financially supported by the National Natural Science Foundation of China (Grant Nos. 31972142 and 31571914), the Shanghai Municipal Science and Technology Project to Enhance the Capabilities of the Platform (Grant No. 19DZ2284000), and Research Start-Up Fund Project for Young Teachers of Shanghai Ocean University (Grant No. A2-2006-21-200316).

- Wang, X., Geng, L., Xie, J., and Qian, Y.-F. (2017). Relationship Between Water Migration and Quality Changes of Yellowfin Tuna (*Thunnus albacares*) During Storage at 0°C and 4°C by LF-NMR. *J. Aquat. Food Prod. T.* 27, 35–47. doi: 10.1080/10498850.2017.1400630
- Wang, X.-Y., and Xie, J. (2019). Evaluation of water dynamics and protein changes in bigeye tuna (*Thunnus obesus*) during cold storage. *LWT* 108, 289–296. doi: 10.1016/j.lwt.2019.03.076
- Wang, X.-Y., and Xie, J. (2020a). Assessment of metabolic changes in *Acinetobacter johnsonii* and *Pseudomonas fluorescens* co-culture from bigeye tuna (*Thunnus obesus*) spoilage by ultra-high-performance liquid chromatography-tandem mass spectrometry. *LWT Food Sci. Technol.* 123:109073. doi: 10.1016/j.lwt.2020.109073
- Wang, X.-Y., and Xie, J. (2020b). Growth Kinetics and Spoilage Potential of Co-culturing *Acinetobacter johnsonii* and *Pseudomonas fluorescens* from Bigeye Tuna (*Thunnus obesus*) During Refrigerated Storage. *Curr. Microbiol.* 77, 1637–1646. doi: 10.1007/s00284-020-01978-5
- Wang, X. Y., and Xie, J. (2020c). Quorum Sensing System-Regulated Proteins Affect the Spoilage Potential of Co-cultured *Acinetobacter johnsonii* and *Pseudomonas fluorescens* From Spoiled Bigeye Tuna (*Thunnus obesus*) as Determined by Proteomic Analysis. *Front. Microbiol.* 11:940. doi: 10.3389/fmicb.2020.00940
- Yan, J., and Xie, J. (2020). Comparative Proteome Analysis of *Shewanella putrefaciens* WS13 Mature Biofilm Under Cold Stress. *Front. Microbiol.* 11:1225. doi: 10.3389/fmicb.2020.01225
- Zhou, J., Wu, X., Chen, Z., You, J., and Xiong, S. (2019). Evaluation of freshness in freshwater fish based on near infrared reflectance spectroscopy and chemometrics. *LWT Food Sci. Technol.* 106, 145–150. doi: 10.1016/j.lwt.2019.01.056
- Zhu, S., Wu, H., Zeng, M., Liu, Z., and Wang, Y. (2015). The involvement of bacterial quorum sensing in the spoilage of refrigerated *Litopenaeus vannamei*. *Int. J. Food Microbiol.* 192, 26–33. doi: 10.1016/j.ijfoodmicro.2014.09.029

Conflict of Interest: The authors declare that the research was conducted in the absence of any commercial or financial relationships that could be construed as a potential conflict of interest.

Publisher's Note: All claims expressed in this article are solely those of the authors and do not necessarily represent those of their affiliated organizations, or those of the publisher, the editors and the reviewers. Any product that may be evaluated in this article, or claim that may be made by its manufacturer, is not guaranteed or endorsed by the publisher.

Copyright © 2021 Wang and Xie. This is an open-access article distributed under the terms of the Creative Commons Attribution License (CC BY). The use, distribution or reproduction in other forums is permitted, provided the original author(s) and the copyright owner(s) are credited and that the original publication in this journal is cited, in accordance with accepted academic practice. No use, distribution or reproduction is permitted which does not comply with these terms.



Evaluating the Effectiveness of Screened Lactic Acid Bacteria in Improving Crop Residues Silage: Fermentation Parameter, Nitrogen Fraction, and Bacterial Community

Liwen He¹, Yimin Wang¹, Xiang Guo², Xiaoyang Chen² and Qing Zhang^{2*}

¹ State Key Laboratory of Animal Nutrition, College of Animal Science and Technology, China Agricultural University, Beijing, China, ² College of Forestry and Landscape Architecture, Guangdong Province Research Center of Woody Forage Engineering Technology, Guangdong Key Laboratory for Innovative Development and Utilization of Forest Plant Germplasm, State Key Laboratory for Conservation and Utilization of Subtropical Agro-Bioresources, South China Agricultural University, Guangzhou, China

OPEN ACCESS

Edited by:

Shalini Gaur Rudra,
Indian Agricultural Research
Institute, India

Reviewed by:

Assar Ali Shah,
Jiangsu University, China
Zhenshang Xu,
Qilu University of Technology, China

*Correspondence:

Qing Zhang
zqing_scau@163.com

Specialty section:

This article was submitted to
Food Microbiology,
a section of the journal
Frontiers in Microbiology

Received: 15 March 2021

Accepted: 08 April 2022

Published: 24 May 2022

Citation:

He L, Wang Y, Guo X, Chen X and
Zhang Q (2022) Evaluating the
Effectiveness of Screened Lactic Acid
Bacteria in Improving Crop Residues
Silage: Fermentation Parameter,
Nitrogen Fraction, and Bacterial
Community.
Front. Microbiol. 13:680988.
doi: 10.3389/fmicb.2022.680988

Ensiling characteristics of sweet potato vine (SPV) and peanut straw (PS), as well as the effects of lactic acid bacteria (LAB) strains, *Lactococcus Lactis* MK524164 (LL) and *Lactobacillus farciminis* MK524159 (LF), were investigated in this study. Fermentation parameters, nitrogen fractions, and bacterial community of SPV and PS were monitored at intervals during the ensiling process. The results showed that inoculating LAB increased lactate production (2.23 vs. 2.73%; 0.42 vs. 1.67% DM), accelerated pH decline (5.20 vs. 4.47; 6.30 vs. 5.35), and decreased butyrate (0.36% DM vs. not detected), ammonia-N (6.41 vs. 4.18% CP), or nonprotein-N (43.67 vs. 35.82% CP). Meanwhile, it altered the silage bacterial community, where the relative abundance of *Lactobacillus* was increased (6.67–32.03 vs. 45.27–68.43%; 0.53–10.45 vs. 38.37–68.62%) and that of undesirable bacteria such as *Clostridium*, *Enterobacter*, *Methylobacterium*, or *Sphingomonas* was much decreased. It is suggested that the screened LAB strains LL and LF can effectively improve the silage quality of SPV and PS silages.

Keywords: bacterial community, lactic acid bacteria, peanut straw, silage quality, sweet potato vine

INTRODUCTION

According to the statistics, almost 92 million tons of sweet potatoes are produced annually, ranking second in the root and tuber crops grown in the world (FAOSTAT, 2020). Sweet potato vine (SPV) is the byproduct of sweet potato, accounting for ~64% of fresh biomass, with a forage yield as high as 14.6 tons/hectare (Aregheore, 2004; Claessens et al., 2009). As well, the peanut is an important cooking oil and protein-producing crop, and its global planting area is as large as 28.52 million hectares with an annual output of 45.95 million tons (FAOSTAT, 2020). It is estimated that peanut straw (PS) yield is also 60 to 65% of the biomass in peanut production (Zhao et al., 2012). China is the main producer of these two crops with a crop yield of 53 million and 17.73 million tons per year (FAOSTAT, 2020), necessarily with large biomass of their byproducts produced, which could be an important feed resource if well used.

In practice, dietary inclusion of fresh SPV could promote follicular development of Chinese Meishan gilt and increase beneficial flora abundance (Xu et al., 2019; Zhang et al., 2019), and supplementing SPV to goats fed grass hay-based diet could improve growth performance and carcass traits, spare conventional concentrate, and improve production benefits (Tadesse et al., 2013). Likewise, PS contains about 60% total digestible nutrients and 14% crude protein along with medium fiber level (Sallam et al., 2019), and it could be used as a sole diet in goat feeding (Yusiati et al., 2016). From the above, exploiting these byproducts in animal feeding can not only relieve the shortage of feed resources but also promote animal growth.

However, a well storage method would be necessary to assure the nutrient preservation and year-round supply of such feed resources. Within the forage preservation methods, ensiling appears to be a more flexible and economic option compared with hay, especially in unfavorable weather seasons (Grant and Ferraretto, 2018). However, few research has focused on profiling their silage fermentation, and it might be a challenge to obtain quality silage given that these byproducts are commonly characterized as seasonal supply, high moisture, low nutrient content, and complicated bacterial community. Inoculating lactic acid bacteria (LAB) is a common way to promote the dominance establishment of LAB fermentation, thereby improving fermentation quality, nutrient preservation, and even aerobic stability. Shah et al. (2017, 2018, 2020, 2021) conducted a series of silage research with king grass, elephant grass, or hybrid pennisetum. The results showed that LAB inoculation could improve the fermentation quality, reduce undesirable microorganisms, and increase *in vitro* rumen gas production. Similarly, a previous study of our group showed that inoculating *Lactococcus Lactis* MK524164 (LL) and *Lactobacillus farciminis* MK524159 (LF) deriving from mature *Moringa oleifera* leaf silage could remarkably increase LAB abundance, lower silage pH value, and reduce dry matter loss in high-moisture (almost 80%) silage (Wang et al., 2019). Thus, it was hypothesized that inoculating LL and LF would improve the fermentation quality of SPV and PS silages. Besides, the effectiveness of LAB strains LL and LF in low-moisture silage had not been studied yet.

Accordingly, the objectives of this study were to (1) investigate the regular changes of SPV silage and PS silage, mainly paying attention to the dynamics of nitrogen distribution and microbial community; and (2) verify the effects of LAB strains LL and LF on improving silage quality of SPV and PS.

MATERIALS AND METHODS

Experimental Design and Silage Preparation

Fresh SPV and PS were collected from the Qilin North test field of South China Agricultural University (Guangzhou, China) and then manually cut into ~2 cm length by a paper cutter. Subsequently, the prepared raw materials were separately subjected to ensiling treatments, that is, inoculating LAB strains *Lactococcus Lactis* MK524164 (LL) and *Lactobacillus farciminis* MK524159 (LF) or their mixture (1:1; MIX, only for SPV silage),

along with the non-inoculated blank (CK). These two strains were previously screened and identified from *Moringa oleifera* leaf silage by the Gram stain, colony morphology, catalase activity test, and 16S rDNA sequencing. They can ferment cellobiose, maltose, sucrose, raffinose, inulin, and lactose, and were able to grow at pH 3.5 to 8.0 and at temperature 15°C to 40°C (Wang et al., 2019). To prepare inoculant powder of LL and LF, the stored strains (-80°C) were activated and incubated for 48 h in MRS broth at 37°C and then centrifuged to get the bacterial biomass, which was finally suspended with skimmed milk and lyophilized. The LAB number was enumerated on MRS agar.

For silage preparation, 200 g of forage was sprayed with given inoculant liquid (1×10^6 colony forming units (CFU) per gram of fresh matter) or deionized water (10 ml), then sealed in a mini bag silo (20 by 30 cm) with a household food vacuum sealer (Lyve DZ280; Dongguan Yijian Packaging Machinery, Dongguan, China). Each treatment was individually prepared in 12 bags (3 replications \times 4 sampling times), and totally 84 bags of silage were produced. During the ensiling fermentation (environmental temperature around 30°C), three bags of each treatment were randomly sampled on days 3, 7, 14, and 30.

Ensiling Characteristic and Nitrogen Distribution Analysis

Each bag silo was sampled (10 g) in triplicate, of which one was used for microbial plate counting, one was prepared for pH and organic acids determination, and the last one was used for bacterial diversity analysis. Finally, the remaining silage was oven-dried at 65°C (48 h) for DM determination. In brief, the silage sample was soaked with sterilized saline and serially diluted, and then the supernatant was used to enumerate LAB, coliform bacteria, yeasts, and molds on Man Rogosa Sharpe (MRS) agar, Violet Red Bile agar, and Rose Bengal agar, respectively. Another sample was extracted with deionized water and filtered to determine pH, ammonia-N, and organic acids. The content of ammonia-N was determined by the colorimetric method of Broderick and Kang (1980). The concentrations of lactic acid, acetic acid, propionic acid, and butyric acid were measured using high-performance liquid chromatography (HPLC) equipped with Shodex RSpak KC-811S-DVB gel C column (8.0 mm \times 30 cm; Shimadzu, Tokyo, Japan) and SPD-M10AVP detector, under the conditions of oven temperature 50°C, mobile phase 3 mmol/L HClO₄, flow rate 1.0 ml/min, and injection volume 5 μ l. The dried sample was ground to pass a 1-mm screen and then used to analyze crude protein (CP) and true protein (TP) using automatic Kjeldahl apparatus (Kjeltec 8400, FOSS), where nonprotein-N was calculated by the difference of CP and TP. The contents of neutral detergent fiber (NDF) and acid detergent fiber (ADF) were determined by an A220 Fiber Analyzer (ANKOM Technology Corp., Macedon, NY, USA), and water-soluble carbohydrates (WSC) content was analyzed with a commercial test kit using the anthrone-sulphuric acid method. All detailed procedures of these analyses referred to He et al. (2019).

16S rDNA Sequencing Analysis of Bacterial Community

The sample was submitted for 16S rDNA sequencing in Guangzhou Gene Denovo Co. Ltd. (Guangzhou, China), and the detailed procedures were the same as He et al. (2019). In brief, bacterial DNA was extracted with DNA Kit (Omega Biotek, Norcross, GA, USA). Then, PCR amplification was conducted with the primers (341F: CCTACGGGNGGCWGCAG; 806R: GGACTACHVGGGTATCTAAT) targeting at V3-V4 regions of 16S rDNA. After purification and quantification, amplicons were sequenced using Illumina Hiseq 2500. As for data analysis, any sequence that contained over 10% of unknown nucleotides (N) or <80% of bases with Q value >20 were removed using FASTP to obtain clean reads, which were then merged as raw tags using FLSAH (v 1.2.11) with the settings of minimum overlap 10 bp and mismatch error rates 2%. Raw tags were denoised using QIIME (V1.9.1) pipeline and chimera-filtered with the UCHIME algorithm. Operational taxonomic units (OTUs) were clustered using the UPARSE pipeline at the similarity level of 97%. Taxonomic classification at the phylum and genus levels was conducted using the RDP classifier (Version 2.2) based on the SILVA database. The alpha-diversity indices covering Sobs, Shannon, Simpson, Chao, Ace, and Goods_coverage were calculated in QIIME (V1.9.1). Principal coordinate analysis (PCoA) of unweighted UniFrac distances and relative abundance comparison was performed in software R. The datasets presented in this study can be found in online repositories. The names of the repositories and accession number(s) can be found below: [PRJNA812632; PRJNA813727] <https://www.ncbi.nlm.nih.gov/bioproject/?term=PRJNA812632> or PRJNA813727.

Statistical Analysis

The effects of ensiling time, LAB inoculant, and their interaction on ensiling characteristics and nitrogen fractions were analyzed using two-way ANOVA on SAS 9.3 with the statistical model:

$$Y_{ij} = \mu + D_i + T_j + (D \times T)_{ij} + e_{ijk}$$

where Y_{ijk} was every observation; μ was the general mean; D_i denoted the effect of ensiling time day i ; T_j represented the effect of LAB inoculant j ; $(D \times T)_{ij}$ accounted for the interaction of ensiling time day i and LAB inoculant j ; and e_{ijk} was random residual error. Duncan's test was used to do multiple comparisons and statistical significance was declared when $P < 0.05$. An online platform (<http://www.omicshare.com/tools>) was used to analyze the sequencing data of the bacterial community.

RESULTS

Characteristics of Raw Sweet Potato Vine and Peanut Straw

The characteristics of raw SPV and PS are shown in **Table 1**. The DM contents of SPV and PS used in this study were separately 11.28 and 48.71, and their CP contents were 13.44 and 9.96% (with true protein proportion of 79.20 and 87.01% CP), along

TABLE 1 | Characteristics of raw sweet potato vine and peanut straw.

Item	Sweet potato vine	Peanut straw
Dry matter (%)	11.28 ± 0.20	48.71 ± 0.17
Crude protein (% DM)	13.44 ± 1.10	9.96 ± 0.62
True protein (%DM)	10.64 ± 0.24	8.67 ± 0.19
Neutral detergent fiber (% DM)	42.19 ± 2.30	39.44 ± 1.96
Acid detergent fiber (% DM)	30.14 ± 1.44	20.75 ± 1.32
Water soluble carbohydrates (% DM)	3.92 ± 0.23	10.35 ± 0.79
Lactic acid bacteria (log ₁₀ CFU/g FM)	5.47 ± 0.43	3.60 ± 0.43
Coliform bacteria (log ₁₀ CFU/g FM)	5.84 ± 0.18	5.43 ± 0.91
Molds (log ₁₀ CFU/g FM)	4.23 ± 0.43	4.31 ± 0.15
Yeasts (log ₁₀ CFU/g FM)	4.33 ± 0.50	4.43 ± 0.10
Sobs	918 ± 30	1,077 ± 25
Shannon	3.46 ± 0.24	1.57 ± 0.10
Simpson	0.74 ± 0.03	0.31 ± 0.03
Chao	1,484 ± 53	1,960 ± 158
Ace	1,535 ± 101	2,002 ± 125
Goods_coverage	0.995 ± 0.001	0.994 ± 0.001

with moderate fiber content (42.19% NDF, 30.14% ADF and 39.44% NDF, 20.75% ADF). The WSC content was 3.92 or 10.35% for SPV and PS, and their plate counts of LAB, coliform bacteria, molds, and yeasts were 5.47, 5.84, 4.23, 4.33 and 3.60, 5.43, 4.31, 4.43 log₁₀ CFU/g FM, respectively. Furthermore, 16S rDNA sequencing analysis of the bacterial community revealed that the Sobs, Shannon, Simpson, Chao, Ace, and Goods_coverage of the bacterial community in SPV and PS silages were 918, 3.46, 0.74, 1484, 1535, 0.995 and 1077, 1.57, 0.31, 1960, 2022, 0.994, respectively.

Ensiling Characteristics of Inoculated or Non-Inoculated SPV and PS Silages

The dynamic changes in pH value, individual organic acid content, and microbial population are presented in **Table 2**. The application of inoculant LL, LF, or MIX decreased ($P < 0.05$) the pH values of SPV and PS silages, especially at the early stage. Consistently, inoculating LAB increased ($P < 0.01$) initial LAB loading and promoted ($P < 0.01$) acid production (lactic acid), thus accelerating ($P < 0.01$) pH decline. In addition, the growth of coliform bacteria was inhibited, and yeasts and molds, as well as propionic acid and butyric acid, were not detected in the inoculated SPV and PS silages.

The nitrogen fractions covering crude protein, true protein, non-protein-N, and ammonia-N of non-inoculated/inoculated SPV and PS silages are summarized in **Table 3**. In this study, the CP content of SPV or PS silage was not affected ($P > 0.05$) by LAB inoculation, but the CP content of SPV silage was decreased when compared to that of fresh SPV. The proportion of true protein decreased ($P < 0.01$) during the ensiling process, which was inhibited ($P < 0.01$) by inoculating LAB for PS silage but not for SPV silage. Meanwhile, ammonia-N proportion gradually increased ($P < 0.01$), and LAB inoculation decelerated ($P < 0.01$)

TABLE 2 | The effect of LAB inoculation on the fermentation characteristics of SPV and PS silages.

Item	Sweet potato vine silage					P-value				Peanut straw silage				P-value			
	Trt	Day 3	Day 7	Day 14	Day 30	SEM	D	T	DT	Day 3	Day 7	Day 14	Day 30	SEM	D	T	DT
DM	CK	11.48 ^a	11.33 ^a	10.48 ^{ab}	10.06 ^b	0.25	**	NS	NS	47.81 ^b	49.13 ^a	49.24 ^a	49.41 ^a	1.41	*	NS	NS
	LL	11.10 ^{ab}	11.34 ^a	10.92 ^{ab}	10.65 ^b					48.47	48.32	49.33	49.18				
	LF	11.38 ^a	11.49 ^a	10.67 ^b	10.42 ^b					48.51 ^b	50.34 ^a	49.78 ^{ab}	50.40 ^a				
	MIX	11.14 ^{ab}	11.52 ^a	10.40 ^b	10.64 ^b												
pH	CK	5.20 ^{Aa}	4.82 ^{Ab}	4.50 ^b	4.58 ^{Ab}	0.07	**	**	**	6.30 ^{Aa}	6.24 ^{Aa}	5.40 ^{Ab}	5.53 ^{Ab}	0.02	**	**	**
	LL	4.59 ^{Ba}	4.38 ^{Bb}	4.39 ^b	4.38 ^{ABb}					5.40 ^{Ba}	4.49 ^{Bb}	4.39 ^{Bb}	4.26 ^{Bb}				
	LF	4.52 ^{Ba}	4.42 ^{Bab}	4.38 ^b	4.38 ^{ABb}					5.35 ^{Ba}	4.57 ^{Bb}	4.36 ^{Bbc}	4.28 ^{Bc}				
	MIX	4.47 ^{Ba}	4.45 ^{ABa}	4.37 ^{ab}	4.30 ^{Bb}												
LAB	CK	7.93 ^{Ba}	8.00 ^a	7.68 ^{ab}	6.80 ^{Bb}	0.16	**	**	NS	6.67 ^{Bc}	7.84 ^{Bab}	8.57 ^{Ba}	7.06 ^{Cb}	0.04	**	**	**
	LL	8.84 ^{Aa}	8.20 ^{ab}	7.77 ^b	7.37 ^{ABb}					8.86 ^{Ab}	9.69 ^{Aa}	9.42 ^{Aa}	8.09 ^{Bc}				
	LF	8.67 ^{ABa}	8.29 ^{ab}	7.71 ^b	7.19 ^{ABb}					8.88 ^{Ab}	9.53 ^{Aa}	9.30 ^{Aa}	9.17 ^{Aab}				
	MIX	8.98 ^{Aa}	8.32 ^{ab}	7.70 ^b	7.63 ^{Ab}												
Coli.	CK	6.25	2.47	<2.00	<2.00	–	–	–	–	4.83	4.03	2.49	3.58	–	–	–	–
	LL	4.25	<2.00	<2.00	<2.00					< 2.00	< 2.00	< 2.00	< 2.00				
	LF	3.23	<2.00	<2.00	<2.00					3.89	< 2.00	< 2.00	< 2.00				
	MIX	3.47	<2.00	<2.00	<2.00												
LA	CK	1.93 ^{Bb}	2.32 ^{Bab}	2.75 ^{Ba}	2.23 ^{Bb}	0.09	**	**	NS	0.04 ^{Cd}	0.13 ^{Cc}	0.55 ^{Ca}	0.42 ^{Bb}	0.24	**	**	**
	LL	2.47 ^{Aa}	2.83 ^{Aa}	2.77 ^{Ba}	2.55 ^{ABab}					0.45 ^{Bd}	1.39 ^{Ac}	1.54 ^{Ab}	1.67 ^{Aa}				
	LF	2.50 ^{Ab}	2.97 ^{Aa}	2.91 ^{Aa}	2.62 ^{ABb}					0.66 ^{Ac}	1.21 ^{Bb}	1.35 ^{Bb}	1.58 ^{Aa}				
	MIX	2.54 ^{Ab}	2.71 ^{ABb}	3.09 ^{Aa}	2.73 ^{Ab}												
AA	CK	0.51 ^b	1.36 ^{ab}	1.60 ^a	1.82 ^a	0.14	**	0.44	NS	ND	ND	0.03	0.03	–	–	–	–
	LL	0.88 ^b	0.96 ^b	1.26 ^{ab}	1.51 ^a					ND	0.15	0.24	0.29				
	LF	0.92 ^b	0.99 ^b	1.38 ^{ab}	1.64 ^a					ND	0.13	0.22	0.30				
	MIX	0.80 ^b	1.17 ^{ab}	1.49 ^a	1.42 ^a												
BA	CK	ND	0.13	0.13	0.36	–	–	–	–	ND	ND	ND	ND	–	–	–	–
	LL	ND	ND	ND	ND					ND	ND	ND	ND				
	LF	ND	ND	ND	ND					ND	ND	ND	ND				
	MIX	ND	ND	ND	ND												

LAB (\log_{10} CFU/g fresh matter), lactic acid bacteria; SPV, sweet potato vine; PS, peanut straw; CK, non-inoculated silage (Control); LL, silage inoculated with *Lactococcus lactis* (LL); LF, silage inoculated with *Lactobacillus farciminis* (LF); MIX, silage inoculated with the mixture (1:1) of LL and LF.

DM (%), dry matter; LA (% DM), lactic acid; AA (% DM), acetic acid; BA (% DM), butyric acid; Coli., coliform bacteria; SEM, standard error of means; D, the effect of ensiling time; T, the effect of LAB inoculation; DT, the interaction of ensiling time and LAB inoculation; ND, not detected; “–”, default. The population of yeast and mold was $<2 \log_{10}$ CFU/g fresh matter, and propionic acid was not detected in this study.

^{A–C} Means in the same column followed by different uppercase letters differ ($P < 0.05$); ^{a–c} Means in the same row followed by different lowercase letters differ ($P < 0.05$). “*” and “**” denotes $P < 0.05$ and $P < 0.01$, respectively, and NS means $P > 0.05$.

TABLE 3 | The effect of LAB inoculation on the nitrogen distribution in SPV and PS silages.

Item	Sweet potato vine silage					P-value				Peanut straw silage				P-value			
	Trt	Day 3	Day 7	Day 14	Day 30	SEM	D	T	DT	Day 3	Day 7	Day 14	Day 30	SEM	D	T	DT
CP	CK	12.81 ^a	12.43 ^a	11.50 ^b	11.12 ^b	0.62	*	NS	NS	9.73	9.63	10.42	9.67	0.78	NS	NS	NS
	LL	12.14 ^a	11.32 ^{ab}	11.17 ^{ab}	10.52 ^b					10.11	10.56	10.33	9.64				
	LF	12.65 ^a	11.65 ^{ab}	11.40 ^b	11.30 ^b					9.87	10.12	10.34	10.21				
	MIX	12.40 ^a	10.63 ^b	10.24 ^b	10.46 ^b												
TPR	CK	66.38 ^{ABa}	60.28 ^{ABb}	56.82 ^{ABc}	55.33 ^{ABc}	1.61	**	**	*	68.26 ^{Ba}	65.11 ^{Ba}	55.78 ^{Cb}	56.33 ^{Bb}	4.93	**	**	*
	LL	67.74 ^{ABa}	58.42 ^{Bb}	57.88 ^{Ab}	56.19 ^{Ac}					72.22 ^{Aa}	67.67 ^{Ab}	61.45 ^{Bc}	61.56 ^{Ac}				
	LF	68.05 ^{ABa}	62.02 ^{Ab}	57.26 ^{Ac}	53.98 ^{Bd}					71.78 ^{Aa}	65.81 ^{ABb}	64.11 ^{Ab}	64.22 ^{Ab}				
	MIX	62.18 ^{Ba}	59.72 ^{Bab}	55.01 ^{Bb}	49.90 ^{Cc}												
NPNR	CK	33.62 ^{Bc}	39.72 ^{ABb}	43.18 ^{ABa}	44.67 ^{BCa}	1.61	**	**	*	31.67 ^{Ac}	34.93 ^{Ab}	44.53 ^{Aa}	43.67 ^{Aa}	4.93	**	**	*
	LL	32.26 ^{Bc}	41.58 ^{Ab}	42.12 ^{Bb}	43.81 ^{Ca}					27.78 ^{Bc}	32.33 ^{Bb}	38.55 ^{Ba}	38.40 ^{Ba}				
	LF	31.95 ^{Bd}	37.98 ^{Bc}	42.74 ^{Bb}	46.02 ^{Ba}					28.22 ^{Bb}	34.22 ^{Aa}	35.89 ^{Ca}	35.82 ^{Ba}				
	MIX	37.82 ^{Ad}	40.28 ^{Ac}	44.99 ^{Ab}	50.10 ^{Aa}												
NHR	CK	1.79 ^{Ac}	3.99 ^{Ab}	5.90 ^{Aa}	6.41 ^{Aa}	0.72	**	**	NS	0.24 ^d	0.38 ^c	0.48 ^b	0.63 ^a	0.09	**	NS	NS
	LL	1.38 ^{ABb}	1.90 ^{Bb}	3.67 ^{Ba}	4.18 ^{Ba}					0.20 ^c	0.35 ^b	0.48 ^b	0.72 ^a				
	LF	0.99 ^{Bd}	2.31 ^{Bc}	4.20 ^{Bb}	5.43 ^{ABa}					0.23 ^c	0.39 ^b	0.51 ^b	0.74 ^a				
	MIX	1.00 ^{Bb}	2.24 ^{Bb}	5.50 ^{Aa}	5.64 ^{ABa}												

LAB, lactic acid bacteria; SPV, sweet potato vine; CK, non-inoculated SPV silage (Control); PS, peanut straw; LL, silage inoculated with *Lactococcus lactis* (LL); LF, silage inoculated with *Lactobacillus farciminis* (LF); MIX, silage inoculated with the mixture (1:1) of LL and LF.

DM (%), dry matter; CP (% DM), crude protein; TPR (% CP), the proportion of true protein; NPNR (% CP), the proportion of nonprotein-N; NHR (% CP), the proportion of ammonia-N (protein equivalent); SEM, standard error of means; D, the effect of ensiling time; T, the effect of LAB inoculation; DT, the interaction of ensiling time and LAB inoculation.

^{A–C} Means in the same column followed by different uppercase letters differ ($P < 0.05$); ^{a–d} Means in the same row followed by different lowercase letters differ ($P < 0.05$). “*” and “**” denotes $P < 0.05$ and $P < 0.01$, respectively, and NS means $P > 0.05$.

its production in SPV silage, while PS silage contained a low ammonia-N proportion.

Bacterial Community Succession of Inoculated or Non-Inoculated SPV and PS Silage

The alpha-diversity indices covering Sobs, Shannon, Simpson, Chao, Ace, and Goods_coverage of the bacterial community in SPV and PS silages are summarized in **Table 4**. The Shannon, Chao, and Ace of the bacterial community in SPV silage varied ($P < 0.05$) during the ensiling process, while the Sobs, Shannon, Simpson, and Goods_coverage of that in PS silage were different ($P < 0.05$) at various time-points. As to the treatments, the bacterial community of inoculated SPV silage had higher ($P < 0.01$) Chao and Ace as well as lower ($P < 0.01$) Goods_coverage relative to the control, while that of inoculated PS silage was lower ($P < 0.01$) in Shannon, Simpson, and Goods_coverage. In addition, there existed an interaction effect ($P < 0.01$) of ensiling time and inoculation on these alpha-diversity indices of the bacterial community in PS silage.

Principal coordinate analysis (PCoA, **Figure 1**) illustrated that the bacterial community of SPV or PS silage was differentiated apparently from that of corresponding fresh material, and inoculating LAB further led to the clear separation of bacterial community between the inoculated silage and non-inoculated silage (CK group), while the bacterial community of LL or LF inoculated silage was similar. Moreover, the bacterial community on day 3 of ensiling in the CK group was separated from those on other time-points, while the bacterial community on various time-points showed cross-distribution in inoculated silages.

As shown in **Figure 2**, *Cyanobacteria* was the dominant phylum (91.46, 88.67%) in the bacterial community of fresh SPV or PS, while *Firmicutes* (27.11–84.40, 0.6–68.7%), *Proteobacteria* (6.30–53.09, 7.13–33.11%), and *Cyanobacteria* (3.00–20.32, 20.71–88.02%) were the top three phyla in the silages. The relative abundance of *Proteobacteria* was lower and that of *Firmicutes* was higher in the inoculated silage relative to that of the control silage.

At the genus level (**Figure 3**), a remarkable difference was found in the bacterial community among the fresh material, the control silage, and the inoculated silage. In general, the majority (>90%) of the bacterial community in fresh SPV or PS was unclassified with the second generation sequencing technology of 16S rDNA, while a high proportion of the bacterial community in their silages can be identified, where the abundance of unclassified bacteria in the inoculated silage (10.66–34.68% and 27.23–52.46%) was lower than that in the control silage (43.38–58.16% and 48.04–84.23%). When focusing on the classified bacteria, the control silage was jointly dominated by several genera like *Lactobacillus*, *Enterococcus*, *Lactococcus*, *Clostridium*, *Methylobacterium*, and *Sphingomonas*. By contrast, *Lactobacillus* was the overwhelming genus in the inoculated silage since day 3 of ensiling. Meanwhile, the undesirable bacteria like *Clostridium*, *Enterobacter*, *Kosakonia*, *Citrobacter*, *Methylobacterium*, or *Sphingomonas* were much decreased in the inoculated silage.

DISCUSSION

Characteristics of Raw Sweet Potato Vine and Peanut Straw

The chemical composition of SPV used in this study was in line with the results of Joo et al. (2018) reporting that SPV was a good feedstuff for ruminants containing 13.5% CP, 50.6% NDF, 33.9% ADF, and 4.68% WSC. The protein content of PS could be also high as 14% DM (Sallam et al., 2019) and PS could be used as a sole diet in goat feeding (Yusiati et al., 2016). The relatively lower protein content (9.96%) of PS in this study might be due to its lower proportion of leaf fraction or the different varieties and agronomic management.

Generally, WSC content is one of the most critical factors determining silage fermentation, and its theoretical requirement for quality silage is 60 to 70 g/kg DM (Smith, 1962). Accordingly, WSC shortage might be an issue when SPV (39.2 g/kg DM) ensiled. Moisture content is another important factor influencing silage fermentation, and a meta-analysis showed that the ideal value for high-quality silage was 65% to 70% (Guyader et al., 2018). In this study, the high-moisture content (88.72%) of SPV would make it bear the high risk of large seepage losses and *Clostridium* proliferation and decelerated pH decline, while the low moisture (51.29%) of PS might inhibit silage fermentation due to the shortage of metabolic water for the growth of LAB, and such dry silage would spoil quickly when exposed to air because of lacking sufficient amount of organic acids (e.g., acetic acid) with antifungal activity (Kung et al., 2018). Meanwhile, the high activities of coliform bacteria, yeasts, and molds might be unfavorable to the dominance establishment of LAB. In addition, bacterial community richness and diversity of fresh SPV and PS were quite different in this study. From the above, inoculating LAB might promote silage fermentation and improve nutrient preservation in SPV and PS silages.

Ensiling Characteristics of Inoculated or Non-Inoculated SPV and PS Silages

The improper moisture content would not benefit the dominance establishment of LAB fermentation or inhibit the growth of LAB, consequently resulting in a low rate of pH decline and microbial inhibition. In this study, inoculating LAB increased initial LAB loading and promoted acid production (lactic acid), inhibiting the growth of undesirable microorganisms, thus accelerating pH decline, even though their final pH values were still slightly higher than the threshold pH 4.20 of high-quality silage (Mcdonald et al., 1991). Such an earlier steady status of silage fermentation would inhibit further DM loss in prolonged silage. It is indicated that inoculating LL or LF could improve the fermentation quality of SPV and PS silages.

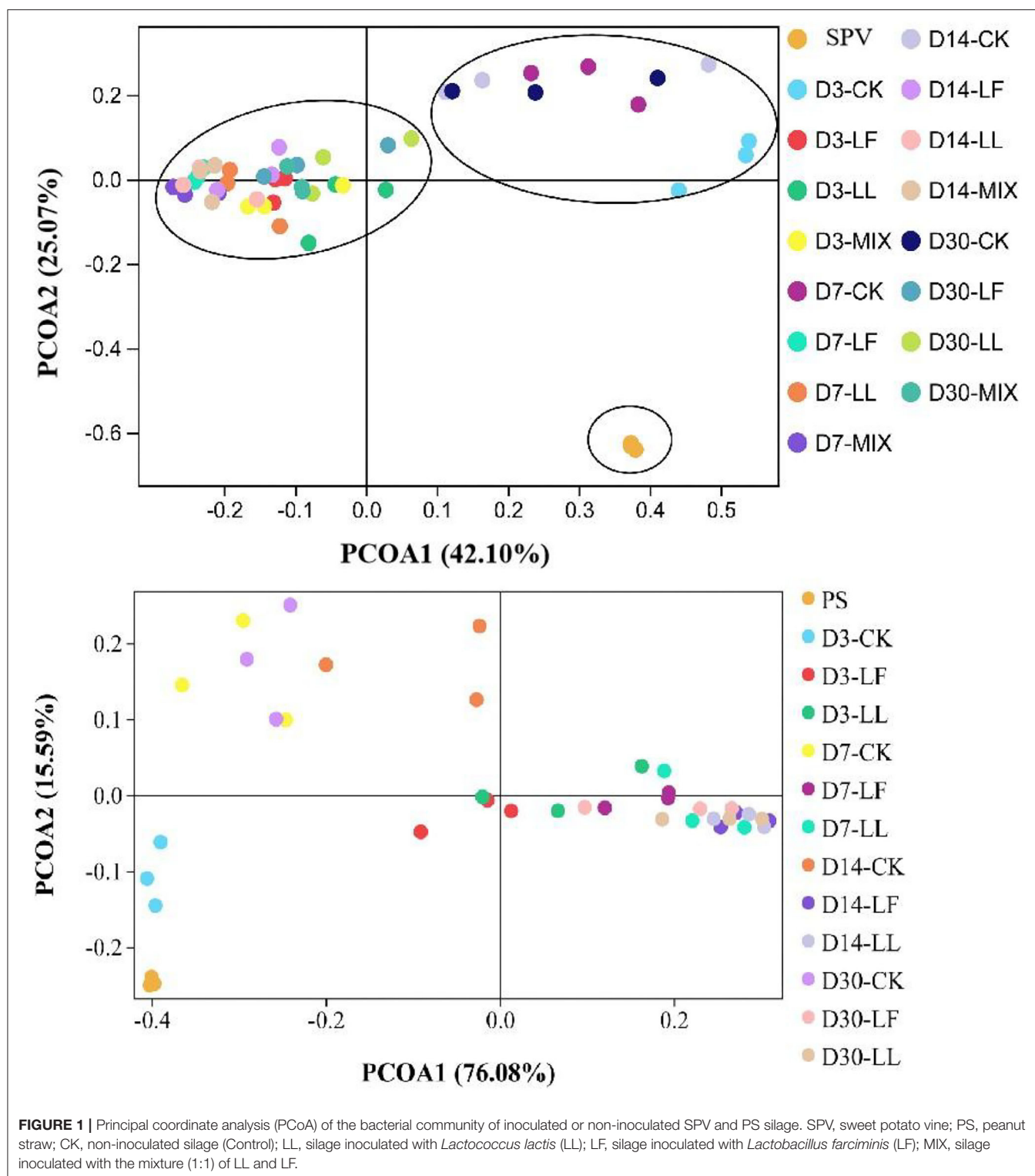
In this study, the CP content of SPV silage was decreased when compared to that of fresh SPV. It might be predominantly caused by the seepage losses due to the high moisture content, which would lead to much loss of soluble N (including soluble protein and ammonia-N). Other than the gross content of CP, the fractions of CP remarkably affect its bioavailability and then determine the feeding value of feed CP. It is

TABLE 4 | The effect of LAB inoculation on the alpha-diversity of bacterial community in SPV and PS silages.

Item	Sweet potato vine silage					P-value				Peanut straw silage				P-value			
	Trt	Day 3	Day 7	Day 14	Day 30	SEM	D	T	DT	Day 3	Day 7	Day 14	Day 30	SEM	D	T	DT
Sobs	CK	1,177	1,001	940	1,182	84	NS	NS	NS	1,232 ^{Bb}	1,499 ^{ab}	1,691 ^{Aa}	1,441 ^{Aab}	62	*	NS	**
	LL	1,202	1,170	1,224	1,444					1,537 ^A	1,404	1,339 ^B	1,233 ^B				
	LF	1,172	1,176	1,021	1,183					1,399 ^{ABb}	1,514 ^a	1,369 ^{Bbc}	1,329 ^{ABc}				
	MIX	1,302	1,087	1,223	1,220												
Shannon	CK	5.58	5.58 ^A	5.14	5.68	0.33	**	NS	NS	2.57b	4.30 ^{Aa}	4.09 ^{Aa}	4.32 ^{Aa}	0.17	*	**	**
	LL	4.98	4.91 ^B	4.96	6.01					2.92a	2.69 ^{Bab}	2.48 ^{Bbc}	2.44 ^{Bc}				
	LF	4.87	4.79 ^B	5.34	5.63					2.89	2.93 ^B	2.42 ^B	2.61 ^B				
	MIX	5.02 ^b	4.50 ^{Bb}	5.08 ^b	5.90 ^a												
Simpson	CK	0.94	0.95	0.92	0.93	0.02	NS	NS	NS	0.51 ^{Bb}	0.79 ^{Aa}	0.81 ^{Aa}	0.78 ^{Aa}	0.02	*	**	**
	LL	0.90	0.91	0.90	0.92					0.68 ^{Aa}	0.66 ^{Ba}	0.56 ^{Bc}	0.61 ^{Bb}				
	LF	0.89	0.91	0.94	0.93					0.68 ^{Aa}	0.61 ^{Bab}	0.56 ^{Bb}	0.58 ^{Bb}				
	MIX	0.91	0.88	0.91	0.95												
Chao	CK	1,649 ^{ab}	1,529 ^{Bab}	1,432 ^{Bb}	1,758 ^a	85	*	**	NS	1,889 ^{Bb}	2,317 ^a	2,631 ^{Aa}	2,305 ^a	112	NS	NS	**
	LL	1,846	1,698 ^A	1,767 ^{AB}	1,868					2,361 ^{AB}	2,540	2,282 ^B	2,347				
	LF	1,789	1,751 ^A	1,563 ^{AB}	1,700					2,594 ^{Aa}	2,400 ^{ab}	2,320 ^{Bb}	2,197 ^b				
	MIX	1,979 ^a	1,627 ^{ABb}	1,865 ^{Aab}	1,768 ^{ab}												
Ace	CK	1,689 ^B	1,537 ^B	1,442 ^B	1,734	82	*	**	NS	1,923 ^{Bb}	2,328 ^a	2,634 ^{Aa}	2,297 ^a	99	NS	NS	**
	LL	1,785 ^{AB}	1,769 ^A	1,595 ^{AB}	1,705					2,345 ^A	2,505	2,305 ^B	2,450				
	LF	1,870 ^{AB}	1,773 ^A	1,817 ^A	1,890					2,686 ^{Aa}	2,496 ^{ab}	2,332 ^{Bbc}	2,218 ^c				
	MIX	1,990 ^{Aa}	1,654 ^{ABb}	1,858 ^{Aab}	1,741 ^{ab}												
Goods_ coverage	CK	0.995 ^A	0.995 ^A	0.995 ^A	0.994	0.000	NS	**	NS	0.995 ^{Aa}	0.993 ^{ab}	0.992 ^{Bb}	0.994 ^a	0.000	**	**	**
	LL	0.994 ^{AB}	0.994 ^B	0.994 ^{AB}	0.994					0.993 ^B	0.992	0.993 ^A	0.993				
	LF	0.993 ^{Bb}	0.993 ^{Bb}	0.994 ^{Bb}	0.995 ^a					0.992 ^{Bc}	0.993 ^b	0.993 ^{ABb}	0.994 ^a				
	MIX	0.993 ^B	0.994 ^{AB}	0.993 ^B	0.994												

LAB, lactic acid bacteria; SPV, sweet potato vine; CK, non-inoculated SPV silage (Control); PS, peanut straw; LL, silage inoculated with *Lactococcus lactis* (LL); LF, silage inoculated with *Lactobacillus farciminis* (LF); MIX, silage inoculated with the mixture (1:1) of LL and LF; SEM, standard error of means; D, the effect of ensiling time; T, the effect of LAB inoculation; DT, the interaction of ensiling time and LAB inoculation.

^{A–B} Means in the same column followed by different uppercase letters differ ($P < 0.05$); ^{a–c} Means in the same row followed by different lowercase letters differ ($P < 0.05$). ** and *** denotes $P < 0.05$ and $P < 0.01$, respectively, and NS means $P > 0.05$.



believed that nonprotein-N, especially ammonia-N, is less-efficient in microbial N synthesis for ruminants relative to true protein, likely increasing the nitrogen emissions in animal production (McDonald et al., 1991; Li et al., 2018). During the ensiling process, true protein would be inevitably degraded into nonprotein-N more or less due to the effects of plant proteases

and microbial activities, thus the variation of nitrogen fractions would reflect the proteolysis extent in silage (He et al., 2019). In this study, remarkable protein hydrolysis occurred during the ensiling process, which might be interpreted as the high-moisture condition or the high-pH environment would benefit the activities of plant proteases and spoilage bacteria (e.g.,

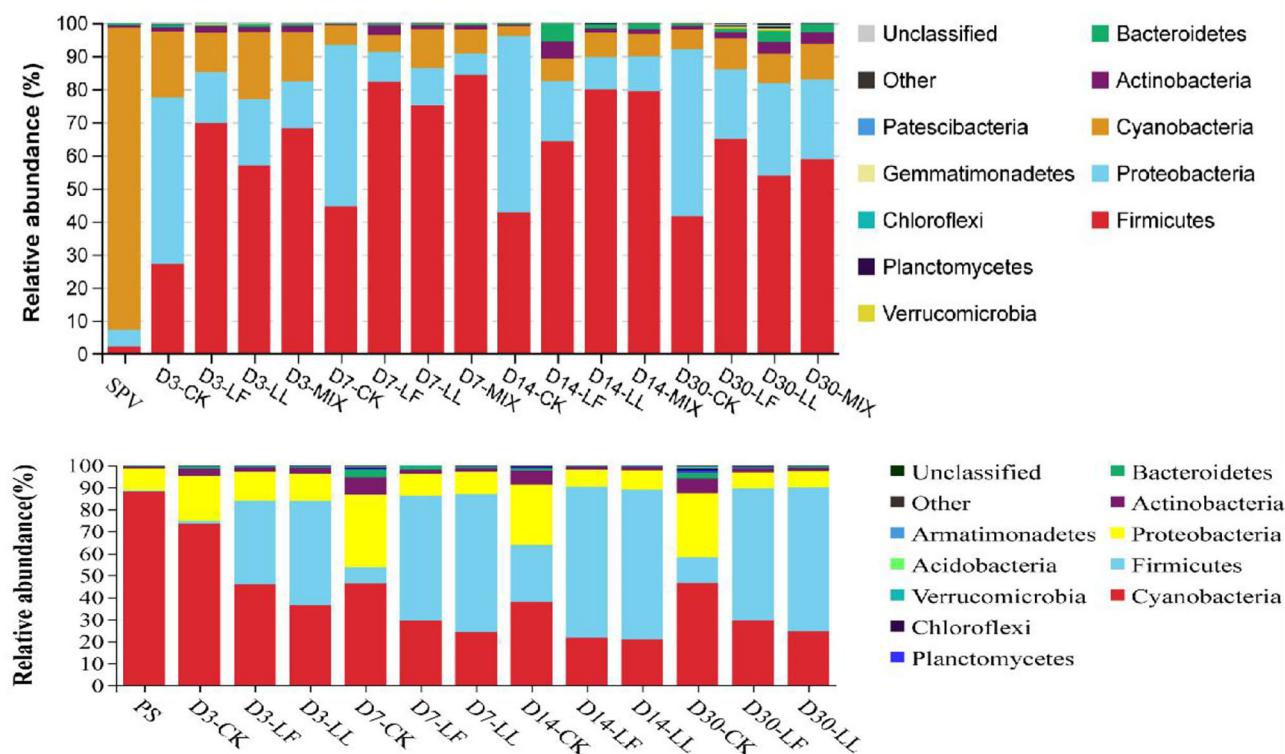


FIGURE 2 | Relative abundance of the bacterial community on phylum level of inoculated or non-inoculated SPV and PS silage. SPV, sweet potato vine; PS, peanut straw; CK, non-inoculated silage (Control); LL, silage inoculated with *Lactococcus lactis* (LL); LF, silage inoculated with *Lactobacillus farciminis* (LF); MIX, silage inoculated with the mixture (1:1) of LL and LF.

proteolytic clostridia) (Muck, 2010; He et al., 2019). Inoculating LAB exerted an improvement effect on protein preservation of PS silage because inoculating LAB increased bacteria loading and lowered pH condition, which might contribute to the acid hydrolysis of protein or the activity of acid proteinase (optimal pH of 4.50 in alfalfa silage) (McKersie, 1981). The specific interpretation of these alterations needs further studies. It is inferred that the profile of raw material such as moisture content and protease activity could affect protein preservation and the effectiveness of silage additive during the ensiling process.

In principle, peptide bonds of plant protein are first hydrolyzed by plant proteases generating free amino acids and peptides (collectively termed nonprotein-N), which are further degraded into ammonia, amines, and others by the deamination of microbial activities (Kung et al., 2018; He et al., 2019). Thus, ammonia-N content could reflect the degree of protein degradation, indicating the activity of undesirable microorganisms like *Clostridium* and *Enterobacter* (Kung et al., 2018). In this study, LAB inoculation decelerated ammonia-N production and slightly decreased its proportion in mature silage of SPV silage. As aforementioned, inoculating LAB promoted acid production and inhibited the activity of spoilage microorganisms like proteolytic clostridia, thus restricting the degree of protein degradation. As ammonia-N is inferior in utilization efficiency relative to true protein and high ammonia-N

content would show a negative effect on animal feed intake (Kung et al., 2018), its proportion is generally recommended as <10% TN, better lower than 5% in mature silage (Zhang et al., 2016). Furthermore, the higher nonprotein-N proportion in inoculated SPV silage did not come with a higher ammonia-N proportion, suggesting that more nonprotein-N existed in the form of amino acids or peptides. From the above, it is suggested that inoculating LAB could improve protein preservation of SPV and PS silage, with higher true protein proportion or less ammonia-N proportion.

Bacterial Community Succession of Inoculated or Non-Inoculated SPV and PS Silage

Analyzing bacterial community succession would contribute to the interpretation of the dynamic changes of silage fermentation, which would further help to specially improve silage quality. As revealed by the alpha-diversity indices, SPV and PS silages had higher bacterial community richness and diversity relative to their raw materials, which varied during ensiling process and were altered by LAB inoculation in this study. Moreover, the alteration of the bacterial community in SPV silage was mainly reflected in community richness (Chao and Ace), while that in PS silage was community diversity (Shannon

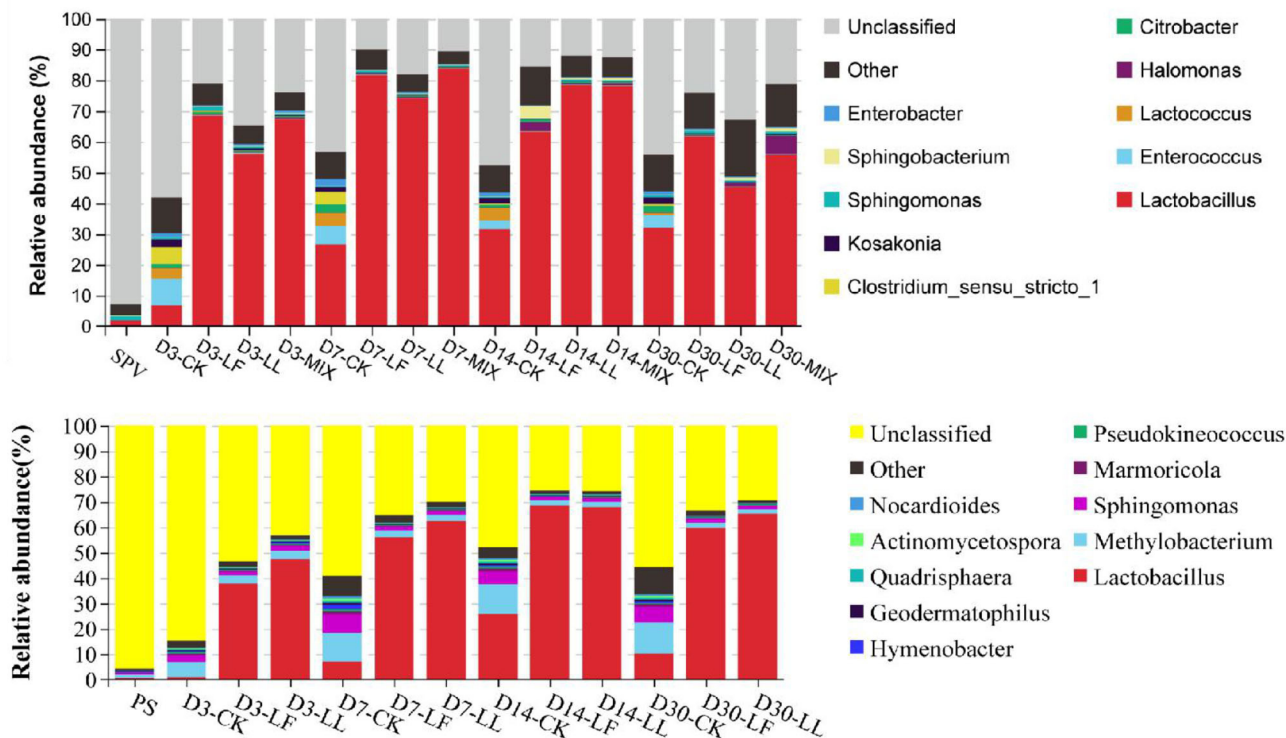


FIGURE 3 | Relative abundance of the bacterial community on genus level of inoculated or non-inoculated SPV and PS silage. SPV, sweet potato vine; PS, peanut straw; CK, non-inoculated silage (Control); LL, silage inoculated with *Lactococcus lactis* (LL); LF, silage inoculated with *Lactobacillus farciminis* (LF); MIX, silage inoculated with the mixture (1:1) of LL and LF.

and Simpson). The Goods_coverage over 0.99 indicated that sequencing abundance was large enough to reflect the profile of the bacterial community. Inoculating LL and LF or MIX increased bacterial community richness of SPV silage but decreased community diversity of PS silage. As ensiling is a process of microbial competition, LAB inoculation would change the initial loading of LAB and its dominance establishment thereby shaping differentiated bacterial communities (He et al., 2020). In general, the greater the abundance of dominant bacteria is, the less diverse the microbial community, and vice versa. The variation in the response of SPV and PS silages might be due to the difference of epiphytic microorganisms and the chemical composition of their raw materials. Consistently, PCoA analysis showed that the bacterial community of SPV or PS silage was differentiated apparently from that of corresponding fresh material, and inoculating LAB remarkably altered the community of silage bacteria, where inoculating LAB strains LL and LF resulted in similar bacterial communities. Moreover, the bacterial community of the CK group might go through a long time to reach a steady status relative to the inoculated silage. Thus, it is believed that inoculating LAB would shape the microbial community more desirable, resulting in quality improvement. Such alterations in bacterial community might well explain the difference in fermentation quality (such

as pH value and DM loss) between inoculated silage and CK silage.

The dominant phylum of the bacterial community of fresh SPV or PS was different from those of their silage. It was indicated that the bacterial community was remarkably changed on the phylum level by ensiling fermentation. Specifically, *Cyanobacteria* is the only known photosynthesizing phylum, which can use a wide nitrogen source with ammonia-N being its preferred source (Esteves-Ferreira et al., 2018), inferring that the relatively low ammonia-N content in PS silage might partly correlate with the high abundance of *Cyanobacteria*. Such bacteria might contribute to the healthy growth of the plant and have gained much attention from the pharmaceutical and biotechnical industries (Heberline, 2017). But not always the good, some *Cyanobacteria* may produce some toxins, such as microcystins, saxitoxins, nodularins, cylindrospermopsin, and anatoxin- α (He et al., 2016). Up to now, there is little study on *Cyanobacteria* in the ensiling process. Li et al. (2019) reported that *Cyanobacteria* was the main phylum in pre-ensiled king grass, paspalum, white popinac, and stylo, but not in the mature silage. The role of *Cyanobacteria* in the ensiling process still needs further study.

Consistently, Ogunade et al. (2018) concluded in a review that the majority of the bacterial community in silage belonged

to the phylum *Firmicutes* and *Proteobacteria*. In this study, inoculating LAB dramatically altered the bacterial communities of SPV and PS silages. The decline of *Proteobacteria* might be attributed to the low pH condition, in that *Proteobacteria* were reported to prefer the neutral environment (Brenner et al., 2005). *Proteobacteria* might play a crucial role in nitrogen cycling given that Li et al. (2020) reported that the abundance of *Proteobacteria* was positively correlated with ammonia-N content in wastewater fermentation. It is inferred that the improvement of protein preservation might somewhat correlate with the alteration of *Proteobacteria*.

The majority (>90%) of the bacterial community in fresh SPV or PS could not be classified on genus level with the second-generation sequencing technology of 16S rDNA, while a high proportion of the bacterial community in their silages can be identified based on the current database. It might be due to the relatively poor development of *Cyanobacterial* taxonomy, where most of the *Cyanobacteria* cannot be cultured in the present knowledge (Palinska and Surosz, 2014). Even though differentiated bacterial communities were illustrated, a higher annotated level of sequencing technology such as PacBio full-length 16S rDNA sequencing might further improve the analysis.

When focusing on the classified bacteria, the control silage was jointly dominated by several genera, showing that LAB could not dominate the silage till the end. By contrast, *Lactobacillus* was the overwhelming genus in the inoculated silage since day 3 of ensiling. It was confirmed that inoculating LAB did promote the dominance establishment of LAB during ensiling fermentation, consequently resulting in more acid production and faster pH decline. *Lactococcus*, *Enterococcus*, *Leuconostoc*, *Weissella*, and *Lactobacillus* are common lactate-producing bacteria in silage (Pahlow et al., 2003), where less acid-tolerant cocci like *Lactococcus* and *Enterococcus* initiate lactic acid fermentation at the early stage of ensiling and the more acid-tolerant bacilli like *Lactobacillus* dominate the community later (Cai et al., 1998). Meanwhile, the undesirable bacteria were much decreased in the inoculated silage. *Enterobacter* and *Clostridium* are undesirable bacteria in silage fermentation in that their activities would cause much protein degradation, dry matter loss, ammonia and butyric acid production, discounting acid fermentation, and pH decline (Pahlow et al., 2003; Muck, 2010). *Kosakonia* is a new genus recently classified from the genus *Enterobacter* (Li, 2016). *Methylobacterium* is strictly aerobic, neutrophilic, and facultative methylophilic bacteria commonly found in plants (Doronina et al., 2002), and their abundance is reported to positively correlate with silage pH (Ogunade et al., 2018).

Its relative high abundance in PS silage should be ascribed to the air residue and high-pH condition caused by the low-moisture content. *Sphingomonas*, belonged to Gram-negative aerobic *Alpha-proteobacteria*, are also detected in agricultural byproducts silage and are considered to cause hydrolysis of soluble protein (Zhou et al., 2019). So their increased abundance in the silage might be undesired and their exact roles in silage fermentation need further research. From the above, inoculating LAB remarkably enlarged the relative abundance of LAB, decreased the abundance of undesirable bacteria, and accelerated the dominance establishment of LAB in the bacterial community of SPV and PS silages.

CONCLUSIONS

The results showed that inoculating screened LAB strains LL and LF increased lactic acid production and accelerated pH decline, and decreased butyric acid and nonprotein-N or ammonia-N content in SPV and PS silages. Meanwhile, it remarkably altered the bacterial community of the silages, where the relative abundance of beneficial bacteria *Lactobacillus* was largely increased and that of undesirable bacteria such as *Clostridium*, *Enterobacter*, *Methylobacterium*, or *Sphingomonas* was much decreased. It is suggested that inoculating screened LAB strains LL and LF can dramatically improve the silage quality of SPV and PS silages.

DATA AVAILABILITY STATEMENT

The datasets presented in this study can be found in online repositories. The name of the repository and accession number can be found below: NCBI; PRJNA812632 and PRJNA813727.

AUTHOR CONTRIBUTIONS

LH: conceptualization, methodology, and writing—reviewing and editing. YW: investigation and data curation and manuscript checking. XG: methodology and investigation. XC: validation and supervision. QZ: conceptualization, methodology, and visualization. All authors contributed to the article and approved the submitted version.

FUNDING

This work was financially supported by the China Agriculture Research System of MOF and MARA (CARS-39), Guangzhou Science and Technology Bureau Project (202102020808), and Guangdong Natural Science Foundation (2020A1515011253).

REFERENCES

Aregheore, E. M. (2004). Nutritive value of sweet potato (*Ipomea batatas* (L) Lam) forage as goat feed: voluntary intake, growth and digestibility of mixed rations

of sweet potato and batiki grass (*Ischaemum aristatum* var. *indicum*). *Small Ruminant Res.* 51, 235–241. doi: 10.1016/S0921-4488(03)00198-6
Brenner, D. J., Krieg, R., and Staley, J. R. (2005). *Bergey's Manual of Systematic Bacteriology*. New York, NY: Springer.

- Broderick, G. A., and Kang, J. H. (1980). Automated simultaneous determination of ammonia and total amino acids in ruminal fluid and in vitro media. *J. Dairy Sci.* 63, 64–75. doi: 10.3168/jds.S0022-0302(80)82888-8
- Cai, Y., Benno, Y., Ogawa, M., Ohmomo, S., Kumai, S., and Nakase, T. (1998). Influence of *Lactobacillus* spp. from an inoculant and of *Weissella* and *Leuconostoc* spp. from forage crops on silage fermentation. *Appl. Environ. Microbiol.* 64, 2982–2987. doi: 10.1128/AEM.64.8.2982-2987.1998
- Claessens, L., Stoorvogel, J. J., and Antle, J. M. (2009). Ex ante assessment of dual-purpose sweet potato in the crop-livestock system of western Kenya: a minimum-data approach. *Agr. Syst.* 99, 13–22. doi: 10.1016/j.agry.2008.09.002
- Doronina, N. V., Trotsenko, Y. A., Kuznetsov, B. B., Tourova, T. P., and Salkinoja-Salonen, M. S. (2002). *Methylobacterium suomiense* sp. nov. and *Methylobacterium lusitanum* sp. nov., aerobic, pink-pigmented, facultatively methylophilic bacteria. *Int. J. Syst. Evol. Micr.* 52, 773–776. doi: 10.1099/00207713-52-3-773
- Esteves-Ferreira, A. A., Inaba, M., Fort, A., Araujo, W. L., and Sulpice, R. (2018). Nitrogen metabolism in *Cyanobacteria*: Metabolic and molecular control, growth consequences and biotechnological applications. *Crit. Rev. Microbiol.* 44, 541–560. doi: 10.1080/1040841X.2018.1446902
- FAOSTAT (2020). <http://www.fao.org/faostat/zh/#data/QC/visualize>
- Grant, R. J., and Ferraretto, L. F. (2018). Silage review: Silage feeding management: Silage characteristics and dairy cow feeding behavior. *J. Dairy Sci.*, 101, 4111–4121. doi: 10.3168/jds.2017-13729
- Guyader, J., Baron, V., and Beauchemin, K. (2018). Corn forage yield and quality for silage in short growing season areas of the Canadian prairies. *Agron.*, 8, 164–172. doi: 10.3390/agronomy8090164
- He, L., Lv, H., Chen, N., Wang, C., Zhou, W., Chen, X., et al. (2019). Improving fermentation, protein preservation and antioxidant activity of *Moringa oleifera* leaves silage with gallic acid and tannin acid. *Bioresource Technol.* 19:122390. doi: 10.1016/j.biortech.2019.122390
- He, L., Lv, H., Xing, Y., Wang, C., and Zhang, Q. (2020). The nutrients in *Moringa oleifera* leaf contribute to the improvement of stylo and alfalfa silage: Fermentation, nutrition and bacterial community. *Bioresource Technol.* 301, 122733. doi: 10.1016/j.biortech.2020.122733
- He, X., Liu, Y. L., Conklin, A., Westrick, J., Weavers, L. K., Dionysiou, D. D., et al. (2016). Toxic *cyanobacteria* and drinking water: impacts, detection, and treatment. *Harmful Algae*. 54, 174–193. doi: 10.1016/j.hal.2016.01.001
- Heberline, J. A. (2017). *Cyanobacteria: omics and manipulation. Environ. Prog. Sustain.* 36, 980–980. Available online at: <https://www.webofscience.com/wos/woscc/full-record/WOS:000388010300015>
- Joo, Y. H., Kim, D. H., Paradhita, D. H. V., Lee, H. J., Amanullah, S. M., Kim, S. B., et al. (2018). Effect of microbial inoculants on fermentation quality and aerobic stability of sweet potato vine silage. *Asian Austral. J. Anim.*, 31, 1897–1902. doi: 10.5713/ajas.18.0264
- Kung, L., Shaver, R. D., Grant, R. J., and Schmidt, R. J. (2018). Silage review: Interpretation of chemical, microbial, and organoleptic components of silages. *J. Dairy Sci.*, 101, 4020–4033. doi: 10.3168/jds.2017-13909
- Li, D., Ni, K., Zhang, Y., Lin, Y., and Yang, F. (2019). Fermentation characteristics, chemical composition and microbial community of tropical forage silage under different temperatures. *Asian Austral. J. Anim.* 32, 665–673. doi: 10.5713/ajas.18.0085
- Li, X., Li, Y., Li, Y., and Wu, J. (2020). *Myriophyllum elatinoides* growth and rhizosphere bacterial community structure under different nitrogen concentrations in swine wastewater. *Bioresour. Technol.* 301, 122776. doi: 10.1016/j.biortech.2020.122776
- Li, X., Tian, J., Zhang, Q., Jiang, Y., Hou, J., Wu, Z., et al. (2018). Effects of applying *Lactobacillus plantarum* and Chinese gallnut tannin on the dynamics of protein degradation and proteases activity in alfalfa silage. *Grass Forage Sci.* 73, 648–659. doi: 10.1111/gfs.12364
- Li, Y. (2016). *Classification of Bacteria of the Genus Kosakonia Based on Genome-wide Sequence Systems*. Hangzhou: Zhejiang University.
- Mcdonald, P., Henderson, A. R., and Heron, S. J. E. (1991). *The Biochemistry of Silage*. Marlow, Bucks: Ed Chalcombe Publication.
- McKersie, B. D. (1981). Proteinases and peptidases of alfalfa herbage. *Can. J. Plant Sci.*, 61, 53–59. doi: 10.4141/cjps81-008
- Muck, R. (2010). Silage microbiology and its control through additives. *Revista Brasileira De Zootecnia* 39, 183–191. doi: 10.1590/S1516-35982010001300021
- Ogunade, I. M., Jiang, Y., Cervantes, A. P., Kim, D. H., Oliveira, A. S., Vyas, D., et al. (2018). Bacterial diversity and composition of alfalfa silage as analyzed by Illumina MiSeq sequencing: Effects of *Escherichia coli* O157: H7 and silage additives. *J. Dairy Sci.* 101, 2048–2059. doi: 10.3168/jds.2017-12876
- Pahlow, G., Muck, R. E., Driehuis, F., Elferink, S. J. W. H., and Spoelstra, S. F. (2003). *Microbiology of Ensiling*. OAI.
- Palinska, K. A., and Surosz, W. (2014). Taxonomy of cyanobacteria: a contribution to consensus approach. *Hydrobiologia* 740, 1–11. doi: 10.1007/s10750-014-1971-9
- Sallam, S. M. A., Kholif, A. E., Amin, K. A., El-Din, A. N. M. N., Attia, M. F. A., Matloup, O. H., et al. (2019). Effects of microbial feed additives on feed utilization and growth performance in growing Barki lambs fed diet based on peanut hay. *Anim. Biotechnol.* 11, 1–8. doi: 10.1080/10495398.2019.1616554
- Shah, A. A., Qian, C., Liu, Z., Wu, J., Sultana, N., Mobashar, M., et al. (2021). Evaluation of biological and chemical additives on microbial community, fermentation characteristics, aerobic stability, and in vitro gas production of SuMu No.2 elephant grass. *J. Sci. Food Agr.* 101, 5429–5436. doi: 10.1002/jsfa.11191
- Shah, A. A., Qian, C., Wu, J., Liu, Z., Khan, S., Tao, Z., et al. (2020). Effects of natamycin and *Lactobacillus plantarum* on the chemical composition, microbial community, and aerobic stability of Hybrid pennisetum at different temperatures. *RSC Adv.* 10, 8692–8702. doi: 10.1039/D0RA00028K
- Shah, A. A., Xianjun, Y., Zhihao, D., Junfeng, L., and Sao, T. (2018). Microbiological and chemical profiles of elephant grass inoculated with and without *Lactobacillus plantarum* and *Pediococcus acidilactici*. *Archives Microbiol.* 200, 311–328. doi: 10.1007/s00203-017-1447-1
- Shah, A. A., Xianjun, Y., Zhihao, D., Siran, W., and Tao, S. (2017). Effects of lactic acid bacteria on ensiling characteristics, chemical composition and aerobic stability of king grass. *J. Anim. Plant Sci.* 3, 747–755. Available online at: https://www.researchgate.net/publication/318118240_Effects_of_lactic_acid_bacteria_on_ensiling_characteristics_chemical_composition_and_aerobic_stability_of_king_grass#fullTextFileContent
- Smith, L. H. (1962). Theoretical carbohydrate requirement for alfalfa silage production. *Agron. J.* 54, 291–293. doi: 10.2134/agronj1962.00021962005400040003x
- Tadesse, M., Mengistu, U., and Ajebu, N. (2013). Effects of feeding sweet potato (*Ipomoea batatas*) vines as a supplement on feed intake, growth performance, digestibility and carcass characteristics of Sidama goats fed a basal diet of natural grass hay. *Trop. Anim. Health Prod.* 45, 593–601. doi: 10.1007/s11250-012-0264-4
- Wang, Y., He, L., Xing, Y., Zhou, W., Pian, R., Yang, F., et al. (2019). Bacterial diversity and fermentation quality of *Moringa oleifera* leaves silage prepared with lactic acid bacteria inoculants and stored at different temperatures. *Bioresource Technol.* 284, 349–358. doi: 10.1016/j.biortech.2019.03.139
- Xu, S., Zhang, P., Cao, M., Dong, Y., and De, W. (2019). Microbial mechanistic insights into the role of sweet potato vine on improving health in Chinese meishan gilt model. *Animals* 9, 632–640. doi: 10.3390/ani9090632
- Yusiati, L. M., Hanim, C., and Putra, D. (2016). “Digestibility and nitrogen balance of male Bligon and Kejombang goat fed peanuts straw,” in *The 17th Asian-Australasian Association of Animal Production Societies Animal Science Congress, Fukuoka, Japan*.
- Zhang, P., Cao, M., Li, J., Lin, Y., and Xu, S. (2019). Effect of sweet potato vine on the onset of puberty and follicle development in Chinese Meishan Gilts. *Animals* 9, 297–305. doi: 10.3390/ani9060297
- Zhang, Y., Yang, J., Wang, J., Zheng, N., Li, S., Zhao, S., et al. (2016). Progress assessment of chemical indicators of silage. *Chinese J. Anim. Husb.* 52, 37–42.
- Zhao, X., Chen, J., and Du, F. L. (2012). Potential use of peanut by-products in food processing: a review. *J. Food Sci. Technol.* 49, 521–529. doi: 10.1007/s13197-011-0449-2
- Zhou, Y., Chen, Y., Guo, J., Shen, Y., and Yang, J. (2019). The correlations and spatial characteristics of microbiome and silage quality by reusing of

citrus waste in a family-scale bunker silo. *J. Clean. Prod.* 226, 407–418. doi: 10.1016/j.jclepro.2019.04.075

Conflict of Interest: The authors declare that the research was conducted in the absence of any commercial or financial relationships that could be construed as a potential conflict of interest.

Publisher's Note: All claims expressed in this article are solely those of the authors and do not necessarily represent those of their affiliated organizations, or those of the publisher, the editors and the reviewers. Any product that may be evaluated in

this article, or claim that may be made by its manufacturer, is not guaranteed or endorsed by the publisher.

Copyright © 2022 He, Wang, Guo, Chen and Zhang. This is an open-access article distributed under the terms of the Creative Commons Attribution License (CC BY). The use, distribution or reproduction in other forums is permitted, provided the original author(s) and the copyright owner(s) are credited and that the original publication in this journal is cited, in accordance with accepted academic practice. No use, distribution or reproduction is permitted which does not comply with these terms.

Advantages of publishing in Frontiers



OPEN ACCESS

Articles are free to read
for greatest visibility
and readership



FAST PUBLICATION

Around 90 days
from submission
to decision



HIGH QUALITY PEER-REVIEW

Rigorous, collaborative,
and constructive
peer-review



TRANSPARENT PEER-REVIEW

Editors and reviewers
acknowledged by name
on published articles

Frontiers

Avenue du Tribunal-Fédéral 34
1005 Lausanne | Switzerland

Visit us: www.frontiersin.org

Contact us: frontiersin.org/about/contact



REPRODUCIBILITY OF RESEARCH

Support open data
and methods to enhance
research reproducibility



DIGITAL PUBLISHING

Articles designed
for optimal readership
across devices



FOLLOW US

@frontiersin



IMPACT METRICS

Advanced article metrics
track visibility across
digital media



EXTENSIVE PROMOTION

Marketing
and promotion
of impactful research



LOOP RESEARCH NETWORK

Our network
increases your
article's readership